frontiers | Research Topics

New frontiers in the application of stable isotopes to ecological and ecophysiological research

Edited by
Keith Alan Hobson, John Whiteman and Seth Newsome

Published in
Frontiers in Ecology and Evolution

ISSN 1664-8714
ISBN 978-2-8325-3240-9
DOI 10.3389/978-2-8325-3240-9

About Frontiers

Frontiers is more than just an open access publisher of scholarly articles: it is a pioneering approach to the world of academia, radically improving the way scholarly research is managed. The grand vision of Frontiers is a world where all people have an equal opportunity to seek, share and generate knowledge. Frontiers provides immediate and permanent online open access to all its publications, but this alone is not enough to realize our grand goals.

Frontiers journal series

The Frontiers journal series is a multi-tier and interdisciplinary set of open-access, online journals, promising a paradigm shift from the current review, selection and dissemination processes in academic publishing. All Frontiers journals are driven by researchers for researchers; therefore, they constitute a service to the scholarly community. At the same time, the *Frontiers journal series* operates on a revolutionary invention, the tiered publishing system, initially addressing specific communities of scholars, and gradually climbing up to broader public understanding, thus serving the interests of the lay society, too.

Dedication to quality

Each Frontiers article is a landmark of the highest quality, thanks to genuinely collaborative interactions between authors and review editors, who include some of the world's best academicians. Research must be certified by peers before entering a stream of knowledge that may eventually reach the public - and shape society; therefore, Frontiers only applies the most rigorous and unbiased reviews. Frontiers revolutionizes research publishing by freely delivering the most outstanding research, evaluated with no bias from both the academic and social point of view. By applying the most advanced information technologies, Frontiers is catapulting scholarly publishing into a new generation.

What are Frontiers Research Topics?

Frontiers Research Topics are very popular trademarks of the *Frontiers journals series*: they are collections of at least ten articles, all centered on a particular subject. With their unique mix of varied contributions from Original Research to Review Articles, Frontiers Research Topics unify the most influential researchers, the latest key findings and historical advances in a hot research area.

Find out more on how to host your own Frontiers Research Topic or contribute to one as an author by contacting the Frontiers editorial office: frontiersin.org/about/contact

New frontiers in the application of stable isotopes to ecological and ecophysiological research

Topic editors

Keith Alan Hobson — Western University, Canada

John Whiteman — Old Dominion University, United States

Seth Newsome — University of New Mexico, United States

Citation

Hobson, K. A., Whiteman, J., Newsome, S., eds. (2023). *New frontiers in the application of stable isotopes to ecological and ecophysiological research*. Lausanne: Frontiers Media SA. doi: 10.3389/978-2-8325-3240-9

Table of contents

frontiers | Frontiers in Ecology and Evolution

TYPE Editorial
PUBLISHED 31 July 2023
DOI 10.3389/fevo.2023.1259402

OPEN ACCESS

EDITED AND REVIEWED BY
Jonathon H. Stillman,
San Francisco State University,
United States

*CORRESPONDENCE
Keith A. Hobson
khobson6@uwo.ca

RECEIVED 15 July 2023
ACCEPTED 24 July 2023
PUBLISHED 31 July 2023

CITATION
Hobson KA, Whiteman JP and Newsome SD (2023) Editorial: New frontiers in the application of stable isotopes to ecological and ecophysiological research. *Front. Ecol. Evol.* 11:1259402. doi: 10.3389/fevo.2023.1259402

Editorial: New frontiers in the application of stable isotopes to ecological and ecophysiological research

Keith A. Hobson[1,2]*, John P. Whiteman[3] and Seth D. Newsome[4]

[1]Western University, London, ON, Canada, [2]Science and Technology Branch, Division of Environment and Climate Change, Government of Canada, Saskatoon, SK, Canada, [3]Department of Biological Sciences, College of Sciences, Old Dominion University, Norfolk, NE, United States, [4]Department of Biology, University of New Mexico, Albuquerque, NM, United States

KEYWORDS

bulk tissues, compound-specific analyses, C,N,O,H,S, metabolic routing, origins of nutrients, metabolism, adding tools

Editorial on the Research Topic

New frontiers in the application of stable isotopes to ecological and ecophysiological research

Application of the measurements of naturally occurring stable isotopes in animal tissues has expanded greatly over the last few decades and has become a firmly established component of the ecologist's toolbox (Hoenig et al., 2022; Hobson, 2023). This is a rapidly evolving field and we are in the midst of new and exciting developments based on creative uses of this technique and on recent technological and computational breakthroughs that enable us to measure stable isotopes of more and more elements. However, applications to ecophysiological research have generally lagged behind more descriptive ecological investigations, despite the tremendous potential to contribute to this field. Our objectives in formulating this set of 15 papers was to provide readers with examples of new and innovative approaches in the use of tissue isotope measurements to investigate animal ecophysiology, or examples which demonstrate creative ways in which the isotope approach can be combined with other tools to provide novel ecological insights, some of which have implications for species conservation. We are delighted to present this special series of papers because they are overwhelmingly diverse and touch upon several avenues of investigation that provide the reader with an impressive update on the current state of isotopic investigations in animal ecophysiology and community ecology.

There are many hundreds of published papers that have used isotopic measurements of animal tissues to reconstruct diet, trophic position, and/or sources of nutrients fueling food webs. As these approaches have become more established, we are witnessing new and creative combinations of isotopic data with information provided by other techniques. For example, Vanderklift et al. combined multiple isotope ($\delta^{13}C$, $\delta^{15}N$, and $\delta^{34}S$) measurements of blood and nails of the turtle *Chelonia mydas* in western Australia with acoustic telemetry to evaluate ontogenetic shifts in diet that could be associated with spatial distributions and habitat use. Importantly, more information was gained using this combination of tools than could be provided by either singly. Similarly, Bloomfield et al.

used acoustic telemetry and stable isotope measurements to link fish diet with thermal guild and space use in several species of freshwater fish during winter in boreal Canada.

Stable isotope measurements provide a unique opportunity to quickly and efficiently evaluate individual isotopic niches within complex communities that can ultimately be related to niche segregation and responses to broad environmental parameters at the landscape scale. These themes are well represented by the papers by Yohannes et al. who, using feather $\delta^{13}C$, $\delta^{15}N$ and $\delta^{34}S$, evaluated how a group of closely related birds in a Madagascar rainforest segregate through diet and space use and by Sekercioglu et al. who examined isotopically dietary responses of forest birds to fragmentation and juxtaposition to agriculture in Costa Rica. Pereira et al. similarly evaluated the effect of land-use practices on caiman in Brazil. Their study importantly made use of varying periods of isotopic integration of different tissue types to extend dietary inferences from the short term (weeks) to many months thereby exploiting one of the key benefits to using an isotope-based approach to reconstruct species diet and habitat use.

Closer to the theme of applying of stable isotope measurements to ecophysiological questions, two papers combined the use of fatty acid profiles with bulk tissue stable isotope measurements of stored lipids. In a captive study, Anparasan et al. made use of natural abundance $\delta^{13}C$ measurements in (C_3) larval diet of a migratory moth to distinguish larval use of essential fatty acids with those derived later during (C_4) consumption of nectar during the adult stage. That study showed essential fatty acids were conserved across life stages and the isotope data provided a means of identifying origins of larval versus adult diets. Genier et al. similarly quantified fatty acid composition of blood plasma in swallows to investigate their acquisition of essential (omega-3) fatty acids and used plasma $\delta^{2}H$ as a marker of where diets were derived. Aquatic emergent insects generally have lower tissue $\delta^{2}H$ compared to upland insects and this study emphasized the utility of hydrogen isotopes in examining local transfer of resources from aquatic habitats to terrestrial (riparian) communities, a key development given the importance of long-chain polyunsaturated fatty acids (PUFAs) in animal nutrition and how access to these essential nutrients may be threatened by climate change (Shipley et al., 2022).

Many studies have used animal tissue $\delta^{2}H$ and $\delta^{18}O$ values as a means of forensically assigning individuals to origin based on the long-term Global Network of Isotopes in Precipitation (GNIP) that can be used to create tissue-specific isoscapes (Hobson and Wassenaar, 2019). Modern assignment algorithms propagate known error based on calibration relationships using tissues from known-origin individuals, but evaluating factors contributing to variance in assignments is of keen interest. Lindroos et al. evaluated variance in the $\delta^{2}H$ of monarch butterfly wings related to metabolically active structures such as hemolymph containing veins and determined experimentally that such contributions are small but can be avoided. Reich et al. similarly investigated the utility of using trace metals and strontium isotopes in monarch wings as a means of geolocation. That investigation unexpectedly uncovered the effect of sex on wing $\delta^{87}Sr$ values that may complicate the use of this isotope for geolocation purposes.

Koehler et al. applied isotopic mapping to estimating origins of illegally traded cheetah cubs seized in east Africa and Dargent et al. combined $\delta^{87}Sr$ and $\delta^{2}H$ measurements to identify local versus migrant spruce budworm. Interestingly, Koehler et al. provide the first evidence that whisker $\delta^{18}O$ measurements can provide information on the nutritional influence of nursing in these cubs, which provided a means of avoiding assignment ambiguity if those researchers had used only whisker $\delta^{2}H$. Apparently, the different metabolic pathways involved in tissue synthesis for oxygen and hydrogen lead to isotopic fractionation differences that can be detected and used to advantage.

The work by Koehler et al. clearly emphasizes the value to ecophysiological studies involving the measurement of $\delta^{18}O$ in animal tissues. However, the work of Navarrete et al. is an exceptional example of the kind of detailed information one can derive from expanding the measurement of this element to $\delta^{16}O$, $\delta^{17}O$, $\delta^{18}O$. This triple-oxygen isotope approach was used in conjunction with $\delta^{13}C$ and $\delta^{15}N$ to evaluate the sources of metabolic water to two passerine species that inhabit coastal habitats in Chile where they consume a mixture of marine and terrestrial resources. That study will have immense impact on future research into the contribution of water sources to the water balance of free-ranging birds, a topic of increasing interest as climate change modifies regional precipitation regimes.

Oxygen isotope measurements ($\delta^{18}O$) were also used by Jones et al. who combined these measurements with $\delta^{13}C$ in fish otoliths to infer metabolic rates in wild populations of plaice. Although that study used an isotopic model provided by Chung et al. (2019) involving the dual isotopic measurement of aragonite in otoliths, theirs was the first application to a wild population. Jones et al. demonstrated that individual fish metabolism was clearly linked to population responses to climate change whereby fish sought out cooler deeper waters and this response had metabolic consequences.

Stable isotope applications to ecological and ecophysiological investigations have undergone a major evolution in recent years due to the more widespread use of compound-specific isotope analyses (CSIA). That work moves beyond bulk tissues to provide isotopic information based on individual fatty acids and amino acids and has provided major insights into metabolic use and origins of key nutrients to animals (Whiteman et al., 2019). Two papers in our Research Topic make use of this approach. Pilecky et al. examined $\delta^{2}H$ and $\delta^{13}C$ values of individual fatty acids stored in the fat body of migrant monarch butterflies. Apart from indicating the extent of bioconversion of essential vs. non-essential fatty acids, of great interest was their finding that larval-derived omega-3 alpha linoleic acid (ALA) $\delta^{2}H$ was correlated with wing chitin $\delta^{2}H$ supporting the idea that such essential fatty acids are linked largely to the larval diet corresponding to provenance of wing formation. The other study using CSIA came out of the well-established CSIA laboratory of Kelton McMahon where Ramirez et al. used amino acid $\delta^{15}N$ measurements of tissues from endangered hawksbill turtles (*Eretmochelys imbricata*) to establish

relative trophic levels of two populations (Florida vs. Texas) that differ dramatically in their growth rates. A major advantage of the CSIA approach is that it can provide trophic information on individuals without the need to assay baseline food web $\delta^{15}N$ values since tissues contain both trophic and source amino acids and the difference between these within an individual provides a self-corrected trophic estimate. This aspect of CSIA allows comparisons of community structure and sources of nutrients to animals separated spatially and temporally.

We maintain the future is bright for the continued application and development of isotopic tools in ecophysiological research. Ecologists have summarized the use of stable isotopes as "You are what you eat", reflecting an emphasis on community studies that has long characterized the field. To that, one might add "You are what you build", reflecting the increasing use of isotopes to understand exchange and transformation within (in addition to between) organisms. We predict a growing number of studies using natural abundance isotope studies that focus on evaluating field metabolic rates, water budgets, and the use and transport of fatty acids and amino acids to fuel metabolism, growth, and reproduction, especially in migratory animals. As demonstrated in our collection of papers, applications are varied and will continue to diversify.

Author contributions

KH: Writing – original draft. JW: Writing – review & editing. SN: Writing – review & editing.

Conflict of interest

The authors declare that the research was conducted in the absence of any commercial or financial relationships that could be construed as a potential conflict of interest.

Publisher's note

References

Chung, M.-T., Trueman, C., Godiksen, J., Holmstrup, M., and Grønkjær, P. (2019). Field metabolic rates of teleost fishes are recorded in otolith carbonate. *Commun. Biol.* 2, 24. doi: 10.1038/s42003-018-0266-5

Hobson, K. A. (2023). Stable isotopes in a changing world. *Oecologia*. doi: 10.1007/s00442-023-05387-w

Hobson, K. A., and Wassenaar, L. I. (Eds.) (2019). *Tracking Animal Migration using Stable Isotopes. 2nd ed.* (London: Academic Press), 253 pp.

Hoenig, B. D., Snider, A. M., Forsman, A. M., Hobson, K. A., Latta, S. C., Miller, E. T., et al. (2022). Current methods and future directions in avian diet analysis. *Ornithology* 139, 1–28. doi: 10.1093/ornithology/ukab077

Shipley, J. R., Twining, C. W., Mathieu-Resuge, M., Parmar, T. P., Kainz, M., Martin-Creuzburg, D., et al. (2022). Climate change shifts the timing of nutritional flux from aquatic insects. *Curr. Biol.* 32, 1342–1349. doi: 10.1016/j.cub.2022.01.057

Whiteman, J. P., Elliott-Smith, E. A., Besser, A. C., and Newsome, S. D. (2019). A guide to using compound-specific stable isotope analysis to study the fates of molecules in organisms and ecosystems. *Diversity* 11, 8. doi: 10.3390/d11010008

frontiers | Frontiers in Ecology and Evolution

TYPE Original Research
PUBLISHED 06 October 2022
DOI 10.3389/fevo.2022.986459

OPEN ACCESS

EDITED BY
John Whiteman,
Old Dominion University, United States

REVIEWED BY
Bryan Maitland,
University of Wisconsin–Madison, United States
Dan Gibson-Reinemer,
Adams State University, United States

*CORRESPONDENCE
Emma J. Bloomfield
emma@sepal.ca

SPECIALTY SECTION
This article was submitted to Ecophysiology, a section of the journal Frontiers in Ecology and Evolution

RECEIVED 05 July 2022
ACCEPTED 15 September 2022
PUBLISHED 06 October 2022

CITATION
Bloomfield EJ, Guzzo MM, Middel TA, Ridgway MS and McMeans BC (2022) Seasonality can affect ecological interactions between fishes of different thermal guilds.
Front. Ecol. Evol. 10:986459.
doi: 10.3389/fevo.2022.986459

Seasonality can affect ecological interactions between fishes of different thermal guilds

Emma J. Bloomfield[1]*, Matthew M. Guzzo[1], Trevor A. Middel[2], Mark S. Ridgway[2] and Bailey C. McMeans[1]

[1]Department of Biology, University of Toronto Mississauga, Mississauga, ON, Canada, [2]Harkness Laboratory of Fisheries Research, Aquatic Research and Monitoring Section, Ontario Ministry of Natural Resources and Forestry, Peterborough, ON, Canada

Seasonality could play a crucial role in structuring species interactions. For example, many ectotherms alter their activity, habitat, and diet in response to seasonal temperature variation. Species also vary widely in physiological traits, like thermal preference, which may mediate their response to seasonal variation. How behavioral responses to seasonality differ between competing species and alter their overlap along multiple niche axes in space and time, remains understudied. Here, we used bulk carbon and nitrogen stable isotopes combined with stomach content analysis to determine the seasonal diet overlap between a native cold-water species [lake trout (*Salvelinus namaycush*)] and a range-expanding warm-water species [smallmouth bass (*Micropterus dolomieu*)] in two north-temperate lakes over 2 years. We coupled these analyses with fine-scale acoustic telemetry from one of the lakes to determine seasonal overlap in habitat use and activity levels. We found that dietary niche overlap was higher in the spring, when both species were active and using more littoral resources, compared to the summer, when the cold-water lake trout increased their reliance on pelagic resources. Telemetry data revealed that activity rates diverged in the winter, when lake trout remained active, but the warm-water smallmouth bass reduced their activity. Combining stable isotopes and stomach contents with acoustic telemetry was a powerful approach for demonstrating that species interactions are temporally and spatially dynamic. In our case, the study species diverged in their diet, habitat, and activity more strongly during certain times of the year than others, in ways that were consistent with their thermal preferences. Despite large differences in thermal preference, however, there were times of year when both species were active and sharing a common habitat and prey source (i.e., resource overlap was greater in spring than summer). Based on our findings, important ecological processes are occurring during all seasons, which would be missed by summer sampling

alone. Our study stresses that quantifying multiple niche axes in both space and time is important for understanding the possible outcomes of altered seasonal conditions, including shorter winters, already arising under a changing climate.

KEYWORDS

seasonality, stable isotope, acoustic telemetry, trophic niche, lake trout, smallmouth bass, thermal guild, coexistence

Introduction

Species coexistence has captivated ecologist for decades. Foundational studies including theoretical modeling (Volterra, 1926; Lotka, 1932), laboratory (Gause, 1934; Park, 1954), and field experiments (Tansley, 1917; Connell, 1961) culminated in the competitive exclusion principle. This principle can be summarized as "complete competitors cannot co-exist" (Hardin, 1960). However, species may coexist if they occupy different habitats (spatial niche partitioning; Macarthur, 1958) or are favored by the physical environment at different times (temporal niche partitioning; Hutchinson, 1961). Species responses to spatial variation has received substantially more research attention than responses to temporal variation, despite the recognition that species can use different resources and be active at different times of the year (Chesson and Huntly, 1997; Shuter et al., 2012; McMeans et al., 2015).

Much of the work on temporal niche partitioning has focused on year-to-year differences in physical conditions (e.g., the amount of precipitation; Angert et al., 2009), but ecosystems also vary dramatically within a year from one season to the next. The role seasonality may play in coexistence has empirical (Shimadzu et al., 2013; McMeans et al., 2020) and theoretical support (Chesson, 2000; Mathias and Chesson, 2013). Central to these coexistence mechanisms are species responding differently to changing conditions. For example, coexistence may be promoted by seasonal patterns in light levels differentially impacting species' foraging efficiency (Helland et al., 2011), or seasonal patterns in temperature and precipitation differentially impacting species' metabolic rates (Szabó, 2016). Further, seasonally mediated coexistence has the potential to be widespread given that many ecosystems experience seasonal variation that impacts species interactions, including wet-dry seasonality in tropical river-floodplains (McMeans et al., 2019) and spring, summer, fall and winter seasonality in north-temperate lakes (Tonn and Magnuson, 1982).

North-temperate lakes (40–60°N) are ideal systems to explore species responses to seasonally changing conditions and consequences for niche overlap in time and space. These lakes undergo drastic seasonal changes in abiotic factors, including temperature and light minima during ice-covered winters ranging from 1 to 6 months (Shuter et al., 2012). For ectothermic organisms, like fish, temperature is a particularly important abiotic factor, affecting growth, locomotory activity, metabolism, and survival (Fry, 1947; Brett, 1971). Temperature influences biochemical processes and different species physiologies are optimized to perform best at specific temperatures (Brett, 1971; Beitinger and Fitzpatrick, 1979). Because of these optimized physiologies, fishes have distinct and well-established thermal preferences (the temperature species occupy when presented with a temperature range), which have been used to assign species to the warm, cool or cold-water thermal guild (Magnuson et al., 1979; Hasnain et al., 2018; Benoit et al., 2021).

Species in different thermal guilds may respond differently to changes in water temperatures as lakes' thermal structure changes seasonally. During the summer, many north-temperate lakes thermally stratify, which can spatially segregate species belonging to different thermal guilds (Guzzo et al., 2016). Cold-water species mainly occupy deeper offshore water, with access to the warmer nearshore area in the summer restricted to short forays (Goyer et al., 2014; Pépino et al., 2015). In the spring, fall, and winter, the nearshore water is cooler, making the area more thermally accessible to cold-water fishes. While cooler nearshore water can increase foraging opportunities for cold-water species (Guzzo et al., 2017), niche overlap with warm-water species may also increase (Vander Zanden et al., 1999). However, during the winter, warm-water fishes are expected to perform poorly and can decrease their activity rates compared to cold-water fishes because of different responses to low temperatures (Shuter et al., 2012). Seasonal changes in water temperature that drives divergent habitat use, diet, or activity rate could therefore be a mechanism for promoting coexistence in north-temperate lakes (Helland et al., 2011; McMeans et al., 2020).

Rapid changes are occurring in north-temperate lakes that may disrupt existing coexistence mechanisms. Increasing air temperature is predicted to cause later ice-on in the fall and earlier ice-off in the spring (Keller, 2007). Predictions about the timing of these key seasonal events are supported by long-term studies of lakes in North America and globally (Benson et al., 2012; Sharma et al., 2016; Guzzo and Blanchfield, 2017;

Woolway et al., 2020). Thus, the winter period in temperate lakes, as defined as a period of ice cover, is shrinking while the open-water period is expanding. To predict how species interactions will be altered under climate change scenarios, the role of current environmental periodicities in structuring competition and predation must be understood. However, current gaps in the literature limit our predictive ability. Many studies on temperate lakes have only considered the ice-free period due to the logistical and safety challenges of winter field work (Block et al., 2019). Studies that consider seasonal changes in both activity rates and resource use of potential competitors are especially rare. Combining existing methods, including stable isotopes and telemetry, is a promising approach for elucidating seasonal habitats, activity, and species interactions (McMeans et al., 2015; Marsden et al., 2021).

Here, we explored the niche overlap between fishes from the cold-water and warm-water thermal guild across all four seasons (spring, summer, fall, and winter) in two north-temperate lakes over a 2-year period. The native lake trout (*Salvelinus namaycush*) is our representative species of the cold-water guild and the range expanding smallmouth bass (*Micropterus dolomieu*) is our representative species of the warm-water guild. The thermal preference of the species differs substantially, with lake trout having a thermal preference of 11.8°C and smallmouth bass having a thermal preference of 25°C (Hasnain et al., 2018). Studies conducted during the open water period suggest that exploitative competition can occur between lake trout and smallmouth bass, where the latter reduce the diversity and abundance of littoral prey fish through predation (Vander Zanden et al., 1999; MacRae and Jackson, 2001). These reductions in prey fish may impact lake trout because they are mobile foragers that feed in both littoral and the pelagic zones (Tunney et al., 2012; Guzzo et al., 2017). In small lakes with smallmouth bass, lake trout consume less littoral prey fish and more pelagic zooplankton (Vander Zanden et al., 1999). Foraging on smaller prey, like zooplankton, has a higher energetic cost (Sherwood et al., 2002; Cruz-Font et al., 2019), so smallmouth bass invasion may negatively impact lake trout (Vander Zanden et al., 2004). Winter periods, when water temperatures decline and smallmouth bass reduce their activity, may therefore be crucial for increasing lake trout access to productive littoral zones (McMeans et al., 2020).

Our study builds on this previous knowledge and is the first to quantify overlap in activity rates, diet and habitat use of lake trout and smallmouth bass in all four seasons and across multiple lakes. Specifically, we ask how the overlap between lake trout and smallmouth bass in (1) habitat use, (2) activity, and (3) diet varies seasonally over two full annual cycles and in two lakes that support different food webs. We addressed our research questions using: (1) depth use and distance to shore from acoustic telemetry to determine habitat overlap, (2) movement rates from acoustic telemetry and the percent of non-empty stomachs as metrics of activity, and (3) stable isotopes of carbon ($\delta^{13}C$) and nitrogen ($\delta^{15}N$) supported by stomach contents to determine diet overlap. Because lake trout and smallmouth bass occupy different thermal guilds with distinct thermal preferences, we expected seasonal changes in niche overlap to be largely a product of different responses to seasonally changing water temperature and lake thermal structure. We expected that overlap in habitat, activity, and diet increases in the spring when both species are expected to be actively foraging in shallower, nearshore habitats. We also expected that winter, relative to summer, is a period of low activity for smallmouth bass and high littoral diet reliance for lake trout.

Materials and methods

Study system

Data were collected from two oligotrophic, dimictic north-temperate lakes that are ice covered for approximately 5 months of the year. The lakes are within Algonquin Provincial Park, Ontario (**Figure 1**), an area well known for lake trout angling opportunities. Lake of Two Rivers (45.5752, −78.4942) has a surface area of 306.4 ha, a maximum depth of 41.5 m and an average depth of 14.5 m (Ontario Ministry of Natural Resources and Forestry, 2022). Lake Opeongo (45.6743, −78.43756) has a surface area of 5154.2 ha, a maximum depth of 49.4 m, and an average depth of 13.7 m (Ontario Ministry of Natural Resources and Forestry, 2022). Hereafter, Lake Opeongo will be referred to as Lake 1 and Lake of Two Rivers will be referred to as Lake 2. Both lakes support self-sustaining populations of lake trout. Additionally, both lakes contain non-native smallmouth bass that have been moved outside of their natural distribution during historical stocking events. The fish communities also include brown bullhead (*Ameiurus nebulosus*), yellow perch (*Perca flavescens*), burbot (*Lota lota*), white sucker (*Catostomus commersonii*), and multiple cyprinid species. However, the fish communities differ in that Lake 1 has the pelagic prey fish, cisco (*Coregonus artedii*) and lake whitefish (*Coregonus clupeaformis*). These lakes were selected to determine if trends in seasonal resource partitioning between lake trout and smallmouth bass were consistent between lakes with different food webs. The presence of cisco combined with a larger surface area were expected to increase pelagic foraging and reduce littoral foraging of lake trout (Vander Zanden and Rasmussen, 1996; Schindler and Scheuerell, 2002) in Lake 1 compared to Lake 2.

Data collection

Water temperatures

Water temperatures were measured year-round throughout the water column. A string of data loggers (HOBO Temp

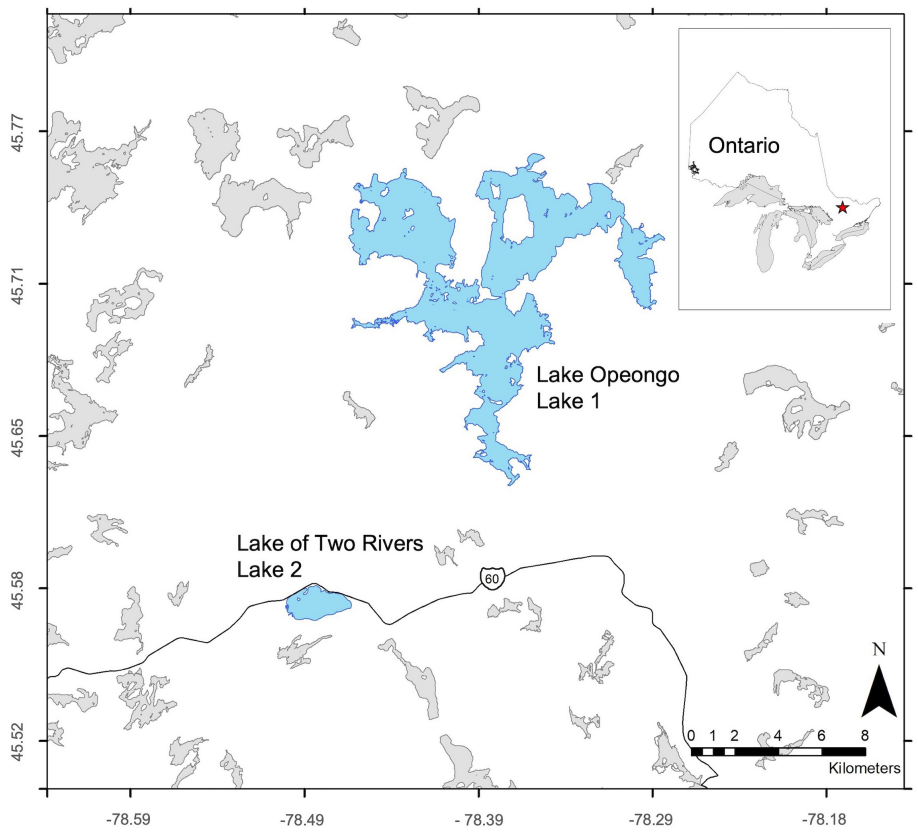

FIGURE 1
Location of Lake Opeongo (Lake 1) and Lake of Two Rivers (Lake 2).

Pro H20-001, Onset, Cape Cod, MA, USA) were deployed centrally in each lake. Data loggers were programmed to record temperature every 15 min and occupied depths of 1.5, 3, 4.5, 6, 7, 8, 9, 10, 11.5, 13, 20, and 27 m. Daily thermal profiles were created by calculating the mean daily temperature at each logger depth and predicting the temperature at 1 m intervals by fitting a spline to the data. Temperature data were also used to delineate seasons based on daily mean surface water temperatures (<6 m depth). Following existing telemetry studies on smallmouth bass and lake trout (Guzzo et al., 2017; McMeans et al., 2020), the period after ice-off but before mean surface temperatures exceeded 15°C was denoted as spring; summer was defined as the period during which surface temperatures were ≥15°C; fall began when lakes cooled to ≤15°C and lasted until winter, defined as ice-on to ice-off (**Figure 2**).

Acoustic telemetry

We used acoustic telemetry to examine seasonal variation in horizontal movement rates and spatial habitat overlap of lake trout and smallmouth bass. Acoustic telemetry was conducted only in Lake 2. A fine-scale positioning system was deployed in Lake 2 for the duration of the study period (spring 2017 to winter 2019). The positioning system included an array of 69 kHz VR2W acoustic receivers with co-located V16 time synchronization tags (InnovaSea Systems, Boston, MA, USA). Receivers and time synchronization tags (n = 54) were deployed at fixed locations designed to optimize acoustic coverage. A grid formation was used with a mean distance of 236 m between receivers. To assess the positioning system's accuracy, six reference tags (V9P tags; InnovaSea Systems, Boston, MA, USA) were deployed at fixed locations within the array at depths of 5 and 18 m.

The positioning system also included acoustic transmitter tags that were surgically implanted in smallmouth bass (n = 17) and lake trout (n = 17). Transmitter tags were equipped with pressure (depth) sensors and were relatively small to minimize behavioral impacts on implanted fish (V9P tags; 9 × 31 mm, 2.8 g in water; InnovaSea Systems, Boston, MA, USA). The tags transmitted every 420 s on average, with a random acoustic transmission rate between 360 and 480 s to reduce signal collisions between tags. The estimated tag battery life was 912 days, exceeding the study duration.

Fish were captured for acoustic tagging with trap nets, gillnets, or angling gear in May 2017, September 2017, and May 2018. Following capture, fish were anaesthetized in a solution of tricaine methanesulfonate (MS-222) and placed on

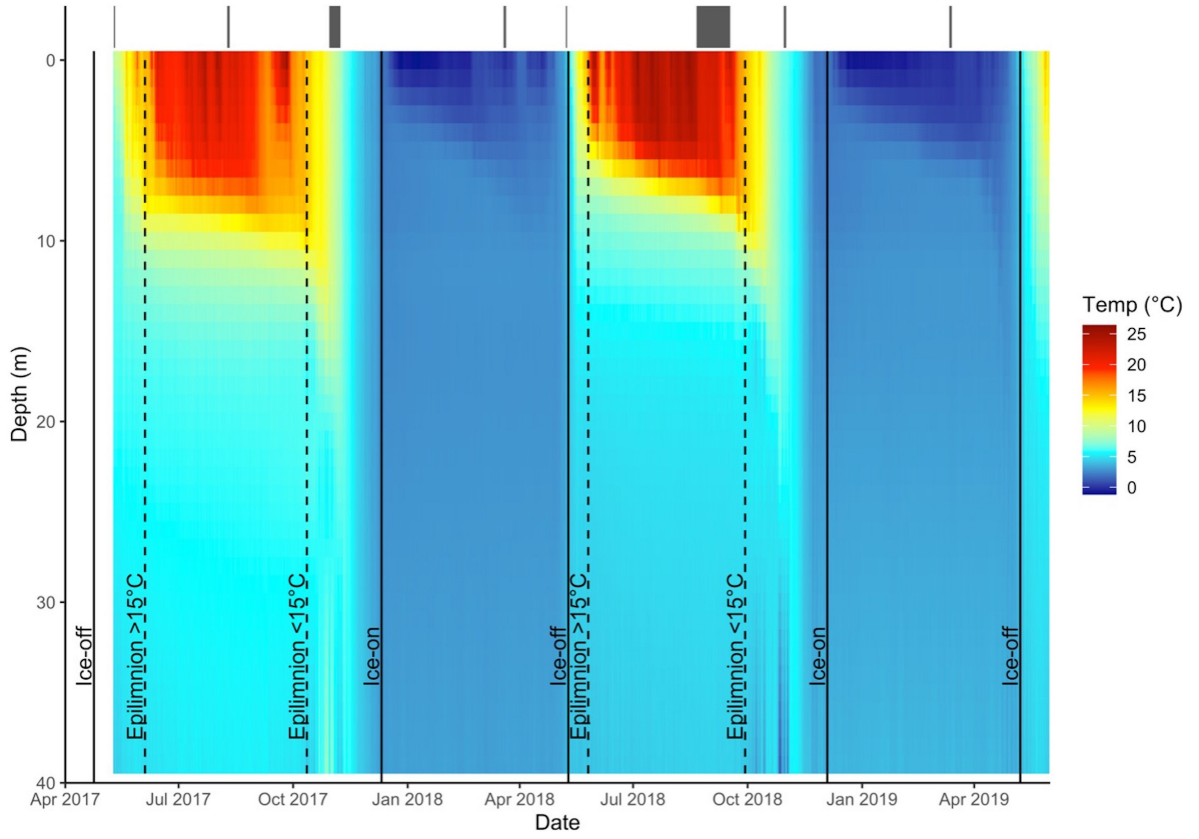

FIGURE 2
Thermal profile of Lake 2 (– cisco) from May 2017 to June 2019. Solid vertical lines indicate ice-on and ice-off events and dashed vertical lines indicate epilimnion water temperatures rising above or falling below 15°C. These lines delineate seasons, with spring between ice-off and water temperature greater than 15°C, summer when water temperatures are 15°C and above, fall between water temperature less than 15°C and ice-on, and winter between ice-on and ice-off. Gray bars at the top of the plot are the sampling periods in each season, spanning from the first to last day that fish were captured for stable isotope and stomach content analysis.

a surgery cradle with a maintenance dose of MS-222 flowing across their gills. Then, a surgical scalpel was used to make an incision posterior to the pectoral fin along the ventral midline, a transmitter tag was inserted into the body cavity, and the incision was stitched closed with 2–3 sutures (3-0 Monocryl synthetic absorbable sutures; Ethicon Inc., Somerville, NJ, USA). Fish total length was also recorded, scale samples were obtained, and an external T-bar anchor tag was applied. Performing the surgery and sampling was normally completed in under 3 min. Then, fish were placed in a cold-water recovery tank and their health was monitored (typically 10–15 min) before being returned to the lake.

Receiver data were processed to determine tagged fish position and depth. Receiver data were downloaded every 6 months and was sent to InnovaSea Systems (Boston, MA, USA) to determine the spatial positions (coordinates) of fish at the time of transmissions using hyperbolic positioning. Hyperbolic positioning involves converting differences in detection time between at least three receivers into differences in fish distance between receivers (Smith, 2013). The fine-scale positioning system produced 887,461 positions between May 23, 2017 and May 7, 2019, of which 63 and 37% were for lake trout and smallmouth bass, respectively. The higher percentage of positions for lake trout could be because lake trout occupy more central positions in the array (see Section "Results"), making tag transmissions more likely to be detected by $\geq$3 receivers (the requirement to calculate position). Each position had a corresponding depth value because pressure sensitive transmitting tags were used. The error on positions calculated from the fine-scale positioning system was assessed using the reference tags. The known position of fixed reference tags was compared to positions calculated from the fine-scale positioning system following Smith (2013). The positional error of reference tags was <6 m in over 95% of detections for reference tags at 5 m depth and over 85% of detections for reference tags at 18 m depth.

Fish and baseline sampling

Lake trout and smallmouth bass were sampled for stomach content and stable isotope analysis between the spring of 2017

and the winter of 2019, four times a year, for a total of eight sampling periods in both lakes. Fishes were captured through short sets of North American standard gill nets, trap nets, and angling. The objective was to sample 20 individuals of each species during each sampling period, however, this target was not always reached (**Table 1**). Lake trout were easily captured during all seasons. However, low numbers of smallmouth bass were captured during the fall and winter in each year, despite similar effort in each sampling period. Following fish capture, fish total length and sex were recorded, and livers were collected for stable isotope analysis. The stomach contents of lake trout and smallmouth bass were also identified during field sampling. Fish were identified to the species level and benthic macroinvertebrates to the order level when possible. It was also noted if stomachs were empty. Snails (Lake 1: n = 13, Lake 2: n = 15) and mussels (Lake 1: n = 13, Lake 2: n = 12) were collected to provide baseline stable isotope information for the benthic and pelagic habitats, respectively. These organisms were collected through snorkeling during the open water period. Attempts to use benthic grabs through the ice to capture snails and mussels failed. Putative prey were also collected using a variety of methods (**Supplementary Note 1**). Putative prey, baseline samples and liver tissue were frozen at −20°C and transferred to −80°C storage at the University of Toronto Mississauga within 2 weeks.

TABLE 1 Sample size (n) and biological data from lake trout (LT) and smallmouth bass (SMB) sampled for stomach contents and stable isotope analysis.

Lake	Species	Year	Season	n	Fork length (mm)	Weight (g)
1	LT	2017	Spr	21	505 (400–610)	1571 (920–2618)
1	LT	2017	Sum	20	492 (365–560)	1416 (534–2082)
1	LT	2017	Fall	21	480 (312–586)	1235 (420–2020)
1	LT	2018	Wint	17	447 (268–591)	1100 (191–2270)
1	LT	2018	Spr	22	482 (394–580)	1290 (626–2074)
1	LT	2018	Sum	22	512 (330–624)	1699 (376–2990)
1	LT	2018	Fall	12	497 (393–610)	1525 (771–2875)
1	LT	2019	Wint	12	481 (295–571)	1323 (276–2100)
1	SMB	2017	Spr	19	287 (252–341)	390 (256–702)
1	SMB	2017	Sum	17	282 (183–428)	407 (90–1210)
1	SMB	2017	Fall	0	NA	NA
1	SMB	2018	Wint	0	NA	NA
1	SMB	2018	Spr	21	234 (169–349)	221 (65–830)
1	SMB	2018	Sum	36	229 (152–335)	224 (53–676)
1	SMB	2018	Fall	5	278 (192–460)	505 (109–1716)
1	SMB	2019	Wint	0	NA	NA
2	LT	2017	Spr	21	402 (331–486)	778 (452–1276)
2	LT	2017	Sum	20	403 (330–518)	756 (370–1510)
2	LT	2017	Fall	23	415 (311–522)	759 (300–1460)
2	LT	2018	Wint	16	379 (310–496)	598 (326–1336)
2	LT	2018	Spr	24	412 (355–479)	808 (507–1303)
2	LT	2018	Sum	31	393 (286–485)	699 (283–1140)
2	LT	2018	Fall	19	394 (278–439)	691 (223–934)
2	LT	2019	Wint	11	365 (242–445)	532 (140–931)
2	SMB	2017	Spr	20	344 (229–470)	677 (160–1420)
2	SMB	2017	Sum	14	340 (204–442)	689 (119–1390)
2	SMB	2017	Fall	3	369 (350–387)	833 (730–900)
2	SMB	2018	Wint	1	288	349
2	SMB	2018	Spr	8	349 (290–380)	675 (389–907)
2	SMB	2018	Sum	21	290 (171–443)	484 (84–1407)
2	SMB	2018	Fall	0	NA	NA
2	SMB	2019	Wint	1	293	395

Fork length and weight are presented as mean (min–max).
Results are divided by Lake 1 (+ cisco) and Lake 2 (− cisco), year, and season.

Stable isotopes

Stable isotopes are naturally occurring, non-decaying elements with different numbers of neutrons. The ratio of the heavy to light forms of stable isotopes in an organism's tissue varies reliably with the isotopic signature of their energy sources (DeNiro and Epstein, 1978; Fry et al., 1978). Thus, stable isotope analysis can be used to characterize niches and determine assimilated energy sources (Boecklen et al., 2011). The ratio of ^{13}C to ^{12}C in a predator's tissue closely resembles its main prey because of limited trophic enrichment (Peterson and Fry, 1987; Post, 2002). Thus, when primary producers have different carbon isotope ratios, energy can be traced from source to consumer. For example, benthic algae, the primary producer in the littoral zone, is enriched in ^{13}C (higher ratio of ^{13}C to ^{12}C) compared to pelagic phytoplankton in the pelagic zone (France, 1995). Unlike carbon isotopes, the ratio of ^{15}N to ^{14}N increases substantially from prey to predator. Because of this trophic enrichment, nitrogen isotope ratios and can be used to estimate an organism's trophic position. Stable isotope analysis is commonly used in ecology because the diet of a consumer is assimilated into its tissue on the timescale of months, allowing a larger window of foraging behavior to be captured than the traditional method of stomach content analysis (Wolf et al., 2009; Boecklen et al., 2011).

To prepare samples for stable isotope analysis, fish liver tissue samples and the soft tissue of snails and mussels were dehydrated for 48 h at 60°C and ground into a powder with a mortar and pestle. Subsamples of between 400 and 600 μg were enclosed in a 5 × 3.5 mm tin capsule for carbon and nitrogen stable isotope analysis. Samples were analyzed at the Fisk Lab Stable Isotope Facility, Great Lakes Institute for Environmental Research, University of Windsor. The facility uses a Costech 4010 Elemental Combustion System coupled with a Thermo Fisher Scientific Delta V Advantage Isotope Ratio Mass Spectrometer and a Thermo Fisher Scientific ConFlo IV Universal Continuous Flow Interface. Stable isotope ratios are expressed in delta (δ) notation, defined as the

difference from a standard reference material in parts per thousand (‰):

$$\delta^{13}C \text{ or } \delta^{15}N = [\frac{R_{Sample}}{R_{Standard}} - 1] \times 1000$$

$$R = {}^{13}C/{}^{12}C \text{ or } R = {}^{15}N/{}^{14}N$$

The standard reference material for nitrogen is atmospheric N_2 and the standard reference material for carbon is Vienna Pee Dee belemnite (V-PBD). Equipment precision was assessed through replicate analyses (n = 25) of four standard materials (NIST1577c, tilapia muscle internal standard, USGS 40 and Urea). The standard deviation of each standard material was ≤0.17‰ for δ^{15}N and ≤0.19‰ for δ^{13}C. Accuracy was determined by analyzing a certified standard (USGS 40) throughout sample runs. The difference between the mean of replicate analyses (n = 25) and the certified value of USGS 40 was 0.04‰ for δ^{15}N and 0.10‰ for δ^{13}C. The carbon to nitrogen ratio (C:N) is also determined through the stable isotope analysis process.

Stable isotope issues and considerations

There are several considerations when using stable isotopes to quantify seasonal shifts in assimilated energy sources. First, the stable isotope turnover in the tissue of focal consumers (i.e., lake trout and smallmouth bass) must be short enough to capture seasonal diet changes (Dalerum and Angerbjörn, 2005). The time it takes for a diet change to be reflected in the isotope signature of a predator's tissue depends on the rate of tissue growth and catabolic replacement of existing tissue (Fry and Arnold, 1982). An animal's tissue isotope turnover rate is often presented as isotope half-life, which is the number of days it takes for an animal's tissue to be at 50% equilibrium with a new diet. The isotope half-life differs between tissues, with internal organs, like the liver, having a faster turnover time than muscle tissue (Boecklen et al., 2011). We used liver tissue instead of muscle tissue in this study because a faster turnover time is better suited for seasonal diet studies. Based on an ectotherm tissue-specific model with body mass as a variable, the isotopic half-life of liver tissue samples from a fish of average weight in our study is 52 days (Vander Zanden et al., 2015). Further, an *in situ* study of rainbow trout (*Oncorhynchus mykiss*) found that it takes ∼5–6 months for the liver tissue of a consumer to be at equilibrium with the stable isotope signature of a new diet (Skinner et al., 2017). Stable isotope turnover time may be slower in the winter than in the fall, spring, and summer because cooler water can decrease the turnover time in fish (Maitland et al., 2021). However, we did not estimate temperature or season specific stable isotope turnover because Vander Zanden et al.'s (2015) isotopic half-life model did not include temperature as a variable due to a weak effect and Skinner et al.'s (2017) study took place only during the open water period. These findings suggests that liver tissue may not fully equilibrate with the stable isotope signature of a seasonal (spring, summer, fall, and winter) diet, but should still begin to reflect seasonal diet shifts, if present. Tissue sample collection was aimed to be late enough in each season so that possible seasonal diet switches were reflected in the stable isotopes of the fish tissue. One exception is the spring, where sampling occurred close to or right at ice-out (the start of spring) because spring is a short season and provided only a limited window of opportunity for sampling. However, spring is also a period of growth and high foraging activity for lake trout (Morbey et al., 2010), potentially increasing isotopic turnover rate and the amount of spring diet integrated into the tissue of our spring sampled fish. Regardless, our spring tissue samples likely reflect the combined late winter and spring diet of the study fishes.

Second, the interpretation of energy source from δ^{13}C can be confounded with lipid content, because lipids are depleted in ^{13}C compared to other macromolecules (DeNiro and Epstein, 1977). Although there is debate on when it is appropriate to perform lipid correction (Arostegui et al., 2019), it is generally recommended when lipid content is high, varies between individuals, and differs between the tissue analyzed and the whole organism (Post et al., 2007; Arostegui et al., 2019). Therefore, we used the C:N ratio of each individual to perform mathematical lipid correction on the liver tissue of lake trout and smallmouth bass using the Post et al. (2007) percent lipid calculation with the Kiljunen et al. (2006) lipid normalization model. Of the commonly used mathematical correction models, these models were found to be the most accurate for correcting liver tissue when tested with taxonomically similar species (Skinner et al., 2016). All lake trout and smallmouth bass δ^{13}C values presented and analyzed are lipid corrected.

Third, both δ^{13}C and δ^{15}N in consumers' tissues can be influenced by stable isotope values of organisms at the base of the food web (Dalerum and Angerbjörn, 2005; Cobain et al., 2022). Phytoplankton are expected to become enriched in δ^{13}C in the summer and δ^{15}N can also be seasonally variable, due to changes in the source of C and N and isotope fractionation during uptake (O'Reilly et al., 2002; Woodland et al., 2012; Sugimoto et al., 2014). The isotope signature of lower trophic levels can also vary by lake (Cabana and Rasmussen, 1996). Baseline variation must therefore be taken into account both between lakes (Cabana and Rasmussen, 1996; Post, 2002) and between different seasons (Woodland et al., 2012; Visconti et al., 2014; Yeakel et al., 2016). Mussels (pelagic baseline) and snails (littoral baseline) were sampled from both lakes in the spring and the summer to explore isotopic variation at the base of the food web that might influence our dietary inferences. We selected unionid mussels instead of zooplankton for the pelagic baseline because mussels are recommended for correcting the stable isotope values of fish, due to their longer life and larger size, reducing short-term stable isotope variation (Cabana and Rasmussen, 1996; Post, 2002). Snails are recommended as littoral baselines for similar reasons

(Post, 2002). Seasonal isotopic variation between summer and spring was minimal for both mussels and snails within each lake (**Supplementary Figure 2**). Therefore, we used the lake specific average $\delta^{15}N$ value of mussels and snails as a baseline value in subsequent calculations.

Data processing and analysis

All data processing and analyses were performed in R version 4.0.2 (R Core Team, 2020).

Habitat divergence: Telemetry

Prior to analyzing the telemetry data, fish positions returned from the fine-scale positioning system were filtered to remove erroneous data. Data from seven fish (three lake trout and four smallmouth bass) were removed, as these fish were deemed dead or to have tag malfunctions. From the remaining 27 fish, ∼1.5% of the positions were removed by filtering out depths above the surface or below the bottom of the lake and positions that fell outside of the lake perimeter. After filtering, 815,148 positions (528,422 from lake trout, 286,726 from smallmouth bass) from 14 lake trout and 13 smallmouth bass remained. The mean fork lengths of the fish that were retained after filtering was 424 mm (range 326–521 mm) for lake trout and 382 mm (range 326–497 mm) for smallmouth bass.

Distance to shore and fish depth were obtained from the filtered telemetry data. A vector map of the lake was used to estimate the minimum distance to shore for each spatial position. Fish depths were already associated with each spatial position and required no additional processing. Distance to shore and fish depth are two meaningful niche axis that have been used to investigate habitat niches of fish, where depth was considered as the vertical axis and distance to shore was the horizontal axis (Guzzo et al., 2016; Versteeg et al., 2021). To calculate seasonal habitat niche overlap between lake trout and smallmouth bass, we used nicheROVER (R package; Swanson et al., 2015). Habitat niche regions for each species-season combination were created as a Bayesian ellipse. Two commonly used ellipse sizes were selected, the standard ellipses (40%) and an expanded ellipse (95%). Then, the probability of habitat overlap between the species was calculated using a Monte Carlo algorithm. Ten thousand independent and identically distributed draws were taken from the distributions of lake trout and overlap was calculated based on how many of those draws fell within the habitat niches of smallmouth bass. Habitat overlap was expressed as the probability that a random lake trout would be found in the habitat niche of smallmouth bass.

Activity divergence: Telemetry and empty stomachs

The average horizontal movement rate of lake trout and smallmouth bass, based on acoustic telemetry in Lake 2, was compared between sampling periods. The distance between successive position detections >20 min apart was divided by the time between detections to determine horizontal movement rate in m min^{-1}. Speeds >40 m min^{-1} were filtered out, as this speed is faster than is likely possible (Cruz-Font et al., 2019). A total of 570,126 horizontal movement rates were obtained (383,965 from lake trout and 186,161 from smallmouth bass). Then, the mean horizontal movement rates for each species during each season-year combination of the study was calculated.

The percent of non-empty stomachs for lake trout and smallmouth bass in each sampling period was also reported to provide further insight into the species' foraging activity. Empty stomach data is commonly used to determine patterns of food consumption (da Silveira et al., 2020), including seasonal changes in foraging activity (Block et al., 2020). Sampling periods with a higher percent of non-empty stomachs were assumed to reflect greater foraging activity than sampling periods with a lower percent of non-empty stomachs.

Diet divergence: Stable isotopes and stomach contents

Stable isotopes were first used to explore the diet overlap between lake trout and smallmouth bass. Isotopic overlap could only be compared in the spring and summer because insufficient numbers of smallmouth bass were captured in the fall and winter. Isotopic overlap was calculated using nicheROVER with $\delta^{13}C$ (lipid corrected, see above) and $\delta^{15}N$ data (R package; Swanson et al., 2015). We took that same approach as we did for calculating habitat niche overlap, with $\delta^{13}C$ and $\delta^{15}N$ instead of fish depth and distance to shore as niche axes. Isotopic overlap is expressed as the probability that a random lake trout will be found in the isotopic niche space of smallmouth bass.

To further explore seasonal trends in lake trout diet, for which we had data for all four seasons, we compared $\delta^{13}C$ (indicating littoral vs. pelagic energy sources) and the trophic position of lake trout across the full 2-year time series (eight sampling periods). We calculated the trophic position of lake trout as:

$$TP_{Consumer} = \left\lfloor \left(\delta^{15}N_{Consumer} - \delta^{15}N_{Baseline}\right)/3.4 \right\rfloor + 2$$

where $\delta^{15}N_{Baseline}$ is the lake specific average $\delta^{15}N$ of secondary consumers (snails and mussels). While the level of enrichment varies due to a number of factors, a trophic enrichment factor of 3.4‰ is widely accepted in freshwater systems (Post, 2002). The choice to use $\delta^{13}C$ values instead of values converted to percent littoral reliance is explained in **Supplementary Note 2**.

We used linear models and pairwise comparisons of estimated marginal means to determine if there were

differences in $\delta^{13}C$ and the trophic position of lake trout between sampling periods (Searle et al., 1980; Lenth, 2020). The Tukey method (using the Studentized range distribution) was used to correct for multiple comparisons (Lenth, 2020). Trophic position and $\delta^{13}C$ were analyzed separately, and separate linear models were used for each lake because of food web differences. Model selection was performed using backward stepwise selection, starting with the possible predictor variables of sampling period, total length, sex, and the interaction between sampling period and total length (James et al., 2013). We used *p*-value as the removal criterion and stopped at a *p*-value threshold of 0.05 (James et al., 2013).

To complement stable isotope data as an indicator of diet, we quantified the stomach contents of lake trout and smallmouth bass. While stable isotope analysis reveals time averaged assimilated energy, stomach content analysis provides a short-term taxonomically specific indicator of diet, on the scale of hours to days. We used percent frequency of occurrence, which is the percentage of stomachs with prey that contain a certain prey type. While many methods of determining the importance of each prey group exist (see reviews by Hynes, 1950; Hyslop, 1980; da Silveira et al., 2020), frequency of occurrence is a simple and robust method. Unlike bulk methods, frequency of occurrence does not suffer from bias introduced by categorizing loose digested material and is less impacted by order of prey ingestion and different rates of prey digestion (Baker et al., 2014). Prey were divided into the broad groups, "fish," "macroinvertebrate," "zooplankton," and "other." Fish were further divided to the species level and macroinvertebrates to the order level, receiving their own group if there were ≥5 occurrences or placed in the "other fish" or "other macroinvertebrate" group if there were <5 occurrences. When identification could be done to the broad grouping (fish and macroinvertebrate) but not to any higher taxonomic resolution due to digestion, the occurrence was added to the "unidentified fish" or "unidentified macroinvertebrate" category.

Results

Habitat divergence: Telemetry

Acoustic telemetry data (only available for Lake 2) reveals that the habitat of lake trout and smallmouth bass, as well as the probability of habitat overlap between the species, changes seasonally. A randomly selected lake trout has a low probability and associated credible interval of being in the habitat niche space of smallmouth bass in the summer (**Table 2**). The low probability of habitat overlap is driven by smallmouth bass occupying shallow positions in the water column in nearshore areas, while lake trout occupy deeper positions in the water column, generally further from shore (**Figure 3**). A randomly selected lake trout has a higher probability of being in the habitat niche of smallmouth bass in the winter than in the summer (**Table 2**). During the winter, the habitat niche of lake trout includes shallow water, in both nearshore and offshore areas, while the habitat niche of smallmouth bass is positioned slightly deeper in the water column and occupies a smaller range on the distance to shore niche axis (**Figure 3**). In the spring and fall, a randomly selected lake trout has the highest probability of being in the habitat niche space of smallmouth bass (**Table 2**). During these seasons, the niche of lake trout includes a wide range on the distances to shore axis and a position on the fish depth axis that is shallower than in the summer (**Figure 3**). During the spring and fall, overlap between the species occurs in the shallow fish depth and nearshore portion of lake trout's habitat niche (**Figure 3**).

TABLE 2 Probability and credible interval (CI) of isotopic and habitat niche overlap between lake trout and smallmouth bass, calculated using nicheROVER (R package; Swanson et al., 2015).

Lake	Season	Isotopic overlap probability % (CI)		Habitat overlap probability % (CI)	
		Standard	Expanded	Standard	Expanded
1	Spr	20.92 (3.98–49.38)	96.67 (86.29–99.96)	–	–
1	Sum	0.15 (0.00–1.16)	63.82 (33.48–87.89)	–	–
1	Fall	–	–	–	–
1	Wint	–	–	–	–
2	Spr	16.44 (5.63–32.27)	79.27 (59.58–94.09)	6.43 (5.93–6.95)	35.59 (34.45–36.74)
2	Sum	1.88 (0.40–4.69)	19.88 (9.05–34.63)	0.09 (0.04–0.16)	0.99 (0.82–1.22)
2	Fall	–	–	12.14 (11.48 –12.80)	52.15 (51.13–53.21)
2	Wint	–	–	5.09 (4.66–5.54)	26.57 (25.69–27.45)

Overlap probability is the probability that a randomly selected lake trout would fall within the elliptical niche space of smallmouth bass. The probability of overlap is presented for standard ellipses (40%) and expanded ellipses (95%).
Results are divided into Lake 1 (+ cisco) and Lake 2 (− cisco), during each season (spring, summer, fall, and winter).

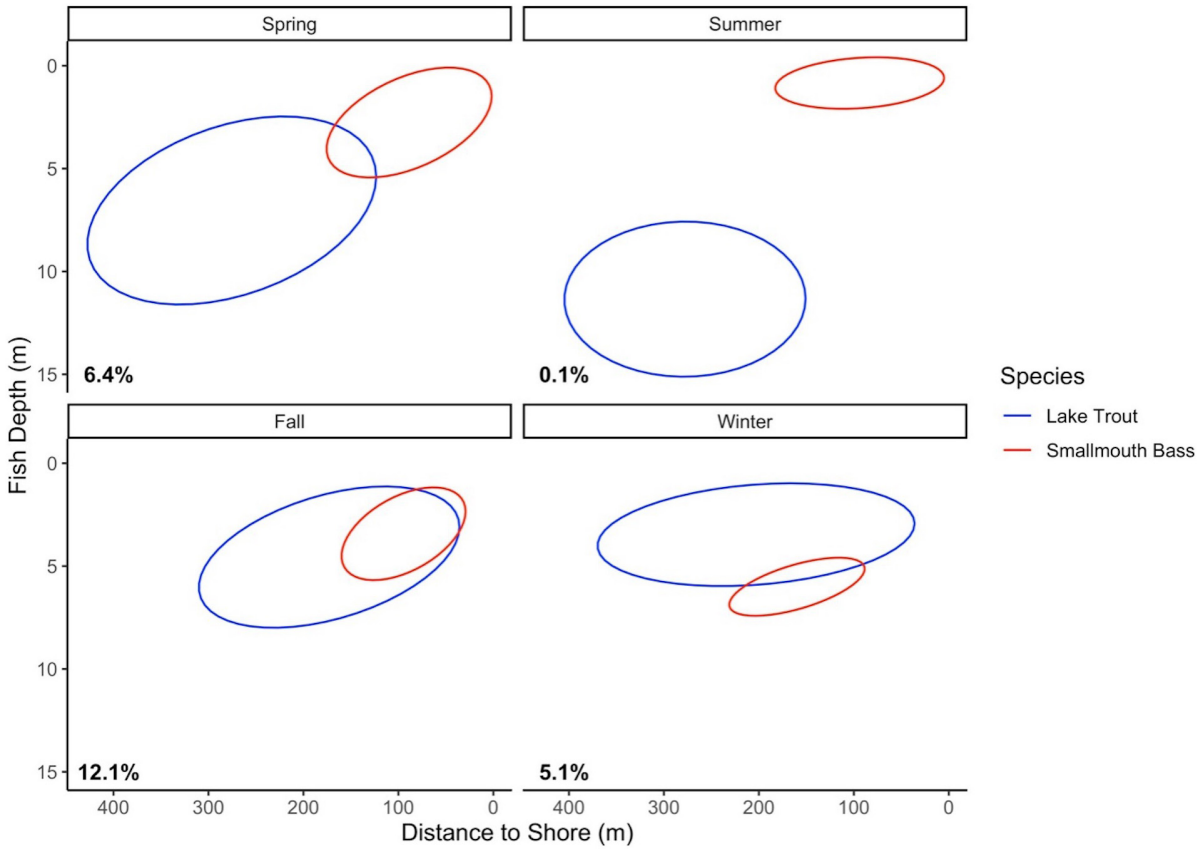

FIGURE 3
Habitat ellipses (40%) for lake trout (blue) and smallmouth bass (red), based on the niche axes fish depth (m) and distance to shore (m). The percent probability that a random lake trout will be in the 40% habitat niche space of smallmouth bass, calculated using the nicheROVER package, is in the lower left corner. Data were collected between spring 2017 and winter 2019 (two annual cycles) from an acoustic telemetry array in Lake 2 (– cisco). Results are separated into spring, summer, fall, and winter.

Activity divergence: Empty stomachs and telemetry

Lake trout were caught in all eight sampling periods and over 40% of stomachs sampled had contents (i.e., non-empty stomachs; Figure 4). The percent of non-empty lake trout stomachs was especially high in the spring, over 85% in each sampling period in both lakes (Figure 4). In contrast, low numbers of smallmouth bass were caught in the fall (n = 8 between both lakes and years) and winter (n = 2 between both lakes and years, Figure 4), despite similar effort across sampling periods. In addition, when smallmouth bass were caught in these seasons, there was a low percentage of stomachs with contents, except for the Fall 2017 sampling period in Lake 2 when all three smallmouth bass caught had stomach contents (Figure 4).

Two years of movement rate data reveal distinct seasonal activity patterns for lake trout and smallmouth bass (Figure 4). The species had similar activity rates (mean ± SD) during the summer (Year 1: lake trout 2.6 m/min ± 4.5, smallmouth bass 3.7 m/min ± 5.1; Year 2: lake trout 3.1 m/min ± 5.4, smallmouth bass 3.4 m/min ± 5.2). In contrast, the mean activity rate of lake trout was higher than smallmouth bass in the fall (Year 1: lake trout 5.4 m/min ± 5.6, smallmouth bass 1.5 m/min ± 2.8; Year 2: lake trout 6.9 m/min ± 7.6, smallmouth bass 1.6 m/min ± 2.9) and the winter (Year 1: lake trout 3.0 m/min ± 3.5, smallmouth bass 1.1 m/min ± 1.9; Year 2: lake trout 5.8 m/min ± 7.1, smallmouth bass 1.2 m/min ± 2.1). In the spring of year 1, lake trout and smallmouth bass had a similar movement rate (lake trout 3.5 m/min ± 4.1, smallmouth bass 3.3 m/min ± 3.8). However, in the spring of year 2, lake trout had a higher movement rate than smallmouth bass (lake trout 6.8 m/min ± 7.0, smallmouth bass 1.5 m/min ± 2.4).

Diet divergence: Stable isotopes and stomach contents

Spring and summer

The diet overlap between lake trout and smallmouth bass was investigated in the spring and summer when both species

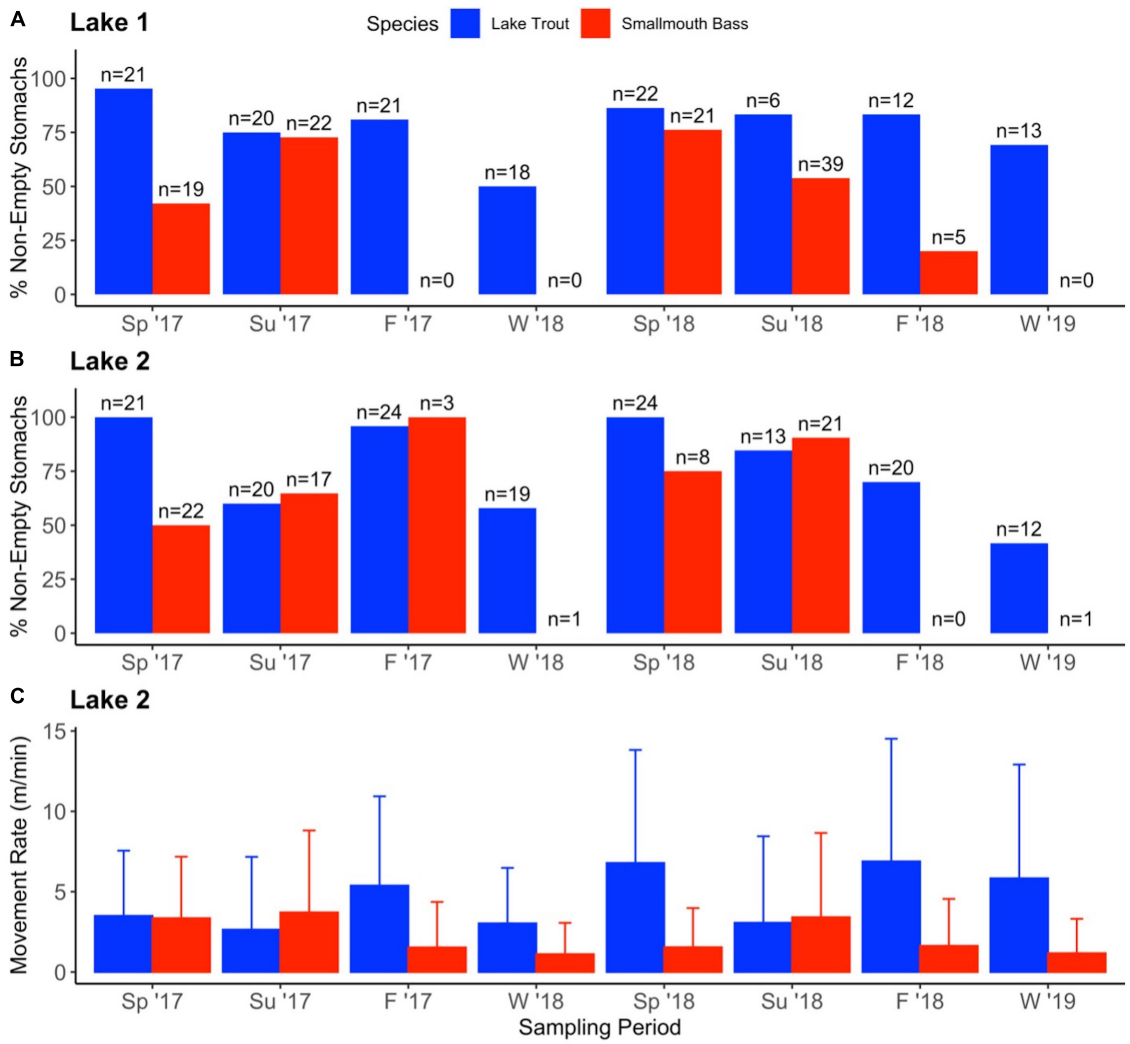

FIGURE 4
Activity of lake trout (blue) and smallmouth bass (red) over four seasons and 2 years. The percent of stomachs sampled that had contents in Lake 1 (+ cisco; **A**) and Lake 2 (– cisco; **B**), with the total number of fish that had stomachs sampled is denoted on top of each bar*. Mean (+ SD) seasonal movement rate of species (m/min) in Lake 2 based on acoustic telemetry data **(C)**. *Note that more lake trout were caught in the summer 2018 sampling period than were sampled for stomach contents because the individuals were used in further study (not presented here).

were actively foraging and successfully captured in sufficient numbers (Table 1 and Supplementary Table 1). Based on analysis using nicheROVER with $\delta^{13}C$ and $\delta^{15}N$ data, a randomly selected lake trout has a higher probability of being in the isotopic niche space of smallmouth bass in the spring compared to the summer (Table 2, Figure 5). The higher probability of niche overlap was largely due to the isotope ellipse of lake trout being higher on the $\delta^{13}C$ axis (higher littoral reliance) and the isotope ellipse of smallmouth bass being higher on the $\delta^{15}N$ axis (higher trophic position) in the spring vs. summer (Figure 5).

The frequency of occurrence of prey items in the stomachs of lake trout and smallmouth bass support the stable isotope data, also suggesting larger dietary overlap in the spring and divergence in the summer (Figure 5). In Lake 1, both lake trout and smallmouth bass consume fish and benthic macroinvertebrates in the spring, with some observations of consuming the same taxa (*Ephemeroptera*, *Odonata*, and crayfish; Supplementary Figures 3, 4). Conversely, in the summer, lake trout were piscivorous, with most identified fish being pelagic cisco. A similar pelagic shift is not observed for smallmouth bass, which continue to feed on benthic macroinvertebrates, especially crayfish (Supplementary Figure 4). In Lake 2 during the spring, lake trout and smallmouth bass both consume yellow perch and benthic macroinvertebrates. In the summer, lake trout consume zooplankton while smallmouth bass do not. Overall, in both lakes there is more similarity in the diet of lake trout and smallmouth bass in the spring and less in the summer as lake trout increase reliance on pelagic prey (cisco in Lake 1

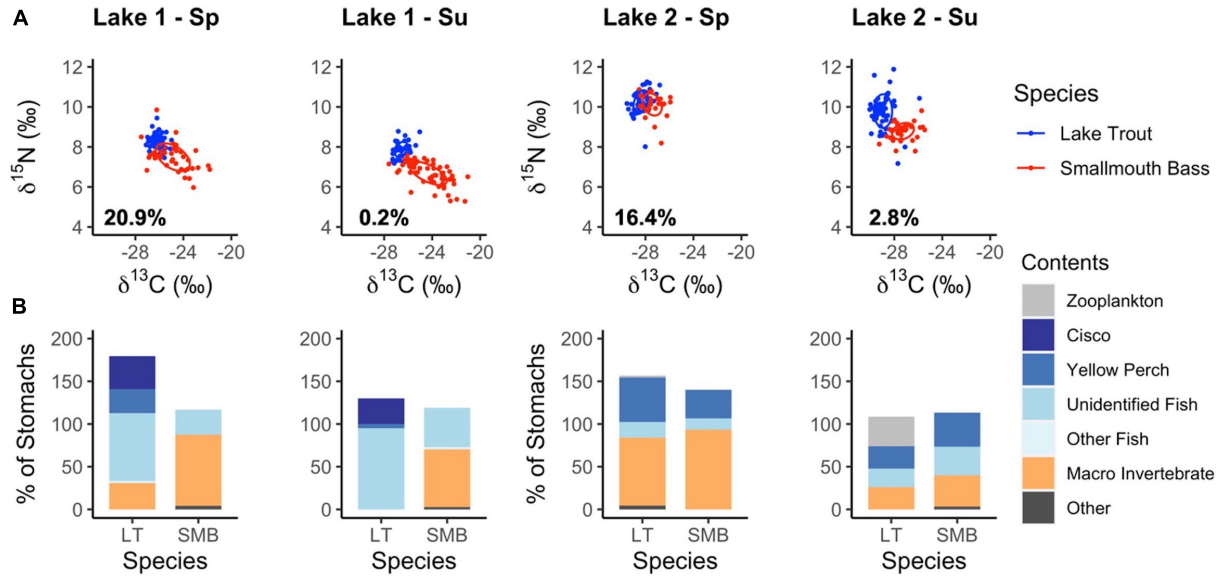

FIGURE 5
Isotope biplot with ellipses where individuals have a 40% probability of being found, with the percent probability that a random lake trout will be in the isotopic niche space of smallmouth bass in the lower left corner **(A)**. The percent of non-empty lake trout and smallmouth bass stomachs that contained certain prey types **(B)**. Results are separated into spring (Sp) and Summer (Su) and Lake 1 (+ cisco) and Lake 2 (– cisco).

and zooplankton in Lake 2). Further, the higher occurrence of potentially littoral prey in lake trout stomachs during the spring is consistent with the isotope ellipses being higher on the $\delta^{13}C$ axis. However, the isotope ellipses of smallmouth bass being higher on the $\delta^{15}N$ axis in the spring is not consistent with the stomach content data, as macroinvertebrates that dominate the spring diet have a lower $\delta^{15}N$ signature than fish (**Supplementary Figures 5, 6**).

Lake trout year-round diet

Factors included in the multiple linear regression models of lake trout trophic position based on backward selection were fish total length, sampling period, and sex. Sampling period had a significant effect on lake trout trophic position in Lake 1 ($F_{7,139} = 22.95$, $p > 0.001$; **Supplementary Table 2**) and Lake 2 ($F_{7,157} = 11.04$, $p > 0.001$; **Supplementary Table 3**). Pairwise comparisons of estimated marginal means (**Supplementary Table 4**) revealed that the trophic position of lake trout in Lake 1 was higher in the winter and spring than the summer (**Figure 6**; **Supplementary Table 5**). In Lake 2, pairwise comparisons of estimated marginal means (**Supplementary Table 6**) showed the same pattern in the first year as Lake 1, but in the second year, trophic position was not statistically significantly different between spring and summer (**Figure 6**; **Supplementary Table 7**).

The linear model of lake trout $\delta^{13}C$ in Lake 1 included only sampling period, while the linear model of Lake 2 included sampling period, fish total length, and an interaction between sampling period and fish total length. Sampling period had a significant effect on the $\delta^{13}C$ value of lake trout in Lake 1 ($F_{7,139} = 9.77$, $p < 0.001$; **Supplementary Table 8**) and Lake 2 ($F_{7,157} = 11.54$, $p < 0.001$; **Supplementary Table 9**). Pairwise comparisons of estimated marginal means (**Supplementary Table 10**) revealed that in Lake 1 the $\delta^{13}C$ value of lake trout was higher (higher reliance on littoral energy) in the winter than the summer and fall in both years (**Figure 6**; **Supplementary Table 11**). In Lake 2, an interaction between fish total length and sampling period ($F_{7,157} = 2.52$, $p = 0.018$; **Supplementary Table 9**) complicates the interpretation of the main effect of sampling period. However, lake trout had a higher $\delta^{13}C$ value in the winter than the summer, except for the largest fish sampled in the first summer (**Supplementary Figure 7**).

The frequency of occurrence of prey items in the stomachs of lake trout support the $\delta^{13}C$ data and indicate a higher consumption of littoral prey in the winter than the summer. In the winter in Lake 1, benthic macroinvertebrates were found in some lake trout stomachs (**Supplementary Figure 3**), which can have a more littoral $\delta^{13}C$ signature than cisco (**Supplementary Figures 5, 6**). In Lake 2, lake trout consumed pelagic zooplankton in the summer, which were not observed in the winter diet (**Supplementary Figure 3**).

Discussion

Exploring seasonal changes in the behavior of interacting species is important for understanding how climate change

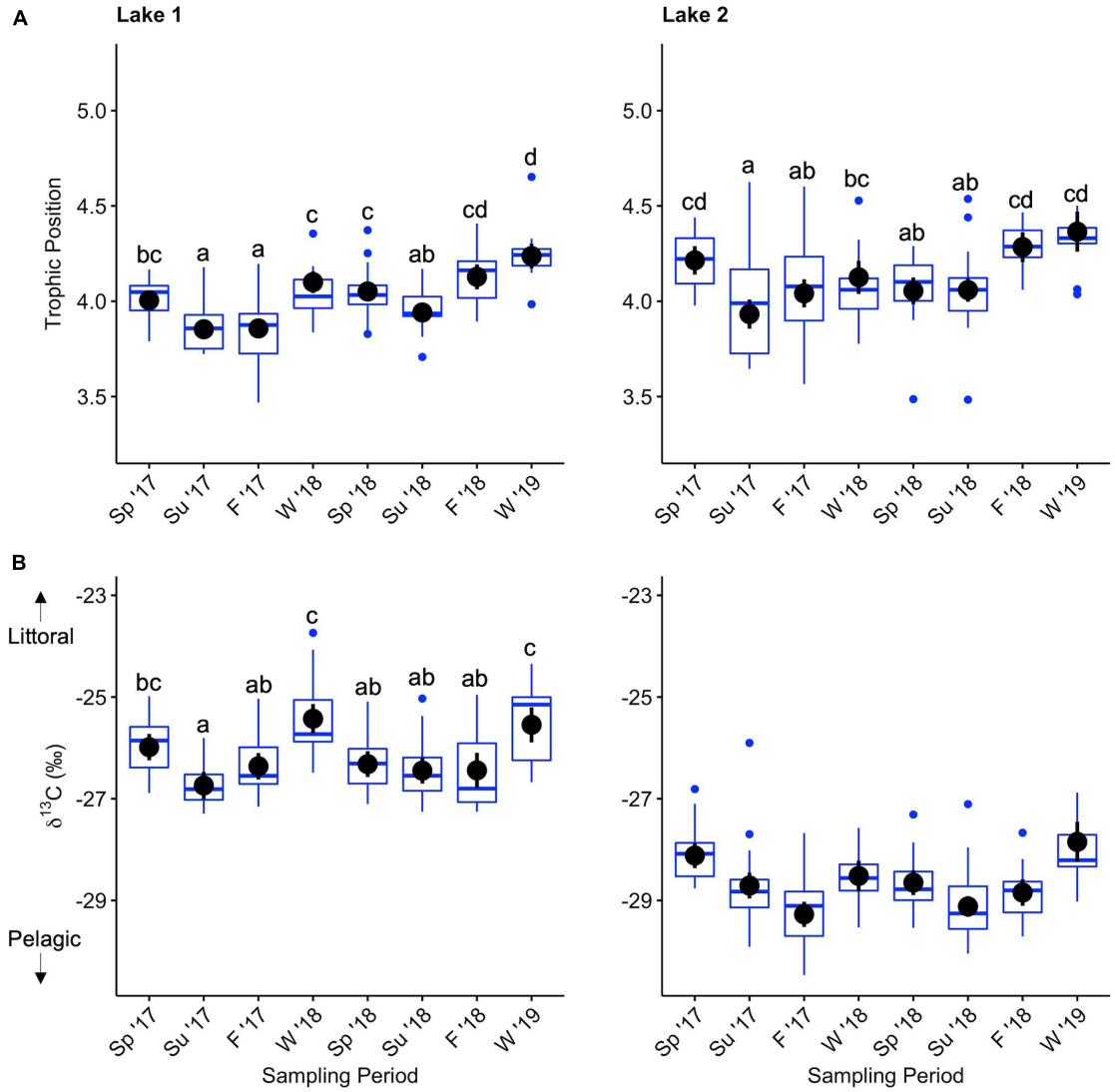

FIGURE 6
Boxplot of trophic position **(A)** and lipid corrected $\delta^{13}C$ **(B)** of lake trout liver in Lake 1 (+ cisco; left) and Lake 2 (− cisco; right) over 2 years of sampling during each season. Black dots are the estimated marginal means and vertical lines through the black dots are the associated confidence intervals. Different letters indicate a significant difference in the mean values between sampling periods. Note that *post-hoc* tests were not performed on $\delta^{13}C$ in Lake 2 due to an interaction between fish length and sampling period that would make results misleading.

might alter species coexistence mechanisms. Despite their importance, seasonal studies on the behavior of interacting species, including in the field of aquatic ecology, are relatively scarce (Helland et al., 2008; McMeans et al., 2015; Sutton et al., 2021). Here, we investigated the seasonal niche overlap in habitat, activity rates, and diet between native lake trout and range-expanding smallmouth bass in north-temperate lakes. As predicted, we found that the niche overlap between lake trout and smallmouth bass changes seasonally. Isotopic and habitat overlap was higher in the spring than the summer and both species were actively foraging during these seasons. Lake trout and smallmouth bass partitioned their habitat and diet more in the summer, when lake trout remained more pelagic. Activity diverged most strongly during winter, when lake trout were actively accessing nearshore habitats and prey, while smallmouth bass were effectively inactive.

Habitat: Low habitat overlap in the summer

Our telemetry data reveal that smallmouth bass and lake trout both seasonally alter their habitats, leading to little habitat overlap in the summer and moderate habitat overlap in the spring, fall, and winter. Our use of "habitat" specifically refers to the depth and distance to shore that fish occupy. Previous

studies of seasonal fish location have similarly found that fishes occupy different depths and habitat types seasonally in both lentic (Suski and Ridgway, 2009) and lotic systems (Gillette et al., 2006).

Smallmouth bass remained at shallow depths and relatively close to shore in the spring, summer, and fall, corresponding to the warmest waters available in the lake. The habitat smallmouth bass occupied was the deepest and furthest offshore in the winter, where the warmest water is available (4°C) due to reverse stratification (i.e., surface water immediately below the ice is the coldest water in the lake). Smallmouth bass have a warm thermal preference (Hasnain et al., 2018) and their habitat use follows the warmer water in the lake. This suggests that behavioral thermoregulation is a primary driver of observed seasonal movements, although factors like spring spawning could also contribute to seasonal habitat use. Other warm-water fishes, like largemouth bass, similarly change their position in the water column seasonally, with the timing of changes concurrent with changes in water temperature (Hanson et al., 2007).

Similarly, lake trout occupied distinct seasonal habitats, which may be due to their thermal preference and changing water temperatures. Water temperature is a primary determinant of suitable lake trout habitat (Plumb and Blanchfield, 2009). Lake trout's summer habitat was offshore in deeper water because nearshore water was too warm to be occupied for extended periods of time. Summer water temperature at shallow depths (above the thermocline) exceeds 15°C, which has been defined as lake trout's usable temperature threshold based on the habitat lake trout occupy in other Canadian Shield lakes (Plumb and Blanchfield, 2009; Guzzo and Blanchfield, 2017). In the spring, fall, and winter, when shallow water is no longer too warm to be usable for extended periods of time, lake trout extend their spatial habitat into shallower, nearshore areas in our study lakes. Lake trout's use of nearshore habitat in the fall could also be due in part to spawning, which occurs in shallow water on cobbled shoals (Callaghan et al., 2016; Riley et al., 2019). In Algonquin Park, lake trout spawn in late October over about 10 days (Martin, 1957).

Due to these species-specific habitat changes, likely driven by changes in water temperature and distinct thermal preferences, the amount of habitat overlap between lake trout and smallmouth bass changes seasonally. Lake trout and smallmouth bass have the lowest habitat overlap in the summer when stratified water creates spatially distinct niches, with warm epilimnetic waters satisfying smallmouth bass's thermal preference and cooler metalimnion and hypolimnion water satisfying lake trout's thermal preference. Key ecological studies on these species' interactions have been confined to this summer period of low habitat overlap (Vander Zanden et al., 1999, but see McMeans et al., 2020). However, we found habitat overlap is the greatest during the spring and fall, when water becomes isothermal and lake trout's habitat is shallower and more nearshore than in the summer.

Activity: Smallmouth bass decrease activity in the fall and winter

While ectotherms like fish can change their habitat to thermoregulate, thermally optimal habitat is not always available. Changing activity rates is another strategy species use to cope with changing water temperature (Shuter et al., 2012). Reductions in movement rate offers fish a massive energy savings due to lower metabolic costs (Speers-Roesch et al., 2018).

We found that smallmouth bass were less active than lake trout in the fall and winter based on lower movement rates from telemetry data. While early studies reported that species in the warm-water thermal guild, like smallmouth bass, were dormant in the winter (Crawshaw, 1984), more recent work describes them as moving minimally and not actively feeding (Shuter et al., 2012). Our results support the more recent findings, as movement rates in the winter are lower than other seasons, but not zero. This is also consistent with previous acoustic telemetry studies on smallmouth bass, including a study in Lake 1, which found that individuals exhibited reduced vertical movement during the winter (Suski and Ridgway, 2009). Smallmouth bass also had a lower average movement rate than lake trout in the fall when water temperature was warmer than in the winter but remained below smallmouth bass's thermal preference.

The finding of lower activity in the fall and winter based on movement rate is supported by low numbers of smallmouth bass caught and generally a greater portion of empty stomachs. Other studies support warm-water fish foraging minimally during these times. For example, warm-water pumpkinseed (*Lepomis gibbosus*) and bluegill (*Lepomis macrochirus*) had empty stomachs more frequently and lower daily energy consumption in the fall and winter compared to the spring and summer (Block et al., 2020). Overall, smallmouth bass are less active and potentially foraging less than lake trout in the fall and winter.

Diet overlap: Higher diet overlap in the spring than the summer

Our seasonally resolved study found that the isotopic niche overlap between lake trout and smallmouth bass is higher in the spring than the summer in both lakes. Consistent with the stable isotope data, the diet of lake trout and smallmouth bass is more similar in the spring than the summer, as both species consume macroinvertebrates more frequently. Increased consumption of macroinvertebrates by lake trout and smallmouth bass in the spring could be due to insect emergences. For example, chironomid pupae emerge and float to the surface in the spring. Ephemeroptera emergence also peaks in the spring (May and June), although some species have a second peak in the late summer (Rowe and Berrill, 1989). The isotopic niche of

lake trout was higher on the $\delta^{13}C$ axis in the spring, as is expected with the increased consumption of potentially littoral benthic macroinvertebrates. In contrast, the isotopic niche of smallmouth bass was higher on the $\delta^{15}N$ axis in the spring than the summer. Despite no increase in the frequency of occurrence of higher trophic position prey (e.g., fish) in spring vs. summer smallmouth bass stomachs, the amount of assimilated energy from higher trophic position prey may have increased. However, this speculation requires more detailed stomach content and energetic analysis. A physiological explanation is also possible. Periods of low food intake can cause protein reserves in the body to be used, leading to ^{14}N being preferentially excreted and a $\delta^{15}N$ enrichment in body tissues (Doi et al., 2017). Thus, the residual effects of limited foraging by smallmouth bass in the winter could have caused the enriched $\delta^{15}N$ we observed in the spring.

Previous studies on the impact of smallmouth bass on lake trout's diet suggest that these species can compete for nearshore prey. In lakes without smallmouth bass, lake trout, on average, have a higher reliance on littoral energy (Vander Zanden et al., 1999). Additionally, after smallmouth bass were removed from a north-temperate lake, lake trout increased their consumption of littoral prey and had a corresponding increase in their reliance on littoral energy (Lepak et al., 2006). Our finding of higher isotopic niche overlap and a more similar diet between lake trout and smallmouth bass in the spring than the summer suggests that potential consumptive competition between the species could be more pronounced in the spring.

Lake effects on seasonal diet overlap

Temperate lakes vastly differ in size, shape, depth, and community composition, potentially impacting food web structure and species interactions. In smaller lakes, mobile top predators like lake trout increase their foraging in the littoral zone (Schindler and Scheuerell, 2002; Tunney et al., 2012). In lakes that lack pelagic prey fish, littoral foraging is also strengthened because lake trout must rely more on littoral food sources (Vander Zanden and Rasmussen, 1996). Variation in lake characteristics that affect the extent of littoral foraging by lake trout may impact diet overlap with nearshore smallmouth bass. We expected lake trout to rely more on littoral prey and have a higher diet overlap with smallmouth bass in the spring and summer in the smaller lake that lacks an offshore forage fish (Lake 2) vs. the larger lake with pelagic cisco (Lake 1).

Counter to our prediction, the probability of lake trout being in the isotopic niche space of smallmouth bass was higher in Lake 1 than Lake 2, in both the spring and summer. The smaller isotopic niche size of lake trout in Lake 1 (with cisco) could be a contributing factor to this surprising finding, because for a set area of niche overlap in isotope space, the probability of overlap will increase with decreasing niche size. The dominance of yellow perch in the diet of lake trout in Lake 2 (no cisco) is also a possible explanation. We found lake trout consumed both young of the year and adult yellow perch. In another Algonquin Park lake without cisco, 80% of yellow perch consumed by lake trout were young of the year (Martin, 1952). Yellow perch consume zooplankton as juveniles (Brown et al., 2009) and the carbon stable isotope signature of young of the year yellow perch in our study is consistent with other pelagic prey (**Supplementary Figures 5, 6**). Therefore, the consumption of young of the year yellow perch with a pelagic stable isotope signature, occupying an analogous position to cisco, could reduce the isotopic niche overlap with smallmouth bass in Lake 2.

Seasonal lake trout diet: Lake trout occupy a higher trophic position and obtain more littoral energy in the winter than the summer

Stable isotope results supported by stomach contents data were explored year-round for lake trout to quantify if and how lake trout diet changed during the winter when smallmouth bass were largely inactive. We found lake trout generally had a higher $\delta^{13}C$ value and occupied a significantly higher trophic position in the winter compared to the summer in both lakes. A higher $\delta^{13}C$ value indicates that more of lake trout's energy ultimately comes from the nearshore environment, either from directly preying on nearshore prey or by consuming prey that have consumed nearshore prey themselves. These stable isotope results are consistent with stomach content data. Lake trout's diet in Lake 1 is dominated by pelagic cisco, but benthic macroinvertebrates are present in the winter and yellow perch were found more frequently in the winter than the summer. Adult yellow perch could contribute to the higher trophic position, based on their ecology and stable isotope signature in Lake 1. Benthic macroinvertebrates, like larval insects, could contribute to the more nearshore signal in the winter in Lake 1 because they mainly occupy the littoral zone (Koroiva and Pepinelli, 2019). However, they can also be found in profundal benthic habitat (e.g., some Diptera larvae), and we did not extensively characterize the stable isotope ecology of larval insects in our study lakes. In the winter in Lake 2, zooplankton, a taxon with a strong pelagic signal and low trophic position, were not detected but higher trophic position and potentially more littoral yellow perch were.

The observed changes in the stable isotope signature and diet of lake trout may align with seasonal changes in prey availability, including pulses in prey abundance, combined with changes in prey thermal accessibility. For example, zooplankton generally have a seasonal pulse of availability in the summer (Sommer et al., 1986; Jensen, 2019), coinciding with when they are detected in lake trout's diet. In addition, nearshore

prey with a more littoral stable isotope signature, are more thermally accessible to lake trout in the winter than the summer. Although lake trout can access the littoral prey by making short forays in summer (Morbey et al., 2006; Plumb et al., 2014; Guzzo et al., 2017), these forays decrease the time lake trout spend at rest, so are not as energetically advantageous as consuming prey that are thermally accessible (Cruz-Font et al., 2019). In addition to the nearshore area being more thermally accessible during the winter, smallmouth bass are largely inactive and thus likely not consumptively drawing down nearshore resources like in the summer (Vander Zanden et al., 1999).

Overall, we find that during the winter, a period of low activity for smallmouth bass, lake trout have a higher trophic position and obtain more energy from the littoral pathway. Lake trout populations that feed on larger higher trophic position organisms (e.g., fish vs. zooplankton) use less energy for foraging, leading to higher growth efficiency and larger adult body sizes (Pazzia et al., 2002; Shuter et al., 2016; Cruz-Font et al., 2019). Other fishes similarly change their diet in the winter to prey that are energetically advantageous (Eloranta et al., 2013; Stockwell et al., 2014). In addition, lake trout's C:N ratio in the liver was generally high in the winter, suggesting that lipids in the liver were not depleted by winter conditions. Thus, winter diet switches could be beneficial for lake trout, but this idea requires further study.

Caveats and future directions

Predator stable isotope signatures not only depend on their own habitat and diet, but on the habitat and diet of their prey. Therefore, considering the seasonal ecology of prey species is important for understanding the stable isotope signature of top predators like lake trout and smallmouth bass. For example, cisco biomass increases nearshore in the late fall, as fish congregate before spawning (Yule et al., 2009). Cisco can also be found in shallow waters in the winter and spring, and while they primarily consume zooplankton, their diet also includes larval insects, crustaceans, and algae (Holm et al., 2009). If cisco feed on more nearshore prey during the winter in our study lakes, this could contribute to the increased littoral stable isotope signal of Lake 1 lake trout in the winter, along with the increased consumption of invertebrates based on stomach contents. Yellow perch were also commonly consumed by both lake trout and smallmouth bass, and yellow perch diet can change seasonally (Block et al., 2020; Duxbury, 2020). For example, yellow perch in Lake Champlain switched their diet from fish and benthic macroinvertebrates in the winter to zooplankton in the summer (Block et al., 2020). We lack data about the seasonal ecology of prey in our study lakes and in general little is known about the seasonal ecology of many prey fish species. Further study of prey fish abundance, habitat, and diet and how these factors change through time would improve our understanding of top predator seasonal niches (Turschak et al., 2022).

There are some potential biases in the stomach content data. It is possible that zooplankton and other small organisms are underrepresented in the diet, as small prey (higher surface area to volume ratio) are digested more quickly than larger prey (Legler et al., 2010). Other organisms may be overrepresented because of features like exoskeletons that slow down digestion (Kionka and Windell, 1972). Stomachs could be found empty less often and contain more prey types in the winter because rates of digestion are slower at colder temperatures (Legler et al., 2010). In addition, the frequency of occurrence of prey may not be representative of assimilated energy because prey types vary in their biomass and energy content. Importantly, stomach contents are only a snapshot of diet, so they can miss temporally constrained but potentially energetically important items (Fernandes and McMeans, 2021). All tools have limitations, which stresses the importance of combining multiple ecological tools (here, stable isotopes, stomach contents and telemetry).

While we quantified seasonal niche overlap, future studies should investigate the impacts of smallmouth bass invasion on lake trout. Previous studies have shown that in the summer, smallmouth bass reduce lake trout's consumption of nearshore prey in lakes without cisco (Vander Zanden et al., 1999). Based on our finding of high diet overlap in the spring in lakes with and without cisco, future studies should include both lake types and be seasonally resolved. A high C:N ratio (**Supplementary Figure 1**) and large size of adult lake trout in Lake 1 compared to lakes without pelagic prey fish (Pazzia et al., 2002), indicates that cisco could buffer the impacts of smallmouth bass invasion on lake trout, as previously suggested (Vander Zanden et al., 2004; Sharma et al., 2009). Studies on the impact of smallmouth bass could include comparing lake trout diet and other factors like abundance (Larocque et al., 2021), bioenergetics, and growth rates in lakes with and without smallmouth bass, throughout an invasion, or through a historical reconstruction (e.g., Morbey et al., 2007).

Lake trout had a higher pelagic reliance and trophic position in Lake 2 (no cisco) than expected. Both results might be explained through the consumption of adult yellow perch and planktivorous young of the year yellow perch based on their stable isotope signature. Yellow perch have a higher $\delta^{15}N$ (trophic position) than other available prey (zooplankton and benthic macroinvertebrates) and young of the year yellow perch have a low (pelagic) $\delta^{13}C$ value (**Supplementary Figure 5**). However, we can only speculate about which diet items caused the observed stable isotope signature based on stomach contents and visually inspecting the stable isotope signatures of predators and prey. Future work should use stable isotope mixing models to determine the specific contributions of each prey type to the overall isotope signature.

Finally, our finding that lake trout trophic positions are higher in the winter than the summer has implication for contaminant modeling. Organisms with a higher trophic position, including lake trout, generally have higher contaminant loads due to bioaccumulation (Vander Zanden and Rasmussen, 1996). Therefore, contaminant models that use trophic positions determined through summer sampling only may underestimate the concentration of contaminants, such as mercury, in lake trout and the human health risks of consumption. Further work is required to explore this idea and seasonal contaminant concentrations overall.

Conclusion and implications

(1) Lake trout and smallmouth bass had a higher isotope and habitat overlap in the spring than the summer. Smallmouth bass also had low activity rates in the fall and winter based on acoustic telemetry in Lake 2, suggesting potential competition is the highest in the spring. Spring is an important time for lake trout to forage as it is the season with the highest energy allocation to growth (Morbey et al., 2010). Increases in air temperature due to climate change in small Boreal Shield lakes may lengthen spring, defined as the period between ice-off and when surface water temperatures reach 15°C (Guzzo and Blanchfield, 2017). While longer access to the littoral area without thermal consequence may be beneficial for lake trout, the impact of a potentially longer period of heightened isotope and habitat overlap with smallmouth bass is unknown.

(2) The isotope overlap and diet similarity between lake trout and smallmouth bass was higher in the spring than the summer in both a lake with and a lake without a pelagic prey fish (i.e., cisco). Based on a previous summer study (Vander Zanden et al., 1999), lake trout in lakes with pelagic prey fish have been classified as not vulnerable to the impacts of smallmouth bass invasion (Sharma et al., 2009). We found high lipid levels in lake trout inhabiting lakes with cisco, potentially supporting their buffering effect against the negative impacts of smallmouth bass. However, the impact of smallmouth bass on lake trout diet and bioenergetics in the spring is unknown but potentially negative given our finding of niche overlap. We suggest that the classification of lake trout lakes with cisco as not vulnerable to the impacts of smallmouth bass invasion should be re-examined using a seasonal perspective.

(3) Our paper supports temporal-mediated coexistence occurring between fishes in different thermal guilds because our study species partitioned a shared resource by accessing it at different times (Chesson, 2000). Physiological traits, such as thermal preference, can drive the different responses to winter that underpin coexistence in freshwater fishes (McMeans et al., 2020). In this study, cold-water lake trout altered their diet and habitat in the winter, with more of their energy coming from the nearshore area in the winter than the summer. In contrast, warm-water smallmouth bass reduced their activity in the winter, decoupling themselves from the nearshore prey they depend on during the summer. Overall, lake trout and smallmouth bass's different responses to cold winters leads to nearshore diet items being partitioned in time (only lake trout access nearshore prey in the winter). Therefore, shorter winters (defined as the period of ice cover) due by climate change (Woolway et al., 2020), may impact coexistence between lake trout and smallmouth bass and between other species in different thermal guilds. Although coexistence mechanisms involve resource partitioning, resource partitioning alone does not guarantee stable species coexistence (Chesson, 2000). To determine if coexistence is stable, future studies should investigate long-term population growth rates and the strength of intraspecific vs. interspecific competition.

(4) Our temporally and spatially resolved study provides an example of how the niches of coexisting species in different thermal guilds are partitioned along multiple niche axes. Niche partitioning was likely driven by different responses to seasonally changing water temperatures. Spatial axes, like diet (consuming littoral or pelagic prey) and habitat (depth and distance to shore) diverged most in the summer, when stratified water creates thermally distinct volumes within lakes. The temporal axis (activity), diverged most in the winter, possibly driven by cold temperatures. Our work suggests that conducting field work exclusively in the summer, as is common practice, can lead to an incomplete understanding of species interactions. Conclusions based on summer work alone, may underestimate the strength of interactions between species in different thermal guilds. Although our study focused on smallmouth bass and lake trout, and centered largely around temperature variation, the findings are broadly applicable to other potential competitors and seasonally variable conditions (e.g., light, dissolved oxygen, resource density). We recommend that a seasonal perspective is also adopted in future studies, to continue to bridge the knowledge gap between species ecology in the summer and other seasons. This improved understanding is increasingly important as the range of warm water species is shifting northward due to climate change, increasing the geographic overlap of warm and cold and cool water species (Sharma et al., 2007).

Data availability statement

The raw data supporting the conclusions of this article will be made available by the authors, without undue reservation.

Ethics statement

The animal study was reviewed and approved by University of Toronto Biological Sciences Local Animal Care Committee.

Author contributions

EB, BM, and MR conceived the study idea. EB and BM processed the stable isotope samples and drafted the original manuscript. MR conducted the telemetry field work. MG and TM managed and processed the telemetry and temperature data. EB curated stomach content data. EB and MG performed the statistical analyses. EB, MG, and TM drafted the figures and tables. MG, TM, and MR provided the feedback and edits. All authors contributed to the article and approved the submitted version.

Funding

EB was supported by a Canada Graduate Scholarship–Master's from the Natural Sciences and Engineering Research Council of Canada and the University of Toronto School of Graduate Studies. BM was funded by a Natural Sciences and Engineering Research Council of Canada Discovery Grant (RGPIN-2017-06794). MG was funded by the Natural Sciences and Engineering Research Council of Canada and The W. Garfield Weston Foundation.

Acknowledgments

We are grateful to Brian Shuter, Cindy Chu, Shannon McCauley, and reviewers BM and DG-R for comments that have improved this manuscript. We thank Tim Fernandes, Nick Lacombe, Krystal Mitchell, Courtney Taylor, Sofia Pereira, and Shazreh Salam for assistance in the field and laboratory.

Conflict of interest

The authors declare that the research was conducted in the absence of any commercial or financial relationships that could be construed as a potential conflict of interest.

Publisher's note

All claims expressed in this article are solely those of the authors and do not necessarily represent those of their affiliated organizations, or those of the publisher, the editors and the reviewers. Any product that may be evaluated in this article, or claim that may be made by its manufacturer, is not guaranteed or endorsed by the publisher.

Supplementary material

The Supplementary Material for this article can be found online at: https://www.frontiersin.org/articles/10.3389/fevo.2022.986459/full#supplementary-material

References

Angert, A. L., Huxman, T. E., Chesson, P., and Venable, L. D. (2009). Functional tradeoffs determine species coexistence via the storage effect. *Proc. Natl. Acad. Sci. U.S.A.* 106, 11641–11645.

Arostegui, M. C., Schindler, D. E., and Holtgrieve, G. W. (2019). Does lipid-correction introduce biases into isotopic mixing models? Implications for diet reconstruction studies. *Oecologia* 191, 745–755. doi: 10.1007/s00442-019-04525-7

Baker, R., Buckland, A., and Sheaves, M. (2014). Fish gut content analysis: Robust measures of diet composition. *Fish Fish.* 15, 170–177. doi: 10.1111/faf.12026

Beitinger, T. L., and Fitzpatrick, L. C. (1979). Physiological and ecological correlates of preferred temperature in fish. *Am. Zool.* 19, 319–329.

Benoit, D. M., Jackson, D. A., and Chu, C. (2021). Partitioning fish communities into guilds for ecological analyses: An overview of current approaches and future directions. *Can. J. Fish. Aquat. Sci.* 78, 984–993. doi: 10.1139/cjfas-2020-0455

Benson, B. J., Magnuson, J. J., Jensen, O. P., Card, V. M., Hodgkins, G., Korhonen, J., et al. (2012). Extreme events, trends, and variability in Northern Hemisphere lake-ice phenology (1855-2005). *Clim. Change* 112, 299–323. doi: 10.1007/s10584-011-0212-8

Block, B. D., Denfeld, B. A., Stockwell, J. D., Flaim, G., Grossart, H. P. F., Knoll, L. B., et al. (2019). The unique methodological challenges of winter limnology. *Limnol. Oceanogr. Methods* 17, 42–57. doi: 10.1002/lom3.10295

Block, B. D., Stockwell, J. D., and Marsden, J. E. (2020). Contributions of winter foraging to the annual growth of thermally dissimilar fish species. *Hydrobiologia* 847, 4325–4341. doi: 10.1007/s10750-020-04428-2

Boecklen, W. J., Yarnes, C. T., Cook, B. A., and James, A. C. (2011). On the use of stable isotopes in trophic ecology. *Annu. Rev. Ecol. Evol. Syst.* 42, 411–440. doi: 10.1146/annurev-ecolsys-102209-144726

Brett, J. R. (1971). Energetic responses of salmon to temperature. A study of some thermal relations in the physiology and freshwater ecology of sockeye salmon (*Oncorhynchus nerka*). *Am. Zool.* 11:99–113.

Brown, T. G., Runciman, B., Bradford, M. J., and Pollard, S. (2009). A biological synopsis of yellow perch (*Perca flavescens*). *Can. Manuscr. Rep. Fish. Aquat. Sci.* 2883, 1–28.

Cabana, G., and Rasmussen, J. B. (1996). Comparison of aquatic food chains using nitrogen isotopes. *Proc. Natl. Acad. Sci. U.S.A.* 93, 10844–10847.

Callaghan, D. T., Blanchfield, P. J., and Cott, P. A. (2016). Lake trout (Salvelinus namaycush) spawning habitat in a northern lake: The role of wind and physical characteristics on habitat quality. *J. Great Lakes Res.* 42, 299–307. doi: 10.1016/j.jglr.2015.07.001

Chesson, P. (2000). Mechanisms of maintenance of species diversity. *Annu. Rev. Ecol. Syst.* 31, 343–366. doi: 10.1146/annurev.ecolsys.31.1.343

Chesson, P., and Huntly, N. (1997). The roles of harsh and fluctuating conditions in the dynamics of ecological communities. *Am. Nat.* 150, 519–553. doi: 10.1086/286080

Cobain, M. R. D., McGill, R. A. R., and Trueman, C. N. (2022). Stable isotopes demonstrate seasonally stable benthic-pelagic coupling as newly fixed nutrients are rapidly transferred through food chains in an estuarine fish community. *J. Fish Biol.* 1–15. doi: 10.1111/jfb.15005

Connell, J. H. (1961). The influence of interspecific competition and other factors on the distribution of the barnacle Chthamalus stellatus. *Ecology* 42, 710–723. doi: 10.2307/1933500

Crawshaw, L. I. (1984). Low-temperature dormancy in fish. *Am. J. Physiol.* 246, 479–486. doi: 10.1152/ajpregu.1984.246.4.R479

Cruz-Font, L., Shuter, B. J., Blanchfield, P. J., Minns, C. K., and Rennie, M. D. (2019). Life at the top: Lake ecotype influences the foraging pattern, metabolic costs and life history of an apex fish predator. *J. Anim. Ecol.* 88, 702–716. doi: 10.1111/1365-2656.12956

da Silveira, E. L., Semmar, N., Cartes, J. E., Tuset, V. M., Lombarte, A., Ballester, E. L. C., et al. (2020). Methods for trophic ecology assessment in rishes: A critical review of stomach analyses. *Rev. Fish. Sci. Aquac.* 28, 71–106. doi: 10.1080/23308249.2019.1678013

Dalerum, F., and Angerbjörn, A. (2005). Resolving temporal variation in vertebrate diets using naturally occurring stable isotopes. *Oecologia* 144, 647–658. doi: 10.1007/s00442-005-0118-0

DeNiro, M. J., and Epstein, S. (1977). Mechanism of carbon isotope fractionation associated with lipid synthesis. *Science* 197, 261–263.

DeNiro, M. J., and Epstein, S. (1978). Influence of diet on the distriution of carbon isotopes in animals. *Ecology* 42, 495–506. doi: 10.1002/mop.25285

Doi, H., Akamatsu, F., and González, A. L. (2017). Starvation effects on nitrogen and carbon stable isotopes of animals: An insight from meta-analysis of fasting experiments. *R. Soc. Open Sci.* 4:170633. doi: 10.1098/rsos.170633

Duxbury, B. (2020). *The effect of seasonality on yellow perch ecology and ecotoxicology within Lake Manganese In Biological Science. [master's thesis]*. Houghton MI: Michigan Technological University.

Eloranta, A. P., Mariash, H. L., Rautio, M., and Power, M. (2013). Lipid-rich zooplankton subsidise the winter diet of benthivorous Arctic charr (*Salvelinus alpinus*) in a subarctic lake. *Freshw. Biol.* 58, 2541–2554. doi: 10.1111/fwb.12231

Fernandes, T., and McMeans, B. C. (2021). Spotty at best: Brook trout exploit large, adult spotted salamanders in the early spring. *Ecology* 102, 1–4. doi: 10.1002/ecy.3202

France, R. L. (1995). Differentiation between littoral and pelagic food webs in lakes using stable carbon isotopes. *Limnol. Oceanogr.* 40, 1310–1313. doi: 10.4319/lo.1995.40.7.1310

Fry, B., and Arnold, C. (1982). Rapid 13C/12C turnover during growth of brown shrimp (*Penaeus aztecus*). *Oecologia* 54, 200–204. doi: 10.1007/BF00378393

Fry, B., Joern, A., and Parker, P. L. (1978). Grasshopper food web analysis: Use of carbon isotope ratios to examine feeding relationships among terrestrial herbivores. *Ecology* 59, 498–506.

Fry, F. E. J. (1947). Effects of the environment on animal activity. *Univ. Toronto Stud. Biol. Ser.* 55, 1–62.

Gause, G. F. (1934). Experimental analysis of Vito Volterra's mathematical theory of the struggle for existence. *Science* 79:1617.

Gillette, D. P., Tiemann, J. S., Edds, D. R., and Wildhaber, M. L. (2006). Habitat use by a Midwestern U.S.A. riverine fish assemblage: Effects of season, water temperature and river discharge. *J. Fish Biol.* 68, 1494–1512. doi: 10.1111/j.0022-1112.2006.001037.x

Goyer, K., Bertolo, A., Pépino, M., and Magnan, P. (2014). Effects of lake warming on behavioural thermoregulatory tactics in a cold-water stenothermic fish. *PLoS One* 9:e92514. doi: 10.1371/journal.pone.0092514

Guzzo, M. M., and Blanchfield, P. J. (2017). Climate change alters the quantity and phenology of habitat for lake trout (*Salvelinus namaycush*) in small Boreal Shield lakes. *Can. J. Fish. Aquat. Sci.* 74, 871–884. doi: 10.1139/cjfas-2016-0190

Guzzo, M. M., Blanchfield, P. J., and Rennie, M. D. (2017). Behavioral responses to annual temperature variation alter the dominant energy pathway, growth, and condition of a cold-water predator. *Proc. Natl. Acad. Sci. U.S.A.* 114, 9912–9917. doi: 10.1073/pnas.1702584114

Guzzo, M. M., Blanchfield, P. J., Chapelsky, A. J., and Cott, P. A. (2016). Resource partitioning among top-level piscivores in a sub-Arctic lake during thermal stratification. *J. Great Lakes Res.* 42, 276–285. doi: 10.1016/j.jglr.2015.05.014

Hanson, K. C., Cooke, S. J., Suski, C. D., Niezgoda, G., Phelan, F. J. S., Tinline, R., et al. (2007). Assessment of largemouth bass (Micropterus salmoides) behaviour and activity at multiple spatial and temporal scales utilizing a whole-lake telemetry array. *Hydrobiologia* 582, 243–256. doi: 10.1007/s10750-006-0549-6

Hardin, G. (1960). The competitive exclusion principle. *Science* 131, 1292–1297.

Hasnain, S. S., Escobar, M. D., and Shuter, B. J. (2018). Estimating thermal response metrics for North American freshwater fish using Bayesian phylogenetic regression. *Can. J. Fish. Aquat. Sci.* 75, 1878–1885. doi: 10.1139/cjfas-2017-0278

Helland, I. P., Finstad, A. G., Forseth, T., Hesthagen, T., and Ugedal, O. (2011). Ice-cover effects on competitive interactions between two fish species. *J. Anim. Ecol.* 80, 539–547. doi: 10.1111/j.1365-2656.2010.01793.x

Helland, I. P., Harrod, C., Freyhof, J., and Mehner, T. (2008). Co-existence of a pair of pelagic planktivorous coregonid fishes. *Evol. Ecol. Res.* 10, 373–390.

Holm, E., Mandrak, N. E., and Burridge, M. E. (2009). *The ROM field guide to freshwater fishes of Ontario*, 6th Edn. Toronto: Royal Ontario Museum.

Hutchinson, G. E. (1961). The paradox of the plankton. *Am. Nat.* 95, 137–145.

Hynes, H. B. N. (1950). The food of fresh-water sticklebacks (*Gasterosteus aculeatus* and *Pygosteus pungitius*), with a review of methods used in studies of the food of fishes. *J. Anim. Ecol.* 19, 36–58. doi: 10.2307/1570

Hyslop, E. J. (1980). Stomach contents analysis – a review of methods and their application. *J. Fish Biol.* 17, 411–429. doi: 10.1111/j.1095-8649.1980.tb02775.x

James, G., Witten, D., Hastie, T., and Tibshirani, R. (2013). *An introduction to statistical learning*. New York, NY: Springer. doi: 10.1007/978-1-4614-7138-7

Jensen, T. C. (2019). Winter decrease of zooplankton abundance and biomass in subalpine oligotrophic Lake Atnsjøen (SE Norway). *J. Limnol.* 78, 348–363. doi: 10.4081/jlimnol.2019.1877

Keller, W. (2007). Implications of climate warming for Boreal Shield lakes: A review and synthesis. *Environ. Rev.* 15, 99–112. doi: 10.1139/A07-002

Kiljunen, M., Grey, J., Sinisalo, T., Harrod, C., Immonen, H., and Jones, R. I. (2006). A revised model for lipid-normalizing δ13C values from aquatic organisms, with implications for isotope mixing models. *J. Appl. Ecol.* 43, 1213–1222. doi: 10.1111/j.1365-2664.2006.01224.x

Kionka, B. C., and Windell, J. T. (1972). Differential movement of digestible and indigestible food fractions in rainbow trout, Salmo gairdneri. *Trans. Am. Fish. Soc.* 101, 112–115.

Koroiva, R., and Pepinelli, M. (2019). "Distribution and habitats of aquatic insects," in *Aquatic insects: Behavior and ecology*, eds K. Del-Claro and R. Guillermo (Cham: Springer International Publishing), 11–33.

Larocque, S. M., Johnson, T. B., and Fisk, A. T. (2021). Trophic niche overlap and abundance reveal potential impact of interspecific interactions on a reintroduced fish. *Can. J. Fish. Aquat. Sci.* 78, 765–774. doi: 10.1139/cjfas-2020-0204

Legler, N. D., Johnson, T. B., Heath, D. D., and Ludsin, S. A. (2010). Water temperature and prey size effects on the rate of digestion of larval and early juvenile fish. *Trans. Am. Fish. Soc.* 139, 868–875. doi: 10.1577/t09-212.1

Lenth, R. (2020). *emmeans: Estimated marginal means, aka least-squares means. R package Version 1.5.2-1*. Available online at: https://CRAN.R-project.org/package=emmeans

Lepak, J. M., Kraft, C. E., and Weidel, B. C. (2006). Rapid food web recovery in response to removal of an introduced apex predator. *Can. J. Fish. Aquat. Sci.* 63, 569–575. doi: 10.1139/f05-248

Lotka, A. J. (1932). The growth of mixed populations: Two species competing for a common food supply. *J. Washingt. Acad. Sci.* 22, 461–469.

Macarthur, R. H. (1958). Population ecology of some warblers of northeastern coniferous forests. *Ecology* 39, 599–619.

MacRae, P. S. D., and Jackson, D. A. (2001). The influence of smallmouth bass (*Micropterus dolomieu*) predation and habitat complexity on the structure of littoral zone fish assemblages. *Can. J. Fish. Aquat. Sci.* 58, 342–351. doi: 10.1139/cjfas-58-2-342

Magnuson, J. J., Crowder, L. B., and Medvick, P. A. (1979). Temperature as an ecological resource. *Am. Zooplogist* 19, 331–343. doi: 10.1093/icb/19.1.331

Maitland, B. M., Del Rio, C. M., and Rahel, F. J. (2021). Effect of temperature on 13C and 15N incoropration rates and discrimation factors in two North American fishes. *Can. J. Fish. Aquat. Sci.* 78, 1833–1840. doi: 10.1139/cjfas-2021-0057

Marsden, J. E., Blanchfield, P. J., Brooks, J. L., Fernandes, T., Fisk, A. T., Futia, M. H., et al. (2021). Using untapped telemetry data to explore the winter biology of freshwater fish. *Rev. Fish Biol. Fish.* 31, 115–134. doi: 10.1007/s11160-021-09634-2

Martin, N. V. (1952). A study of the lake trout, Salvelinus Namaycush, in two Algonquin Park, Ontario, lakes. *Trans. Am. Fish. Soc.* 81, 111–137.

Martin, N. V. (1957). Reproduction of lake trout in Algonquin Park, Ontario. *Trans. Am. Fish. Soc.* 86, 231–244.

Mathias, A., and Chesson, P. (2013). Coexistence and evolutionary dynamics mediated by seasonal environmental variation in annual plant communities. *Theor. Popul. Biol.* 84, 56–71. doi: 10.1016/j.tpb.2012.11.009

McMeans, B. C., Kadoya, T., Pool, T. K., Holtgrieve, G. W., Lek, S., Kong, H., et al. (2019). Consumer trophic positions respond variably to seasonally fluctuating environments. *Ecology* 100, 1–10. doi: 10.1002/ecy.2570

McMeans, B. C., McCann, K. S., Guzzo, M. M., Bartley, T. J., Bieg, C., Blanchfield, P. J., et al. (2020). Winter in water: Differential responses and the maintenance of biodiversity. *Ecol. Lett.* 23, 922–938. doi: 10.1111/ele.13504

McMeans, B. C., McCann, K. S., Humphries, M., Rooney, N., and Fisk, A. T. (2015). Food web structure in temporally-forced ecosystems. *Trends Ecol. Evol.* 30, 662–672. doi: 10.1016/j.tree.2015.09.001

Morbey, Y. E., Addison, P., Shuter, B. J., and Vascotto, K. (2006). Within-population heterogeneity of habitat use by lake trout Salvelinus namaycush. *J. Fish Biol.* 69, 1675–1696. doi: 10.1111/j.1095-8649.2006.01236.x

Morbey, Y. E., Couture, P., Busby, P., and Shuter, B. J. (2010). Physiological correlates of seasonal growth patterns in lake trout Salvelinus namaycush. *J. Fish Biol.* 77, 2298–2314. doi: 10.1111/j.1095-8649.2010.02804.x

Morbey, Y. E., Vascotto, K., and Shuter, B. J. (2007). Dynamics of piscivory by lake trout following a smallmouth bass invasion: A historical reconstruction. *Trans. Am. Fish. Soc.* 136, 477–483. doi: 10.1577/t06-070.1

O'Reilly, C. M., Hecky, R. E., Cohen, A. S., and Plisnier, P. D. (2002). Interpreting stable isotopes in food webs: Recognizing the role of time averaging at different trophic levels. *Limnol. Oceanogr.* 47, 306–309. doi: 10.4319/lo.2002.47.1.0306

Ontario Ministry of Natural Resources and Forestry (2022). *Fish ON-Line*. Available online at: https://www.lioapplications.lrc.gov.on.ca/fishonline/Index.html?viewer=FishONLine.FishONLine (accessed January 10, 2021)

Park, T. (1954). Experimental studies of interspecies competition II. Temperature, humidity, and competition in two species of Tribolium. *Physiol. Zool.* 27, 177–238.

Pazzia, I., Trudel, M., Ridgway, M., and Rasmussen, J. B. (2002). Influence of food web structure on the growth and bioenergetics of lake trout (*Salvelinus namaycush*). *Can. J. Fish. Aquat. Sci.* 59, 1593–1605. doi: 10.1139/f02-128

Pépino, M., Goyer, K., and Magnan, P. (2015). Heat transfer in fish: Are short excursions between habitats a thermoregulatory behaviour to exploit resources in an unfavourable thermal environment? *J. Exp. Biol.* 218, 3461–3467. doi: 10.1242/jeb.126466

Peterson, B. J., and Fry, B. (1987). Stable isotopes in ecosystem studies. *Annu. Rev. Ecol. Syst.* 18, 293–320.

Plumb, J. M., and Blanchfield, P. J. (2009). Performance of temperature and dissolved oxygen criteria to predict habitat use by lake trout (*Salvelinus namaycush*). *Can. J. Fish. Aquat. Sci.* 66, 2011–2023. doi: 10.1139/F09-129

Plumb, J. M., Blanchfield, P. J., and Abrahams, M. V. (2014). A dynamic-bioenergetics model to assess depth selection and reproductive growth by lake trout (*Salvelinus namaycush*). *Oecologia* 175, 549–563. doi: 10.1007/s00442-014-2934-6

Post, D. M. (2002). Using stable isotopes to estimate trophic position: Models, methods, and assumptions. *Ecology* 83, 703–718. doi: 10.2307/3071875

Post, D. M., Layman, C. A., Arrington, D. A., Takimoto, G., Quattrochi, J., and Montaña, C. G. (2007). Getting to the fat of the matter: Models, methods and assumptions for dealing with lipids in stable isotope analyses. *Oecologia* 152, 179–189. doi: 10.1007/s00442-006-0630-x

R Core Team (2020). *R: A language and environment for statistical computing*. Vienna: R Foundation for Statistical Computing.

Riley, S. C., Marsden, J. E., Ridgway, M. S., Konrad, C. P., Farha, S. A., Binder, T. R., et al. (2019). A conceptual framework for the identification and characterization of lacustrine spawning habitats for native lake charr *Salvelinus namaycush*. *Environ. Biol. Fishes* 102, 1533–1557. doi: 10.1007/s10641-019-00928-w

Rowe, L., and Berrill, M. (1989). The life cycles of five closely related mayfly species (Ephemeroptera: Heptageniidae) coexisting in a small southern Ontario stream pool. *Aquat. Insects* 11, 73–80. doi: 10.1080/01650428909361351

Schindler, D. E., and Scheuerell, M. D. (2002). Habitat coupling in lake ecosystems. *Oikos* 98, 177–189. doi: 10.1034/j.1600-0706.2002.980201.x

Searle, S. R., Speed, F. M., and Milliken, G. A. (1980). Population marginal means in the linear model: An alternative to least squares means. *Am. Stat.* 34, 216–221. doi: 10.1080/00031305.1980.10483031

Sharma, S., Jackson, D. A., and Minns, C. K. (2009). Quantifying the potential effects of climate change and the invasion of smallmouth bass on native lake trout populations across Canadian lakes. *Ecography* 32, 517–525. doi: 10.1111/j.1600-0587.2008.05544.x

Sharma, S., Jackson, D. A., Minns, C. K., and Shuter, B. J. (2007). Will northern fish populations be in hot water because of climate change? *Glob. Chang. Biol.* 13, 2052–2064. doi: 10.1111/j.1365-2486.2007.01426.x

Sharma, S., Magnuson, J. J., Batt, R. D., Winslow, L. A., Korhonen, J., and Aono, Y. (2016). Direct observations of ice seasonality reveal changes in climate over the past 320-570 years. *Sci. Rep.* 6, 1–11. doi: 10.1038/srep25061

Sherwood, G. D., Pazzia, I., Moeser, A., Hontela, A., and Rasmussen, J. B. (2002). Shifting gears: Enzymatic evidence for the energetic advantage of switching diet in wild-living fish. *Can. J. Fish. Aquat. Sci.* 59, 229–241. doi: 10.1139/f02-001

Shimadzu, H., Dornelas, M., Henderson, P. A., and Magurran, A. E. (2013). Diversity is maintained by seasonal variation in species abundance. *BMC Biol.* 11:98. doi: 10.1186/1741-7007-11-98

Shuter, B. J., Finstad, A. G., Hellend, I. P., Zweimüller, I., and Hölker, F. (2012). The role of winter phenology in shaping the ecology of freshwater fish and their sensitivities to climate change. *Aquat. Sci.* 74, 637–657. doi: 10.1007/s00027-012-0274-3

Shuter, B. J., Giacomini, H. C., de Kerckhove, D., and Vascotto, K. (2016). Fish life history dynamics: Shifts in prey size structure evoke shifts in predator maturation traits. *Can. J. Fish. Aquat. Sci.* 73, 693–708. doi: 10.1139/cjfas-2015-0190

Skinner, M. M., Cross, B. K., and Moore, B. C. (2017). Estimating in situ isotopic turnover in rainbow trout (*Oncorhynchus mykiss*) muscle and liver tissue. *J. Freshw. Ecol.* 32, 209–217. doi: 10.1080/02705060.2016.1259127

Skinner, M. M., Martin, A. A., and Moore, B. C. (2016). Is lipid correction necessary in the stable isotope analysis of fish tissues? *Rapid Commun. Mass Spectrom.* 30, 881–889. doi: 10.1002/rcm.7480

Smith, F. (2013). *Understanding HPE in the VEMCO positioning system (VPS)*. Boston, MA: VEMCO.

Sommer, U., Gliwicz, Z., Lampert, W., and Duncan, A. (1986). The PEG-model of seasonal succession of planktonic events in fresh waters. *Arch. Für Hydrobiol.* 106, 433–471.

Speers-Roesch, B., Norin, T., and Driedzic, W. R. (2018). The benefit of being still: Energy savings during winter dormancy in fish come from inactivity and the cold, not from metabolic rate depression. *Proc. R. Soc. B Biol. Sci.* 285:20181593. doi: 10.1098/rspb.2018.1593

Stockwell, J. D., Yule, D. L., Hrabik, T. R., Sierszen, M. E., and Isaac, E. J. (2014). Habitat coupling in a large lake system: Delivery of an energy subsidy by an offshore planktivore to the nearshore zone of Lake Superior. *Freshw. Biol.* 59, 1197–1212. doi: 10.1111/fwb.12340

Sugimoto, R., Sato, T., Yoshida, T., and Tominaga, O. (2014). Using stable nitrogen isotopes to evaluate the relative importance of external and internal nitrogen loadings on phytoplankton production in a shallow eutrophic lake (Lake Mikata Japan). *Limnol. Oceanogr.* 59, 37–47. doi: 10.4319/lo.2014.59.1.0037

Suski, C. D., and Ridgway, M. S. (2009). Seasonal pattern of depth selection in smallmouth bass. *J. Zool.* 279, 119–128. doi: 10.1111/j.1469-7998.2009.00595.x

Sutton, A. O., Studd, E. K., Fernandes, T., Bates, A. E., Bramburger, A. J., Cooke, S. J., et al. (2021). Frozen out: Unanswered questions about winter biology. *Environ. Rev.* 29, 431–442. doi: 10.1139/er-2020-0127

Swanson, H. K., Lysy, M., Power, M., Stasko, A. D., Johnson, J. D., and Reist, J. D. (2015). A new probabilistic method for quantifying n-dimensional ecological niches and niche overlap. *Ecology* 96, 318–324.

Szabó, P. (2016). Ideal free distribution of metabolic activity: Implications of seasonal metabolic-activity patterns on competitive coexistence. *Theor. Popul. Biol.* 111, 1–8. doi: 10.1016/j.tpb.2016.05.001

Tansley, A. G. (1917). On competition between *Galium saxatile* L. (G. *hercynicum* Weig.) and *Galium sylvestre* Poll. (G. *Asperum Schreb.*) on different types of soil. *J. Ecol.* 5, 173–179. doi: 10.2307/2255655

Tonn, W. M., and Magnuson, J. J. (1982). Patterns in the species composition and richness of fish assemblages in northern Wisconsin lakes. *Ecology* 63, 1149–1166. doi: 10.2307/1937251

Tunney, T. D., McCann, K. S., Lester, N. P., and Shuter, B. J. (2012). Food web expansion and contraction in response to changing environmental conditions. *Nat. Commun.* 3, 1–9. doi: 10.1038/ncomms2098

Turschak, B., Bronte, C. R., Czesny, S., Gerig, B., Happel, A., Höök, T. O., et al. (2022). Temporal variation in the niche partitioning of Lake Michigan salmonines as it relates to alewife abundance and size structure. *Can. J. Fish. Aquat. Sci.* 79, 487–502. doi: 10.1139/cjfas-2021-0027

Vander Zanden, J. M., and Rasmussen, J. B. (1996). A trophic position model of pelagic food webs: Impact on contaminant bioaccumulation in lake trout. *Ecol. Monogr.* 66, 451–477.

Vander Zanden, M. J., Casselman, J. M., and Rasmussen, J. B. (1999). Stable isotope evidence for the food web consequences of species invasions in lakes. *Nature* 401, 464–467. doi: 10.1038/46762

Vander Zanden, M. J., Clayton, M. K., Moody, E. K., Solomon, C. T., and Weidel, B. C. (2015). Stable isotope turnover and half-life in animal tissues: A literature synthesis. *PLoS One* 10:e0116182. doi: 10.1371/journal.pone.0116182

Vander Zanden, M. J., Olden, J. D., Thorne, J. H., and Mandrak, N. E. (2004). Predicting occurrences and impacts of smallmouth bass introductions in north temperate lakes. *Ecol. Appl.* 14, 132–148.

Versteeg, E. J., Fernandes, T., Guzzo, M. M., Laberge, F., Middel, T., Ridgway, M., et al. (2021). Seasonal variation of behavior and brain size in a freshwater fish. *Ecol. Evol.* 11, 14950–14959. doi: 10.1002/ece3.8179

Visconti, A., Volta, P., Fadda, A., Di Guardo, A., and Manca, M. (2014). Seasonality, littoral versus pelagic carbon sources, and stepwise 15N-enrichment of pelagic food web in a deep subalpine lake: The role of planktivorous fish. *Can. J. Fish. Aquat. Sci.* 71, 436–446. doi: 10.1139/cjfas-2013-0178

Volterra, V. (1926). Fluctuations in the abundance of a species considered mathematically. *Nature* 118, 558–560. doi: 10.1038/118558a0

Wolf, N., Carleton, S. A., and del Rio, C. M. (2009). Ten years of experimental animal isotopic ecology. *Funct. Ecol.* 23, 17–26. doi: 10.1111/j.1365-2435.2008.01529.x

Woodland, R. J., Rodríguez, M. A., Magnan, P., Glémet, H., and Cabana, G. (2012). Incorporating temporally dynamic baselines in isotopic mixing models. *Ecology* 93, 131–144. doi: 10.1890/11-0505.1

Woolway, R. I., Kraemer, B. M., Lenters, J. D., Merchant, C. J., O'Reilly, C. M., and Sharma, S. (2020). Global lake responses to climate change. *Nat. Rev. Earth Environ.* 1, 388–403. doi: 10.1038/s43017-020-0067-5

Yeakel, J. D., Bhat, U., Smith, E. A. E., and Newsome, S. D. (2016). Exploring the isotopic niche: Isotopic variance, physiological incorporation, and the temporal dynamics of foraging. *Front. Ecol. Evol.* 4:1. doi: 10.3389/fevo.2016.00001

Yule, D. L., Stockwell, J. D., Schreiner, D. R., Evrard, L. M., Balge, M., and Hrabik, T. R. (2009). Can pelagic forage fish and spawning cisco (*Coregonus artedi*) biomass in the western arm of Lake Superior be assessed with a single summer survey? *Fish. Res.* 96, 39–50. doi: 10.1016/j.fishres.2008.09.012

frontiers | Frontiers in Ecology and Evolution

TYPE Original Research
PUBLISHED 18 November 2022
DOI 10.3389/fevo.2022.1006928

OPEN ACCESS

EDITED BY
Perry S. Barboza,
Texas A&M University, United States

REVIEWED BY
Craig Stricker,
United States Department of the Interior, United States
Jeremy Ryan Shipley,
Max Planck Institute of Ornithology, Germany

*CORRESPONDENCE
Corrine S. V. Génier
cgenier@uwo.ca

SPECIALTY SECTION
This article was submitted to Ecophysiology, a section of the journal Frontiers in Ecology and Evolution

RECEIVED 29 July 2022
ACCEPTED 31 October 2022
PUBLISHED 18 November 2022

CITATION
Génier CSV, Guglielmo CG and Hobson KA (2022) Combining bulk stable H isotope (δ^2H) measurements with fatty acid profiles to examine differential use of aquatic vs. terrestrial prey by three sympatric species of aerial insectivorous birds.
Front. Ecol. Evol. 10:1006928.
doi: 10.3389/fevo.2022.1006928

Combining bulk stable H isotope (δ^2H) measurements with fatty acid profiles to examine differential use of aquatic vs. terrestrial prey by three sympatric species of aerial insectivorous birds

Corrine S. V. Génier[1]*, Christopher G. Guglielmo[1] and Keith A. Hobson[1,2]

[1]Department of Biology, Centre for Animals on the Move, Advanced Facility for Avian Research, University of Western Ontario, London, ON, Canada, [2]Environment and Climate Change Canada, Saskatoon, SK, Canada

Aerial insectivorous songbirds such as swallows and martins have declined substantially in North America in recent decades. Aquatic-emergent insects provide more beneficial omega-3 fatty acids than terrestrial insects, and thus, diet quality is expected to vary among aerial insectivores with differential access to aquatic-emergent insects. We compared the stable hydrogen isotope (δ^2H) values of feathers and bulk blood plasma fatty acids of nestling purple martins (*Progne subis*), tree swallows (*Tachycineta bicolor*), and barn swallows (*Hirundo rustica*), at lakeshore and inland sites near Lake Erie, Ontario, Canada. We found that diet quality differed between inland and lakeshore nesting habitats, but differences depended on species. Overall, purple martin and tree swallow nestlings had lower feather δ^2H values, indicating a more aquatic-emergent diet, and lakeshore populations of both species had higher omega-3 fatty acid levels in their blood plasma compared to inland populations. Conversely, higher plasma levels of omega-6 fatty acids were found in inland birds. Tree swallows have a low omega-3 conversion efficiency from precursor substrates and so depend on aquatic subsidies to fulfill their nutritional needs. We suggest this may also be the case with purple martins. Barn swallows had the most positive feather δ^2H values, regardless of proximity to the lakeshore, indicating a more terrestrial diet. However, barn swallow nestlings had consistently higher plasma omega-3 docosahexaenoic acid (DHA) regardless of nesting location, suggesting that barn swallows can efficiently convert omega-3 precursors into their beneficial elongated fatty acid chains. Our study indicates the benefit of combining plasma fatty acid compositional analyses with bulk feather δ^2H values to decipher interspecific differences in adaptations to availability of aquatic-emergent insects.

KEYWORDS

aerial insectivore, diet quality, stable hydrogen isotopes, fatty acids, nutritional landscapes

Introduction

Aerial insectivorous songbirds have declined more than any other avian guild in North America in recent decades (Smith et al., 2015; Sauer et al., 2017; North American Bird Conservation Initiative Canada, 2019; Rosenberg et al., 2019). As these species all forage on insects in the air column, insect population declines have been considered among the likely factors influencing these trends (Hallmann et al., 2017; Møller, 2019; Sánchez-Bayo and Wyckhuys, 2019; Stepanian et al., 2020). However, the role of insect abundance as a limiting factor for aerial insectivore populations remains an open question (Imlay et al., 2017; McClenaghan et al., 2019a; Spiller and Dettmers, 2019). Instead, a growing literature on the effects of diet quality versus quantity on aerial insectivore health suggests a need to identify if diet quality is a contributor to population declines (Twining et al., 2016, 2018b, 2021; Spiller and Dettmers, 2019).

Fatty acids (FA) are nutrients essential to many physiological processes. Omega-3 eicosapentaenoic acid (EPA) and docosahexaenoic acid (DHA) are long-chain polyunsaturated fatty acids (PUFA) known to promote brain development and provide anti-inflammatory properties in humans (Simopoulos, 2011). In contrast to omega-3 FAs, omega-6 arachidonic acid (ARA) competes with EPA in cell membranes and has pro-inflammatory properties in humans, yet ARA is necessary in organ development and gene expression (Simopoulos, 2011). A low omega-6/omega-3 ratio is thought to have positive benefits, while a high ratio may cause susceptibility to inflammatory responses (Roy et al., 2008; Andersson et al., 2015; Isaksson et al., 2017). Insect lipids have high levels of saturated FAs, but also unsaturated FA, the most abundant being oleic acid and linoleic (LA) (Rumpold and Schlüter, 2013; Sosa and Fogliano, 2017). Many terrestrial insects can also be high in ARA (Rumpold and Schlüter, 2013). Depending on the study, LA and alpha-linolenic acid (ALA) can be high in terrestrial and aquatic insects (Rumpold and Schlüter, 2013; Hixson et al., 2015; Twining et al., 2018a, 2019, 2021). More importantly for insectivorous birds, these studies show that aquatic insects are a rich source of omega-3 FAs such as EPA and DHA compared to terrestrial insects (Rumpold and Schlüter, 2013; Hixson et al., 2015; Twining et al., 2018a, 2019, 2021; Shipley et al., 2022). Tree swallows (TRES; *Tachycineta bicolor*) with higher omega-3 FAs benefit from associated increases in nestling health, growth, and fledging success compared to nestlings provisioned with more terrestrial insects or a lower omega-3 diet (Twining et al., 2016, 2018b). Furthermore, a high EPA and DHA diet fed to nestling eastern phoebe (*Sayornis phoebe*) increased mass growth 2–3 times more than a high ALA diet (Twining et al., 2019).

Habitat can determine diet composition in birds, as the spatial distribution of prey quality and nutrient content varies across landscapes. Swallows forage close (~1 km) to their nests during the breeding season (Waugh, 1979; McCarty and Winkler, 1999; Evans et al., 2007). Breeding purple martins (PUMA; *Progne subis*) also forage in proximity (~3 km) to their nest (Lalla, 2022). Thus, birds nesting in one location may differ in diet composition and quality from birds nesting in another nearby location. For example, bank swallows (*Riparia riparia*) nesting at lakeshore sites in southern Ontario fed on a more aquatic-emergent insect diet represented by low feather stable hydrogen isotope values (δ^2H) and had higher plasma EPA than inland birds (Génier et al., 2021). Similarly, spider, reptile, and amphibian diets have been shown to isotopically shift from an aquatic-derived diet to a more terrestrial diet as they became more distant from the riparian zone (Walters et al., 2008; Twining et al., 2021).

Songbirds can compensate for variation in diet quality by internally synthesizing some FAs. This has been demonstrated in nestling tree swallows and blue tits (*Cyanistes caeruleus*) that are able to convert the 18-carbon omega-3 precursor ALA to its longer EPA and DHA chains (Twining et al., 2018a, 2021). However, this conversion efficiency in nestling tree swallows was not adequate to meet their high omega-3 PUFA demand, whereas blue tits were not limited (Twining et al., 2018a, 2021). A balance likely exists between conversion efficiency, the physiological costs of such conversion and prey quality, where the ability to efficiently convert omega-3 precursors to their long-chain PUFA may alleviate the dependency on aquatic-emergent insects.

It is still unknown how different aerial insectivores occurring in sympatry compare in their diet composition within or between riparian and inland nesting habitats. In general, we expect closely-related species to segregate diets (Orłowski and Karg, 2013; Collins, 2015; Bumelis et al., 2021) depending on relative abundance of prey and density of avian consumers. Furthermore, purple martins, tree swallows, and barn swallows forage in different aerial strata (Dreelin et al., 2018). Swallows feed generally on aerial insects, but there is evidence of dietary segregation occurring among them (Bumelis et al., 2021). Unfortunately, determining origins of prey and their nutritional quality, especially in the context of multispecies communities, is extremely challenging.

In combination with tissue FA profiles that provide insight into diet quality, measurements of naturally occurring ratios of stable hydrogen isotopes (δ^2H) in animal tissues provide a strong tool to differentiate between aquatic and terrestrial dietary sources (Voigt et al., 2015; Vander Zanden et al., 2016; Génier et al., 2021). In general, terrestrial plants tend to be enriched in ^{2}H (i.e., have higher δ^2H) due to local evaporative conditions compared to aquatic plants that occur in water (Fogel and Cifuentes, 1993; Doucett et al., 2007). Unless a water source is prone to seasonal evaporation, aquatic consumers are expected to have lower δ^2H values than terrestrial consumers and the use of this isotope appears more useful for this purpose than stable carbon isotopes (δ^{13}C, Doucett et al., 2007; Voigt et al., 2015; Génier et al., 2021). Combining FA and δ^2H measurements in sympatric aerial insectivores, we sought to understand diet composition and the relative use of aquatic-emergent insects by these birds across a broad landscape in southern Ontario.

Following on from our earlier work on bank swallows, we compared plasma FA profiles and feather δ^2H among nestling

barn swallows (BARS; *Hirundo rustica*), tree swallows and purple martins nesting inland and in close proximity to Lake Erie, Ontario. All species have broad diets but previous research elsewhere and in our study area confirms that barn swallows have the most terrestrial diet compared to tree swallows and purple martins (McCarty and Winkler, 1999; Helms et al., 2016; McClenaghan et al., 2019b; Bumelis et al., 2021). We used the eastern bluebird (EABL; *Sialia sialis*) as a "control" species as it feeds largely on terrestrial invertebrates (Weinkam et al., 2017). We expected that all aerial insectivores would consume more aquatic-emergent insects with proximity to major waterbodies, showing low δ^2H, high EPA, and low ARA at lakeshore sites compared to more terrestrial locations. In general, we expected segregation within sites with barn swallows the most terrestrial and tree swallows and purple martins the most riparian. However, we had no *a priori* expectations regarding interactions between species and proximity to lake.

Materials and methods

Field sampling

In 2020, nestlings of barn swallow ($n = 101$), tree swallow ($n = 162$), purple martin ($n = 66$), and eastern bluebird ($n = 33$) were sampled from colonies in the Lake Erie region (LAT: 42.58° to 43.10°, LON: −80.40° to-81.51°) of southwestern Ontario, Canada (Figure 1). We categorized sites within 5 km of Lake Erie or Lake Huron as lakeshore sites, and all other sites (i.e., 5–70 km from the lakes) as inland. Nestlings, at day 12–18 depending on species, were sampled for blood for FA profiles and tail feathers for δ^2H analysis. Blood was taken by brachial vein puncture and separated into cellular and plasma fractions in the field using a portable centrifuge (Scilogex® Model D1008 EZeeMini, Rocky Hill, United States). In the field, plasma was stored in a liquid nitrogen Dewar (−135 to-190°C). Within 7 h, samples were then transferred to an ultracold (−80°C) and regular (−25°C) freezer for plasma and cellular fractions, respectively. Tail feathers were pulled and placed into a labelled paper envelope and kept dry at room temperature. All animal work was approved by the University of Western Ontario Animal Care Committee (AUP 2017–005) and the Canadian Wildlife Service (10613G).

Insects were collected for δ^2H from lakeshore and inland sites using a combination of sweep netting, a Malaise trap (Bugdorm, TWN), and a light trap (University of Western Ontario, Department of Physics, London, CAN). In 2020, we installed the Malaise trap twice at inland and lakeshore sites for 5 days each (May 26 and June 2, 11, 16) while alternating between locations throughout the breeding season. In 2021, we installed the Malaise trap among 3 inland and 3 lakeshore sites for 5-day periods (May–July). Sampling was further increased through opportunistic sweep netting over the vegetation surrounding our sites and insect collection from Western's light trap at the Environmental Sciences Western Field Station. The daily decanting of the Malaise trap

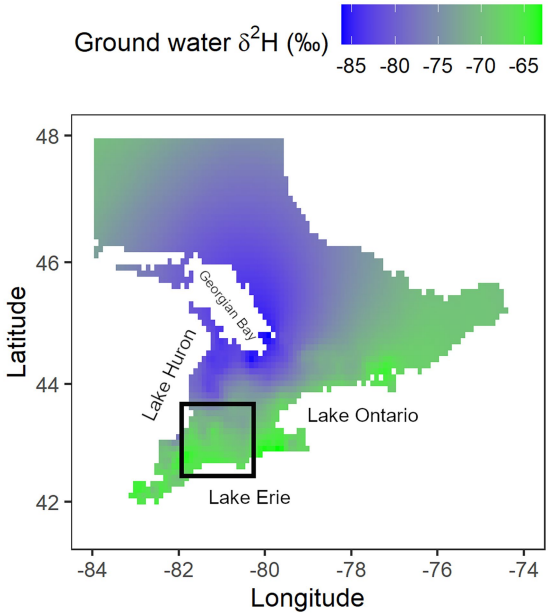

FIGURE 1
Kriged plot of groundwater δ^2H values (‰) from shallow well data (less than 32m) for southern Ontario. Data were extracted from the waterisotopes.org database (n=703). Black square represents the study area.

targeted smaller flying insects, while sweep netting collected additional insect orders such as orthopterans and odonates and the light trap allowed the collection of nocturnal insects such trichopterans. Insects were transferred at the end of the day and stored in a-80°C freezer. We separated the insects based on orders and further separated aquatic insects of interest (e.g., chironomids from other dipterans).

Stable hydrogen isotope analyses

Tail feathers (2020: n = 266) were soaked in 2:1 chloroform:methanol solution overnight, decanted, rinsed, and dried at ambient temperature in a fume hood. Dragonfly, damselfly (Odonata), and mayfly (Ephemeroptera) wings were separated from their body for soaking, while all other insect groups were soaked with bodies intact (2020: n = 132; 2021: n=510). Grasshopper and cricket (Orthoptera) samples involved the use of legs in addition to wings. In 2021, whole midges (Chironomidae) were dried at 50°C for 24 h and powdered. Feather barbs, insect wing or powdered insect bodies were weighed to 0.33–0.35 mg into silver capsules (Mettler Toledo® XP6 Excellence Plus XP Micro Balance, Greifensee, CHE). Individuals of larger insects such as dragonflies and damselflies were used whereas smaller insects such as flies required multiple individuals for a single composite sample.

Samples were measured by KAH for δ^2H at the LSIS-AFAR stable isotope facility at the University of Western Ontario.

Compressed silver capsules were loaded onto a UNI-Prep (Eurovector®, Milan, ITA) heated carousel at 60°C coupled with a Eurovector 3,000 elemental analyzer. The samples were combusted pyrolytically at 1350°C on a glassy carbon reactor. The resulting H_2 gas was analyzed on a Thermo Delta V Plus (Thermo Scientific®, Bremen, DEU) continuous-flow isotope ratio mass spectrometer *via* a Conflo device (Thermo Scientific®). Results were expressed in the standard delta notation (δ) in parts per thousand (‰) and normalized using two in-house keratin standards (CBS: −197 ‰; KHS: −54 ‰). We derived our δ^2H values from the non-exchangeable H fraction using the comparative equilibrium approach (Wassenaar and Hobson, 2003) and expressed them relative to the Vienna Standard Mean Ocean Water (VSMOW). Within-run standards CBS ($n = 5$) and KHS ($n = 5$) measured error to be ±2 ‰.

Fatty acid analyses

Aerial insectivore plasma samples (2020, $n = 264$) underwent a solvent extraction and derivatization, a protocol modified from Bligh and Dyer (1959) and loaded onto the gas chromatograph (GC)/flame ionization detector (FID) (see Supplementary material for full protocol). Briefly, we mixed the plasma and an internal 17:0 standard in culture tubes with a chloroform:methanol solution containing butylated hydroxytoluene. After centrifuging, the supernatant was mixed with potassium chloride and placed in a 70°C water bath. The organic phase was filtered into vials and dried under N_2. Methanolic hydrogen chloride was added and vials were placed in a 90°C oven to derivatize fatty acid methyl esters. Ultrapure water and hexane were added to the vials and the top hexane layer was transferred to GC vials containing dimethoxypropane. Vials were dried under N_2 and resuspended in hexane.

We loaded GC vials on a carousel with dichloromethane blank and two standards (Supelco® PUFA and 37 components) and analyzed FA profiles using a GC/FID (Agilent Technologies® 6,890 N G1530N, Santa Clara, United States) equipped with a DB23 column (Agilent Technologies® DB23 122–2,332; see Supplementary material for temperature settings). The retention times of both standards across all runs were averaged for each known FA. We then manually identified each distinct FA peak in a given sample chromatograph by comparing the retention time to our FA library. Relative to the internal 17:0 standard, mass percent was calculated for each FA.

Statistical analyses

Our goal was to examine if aerial insectivores differed in use of aquatic-versus terrestrially-derived insects by comparing feather δ^2H values and plasma FA percentages. We also assessed the δ^2H values and FA percentages of presumed insect prey (see Supplementary material). All figures and statistical analyses were performed with RStudio Version 1.4.1717 and R 4.0.5 statistical software (RStudio Team, 2018; R Core Team, 2019). Significance level was $p < 0.05$.

Terrestrial foodwebs near large lakes can receive input from meteoric precipitation and from reprecipitated lakewater. If there was significant input of water driving the terrestrial foodweb from Lake Erie, then this would tend to drive that foodweb to lower δ^2H values than expected from expected precipitation isotope data alone (i.e., the long-term database of the International Atomic Energy Agency – Global Network of Isotopes in Precipitation IAEA-GNIP and other sources summarized in waterisotopes.org). If this were the case, it would interfere with our ability to test for the relative abundance of aquatic-derived prey in the diet because diets near lakes might simply be naturally labelled as being lower in ^{2}H regardless of actual diet. Unfortunately, there are relatively few GNIP sites in our study area and so the only way to gain an idea of H inputs to the terrestrial foodweb at the spatial resolution needed was to consider a proxy for amount-weighted precipitation. We followed the example of Bowen et al. (2012) by mapping published δ^2H values of shallow groundwater (Waterisotopes Database, 2020) in our study area. Bowen et al. (2012) used this approach to investigate the relative contribution of reprecipitated lakewater from Lake Michigan to downwind terrestrial regions. They used shallow groundwater as a proxy for mean annual precipitation and used the deuterium excess values based on both δ^2H and δ^{18}O values in water to trace evaporated lakewater. We were simply interested in a proxy for all precipitation driving terrestrial foodwebs and so only focussed on shallow groundwater δ^2H values. We extracted groundwater data from a latitude of 41.8° to 45° and longitude of-83° to-75°. We filtered the data to shallow wells of no more than 32 m depth and removed 11 outliers (with δ^2H values < −100‰). Shallow wells represented an integration of annual precipitation. The resultant data included 703 groundwater samples dated from 2007 to 2014 and was then auto kriged and mapped onto a raster grid of southern Ontario. We wished to investigate if a gradient in precipitation δ^2H from lakeshores to inland sites was present in our study area and if this was of a magnitude great enough to interfere with our hypotheses regarding the use of aquatic-emergent insects by aerial insectivores.

For δ^2H values of nestling tail feathers, we performed a linear mixed effect model (LMM) that included location type (inland versus lakeshore) and species (PUMA, TRES, BARS, and EABL) as fixed effects and site (within the landscape) as a random effect. To see if there was an interaction between species and location (lakeshore versus inland), we used an ANOVA to compare two models including and excluding the interaction. While keeping site as the random effect, we manually performed a post-hoc test by running multiple LMM models. We reorganized our data into eight groups that combined species and location (e.g., inland BARS) and ran multiple LMMs by changing the reference group each time to force all possible group comparisons (see Supplementary material for all combinations). We fitted our LMMs with the nlme package (Pinheiro et al., 2019). We used Akaike information criterion corrected for small sample size from

the R package MuMIn (Bartoń, 2019) for model selection. The residuals were verified for normality, equal variance, and leverage.

In combination with δ^2H, fatty acid profiles confirm diet differences among species across locations and can be used to infer diet quality. We created a matrix for δ^2H values of feathers and relative abundance of 8 notable plasma fatty acids (palmitic acid, stearic acid, oleic acid, LA, ALA, ARA, EPA, and DHA) that were standardized (Routti et al., 2012; Gong et al., 2020) to a mean of zero and a standard deviation of one using the vegan R package (Oksanen et al., 2019). Using Euclidean distances, a redundancy analysis compared δ^2H values and FA percentages among species and between locations using the vegan package. We finally ran a permutation test on our model that included a species and location interaction.

For insect δ^2H, we performed a LMM where the insect group (aquatic, terrestrial and odonates) and year of collection were fixed effects, and site was the random effect. Odonates were grouped separately to reflect their active feeding on both aquatic and terrestrial insect prey as winged (volant) adults and possibly of distant origin. We changed the reference group to include all possible insect comparisons. We then performed an ANOVA to compare two models including and excluding the interaction between insect group and year.

Results

Groundwater stable hydrogen isotopes

To evaluate if there was a gradient in δ^2H in our terrestrial foodweb related to proximity to lake vs. aquatic-emergent prey contributions *per se*, we analyzed groundwater isotopic data in the region of southern Ontario. Over the larger region, shallow groundwater ($n = 703$) δ^2H values ranged from-47 ‰ in the lower latitudes to-98 ‰ in the high latitudes (Figure 1). However, in our study area ($n = 43$), the groundwater δ^2H values (−67.76 ‰ ± 5.12 ‰) remained relatively constant (Figure 1).

Aerial insectivore stable hydrogen isotopes

Nestling feather δ^2H values of eastern bluebirds were lower than those of barn swallows (LMM; $df = 244$, $t = 2.92$, $p < 0.01$) and tree swallows (LMM; $df = 244$, $t = 6.94$, $p < 0.01$), but did not differ from those of purple martins (LMM; $df = 244$, $t = 1.17$, $p = 0.24$; Figure 2). Feather δ^2H values of all inland nestlings (controlling for species) were not different from those of nestlings at lakeshore sites (LMM; $df = 14$, $t = -0.90$, $p = 0.38$; Figure 2).

We found an interaction between location and species when comparing models of feather δ^2H values (ANOVA; LR$t = 70.18$, $p < 0.01$; model-1: AIC = 1,690, $df = 10$; model-2: AIC = 1,755, $df = 7$; Figure 2). That is, how different feather δ^2H values are between lakeshore and inland birds depended on the species of interest. We further compared the effect of location within and between each species (see Supplementary material for stable isotope data).

Within each species, only tree swallow nestlings differed in feather δ^2H values between inland and lakeshore nesting sites (LMM; $df = 243$, $t = -6.54$, $p < 0.01$; Figure 2). As expected, lakeshore purple martin nestlings had the lowest feather δ^2H values and differed from all barn swallows and inland tree swallows ($p < 0.01$ to 0.04). In contrast, inland barn swallow nestlings had the highest feather δ^2H values and differed from every group ($p < 0.01$ to 0.06), except other barn swallows at lakeshore sites. Inland tree swallows had similar feather δ^2H values to lakeshore barn swallows ($p = 0.29$). Inland purple martins were similar to lakeshore barn swallows ($p = 0.32$) in their feather δ^2H values, but surprisingly still differed from lakeshore tree swallows ($p < 0.01$). We had expected that eastern bluebird nestlings to have more positive feather δ^2H values similar to barn swallows, but instead they were most similar to purple martins ($p > 0.05$) with more negative feather δ^2H values.

Fatty acid and stable isotope ordination

We combined isotope and fatty acid data using a redundancy analysis (Oksanen et al., 2019). The redundancy analysis had four significant axes and so we retained the first two axes (Axis1: $F = 70.91$, $p < 0.01$; Axis2: $F = 57.58$, $p < 0.01$; Figure 3). The first axis divided individual birds based on inland versus lakeshore and species, while the second axis further divided species. The final model explained 38% of the data variation (adj $r^2 = 0.38$). A permutation test on the redundancy analysis found an interaction between location and species (ANOVA; $df = 7$, $F = 23.49$, $p < 0.01$, Figure 3).

Each species of aerial insectivore had some overlap in ordination space (see Supplementary material for fatty acid profiles). As expected, we found a pattern of lower feather δ^2H values with higher plasma omega-3 FAs in lakeshore locations and higher feather δ^2H values with higher plasma omega-6 FAs in terrestrial locations. Inland birds were associated with more positive feather δ^2H values, higher plasma ARA, DHA, oleic acid and LA as seen on the left of the ordination (Figure 3). Lakeshore birds were associated with lower feather δ^2H values, higher ALA, palmitic acid, stearic acid, and EPA as shown on the right of the ordination (Figure 3).

Purple martins were the most isotopically variable among the four species and were characterized primarily by more negative feather δ^2H values. While this species largely overlapped with eastern bluebirds and tree swallows in the top and middle of the ordination, they were distinct from inland barn swallows found in the lower part of the ordination (Figure 3). Inland purple martins had higher plasma oleic acid (22.75 ± 5.24%) and LA (14.13 ± 3.88%) than other species, while lakeshore purple martins had higher plasma ALA (5.42 ± 2.54%). There was no location difference in eastern bluebirds and they overlapped with lakeshore

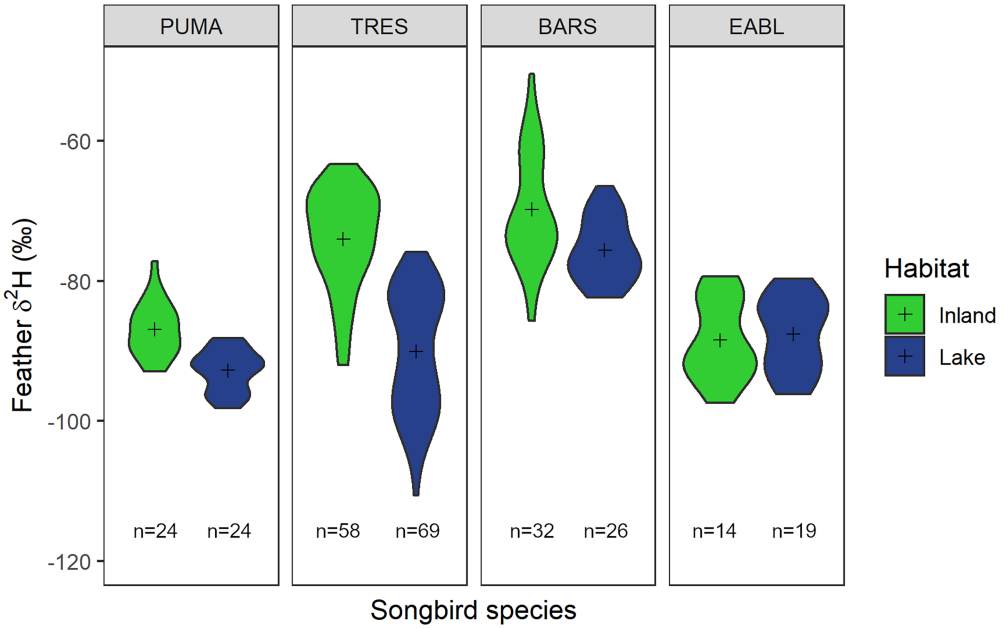

FIGURE 2
Violin plot showing the distribution of feather δ^2H values (‰) from purple martin (PUMA), tree swallow (TRES), barn swallow (BARS), and eastern bluebird (EABL) nestlings from inland (green) or lakeshore (blue) sites. Sample sizes are as shown on the plot and means are represented by (+) symbol.

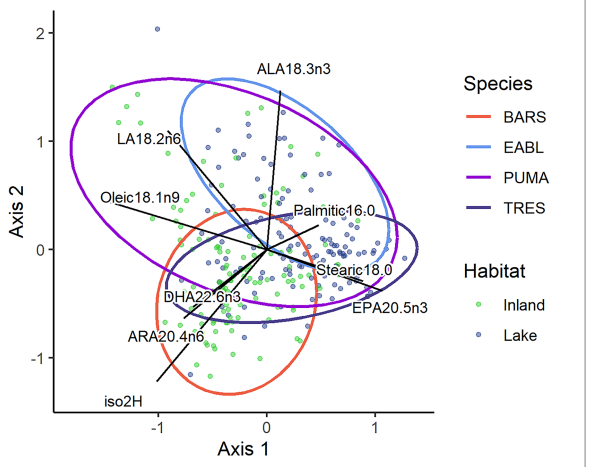

FIGURE 3
Redundancy analysis of standardized feather δ^2H values (‰) and 8 notable plasma fatty acid percentages from purple martin (PUMA), tree swallow (TRES), barn swallow (BARS), and eastern bluebird (EABL) nestlings from inland (green) or lakeshore (blue) sites (n=261).

purple martins. Eastern bluebirds in either location were associated with higher plasma palmitic acid (~18%) and ALA (~ 4%).

Barn swallows and tree swallows overlapped with other species in the center of the ordination, but deviated based on location (Figure 3). However, inland barn swallows and lakeshore tree swallows differed from any other group. Barn swallows were mainly characterized by their more positive feather δ^2H values and higher plasma DHA (~7%). Inland barn swallows had also high plasma ARA (12.04 ± 3.66%), though inland purple martins and tree swallows had high ARA as well (~11%). Lakeshore tree swallows on the other hand had higher plasma EPA (6.65 ± 3.18%) than any other species, though following close behind were lakeshore purple martins (4.36 ± 1.66%).

Insect stable hydrogen isotopes

As predicted, values of δ^2H of aquatic insects were lower than those of terrestrial insects (LMM; df = 622, t = 5.82, p < 0.01; Figure 4). Odonate δ^2H values were between those of aquatic (LMM; df = 622, t = 1.86, p = 0.06; Figure 4) and terrestrial insects (LMM; df = 622, t = −1.44, p = 0.15; Figure 4). However, the difference between these insect groups changed in magnitude depending on the year (ANOVA; AIC_1 = 5,946, df_1 = 8, AIC_2 = 5,958, df_2 = 6, LRt = 16.69, p < 0.01; Figure 4).

Discussion

Shallow groundwater δ^2H values remained consistent through our study area, suggesting little evidence for a precipitation δ^2H gradient driven by proximity to lake. This provided a firm basis for testing the effects of aquatic versus terrestrial insects in the diets of aerial insectivorous birds using feather δ^2H values since we suggest shallow groundwater was a good proxy for long-term

precipitation H driving the terrestrial foodweb. We found that aerial insectivore diet composition differed based on nesting location and species. There was an interaction between location and species in both feather δ^2H values and in plasma FA. In the following sections, we discuss in detail diet differences among aerial insectivore species and the implications that diet quality and FA conversion can have on aerial insectivore vulnerability to changes in nutritional landscapes.

Groundwater and insect stable isotopes

Using predicted isoscapes developed by Terzer et al. (2013), the amount-weighted mean growing-season (months with average temperature > 0°C) δ^2H in precipitation for southern Ontario is expected to range between-48 to-79.9 ‰ following a latitudinal gradient. Shallow groundwater can also be used as a proxy for the mean annual δ^2H in precipitation and while not necessarily conforming precisely to the precipitation driving the foodweb leading to birds in our study area, nonetheless it was useful in evaluating high resolution spatial patterning of precipitation δ^2H that might have been related to inputs of re-precipitated lakewater (Bowen et al., 2012). For example, using shallow groundwater isotope data, Bowen et al. (2012) showed that up to 18% of the evaporated lakewater was re-precipitated in downwind regions of nearby Lake Michigan. Similarly, we found a northward depletion in groundwater δ^2H for our southern Ontario study region (Waterisotopes Database, 2020). However, groundwater δ^2H values were remarkably constant, around-68 ± 5 ‰ for our study sites regardless of proximity to Lake Erie (Waterisotopes Database, 2020). We concluded that any difference observed in δ^2H of aerial insectivore feathers in our region was thus influenced by the relative contribution of aquatic-emergent insects. In other words, feather δ^2H values were associated primarily with diet instead of any underlying baseline precipitation δ^2H effects related to proximity to lake.

Feather δ^2H values reflect the isotopic value in diet and drinking water during growth (Hobson et al., 1999). For aerial insectivores, feather δ^2H will largely reflect the values in their insect prey. As expected, we found δ^2H values of aquatic-emergent insects were lower than terrestrial insects. Odonates (i.e., dragonflies and damselflies) were the exception and had δ^2H values intermediate between aquatic and terrestrial sources. The wings of odonates represent the isotopic signature of the aquatic larval stage that is dependent on the isotopic composition of the waterbody. Lakes typically have more consistent isotopic compositions than smaller waterbodies such as ponds that may be influenced by evaporation.

Purple martins

Nestling purple martins had lower feather δ^2H values than the swallows, suggesting a more aquatic-emergent diet, but there was no difference in feather δ^2H values between lakeshore and inland populations. Purple martins forage on a variety of terrestrial and

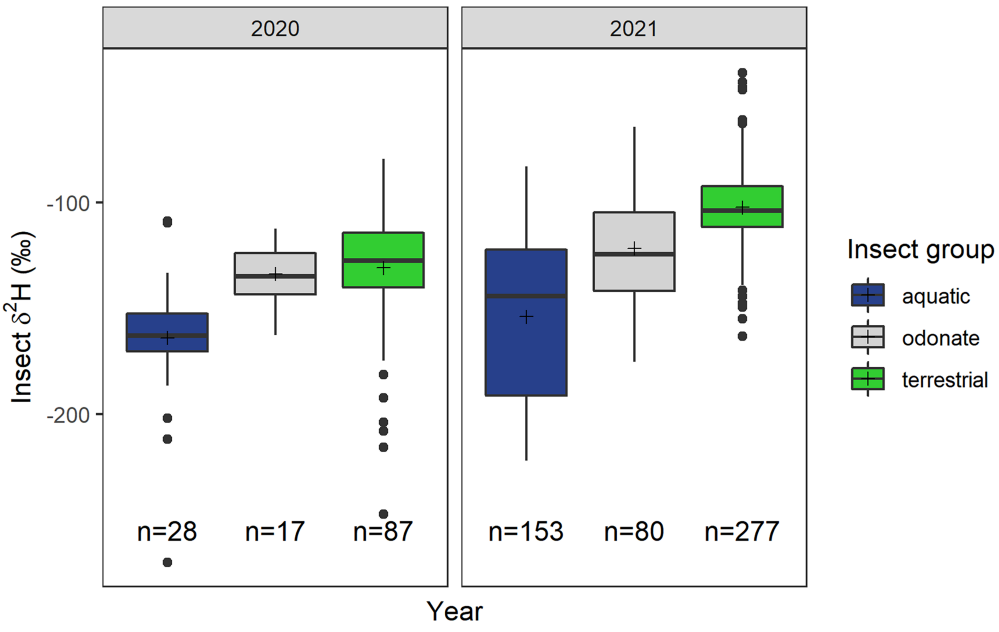

FIGURE 4
Boxplot showing insect δ^2H values (‰) from different insect groups. These groups include smaller aquatic insects, odonates, and terrestrial insects sampled in the study area. Sample sizes are as shown on the plot and means are represented by (+) symbol. Refer to Supplementary material for data of insects included in each group.

aquatic insects (Helms et al., 2016) and dragonflies are frequently fed to nestlings. Though the wings of odonates reflect aquatic origin, the body could have variable δ^2H values due to their broad (terrestrial to aquatic) diets (Chari et al., 2018) and some may move between waterbodies. Thus, the diet of odonates can obscure tracing of the terrestrial versus aquatic signature in martins even though odonates are themselves aquatic-emergent.

Purple martins differed in fatty acid profiles between inland and lakeshore sites. Inland martins had high plasma oleic acid, LA and ARA, while lakeshore martins had high plasma ALA and EPA. In general, aquatic ecosystems are known as a better source of omega-3 EPA and DHA (Rumpold and Schlüter, 2013; Hixson et al., 2015; Twining et al., 2018a, 2019, 2021; Shipley et al., 2022). Inland purple martins likely acquired oleic acid, LA, and ARA from terrestrial insects and odonates that are lower in the omega-3 FAs compared to their lakeshore counterparts. Lakeshore purple martins may benefit from a mix of terrestrial and aquatic insects (including odonates that forage on other aquatic insects) and acquire high amounts of ALA and EPA from aquatic subsidies. Odonates themselves, an undoubtable source of omega-3 FAs from their aquatic life stage, are still dependent on the insect prey available in their habitat (Chari et al., 2018). Thus, we suspect that odonates through trophic enrichment may have enhanced the amount of omega-6 and omega-3 FAs that inland and lakeshore purple martins consumed, respectively. Purple martins select riparian habitats (Lalla, 2022) and forage on diverse insects including aquatic-emergent insects (Helms et al., 2016). Hence, we suspect that martins have a low conversion ability, unable to efficiently synthesize large amounts of omega-3 EPA and DHA similar to the low conversion efficiency of tree swallows (Twining et al., 2018a). Our results suggest that diet quality of purple martins is dependent on nesting habitat. However, the use of odonates that can vary considerably in their use of terrestrial versus aquatic-emergent prey makes the assignment of purple martins to foraging site type more complex.

Tree swallows

Feather δ^2H values of nestling tree swallows differed between inland and lakeshore sites according to our expectation of greater use of aquatic-emergent prey near the lakeshore. This result was similar to our previous findings for bank swallow (Génier et al., 2021) in our study area, where lakeshore bank swallows had lower feather δ^2H values than inland birds.

Fatty acid profiles of blood plasma further supported the dietary differences we inferred between inland and lakeshore locations. Lakeshore tree swallows had high plasma EPA, while inland tree swallows had high plasma ARA. Aquatic insects are vital sources of omega-3 PUFAs, but chironomids have among the highest amounts of EPA and DHA (Gladyshev et al., 2019; Shipley et al., 2022). Thus, tree swallows foraging on aquatic insects such as chironomids emerging from Lake Erie can benefit from a higher diet quality that is high in omega-3 FAs. Our results align well with the high omega-3 FAs found in tree swallow tissues in Twining et al. (2018a,b) studies in Ithaca, NY, showing the importance of obtaining omega-3 FAs directly from diet. Inland tree swallows, however, could acquire high amounts of ARA from terrestrial insects, but miss an important source of omega-3 FAs.

Barn swallows

More than the other species we examined, barn swallows are typically associated with agro-ecosystems and are the least riparian (McClenaghan et al., 2019b; Bumelis et al., 2021). Our stable isotope and fatty acid results were consistent with this behaviour. Barn swallows had the highest feather δ^2H values, representing the most terrestrial diet. Although feather δ^2H values of barn swallow nestlings did not differ between inland and lakeshore locations, inland birds had higher plasma ARA, presumably derived from terrestrial insects. Barn swallows forage at lower altitudes than purple martins and tree swallows, and could be targeting different insects than those in higher altitudes (Dreelin et al., 2018). Just as blue tit nestlings in Europe were provisioned with terrestrial insects regardless of aquatic insect availability and distance from lake (Twining et al., 2021), barn swallows in our study area appeared to maintain a terrestrial insect diet regardless of proximity to Lake Erie. Most importantly, barn swallows had high plasma DHA in both inland and lakeshore habitats, more so than the purple martins and tree swallows. We speculate that this high DHA can only be a result of a high omega-3 conversion efficiency, as seen in the blue tits (Twining et al., 2021).

Eastern bluebirds

The diet of eastern bluebirds differed from swallows and martins possibly because they arrive earlier to our study area, breeding in late April through May, and are primarily ground foragers. Based on feather δ^2H, we expected nestling bluebirds to have the most terrestrial diet similar to barn swallows. Bluebird diet did not differ between lakeshore and inland habitats and instead had low feather δ^2H values similar to purple martins. We speculate that these low values were due to a fossorial diet possibly influenced by early spring snowmelt that was relatively depleted in ^{2}H (Rohwer et al., 2011). Snow was indeed observed at our site during egg laying and chick rearing of bluebirds. In this sense, this species was likely not a good "control" species to compare to later-breeding aerial insectivores.

Plasma of nestling bluebirds was high in palmitic and stearic acid as well as ALA. Many insects have high levels of saturated FA, mostly palmitic, but also stearic acid (Rumpold and Schlüter, 2013; Sosa and Fogliano, 2017). Since both aquatic and terrestrial primary producers can synthesize ALA and LA, insects can also provide sufficient ALA (Hixson et al., 2015; Shipley et al., 2022). Nonetheless, the lack of omega-3 PUFAs suggest a more terrestrial

diet. Berries and seeds can also be excellent sources of saturated and unsaturated FAs that could contribute to the fatty acid profiles of bluebirds (Weinkam et al., 2017). Several wild and cultivated northern berries have seed oils high in ALA and LA (Yang et al., 2011).

Implications

In North America, declines in populations of aerial insectivores vary among species (Sauer et al., 2017; North American Bird Conservation Initiative Canada, 2019). We speculate that changes in diet quality may be a contributing factor. In our study area, Bumelis et al. (2021) showed strong evidence of dietary segregation among sympatric swallow species, despite all foraging on flying insects. Dreelin et al. (2018) found that purple martins foraged at the highest altitude, followed by tree swallows and barn swallows, suggesting that these species forage on different insect assemblages found in their respective aerial band. In Japan, the contribution of aquatic subsidies to the annual energy budget of forest birds vastly differed among species (Nakano and Murakami, 2001). As aquatic insects emerge earlier than terrestrial insects, diet is also influenced by the timing of a species breeding season (Nakano and Murakami, 2001; Shipley et al., 2022; Twining et al., 2022). Our previous work has shown that prey quality also varies across the landscape and habitat can be a strong factor in determining diet composition (Génier et al., 2021). Together, time, location and species ecology can determine nutrient availability for provisioning adults and these factors may be related to population dynamics in anthropogenically influenced landscapes.

Our study used nestling feather δ^2H measurements and plasma FA profiles jointly to infer diet quality and source to elucidate how certain FAs are being acquired or synthesized. Omega-3 FAs can confer health benefits to nestlings (Twining et al., 2016, 2018b, 2019), but too little omega-3 or too much omega-6 FAs can lead to harmful effects for many bird species (Andersson et al., 2015; Isaksson et al., 2017). Omega-3 and omega-6 PUFAs can be acquired through diet, but also some birds have the ability to synthesize these PUFAs from precursor molecules. A delicate balance between diet quality, conversion efficiency, and hence foraging location, must exist to fulfill the dietary needs of these aerial insectivores.

Barn swallows had a more terrestrial diet regardless of nesting habitat. Lacking in a source of EPA and DHA, we suspect the high plasma DHA observed for this species was a result of conversion of omega-3 precursors. Similar to blue tits (Twining et al., 2021), barn swallows could fulfill their omega-3 FA demand through conversion instead of foraging on aquatic insects. Eastern bluebirds appear to have a mixed diet that had neither high plasma ARA nor EPA or DHA. It is possible that bluebirds do not have a high demand for PUFAs. Bluebirds could also be compensating for the lack in PUFAs in their diet by synthesizing their own supply when needed.

Just as lakeshore bank swallows forage on a more aquatic-emergent insects high in omega-3 FAs (Génier et al., 2021), lakeshore tree swallow and purple martin nestlings were fed more aquatic-emergent insects than their inland counterparts. We suspect, however, that purple martins like tree swallows have a low omega-3 FA conversion efficiency, relying on high-quality aquatic diets to acquire their needed supply of EPA and DHA (Twining et al., 2018a). Purple martins and tree swallows nesting in riparian habitats would benefit from the high EPA and DHA in aquatic-emergent insects, however, in more terrestrial habitats diet quality may decrease. In our study area, Génier et al. (2021) has shown how the distance from Lake Erie decreased the diet quality of bank swallows. Furthermore, Twining et al. (2019) demonstrated that eastern phoebe nestlings fed both aquatic and terrestrial insects depended on the aquatic insects for EPA.

As aquatic-emergent insects decline globally (Gladyshev et al., 2019; Sánchez-Bayo and Wyckhuys, 2019) and locally (Stepanian et al., 2020), a valuable source of omega-3 FAs to terrestrial consumers becomes increasingly limited. Over a 25-year study period, Shipley et al. (2022) also found that insect emergence had advanced and in shorter pulses, outpacing the egg laying phenology of many aerial insectivore species. During energetically demanding life stages such as early development, nestlings can be particularly sensitive to phenological mismatches (Twining et al., 2022). Unable to acquire the necessary omega-3 FAs, aerial insectivores can be vulnerable to such changes in the nutritional landscape and aquatic insect population declines. North America has lost a considerable amount in the aerial insectivore population, even in more recent decades from 1993 to 2015 tree swallows and purple martins have been declining by 0.5 and 0.1% per year, respectively (Sauer et al., 2017). For many aerial insectivores, including tree swallows and purple martins, these declines are more pronounced in the northeast part of their range (Nebel et al., 2010) such as our study area. In addition to previous work on bank swallows (Génier et al., 2021), we identified tree swallows and purple martins to be potentially vulnerable to spatial and temporal loses of aquatic subsidies (Shipley et al., 2022) and highlight the need to support such vitally important aquatic ecosystems.

Clearly, the use of δ^2H measurements was crucial to evaluate actual source of insects (aquatic versus terrestrial) to nestlings. This allowed us to evaluate to what degree proximity to Lake Erie had on the nutritional condition of swallows and martins, and permitted much more informed inferences of factors driving fatty acid acquisition and synthesis. Future isotopic studies that investigate other isotopic or elemental tracers of aquatic versus terrestrial foods are thus encouraged to further this area of ecophysiological research. Another particularly useful tool is the use of compound-specific isotope analyses of individual fatty acids (Pilecky et al., 2023). By assessing or tracing ^{13}C of individual fatty acids, we could infer fatty acid conversion efficiencies (Twining et al., 2018a) and dietary sources of each PUFAs with great precision. Ultimately being able to link diet quality to lifetime fitness in these declining aerial insectivores should be a priority of

future research. Such research could manipulate breeding location in those species amenable to nest box use (tree swallows and purple martins) and hence proximity to aquatic-derived prey.

Data availability statement

The original contributions presented in the study are included in the article/Supplementary material, further inquiries can be directed to the corresponding author.

Ethics statement

The animal study was reviewed and approved by Animal Care Committee, University of Western Ontario (AUP 2017–005).

Author contributions

All authors conceived the project. CSVG performed the field work, lab work, quantified, and analyzed the data. KAH also analyzed the samples for stable hydrogen isotopes. KAH and CGG supported and funded the research. The manuscript was drafted by CSVG, but was edited and finalized by KAH and CGG. All authors contributed to the article and approved the submitted version.

Funding

This work was supported by an NSERC Discovery Grant (2017-04430) to KAH, by operating grants from Environment and Climate Change Canada to KAH. This work was also supported by an NSERC Discovery Grant (2020-07204) to CGG.

Acknowledgments

We thank the many landowners and Long Point Bird Observatory that kindly allowed us to access bird breeding colonies. We are thankful for the help of our field assistants Chris Posliff and Celina Tang, and colleague Jackson Kusack. We greatly appreciate the assistance of Blanca X. Mora Alvarez with sample preparation for stable isotope analyses. Two reviewers made valuable comments that improved an earlier draft of this manuscript.

Conflict of interest

The authors declare that the research was conducted in the absence of any commercial or financial relationships that could be construed as a potential conflict of interest.

Publisher's note

Supplementary material

The Supplementary material for this article can be found online at: https://www.frontiersin.org/articles/10.3389/fevo.2022.1006928/full#supplementary-material

References

Andersson, M. N., Wang, H.-L., Nord, A., Salmon, P., and Isaksson, C. (2015). Composition of physiologically important fatty acids in great tits differs between urban and rural populations on a seasonal basis. *Front. Ecol. Evol.* 3:93. doi: 10.3389/fevo.2015.00093

Barton, K. (2019). MuMIn: multi-model inference. Available at: https://CRAN.R-project.org/package=MuMIn (Accessed May, 2022).

Bligh, E. G., and Dyer, W. J. (1959). A rapid method of total lipid extraction and purification. *Can. J. Biochem. Physiol.* 37, 911–917. doi: 10.1139/y59-099

Bowen, G. J., Kennedy, C. D., Henne, P. D., and Zhang, T. (2012). Footprint of recycled water subsidies downwind of Lake Michigan. *Ecosphere* 3:art53. doi: 10.1890/ES12-00062.1

Bumelis, K. H., Cadman, M. D., and Hobson, K. A. (2021). Endogenous biomarkers reveal diet partitioning among three sympatric species of swallows. *Ornithology* 139:ukab078. doi: 10.1093/ornithology/ukab078

Chari, L. D., Moyo, S., and Richoux, N. B. (2018). Trophic ecology of adult male Odonata. I. Dietary niche metrics by foraging guild, species, body size, and location. *Ecol. Entomol.* 43, 1–14. doi: 10.1111/een.12458

Collins, C. T. (2015). Food habits and resource partitioning in a guild of Neotropical swifts. *Wilson J. Ornithol.* 127, 239–248. doi: 10.1676/wils-127-02-239-248.1

Doucett, R. R., Marks, J. C., Blinn, D. W., Caron, M., and Hungate, B. A. (2007). Measuring terrestrial subsidies to aquatic food webs using stable isotopes of hydrogen. *Ecology* 88, 1587–1592. doi: 10.1890/06-1184

Dreelin, R. A., Shipley, J. R., and Winkler, D. W. (2018). Flight behavior of individual aerial insectivores revealed by novel altitudinal dataloggers. *Front. Ecol. Evol.* 6:182. doi: 10.3389/fevo.2018.00182

Evans, K. L., Wilson, J. D., and Bradbury, R. B. (2007). Effects of crop type and aerial invertebrate abundance on foraging barn swallows *Hirundo rustica*. *Agric. Ecosyst. Environ.* 122, 267–273. doi: 10.1016/j.agee.2007.01.015

Fogel, M. L., and Cifuentes, L. A. (1993). "Isotope fractionation during primary production," in *Organic Geochemistry*. eds. M. H. Engel and S. A. Macko (Boston: Springer).

Génier, C. S. V., Guglielmo, C. G., Mitchell, G. W., Falconer, M., and Hobson, K. A. (2021). Nutritional consequences of breeding away from riparian habitats in Bank swallows: new evidence from multiple endogenous markers. *Conserv. Phys.* 9:coaa140. doi: 10.1093/conphys/coaa140

Gladyshev, M. I., Gladysheva, E. E., and Sushchik, N. N. (2019). Preliminary estimation of the export of omega-3 polyunsaturated fatty acids from aquatic to terrestrial ecosystems in biomes via emergent insects. *Ecol. Complex.* 38, 140–145. doi: 10.1016/j.ecocom.2019.03.007

Gong, Y., Li, Y., Chen, X., and Yu, W. (2020). Trophic niche and diversity of a pelagic squid (*Dosidicus gigas*): a comparative study using stable isotope, fatty acid, and feeding apparatuses morphology. *Front. Mar. Sci.* 7:642. doi: 10.3389/fmars.2020.00642

Hallmann, C. A., Sorg, M., Jongejans, E., Siepel, H., Hofland, N., Schwan, H., et al. (2017). More than 75 percent decline over 27 years in total flying insect biomass in protected areas. *PLoS One* 12:e0185809. doi: 10.1371/journal.pone.0185809

Helms, J. A., Godfrey, A. P., Ames, T., and Bridge, E. S. (2016). Predator foraging altitudes reveal the structure of aerial insect communities. *Sci. Rep.* 6:28670. doi: 10.1038/srep28670

Hixson, S. M., Sharma, B., Kainz, M. J., Wacker, A., and Arts, M. T. (2015). Production, distribution, and abundance of long-chain omega-3 polyunsaturated fatty acids: a fundamental dichotomy between freshwater and terrestrial ecosystems. *Environ. Rev.* 23, 414–424. doi: 10.1139/er-2015-0029

Hobson, K. A., Atwell, L., and Wassenaar, L. I. (1999). Influence of drinking water and diet on the stable-hydrogen isotope ratios of animal tissues. *Proc. Natl. Acad. Sci. U. S. A.* 96, 8003–8006. doi: 10.1073/pnas.96.14.8003

Imlay, T., Mann, H., and Leonard, M. (2017). No effect of insect abundance on nestling survival or mass for three aerial insectivores. *Avian Conserv. Ecol.* 12:19. doi: 10.5751/ACE-01092-120219 17

Isaksson, C., Andersson, M. N., Nord, A., von Post, M., and Wang, H.-L. (2017). Species-dependent effects of the urban environment on fatty acid composition and oxidative stress in birds. *Front. Ecol. Evol.* 5:44. doi: 10.3389/fevo.2017.00044

Lalla, K. M. (2022). Purple martin (*Progne subis*) movement ecology during three stages of the annual cycle. [master's thesis]. Montréal, QC: McGill University.

McCarty, J. P., and Winkler, D. W. (1999). Foraging ecology and diet selectivity of tree swallows feeding nestlings. *Condor* 101, 246–254. doi: 10.2307/1369987

McClenaghan, B., Kerr, K. C. R., and Nol, E. (2019a). Does prey availability affect the reproductive performance of barn swallows (*Hirundo rustica*) breeding in Ontario, Canada? *Can. J. Zool.* 97, 979–987. doi: 10.1139/cjz-2019-0001

McClenaghan, B., Nol, E., and Kerr, K. C. R. (2019b). DNA metabarcoding reveals the broad and flexible diet of a declining aerial insectivore. *Auk* 136, 1–11. doi: 10.1093/auk/uky003

Møller, A. P. (2019). Parallel declines in abundance of insects and insectivorous birds in Denmark over 22 years. *Ecol. Evol.* 9, 6581–6587. doi: 10.1002/ece3.5236

Nakano, S., and Murakami, M. (2001). Reciprocal subsidies: dynamic interdependence between terrestrial and aquatic food webs. *Proc. Natl. Acad. Sci. U. S. A.* 98, 166–170. doi: 10.1073/pnas.98.1.166

Nebel, S., Mills, A., McCracken, J., and Taylor, P. (2010). Declines of aerial insectivores in North America follow a geographic gradient. *Avian. Conserv. Ecol.* 5:1. doi: 10.5751/ACE-00391-050201

North American Bird Conservation Initiative Canada (2019). *The State of Canada's Birds, 2019. Environment and Climate Change Canada*, Ottawa: North American Bird Conservation Initiative Canada.

Oksanen, J., Blanchet, F. G., Friendly, M., Kindt, R., Legendre, P., McGlinn, D., et al. (2019). Vegan: Community ecology package. Available at: https://CRAN.R-project.org/package=vegan (Accessed May, 2022).

Orłowski, G., and Karg, J. (2013). Diet breadth and overlap in three sympatric aerial insectivorous birds at the same location. *Bird Study* 60, 475–483. doi: 10.1080/00063657.2013.839622

Pilecky, M., Wassenaar, L. I., Kainz, M. J., Anparasan, L., Ramirez, I., McNeil, J. M., et al. (2023). Isotopic (δ^2H, δ^{13}C) tracing of the origin and fate of individual fatty acids fueling migrating animals: A case study of the monarch butterfly (*Dannaus plexippus*). *Front. Ecol. Evol.* 8:572140. doi: 10.3389/fevo.2020.572140

Pinheiro, J., Bates, D., DebRoy, S. Sarkar, D., and R Core Team. (2019). Nlme: Linear and nonlinear mixed effects models. Available at: https://CRAN.R-project.org/package=nlme (Accessed May, 2022).

R Core Team (2019). *R: A Language and environment for Statistical Computing*. Vienna, AT: R Foundation for Statistical Computing.

RStudio Team (2018). RStudio: integrated development for R. RStudio Inc., Boston, USA. Available at: http://www.rstudio.com/

Rohwer, S., Hobson, K. A., and Yang, S. (2011). Stable isotopes (δD) reveal east—west differences in scheduling of molt and migration in Northern rough-winged swallows (*Stelgidopteryx serripennis*). *Auk* 128, 522–530. doi: 10.1525/auk.2011.10273

Rosenberg, K. V., Dokter, A. M., Blancher, P. J., Sauer, J. R., Smith, A. C., Smith, P. A., et al. (2019). Decline of the north American avifauna. *Science* 366, 120–124. doi: 10.1126/science.aaw1313

Routti, H., Letcher, R. J., Born, E. W., Branigan, M., Dietz, R., Evans, T. J., et al. (2012). Influence of carbon and lipid sources on variation of mercury and other trace elements in polar bears (*Ursus maritimus*) environ. *Toxicol. Chem.* 31, 2739–2747. doi: 10.1002/etc.2005

Roy, R., Singh, S., and Pujari, S. (2008). Dietary role of omega-3 polyunsaturated fatty acid (PUFA): a study with growing chicks, *Gallus domesticus*. *Int. J. Poult. Sci.* 7, 360–367. doi: 10.3923/ijps.2008.360.367

Rumpold, B. A., and Schlüter, O. K. (2013). Nutritional composition and safety aspects of edible insects. *Mol. Nutr. Food Res.* 57, 802–823. doi: 10.1002/mnfr.201200735

Sánchez-Bayo, F., and Wyckhuys, K. A. G. (2019). Worldwide decline of the entomofauna: a review of its drivers. *Biol. Conserv.* 232, 8–27. doi: 10.1016/j.biocon.2019.01.020

Sauer, J. R., Pardieck, K. L., Ziolkowski, D. J., Smith, A. C., Hudson, M.-A. R., Rodriguez, V., et al. (2017). The first 50 years of the North American breeding bird survey. *Condor* 119, 576–593. doi: 10.1650/CONDOR-17-83.1

Shipley, J. R., Twining, C. W., Mathieu-Resuge, M., Parmar, T. P., Kainz, M., Martin-Creuzburg, D., et al. (2022). Climate change shifts the timing of nutritional flux from aquatic insects. *Curr. Biol.* 32, 1342.e3–1349.e3. doi: 10.1016/j.cub.2022.01.057

Simopoulos, A. P. (2011). Evolutionary aspects of diet: the omega-6/omega-3 ratio and the brain. *Mol. Neurobiol.* 44, 203–215. doi: 10.1007/s12035-010-8162-0

Smith, A. C., Hudson, M.-A. R., Downes, C. M., and Francis, C. M. (2015). Change points in the population trends of aerial-insectivorous birds in North America: synchronized in time across species and regions. *PLoS One* 10:e0130768. doi: 10.1371/journal.pone.0130768

Sosa, D. A. T., and Fogliano, V. (2017). "Potential of insect-derived ingredients for food applications," in *Insect Physiology and Ecology* (HR InTech: Rijekay).

Spiller, K. J., and Dettmers, R. (2019). Evidence for multiple drivers of aerial insectivore declines in North America. *Condor* 121, 1–13. doi: 10.1093/condor/duz010

Stepanian, P. M., Entrekin, S. A., Wainwright, C. E., Mirkovic, D., Tank, J. L., and Kelly, J. F. (2020). Declines in an abundant aquatic insect, the burrowing mayfly, across major North American waterways. *Proc. Natl. Acad. Sci. U. S. A.* 117, 2987–2992. doi: 10.1073/pnas.1913598117

Terzer, S., Wassenaar, L. I., Araguás-Araguás, L. J., and Aggarwal, P. K. (2013). Global isoscapes for δ^{18}O and δ^2H in precipitation: improved prediction using regionalized climatic regression models. *Hydrol. Earth Syst. Sci.* 17, 4713–4728. doi: 10.5194/hess-17-4713-2013

Twining, C. W., Brenna, J. T., Lawrence, P., Shipley, J. R., Tollefson, T. N., and Winkler, D. W. (2016). Omega-3 long-chain polyunsaturated fatty acids support aerial insectivore performance more than food quantity. *Proc. Natl. Acad. Sci. U. S. A.* 113, 10920–10925. doi: 10.1073/pnas.1603998113

Twining, C. W., Brenna, J. T., Lawrence, P., Winkler, D. W., Flecker, A. S., and Hairston, N. G. (2019). Aquatic and terrestrial resources are not nutritionally reciprocal for consumers. *Funct. Ecol.* 33, 2042–2052. doi: 10.1111/1365-2435.13401

Twining, C. W., Lawrence, P., Winkler, D. W., Flecker, A. S., and Brenna, J. T. (2018a). Conversion efficiency of α-linolenic acid to omega-3 highly unsaturated fatty acids in aerial insectivore chicks. *J. Exp. Biol.* 221:jeb165373. doi: 10.1242/jeb.165373

Twining, C. W., Parmar, T. P., Mathieu-Resuge, M., Kainz, M. J., Shipley, J. R., and Martin-Creuzburg, D. (2021). Use of fatty acids from aquatic prey varies with foraging strategy. *Front. Ecol. Evol.* 9:735350. doi: 10.3389/fevo.2021.735350

Twining, C. W., Shipley, J. R., and Matthews, B. (2022). Climate change creates nutritional phenological mismatches. *Trends Ecol. Evol.* 37, 736–739. doi: 10.1016/j.tree.2022.06.009

Twining, C. W., Shipley, J. R., and Winkler, D. W. (2018b). Aquatic insects rich in omega-3 fatty acids drive breeding success in a widespread bird. *Ecol. Lett.* 21, 1812–1820. doi: 10.1111/ele.13156

Vander Zanden, H. B., Soto, D. X., Bowen, G. J., and Hobson, K. A. (2016). Expanding the isotopic toolbox: applications of hydrogen and oxygen stable isotope ratios to food web studies. *Front. Ecol. Evol.* 4:20. doi: 10.3389/fevo.2016.00020

Voigt, C. C., Lehmann, D., and Greif, S. (2015). Stable isotope ratios of hydrogen separate mammals of aquatic and terrestrial food webs. *Methods Ecol. Evol.* 6, 1332–1340. doi: 10.1111/2041-210X.12414

Walters, D. M., Fritz, K. M., and Otter, R. R. (2008). The dark side of subsidies: adult stream insects export organic contaminants to riparian predators. *Ecol. Appl.* 18, 1835–1841. doi: 10.1890/08-0354.1

Wassenaar, L. I., and Hobson, K. A. (2003). Comparative equilibration and online technique for determination of non-exchangeable hydrogen of keratins for use in animal migration studies. *Isot. Environ. Health Stud.* 39, 211–217. doi: 10.1080/1025601031000096781

Waterisotopes Database (2020). Query: Country=CA, type=groundwater. Available at: http://waterisotopesDB.org (Accessed December, 2020).

Waugh, D. R. (1979). The diet of sand martins during the breeding season. *Bird Study* 26, 123–128. doi: 10.1080/00063657909476629

Weinkam, T. J., Janos, G. A., and Brown, D. R. (2017). Habitat use and foraging behavior of eastern bluebirds (*Sialia sialis*) in relation to winter weather. *Northeast. Nat.* 24, B1–B18. doi: 10.1656/045.024.s704

Yang, B., Ahotupa, M., Määttä, P., and Kallio, H. (2011). Composition and antioxidative activities of supercritical CO2-extracted oils from seeds and soft parts of Northern berries. *Food Res. Int.* 44, 2009–2017. doi: 10.1016/j.foodres.2011.02.025

frontiers | Frontiers in Ecology and Evolution

TYPE Original Research
PUBLISHED 25 November 2022
DOI 10.3389/fevo.2022.1051782

OPEN ACCESS

EDITED BY
Todd Jason McWhorter,
University of Adelaide, Australia

REVIEWED BY
Louie Yang,
University of California, Davis,
United States
David Nelson,
University of Maryland, College Park,
United States

*CORRESPONDENCE
Matthias Pilecky
matthias.pilecky@donau-uni.ac.at

SPECIALTY SECTION
This article was submitted to Ecophysiology,
a section of the journal
Frontiers in Ecology and Evolution

RECEIVED 23 September 2022
ACCEPTED 14 November 2022
PUBLISHED 25 November 2022

CITATION
Pilecky M, Wassenaar LI, Kainz MJ, Anparasan L, Ramirez MI, McNeil JN and Hobson KA (2022) Isotopic (δ ^{2}H and δ ^{13}C) tracing the provenance and fate of individual fatty acids fueling migrating animals: A case study of the monarch butterfly (*Danaus plexippus*).
Front. Ecol. Evol. 10:1051782.
doi: 10.3389/fevo.2022.1051782

Isotopic (δ ^{2}H and δ ^{13}C) tracing the provenance and fate of individual fatty acids fueling migrating animals: A case study of the monarch butterfly (*Danaus plexippus*)

Matthias Pilecky[1,2]*, Leonard I. Wassenaar[1,3], Martin J. Kainz[1,2], Libesha Anparasan[4], M. Isabel Ramirez[5], Jeremy N. McNeil[4] and Keith A. Hobson[4,6]

[1]WasserCluster Lunz - Biologische Station, Inter-University Center for Aquatic Ecosystem Research, Lunz am See, Austria, [2]Department for Biomedical Research, Donau-Universität Krems, Krems an der Donau, Austria, [3]Department of Geological Science, University of Saskatchewan, Saskatoon, SK, Canada, [4]Department of Biology, University of Western Ontario, London, ON, Canada, [5]Centro de Investigaciones en Geografía Ambiental, Universidad Nacional Autónoma de México, Morelia, Mexico, [6]Environment and Climate Change Canada, Saskatoon, SK, Canada

Introduction: Among long-distance migratory insects, the monarch butterfly (*Danaus plexippus*) is one of the most iconic, whose journey is fueled by nectar from flowering plants along the migratory route which may involve up to 3,500 km. Understanding how and where monarchs obtain their dietary resources to fuel migratory flight and ensure overwintering stores would provide new insights into the migratory strategy of this species and subsequently help focus conservation efforts.

Methods: This pilot study was designed as a first attempt to assess the composition, dynamics, and isotopic ($\delta^{2}H$, $\delta^{13}C$) composition of essential and non-essential fatty acids (FA) acquired or manufactured *de novo* from larval host milkweed (*Asclepias* spp.) by monarch butterflies and from adult emergence to overwintering.

Results: Data from controlled laboratory isotopic tracer tests suggested that adult monarchs convert their dietary energy mainly into 16:0 and 18:1 fatty acids and store them as neutral lipids in their abdomen. FA isotopic composition reflects not only dietary sources but also subsequent isotopic fractionation from metabolism. On the other hand, $\delta^{2}H$ values of essential omega-3 fatty acid alpha-linolenic acid (ALA) correlated with $\delta^{2}H_{Wing}$, as markers of an individual's geographic origin and indicated the importance of larval diet. Additionally, in wild-type females, high isotopic fractionation in $\delta^{13}C_{ALA}$ between neutral and polar lipids might indicate increased bioconversion activity during gravidity. Finally, $\delta^{2}H_{LIN}$ showed positive H isotope fractionation from larval dietary sources, indicating that catabolic processes were involved in their manufacture. Furthermore, $\delta^{2}H_{LIN}$ showed

a negative correlation with δ^2H_{Wing} values, which could potentially be useful when investigating individual life-history traits, such as migratory catabolic efforts or periods of fasting.

Discussion: This interpretation was supported by significant larger variations in δ^2H_{LIN} and δ^2H_{LIN} overwintering monarchs compared to other FA. Altogether, our results provide the first evidence that the H isotopic analysis of individual fatty acids in migrating and overwintering monarchs can be used to infer the nutritional history of individuals including the provenance of nectaring sites used to fuel key life history events.

KEYWORDS

lipids, migration, habitat conservation, stable isotopes, fatty acids, deuterium, ^{13}C

Introduction

Migratory animals have evolved numerous morphometric, physiological, and behavioral adaptations to successfully achieve seasonal habitat movements, often involving impressive transcontinental passages (Dingle, 2014; Hobson et al., 2019). Independent of biome, vertebrate, and invertebrate adult migrants using terrestrial and aquatic habitats fuel their migratory journeys using energy-dense lipids, mainly triacyclglycerols (storage lipids), which are acquired directly from diet or are synthesized *de novo*, for example, from carbohydrates (McWilliams et al., 2004). Fats are typically accumulated and stored to fuel the entire migratory episode, or are obtained at stopover refueling sites. The dietary quality for animals at pre-migratory staging sites and along stopovers used during migration, along with the ability of animals to convert food into fuel, are crucial factors influencing the overall success of their migration cycle (Lennox et al., 2016).

Among long-distance migratory insects, the monarch butterfly (*Danaus plexippus*) is the most iconic. The eastern population of this species in North America undergoes a continental-scale fall migration of up to 3,500 km to overwinter in high altitude (3,000–4,000 m.a.s.l.) colonies in the oyamel (*Abies religiosa*) forests of the transvolcanic belt of central Mexico (Slayback et al., 2007). After reaching the overwintering colony, monarchs fast and rely on their accumulated fats to sustain them from December to March. Only successful gravid females begin re-migration north in the springtime reaching as far as Texas where they oviposit on milkweed (*Asclepia* sp.) plants. Successive generations continue northward, making use of newly available milkweed until the late summer cohort of individuals is produced, many of which migrate south to Mexico. The monarch's fall migratory journey is fueled by nectar (Brown and Chippendale, 1974; Brower et al., 2006) obtained from flowering plants along the migratory route (Beall, 1948; Gibo and McCurdy, 1993; Brower et al., 2006). It has been proposed that nectaring resources in Texas provide the bulk of the lipids required to sustain both overwintering and subsequent reproduction the following spring (Brower, 1985). However, in a year of record drought in Texas (Brower et al., 2015) found that butterflies collected there contained lipid contents well below normal, while butterflies collected from overwintering sites had higher contents. They hypothesized that there should be other areas in Mexico where they could have access to abundant nectar. Recently, Hobson et al. (2020) provided hydrogen isotopic evidence contrasting total lipid δ^2H and wing δ^2H values that suggested migrant monarchs acquire overwintering storage lipids much closer to their winter roost sites than expected, rather than gradual by accumulation along the migratory route. Understanding where and how monarchs obtain the dietary fat resources to fuel migratory flight and to ensure overwintering stores would provide new insights into the migratory strategy of this species and subsequently inform conservation strategies (Brower et al., 2006).

Besides non-essential saturated and monounsaturated fatty acids composing the majority of energy storage in lipids, attention has turned to polyunsaturated fatty acids (PUFA) in animal nutritional ecology, and especially omega-3 polyunsaturated fatty acids (n-3 PUFA), such as the essential alpha-linolenic acid (18:3n-3, ALA), as well as the conditionally indispensable eicosapentaenoic acid (20:5n-3, EPA) and docosahexaenoic acid (22:6n-3, DHA), which are physiologically crucial but of limited dietary availability in nature (reviewed by Twining et al., 2016). Animals vary in their ability to convert essential ALA into EPA and DHA but they cannot synthesize ALA *de novo*. Currently, our understanding of animal lipid biochemistry and physiology is biased to marine food webs (Baird, 2022), with far less information available for freshwater, terrestrial, or insect food webs (but see Twining et al., 2016; Génier et al., 2021; Parmar et al., 2022). Little attention has been given to understanding the interactions between the physiological demands of long-distance migration (e.g., for insects, birds), spatial origin of lipids and subsequent storage, utilization, and conservation and dynamics of PUFA and the

essential precursors such as linoleic acid (18:2n-6, LIN) and ALA.

Increasingly, efforts are underway to gain a better understanding of the spatio-temporal environmental conditions experienced by migrating monarchs (and other animals) during migration with respect to understanding population demographic trends and conservation (Saunders et al., 2019; Taylor et al., 2019). The findings of Hobson et al. (2020) were based on H isotopic measurements of "total" lipids in migrant monarchs, which for adult monarchs predominantly reflects the abundant non-essential oleic (18:1n-9) and palmitic acids (16:0) (Cenedella, 1971). Here we explore the idea that fatty acid profiles combined with compound-specific fatty acid isotopic ($\delta^{13}C$ and $\delta^{2}H$) analyses of storage lipids could provide new information on energy provenance because lipids are composed of carbon and hydrogen atoms derived from spatially-distributed plant nectars [see West et al. (2008, 2010) regarding plant-based H and C isoscape patterns]. We hypothesized that the essential PUFA (i.e., ALA and LIN) would be derived exclusively from the larval milkweed host plant diet, because no notable amounts are taken up by the nectar feeding adults, and these PUFA should retain the isotopic composition of their geographical provenance (O'Brien et al., 2000; but see Levin et al., 2017), whereas non-essential fatty acids, such as palmitic acid (16:0), stearic acid (18:0), or oleic acid (18:1n-9) would be synthesized from dietary sources like nectar taken up along the migratory route, and simultaneously being used during flight. However, carbon and hydrogen isotope discrimination of stored fatty acids through mobilization kinetics (e.g., burning of fat) and by other biochemical processes are possible and could complicate isotopic-based inferences of these fatty acid spatial origins (Soto et al., 2013). Regardless, the measurement of the stable isotopic composition of stored lipids could be a powerful new method to infer origins of nectaring sites of migratory insects and potentially (re)fueling sites for migratory birds, other insects, and vertebrates (Hobson et al., 2020).

We designed this pilot study in a first attempt to assess the composition, trophic dynamics (i.e., trophic discrimination factors), and isotopic ($\delta^{2}H$ and $\delta^{13}C$) structure of essential and non-essential fatty acids acquired or manufactured *de novo* from larval hostplant milkweed by monarch butterflies from adult emergence stage to overwintering. We used controlled captive experiments to raise monarchs from eggs on swamp (*A. incarnata*) and common (*A. syriaca*) milkweed hostplants to the eclosed adult butterfly. This experiment allowed us to examine stable isotopic relationships between the natal host plant and larval dietary fatty acids and those in newly emerged adults. With later diet-switching of newly eclosed adults to an isotopically spiked ($\delta^{2}H$) nectar we were able to infer which FAs were produced *de novo* and which were obtained directly via the larvae from the larval milkweed hostplant.

Using analyses of polar and neutral lipids, the compositional and isotopic structure of fatty acids derived from the head and thorax (i.e., functional compartments) were compared to those in the abdominal fat body (i.e., storage compartment) of the captive-raised monarchs. We examined the lipid composition and isotopic ($\delta^{13}C$ and $\delta^{2}H$) structure of a small sample (n = 20) of wild monarchs obtained from an overwintering colony in Mexico in February 2022, and correlated wing $\delta^{2}H$ measurements (e.g., proxy for migratory distance) to individual fatty acids to determine whether $\delta^{2}H$ values of larval-derived essential fatty acids also provided information on spatial origins of individuals (Wassenaar and Hobson, 1998; Flockhart et al., 2013). The isotopic structure ($\delta^{13}C$ and $\delta^{2}H$) of non-essential fatty acids, which were presumably derived from southern nectaring sites close to the winter colonies (Hobson et al., 2020) were examined to evaluate their potential for spatial inferences of where monarchs acquired the key storage lipids required to sustain overwintering.

Materials and methods

Captive rearing and tracer experiments

In a first experiment, swamp milkweed was grown in planter pots in a greenhouse and randomly assigned to two groups (10 pots per treatment). One group was watered for 4 weeks using tap water ($\sim\delta^{2}H$-54‰) and the other on water spiked with 99% deuterated water (Sigma-Aldrich) to achieve a watering $\delta^{2}H$ value of ∼+350‰. Milkweed leaves from these spiked and tap water groups were thereafter used to raise monarchs from eggs through the larval stage and pupa to the eclosed adult monarch. Eclosed adult monarchs (n = 8 per treatment) were sampled immediately after emergence without any subsequent nectaring.

In a second experiment, monarchs were raised on a single batch of wild-sourced common milkweed from Manitoulin Island, ON, Canada. Similar to those raised in captivity on the swamp milkweed, we sampled eclosed adults without any nectaring. A second group of the emerged adults were kept for seven additional days and fed a ^{2}H spiked nectar consisting of a 3:1 water:sugar solution using spiked dilution water ($\delta^{2}H$ = ∼+350‰).

Adult monarchs were euthanized and stored in a −80°C freezer and freeze-dried before conducting isotopic analyses. Subsamples of milkweed leaves representing (equally) all treatments were freeze-dried and powdered for subsequent stable isotope and lipid analyses.

Overwintering monarchs (Mexico)

A small sampling of 20 (10 M and 10 F) overwintering monarchs were collected live in late January 2022, at the Sierra

Chincua wintering colony in Michoacan, Mexico. These wild monarch samples were transported cold on the collection day to the UNAM-Campus Morelia where they were euthanized and immediately freeze dried. These monarchs were stored whole at −20°C before being transported to the laboratory for lipid composition and stable isotopic analysis.

Monarch wing H isotopic analyses

Samples (0.35 ± 0.02 mg) of monarch wing chitin were weighed into 3.5 mm × 5 mm silver capsules, placed in a Uni-Prep autosampler (Eurovector, Milan, Italy, Wassenaar et al., 2015) and subsequently analyzed in a Eurovector 3000 Elemental Analyzer, coupled to a Thermo Delta V Plus isotope ratio mass spectrometer (Bremen, Germany) in continuous flow mode at the University of Western Ontario. After the samples were loaded, the Uniprep autosampler was heated to 60°C and evacuated and subsequently flushed with dry helium to remove adsorbed atmospheric moisture from the samples. Two USGS keratin standards, CBS: Caribou Hoof Standard and KHS: Kudu Horn Standard were included every ten samples. Samples were combusted at 1,350°C using a glassy carbon reactor. Values of δ^2H of non-exchangeable hydrogen were derived using the comparative equilibration approach of Wassenaar and Hobson (2003) and calibrated to Vienna Standard Mean Ocean Water (VSMOW) using CBS (±1.9‰ 1 SD, n = 18, accepted δ^2H = −197.0‰) and KHS (±1.6‰, n = 17, accepted δ^2H = −54.1‰). Overall (within-run) measurement error for CBS and KHS δ^2H was <∼2‰.

For the laboratory experiments, the δ^2H analyses of water were done using a DLT-100 laser spectrometer (ABB/Los Gatos Research, Mountain View, CA, USA) using laboratory standards INV1 δ^2H = −217.7‰ and ROD3 δ^2H = −3.9‰, respectively, to normalize delta values to the VSMOW-SLAP scale. Accuracy as determined by replicate analyses of samples and reference waters was <±1 and 0.1‰, respectively.

Fatty acid quantification and stable isotope analysis

Lipids of the selected monarch body tissues and milkweed hostplants were extracted as in Heissenberger et al. (2010) and the lipid content was determined gravimetrically. Briefly, freeze-dried monarch and milkweed samples were homogenized and mixed with chloroform:methanol (2:1 vol/vol) and after sonication, vortexed and centrifuged three times to remove non-lipid material. Solvent-extracted lipids were evaporated to a final volume of 1.5 mL under N_2 flow. Lipids were then separated into neutral lipids (NL), free-fatty acids (FF), and polar lipids (PL) using solid phase extraction (SPE; Bond Elut LRC–SI, Agilent Technologies, Santa Clara, CA, USA). The SPE columns were conditioned using hexane and loaded using 0.5 mL of the sample extract. NL were eluded using Chloroform:2-propanol (2:1 v/v), followed by elution of the FF using 2% acetic acid in diethyl ether and PL using methanol (Kaluzny et al., 1985). For fatty acid methyl ester (FAME) formation, lipid samples were incubated with a sulfuric acid:methanol mixture (1:100 vol/vol) for 16 h at 50°C, following the addition of $KHCO_3$ and hexane. Samples were shaken, vortexed, and centrifuged and the upper organic layers collected, pooled, and concentrated under N_2 gas flow.

All δ^{13}C and δ^2H analyses of FA were performed following the analytical methodology described previously (Pilecky et al., 2021a). Briefly, a Thermo Trace 1310 GC (ThermoFisher Scientific, Waltham, MA, USA) was connected via a ConFlo IV combustion or reduction interface (ThermoFisher Scientific) to an Isotope Ratio Mass Spectrometer (IRMS, DELTA V Advantage, ThermoFisher Scientific). FAMEs were separated using a VF-WAXms 30 m column, 0.32 mm ID, film thickness 1 μm (Agilent) and then for δ^{13}C analysis oxidized to CO_2 gas in a combustion reactor, filled with Ni, Pt, and Cu wires, at a temperature of 1,000°C, or for δ^2H analysis reduced to H_2 gas by passing through a high thermal conversion (HTC) ceramic reactor at 1,420°C.

Lipid samples were reference scale-normalized using three-point calibration with FAME stable isotope (Me-C20:0) reference materials (USGS70: δ^{13}C = –30.53‰, δ^2H = –183.9‰, USGS71: δ^{13}C = –10.5‰, δ^2H = –4.9‰, and USGS72: δ^{13}C = –1.54‰, δ^2H = +348.3‰). FA δ^{13}C and δ^2H values (δI_{FA}) were corrected for methylation according to the formula (Pilecky et al., 2021a):

$$\delta I_{FA} = ((n+1) \times \delta I_{FAME} - \delta I_{MeOH})/n$$

Where δI_{FAME} are the δ^2H or δ^{13}C values of the measured FAME and δI_{MeOH} the δ^2H or δ^{13}C values of the methanol used during methylation and n equals the total number of H-/C-atoms of the FAME molecule. Values for δ^{13}C are referenced to Vienna PeeDee Belemite (VPDB).

$$\delta^{13}C_{FA} = \left(\frac{^{13}C/^{12}C_{Sample}}{^{13}C/^{12}C_{VPDB}} - 1\right) \times 1000$$

Values for δ^2H are standardized against Vienna Standard Mean Ocean Water (VSMOW).

$$\delta^2H_{FA} = \left(\frac{^{2}H/^{1}H_{Sample}}{^{2}H/^{1}H_{VSMOW}} - 1\right) \times 1000$$

Data analysis

All data and graphical analyses were performed in R (Version 4.1.0) using the packages rstatix, ggplot2, and ggpubr. Data were presented as mean ± standard deviation including

10.3389/fevo.2022.1051782

propagated errors wherever applicable. A student's *t*-test, or one-way ANOVA with Tukey post-hoc test was used for two or multiple group comparison, respectively. The Pearson method was used for linear correlation analysis. Z-scores for individual FA relative abundance (% of total FAME of a sample) were calculated by normalization to the global study mean and standard deviation within this study.

Results

Fatty acid profiles of milkweed, wild, and captive monarchs

Milkweed host plant leaves had an average lipid content of 120.5 ± 12.3 μg mg^{-1} of dry weight. The most abundant FA in milkweed leaves were palmitic acid 16:0 (11.3 ± 6.6 μg mg^{-1}) and ALA (10.3 ± 5.8 μg mg^{-1}), followed by LIN (2.7 ± 1.5 μg mg^{-1}), 18:1n-9 (2.2 ± 0.9 μg mg^{-1}), 18:0 (1.6 ± 0.9 μg mg^{-1}), and 16:1n-7 (0.7 ± 0.6 μg mg^{-1}). Furthermore, only traces of 16:1n-9, GLA, 18:1n-7, and 14:0 could be identified.

For monarchs, the lipid content was dependent on the sample type (ANOVA, $F_{4,31} = 19.8$, $p < 0.001$). The lipid content of overwintering wild monarchs was approximately double for females (628 ± 208 μg mg^{-1}) compared to males (313 ± 136 μg mg^{-1}, Tukey, $p < 0.001$). Adults eclosed under controlled laboratory conditions and without any subsequent nectaring began life with an average lipid content of 136 μg mg^{-1} ± 52, and the abdomen had twice the lipid content (214 ± 54 μg mg^{-1}) of the head/thorax tissue (94 ± 10 μg mg^{-1}).

Neutral lipids (NL) were positively correlated with total lipids ($R^2 = 0.5$, $p < 0.001$). The marked increase in the NL fraction of the wild individuals was due to the accumulation of 16:0 and 18:1n-9. The phospholipid (PL) mass fraction was slightly higher in the captive monarch adults (13.8 ± 3.2 μg mg^{-1}) compared to the overwintering individuals (female: 9.7 ± 4.6 μg mg^{-1}, male: 10.6 ± 3.7 μg mg^{-1}), with head and thorax tissue particularly rich in PL (21.2 ± 9.7 μg mg^{-1}).

Mass fractions of LIN (*t*-test, $p < 0.001$), ALA (*t*-test, $p < 0.001$) and EPA (*t*-test, $p < 0.001$) were significantly higher in the captive monarchs compared to wild overwintering individuals. The EPA content did not differ (paired *t*-test, $p = 0.75$) between NL and PL, however, higher mass fractions were found in the newly emerged adults (∼0.4 μg mg^{-1}) compared to wild overwintering monarchs (∼0.1 μg mg^{-1}), as well as having higher mass fractions in the head/thorax tissue (∼0.4 μg mg^{-1}) compared to the abdomen (∼0.1 μg mg^{-1}). Other PUFA detected in trace amounts were gamma-linoleic acid (GLA, 18:3n-6), 20:3n-3, and 20:4n-6, however, no SDA or PUFA with >20 carbon atoms were found (Table 1 and Figure 1). In total, six fatty acids were found to be abundant enough to allow for compound-specific stable isotope analysis: 16:0, 16:1 (sum of all isomers), 18:0, 18:1 (sum of all isomers), LIN and ALA. The C and H isotopic composition of EPA could only be measured in the PL fraction.

Isotope fractionation in fatty acids of freshly eclosed adults compared to larval diet

The captive-raised milkweed and monarchs treated with ^2H enriched (∼+350‰) water resulted in a ∼50–100‰ increase in the δ^2H values of the fatty acids of milkweed and correspondingly of the fatty acids of monarch larvae, as reflected in the eclosed non-nectaring adults feeding on them (Figure 2A). Non-essential FA were significantly lower in δ^2H values in the newly eclosed adults compared to larval milkweed diet ($\Delta\delta^2H$: 16:0: −79.7 ± 23.8‰; 16:1: −193.2 ± 31.5‰; 18:0: −72.5 ± 20.2‰; 18:1: −251.0 ± 26.8‰; all *t*-test, $p < 0.001$), while LIN was significantly enriched ($\Delta\delta^2H$ +54.8 ± 12.4‰; *t*-test, $p < 0.001$). ALA showed a slight but insignificant positive trend ($\Delta\delta^2H$ 7.8 ± 18.2‰; *t*-test, $p = 0.665$). There was no significant difference in the δ^2H values between fatty acids of NL and PL of eclosed adults, except for 16:0, which were slightly enriched in ^2H in PL compared to NL ($\Delta\delta^2H$ −241.9 ± 5.9 vs. −267.8 ± 11.2‰, *t*-test, $p = 0.007$). The δ^2H values of EPA could only be measured in PL and were approximately 40‰ higher compared to ALA when feeding on leaves from milkweed raised on tap water ($\Delta\delta^2H$ −111.1 ± 7.7 vs. −149.7 ± 3.2‰) and ca. 60‰ enriched in individuals feeding on ^2H-enriched leaves ($\Delta\delta^2H$ −46.3 ± 0.8 vs. −111.8 ± 0.8‰) (Figure 2A).

Integration of deuterium into fatty acids in adults feeding on enriched nectar

Significant integration of the ^2H tracer into the fatty acids of individuals feeding on ^2H_2O enriched nectar was observed in 16:0 of NL ($\Delta\delta^2H$ abdomen: 31.1 ± 13.8‰; *t*-test, $p = 0.017$; head/thorax: 31.7 ± 9.3‰; *t*-test, $p = 0.004$) but not for PL. Non-significant trends were observed in 18:1 in PL of the abdomen ($\Delta\delta^2H$ 25.7 ± 18.7‰; *t*-test, $p = 0.12$) as well as ALA and EPA of all tissues and lipid classes ($\Delta\delta^2H$ ∼+10‰). A negative trend was observed in 18:0 of NL of abdominal tissue (spiked – tap water $\Delta\delta^2H$ −69.2 ± 22.9‰; *t*-test, $p = 0.019$; Figure 2B).

A significant positive H isotopic fractionation between the head/thorax and abdominal tissue was found in 16:0 of NL ($\Delta\delta^2H$ 31.5 ± 11.2‰; *t*-test, $p = 0.016$), while a corresponding negative isotope fractionation was observed for 16:0 of PL ($\Delta\delta^2H$ −34.1 ± 20.9‰; *t*-test, $p = 0.003$). Furthermore, in PL δ^2H_{LIN} ($\Delta\delta^2H$ −30.4 ± 14.0‰; *t*-test, $p = 0.017$), δ^2H_{ALA} ($\Delta\delta^2H$ −36.6 ± 15.2‰; *t*-test, $p = 0.002$), and δ^2H_{EPA} ($\Delta\delta^2H$ −22.4 ± 11.1‰; *t*-test, $p = 0.018$) values were lower in the head/thorax than in the abdomen.

TABLE 1 Fatty acid mass fractions (μg mg^{-1}) in individual lipid classes for monarchs raised in captivity and over-wintering in Mexico.

	Eclosed adult			Abdomen			Head/Thorax			Wild (female), Mexico			Wild (male), Mexico		
Total lipids	**136 ± 51**			**213 ± 54**			**93 ± 10**			**628 ± 208**			**313 ± 136**		
(μ g mg^{-1})	**FF**	**NL**	**PL**	**FF**	**NL**	**PL**	**FF**	**NL**	**PL**	**FF**	**NL**	**PL**	**FF**	**NL**	**PL**
14	N/D	0.46 ± 0.09	0.02 ± 0.00	N/D	0.57 ± 0.16	0.01 ± 0.01	N/D	0.13 ± 0.19	0.02 ± 0.02	N/D	0.80 ± 0.28	N/D	N/D	0.60 ± 0.33	0.01 ± 0.01
16	0.23 ± 0.16	28.4 ± 5.7	1.55 ± 0.38	0.15 ± 0.06	47.8 ± 11.6	1.82 ± 1.14	0.15 ± 0.17	15.1 ± 11.2	3.42 ± 2.22	0.89 ± 0.66	141.5 ± 62.8	1.33 ± 0.63	0.32 ± 0.32	101.3 ± 59.2	1.32 ± 0.87
16.1.7c	0.01 ± 0.01	1.84 ± 0.37	0.04 ± 0.01	0.01 ± 0.01	10.0 ± 6.0	0.23 ± 0.17	N/D	2.4 ± 3.0	0.31 ± 0.24	0.09 ± 0.08	16.62 ± 9.14	0.19 ± 0.09	0.04 ± 0.03	14.2 ± 7.7	0.31 ± 0.23
16.1.9c	N/D	0.31 ± 0.08	0.01 ± 0.00	N/D	0.34 ± 0.09	0.01 ± 0.01	N/D	0.10 ± 0.08	0.02 ± 0.01	N/D	0.88 ± 0.38	0.01 ± 0.00	N/D	0.77 ± 0.48	0.01 ± 0.01
17	N/D	0.10 ± 0.22	0.01 ± 0.02	N/D	0.03 ± 0.04	0.00 ± 0.01	N/D	N/D	0.02 ± 0.02	N/D	0.02 ± 0.02	N/D	N/D	0.02 ± 0.04	N/D
17.1.7c	0.01 ± 0.00	1.37 ± 0.58	0.02 ± 0.01	0.01 ± 0.01	0.35 ± 0.05	0.02 ± 0.02	0.01 ± 0.01	0.49 ± 0.12	0.04 ± 0.02	N/D	0.22 ± 0.03	0.01 ± 0.00	N/D	0.31 ± 0.10	0.01 ± 0.00
18	0.12 ± 0.08	8.5 ± 1.7	1.88 ± 0.45	0.06 ± 0.04	4.84 ± 3.07	0.89 ± 0.68	0.09 ± 0.10	4.4 ± 1.0	1.89 ± 1.26	0.08 ± 0.07	8.43 ± 4.65	0.65 ± 0.33	0.04 ± 0.03	5.48 ± 2.58	0.63 ± 0.25
18.1.7c	N/D	0.38 ± 0.09	0.03 ± 0.01	N/D	0.41 ± 0.21	0.02 ± 0.01	N/D	0.14 ± 0.07	0.04 ± 0.02	0.01 ± 0.01	1.35 ± 0.80	0.03 ± 0.01	N/D	1.44 ± 0.65	0.03 ± 0.02
18.1.9c	0.18 ± 0.12	23.7 ± 4.9	2.07 ± 0.40	0.09 ± 0.04	48.7 ± 15.3	2.83 ± 2.09	0.05 ± 0.06	20.2 ± 10.1	5.64 ± 3.90	1.64 ± 1.23	282.9 ± 90.2	3.95 ± 1.87	0.53 ± 0.59	150.6 ± 97.0	5.0 ± 2.7
LIN 18.2.6c	0.02 ± 0.01	6.0 ± 1.7	0.81 ± 0.23	0.02 ± 0.01	11.2 ± 2.9	0.92 ± 0.86	0.01 ± 0.02	6.0 ± 2.4	2.13 ± 1.24	0.01 ± 0.01	1.31 ± 0.53	0.51 ± 0.23	0.00 ± 0.00	1.31 ± 0.49	0.59 ± 0.42
ALA 18.3.3c	0.19 ± 0.08	35.6 ± 16.3	6.3 ± 1.5	0.06 ± 0.03	34.7 ± 7.8	2.56 ± 3.42	0.04 ± 0.05	18.9 ± 5.1	5.8 ± 4.0	0.03 ± 0.02	6.47 ± 2.65	2.58 ± 1.34	0.02 ± 0.01	5.9 ± 3.2	2.3 ± 1.3
GLA 18.3.6c	N/D	0.33 ± 0.04	0.03 ± 0.01	N/D	0.16 ± 0.05	N/D	N/D	0.10 ± 0.03	0.03 ± 0.02	N/D	0.01 ± 0.01	0.01 ± 0.00	N/D	0.01 ± 0.01	N/D
SDA 18.4.3c	N/D	N/D	N/D	N/D	N/D	N/D	N/D	N/D	N/D	N/D	N/D	N/D	N/D	N/D	N/D
20.1.9c	N/D	0.04 ± 0.06	N/D	N/D	0.02 ± 0.02	N/D	N/D	0.01 ± 0.01	0.02 ± 0.01	N/D	0.25 ± 0.16	0.01 ± 0.01	N/D	0.21 ± 0.07	0.02 ± 0.01
20.3.3c	N/D	0.23 ± 0.05	0.02 ± 0.01	N/D	0.19 ± 0.10	0.01 ± 0.01	N/D	0.07 ± 0.01	0.02 ± 0.02	N/D	0.11 ± 0.06	0.01 ± 0.01	N/D	0.09 ± 0.04	0.01 ± 0.01
ARA 20.4.6c	0.01 ± 0.01	0.08 ± 0.04	0.01 ± 0.01	N/D	0.06 ± 0.02	0.00 ± 0.01	N/D	0.07 ± 0.02	0.01 ± 0.01	N/D	0.02 ± 0.01	N/D	N/D	0.03 ± 0.02	N/D
EPA 20.5.3c	N/D	0.48 ± 0.12	0.37 ± 0.10	N/D	0.10 ± 0.05	0.13 ± 0.18	N/D	0.37 ± 0.19	0.41 ± 0.43	N/D	0.13 ± 0.04	0.11 ± 0.05	N/D	0.11 ± 0.08	0.10 ± 0.06
22	N/D	0.24 ± 0.05	0.02 ± 0.01	N/D	0.07 ± 0.04	0.01 ± 0.01	N/D	0.11 ± 0.03	0.03 ± 0.03	N/D	0.11 ± 0.05	0.01 ± 0.01	N/D	0.21 ± 0.09	0.01 ± 0.00
24	0.01 ± 0.01	0.15 ± 0.03	0.01 ± 0.01	N/D	0.04 ± 0.02	0.04 ± 0.05	N/D	0.11 ± 0.05	0.03 ± 0.03	N/D	0.07 ± 0.04	N/D	N/D	0.10 ± 0.06	N/D
Total FA	1.5 ± 1.2	111 ± 30	13.8 ± 3.2	0.7 ± 0.1	161 ± 35	10.6 ± 5.7	0.8 ± 0.6	70 ± 31	21.2 ± 9.7	3.0 ± 2.2	463 ± 163	9.7 ± 4.6	1.2 ± 1.0	284 ± 140	10.6 ± 3.7

Values indicate mean ± standard deviation (n = 10 for each group). FF, free fatty acids; PL, polar lipids; NL, neutral lipids.

10.3389/fevo.2022.1051782

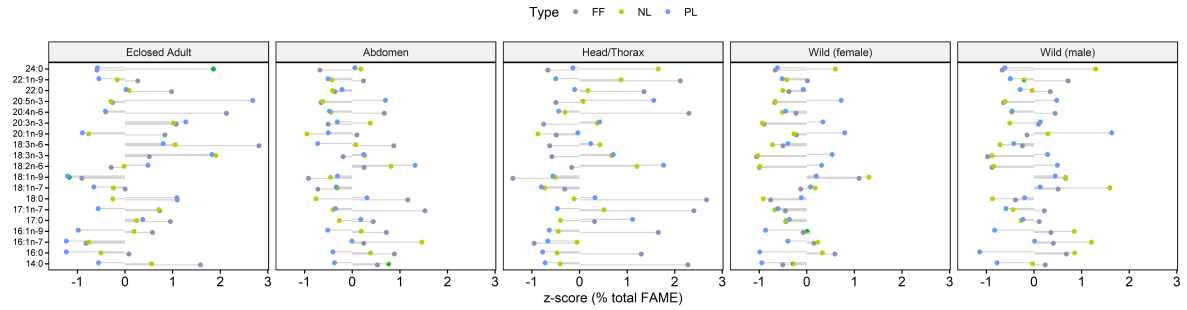

FIGURE 1
Z-scores (for all samples in this study) of relative fatty acid abundance (% total FAME) for each sample and corresponding mass fractions (μg mg^{-1} dw). Wild monarchs, especially females, contained higher lipid fractions than males or monarchs raised in the lab, in which the abdomen had ca. twice the lipid content compared to the head/thorax region. Polar lipids (PL) content was comparable for all monarchs but particularly concentrated in head/thorax. Neutral lipids (NL) correlated with lipid content, mainly driven by the increase in 16:0 and 18:1n-9. Notably, EPA was concentrated in PL, while 18:1 and 24 were enriched in the NL. Relative EPA contents in the PL were lower in freshly emerged monarchs for both head/thorax and abdomen compared to those migrant individuals overwintering in Mexico. Relative fatty acid content of LIN and ALA was comparable between NL and PL.

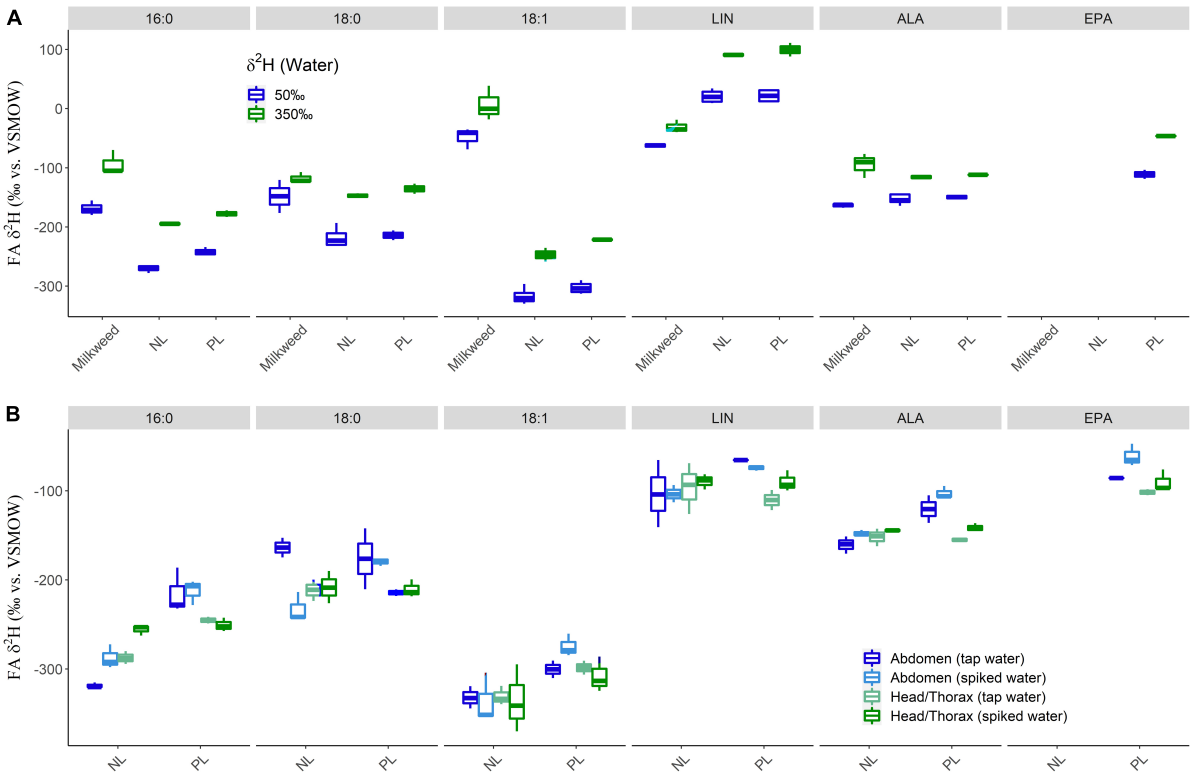

FIGURE 2
Hydrogen isotopic fractionation between diet and fatty acids (FA) of **(A)** eclosed monarchs after feeding on milkweed grown under two different water treatments at larval stage (experiment 1) and **(B)** adult monarchs feeding on nectar with or without spiked D_2O (experiment 2). **(A)** While the effect of ^2H spiked water was universally seen, the saturated and monounsaturated fatty acids were significantly lighter in larvae compared to diet, while LIN was significantly enriched. Alpha-linoleic acid (ALA) closely reflected the diet. There were no differences in δ^2H values between neutral lipids (NL) and polar lipids (PL). δ^2H_{EPA} could only be determined in PL and was enriched compared to the corresponding ALA values. **(B)** 16:0 and 18:1 in PL were isotopically enriched compared to NL and $\delta^2H_{16:0}$ values of NL were lower in the abdomen, compared to head/thorax tissue, while the opposite held for PL. In addition, 16:0 was the only FA showing significant integration of deuterium, although slight isotopic effects could also be observed for ALA and EPA. LIN, ALA, and EPA in PL of the abdomen were isotopically enriched compared to NL or both PL and NL of head/thorax tissue.

Significant inter-class H isotopic fractionation between NL and PL was observed in 16:0 in abdominal tissue ($\Delta\delta^2$H 89.1 ± 22.4‰; *t*-test, $p < 0.001$), but also in head/thorax tissue ($\Delta\delta^2$H 23.6 ± 9.3‰; *t*-test, $p = 0.027$) as well as to a lesser extend in 18:1 ($\Delta\delta^2$H abdominal: 46.8 ± 24.7‰; *t*-test, $p = 0.002$; head/thorax: 29.7 ± 28.9‰; *t*-test, $p = 0.05$). Finally, δ^2H_{ALA} values were lower in NL than PL in abdominal tissue ($\Delta\delta^2$H 42.6 ± 15.9‰; *t*-test, $p < 0.001$; **Figure 2B**).

Compound-specific isotope analyses (CSIA) of fatty acids in overwintering monarchs

Compared to monarchs raised in captivity in the laboratory, the samples of overwintering monarchs from Mexico had lower $\delta^2H_{16:0}$ (−328 ± 222 vs. −250 ± 15‰), $\delta^2H_{16:1}$ (−362 ± 25 vs. −310 ± 46‰) and $\delta^2H_{18:1}$ (−354 ± 11 vs. −307 ± 17‰), but higher $\delta^2H_{18:0}$ (−133 ± 46 vs. −203 ± 28‰) and δ^2H_{ALA} values (−101 ± 27 vs. −135 ± 25‰). As observed in the captive study, the $\delta^2H_{16:0}$ values were lower in NL than PL, whereby the H isotopic fractionation was slightly higher in male than female monarchs ($\Delta\delta^2$H: 39.6 ± 11.6 vs. 27.9 ± 8.1‰), but in addition the $\Delta\delta^2H_{18:0}$ values were higher in NL than in PL ($\Delta\delta^2$H: female: −79.9 ± 34.3‰; male: −89.1 ± 53.4‰). The standard deviation of H isotopic fractionation between NL and PL in all 20 monarchs was lower in $\delta^2H_{16:0}$ (11.3‰), $\delta^2H_{18:1}$ (7.7‰), and δ^2H_{ALA} (9.0‰) than in $\delta^2H_{18:0}$ (47.5‰) and δ^2H_{LIN} (56.2‰). The δ^2H_{ALA} values of both lipid classes strongly correlated with wing chitin δ^2H values (Pearson, NL: $R^2 = 0.78$; PL: $R^2 = 0.64$). No significant correlation with wing chitin was observed for δ^2H values of any other FA (**Figure 3A**).

Regarding δ^{13}C, all saturated and monounsaturated FA had slightly lower values in NL compared to PL (δ^{13}C 16:0 −2.1 ± 1.2‰; 18:0 −1.5 ± 2.0‰; 18:1 −2.0 ± 1.9‰). About half of the female monarchs had up to 6‰ higher $\delta^{13}C_{ALA}$ values in NL than in PL, while no carbon isotopic fractionation in ALA between lipid classes was observed in males (**Figures 3B,C**).

Discussion

This is the first study investigating fatty acids in monarchs (or any migratory insect) using compound-specific δ^2H and δ^{13}C and controlled tracer test analysis. Data from controlled laboratory isotope tracer tests and from overwintering individuals suggested that adult monarchs convert their dietary energy mainly into 16:0 and 18:1 FA and store them as NL in their abdomen. Accordingly, the H and C isotopic values of the non-essential saturated and monounsaturated fatty acids should not correlate with the δ^2H of monarch wings, a proxy of the natal origin of each individual (Wassenaar and Hobson, 1998; Flockhart et al., 2013), but are instead expected to correlate to the spatial origins of their nectar sources. On the other hand, the δ^2H values of the essential omega-3 PUFA ALA were correlated with the δ^2H_{Wing}, underscoring the physiological importance of ALA because it is retained by the migratory individual throughout its entire life cycle. Finally, δ^2H_{LIN} showed a ^{2}H enrichment compared to the larval milkweed diet, indicating the predominance of catabolic processes. In fact, we found considerable variations in the isotopic fractionation of δ^2H_{LIN} and $\delta^{13}C_{LIN}$ between NL and PL of overwintering monarchs. The absolute $\Delta\delta^2H_{LIN}$ values of NL revealed a negative correlation with δ^2H values of wing chitin which could potentially be useful when investigating individual life-history traits, such as past catabolic events or periods of fasting. Taken altogether, our results provide evidence that H and C isotopic analyses of individual fatty acids in migrating and overwintering monarchs can be used to gain new insights into the nutritional history of individuals including provenance of nectaring sites used to fuel key life history events.

Monarch larvae feeding on ^{2}H-labeled milkweed leaves accordingly integrated the isotope tracer into all FA. The δ^2H values of saturated and monounsaturated FA were significantly lower in the larvae than the hostplant milkweed, indicating predominant anabolic processes, that is, ongoing fatty acid synthesis. Conversely, δ^2H_{ALA} closely reflected the milkweed hostplant diet, and those of LIN were significantly higher, indicating a predominance of catabolic processes. We were able to detect low contents of EPA, whose δ^2H values were slightly higher compared to ALA (∼40‰), but even higher when feeding on the ^{2}H-labeled leaves (∼60‰). This could be explained by the integration of the liquid water hydrogen/deuterium atoms into the FA molecule during the conversion process of ALA to EPA (Pilecky et al., 2022), which monarchs must perform because terrestrial plants do not contain any PUFA with more than 18 C atoms (Twining et al., 2016). Bioconversion is likely initiated by an elongation of ALA to 20:3n-3, followed by double desaturation to EPA as has been found in other hexapods (Strandberg et al., 2020) and because we did not detect any traces of stearidonic acid (18:4n-3) in monarchs in this study. Integration of deuterium atoms into EPA and into ALA of PL of head/thorax tissue also occurred for adults feeding on a sugar solution with ^{2}H-enriched water but without any FA, which revealed that bioconversion of ALA to EPA is not only performed in monarch larvae, but also in adults, and that EPA in monarchs is potentially subjected to retro-conversion to ALA in head/thorax tissue. Still, the monarch larval stage appeared to be the only possibility for monarch adults to obtain this essential fatty acid. A recent study by Pocius et al. (2022) found a correlation between larval diet, *i.e.*, milkweed species, and the free-flight energetics of monarch adults, hence it would be of great interest to establish whether the species of milkweed host plant (and its distribution) impacts the EPA quantity in freshly eclosed monarch adults. In many animal species, EPA increases the efficacy of neuronal

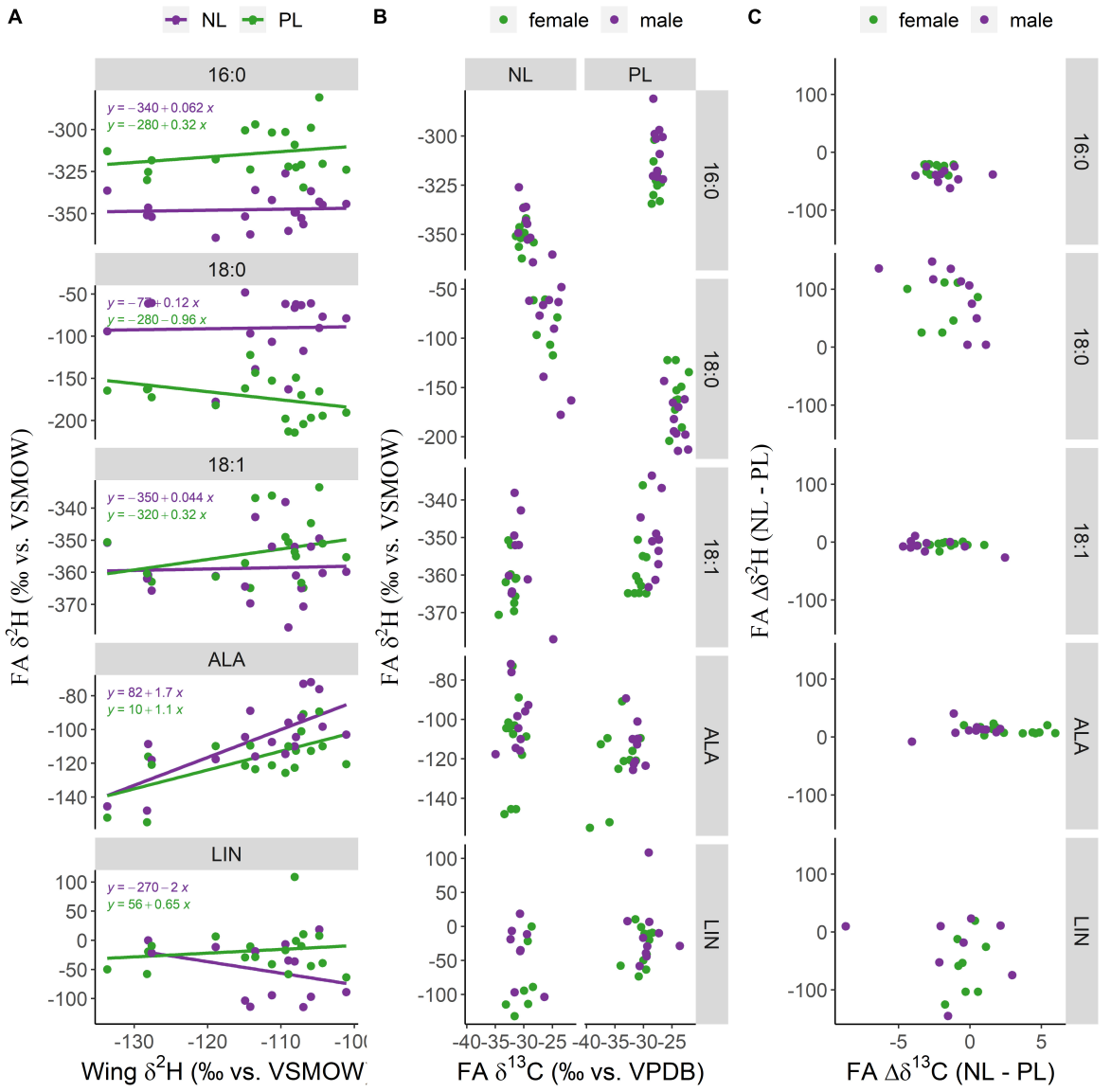

FIGURE 3
Compound specific isotope analysis fatty acids (FA) for 20 monarchs at their overwintering habitat in Mexico. **(A)** In contrast to all other FA, δ^2H_{ALA} correlated with wing δ^2H suggesting strict conservation of this FA from their natal provenance. **(B)** δ^2H and $\delta^{13}C$ fatty acid specific biplots of 10 female and 10 male monarchs from the overwintering site in Mexico. Distinct groups in an isotopic biplot, indicating different nectaring provenance, could not be identified in this small dataset. **(C)** The individual isotopic fractionation between neutral lipids (NL) and polar lipids (PL).

tissue (e.g., providing higher visual acuity, memory capacity, or spatial navigation) and promotes reproduction, and is therefore particularly biosynthesized by females for maternal provision to offspring (Pilecky et al., 2021b). In our small pilot dataset of 20 wild overwintering monarchs, we found that about half of females showed a high carbon isotopic fractionation in $\delta^{13}C_{ALA}$ between NL and PL, which suggest increased bioconversion activity during gravidity, although our sample size is too small to solidly support this idea. Unfortunately, determining δ^2H_{EPA} and $\delta^{13}C_{EPA}$ is analytically challenging in adult monarch lipid extracts due to the extremely low ratio of these EPA to total FAME, particularly in NL and abdominal tissue. As a result, we were unable to reliably measure δ^2H_{EPA} and $\delta^{13}C_{EPA}$ in the wild overwintering monarchs. Further methodological improvements will be required for studying EPA bioconversion rates in the wild monarch populations.

The large isotopic fractionation in $\delta^2H_{16:0}$ between PL and NL in abdominal tissue revealed a high rate of fatty acid synthesis and thereby underscores its importance for dietary energy conversion from carbohydrates to storage lipids. Unfortunately, our overwintering monarch sample size was too

small to fully validate the suitability of compound-specific non-essential stable isotope analysis for linking wintering individual's FA to different food sources spatially, and we were unable to identify any subgroups by dual (C + H) isotope plots of any FA to potentially differentiate nectaring locations. However, data from the controlled experiments showed that nectar sources were clearly reflected in the $\delta^2H_{16:0}$ values and may be integrated into $\delta^2H_{18:0}$ and $\delta^2H_{18:1}$ over a longer period of time, encouraging further studies investigating the suitability of this FA as food provenance and energy source marker.

Linoleic acid was the only fatty acid whose δ^2H values were significantly enriched compared to diet and showed the largest variation in δ^2H values in the 20 wild overwintering monarchs from Mexico, both in their absolute values but particularly in the isotopic fractionation between NL and PL. Furthermore, the δ^2H_{LIN} of NL showed a negative correlation with wing chitin δ^2H values (e.g., natal origin). We found low mass fractions of arachidonic acid (20:4n-6, ARA) mainly in the NL and almost none in PL, which suggested that ARA was a by-product of fatty acid bioconversion of the non-selective (between n-3 and n-6) bioconversion, rather than having an ARA-demanding physiological function. LIN is taken up together with ALA from milkweed leaves at the larval stage, whereas adults have no significant access to both PUFA. Omega-3 PUFA are vital for functioning of the neuronal system including vision and navigation and are thus particularly retained rather than catabolized (Pilecky et al., 2021b), while no similar biological function for LIN is known. We therefore postulate that LIN is accumulated at the larval stage up to eclosure of the adult. From that time on, LIN is partially used for energy production, particularly when running low on non-essential fatty acids. This is likely the cause of the observed increase in δ^2H_{LIN} values in all samples, because fatty acids with lighter isotopic composition are mobilized faster, rendering the residual unused pool with heavier isotopic composition. It could be speculated that δ^2H_{LIN} values are an energetics marker for individual life-history of migrant monarchs, but it remains to be tested whether directly or indirectly, for example by correlation of isotopic fractionation between LIN_{NL} and LIN_{PL} with spatiotemporal parameters such as total flight time or migratory distance and/or the number of over-wintering fasting days.

Conclusion

The controlled laboratory and field results of this pilot study encourage further investigation on the application of compound-specific ^2H and ^{13}C analysis investigations of the migration routes and nectaring energy sources of monarchs and for other migratory Lepidoptera or insects. Further studies using appropriately larger population samples sizes are warranted to better understand the physiological processes altering isotopic values of saturated and mono-unsaturated FA in addition to isotopic values of food sources. Larger datasets are also needed to correct for isotopic "noise" introduced by each individuals' life-history (i.e., catabolism), which may blur the energy source signal from diet. Within this context, we suggest δ^2H_{LIN} could potentially be useful as life-history marker, and our results establish an encouraging basis for future studies with flight-time/distance and/or fasting periods. Finally, our study reveals the power of compound-specific isotope analyses (CSIA) for a detailed investigation of the migration routes and fuel sources of insects and other migrating species.

Data availability statement

The original contributions presented in this study are included in the article, further inquiries can be directed to the corresponding author.

Author contributions

KH and JM designed the study and provided financial support. MP, LW, and KH performed the data analysis and led wrote the manuscript. KH, JM, and MR collected the samples. LW, KH, MK, JM, and MR assisted with manuscript editing. All authors critically assessed the manuscript and approved the submitted version.

Funding

This work was supported by discovery grant to KH from the Natural Sciences and Engineering Council (NSERC) of Canada (grant 2017-04430). The open access fee was covered by Donau-Universität Krems. Funding was provided in part by a grant from Environment and Climate Change Canada to JM.

Conflict of interest

The authors declare that the research was conducted in the absence of any commercial or financial relationships that could be construed as a potential conflict of interest.

Publisher's note

References

Baird, P. (2022). Diatoms and fatty acid production in arctic and estuarine ecosystems—a reassessment of marine food webs, with a focus on the timing of shorebird migration. *Mar. Ecol. Prog. Ser.* 688, 173–196. doi: 10.3354/meps14025

Beall, G. (1948). The fat content of a butterfly, *Danaus Plexippus* Linn., As affected by migration. *Ecology* 29, 80–94. doi: 10.2307/1930346

Brower, L. P. (1985). "New perspectives on the migration biology of the monarch butterfly, *Danaus plexippus* L," in *Contributions in marine science*, Vol. 27, (Austin: The University of Texas Libraries), 748–786.

Brower, L. P., Fink, L. S., and Walford, P. (2006). Fueling the fall migration of the monarch butterfly. *Integr. Comp. Biol.* 46, 1123–1142. doi: 10.1093/icb/icl029

Brower, L., Fink, L., Kiphart, R., Pocius, V., Zubieta, R., and Ramírez, M. (2015). "The effect of the 2010-2011 drought on the lipid content of monarch butterflies (*Danaus plexippus* L., Danainae) migrating through Texas to their overwintering sites in Mexico," in *Monarchs in a changing world: Biology and conservation of an iconic butterfly*, eds K. S. Obserhauser, K. R. Nail, and S. Altizer (Ithaca, NY: Cornell University Press), 117–129.

Brown, J. J., and Chippendale, G. M. (1974). Migration of the monarch butterfly, *Danaus plexippus*: Energy sources. *J. Insect Physiol.* 20, 1117–1130. doi: 10.1016/0022-1910(74)90218-2

Cenedella, R. J. (1971). The lipids of the female monarch butterfly, *Danaus plexippus*, during fall migration. *Insect Biochem.* 1, 244–247. doi: 10.1016/0020-1790(71)90077-1

Dingle, H. (2014). *Migration: The biology of life on the move*. Oxford: Oxford University Press.

Flockhart, D. T. T., Wassenaar, L. I., Martin, T. G., Hobson, K. A., Wunder, M. B., and Norris, D. R. (2013). Tracking multi-generational colonization of the breeding grounds by monarch butterflies in eastern North America. *Proc. Biol. Sci.* 280:20131087. doi: 10.1098/rspb.2013.1087

Génier, C. S. V., Guglielmo, C. G., Mitchell, G. W., Falconer, M., and Hobson, K. A. (2021). Nutritional consequences of breeding away from riparian habitats in Bank Swallows: New evidence from multiple endogenous markers. *Conserv. Physiol.* 9:coaa140. doi: 10.1093/conphys/coaa140

Gibo, D. L., and McCurdy, J. A. (1993). Lipid accumulation by migrating monarch butterflies (*Danaus plexippus* L.). *Can. J. Zool.* 71, 76–82. doi: 10.1139/z93-012

Heissenberger, M., Watzke, J., and Kainz, M. J. (2010). Effect of nutrition on fatty acid profiles of riverine, lacustrine, and aquaculture-raised salmonids of pre-alpine habitats. *Hydrobiologia* 650, 243–254. doi: 10.1007/s10750-010-0266-z

Hobson, K. A., García-Rubio, O. R., Carrera-Treviño, R., Anparasan, L., Kardynal, K. J., McNeil, J. N., et al. (2020). Isotopic (δ2H) analysis of stored lipids in migratory and overwintering monarch butterflies (*Danaus plexippus*): Evidence for Southern critical late-stage nectaring sites? *Front. Ecol. Evol.* 8:572140. doi: 10.3389/fevo.2020.572140

Hobson, K. A., Norris, D. R., Kardynal, K. J., and Yohannes, E. (2019). "Chapter 1 - animal migration: A context for using new techniques and approaches," in *Tracking animal migration with stable isotopes (Second Edition)*, eds K. A. Hobson and L. I. Wassenaar (Cambridge: Academic Press), 1–23. doi: 10.1016/B978-0-12-814723-8.00001-5

Kaluzny, M. A., Duncan, L. A., Merritt, M. V., and Epps, D. E. (1985). Rapid separation of lipid classes in high yield and purity using bonded phase columns. *J. Lipid Res.* 26, 135–140. doi: 10.1016/S0022-2275(20)34412-6

Lennox, R. J., Chapman, J. M., Souliere, C. M., Tudorache, C., Wikelski, M., Metcalfe, J. D., et al. (2016). Conservation physiology of animal migration. *Conserv. Physiol.* 4:cov072. doi: 10.1093/conphys/cov072

Levin, E., McCue, M. D., and Davidowitz, G. (2017). More than just sugar: Allocation of nectar amino acids and fatty acids in a Lepidopteran. *Proc. Biol. Sci.* 284:20162126. doi: 10.1098/rspb.2016.2126

McWilliams, S. R., Guglielmo, C., Pierce, B., and Klaassen, M. (2004). Flying, fasting, and feeding in birds during migration: A nutritional and physiological ecology perspective. *J. Avian Biol.* 35, 377–393. doi: 10.1111/j.0908-8857.2004.03378.x

O'Brien, D. M., Schrag, D. P., and del Rio, C. M. (2000). Allocation to reproduction in a Hawkmoth: A quantitative analysis using stable carbon isotopes. *Ecology* 81, 2822–2831. doi: 10.1890/0012-96582000081[2822:ATRIAH]2.0.CO;2

Parmar, T. P., Kindinger, A. L., Mathieu-Resuge, M., Twining, C. W., Shipley, J. R., Kainz, M. J., et al. (2022). Fatty acid composition differs between emergent aquatic and terrestrial insects—A detailed single system approach. *Front. Ecol. Evol.* 10:952292. doi: 10.3389/fevo.2022.952292

Pilecky, M., Kämmer, S. K., Mathieu-Resuge, M., Wassenaar, L. I., Taipale, S. J., Martin-Creuzburg, D., et al. (2022). Hydrogen isotopes (δ2H) of polyunsaturated fatty acids track bioconversion by zooplankton. *Funct. Ecol.* 36, 538–549. doi: 10.1111/1365-2435.13981

Pilecky, M., Winter, K., Wassenaar, L. I., and Kainz, M. J. (2021a). Compound-specific stable hydrogen isotope (δ2H) analyses of fatty acids: A new method and perspectives for trophic and movement ecology. *Rapid Commun. Mass Spectrom.* 35:e9135. doi: 10.1002/rcm.9135

Pilecky, M., Závorka, L., Arts, M. T., and Kainz, M. J. (2021b). Omega-3 PUFA profoundly affect neural, physiological, and behavioural competences – implications for systemic changes in trophic interactions. *Biol. Rev.* 96, 2127–2145. doi: 10.1111/brv.12747

Pocius, V. M., Cibotti, S., Ray, S., Ankoma-Darko, O., McCartney, N. B., Schilder, R. J., et al. (2022). Impacts of larval host plant species on dispersal traits and free-flight energetics of adult butterflies. *Commun. Biol.* 5:469. doi: 10.1038/s42003-022-03396-8

Saunders, S. P., Ries, L., Neupane, N., Ramírez, M. I., García-Serrano, E., Rendón-Salinas, E., et al. (2019). Multiscale seasonal factors drive the size of winter monarch colonies. *Proc. Natl. Acad. Sci. U.S.A.* 116, 8609–8614. doi: 10.1073/pnas.1805114116

Slayback, D., Brower, L., Ramírez, M., and Fink, L. (2007). Establishing the presence and absence of overwintering colonies of the monarch butterfly in Mexico by the use of small aircraft. *Am. Entomol.* 53, 28–40. doi: 10.1093/ae/53.1.28

Soto, D. X., Hobson, K. A., and Wassenaar, L. I. (2013). The influence of metabolic effects on stable hydrogen isotopes in tissues of aquatic organisms. *Isotopes Environ. Health Stud.* 49, 305–311. doi: 10.1080/10256016.2013.820727

Strandberg, U., Vesterinen, J., Ilo, T., Akkanen, J., Melanen, M., and Kankaala, P. (2020). Fatty acid metabolism and modifications in Chironomus riparius. *Philos. Trans. R. Soc. B Biol. Sci.* 375:20190643. doi: 10.1098/rstb.2019.0643

Taylor, O. R., Lovett, J. P., Gibo, D. L., Weiser, E. L., Thogmartin, W. E., Semmens, D. J., et al. (2019). Is the timing, pace, and success of the monarch migration associated with sun angle? *Front. Ecol. Evol.* 7:442. doi: 10.3389/fevo.2019.00442

Twining, C. W., Brenna, J. T., Hairston, N. G., and Flecker, A. S. (2016). Highly unsaturated fatty acids in nature: What we know and what we need to learn. *Oikos* 125, 749–760. doi: 10.1111/oik.02910

Wassenaar, L. I., and Hobson, K. A. (1998). Natal origins of migratory monarch butterflies at wintering colonies in Mexico: New isotopic evidence. *Proc. Natl. Acad. Sci. U.S.A.* 95, 15436–15439. doi: 10.1073/pnas.95.26.15436

Wassenaar, L. I., and Hobson, K. A. (2003). Comparative equilibration and online technique for determination of non-exchangeable hydrogen of keratins for use in animal migration studies. *Isotopes Environ. Health Stud.* 39, 211–217. doi: 10.1080/1025601031000096781

Wassenaar, L. I., Hobson, K. A., and Sisti, L. (2015). An online temperature-controlled vacuum-equilibration preparation system for the measurement of δ2H values of non-exchangeable-H and of δ18O values in organic materials by isotope-ratio mass spectrometry. *Rapid Commun. Mass Spectrom.* 29, 397–407. doi: 10.1002/rcm.7118

West, J. B., Sobek, A., and Ehleringer, J. R. (2008). A simplified GIS approach to modeling global leaf water isoscapes. *PLoS One* 3:e2447. doi: 10.1371/journal.pone.0002447

West, J., Kreuzer, H., and Ehleringer, J. (2010). *Approaches to plant hydrogen and oxygen isoscapes generation*. Berlin: Springer. doi: 10.1007/978-90-481-3354-3_8

frontiers | Frontiers in Ecology and Evolution

TYPE Original Research
PUBLISHED 09 February 2023
DOI 10.3389/fevo.2023.1060836

OPEN ACCESS

EDITED BY
Seth Newsome,
University of New Mexico,
United States

REVIEWED BY
Kaycee Morra,
Northwestern University,
United States
David Nelson,
University of Maryland,
United States

*CORRESPONDENCE
Eve E. Lindroos
✉ elind015@uottawa.ca
Megan S. Reich
✉ megan.reich@uottawa.ca

SPECIALTY SECTION
This article was submitted to Ecophysiology, a section of the journal Frontiers in Ecology and Evolution

RECEIVED 03 October 2022
ACCEPTED 11 January 2023
PUBLISHED 09 February 2023

CITATION
Lindroos EE, Bataille CP, Holder PW, Talavera G and Reich MS (2023) Temporal stability of δ^2H in insect tissues: Implications for isotope-based geographic assignments. *Front. Ecol. Evol.* 11:1060836. doi: 10.3389/fevo.2023.1060836

Temporal stability of δ^2H in insect tissues: Implications for isotope-based geographic assignments

Eve E. Lindroos[1]*, Clément P. Bataille[1,2], Peter W. Holder[3], Gerard Talavera[4] and Megan S. Reich[2]*

[1]Department of Earth and Environmental Sciences, University of Ottawa, Ottawa, ON, Canada, [2]Department of Biology, University of Ottawa, Ottawa, ON, Canada, [3]Bio-Protection Research Centre, Lincoln University, Canterbury, New Zealand, [4]Institut Botànic de Barcelona (IBB), CSIC-Ajuntament de Barcelona, Barcelona, Catalonia, Spain

Hydrogen isotope geolocation of insects is based on the assumption that the chitin in the wings of adult migratory insects preserves the hydrogen isotope composition (δ^2H) of the larval stages without influence of adult diet. Here, we test this assumption by conducting laboratory feeding experiments for monarch butterflies (*Danaus plexippus*) including: (1) a starvation treatment where adults were not fed and (2) an enriched treatment where adults were fed a diet isotopically enriched in deuterium (~ +78‰) compared to the larval diet. The δ^2H values of adult wings were measured at different time steps along the 24-day experiment. We also investigated intra-wing differences in δ^2H values caused by wing pigmentation, absence of wing scales, and presence of major wing veins. We conclude that, although the magnitude of the changes in δ^2H values are small (~6‰), wing δ^2H values vary based on adult diet and insect age, particularly early after eclosion (i.e., 1–4 days). We found that wing shade, wing pigmentation, and the presence of wing scales do not alter wing δ^2H values. However, wing samples containing veins had systematically higher δ^2H values (~9‰), suggesting that adult diet influences the hemolymph that circulates in the wing veins. We hypothesise that there is a stronger influence of adult diet on the isotope signal of wings during early adult life relative to later life because of increased metabolic and physiologic activity in young insect wings. We argue that the influence of the isotopic contribution of adult diet is generally small and is likely minimal if the wings are carefully sampled to avoid veins. However, we also demonstrated that wings are not inert tissues, and that adult feeding contributes to some of the intra-population δ^2H variance. We conclude that δ^2H geolocation using insect wings remains valid, but that adult feeding, butterfly age and wing vein sampling generate an inherent uncertainty limiting the precision of geolocation.

KEYWORDS

migratory insect, monarch butterfly, hydrogen isotope, fractionation, geolocation, isoscape, diet

1. Introduction

Investigating, understanding and predicting migration patterns has critical implications for species conservation, biosecurity and ecology (Meretsky et al., 2011; Lohmann, 2018; Satterfield et al., 2020). One effective tool to track migratory animals is through endogenous biochemical markers such as stable isotopes (Hobson et al., 2010). Biological and physical processes drive predictable variations of isotope compositions across the landscape (West et al., 2010), which can be used to generate isotopic baseline maps, referred to as isoscapes (e.g., Bowen and Revenaugh,

2003; West et al., 2010; Bataille et al., 2018, 2020). The principle behind stable isotope geolocation is that metabolically inert tissues (e.g., enamel and keratin) will preserve the isotopic signature of the location where the tissue developed through the isotopic composition from local diet (Hobson and Wassenaar, 1996; Holder, 2012). To track the mobility and determine the natal origin of migratory individuals, the isotope composition of the metabolically inert tissue is compared to isoscapes of the study area to generate probabilistic maps of potential origin (Wunder, 2010).

Hydrogen isotopes have been used to track animal migrations for decades (e.g., Hobson and Wassenaar, 1996; Cryan et al., 2004; Britzke et al., 2012; Holder, 2012; Popa-Lisseanu et al., 2012; Flockhart et al., 2013, 2017; Talavera et al., 2018; Hobson et al., 2020; Reich et al., 2021). The hydrogen isotope composition (δ^2H) is provided in a delta notation: $\delta(‰) = \left(\frac{R_{sample}}{R_{standard}} - 1\right) \times 1000$, with R corresponding to the ratio of heavy isotopes to light isotopes of the sample (R_{sample}) or standard ($R_{standard}$) (Coplen, 2011). Hydrogen isotopes fractionate in precipitation and vary across the landscape following climate patterns as hydrogen fractionates due to the rainout effect and temperature (Bowen and Revenaugh, 2003). Hydrogen isotopes tend to become more depleted in heavy isotopes in cooler (higher latitudes), more inland and higher altitude conditions (Bowen and Revenaugh, 2003; Bowen et al., 2005), creating distinctive and predictable δ^2H precipitation patterns. These unique δ^2H precipitation patterns are inherited by local plants and animals in a predictable manner through diet, allowing tissue-specific δ^2H isoscapes to be calibrated using the relationship between known-origin tissue δ^2H values and δ^2H in precipitation (Yapp and Epstein, 1982; Bowen, 2008; Hobson, 2019). Consequently, in migratory individuals, the δ^2H values of inert tissues that developed at a specific location can be compared to tissue-specific δ^2H isoscapes to estimate an individual's potential geographic origin (Bowen, 2008; Hobson, 2019; Hobson et al., 2010). Studies using the δ^2H values of inert tissues including enamel or keratinous tissues (e.g., hair, feather and nail) have been used to track the mobility of many vertebrate species (e.g., Britzke et al., 2012;Popa-Lisseanu et al., 2012; Nordell et al., 2016; Voigt and Lehnert, 2019; Hu et al., 2020; Fauberteau et al., 2021; Kruszynski et al., 2021).

However, estimating the natal origin of migratory invertebrates using δ^2H values requires the existence of inert tissues in which the δ^2H value of the earlier stages of life (i.e., larval stage) is preserved as the animal migrates (Hobson et al., 2010). In insects, neither enamel nor keratin is present (McKittrick et al., 2012). When applying isotope geolocation to track migratory insects, it has long been assumed that the δ^2H values of chitinous insect wing tissues reflect the location of natal origin (i.e., larval stage; e.g., Hobson, 1999; Flockhart et al., 2013; Stefanescu et al., 2016; Talavera et al., 2018; Vander Zanden et al., 2018; Hobson et al., 2019). However, the assumption that insect wing tissues preserve the isotope signal of the larval stage has not been properly verified (but see Holder, 2012; Hungate et al., 2016; Morra et al., 2021). This assumption is based on the idea that insect wings are analogous to bird feathers and mammal hair, which are metabolically inert after tissue formation and are mainly composed of keratin, a structural scleroprotein (Hobson, 1999; Holder, 2012). Hair and feathers are inert (i.e., "dead") tissues that preserve the δ^2H of the location of tissue formation, allowing isotope geolocation principles to be applied (Ehleringer et al., 2008; Hu et al., 2020). As hair grows continuously and feathers moult regularly, isotope geolocation principles can be applied to the hair and feathers to track adult migration and movement (e.g., Cryan et al., 2004; Fauberteau et al., 2021). In the case of insect wing tissues, it is assumed that isotope geolocation principles can also be applied because the tissues developed at the larval/pupa stage and were subsequently inert during adult life (Wassenaar and Hobson, 1998; Hobson, 1999). However, chitin, a structural polysaccharide (Ravi Kumar, 2000; Resh and Carde, 2009), fundamentally differs from keratin.

Although insect wings do not continuously grow or repair themselves following formation, these tissues are known to be metabolically active and do not qualify as inert tissues (Pass, 2018; Tsai et al., 2020). Insect wings are irrigated with hemolymph, the equivalent of blood in insects, which circulates in the insect for thermoregulation (Rawlins, 1980; Tsai et al., 2020) and for replacing water loss from evaporation (Wasserthal, 1983). Insect wings also require oxygen, water, nutrients, hormones, and, waste removal due to the presence of active "living" tissues, such as the epidermis and pheromone glands (Pass, 2018). The cuticle that makes up the wing membrane remains active during early adult life and undergoes sclerotization following eclosion. In the cuticle, hydrogen (in the form of OH) is used for cross-linking cuticular proteins during sclerotization (Wright, 1987; Hopkins and Kramer, 1992; Andersen, 2010). Due to the continued development of wing structures in the adult phase (i.e., tissue turn-over and tissue activity; Wright, 1987; Hopkins and Kramer, 1992; Andersen, 2010; Pass, 2018), food intake (Wyatt, 1961), and effects from metamorphosis (Morra et al., 2021), it is likely that the isotopic composition of the wing will change through time. As hydrogen isotopes, other isotope systems and trace elements are increasingly used in insect ecology studies, it is critical to investigate the potential influence of adult diet, insect age and, metabolic processes on insect wing isotope values.

In this study, we propose to revisit the assumption that the δ^2H values of wing tissues of migratory insects are not altered by adult diet and/or insect age. We use monarch butterflies (*Danaus plexippus*) as our study species for a series of laboratory feeding experiments. Monarch butterflies are an ideal species for this study as: (1) they are easily sexed, (2) they have large wings allowing the same individual to be sampled multiple times to test intra-wing differences, (3) they can live up to 8 months allowing changes in isotope composition to be tested across several weeks of adult feeding, and (4) caterpillars develop on a single host plant (*Asclepias* spp.). Additionally, hydrogen isotope geolocation has been used for decades to investigate the multi-generational annual round trip of the species between Mexico, the United States, and Canada (e.g., Hobson, 1999; Flockhart et al., 2013; Vander Zanden et al., 2018; Hobson et al., 2019; Reich et al., 2021). The assumption behind these studies is that the wings of monarch butterflies are inert after eclosion and preserve the δ^2H value of the larval stage throughout adult life (Hobson et al., 1999). Adult monarchs often travel across long distances and feed throughout their adult life on flower nectar found along their migratory paths (Brown and Chippendale, 1974). As the monarch butterfly migrates, the isotopic composition of the nectar along its path likely diverges from that of the site of larval development (Yapp and Epstein, 1982; Bowen, 2008; Hobson, 2019). We hypothesise that wing δ^2H may change through time and if some of the hydrogen ingested during adult feeding is incorporated into the wing tissue, it could influence the δ^2H value of the wing.

The secondary focus of this study is to further test if wing δ^2H values vary based on the wing sampling location by testing if there are intra-wing differences in δ^2H values in wings of migratory insects (i.e., monarch butterflies). As migratory insect wings are used for δ^2H geolocation, the wing sampling procedure and sampling location on the wing can vary based on wing wear, wing shade, wing pigmentation, insect species and wing size. To know if wing δ^2H can reliably be used

as a geolocation tool for migratory insects, it is essential to test if wing variations (i.e., shade, pigmentation, size, etc.) will affect wing δ^2H values. Previous studies have shown that wing δ^2H values vary based on the pigmentation within the sampling region (Hobson et al., 2017). In this study, we test if δ^2H values vary based on wing pigmentation (orange vs. black), wing shade (dark orange vs. light orange), the presence of major veins and the absence of wing scales in the wing sample. As insect wing tissues are not metabolically inert (Pass, 2018; Tsai et al., 2020), we predict that wing δ^2H values of migratory insects, specifically butterflies, will vary with the sampling location on the wing.

2. Materials and methods

2.1. Feeding experiment

To test if the wings of migratory insects preserve the δ^2H values of the larval stage, feeding experiments for monarch butterflies were designed. In summary, monarch caterpillars were fed a diet with a distinct δ^2H value, then upon emerging from the chrysalis as adults (i.e., eclosion) they are either provided with no food or provided with an enriched deuterium diet. The approach used in this study is summarised in Figure 1.

2.1.1. Larval stage

In August 2021, 67 eggs were collected from laboratory-raised monarch butterflies from the Department of Biology at the University of Ottawa. All of the 67 eggs were collected from the same female monarch butterfly. The eggs were harvested and transferred to fresh milkweed leaves. At the larval stage, caterpillars were fed every day with wild common milkweed (*Asclepias syriaca*) collected daily from the same urban green area in Ottawa, Ontario (45°24′48″ N, 75°39′53″ W) between August and September 2021. The caterpillars were contained individually in mason jars with a screen netting and frass was removed daily. The caterpillars were kept at room temperature and exposed to natural daylight cues. A humidifier was placed in the room to mimic natural humidity to promote successful ecdysis. We expect that any surficial absorption of hydrogen by the milkweed leaves from the humidifier will have little to no influence on the δ^2H of the caterpillars. Holder (2012) showed that the δ^2H in insect wings, specifically Lepidoptera, are largely derived from plant or leaf solid and only minimally influenced by plant or leaf water. Additionally, the hydrogen provided by the leaf solid and plant water will far outweigh contributions of hydrogen absorbed on the leaf surface from the ambient environment, thus minimising any contribution of hydrogen from water vapour provided by the humidifier. One day after the caterpillars entered the pupal phase, the chrysalises were tied at the base and strung to ensure that the chrysalis would not fall or be squished by the side of the mason jar. As the mason jar may not be sufficient for the butterflies to grip, a thin piece of fabric was placed in the mason jar. By tying the chrysalises and placing fabric in the mason jar, the butterflies will have ample space to hang and pump their wings following eclosion. The larval and pupal stages took place from the end of August to mid-October 2021. The monarch butterflies enclosed from the chrysalises throughout September and October 2021. Of the 67 eggs, 56 monarchs reached the adult stage.

2.1.2. Adult stage

To test if an isotopically distinct adult diet from that of the larval stage alters the δ^2H values in the wings of monarch butterflies, monarchs

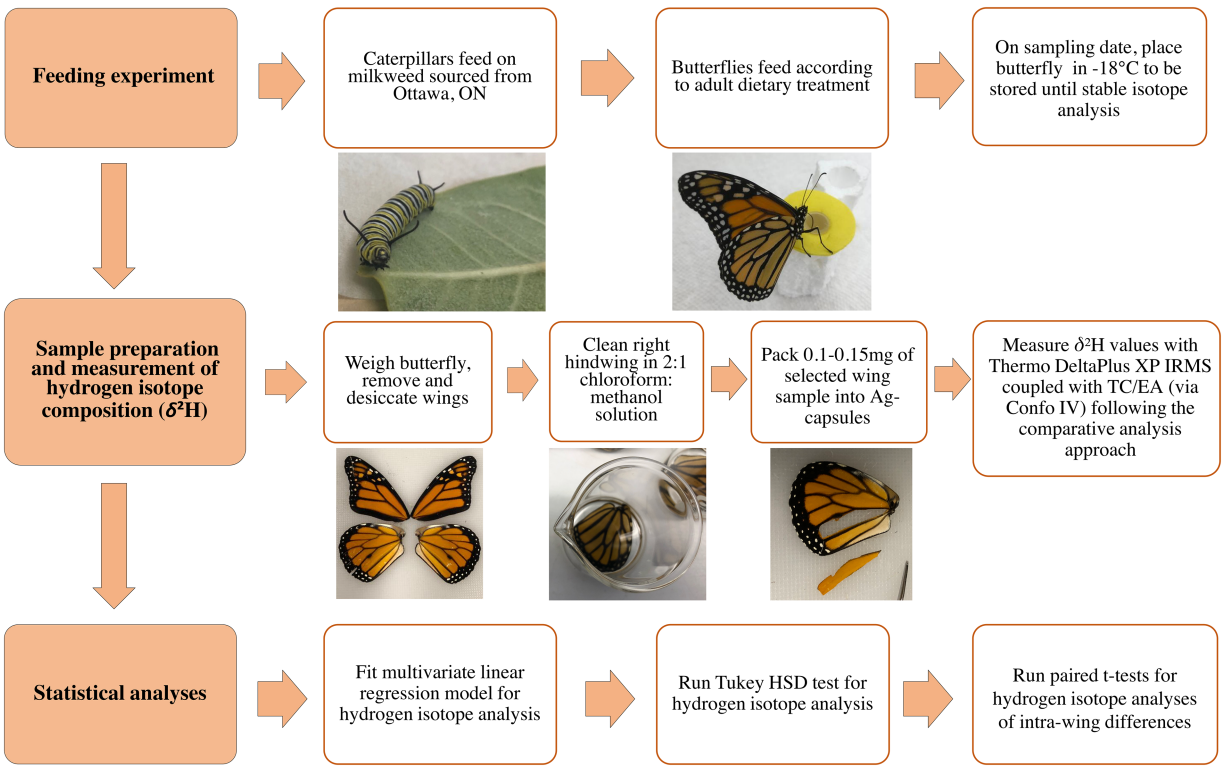

FIGURE 1
Flow chart summarising the methodology used in this study into three main stages with sub-steps depicting the procedure used to rear monarch butterflies in the feeding experiment, prepare wing samples, measure δ^2H and perform statistical analyses.

were assigned to one of two adult dietary treatments. In the first adult dietary treatment, the "enriched treatment," adult monarch butterflies were fed a solution of 2:1 deuterium-enriched water (δ^2H = +78‰): New Zealand honey. The deuterium-enriched water was obtained by boiling sequentially several litres of water to distil the heavy isotopes and regularly measured δ^2H values using a Los Gatos Cavity Ringdown Spectroscopy instrument at the University of Ottawa. The δ^2H value of the adult diet water (δ^2H = +78‰) was highly enriched in deuterium relative to estimates for the larval diet water (δ^2H = −62 ± 2.1‰; Bowen et al., 2005). We estimated the larval diet water based on the δ^2H value for the Ottawa region of the global growing season precipitation hydrogen isoscape (Bowen et al., 2005). We assumed that plant tissues preserve the δ^2H value of local precipitation with minimal change (Hobson et al., 2010; Holder, 2012). In the second adult dietary treatment, the "starvation treatment," adult monarch butterflies were not provided with food or water. This treatment was used to test the influence of physiology on the wing δ^2H values with no influence from the adult diet. To test if wing δ^2H values are influenced by the butterfly's age following eclosion, henceforth referred to as butterfly age (days), the monarch butterflies were assigned to a specific sampling date (0–24 days following eclosion). In total, six monarch butterflies (three females, three males) were sampled on the day of their eclosion (i.e., day 0), which is the reference δ^2H value for the larval stage without alteration from butterfly age and/or adult diet. The monarch butterflies in the starvation treatment were sampled at 2, 4 and 6 days following eclosion, whilst the monarch butterflies in the enriched treatment were sampled at 4, 6, 12, 18 and 24 days following eclosion. The design was unbalanced to accommodate the expectation that monarchs in the starvation treatment would show increasing rates of natural mortality with time. In total, 31 monarch butterflies (14 females, 17 males) were assigned to the enriched treatment and 19 monarch butterflies (10 females, 9 males) were assigned to the starvation treatment.

Upon eclosion, the monarch butterflies that were not assigned to a day 0 sampling date were carefully transferred to netting cages. Each small and medium-sized cage contained one monarch butterfly, whereas the large cages contained two monarch butterflies that were separated by a piece of fabric. The adults were kept at room temperature and were not exposed to a humidifier or natural daylight, so there was a strict lights schedule paired with lights on a timer to mimic natural daylight cues (~12:12). The monarch butterflies in the enriched treatment were encouraged to feed on the 2:1 deuterium-enriched water: New Zealand honey mixture daily for a minimum of 2 minutes. Since the butterflies do not always recognise the artificial food source, they were hand-fed to ensure they would ingest the deuterium-enriched diet. To feed the monarch butterflies, the deuterium-enriched water and honey solution was put into small faux-flower tubes at the centre of a butterfly feeder. The monarch butterfly was gently captured and placed on the feeder, where a thin paintbrush was used to expose the proboscis and hold it in the deuterium-enriched water and honey mixture. If the butterfly began to feed on its own, the paintbrush was removed. No monarch butterflies were fed on the day of eclosion as the wings and proboscis were too delicate to be handled.

On the assigned sampling date, sampled monarch butterflies were not fed, irrespective of treatment, and were placed in an envelope. The envelope and butterfly were then weighed to obtain the butterfly wet weight. The monarch butterflies were killed by freezing and were stored at −18°C until stable isotope analysis. The monarch butterflies sampled on day 0 (i.e., day of eclosion), were killed by freezing 2–4 hours after emergence from the chrysalis.

2.2. Sample preparation

Before the δ^2H values of the wings were measured, the wings underwent a sampling preparation procedure (Figure 1) and a location on the wing was selected to undergo stable isotope analysis (Figure 2). The wings were assigned a wing wear score (1–5) which represents the physical condition of the wing, 1 being wings in perfect condition and 5 being wings in which the majority of scales were removed and there is significant tearing of the wing (Flockhart et al., 2013). The wings were then removed from the thorax. The wings and bodies were desiccated at 65°C and the bodies were weighed (i.e., butterfly dry weight), including only the head, thorax, and abdomen to account for differences in physical damage (e.g., loss of scales and torn wings).

Next, the wings were cleaned using the 2:1 chloroform:methanol solution to remove lipids, dust, and contaminates from the wings that could have impacted the δ^2H values of the wing samples (Paritte and Kelly, 2009; Hobson et al., 2017). The wings were washed three times for 60, 30, and 15 minutes, respectively, with agitation and were flipped halfway through each wash. The wings were air dried in a class-100 fume hood before the wing sample is taken.

A standard wing sample was taken in the lower distal portion of the wing that is dark orange, veinless, and scaled (location S, Figure 2). To test if there are intra-wing differences in δ^2H values based on wing pigmentation, wing shade, presence of major veins, or the absence of scales in the wing sample, for each butterfly, a second sample of the wing was taken to be compared to the standard wing sample (Figure 2). The butterflies were accordingly assigned a secondary sample (i.e., black wing sample, light orange wing sample, wing sample containing vein and wing sample without scales) to ensure that age (i.e., 0–24 days), sex and dietary treatment (i.e., starvation or enriched) were distributed for all of the secondary samples. To test for differences in pigmentation, a black

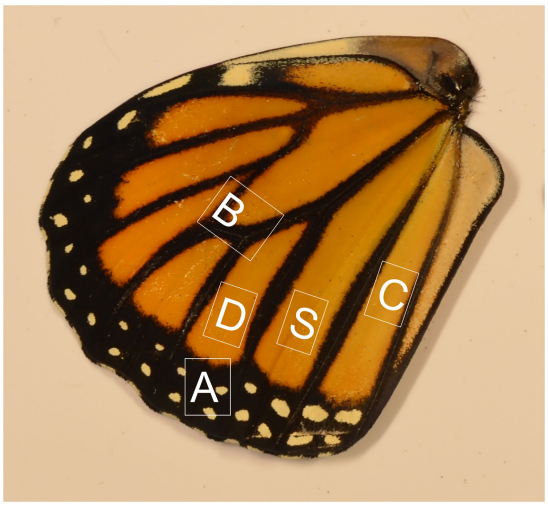

FIGURE 2
Annotated photo depicting the location of samples on the right hindwing. S is the location of the standard samples (dark orange, no vein and scaled), A is the location of black samples, B is the location of samples with vein, C is the location of light orange samples, and D is the location of samples with no scales (scales were manually removed). Results from samples from location S were used for linear regression modelling and the Tukey HSD test for the δ^2H of wing samples analysis. Results from samples from locations S, A, B, C, and D were used for the paired *t*-tests for the analysis of intra-wing differences.

pigmented wing sample was taken (location A, Figure 2). A sample was taken from a light orange section of the wing (location C, Figure 2), in contrast with the dark orange shade of the standard sample, to look for differences due to wing shade. To explore the influence of wing veins on intra-wing δ^2H values, samples were taken across a prominent wing vein (location B, Figure 2). Finally, scales were manually removed with a paintbrush (location D, Figure 2) to detect any influence of wing wear scores on δ^2H values.

2.3. Stable isotope analysis

For each individual, we sampled 0.10–0.15 mg of wing tissues packed into silver capsules. The δ^2H values of the non-exchangeable hydrogen of butterfly wings were determined at the Ján Veizer Stable Isotope Laboratory at the University of Ottawa using the comparative analysis approach similar to Wassenaar and Hobson (2003). We performed hydrogen isotopic measurements on H_2 gas derived from high-temperature (1,400°C) flash pyrolysis (TCEA, Thermo, Germany) of 0.15 ± 0.10 mg of wing subsamples, along with keratin standards: Caribou Hoof Standard (CBS; $\delta^2H = -157.0 \pm 0.9$‰), Kudo Horn Standard (KHS; $\delta^2H = -35.3 \pm 1.1$‰; Soto et al., 2017), USGS42 hair ($\delta^2H = -72.9 \pm 2.2$‰), USGS43 hair ($\delta^2H = -44.4 \pm 2.0$‰; Coplen and Qi, 2012), and two internal standards made of chitin material: ground and homogenised spongy moths (*Lymantria dispar dispar,* Linnaeus, 1,758; $\delta^2H = -64 \pm 0.8$‰) and Alfa Aesar chitin ($\delta^2H = -22 \pm 1.2$‰). The resultant separated H_2 flowed to a Conflow IV (Thermo, Germany) interfaced to a Delta V Plus IRMS (Thermo, Germany) for δ^2H analysis. The USGS42 hair sample was calibrated with a three-point calibration curve to the reference materials (i.e., CBS, KHS and USGS43), whilst USGS42 and the two chitin internal standards were used as quality checks. The measured δ^2H values for USGS42 (-73 ± 1.0, $n = 4$), spongy moths (-64 ± 0.8, $n = 6$), and Alfa Aesar chitin (-23 ± 1.0, $n = 4$) were within the reported value and uncertainty. The analytical precision of these measurements is based on the reproducibility of USGS42 and the chitin internal standards and is better than ±2‰. All δ^2H measurements are reported following the international scale VSMOW-SLAP.

2.4. Statistical analysis

We subdivided the dataset into four categories: (1) starvation, which were butterflies in the starvation treatment aged 2–6 days ($n = 19$), (2) early enriched, which were butterflies in the enriched treatment aged 2–6 days ($n = 14$), (3) late enriched, which were butterflies in the enriched treatment older than 6 days ($n = 15$) and (4) day 0, which can be considered the control treatment as they were not aged or exposed to the adult diet ($n = 5$). These four categories subdivide the dataset into comparable groups based on adult dietary treatment and time and are henceforth referred to as treatment-time. To test if the deuterium-enriched diet and/or insect age altered the δ^2H values of wing tissues of monarch butterflies, a multivariate linear regression and Tukey HSD test were applied to compare the wing δ^2H values of the monarch butterflies in the four treatment-time categories. To test if there are intra-wing differences in δ^2H values based on wing pigmentation (orange vs. black), wing shade (dark orange vs. light orange), the presence of major veins, and the absence of wing scales in the wing sample, paired *t*-tests were applied to compare the δ^2H values of these groups. All of the data collected and used for statistical analysis can be found in Supplementary Table 1.

2.4.1. Multivariate linear regression

We ran a multivariate linear regression model to test the correlation between categorical, continuous and discrete predictor variables (i.e., adult dietary treatment and time categories, sex, dry butterfly weight (g), percent hydrogen of the wing sample and date of eclosion) and wing δ^2H. For the multivariate linear regression samples, EL20, EL22 and EL23 were removed as outliers. EL20 is a monarch butterfly that was sampled on the day of eclosion and yielded a δ^2H value of −115‰, which is an outlier from the rest of the dataset as seen in Supplementary Figure 1. EL22 and EL23 were lost during isotope analysis due to autosampler malfunction. The linear regression model was performed using the *ols* linear model function of the *statsmodels.formula.api* package in Python3 (Seabold and Perktold, 2010).

To test whether wing δ^2H values (from sampling location S; Figure 2) are correlated to adult dietary treatment and time categories, sex, dry butterfly weight (g), percent hydrogen of the wing sample, and date of eclosion, a multivariate linear regression model was applied. Model assumptions of normality and homoscedasticity were visually confirmed before running the multivariate linear regression model (Supplementary Figure 2).

As there is a sample size of 53, five independent variables were selected for the linear regression model (abiding by the recommended 10 samples:1 variable ratio; Peduzzi et al., 1996). Sex and dry butterfly weight were selected as independent variables to test if the sex or size of the butterfly were correlated to wing δ^2H values. Dry butterfly weight and wet butterfly weight have a direct linear correlation (Supplementary Figure 3), so either can be used as an independent variable in the model. The independent variables all had a normal or close to a normal distribution, but a log transformation was applied to dry butterfly weight (Supplementary Figure 4). The percent hydrogen of the wing sample (Supplementary Figure 5) was selected as an independent variable to test if the proportion of hydrogen in an individual wing sample is correlated with δ^2H values, as the quantity of hydrogen in a given sample may differ based on adult dietary treatment. As individuals enclosed across 3 weeks and were fed milkweed collected during their larval stages, we tested whether the date of eclosion affected wing δ^2H values (Supplementary Figure 6). The date of eclosion variable was first converted to a DateTime data type using the *datetime* function in Python3 (Van Rossum and Drake, 2009). Weight of wing sample and wing wear score were excluded as independent variables as they showed no univariate correlations to wing δ^2H values, with an r^2 of 0.019 and 0.000, respectively (Supplementary Figures 7, 8).

2.4.2. Tukey HSD test

A *post hoc* multiple comparison Tukey HSD test was used to identify differences between the four treatment-time categories: (1) starvation, (2) early enriched, (3) late enriched and (4) day 0. Since the δ^2H values of wing samples had a close to normal distribution, as seen in Supplementary Figure 2, a Tukey HSD test could reliably be applied to this dataset. The outliers removed for the multivariate linear regression model were also removed for the Tukey HSD test. The Tukey HSD test was performed using the *stats* pairwise Tukey function from the *statsmodels. Regression.linear_model.OLSResults.t_test_pairwise* package in Python3 (Seabold and Perktold, 2010).

2.4.3. Paired *t*-tests

Paired *t*-tests were applied to test the intra-wing differences in δ^2H values based on different wing sample locations. We compared the δ^2H values of the standard sample (i.e., dark orange, vein-less, scaled;

location S, Figure 2), to the δ^2H of either a black wing sample ($n = 12$, location A, Figure 2), a light orange wing sample ($n = 13$, location C, Figure 2), a wing sample containing vein ($n = 13$, location B, Figure 2), or a wing sample with no scales ($n = 12$, location D, Figure 2), on the same individual. In addition to the previously removed outliers, EL2, EL19 and, EL54 were removed for the paired *t*-tests. EL2 had a sample weight of 0 mg likely due to an error during sample capsule packing. EL19 was removed as an outlier as it had a much higher wet butterfly weight (0.64 mg) compared to that of the others. EL54 was lost during isotope analysis due to autosampler malfunction. The paired *t*-tests were performed using the *stats t*-test function of the *scipy* package in Python3 (Virtanen et al., 2020).

3. Results

3.1. Trends in wing δ^2H based on adult diet and insect age

The trends for wing δ^2H values from the standard location (location S, Figure 2) are observed in Figure 3. The mean δ^2H value of wings from monarch butterflies sampled on the day of eclosion (day 0) was -104 ± 1.7‰ ($n = 5$; Figure 3). This is the reference δ^2H value of the larval stages with no influence from adult diet, butterfly age and/or physiology. The δ^2H values of the wings of monarch butterflies from the enriched treatment were higher than those of the starvation treatment (Figure 3). The mean wing δ^2H value from the enriched treatment was -100 ± 4.8‰ ($n = 29$) and for the starvation treatment was -104 ± 4.0‰ ($n = 19$). The δ^2H values of the wing samples appeared to vary based on the butterfly's age for both adult dietary treatments (Figure 3). The most notable changes to δ^2H values occurred during the first 4 days following eclosion (Figure 3). δ^2H values in both adult dietary treatments peaked at days 2 and 4, before leveling off towards the expected δ^2H value from the larval stage (i.e., −104‰; Figure 3).

The linear regression model explained approximately half of the variance in wing δ^2H values (Adj. $r^2 = 0.51$; Table 1). The correlation of wing δ^2H values with sex, dry butterfly weight, and percent hydrogen were not statistically significant (i.e., *p*-values of 0.958, 0.267 and 0.168, respectively; Table 1). Day of eclosion was significantly associated with wing δ^2H values, with an average increase of ~0.4‰ per day ($\beta = 0.37 \pm 0.09$, $p < 0.001$; Table 1 and Supplementary Figure 6). The treatment-time categorical variable was also significantly associated with wing δ^2H values (Table 2; Figure 3). The comparisons of treatment-time groups using the post-hoc Tukey HSD test found significant differences between the early enriched and day 0 categories ($p = 0.004$), and the early enriched and starvation categories ($p = 0.03$) (Table 2). The early enriched category was on average more enriched than the day 0 category by ~6‰ and more enriched than the starvation category

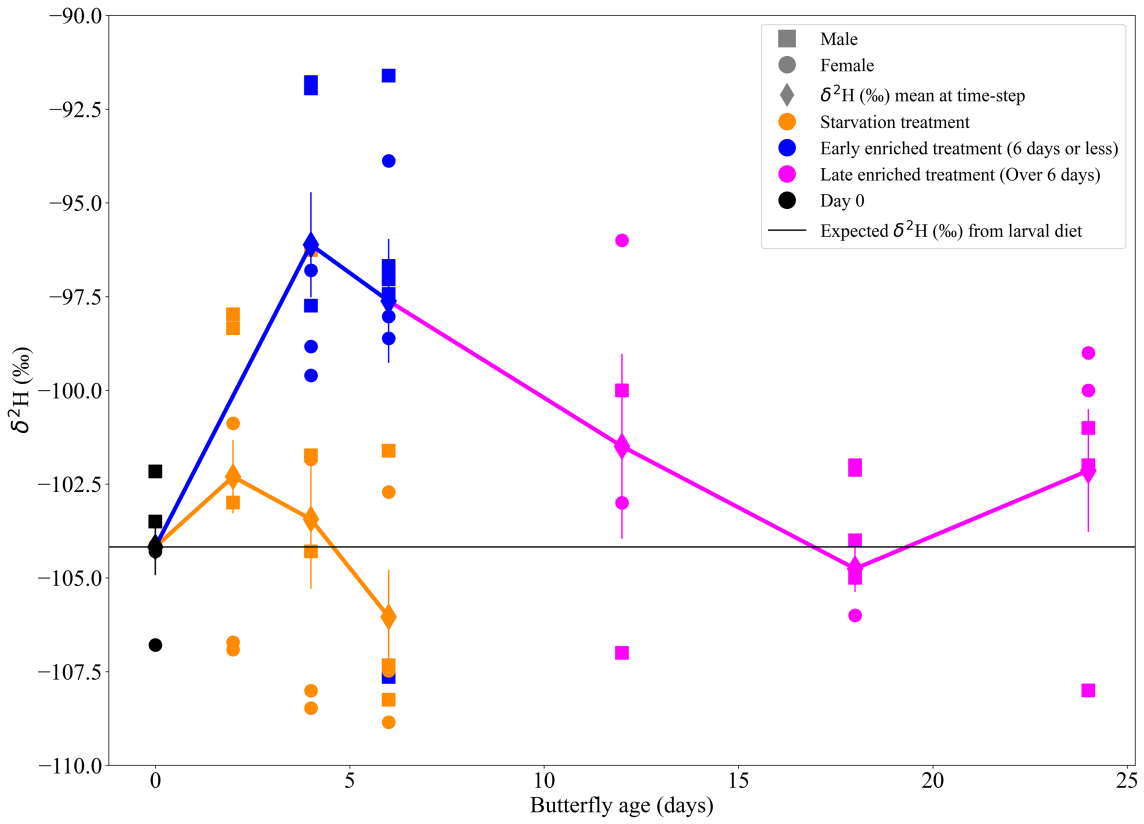

FIGURE 3
Scatter plot of δ^2H (‰) of wing samples (from location S), shown over butterfly age (days) depicted by sex and adult dietary treatments (starvation and enriched) which are organised into four categories [(1) starvation, n=19; (2) early enriched, n=14; (3) late enriched, n=15; and (4) day 0, n=5]. The trendlines show the mean δ^2H values of the two adult dietary treatments over butterfly age. The error bars represent the standard error of the mean for each treatment on a specific day. The horizontal line at –104‰ depicts the day 0 δ^2H mean, which is assumed to be the δ^2H reflecting that of larval stages with no influence from adult diet or physiology.

TABLE 1 Table showing the results of the multivariate fixed effect linear regression model for wing δ^2H with the independent variables (sex, treatment-time, percent hydrogen of wing sample, date of eclosion and dry weight of butterfly), coefficient of variable in linear regression, and *p*-value depicting the significance of the correlation, and the standard error for the variable.

Independent variable	Coefficient	*p*-value ($p > \|t\|$)	Standard error
Treatment-time (Early enriched)	6.192	0.001	1.685
Treatment-time (Late enriched)	2.754	0.131	1.790
Treatment-time (Starvation)	2.289	0.186	1.706
Sex (Male)	0.048	0.958	0.921
Percent hydrogen of wing sample	−1.089	0.168	0.778
Dry butterfly weight (g)	6.751	0.267	6.003
Date of eclosion	0.365	<0.001	0.086

This multivariate linear regression model has an intercept of −2.693e^5 and an adjusted r^2 of 0.519.

TABLE 2 Table showing the Tukey HSD test results based on wing δ^2H between the four categories: (1) early enriched, (2) late enriched, (3) starvation, and (4) day 0. The table shows the compared categories (Group 1−Group 2), the mean δ^2H difference between the compared groups, the adjusted *p*-value and if the null hypothesis (H0) is rejected.

Group 1	Group 2	Mean difference	Adjusted *p*-value	Reject H0
Early enriched	Day 0	6.192	0.004	True
Late enriched	Day 0	2.754	0.372	False
Starvation	Day 0	2.289	0.372	False
Late enriched	Early enriched	−3.437	0.102	False
Starvation	Early enriched	−3.903	0.028	True
Starvation	Late enriched	−0.465	0.700	False

The null hypothesis (H0) for the Tukey HSD tests states that the groups being compared have equal means.

by ~4‰ (Table 2; Figure 4). All other comparisons were not statistically significant, with late enriched and day 0 ($p = 0.4$), starvation and day 0 ($p = 0.4$), late enriched and early enriched ($p = 0.1$), starvation and late enriched ($p = 0.7$) (Table 2; Figure 4).

3.2. Intra-wing differences in δ^2H values

Tests of intra-wing δ^2H variability found that the δ^2H values between the paired variables of wing shade (dark orange vs. light orange), wing pigmentation (orange vs. black) and scaled vs. non-scaled wing samples were not significantly different (*t*-test; *p*-values of 0.276, 0.065 and 0.950, respectively; Table 3), with mean wing δ^2H differences of −1.1‰, −2.1‰, and, 0.06‰, respectively, (Table 3; Figure 5). The mean δ^2H of wing samples with veins compared to wing samples without veins on the same individual were significantly different (*t*-test; $p < 0.001$; Table 3), with samples with veins having δ^2H values ~9‰ more enriched than those without veins (Table 3; Figure 5).

4. Discussion

4.1. Identifying non-significant controls on δ^2H values in butterfly wings

As indicated by the multivariate linear regression model, sex, percent hydrogen of wing sample and dry weight of the butterfly do not have a significant influence on δ^2H values in wings (Table 1). This experiment demonstrates that if metabolism influences the fractionation of hydrogen isotopes in wings, this influence is not related to the adult body mass and/or sex of the individual, which supports the findings of Hobson et al. (2017). When using isotopes to trace the migration of butterfly species, the sample set often includes individuals of different sizes. For example, monarch butterflies have different phenotypes depending on the summer or overwintering generations (Altizer and Davis, 2010; Flockhart et al., 2017). Similarly, sex is often challenging to identify for some butterfly species (e.g., *Papilio victorinus and Papilio glaucus*; Glassberg, 2017). The lack of influence of morphology and sex validates the use of δ^2H geolocation tools for a sample set composed of randomly collected individuals (e.g., Flockhart et al., 2013).

Wing shade (dark orange vs. light orange), wing pigmentation (orange vs. black) and the absence of scales show an insignificant and negligible isotopic effect on wing δ^2H values (Table 3; Figure 5). Our findings differ from those of Hobson et al. (2017), who demonstrated that wing pigmentation (i.e., black vs. orange) and the absence of wing scales influenced wing δ^2H values, though this effect was small with little variation between wing quadrants. Hobson et al. (2017) also demonstrated that proper sampling procedures and wing washing (i.e., 2:1 chloroform:methanol solution) minimised the intra-wing variations of δ^2H values (Hobson et al., 2017). We demonstrate that worn wings have approximately the same isotopic composition as fresh wings (Figure 5). This is important because migratory insects travel great distances, and their wings tend to be worn with significant scale loss (Flockhart et al., 2017). Similarly, sampling different portions of the wings with distinct pigmentation and shades will have only a small impact on the measured δ^2H values as long as veins are avoided (Figure 5). The combined findings of this study and Hobson et al. (2017) further support the applicability of hydrogen isotope geolocation of migratory insects' wings.

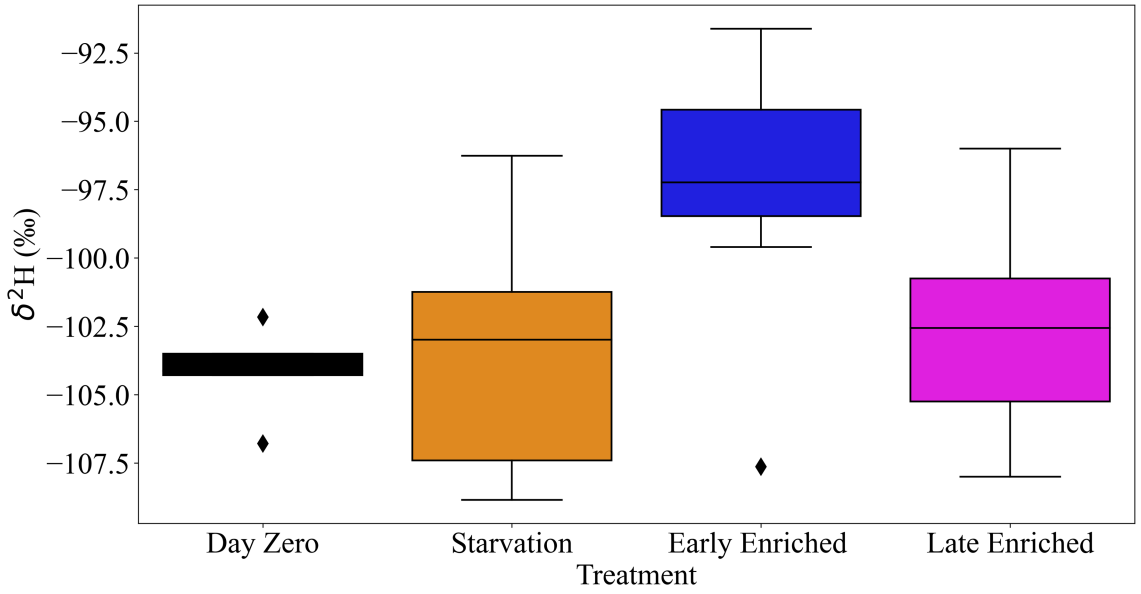

FIGURE 4
Box and whisker plot of δ^2H (‰) of wing samples (from location S), for the four categories of the treatment-time variable [(1) starvation, n=19; (2) early enriched, n=14; (3) late enriched, n=15; and (4) day 0, n=5]. The starvation and early enriched categories have a mean difference of 4‰ and the day 0 and early enriched categories have a mean difference of ~6‰. Black diamond points indicate outliers.

TABLE 3 Table showing the paired *t*-test results for intra-wing differences in δ^2H of wing samples based on wing colour (orange vs. black), wing pigmentation (dark orange vs. light orange), vein vs. no vein in wing sample and scaled vs. non-scaled wing samples within an individual.

Paired variables	Degrees of freedom	Difference [*t*(df)]	*p*-value
Orange vs. black	11	−2.050	0.065
Dark orange vs. light orange	12	−1.142	0.276
No vein vs. vein	12	−9.142	< 0.001
Scaled vs. non-scaled	11	0.064	0.950

The table shows the paired variables, the degrees of freedom (df; i.e., $n-1$), the mean difference [*t*(df)] between the paired variables and the associated *p*-value showing the significance of the difference.

4.2. Identifying significant controls on δ^2H values in butterfly wings

On day 0 (day of eclosion), most individuals have a similar wing δ^2H value of -104 ± 1.7‰ ($n=5$; Figure 3). If we calculate the expected δ^2H values in wings using an existing calibration equation (i.e., $\delta^2H_{wing} = 0.78 \times \delta^2H_{GSP} - 51.63$) from known-origin monarch butterfly individuals from Hobson et al. (2019) and local growing season precipitation (GSP) in Ottawa (-62 ± 2.1‰; Bowen et al., 2005), we find an expected δ^2H value of -101 ± 3.5‰ for local monarch butterfly wings. This value is within the uncertainty of the measured δ^2H values, confirming the major and predictable influence of larval diet on the wing δ^2H value. However, we also notice that at a single location with a well-controlled laboratory setting the intra-population δ^2H variance at day 0 is only slightly larger (~2.27‰, $n=5$) than the analytical uncertainty (>2.00‰; Figure 3). Interestingly, we also notice that the δ^2H variance is larger on most days (e.g., starvation treatment days 4 and 6, enriched treatment days 4, 6, 12 and, 24) than on day 0, underlining the probable role of metabolic processes in fractionating the isotopes differently in each adult (Figure 3).

We found that wing δ^2H values increase with later eclosion dates (Table 1; Supplementary Figure 6). As the milkweed leaves were collected daily throughout August and September 2021, changes in milkweed senescence and local weather events (i.e., thunderstorms, changes in temperature and/or humidity) may have altered milkweed δ^2H values throughout the feeding experiment, potentially altering larval diet δ^2H values and driving the observed changes in wing δ^2H values associated with the date of eclosion. Considering that all milkweed leaves were collected within a month and on the same 30 m^2 patch of land, this is a surprising result but underlines the potentially rapid changes in δ^2H values in soil water influencing larval diet and δ^2H values of known origin individuals. Alternatively, but less likely, the effect of eclosion dates on δ^2H values might be a result of the conditions in which the larvae were reared which were not perfectly controlled, such as the δ^2H value of ambient water vapour (e.g., from the humidifier). To avoid such an effect, we recommend that future studies rear the caterpillars and butterflies in growth chambers where temperature and humidity can be tightly controlled.

As the early enriched and starvation categories occur over the same time span (6 days or less), the significant difference of ~4‰ in wing δ^2H values between these categories provides evidence that adult diet influences wing δ^2H values and thus wings are not inert tissues (Tables 1, 2; Figures 3, 4). Our work investigating the δ^2H values based on wing sampling location further supports the hypothesis that adult diet

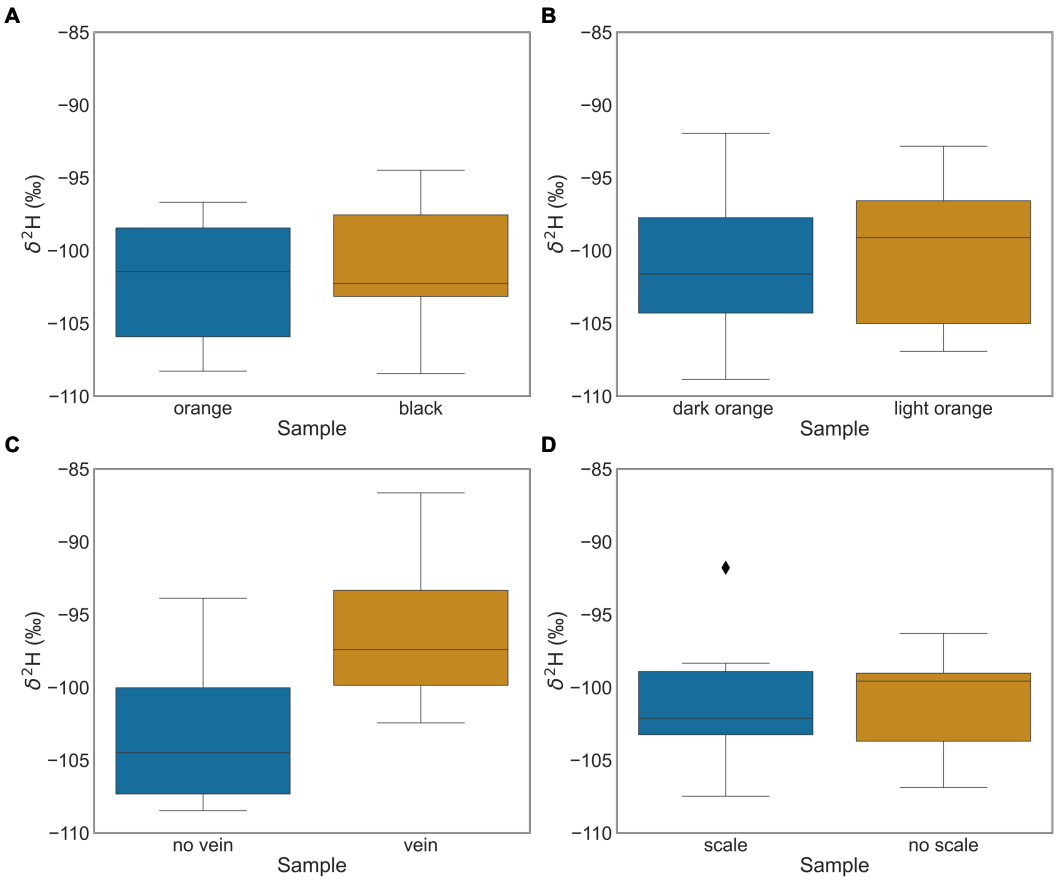

FIGURE 5
Box and whisker plots of intra-wing differences in δ^2H (‰), comparing the standard wing samples (from location S) to **(A)** wing pigmentation (orange vs. black), n=12; **(B)** wing shade (dark orange vs. light orange), n=13; (**C***) vein or no vein wing samples, n=13; and **(D)** scaled or non-scaled wing samples, n=12. There is a mean difference of ~9‰ between samples containing veins and samples with no veins. Panel C* has an asterix to indicate statistical significance between the compared intra-wing differences in δ^2H (‰; i.e., vein or no vein wing samples). Black diamond points indicate outliers.

influences wing δ^2H values. There is a significant difference of ~9‰ in the δ^2H values of wing samples containing a high density of veins to wing samples with no veins (Table 3; Figure 5). We suggest that wing veins have greater variation in δ^2H values, and greater influence from the adult diet because they are made of metabolically active endocuticle tissues. Endocuticle tissues undergo active physiological processes (Pass, 2018; Tsai et al., 2020) and contain a large volume of metabolically active hemolymph (Wyatt, 1961; Emmel, 2012; Pass, 2018) which provides constant hydration to the wing veins (Wasserthal, 1983); therefore, it is expected that the δ^2H value of the wing veins may vary from that of the rest of the wing, as observed in this study. This second experiment confirms that hemolymph and veins have a significant portion of newly metabolised hydrogen influenced by the adult diet and/or metabolic processes. We recommend that, as much as possible, veins should be avoided when using insect tissues for geolocation. This might not be currently feasible for small species where entire wings are needed for δ^2H analysis or for other isotope analyses that require larger wing samples (e.g., Sr wing analysis; Reich et al., 2021). However, with advances in mass spectrometry, the required sampling mass is rapidly decreasing and avoiding veins should become a more common practise.

We suggest that the pronounced δ^2H change during early adult life (i.e., 2–6 days post-eclosion) is strengthened by early adult wing formation processes (Figure 3). The early enriched and day 0 categories had the greatest significant mean δ^2H difference (~6‰) relative to any of the other compared categories, but the early enriched category was only enriched over the starvation category by ~4‰ (Table 2; Figure 3). We suggest that the remaining difference between the day 0 and starvation categories (~2‰), although not significant, is likely due to an additional influence from non-dietary related processes, which also further enriched the wing δ^2H values in the early enriched treatment. Following eclosion, the wings are wet and fragile, and an increased hemolymph volume is pumped through the wing veins to facilitate hardening (Andersen, 2010; Emmel, 2012), whereas hardened mature wings do not have as great a volume of hemolymph circulating through the veins (Wasserthal, 1983; Emmel, 2012). We argue that during early adult wing formation, physiological processes (e.g., sclerotization, wing hardening) also fractionate hydrogen isotopes creating further isotope variations in the wing in early adult life. This is demonstrated as wing δ^2H values appeared to vary the most between 2 and 4 days following eclosion before converging towards the day 0 δ^2H mean (Figure 3). The hemolymph circulating in the wings is a fluid partially metabolised from the recent adult diet (Wyatt, 1961). We suggest that the decreased hemolymph volume in hardened mature wings (Wasserthal, 1983; Emmel, 2012) limits the influence of adult diet and/or physiology on wing δ^2H values. Thus, the δ^2H values of wings in the early enriched treatment increasingly diverge from their initial values towards those of the adult diet due to the high volume of deuterium-enriched hemolymph filling the wings (Wyatt, 1961; Wasserthal, 1983; Emmel, 2012).

However, as the individual ages, the δ^2H value of the wings trends back towards the initial values (Table 2; Figure 3). Fortunately, most sampling of migratory insects occurs at later stages of adult life after the individual migrated or dispersed. Alternatively, as observed in previous studies (e.g., McCue and Pollock, 2008; Doi et al., 2017) starvation conditions can lead to an isotopic starvation effect, where in our study this could account for the difference in δ^2H values between the day 0 and starvation categories. However, the starvation treatment was short (fewer than 6 days) and, prior to euthanizing the butterflies by freezing, all individuals were active and in overall good health. Therefore, we do not expect that the effects of starvation are driving our isotopic results. Nevertheless, as insect wings are not inert, as shown in this study and by Pass (2018), Tsai et al. (2020), and Morra et al. (2021), when an individual travels across large distances with varying isotopic values, adult diet and physiology could contribute a small amount to the isotope variability.

4.3. Isotope element cycling and isotope-based geographic assignments for migratory insects

We conclude that there is cycling of hydrogen isotopes in the wings of monarch butterflies which is influenced by the butterfly's age and adult diet. Our results support those of a previous feeding experiment performed using moths (*Helicoverpa. armigera*; Holder, 2012). We calculated that, for monarch butterflies, up to 8% of hydrogen isotopes in wing tissues are sourced from the adult diet (3.0 ± 3.2%; Supplementary Figure 9). We also found that early adult wing formation alters hydrogen isotopes by up to 2% (0.7 ± 0.9%; Supplementary Figure 10). These proportions may differ from those found by Holder (2012) for moths due to physiological differences between the insect species, and/or differences between experiments. However, the results from these studies support our hypothesis that wing tissues of migratory insects are not metabolically inert and that wing δ^2H will be altered by the isotopic composition of the adult diet and/or the insect's age.

We found that the influence of adult diet and physiology is small (average ~6‰ for an isotopic difference of ~140‰ between larval and adult stage diets) relative to the uncertainty generally associated with hydrogen-based geographic assignments of migratory insects. For example, the spatially explicit map of isoscape uncertainty in Reich et al. (2021) ranges from 6 to 19‰. This high uncertainty is due, in part, to the high intra-site δ^2H variance of known-origin individuals used to calibrate the tissue isoscape (Ma et al., 2020). Adult diet and physiology likely contribute to the high intra-site δ^2H variance observed in previous studies (e.g., Hobson et al., 1999, 2019; Morra et al., 2021). Whilst this high intra-site variance does not preclude using δ^2H geolocation, it sets inherent limits of this geolocation tool to provide specific geographic assignments for migratory insects. Other possible sources of intra-site isotope variance such as variations in the δ^2H of plants and water at one given site, should be further explored to develop a better understanding and prediction of this uncertainty (e.g., Magozzi et al., 2020). To minimise the uncertainty identified in this study, researchers should be careful to avoid sampling wing portions with veins, and they should also consider sampling individuals of similar ages (using for instance similar wing worn indices). Additionally, appropriate uncertainty propagation should be performed when relating the δ^2H of wing chitin and precipitation isoscapes to account for the inherent uncertainty of this geolocation tool (Ma et al., 2020). Using simple transfer equations relating δ^2H of wings with that of precipitation without accounting for the full uncertainty propagation (Ma et al., 2020) will yield overly optimistic geographic assignments.

4.4. Limitations and future studies

This study used a sample size of 53 monarch butterflies collected from the same mating pair. Future studies could test the isotope effect in a feeding experiment on individuals selected from different mating pairs to evaluate if natural population diversity would incorporate additional isotope uncertainty. As the date of eclosion had a significant effect on our study, individuals with identical dates of eclosion should be used in future studies to better control for potential isotopic differences in larval diets. Additionally, the monarch butterflies raised in this study could have been raised in growth chambers to minimise physiological and environmentally driven isotope fractionation. Studies testing the role of adult diet and physiology could also be conducted for other insect species of interest, given the diversity of natural-history strategies, including diets, in this large taxonomic group. The mechanisms of δ^2H changes over time could also be explored by expanding on recent work by Morra et al. (2021) by looking at how compound-specific (e.g., amino acids, lipids) δ^2H values of different life stages and tissues (e.g., caterpillars, frass, exuviae and wings) change over time. We also recommend testing other isotope systems [e.g., Sr (e.g., Reich et al. this issue), C, O, S etc.] in wings to further ensure that wings preserve the isotopic signal of the location of larval development over time. As there were only two adult dietary treatments, we propose further studies with multiple adult dietary treatments of varying isotopic compositions to have a deeper understanding of the role of adult diet in wing tissues of migratory insects, especially under natural conditions.

4.5. Summary

Through a feeding experiment with two adult dietary treatments, we tested whether the δ^2H values of wing tissues of migratory insects (i.e., monarch butterflies) were altered by adult diet and/or insect age. We found that the δ^2H value of the wings did not vary based on sex and body mass but showed significant effects from the adult diet, age, and the date of eclosion. We also showed that the intra-wing δ^2H values did not vary based on condition or pigmentation/shade of the wing but varied based on the presence of veins. We conclude that the effect of adult diet and age remains small and that the δ^2H values of wings can reasonably be used as an endogenous biochemical marker to track migratory insect species. We predict that for wild monarch butterflies where the difference between larval and adult diet is likely much smaller than in this study, the influence of adult diet will be minimal and potentially negligible (<4‰). However, our results suggest that wings cannot be assumed to be "dead" or "inert" tissues, and should no longer be referred to as such in isotope literature. We also caution researchers that adult diet and physiological processes contribute to a fraction of the large intra-site isotope variance observed in this isotopic system. Interestingly, the changes in δ^2H values based on eclosion dates underline the rapid isotopic variation of the larval diet and its impact on δ^2H values of known-origin individuals. In summary, we recommend that researchers carefully select wing samples from individuals of approximately the same age, collect samples from the same location and time period, avoid sampling veins, and take samples from the

same location on the wing to minimise δ^2H variation and the differential isotopic contribution from adult diet and insect age. We also recommend that researchers fully propagate the δ^2H uncertainty in their isoscapes as proposed by Ma et al. (2020). Whilst δ^2H geolocation has clear limitations and uncertainties, it remains a powerful tool for tracking the mobility and the natal origin of monarch butterflies and other migratory insect species in biological, ecological and conservation studies.

Data availability statement

The original contributions presented in the study are included in the article/Supplementary material; further inquiries can be directed to the corresponding authors.

Author contributions

CB, PH, and MR designed the experiment inspired by PH, 2012 Ph.D. Thesis. EL and MR reared monarch butterflies and carried out the feeding experiment. Sample preparation for stable isotope analysis and statistical analyses was performed by EL. EL led the writing of the manuscript. All authors contributed to the article and approved the submitted version.

Funding

CB and GT acknowledge funding from the SSHRC CRSH New Frontiers in Research Fund 2018 (NFRFE-2018-00738). MR acknowledges funding from the Ontario Graduate Scholarship 2021–2022. GT acknowledges funding from the grant PID2020-117739GA-I00 from MCIN/AEI/10.13039/501100011033 and the grant LINKA20399 from the CSIC iLink program. EL acknowledges funding from the G.G. Hatch Award of the Ján Veizer Stable Isotope Laboratory Scholarship, University of Ottawa, 2022, the TD Green Bursaries, 2021 and the O'Connor Associates Environmental Scholarship, 2021.

Acknowledgments

Monarchs for the feeding experiment were collected under Ontario Ministry of Natural Resources collection authorization #1098187. We would like to acknowledge members of the SAIVE Laboratory, Kharouba Laboratory and the Ján Veizer Stable Isotope Laboratory at the University of Ottawa for their guidance and assistance in this project. We would also like to thank Julien Martin for his advice on the statistical analyses.

Conflict of interest

The authors declare that the research was conducted in the absence of any commercial or financial relationships that could be construed as a potential conflict of interest.

Publisher's note

Supplementary material

The Supplementary material for this article can be found online at: https://www.frontiersin.org/articles/10.3389/fevo.2023.1060836/full#supplementary-material

References

Altizer, S., and Davis, A. K. (2010). Populations of monarch butterflies with different migratory behaviors show divergence in wing morphology. *Evolution* 64, 1018–1028. doi: 10.1111/j.1558-5646.2009.00946.x

Andersen, S. O. (2010). Insect cuticular sclerotization: a review. *Insect Biochem. Mol. Biol., Insect Cuticle* 40, 166–178. doi: 10.1016/j.ibmb.2009.10.007

Bataille, C. P., Crowley, B. E., Wooller, M. J., and Bowen, G. J. (2020). Advances in global bioavailable strontium isoscapes. *Palaeogeogr. Palaeoclimatol. Palaeoecol.* 555:109849. doi: 10.1016/j.palaeo.2020.109849

Bataille, C.P., Holstein, I.C.C.Von, Laffoon, J.E., Willmes, M., Liu, X.-M., and Davies, G.R. (2018). A bioavailable strontium isoscape for Western Europe: a machine learning approach. *PLoS One* 13:e0197386. doi:10.1371/journal.pone.0197386

Bowen, G. J. (2008). Spatial analysis of the intra-annual variation of precipitation isotope ratios and its climatological corollaries. *J. Geophys. Res. Atmos.* 113, 1–9. doi: 10.1029/2007JD009295

Bowen, G. J., and Revenaugh, J. (2003). Interpolating the isotopic composition of modern meteoric precipitation. *Water Resour. Res.* 39, 2–12. doi: 10.1029/2003WR002086

Bowen, G. J., Wassenaar, L. I., and Hobson, K. A. (2005). Global application of stable hydrogen and oxygen isotopes to wildlife forensics. *Oecologia* 143, 337–348. doi: 10.1007/s00442-004-1813-y

Britzke, E. R., Loeb, S. C., Romanek, C. S., Hobson, K. A., and Vonhof, M. J. (2012). Variation in catchment areas of Indiana bat (Myotis sodalis) hibernacula inferred from stable hydrogen ([[delta].Sup.2]H) isotope analysis. *Can. J. Zool.* 90, 1243–1250. doi: 10.1139/Z2012-093

Brown, J. J., and Chippendale, G. M. (1974). Migration of the monarch butterfly, *Danaus plexippus*: energy sources. *J. Insect Physiol.* 20, 1117–1130. doi: 10.1016/0022-1910(74)90218-2

Coplen, T. B. (2011). Guidelines and recommended terms for expression of stable-isotope-ratio and gas-ratio measurement results. *Rapid Commun. Mass Spectrom.* 25, 2538–2560. doi: 10.1002/rcm.5129

Coplen, T. B., and Qi, H. (2012). USGS42 and USGS43: human-hair stable hydrogen and oxygen isotopic reference materials and analytical methods for forensic science and implications for published measurement results. *Forensic Sci. Int.* 214, 135–141. doi: 10.1016/j.forsciint.2011.07.035

Cryan, P. M., Bogan, M. A., Rye, R. O., Landis, G. P., and Kester, C. L. (2004). Stable hydrogen isotope analysis of bat hair as evidence for seasonal molt and long-distance migration. *J. Mammal.* 85, 995–1001. doi: 10.1644/BRG-202

Doi, H., Akamatsu, F., and González, A. L. (2017). Starvation effects on nitrogen and carbon stable isotopes of animals: an insight from meta-analysis of fasting experiments. *R. Soc. Open Sci.* 4:170633. doi: 10.1098/rsos.170633

Ehleringer, J. R., Bowen, G. J., Chesson, L. A., West, A. G., Podlesak, D. W., and Cerling, T. E. (2008). Hydrogen and oxygen isotope ratios in human hair are related to geography. *Proc. Natl. Acad. Sci.* 105, 2788–2793. doi: 10.1073/pnas.0712228105

Emmel, T. C. (2012). Veterinary pediatrics of butterflies, moths, and other invertebrates. *Vet. Clin. Exot. Anim. Pract.* 15, 279–288. doi: 10.1016/j.cvex.2012.02.003

Fauberteau, A. E., Chartrand, M. M. G., Hu, L., St-Jean, G., and Bataille, C. P. (2021). Investigating a cold case using high-resolution multi-isotope profiles in human hair. *Forensic Chem.* 22:100300. doi: 10.1016/j.forc.2020.100300

Flockhart, D. T. T., Fitz-gerald, B., Brower, L. P., Derbyshire, R., Altizer, S., Hobson, K. A., et al. (2017). Migration distance as a selective episode for wing morphology in a migratory insect. *Mov. Ecol.* 5, 7–9. doi: 10.1186/s40462-017-0098-9

Flockhart, D. T. T., Wassenaar, L. I., Martin, T. G., Hobson, K. A., Wunder, M. B., and Norris, D. R. (2013). Tracking multi-generational colonization of the breeding grounds by monarch butterflies in eastern North America. *Proc. R. Soc. B Biol. Sci.* 280:20131087. doi: 10.1098/rspb.2013.1087

Glassberg, J. (2017). (eds.) *A Swift Guide to Butterflies of North America: 2nd Edn.* (Princeton: Princeton University: University Press), 18–29.

Hobson, K. A. (1999). Tracing origins and migration of wildlife using stable isotopes: a review. *Oecologia* 120, 314–326. doi: 10.1007/s004420050865

Hobson, K. A. (2019). *Chapter 4- Application of Isotopic Methods to Tracking Animal Movement Tracking Animal Migration with Stable Isotopes. 2nd Edn.* eds. K. A. Hobson and L. I. Wassenaar, (Amsterdam: Academic Press), 85–115.

Hobson, K. A., Barnett-Johnson, R., Cerling, T., and Hobson, K. A. (2010). "Using isoscapes to track animal migration," in *Isoscapes, Understanding Movement, Pattern, and Process on Earth Through Isotope Mapping*. eds. J. B. West, G. J. Bowen, T. E. Dawson and K. P. Tu (Dordrecht: Springer Netherlands), 273–298.

Hobson, K. A., Jinguji, H., Ichikawa, Y., Kusack, J. W., and Anderson, R. C. (2020). Long-distance migration of the globe skimmer dragonfly to Japan revealed using stable hydrogen (δ2H) isotopes. *Environ. Entomol.* 50, 247–255. doi: 10.1093/ee/nvaa147

Hobson, K. A., Kardynal, K. J., and Koehler, G. (2019). Expanding the isotopic toolbox to track monarch butterfly (*Danaus plexippus*) origins and migration: on the utility of stable oxygen isotope (δ18O) measurements. *Front. Ecol. Evol.* 7, 2–7. doi: 10.3389/fevo.2019.00224

Hobson, K. A., Plint, T., Serrano, E. G., Alvarez, X. M., Ramirez, I., and Longstaffe, F. J. (2017). Within-wing isotopic (δ2H, δ13C, δ15N) variation of monarch butterflies: implications for studies of migratory origins and diet. *Anim. Migr.* 4, 9–13. doi: 10.1515/ami-2017-0002

Hobson, K. A., and Wassenaar, L. I. (1996). Linking breeding and wintering grounds of neotropical migrant songbirds using stable hydrogen isotopic analysis of feathers. *Oecologia* 109, 142–148. doi: 10.1007/s004420050068

Hobson, K. A., Wassenaar, L. I., and Taylor, O. R. (1999). Stable isotopes (δD and δ13C) are geographic indicators of natal origins of monarch butterflies in eastern North America. *Oecologia* 120, 397–404. doi: 10.1007/s004420050872

Holder, (2012). *Isotopes and Trace Elements as Geographic Origin Markers for Biosecurity Pests*. New Zealand: Lincoln University

Hopkins, T. L., and Kramer, K. J. (1992). Insect cuticle sclerotization. *Annu. Rev. Entomol.* 37, 273–302. doi: 10.1146/annurev.en.37.010192.001421

Hu, L., Chartrand, M. M. G., St-Jean, G., Lopes, M., and Bataille, C. P. (2020). Assessing the reliability of mobility interpretation from a multi-isotope hair profile on a traveling individual. *Front. Ecol. Evol.* 8, 3–14. doi: 10.3389/fevo.2020.568943

Hungate, B. A., Kearns, D. N., Ogle, K., Caron, M., Marks, J. C., and Rogg, H. W. (2016). Hydrogen isotopes as a sentinel of biological invasion by the Japanese beetle, Popillia japonica (Newman). *PLoS One* 11:e0149599. doi: 10.1371/journal.pone.0149599

Kruszynski, C., Bailey, L. D., Courtiol, A., Bach, L., Bach, P., Göttsche, M., et al. (2021). Identifying migratory pathways of Nathusius' pipistrelles (Pipistrellus nathusii) using stable hydrogen and strontium isotopes. *Rapid Commun. Mass Spectrom.* 35:e9031. doi: 10.1002/rcm.9031

Lohmann, K. J. (2018). Animal migration research takes wing. *Curr. Biol.* 28, R952–R955. doi: 10.1016/j.cub.2018.08.016

Ma, C., Vander Zanden, H. B., Wunder, M. B., and Bowen, G. J. (2020). AssignR: an r package for isotope-based geographic assignment. *Methods Ecol. Evol.* 11, 996–1001. doi: 10.1111/2041-210X.13426

Magozzi, S., Vander Zanden, H. B., Wunder, M. B., Trueman, C. N., Pinney, K., Peers, D., et al. (2020). Combining models of environment, behavior, and physiology to predict tissue hydrogen and oxygen isotope variance among individual terrestrial animals. *Front. Ecol. Evol.* 8:536109. doi: 10.3389/fevo.2020.536109

McCue, M. D., and Pollock, E. D. (2008). Stable isotopes may provide evidence for starvation in reptiles. *Rapid Commun. Mass Spectrom.* 22, 2307–2314. doi: 10.1002/rcm.3615

McKittrick, J., Chen, P.-Y., Bodde, S. G., Yang, W., Novitskaya, E. E., and Meyers, M. A. (2012). The structure, functions, and mechanical properties of keratin. *JOM* 64, 449–468. doi: 10.1007/s11837-012-0302-8

Meretsky, V. J., Atwell, J. W., and Hyman, J. B. (2011). Migration and conservation: frameworks, gaps, and synergies in science, law, and management. *Environ. Law Northwest. Sch. Law* 41, 447–534.

Morra, K. E., Newsome, S. D., Graves, G. R., and Fogel, M. L. (2021). Physiology drives reworking of amino acid δ2H and δ13C in butterfly tissues. *Front. Ecol. Evol.* 9:729258. doi: 10.3389/fevo.2021.729258

Nordell, C. J., Haché, S., Bayne, E. M., Sólymos, P., Foster, K. R., Godwin, C. M., et al. (2016). Within-site variation in feather stable hydrogen isotope (δ2Hf) values of boreal songbirds: implications for assignment to molt origin. *PLoS One* 11:e0163957. doi: 10.1371/journal.pone.0163957

Paritte, J. M., and Kelly, J. F. (2009). Effect of cleaning regime on stable-isotope ratios of feathers in Japanese quail (*Coturnix japonica*). *Auk* 126, 165–174. doi: 10.1525/auk.2009.07187

Pass, G. (2018). Beyond aerodynamics: the critical roles of the circulatory and tracheal systems in maintaining insect wing functionality. *Arthropod. Struct. Dev.* 47, 391–407. doi: 10.1016/j.asd.2018.05.004

Peduzzi, P., Concato, J., Kemper, E., Holford, T. R., and Feinstein, A. R. (1996). A simulation study of the number of events per variable in logistic regression analysis. *J. Clin. Epidemiol.* 49, 1373–1379. doi: 10.1016/S0895-4356(96)00236-3

Popa-Lisseanu, A. G., Sörgel, K., Luckner, A., Wassenaar, L. I., Ibáñez, C., Kramer-Schadt, S., et al. (2012). A triple-isotope approach to predict the breeding origins of European bats. *PLoS One* 7:e30388. doi: 10.1371/journal.pone.0030388

Ravi Kumar, M. N. V. (2000). A review of chitin and chitosan applications. *React. Funct. Polym.* 46, 1–27. doi: 10.1016/S1381-5148(00)00038-9

Rawlins, J. E. (1980). Thermoregulation by the black swallowtail butterfly, Papilio Polyxenes (Lepidoptera: Papilionidae). *Ecology* 61, 345–357. doi: 10.2307/1935193

Reich, M. S., Flockhart, D. T. T., Norris, D. R., Hu, L., and Bataille, C. P. (2021). Continuous-surface geographic assignment of migratory animals using strontium isotopes: a case study with monarch butterflies. *Methods Ecol. Evol.* 12, 2445–2457. doi: 10.1111/2041-210X.13707

Resh, V.H., and Carde, R.T. (2009). *Encyclopedia of Insects*. San Diego, United States: Elsevier Science & Technology

Van Rossum, G., and Drake, F.L. (2009). *Python 3 Reference Manual*. (Scotts Valley, CA: CreateSpace)

Satterfield, D. A., Sillett, T. S., Chapman, J. W., Altizer, S., and Marra, P. P. (2020). Seasonal insect migrations: massive, influential, and overlooked. *Front. Ecol. Environ.* 18, 335–344. doi: 10.1002/fee.2217

Seabold, S., and Perktold, J.. "*Statsmodels: Econometric and Statistical Modeling with Python. Presented at the Python in Science Conference*"; Austin, Texas (2010). pp. 92–96

Soto, D. X., Koehler, G., Wassenaar, L. I., and Hobson, K. A. (2017). Re-evaluation of the hydrogen stable isotopic composition of keratin calibration standards for wildlife and forensic science applications: measurements of H isotopes of keratin calibration standards. *Rapid Commun. Mass Spectrom.* 31, 1193–1203. doi: 10.1002/rcm.7893

Stefanescu, C., Soto, D. X., Talavera, G., Vila, R., and Hobson, K. A. (2016). Long-distance autumn migration across the Sahara by painted lady butterflies: exploiting resource pulses in the tropical savannah. *Biol. Lett.* 12:20160561. doi: 10.1098/rsbl.2016.0561

Talavera, G., Bataille, C., Benyamini, D., Gascoigne-Pees, M., and Vila, R. (2018). Round-trip across the Sahara: afrotropical painted lady butterflies recolonize the mediterranean in early spring. *Biol. Lett.* 14:20180274. doi: 10.1098/rsbl.2018.0274

Tsai, C.-C., Childers, R. A., Nan Shi, N., Ren, C., Pelaez, J. N., Bernard, G. D., et al. (2020). Physical and behavioral adaptations to prevent overheating of the living wings of butterflies. *Nat. Commun.* 11:551. doi: 10.1038/s41467-020-14408-8

Vander Zanden, H. B., Chaffee, C. L., González-Rodríguez, A., Flockhart, D. T. T., Norris, D. R., and Wayne, M. L. (2018). Alternate migration strategies of eastern monarch butterflies revealed by stable isotopes. *Anim. Migr.* 5, 74–83. doi: 10.1515/ami-2018-0006

Virtanen, P., Gommers, R., Oliphant, T. E., Haberland, M., Reddy, T., Cournapeau, D., et al. (2020). SciPy 1.0: fundamental algorithms for scientific computing in python. *Nat. Methods* 17, 261–272. doi: 10.1038/s41592-019-0686-2

Voigt, C. C., and Lehnert, L. S. (2019). "Chapter 5—tracking of movements of terrestrial mammals using stable isotopes," in *Tracking Animal Migration With Stable Isotopes*. eds. K. A. Hobson and L. I. Wassenaar. *2nd* ed (Amsterdam: Academic Press), 117–135.

Wassenaar, L. I., and Hobson, K. A. (1998). Natal origins of migratory monarch butterflies at wintering colonies in Mexico: new isotopic evidence. *Proc. Natl. Acad. Sci.* 95, 15436–15439. doi: 10.1073/pnas.95.26.15436

Wassenaar, L. I., and Hobson, K. A. (2003). Comparative equilibration and online technique for determination of non-exchangeable hydrogen of keratins for use in animal migration studies. *Isotopes in Environmental and Health Studies* 39, 211–217. doi: 10.1080/1025601031000096781

Wasserthal, L. (1983). Haemolymph flows in the wings of pierid butterflies visualized by vital staining (insecta, lepidoptera). *Zoomorphology* 103, 177–192. doi: 10.1007/BF00310476

West, J.B., Bowen, G.J., Dawson, T.E., and Tu, K.P. (eds.) (2010). *Isoscapes, Understanding Movement, Pattern, and Process on Earth Through Isotope Mapping*. Netherlands, Dordrecht: Springer

Wright, T. R. F. (1987). "The genetics of biogenic amine metabolism, sclerotization, and melanization in Drosophila melanogaster," in *This review is dedicated to Professor Ernst Caspari in recognition of his pioneering research in biochemical genetics Advances in Genetics* eds. J. G. Scandalios and E. W. Caspari (Amsterdam: Academic Press), 127–222.

Wunder, M. B. (2010). "Using isoscapes to model probability surfaces for determining geographic origins," in *Isoscapes*. eds. J. B. West, G. J. Bowen, T. E. Dawson and K. P. Tu (Dordrecht: Springer Netherlands), 251–270.

Wyatt, G. R. (1961). The biochemistry of insect Hemolymph. *Annu. Rev. Entomol.* 6, 75–102. doi: 10.1146/annurev.en.06.010161.000451

Yapp, C. J., and Epstein, S. (1982). A reexamination of cellulose carbon-bound hydrogen δD measurements and some factors affecting plant-water D/H relationships. *Geochim. Cosmochim. Acta* 46, 955–965. doi: 10.1016/0016-7037(82)90051-5

frontiers | Frontiers in Ecology and Evolution

TYPE Original Research
PUBLISHED 10 February 2023
DOI 10.3389/fevo.2023.1058985

OPEN ACCESS

EDITED BY
Gábor Árpád Czirják,
Leibniz Institute for Zoo and Wildlife Research (LG), Germany

REVIEWED BY
Stefania Milano,
Leibniz Institute for Zoo and Wildlife Research (LG), Germany
Stephan Woodborne,
TAMS Laboratory, South Africa

*CORRESPONDENCE
Geoff Koehler
✉ geoff.koehler@usask.ca

SPECIALTY SECTION
This article was submitted to Ecophysiology, a section of the journal Frontiers in Ecology and Evolution

RECEIVED 30 September 2022
ACCEPTED 24 January 2023
PUBLISHED 10 February 2023

CITATION
Koehler G, Schmidt-Küntzel A, Marker L and Hobson KA (2023) Delineating origins of cheetah cubs in the illegal wildlife trade: Improvements based on the use of hair δ^{18}O measurements.
Front. Ecol. Evol. 11:1058985.
doi: 10.3389/fevo.2023.1058985

Delineating origins of cheetah cubs in the illegal wildlife trade: Improvements based on the use of hair δ^{18}O measurements

Geoff Koehler[1]*, Anne Schmidt-Küntzel[2], Laurie Marker[2] and Keith A. Hobson[1,3]

[1]NHRC Stable Isotope Laboratory, Environment and Climate Change Canada, Saskatoon, SK, Canada, [2]Cheetah Conservation Fund, Otjiwarongo, Namibia, [3]Department of Biology, University of Western Ontario, London, ON, Canada

All African felids are listed as vulnerable or endangered according to the IUCN (International Union for Conservation of Nature) Red List of Threatened Species. Cheetahs (*Acinonyx jubatus*) in particular have declined rapidly as a result of human impacts so that development of effective strategies and tools for conservation of this highly vulnerable species, as well as African felids in general, are essential for their survival in the wild. Here we use the oxygen stable isotopic compositions of cheetah hair to determine origins of cheetah cubs destined for the illegal exotic pet trade by associating individual cubs with predicted δ^{18}O isoscape locations. We found that cheetah cubs most likely originated in East Africa, close to the corridors responsible for this aspect of the illegal wildlife trade to the Middle East. Further refinement of these assignments using a two isotope analysis (δ^{18}O and δ^{13}C values) indicate that these cubs were likely sourced in Southern Ethiopia or possibly as far as Tanzania. We also demonstrate that δ^{18}O values in tissues can provide provenance information in cases where results of δ^{2}H analyses may be obscured by the effects of metabolic routing of nutrients during nursing, starvation, or dehydration. This study demonstrates the utility of stable isotopic tools for conservation and forensic uses for endangered mammalian species.

KEYWORDS

hydrogen, oxygen, stable isotope, conservation, cheetah, maternal nutrients, metabolic routing

1. Introduction

The cheetah (*Acinonyx jubatus*) is one of the most endangered felids in the world. Once wide ranging, they are now only extant in parts of Africa, except for a very small, critically endangered, population of the sub-species *Acinonyx jubatus venaticus* (Asiatic cheetah) in Iran (Farhadinia, 2004). Asiatic cheetahs were hunted to extinction in India, the last three likely to have been killed in 1948 (Velho et al., 2012). The subsequent half century has seen the remaining cheetah distributions contract sharply to only about 10% of their historical range and their numbers similarly decline to only about 7,000 individuals, with over half of the worlds remaining cheetahs resident in southwest Africa (Durant et al., 2017). Other populations are fragmented and small, with numbers of 200 or fewer. The threats to cheetahs are many and, like other wild felids, are primarily the result of anthropogenic pressures. Sub-Saharan Africa has one of the largest growing human populations (Cilliers, 2017) and this has resulted in decimation of wild felid numbers as a consequence of habitat destruction, agricultural expansion, prey reduction, livestock related conflicts, and direct hunting for food, trophies, or curatives (Ripple et al., 2014; Di Minin et al., 2016; Wolf and Ripple, 2017). Cheetahs are in direct competition for prey with other, larger, carnivores, such as lions (*Panthera leo*), leopards (*Panthera pardus*) and hyenas (Hyaenidae) and thus naturally occur in low numbers and are widely dispersed, a situation

that makes conservation by inclusion in national parks difficult. Moreover, their low densities, declining numbers, and solitary nature has resulted in species genetic fragility (O'Brien et al., 1985). These combination of factors make the cheetah, perhaps of all the wild felids, especially vulnerable to existing and growing anthropogenic impacts (Cardillo et al., 2004).

An additional and emerging concern for conservation of cheetahs as well as other charismatic species is the illegal trade of wildlife parts and, more recently, as exotic pets. In some cases, the number of animals affected by the illegal pet market exceeds those from the smuggling of animal parts (Pires, 2012; Daut et al., 2015). Animals entering the exotic pet trade are distributed through illegal criminal organizations and are usually poached from wild populations, although some captive breeding facilities exist (Pires and Moreto, 2011; Dalberg, 2012; Ayling, 2013).

Cheetahs (once called "hunting leopards") were historically kept and used for hunting in India because they are relatively less ferocious, smaller bodied, and easier to domesticate than other big cats (O'Brien et al., 1986; Bothma and Walker, 1999). Although no longer used for hunting, they are still captured by the modern illegal wildlife trade in Africa whereby cubs are taken alive, usually after killing the mother, and subsequently sold into middle Eastern markets to be kept as "status" pets by the very wealthy (Warchol, 2004; Tricorache et al., 2018; Marker, 2019). Cub mortality during the smuggling process is high with most cubs dying before reaching market (Warchol et al., 2003). Kept as domestic pets, the outlook is similarly grim because cheetahs do poorly in captivity, surviving only a few years without large spatial freedom and specialized diets that mimic those of wild cheetahs (Marker-Kraus, 1997; Tordiffe et al., 2016). Cheetahs are difficult to breed in captivity (O'Brien et al., 1985) so that cubs for the pet trade must be continuously supplied from wild populations, already fragmented and vulnerable. As a result, along with increasing habitat loss, this particular aspect of illegal wildlife trade is now one of the largest current threats to cheetah conservation and survival.

Poached cheetah cubs are funneled through the horn of Africa, across the Gulf of Aden, and into the Arabian Peninsula on their way to illegal markets for exotic pets. The semi-autonomous region of Somaliland, in conjunction with other wildlife agencies, manage to intercept some of these shipments and confiscate a few of the over 300 cheetah cubs that are estimated to move along trafficking routes and into the pet trade every year (Tricorache et al., 2018; Marker, 2019). However, while rescued in Somaliland, the origins of these cubs remain unknown. This is of great concern to conservation and law enforcement agencies, because it is important to know where these cubs are captured so that they may focus their conservation efforts. To address this, we measured the H, O, N, and C stable isotopic compositions of hair from rescued cheetah cubs to try to determine their origins.

The stable isotopic compositions of animal tissues hold great potential for conservation because they may be linked to provenance (Meier-Augenstein et al., 2013; Chesson et al., 2018) or determination of migration patterns of wildlife (Hobson and Wassenaar, 2008). The H and O stable isotopic compositions of hair are related to those of body water, and thus ingested environmental waters (Hobson et al., 1999). Because the H and O stable isotopic compositions of water varies regionally, so do those of animal tissues. Similarly, the carbon isotopic compositions of tissues are related to those of regional vegetation which varies with the relative distribution of C3 and C4 plants and is transferred upwards through the food web. The resulting isotopic landscapes, or "isoscapes," can be used to link organisms with their environment (West et al., 2009; Hobson and Wassenaar, 2018; Vander Zanden et al., 2018). Because of their water conserving nature and obligate carnivore physiology, isotopic linking of felids to environmental water and thus location was not considered feasible (Pietsch et al., 2011). However, a recent study by Koehler and Hobson (2019) has determined that a relationship between environmental water and felid hair does indeed hold for domestic and wild cats and therefore may be used for provenance estimation. A remaining issue pertains to the use of cub hair because young mammals may be influenced by maternal nutrient inputs through nursing and such maternal effects have not been previously considered in isotopic assignments. Our objective, then, was to use isotopic techniques to establish the provenance of cheetah cubs confiscated in Somaliland and to explore means to resolve the maternal nutrient transfer issue. Ultimately though, it is our hope that this proof of concept can be further expanded to other terrestrial mammals, particularly those that are currently threatened by illegal activities.

2. Methods

Hair samples (*ca.* 20 mg) were collected from 2015 to 2021 during veterinary health checks from lawfully confiscated cheetah cubs (n = 96) after rescue in Somaliland. The ages of cubs ranged between 3 and 7 months, as determined by veterinary assessments after rescue. All hair samples were shipped to the NHRC Stable Isotope Laboratory under CITES export permits 0061077 and 0063888 and imported with Canadian CITES import permit 21CA01252/CWHQ. This study was approved by the University of Saskatchewan Research Services and Ethics Office, RSEO Reference number 003Exempt2020.

2.1. Stable isotope analysis

Stable isotopic compositions of all hair samples were performed at the NHRC Stable Isotope Laboratory of Environment and Climate Change Canada in Saskatoon, SK, Canada. Prior to analyses, hair samples were cleaned of adherent debris and any surface oils were removed by rinsing in 2:1 chloroform:methanol. Hair was homogenized to powder with a ball grinder (Retsch model MM-301, Haan, Germany). The root end of the hairs were discarded as these will reflect the most recent growth and may include hair grown in captivity prior to rescue. For hydrogen and oxygen, our approach involved the measurement of both δ^2H and δ^{18}O values with the same analytical run (i.e., both H_2 and CO gases were analyzed from the same pyrolysis) (Hobson and Koehler, 2015). Samples and standards were weighed to 350 $\pm$ 20 μg in silver capsules and analyzed using a Delta V Plus IRMS system (Thermo Finnigan, Bremen, Germany) equipped with a Costech Zero-Blank autosampler. The helium carrier gas rate was set to 120 mL/min. We used a HTC 1.5 m 0.25 inch 5 Å molecular sieve (80–100 mesh) GC column. The glassy carbon reactor was operated at a temperature of 1,400°C, and the GC column temperature was set to 90 °C. After separation, the gases were introduced into a Delta V plus isotope-ratio mass spectrometer *via* a ConFlo IV interface (Thermo Finnigan, Bremen, Germany). The eluted N_2 was flushed to waste by withdrawing the CF capillary from the ConFlo interface. We

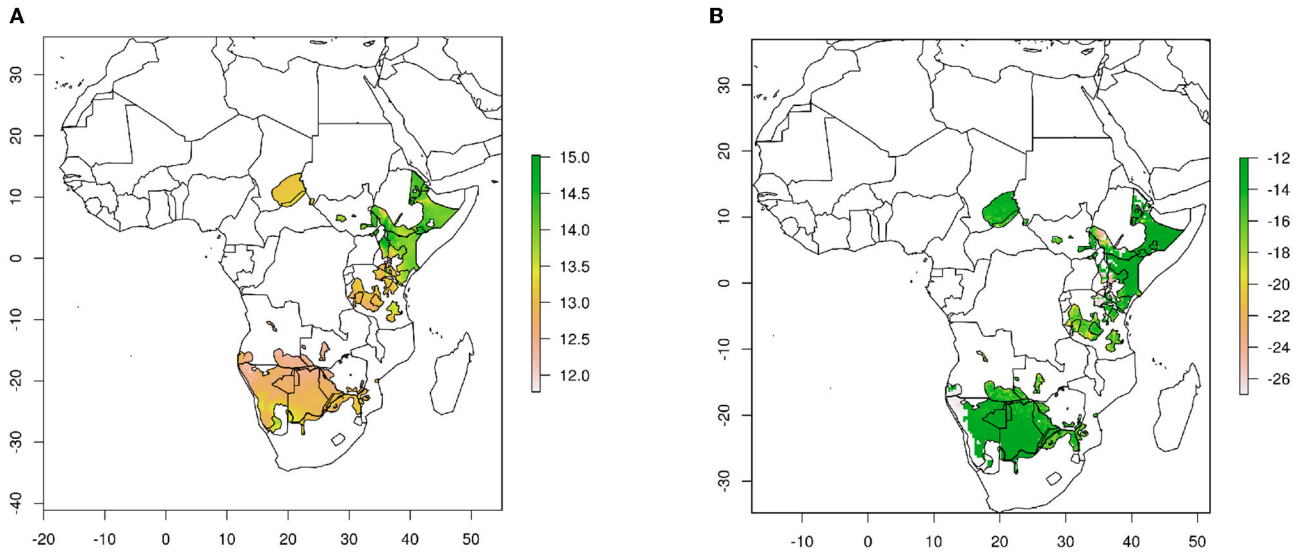

FIGURE 1
Cheetah hair isoscapes used in this study. **(A)** δ^{18}O values. **(B)** δ^{13}C values. Base maps produced from data of Terzer et al. (2013) and Terzer-Wassmuth et al. (2021) for δ^{18}O and Still and Powell (2010) for δ^{13}C.

used Environment Canada keratin reference standards CBS (Caribou hoof) and KHS (Kudu horn) to calibrate sample δ^2H (–197 and –54.1 per mil, respectively) and δ^{18}O values (+2.50 and +21.46 per mil, respectively Qi et al., 2011). This normalization with calibrated keratins also corrects for any hydrogen isotope measurement artifact caused by production of HCN (Gehre et al., 2015) in the glassy carbon reactor as described by Soto et al. (2017). Based on replicate (n = 10) within-run measurements of keratin standards and from historical analyses of an in-house QA/QC reference (SPK keratin), sample measurement error was estimated at ±2 per mil for δ^2H and ± 0.4 per mil for δ^{18}O. All H results are reported for nonexchangeable H and for both H and O in the standard delta notation, normalized on the Vienna Standard Mean Ocean Water—Standard Light Antarctic Precipitation (VSMOW-SLAP) scale.

For carbon and nitrogen isotope analyses, we weighed 1 mg of ground hair into precombusted tin capsules. Encapsulated hair was combusted at 1,030°C in a Carlo Erba NA1500 elemental analyser. The resulting N_2 and CO_2 were separated chromatographcally and introduced to an Elementar Isoprime isotope ratio mass spectrometer (Langenselbold, Germany–www.elementar.de). We used two calibrated in–house reference materials to normalize the results to VPDB and AIR: BWBIII keratin (δ^{13}C = –20.18, δ^{15}N = 14.31 per mil, respectively) and PRCgel (δ^{13}C = –13.64, δ^{15}N = 5.07 per mil, respectively). Precisions as determined from both reference and sample duplicate analyses and from within-run analyses of QA/QC bovine gelatin (BVgel) were ± 0.1 per mil for both δ^{13}C and δ^{15}N. For both HO and CN stable isotope analyses, most samples were run in duplicate.

2.2. Assignment to origin

We used geographical assignment algorithms as described in Van Wilgenburg and Hobson (2011). Briefly, we used rastered δ^{18}O hair-specific isoscapes as a basis for predicting origins of cheetah cubs produced from the rescaling factors measured for known–origin cats across North America (Figure 1A) (Koehler and Hobson, 2019). These hair δ^{18}O isoscapes were then imported into custom R scripts using the rgdal, sp and raster packages and used to plot 2-D spatial data in map form, and perform spatial statistics on the raster surfaces. We used current cheetah range shapefiles from the IUCN, but did not include the ranges of two critically endangered (i.e., < 30 individuals) cheetah subspecies, the Asiatic cheetah (*A. j. venaticus*) and the North African cheetah (*A. j. hecki*). We then applied a normalized probability density method (Hobson et al., 2009) to estimate the probability that individual cells in the calibrated felid isoscape represented a potential origin for each cub at the 67% (i.e., 2:1 odds ratio) confidence level. Digital file manipulation and assignment to origin analyses were conducted using multiple packages including "raster" v.3.6-3 (Hijmans and Van Etten, 2015) and "maptools" v. 1.1-4 (Bivand and Lewin-Koh, 2015) in the R statistical computing environment v.4.1.2 (R Core Team, 2021).

For carbon isotopes, we used δ^{13}C isoscapes for Africa produced from the theoretical spatial distribution of plants obtained from C3/C4 plant abundance remote sensing maps (Still and Powell, 2010; Hobson et al., 2012). We did not use a rescaling factor because previous studies have indicated that cheetah fur has similar δ^{13}C values to those of food (Voigt et al., 2014), whereas an enrichment of 1 to 4 per mil is measured for other felids (Parng et al., 2014; Montanari and Amato, 2015) (Figure 1B).

3. Results and discussion

The δ^2H, δ^{18}O, δ^{13}C, and δ^{15}N values of hair from 96 cheetah cubs are shown in Table 1. Values of δ^{15}N of these cubs ranged from +8.6 to +16.9 per mil, and are significantly higher (mean = 13.4, σ = 1.7 per mil) than those reported values for African lions or leopards (Codron et al., 2007). Adult cheetahs from Namibia have similar δ^{15}N values (+12.3 per mil) to those of other African felids (Voigt et al., 2014), largely because most felid species tend to prey on

TABLE 1 Nitrogen, carbon, hydrogen, and oxygen stable isotopic compositions of hair from cheetah cubs confiscated from the illegal pet trade, Somaliland.

Name	$\delta^{13}C$	$\delta^{15}N$	$\delta^{2}H$	$\delta^{18}O$	Name	$\delta^{13}C$	$\delta^{15}N$	$\delta^{2}H$	$\delta^{18}O$
Cloud	−21.5	14.1	−45	16.4	Kiana	—13.2	10.9	−15	14.8
Star	−20.7	14.9	−35	15.4	Serge	−20.9	11.8		
Mist	−22.1	13.6	−44	16.1		−22.1	12.9		
Moonlight	−21.1	14.1	−49	16.6	Amiin			−6	15.1
Sunshine	−23.1	15.4	−61	17.1	Zelda	−22.4	13.8	−27	14.2
Libbo	−21.1	16.7	−14	15.2	Amiir	−22.2	16.9	−12	15.4
Lyaru	−21.0	16.3	−3	15.9	Moxie	−19.1	12.8	−37	14.5
Leo	−21.2	16.4	−7	15.3	Zero	−19.7	12.8	−7	16.6
Galol	−22.2	14.6	−25	15.9	Johnny-2,750	−18.5	13.1	−32	14.7
Kidi	−22.3	14.4	−31	14.5	Olivia			−16	15.6
Kulan	−22.3	14.7	−23	16.6	Sol	−21.1	11.8	−24	17.5
Lion	−19.5	10.5	−34	13.5	Fush	−22.7	14.7	−22	15.2
Libra	−14.7	12.7	−43	15.0	Rocket	−22.1	14.1	−27	13.9
Abbo	−21.2	14.4	−6	16.0	Mischief	−21.5	14.9	−5	16.0
Mariam	−19.1	14.7	−10	15.5	Phil	−21.1	14.1	−39	15.6
Libbo	−20.3	13.0	−36	13.2	Frigga	−20.1	13.3	3	16.5
Leo	−20.6	13.8	−25	13.7	Freya	−20.0	13.4	−25	17.1
Lyam	−20.5	12.8	−41	13.6	Sif	−20.5	11.4	−12	16.9
Kalli	−21.5	14.3	−13	15.5	Magan	−20.1	14.1	3	15.5
Guhad	−19.2	14.8	−2	16.6		−21.7	14.1	−44	15.2
Ayanna	−20.4	14.0	−16	16.3	Link	−20.4	15.2	−9	14.9
Kurro	−21.3	14.4	−7	16.1	Duma	−18.5	12.3	−28	13.9
Dominic	−13.0	11.5	−38	13.3		−21.8	14.7	−45	16.2
Savanna	−18.5	12.4	2	19.7	Teresa	−20.1	14.8	2	16.4
Smartman	−13.2	10.8	−28	14.3	Yasir	−20.3	14.9	8	15.8
Polly	−13.3	10.1	−31	14.3	Vicki 2	−19.2	13.6	−2	16.8
B2	−13.1	8.6	−38	12.9	Major	−19.9	13.2	−33	15.6
Little C	−12.8	9.1	−41	16.8	Koya	−19.9	14.0	−49	14.1
Ron	−12.8	9.5	−32	11.9	Janet	−18.3	13.9	−27	15.6
Hermione	−13.6	10.2	−38	14.4	Faduma	−18.4	13.4	−29	15.1
Max	−13.0	10.6	−45	13.7	Meeko	−18.3	13.7	−42	13.8
Thor	−12.8	11.0	−35	13.5	Shamsi	−20.7	14.0	−33	16.1
West	−12.9	11.2	−42	14.3	DJ	−18.3	14.1	−32	13.9
Ben	−12.8	10.9	−39	13.6	Micket	−18.4	13.5	−33	14.6
Mike	−12.9	11.3	−39	14.3	James–4269	−18.2	13.5	−35	15.0
Darwin	−13.0	10.7	−31	14.0	Idris	−20.0	14.5	−10	15.6
Nico	−13.0	10.8	−29	13.8	Elba	−19.6	13.8	−7	17.6
Kayla	−12.7	11.8	−31	12.9	Astur	−20.4	14.3	1	12.8
Merlot	−13.3	10.8	−21	15.7	Kaiir	−20.7	14.7	9	13.8
Romeo	−14.5	11.1	−11	15.8	Jaleelo	−19.9	14.0		
Khayjay	−13.0	11.3	−18	14.9	Galiil	−20.5	15.0	−4	14.9
Rosy	−13.3	11.2	−15	15.4	Rajo	−18.5	13.4	−21	12.3

(Continued)

TABLE 1 (Continued)

Name	$\delta^{13}C$	$\delta^{15}N$	$\delta^{2}H$	$\delta^{18}O$	Name	$\delta^{13}C$	$\delta^{15}N$	$\delta^{2}H$	$\delta^{18}O$
Solo	−13.1	11.1	−10	15.3	Cizi	−18.6	13.0	4	14.7
Amani	-13.2	10.6	-10	14.7	Emmeh	−18.5	13.8	−38	13.0
Harry	−13.6	11.4	−12	15.2	Margarita	−18.4	13.8	−31	12.2
Blondeman	−13.8	11.4	−43	16.2	Bagheer	−18.4	13.0	−31	12.7
Phoenix	−14.6	11.4	−21	16.1	Darth	−18.4	13.2	−36	11.8
Fossey	−14.5	11.5	−26	15.3	Dead cheetah	−19.7	13.2	−20	15.4

ungulates or other small bodied herbivores (Eaton, 1970; Mills, 1984). The most likely reason for the observed high $\delta^{15}N$ values in these cheetah cubs is the well known trophic effect from nursing young to offspring, although other effects such as malnutrition, cannot be ruled out. Adult mammals isotopically integrate their environment through coupling of H, O, C, and N isotopes into tissues by direct ingestion of food and water (Hobson and Wassenaar, 2018). For nursing young, however, this relationship is complicated because young mammals obtain a significant amount of environmental water and nutrients indirectly through maternal milk thereby placing young at a higher trophic position (i.e., higher $\delta^{15}N$ values) than their mothers. The high lipid content of milk also tends to drive cub tissue $\delta^{13}C$ values lower than those formed after weaning.

With the exception of humans, there is very little information in the literature on the relative discrimination of stable isotopes between tissues of mothers and nursing young. A few studies have compared the stable isotopic compositions of herbivores, generally cows (*Bos taurus*), with diet (Kornexl et al., 1997; Camin et al., 2008), or location (Chesson et al., 2010), mostly for detection of food adulteration. Jenkins et al. (2001) determined that isotopic differences between maternal and offspring plasma were variable and species dependent. Lipids are generally ^{13}C depleted relative to other animal tissues (Tieszen et al., 1983) and also to the rest of the components in milk (Melzer and Schmidt, 1987; Wilson et al., 1988), so that we would expect tissues of nursing offspring to have lower $\delta^{13}C$ values than those of the mother. The low $\delta^{13}C$ values of many of these cheetah cubs (Table 1) compared with Namibian cheetahs ($\delta^{13}C = -14.8$ per mil Voigt et al., 2014) are consistent with this, however the $\delta^{13}C$ values of the maternal diet are unknown so it is impossible to make comparisons.

Polar bear (*Ursus maritimus*) cubs have higher $\delta^{15}N$ values and lower $\delta^{13}C$ values than do adults from the same subpopulations (Polischuk et al., 2001; Koehler et al., 2019). Hair $\delta^{13}C$ and $\delta^{2}H$ values of polar bear cubs are typically lower than those of adults (Koehler et al., 2019), most likely because of the high lipid content of maternal milk with correspondingly low $\delta^{13}C$ and $\delta^{2}H$ values. The amount of the differences in these isotopic compositions is likely dependent on the relative ages of cubs, and thus amount of nursing, and of the lipid content of the milk. The fat content of cheetah milk (64 g/kg) is lower than milk from polar bears (350 g/kg Derocher et al., 1993) and slightly lower than lions or domestic cats (*Felis catus*) (De Waal et al., 2004; Osthoff et al., 2006). Therefore compared to polar bears, we would certainly expect a smaller or perhaps no difference in $\delta^{2}H$ and $\delta^{13}C$ values between adult cheetahs and cheetah cubs. Ultimately, though, there is no way to determine this other than using controlled diet studies.

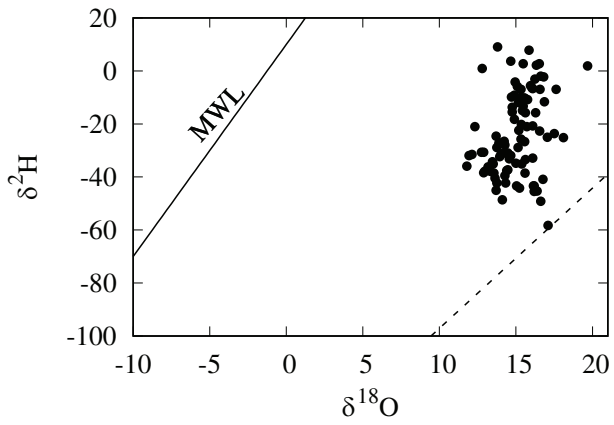

FIGURE 2
$\delta^{2}H$ and $\delta^{18}O$ values in per mil (SMOW) of cheetah cub hair. The dashed line is the relationship for domestic and wild cats in North America (Koehler and Hobson, 2019). Also shown is the global meteoric water line (MWL) of Craig (1961).

Values of hair $\delta^{2}H$ for these Cheetah cubs were more variable and positive than we anticipated, ranging from −61 to +9 per mil. Because the $\delta^{2}H$ values of lipids are much lower than that of other macromolecules (Sessions et al., 1999; Sachse et al., 2012), we expected the $\delta^{2}H$ values of nursing cub hair to be lower than those of adult cats relative to their oxygen isotopic compositions, however this was clearly not the case (Figure 2). One possible explanation for this observation is that the relative enrichment in ^{2}H in hair in cubs is the result of a trophic effect between mother and cub. Because these cubs were generally young (3–7 months), it is likely that a portion of the hair was grown before birth and prior to nursing and introduction of the lipid-rich milk diet.

For placental mammals, *in utero* nutrient and gas exchange occurs across the fetal villi without exchange of blood. In humans, fetal amino acid concentrations are generally higher than maternal levels (Cetin et al., 1992), reflecting an active transport mechanism across the placental membranes. It seems unlikely that active transport of large molecules such as amino acids will result in significant isotopic fractionation, and thus we would expect the familiar trophic effect *in utero* that is observed in nursing young, and is consistent with the $\delta^{15}N$ values of cubs in this survey. This has been observed in humans, where $\delta^{15}N$ and $\delta^{13}C$ values of newborn infant hair were higher than those of the mother (De Luca et al., 2012). For hydrogen isotopes, a trophic enrichment of 30 to 50 per mil is predicted from mechanistic models (Magozzi et al., 2019) and

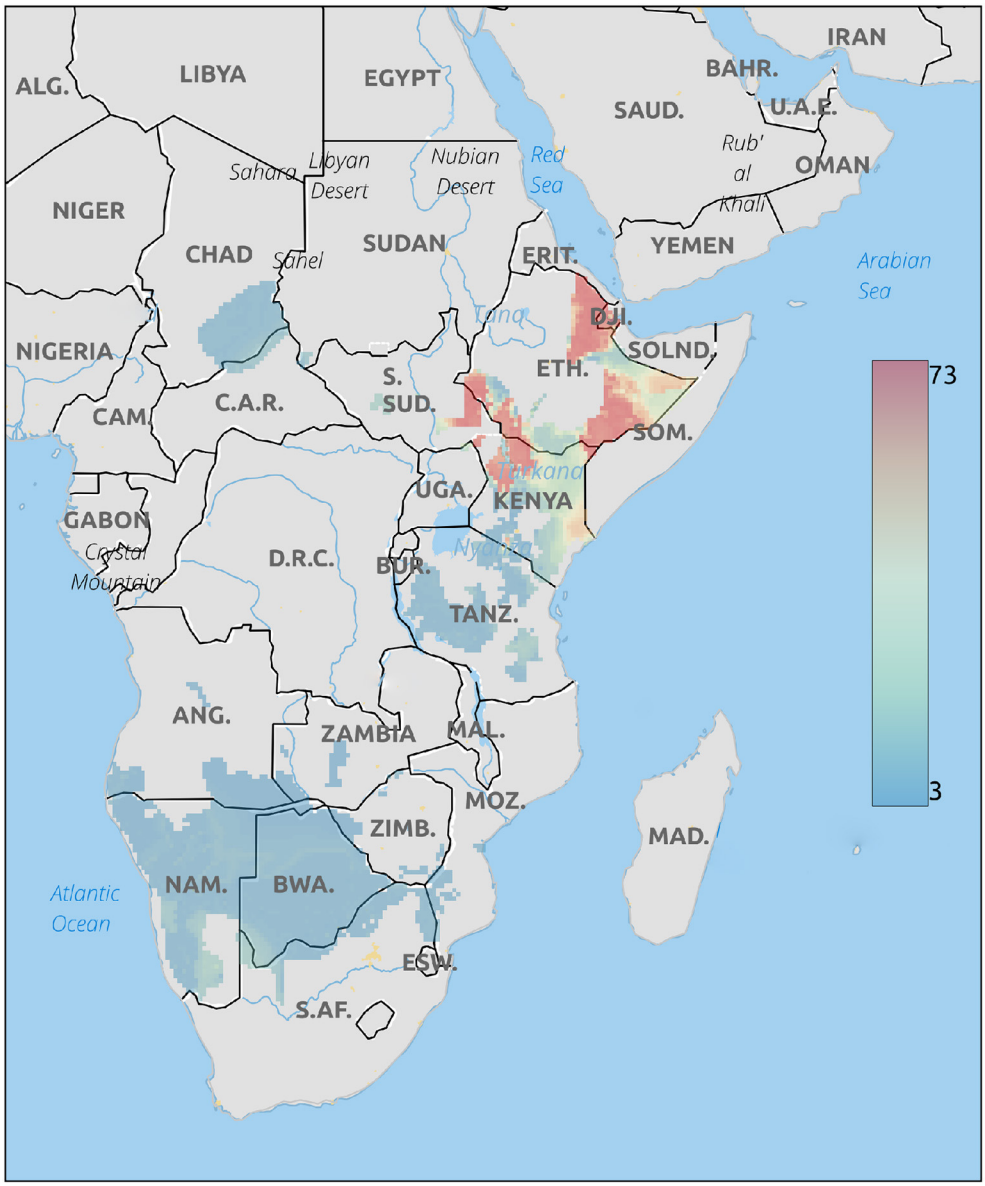

FIGURE 3
Probable origins of cheetah cubs rescued from the illegal pet trade based on δ^{18}O isoscapes. Legend is the number of individuals assigned to a pixel based on the odds ratio criterion used.

observed in a few studies (Birchall et al., 2005; Topalov et al., 2013). If this is the case for cheetahs, the variability in hydrogen isotope enrichment in cheetah cubs may be related to their variable ages where the δ^2H values of older cubs would be more negative, reflecting more a contribution of nursing in the hair. Unfortunately, we do not have exact ages for the cubs and, historically, it is has been difficult to separate a hydrogen isotopic trophic effect from other metabolic and dietary processes with any certainty (reviewed by Vander Zanden et al., 2016).

Another complication with the cheetah cubs we examined was that they are usually extremely malnourished and dehydrated when rescued. Starvation in humans generally increases the δ^{13}C and δ^{15}N of hair by recycling of proteins within the body pool (Hatch et al., 2006; Mekota et al., 2006), a phenomenon also noted in birds (Hobson et al., 1993; Cherel et al., 2005). Nutritional and water stress has been suggested as the mechanism for large increases in the δ^{15}N values in bone collagen in African herbivores (Ambrose and DeNiro, 1986). For hydrogen and oxygen isotopes, however, there appears to be very little in the literature on the effects of starvation on the isotopic compositions of animal protein. For dehydration, it seems intuitive that evaporation concurrent with respiration and diffusive water loss would result in higher δ^2H and δ^{18}O values of the body water pool with corresponding increases of those of hair. Indeed, McKechnie et al. (2004) observed that feathers of water-stressed Rock Doves (*Columba livia*) were enriched in ^2H, similar to previous observations in humans (Schoeller et al., 1986). However, the picture is not as clear for oxygen isotopes for which there are very few measurements. Storm-Suke et al. (2012) observed similar hydrogen isotope results in Japanese quail (*Coturnix japonica*) as was observed for Rock Doves by McKechnie et al. (2004),

but did not see any differences for oxygen isotopes. Ultimately, though, whether it can be attributed to maternal trophic effects, malnutrition, or dehydration, the relatively high δ^2H values of these cubs remain enigmatic.

For geographical assignments, tissue δ^2H values in consumers are generally preferred over δ^{18}O values because of their greater range and smaller relative error (Hobson and Koehler, 2015). But, because of all the aforementioned uncertainties involved with the use of δ^2H values of hair from cheetah cubs, we decided to avoid these complexities altogether and instead use hair δ^{18}O values for geographical placement. The δ^{18}O values of adult and cub hair from polar bears from the same locations did not show any significant difference, although there were large differences in δ^2H, δ^{15}N, and δ^{13}C values (Koehler et al., 2019). This is most likely because lipids in maternal milk contain little oxygen and the δ^{18}O values of milk protein is similar to those of the maternal diet. Because oxygen is more weakly routed from diet to consumer tissues, it is likely that the isotopic compositions of oxygen in these tissues will be less confounded by environmental and dietary considerations than hydrogen (Bowen et al., 2009; Soto et al., 2011; Wolf et al., 2015), and thus will more closely reflect the isotopic compositions of environmental water. It is currently unknown whether malnutrition or dehydration can cause changes to the δ^{18}O values of mammal hair.

3.1. Geographical origins of cheetah cubs

Cheetah females are polyesterous and are thus non-seasonal breeders (Crosier et al., 2018, 2022). As a result, cubs are captured in the illegal trade throughout the year, with a slight bias to dry season (Jul-Aug), perhaps as a result of easier transport along illegal trade routes. Assuming the cubs are, on average, 6 months old, this indicates they were likely born during a wet season in East Africa. Here, with the exception of northern Ethiopia, the majority of precipitation falls during two wet seasons (Levin et al., 2009). In this case, the mean annual oxygen isoscape is appropriate because the bulk of the precipitation occurs in the wet seasons and the isoscape is representative of this. Considering the wide range of ages of the cubs and that cubs can be taken at any time during the year, it is impossible to associate a particular season with most of the cubs with any accuracy.

For geographic placement, we cannot assume a single batch of cubs captured at a single time. In reality, cubs were captured in small batches (1 to a few) from 2015 to 2021. We also have to consider the isotopic integration that occurs through the foodweb which will tend to average out wet season-dry season differences in stable isotopic compositions of hair. While prey species are more closely coupled to the underlying precipitation isoscape, they will also tend to average out yearly precipitation to some extent based on growth characteristics and seasonal isotope patterns in plants. Considering all of this, we treated all 96 cubs as a single batch of time-integrated samples and assigned them to origin using the mean amount averaged oxygen isoscape. This approach provides an estimation of the total geographic range of cub origins, an important consideration for law enforcement and conservation.

Because oxygen isotopic compositions are rarely used, it is important to take into account the error envelope involved in geographical placement of cheetah cubs. If we examine the standard error of δ^{18}O values reported for the RCWIP dataset and translate

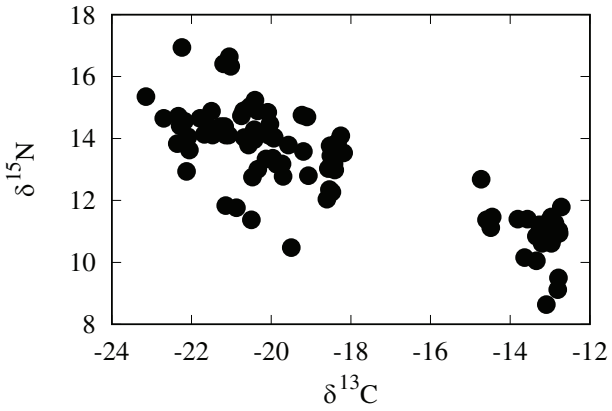

FIGURE 4
Carbon and nitrogen stable isotopic compositions of cheetah cub fur in per mil PDB and AIR, respectively.

those to the cheetah isoscape as seen on Figure 1A, oxygen isotopic compositions of cheetah fur are only expected to vary by about 0.4 per mil at any single location in east Africa, similar to our measurement error for δ^{18}O values. Our measured range of δ^{18}O values in cheetah fur exceeds 5 per mil (Table 1) so that we are confident that geographic placement is outside the analytical error. In addition, the assignment algorithm takes this error into account so that the oxygen isotopic composition of any cub that matches the isoscape does so at the 2:1 odds ratio or the 67% (1σ) confidence interval.

The Geographical placement of cheetah cubs based on δ^{18}O values of hair are shown in Figure 3. This analysis places these cubs in northwestern Kenya, northern Ethiopia, or southern Ethiopia close to the border with Somalia. These areas, particularly along the Somalian border are close to the expected routes for the illegal trade in live cubs (Marker, 2019).

Although regionally accurate, assignments of cheetah cubs to geographic origin are fairly broad based only on δ^{18}O values. To further refine these assignments we examined the utility of a multivariate placement using both δ^{18}O and δ^{13}C values. Values of δ^{13}C of cheetah cubs range from −22.7 to −12.7 per mil and show a clear bimodal distribution (Figure 4 and Table 1). While relatively high δ^{13}C values of cubs were expected from the east African savannahs where the C4 grasses dominate in the warm, arid lowlands (Tieszen et al., 1979b), many cubs had unexpectedly low δ^{13}C values. At first, we attributed these low δ^{13}C values of these cubs to consumption of a high lipid diet during nursing, but on further analysis this seems unlikely. Polar bear cubs have δ^{13}C hair values that are only 1–3 per mil lower than those of adults (Koehler et al., 2019) concurrent with very high concentrations of lipids in maternal milk. Cheetahs have lower amounts of lipids in maternal milk, so it seems unlikely that there would be asimilar large negative offset in δ^{13}C values between cheetahs adults and nursing young. If ingestion of lipid rich milk were responsible for the low δ^{13}C values observed, we would also expect a similar decrease in δ^2H values, but we see the opposite. Furthermore, fur from free ranging Namibian cheetahs have δ^{13}C values about −14.8 per mil (Voigt et al., 2014), very close to the −12 to −13 per mil predicted from the African carbon isoscape (Figure 1B), which reflects the abundance of C4 plants and therefore C4-eating prey in tropical grasslands. Feeding

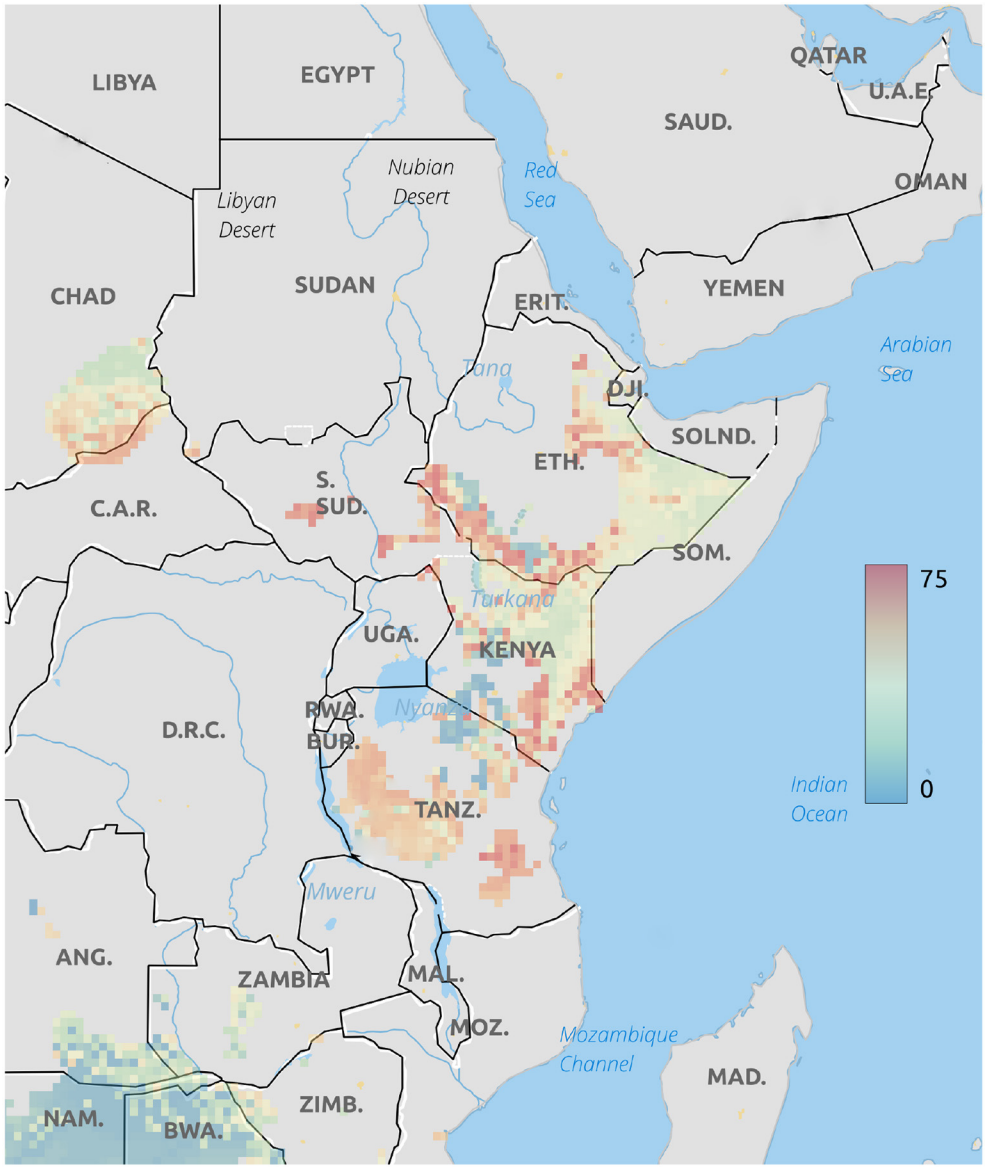

FIGURE 5
Multivariate isotope assignment of cheetah cubs to location based on a $\delta^{18}O$ and $\delta^{13}C$ values. Legend is the number of individuals assigned to a pixel based on the odds ratio criterion used.

studies of adult cheetahs also indicate there only minor differences in $\delta^{13}C$ values between cheetahs and food sources (Voigt et al., 2014). These observations suggest that, overall, the isotopic discrimination of carbon isotopes is close to 0 per mil between cheetahs and their environment. Therefore, if the consumption of a lipid rich milk is responsible for the low $\delta^{13}C$ values measured in these cubs, we would expect that hair from cheetah cubs should have $\delta^{13}C$ values around −15 per mil.

An important consideration is that accurate transfer of carbon isoscapes based on terrestrial foodwebs have never been ground-tested for mammals. Stable carbon isoscapes are based on the predicted spatial proportions of C4 and C3 plants obtained from remote sensing and, as a result, there is a uncertainty differentiating between grasses and non-tree herbaceous layers in the present carbon isoscapes (Still and Powell, 2010). In theory, carnivores should integrate the total carbon isotopic compositions of these relative proportions and therefore should closely reflect their ^{13}C environment. Herbivores tend to be selective and can be classified as grazers (C4-eating) or browsers (C3-eating). Therefore, provided that browsers and grazers are in proportion to the relative proportions of C3 to C4 plants and that predators are non-selective, the carbon isotopic compositions of predator tissues should be similar to those of the carbon isotope biome in which they inhabit.

In practice, however, it is undoubtedly more complicated. The $\delta^{13}C$ values of tissues in carnivores will be a function not just of the underlying carbon isoscape, but will also be compounded by trophic discrimination factors, hunting behavior, and foraging behavior of prey. For higher level taxa, such as felids or canids, we would also expect a variation of hunting behaviors depending on availability and/or individual preferences. Indeed, we know that cheetahs can

develop strategies to overcome particular prey animals (Mills, 1984; Marker et al., 2003) and this may account for the clear exploitation of either grazers or browsers as prey in a mixed tree/grass savannah (Figure 4). Higher δ^{15}N values in cub hair with low δ^{13}C values seem to confirm this as mixed feeding gazelles have relatively high δ^{15}N values compared to grazers (Ambrose and DeNiro, 1986).

Impalas (*Aepyceros melampus*), Grants gazelles (*Nanger granti*) and Thompsons gazelles (*Eudorcas thomsonii*) comprise a large part of the diet of East African cheetahs (Eaton, 1970), all of which are mixed feeders wherein their diet consists of both C3 and C4 plants and varies temporally depending on species and the season (Spinage et al., 1980). Grants gazelles, which tend to browse more than they graze, occur in Ethiopia and South Sudan, whereas Thomsons gazelles and impalas, which can graze or browse, are more common in Kenya and Tanzania (Arctander et al., 1996). Consequently the δ^{13}C values of the stomach contents of these prey species can vary from average values of –21.9 per mil for Grants gazelles to –17 per mil for Thompsons gazelles, with Impalas averaging about –19 per mil (Tieszen et al., 1979a). Therefore, it is likely that the bimodal δ^{13}C and δ^{15}N values of these cubs simply reflect prey preference of the mother and thus are only loosely coupled to the underlying carbon isoscape.

An alternate, but less likely, explanation is that the C3 group of cubs are younger because they were captured closer to the trafficking routes in the Horn of Africa in the mixed savannah proximal to the Ethiopian highlands. In this case, the low δ^{13}C values will be augmented by lipids in milk and the elevated δ^{15}N values may be partially the result of maternal trophic effects.

The dual-isotope model places the origins of these cubs primarily in south western Ethiopia, as do the assignments based only on δ^{18}O values (Figure 5). However, the abundance of low δ^{13}C values in cheetah cub hair suggests many cubs originated in the savannah highlands where most of the forbs, shrubs, and trees are C3 types or, possibly, as far south as the great rift region of Tanzania. Considering all of the complexity involved in transfer of the carbon isotopes into predator tissues, however, this analysis cannot be taken as diagnostic and is of limited usefulness. While it is unlikely that these cubs could survive transport over the >1,000 km between Tanzania and Somalia, it is certainly possible that many could have been captured in southwestern Ethiopia where, presumably, Grants gazelles would make up a larger part of the adult diet.

4. Conclusions

Based on δ^{18}O values only, it is evident that cheetah cubs destined for the illegal pet trade are sourced from East Africa, primarily northern Ethiopia, western Kenya, and along the Somali border with Kenya. Further refining these placements by using a two isotope multivariate assignment suggests that it is possible that these cubs could have been sourced as far south as Tanzania. The two isotope analysis is, at best, uncertain because of complexities relating the underlying carbon isoscape to the terrestrial foodweb. It seems obvious that geographic placement of cheetah cubs places them proximal to the illegal trade routes. However, this appoach also demonstrates the general usefulness of stable isotopic placement for forensic analyses in terrestrial mammals, particularly the carnivores. In addition, it is our strong recommendation that oxygen isoscapes be considered for geographic placement in cases where the normal transfer of nutrients into tissues are complicated by the effects of nursing or nutritional stress.

Moving forward, it is our hope that these isotopic techniques can be developed into a robust analytical protocol that can be used by law enforcement and conservation agencies to address the many aspects of the illegal wildlife trade, not just for cheetahs, but for other vulnerable or endangered species. To this end, the addition of other intrinsic markers, such as genetic or chemical information, will help to refine geographical placement or identification of individuals for forensic applications. In the short term, automatic sampling and archiving of all confiscated illegally captured cheetahs is needed. Ultimately though, successful development and use of stable isotopic techniques will require a concerted effort from scientists, law enforcement, conservation groups, and policy makers. Like cheetahs, many of the worlds iconic species are currently under threat and these novel avenues for wildlife conservation may contribute to their very survival.

Data availability statement

The original contributions presented in the study are included in the article/supplementary material, further inquiries can be directed to the corresponding author.

Ethics statement

This animal study was reviewed and approved by the University of Saskatchewan, 003Exempt2020.

Author contributions

GK and KH contributed to conception and design of the study. AS-K and LM orchestrated sampling and logistics. GK collected the data, performed the statistical analysis, and wrote the first draft of the manuscript. GK and KH contributed equally to manuscript revision and all authors approved the submitted version.

Funding

This study was funded by Environment and Climate Change Canada.

Acknowledgments

The contributions of Andrei Mihalca, Carolyn Farquhar, and Patricia Tricorache were essential for sample collection, CITES permits, and logistics. The help and guidance of the Cheetah Conservation Fund was invaluable and we look forward to working with them in the future. We thank Chantel Gryba and Jessica Fehr for sample preparation and for assistance in stable isotope analyzes.

Conflict of interest

The authors declare that the research was conducted in the absence of any commercial or financial relationships that could be construed as a potential conflict of interest.

Publisher's note

References

Ambrose, S. H., and DeNiro, M. J. (1986). The isotopic ecology of east african mammals. *Oecologia* 69, 395–406. doi: 10.1007/BF00377062

Arctander, P., Kat, P. W., Aman, R. A., and Siegismund, H. R. (1996). Extreme genetic differences among populations of gazella granti, grant's gazelle, in kenya. *Heredity* 76, 465–475. doi: 10.1038/hdy.1996.69

Ayling, J. (2013). What sustains wildlife crime? rhino horn trading and the resilience of criminal networks. *J. Int. Wildlife Law Policy* 16, 57–80. doi: 10.1080/13880292.2013.764776

Birchall, J., O'Connell, T. C., Heaton, T. H. E., and Hedges, R. E. M. (2005). Hydrogen isotope ratios in animal body protein reflect trophic level. *J. Anim. Ecol.* 74, 877–881. doi: 10.1111/j.1365-2656.2005.00979.x

Bivand, R., and Lewin-Koh, N. (2015). maptools: Tools for reading and handling spatial objects. *R package version 0.8–39*.

Bothma, J., d,. P., and Walker, C. (1999). "The cheetah," in *Larger Carnivores of the African Savannas* (Springer), 92–115.

Bowen, G. J., Ehleringer, J. R., Chesson, L. A., Thompson, A. H., Podlesak, D. W., and Cerling, T. E. (2009). Dietary and physiological controls on the hydrogen and oxygen isotope ratios of hair from mid-20th century indigenous populations. *Am. J. Phys. Anthropol.* 139, 494–504. doi: 10.1002/ajpa.21008

Camin, F., Perini, M., Colombari, G., Bontempo, L., and Versini, G. (2008). Influence of dietary composition on the carbon, nitrogen, oxygen and hydrogen stable isotope ratios of milk. *Rapid Commun. Mass Spectrometry* 22, 1690–1696. doi: 10.1002/rcm.3506

Cardillo, M., Purvis, A., Sechrest, W., Gittleman, J. L., Bielby, J., and Mace, G. M. (2004). Human population density and extinction risk in the world's carnivores. *PLoS Biol.* 2, e197. doi: 10.1371/journal.pbio.0020197

Cetin, I., Marconi, A., Corbetta, C., Lanfranchi, A., Baggiani, A., Battaglia, F., et al. (1992). Fetal amino acids in normal pregnancies and in pregnancies complicated by intrauterine growth retardation. *Early Hum. Dev.* 29, 183–186. doi: 10.1016/0378-3782(92)90136-5

Cherel, Y., Hobson, K. A., Bailleul, F., and Groscolas, R. (2005). Nutrition, physiology, and stable isotopes: new information from fasting and molting penguins. *Ecology* 86, 2881–2888. doi: 10.1890/05-0562

Chesson, L. A., Barnette, J. E., Bowen, G. J., Brooks, J. R., Casale, J. F., Cerling, T. E., et al. (2018). Applying the principles of isotope analysis in plant and animal ecology to forensic science in the americas. *Oecologia* 187, 1077–1094. doi: 10.1007/s00442-018-4188-1

Chesson, L. A., Valenzuela, L. O., O'Grady, S. P., Cerling, T. E., and Ehleringer, J. R. (2010). Hydrogen and oxygen stable isotope ratios of milk in the united states. *J. Agric. Food Chem.* 58, 2358–2363. doi: 10.1021/jf904151c

Cilliers, J. (2017). "Fertility, growth and the future of aid in sub-Saharan Africa," in *Growth and the Future of Aid in Sub-Saharan Africa* (New York: Springer).

Codron, D., Codron, J., Lee-Thorp, J. A., Sponheimer, M., Ruiter, D., and Brink, J. S. (2007). Stable isotope characterization of mammalian predator-prey relationships in a South African savanna. *Eur. J. Wildl Res.* 3, 161–170. doi: 10.1007/s10344-006-0075-x

Craig, H. (1961). Isotopic variations in meteoric waters. *Science* 133, 1702–1703. doi: 10.1126/science.133.3465.1702

Crosier, A., Byron, M., and Comizzoli, P. (2022). Connecting the spots: understanding cheetah reproduction to improve assisted breeding and population management. *Theriogenology* 185, 70–77. doi: 10.1016/j.theriogenology.2022.03.025

Crosier, A. E., Wachter, B., Schulman, M., Luders, I., Koester, D., Wielebnowski, N., et al. (2018). "Reproductive physiology of the cheetah and assisted reproductive techniques," in *Cheetahs: Biology and Conservation*; ed A. Valutkevich (London: Elsevier Inc.), 385–402.

Dalberg, W. (2012). *Fighting Illicit Wildlife Trafficking*. Gland: WWF International.

Daut, E. F., Brightsmith, D. J., and Peterson, M. J. (2015). Role of non-governmental organizations in combating illegal wildlife-pet trade in peru. *J. Nat. Conservat.* 24, 72–82. doi: 10.1016/j.jnc.2014.10.005

De Luca, A., Boisseau, N., Tea, I., Louvet, I., Robins, R. J., Forhan, A., et al. (2012). $\delta^1$5N and $\delta^1$3C in hair from newborn infants and their mothers: a cohort study. *Pediatr. Res.* 71, 598–604. doi: 10.1038/pr.2012.3

De Waal, H., Osthoff, G., Hugo, A., Myburgh, J., and Botes, P. (2004). The composition of African lion (Panthera leo) milk collected a few days postpartum. *Mammalian Biol.* 69, 375–383. doi: 10.1078/1616-5047-00159

Derocher, A. E., Andriashek, D., and Arnould, J. P. (1993). Aspects of milk composition and lactation in polar bears. *Can. J. Zool.* 71, 561–567. doi: 10.1139/z93-077

Di Minin, E., Slotow, R., Hunter, L. T., Pouzols, F. M., Toivonen, T., Verburg, P. H., et al. (2016). Global priorities for national carnivore conservation under land use change. *Sci. Rep.* 6, 23814. doi: 10.1038/srep23814

Durant, S. M., Mitchell, N., Groom, R., Pettorelli, N., Ipavec, A., Jacobson, A. P., et al. (2017). The global decline of cheetah Acinonyx jubatus and what it means for conservation. *Proc. Natl. Acad. Sci. U.S.A.* 114, 528–533. doi: 10.1073/pnas.1611122114

Eaton, R. L. (1970). Hunting behavior of the cheetah. *J. Wildlife Manag.* 34, 56–67. doi: 10.2307/3799492

Farhadinia, M. (2004). The last stronghold: cheetah in Iran. *Cat News* 40, 11–14.

Gehre, M., Renpenning, J., Gilevska, T., Qi, H., Coplen, T. B., Meijer, H. A., et al. (2015). On-line hydrogen-isotope measurements of organic samples using elemental chromium: an extension for high temperature elemental-analyzer techniques. *Anal. Chem.* 87, 5198–5205. doi: 10.1021/acs.analchem.5b00085

Hatch, K. A., Crawford, M. A., Kunz, A. W., Thomsen, S. R., Eggett, D. L., Nelson, S. T., et al. (2006). An objective means of diagnosing anorexia nervosa and bulimia nervosa using ^{1}5N/^{1}4N and ^{1}3C/^{1}2C ratios in hair. *Rapid Commun. Mass Spectrom.* 20, 3367–3373. doi: 10.1002/rcm.2740

Hijmans, R. J., and Van Etten, J. (2015). Raster: geographic data analysis and modeling. *R package version 2.3–40*.

Hobson, K., Van Wilgenburg, S., Wassenaar, L., Powell, R., Still, C., and Craine, J. (2012). A multi-isotope (δ13c, δ15n, δ2h) feather isoscape to assign afrotropical migrant birds to origins. *Ecosphere* 3, 1–20. doi: 10.1890/ES12-00018.1

Hobson, K. A., Alisauskas, R. T., and Clark, R. G. (1993). Stable-nitrogen isotope enrichment in avian tissues due to fasting and nutritional stress: Implications for isotopic analyses of diet. *Condor* 95, 388–394. doi: 10.2307/1369361

Hobson, K. A., Atwell, L., and Wassenaar, L. I. (1999). Influence of drinking water and diet on the stable-hydrogen isotope ratios of animal tissues. *Proc. Natl. Acad. Sci. U.S.A.* 96, 8003–8006. doi: 10.1073/pnas.96.14.8003

Hobson, K. A., and Koehler, G. (2015). On the use of stable oxygen isotope ($\delta^1$8O) measurements for tracking avian movements in North America. *Ecol. Evol.* 5, 799–806. doi: 10.1002/ece3.1383

Hobson, K. A., and Wassenaar, L. I. (2008). *Tracking Animal Migration With stable Isotopes*. Academic Press. doi: 10.1016/S1936-7961(07)00006-1

Hobson, K. A., and Wassenaar, L. I. (2018). *Tracking Animal Migration With Stable Isotopes*. Academic Press.

Hobson, K. A., Wunder, M. B., Van Wilgenburg, S. L., Clark, R. G., and Wassenaar, L. I. (2009). A method for investigating population declines of migratory birds using stable isotopes: origins of harvested lesser scaup in North America. *PLoS ONE* 4, e7915. doi: 10.1371/journal.pone.0007915

Jenkins, S. G., Partridge, S. T., Stephenson, T. R., Farley, S. D., and Robbins, C. T. (2001). Nitrogen and carbon isotope fractionation between mothers, neonates, and nursing offspring. *Oecologia* 129, 336–341. doi: 10.1007/s004420100755

Koehler, G., and Hobson, K. A. (2019). Tracking cats revisited: placing terrestrial mammalian carnivores on δ2H and δ18O isoscapes. *PLoS ONE* 14, e0221876. doi: 10.1371/journal.pone.0221876

Koehler, G., Kardynal, K. J., and Hobson, K. A. (2019). Geographical assignment of polar bears using multi-element isoscapes. *Sci. Rep.* 9, 9390. doi: 10.1038/s41598-019-45874-w

Kornexl, B. E., Werner, T., Roßmann, A., and Schmidt, H.-L. (1997). Measurement of stable isotope abundances in milk and milk ingredients–a possible tool for origin assignment and quality control. *Zeitschrift für Lebensmitteluntersuchung und-Forschung A* 205, 19–24. doi: 10.1007/s002170050117

Levin, N. E., Zipser, E. J., and Cerling, T. E. (2009). Isotopic composition of waters from ethiopia and kenya: Insights into moisture sources for eastern africa. *J. Geophys. Res. Atmospheres* 114, D23. doi: 10.1029/2009JD012166

Magozzi, S., Vander Zanden, H., Wunder, M., and Bowen, G. (2019). Mechanistic model predicts tissue-environment relationships and trophic shifts in animal hydrogen and oxygen isotope ratios. *Oecologia* 191, 777. doi: 10.1007/s00442-019-04532-8

Marker, L. (2019). Loving a species to death. *Biodiversity* 20, 50–55. doi: 10.1080/14888386.2019.1591300

Marker, L. L., Muntifering, J., Dickman, A., Mills, M., and Macdonald, D. (2003). Quantifying prey preferences of free-ranging namibian cheetahs. *South Afr. J. Wildlife Res*. 33, 43–53.

Marker-Kraus, L. (1997). History of the Cheetah: *Acinonyx jubatus* in zoos 1829-1994. *Int. Zoo Yearbook* 35, 27–43. doi: 10.1111/j.1748-1090.1997.tb01186.x

McKechnie, A. E., Wolf, B. O., and Del Rio, C. M. (2004). Deuterium stable isotope ratios as tracers of water resource use: an experimental test with rock doves. *Oecologia* 140, 191–200. doi: 10.1007/s00442-004-1564-9

Meier-Augenstein, W., Hobson, K. A., and Wassenaar, L. I. (2013). Critique: measuring hydrogen stable isotope abundance of proteins to infer origins of wildlife, food and people. *Bioanalysis* 5, 751–767. doi: 10.4155/bio.13.36

Mekota, A.-M., Grupe, G., Ufer, S., and Cuntz, U. (2006). Serial analysis of stable nitrogen and carbon isotopes in hair: monitoring starvation and recovery phases of patients suffering from anorexia nervosa. *Rapid Commun. Mass Spectrom*. 20, 1604–1610. doi: 10.1002/rcm.2477

Melzer, E., and Schmidt, H. (1987). Carbon isotope effects on the pyruvate dehydrogenase reaction and their importance for relative carbon-13 depletion in lipids. *J. Biol. Chem*. 262, 8159–8164. doi: 10.1016/S0021-9258(18)47543-6

Mills, M. L. (1984). Prey selection and feeding habits of the large carnivores in the southern Kalahari. *Koedoe* 27, 281–294. doi: 10.4102/koedoe.v27i2.586

Montanari, S., and Amato, G. (2015). Discrimination factors of carbon and nitrogen stable isotopes from diet to hair and scat in captive tigers (*Panthera tigris*) and snow leopards (uncia uncia). *Rapid Commun. Mass Spectrom*. 29, 1062–1068. doi: 10.1002/rcm.7194

O'Brien, S. J., Roelke, M. E., Marker, L., Newman, A., Winkler, C., Meltzer, D., et al. (1985). Genetic basis for species vulnerability in the cheetah. *Science* 227, 1428–1434. doi: 10.1126/science.2983425

O'Brien, S. J., Wildt, D. E., and Bush, M. (1986). The cheetah in genetic peril. *Sci. Am*. 254, 84–95. doi: 10.1038/scientificamerican0586-84

Osthoff, G., Hugo, A., and De Wit, M. (2006). The composition of cheetah (*Acinonyx jubatus*) milk. *Comparat. Biochem. Physiol. B Biochem. Mol. Biol*. 145, 265–269. doi: 10.1016/j.cbpb.2006.05.016

Parng, E., Crumpacker, A., and Kurle, C. M. (2014). Variation in the stable carbon and nitrogen isotope discrimination factors from diet to fur in four felid species held on different diets. *J. Mammal*. 95, 151–159. doi: 10.1644/13-MAMM-A-014.1

Pietsch, S. J., Hobson, K. A., Wassenaar, L. I., and Tütken„ T. (2011). Tracking cats: problems with placing feline carnivores on $\delta^1$8O, δD isoscapes. *PLoS ONE* 6, e24601. doi: 10.1371/journal.pone.0024601

Pires, S. F. (2012). The illegal parrot trade: a literature review. *Global Crime* 13, 176–190. doi: 10.1080/17440572.2012.700180

Pires, S. F., and Moreto, W. D. (2011). Preventing wildlife crimes: solutions that can overcome the 'tragedy of the commons'. *Eur. J. Crim. Policy Res*. 17, 101–123. doi: 10.1007/s10610-011-9141-3

Polischuk, S. C., Hobson, K. A., and Ramsay, M. A. (2001). Use of stable-carbon and-nitrogen isotopes to assess weaning and fasting in female polar bears and their cubs. *Can. J. Zool*. 79, 499–511. doi: 10.1139/z01-007

Qi, H., Coplen, T. B., and Wassenaar, L. I. (2011). Improved online $\delta^1$8O measurements of nitrogen-and sulfur-bearing organic materials and a proposed analytical protocol. *Rapid Commun. Mass Spectrom*. 25, 2049–2058. doi: 10.1002/rcm.5088

R Core Team (2021). *R: A Language and Environment for Statistical Computing*. Vienna: R Foundation for Statistical Computing.

Ripple, W. J., Estes, J. A., Beschta, R. L., Wilmers, C. C., Ritchie, E. G., Hebblewhite, M., et al. (2014). Status and ecological effects of the world's largest carnivores. *Science* 343, 1241484. doi: 10.1126/science.1241484

Sachse, D., Billault, I., Bowen, G. J., Chikaraishi, Y., Dawson, T. E., Feakins, S. J., et al. (2012). Molecular paleohydrology: interpreting the hydrogen-isotopic composition of lipid biomarkers from photosynthesizing organisms. *Annu. Rev. Earth Planet. Sci*. 40, 221–249. doi: 10.1146/annurev-earth-042711-105535

Schoeller, D. A., Leitch, C. A., and Brown, C. (1986). Doubly labeled water method: in vivo oxygen and hydrogen isotope fractionation. *Am. J. Physiol. Regulat. Integr. Compar. Physiol*. 251, R1137-R1143. doi: 10.1152/ajpregu.1986.251.6.R1137

Sessions, A. L., Burgoyne, T. W., Schimmelmann, A., and Hayes, J. M. (1999). Fractionation of hydrogen isotopes in lipid biosynthesis. *Org. Geochem*. 30, 1193–1200. doi: 10.1016/S0146-6380(99)00094-7

Soto, D. X., Koehler, G., Wassenaar, L. I., and Hobson, K. A. (2017). Re-evaluation of the hydrogen stable isotopic composition of keratin calibration standards for wildlife and forensic science applications. *Rapid Commun. Mass Spectrom*. 31, 1193–1203. doi: 10.1002/rcm.7893

Soto, D. X., Wassenaar, L. I., Hobson, K. A., and Catalan, J. (2011). Effects of size and diet on stable hydrogen isotope values (δD) in fish: implications for tracing origins of individuals and their food sources. *Can. J. Fish. Aquat. Sci*. 68, 2011–2019. doi: 10.1139/f2011-112

Spinage, C., Ryan, C., and Shedd, M. (1980). Food selection by the Grant's gazelle. *Afr. J. Ecol*. 18, 19–25. doi: 10.1111/j.1365-2028.1980.tb00267.x

Still, C. J., and Powell, R. L. (2010). "Continental-scale distributions of vegetation stable carbon isotope ratios," in *Isoscapes*, eds J. West, G. Bowen, T. Dawson, and K. Tu (Dordrecht: Springer). doi: 10.1007/978-90-481-3354-3_9

Storm-Suke, A., Wassenaar, L. I., Nol, E., and Norris, D. R. (2012). The influence of metabolic rate on the contribution of stable-hydrogen and oxygen isotopes in drinking water to quail blood plasma and feathers. *Funct. Ecol*. 26, 1111–1119. doi: 10.1111/j.1365-2435.2012.02014.x

Terzer, S., Wassenaar, L., Araguás-Araguás, L., and Aggarwal, P. (2013). Global isoscapes for $\delta^1$8O and δ^2H in precipitation: improved prediction using regionalized climatic regression models. *Hydrol. Earth Syst. Sci*. 17, 4713. doi: 10.5194/hess-17-4713-2013

Terzer-Wassmuth, S., Wassenaar, L. I., Welker, J. M., and Araguás-Araguás, L. J. (2021). Improved high-resolution global and regionalized isoscapes of $\delta^1$8o, δ^2h and d-excess in precipitation. *Hydrol. Process*. 35, e14254. doi: 10.1002/hyp.14254

Tieszen, L. L., Boutton, T. W., Tesdahl, K. G., and Slade, N. A. (1983). Fractionation and turnover of stable carbon isotopes in animal tissues: implications for $\delta^1$3C analysis of diet. *Oecologia* 57, 32–37. doi: 10.1007/BF00379558

Tieszen, L. L., Hein, D., Qvortrup, S., Troughton, J., and Imbamba, S. (1979a). Use of $\delta^1$3C values to determine vegetation selectivity in East African herbivores. *Oecologia* 37, 351. doi: 10.1007/BF00347911

Tieszen, L. L., Senyimba, M. M., Imbamba, S. K., and Troughton, J. H. (1979b). The Distribution of C3 and C4 grasses and carbon isotope discrimination along an altitudinal and moisture gradient in Kenya. *Oecologia* 37, 337–350. doi: 10.1007/BF00347910

Topalov, K., Schimmelmann, A., Polly, P. D., Sauer, P. E., and Lowry, M. (2013). Environmental, trophic, and ecological factors influencing bone collagen δ^2H. *Geochim. Cosmochim. Acta* 111, 88–104. doi: 10.1016/j.gca.2012.11.017

Tordiffe, A. S., Wachter, B., Heinrich, S. K., Reyers, F., and Mienie, L. J. (2016). Comparative serum fatty acid profiles of captive and free-ranging cheetahs (*Acinonyx jubatus*) in Namibia. *PLoS ONE* 11, e0167608. doi: 10.1371/journal.pone.0167608

Tricorache, P., Nowell, K., Wirth, G., Mitchell, N., Boast, L. K., and Marker, L. (2018). "Pets and pelts: Understanding and combating poaching and trafficking in cheetahs," in *Biodiversity of the World-Cheetahs: Biology and Conservation*, 1st Edn (San Diego, CA: Elsevier), 191–205.

Van Wilgenburg, S. L., and Hobson, K. A. (2011). Combining stable-isotope (δD) and band recovery data to improve probabilistic assignment of migratory birds to origin. *Ecol. Appl*. 21, 1340–1351. doi: 10.1890/09-2047.1

Vander Zanden, H. B., Nelson, D. M., Wunder, M. B., Conkling, T. J., and Katzner, T. (2018). Application of isoscapes to determine geographic origin of terrestrial wildlife for conservation and management. *Biol. Conserv*. 228, 268–280. doi: 10.1016/j.biocon.2018.10.019

Vander Zanden, H. B., Soto, D. X., Bowen, G. J., and Hobson, K. A. (2016). Expanding the isotopic toolbox: applications of hydrogen and oxygen stable isotope ratios to food web studies. *Front. Ecol. Evol*. 4, 20. doi: 10.3389/fevo.2016.00020

Velho, N., Karanth, K. K., and Laurance, W. F. (2012). Hunting: a serious and understudied threat in India, a globally significant conservation region. *Biol. Conserv*. 148, 210–215. doi: 10.1016/j.biocon.2012.01.022

Voigt, C. C., Thalwitzer, S., Melzheimer, J., Blanc, A.-S., Jago, M., and Wachter, B. (2014). The conflict between cheetahs and humans on Namibian farmland elucidated by stable isotope diet analysis. *PLoS ONE* 9, e101917. doi: 10.1371/journal.pone.0101917

Warchol, G. L. (2004). The transnational illegal wildlife trade. *Crim. Justice Stud*. 17, 57–73. doi: 10.1080/0888431042000167933 4

Warchol, G. L., Zupan, L. L., and Clack, W. (2003). Transnational criminality: an analysis of the illegal wildlife market in Southern Africa. *Int. Crim. Justice Rev*. 13, 1–27. doi: 10.1177/105756770301300101

West, J. B., Bowen, G. J., Dawson, T. E., and Tu, K. P. (2009). *Isoscapes: Understanding Movement, Pattern, and Process on Earth Through Isotope Mapping*. Dordrecht: Springer. doi: 10.1007/978-90-481-3354-3

Wilson, G., Mackenzie, D., Brookes, I., and Lyon, G. (1988). Importance of body tissues as sources of nutrients for milk synthesis in the cow, using ^{1}3C as a marker. *Br. J. Nutr*. 60, 605–617. doi: 10.1079/BJN19880131

Wolf, C., and Ripple, W. J. (2017). Range contractions of the world's large carnivores. *R. Soc. Open Sci*. 4, 170052. doi: 10.1098/rsos.170052

Wolf, N., Newsome, S. D., Peters, J., and Fogel, M. L. (2015). Variability in the routing of dietary proteins and lipids to consumer tissues influences tissue-specific isotopic discrimination. *Rapid Commun. Mass Spectrom*. 29, 1448–1456. doi: 10.1002/rcm.7239

frontiers | Frontiers in Ecology and Evolution

TYPE Original Research
PUBLISHED 13 February 2023
DOI 10.3389/fevo.2023.1085903

OPEN ACCESS

EDITED BY
Keith Alan Hobson,
Western University,
Canada

REVIEWED BY
Stefan Siebert,
North-West University,
South Africa
Michał Filipiak,
Jagiellonian University,
Poland

*CORRESPONDENCE
Megan S. Reich
✉ megan.reich@uottawa.ca
Clément P. Bataille
✉ cbataill@uottawa.ca

SPECIALTY SECTION
This article was submitted to Ecophysiology, a section of the journal Frontiers in Ecology and Evolution

RECEIVED 31 October 2022
ACCEPTED 13 January 2023
PUBLISHED 13 February 2023

CITATION
Reich MS, Kindra M, Dargent F, Hu L, Flockhart DTT, Norris DR, Kharouba H, Talavera G and Bataille CP (2023) Metals and metal isotopes incorporation in insect wings: Implications for geolocation and pollution exposure.
Front. Ecol. Evol. 11:1085903.
doi: 10.3389/fevo.2023.1085903

Metals and metal isotopes incorporation in insect wings: Implications for geolocation and pollution exposure

Megan S. Reich[1]*, Mira Kindra[2], Felipe Dargent[2,3], Lihai Hu[2], D. T. Tyler Flockhart[4], D. Ryan Norris[4], Heather Kharouba[1], Gerard Talavera[5] and Clément P. Bataille[1,2]*

[1]Department of Biology, University of Ottawa, Ottawa, ON, Canada, [2]Department of Earth and Environmental Sciences, University of Ottawa, Ottawa, ON, Canada, [3]Great Lakes Forestry Centre, Canadian Forest Service, Natural Resources Canada, Sault Ste. Marie, ON, Canada, [4]Department of Integrative Biology, University of Guelph, Guelph, ON, Canada, [5]Institut Botànic de Barcelona (IBB), CSIC-Ajuntament de Barcelona, Barcelona, Catalonia, Spain

Anthropogenic activities are exposing insects to elevated levels of toxic metals and are altering the bioavailability of essential metals. Metals and metal isotopes have also become promising tools for the geolocation of migratory insects. Understanding the pathways of metal incorporation in insect tissues is thus important for assessing the role of metals in insect physiology and ecology and for the development of metals and metal isotopes as geolocation tools. We conducted a diet-switching experiment on monarch butterflies [*Danaus plexippus* (L.)] with controlled larval and adult diets to evaluate the sources of 23 metals and metalloids, strontium isotopes, and lead isotopes to insect wing tissues over a period of 8 weeks. Concentrations of Ca, Co, Mo, and Sb differed between the sexes or with body mass. Ni and Zn bioaccumulated in the insect wing tissues over time, likely from the adult diet, while increases in Al, Cr, Cd, Cu, Fe, and Pb were, at least partially, from external sources (i.e., dust aerosols). Bioaccumulation of Pb in the monarch wings was confirmed by Pb isotopes to mainly be sourced from external anthropogenic sources, revealing the potential of Pb isotopes to become an indicator and tracer of metal pollution exposure along migratory paths. Concentrations of Ba, Cs, Mg, Na, Rb, Sr, Ti, Tl, and U appeared to be unaffected by intrinsic factors or additions of metals from adult dietary or external sources, and their potential for geolocation should be further explored. Strontium isotope ratios remained indicative of the larval diet, at least in males, supporting its potential as a geolocation tool. However, the difference in strontium isotope ratios between sexes, as well as the possibility of external contamination by wetting, requires further investigation. Our results demonstrate the complexity of metal incorporation processes in insects and the value of studying metals to develop new tools to quantify pollution exposure, metal toxicity, micronutrient uptake, and insect mobility.

KEYWORDS

metal isotopes, strontium isotopes (87Sr/86Sr), lead isotopes, isotope-based geographic assignment, chemoprint, monarch butterfly (*Danaus plexippus*), metal pollution

1. Introduction

Some metals are important micronutrients that sustain life while others have profound implications as toxic metals that reduce survival and fitness. Essential metals are required for metabolic functions such as that the organism cannot survive when the metal is removed from the diet. Essential metals participate in enzyme catalysis, protein structure, cellular signaling, and the creation of electrochemical potentials at membranes (Maret, 2016; Dow, 2017) and it is estimated that up to 30% of proteins are metalloproteins (Aptekmann et al., 2022). Within organisms, these essential metals follow a dose–response curve, in which low doses cause morbidity due to metal deficiency and high doses cause toxicological effects. Conversely, many non-essential metals are toxic even at low doses. However, despite the fundamental importance of metals, little is known about the pathways of metal incorporation into insects in comparison to non-metal macronutrients like C, H, N, and S (Dow, 2017; Kaspari, 2021).

Insects incorporate essential and non-essential metals through their larval and adult diets. When some of these essential metals are limited in the environment, populations of herbivorous insect species can be strongly affected (Kaspari, 2020; Reihart et al., 2021), whereas abundant essential metals in the environment can boost population sizes (Prather et al., 2018). For example, the community composition and abundance of grasshoppers is influenced by plant concentrations of N, P, Mg, Na and K in grasslands (Joern et al., 2012). Some toxic metals are also bioaccumulated through dietary sources with detrimental effects on insect populations. For example, experiments have demonstrated that *Spodoptera litura* Fabricius moths bioaccumulate Ni from their adult diet with negative impacts on growth rate and fecundity (Sun et al., 2013). However, diet might not be the only source of metal incorporation into insect tissues. Unlike vertebrates, insects respire through a system of tubes called tracheae that form a complex network of gas-filled vessels throughout the body. Many metals, such as Pb and Cd, are concentrated in anthropogenic aerosols and can potentially circulate within the tracheal system (Negri et al., 2015). In addition, chitin, a structural polysaccharide, forms insect exoskeletons and is a powerful metal absorbent (Anastopoulos et al., 2017) that could facilitate metal incorporation in insect tissues through adhesion to the surface of the exoskeleton (Negri et al., 2015). Some elements, such as Sr, Ca, Mg, and Ba, are highly soluble in water and it is possible that they could exchange and diffuse deeper into insect tissues when wetted. Recent controlled studies on metabolically inert keratinous tissues of vertebrates (e.g., Feathers: Crowley et al., 2021; hair: Fauberteau et al., 2021) demonstrated that many metals in keratin are rapidly exchanged and concentrated from external sources (e.g., wet absorption, pollution, dust aerosols; Hu et al., 2018, 2019, 2020; Rodiouchkina et al., 2022). In addition to their incorporation through diet, exogenous bioaccumulation could influence the concentration of metals in chitinous insect tissues.

Understanding the sources and mechanisms of metal incorporation into insect tissues is especially urgent in the context of anthropogenic habitat alteration because human activities have changed the concentrations of toxic and essential metals in the environment. Human activities such as smelting, mining, industrialization, and agriculture are causing insects to be increasingly exposed to toxic metals at rates above the natural baselines they evolved to tolerate (Monchanin et al., 2021). Even when regulated, these activities can have adverse effects on insects because invertebrates are more susceptible than vertebrates to toxic metals like Cd and Pb and, therefore, often experience adverse effects well below anthropocentric permissible concentration limits (Hopkin, 1990; Mogren and Trumble, 2010; Monchanin et al., 2021). Similarly, activities such as CO_2 enrichment or the application of nitrogen and phosphate fertilizers can alter the availability of essential metals to insects though the nutrient dilution of plants (Welti et al., 2020; Nessel et al., 2021). Limited availability of essential metals can inhibit growth and development and reduce fitness; thus, conservation efforts need to consider both changes to the bioavailability of essential metals to organisms (Filipiak and Filipiak, 2022) and exposure to toxic metals.

Besides these toxicological and micronutrient availability concerns, understanding the mechanisms of metal incorporation into insect tissues is essential to develop new geolocation tools for insect population ecology. The analysis of metal and metal isotopes in insect tissues has become a promising avenue for developing tools aimed at understanding insect migration. Metals (e.g., Tigar and Hursthouse, 2016), metal ratios (e.g., Holder et al., 2014), combined metal composition (i.e., chemoprints, mineral component analysis, chemometrics; e.g., Lin et al., 2019) and metal isotopes (Holder et al., 2014; Reich et al., 2021) have been used to assess long-term patterns of insect dispersal. Insect wings are the primary tissue used to develop these geolocation tools. It has been demonstrated that, for some metal and metal isotopes, the insect wings reflect the chemical signature of the larval diet (e.g., Flockhart et al., 2015). By comparing the chemical signature of the metal or metal isotopes of the insect tissue to metal-specific baseline maps (called "metalscapes" or isoscapes), one can then estimate the location where the tissue formation occurred (i.e., the natal origin). However, making proper geolocation inferences with these metals requires a clear understanding of metal and metal isotope incorporation into insect tissue over time because alteration of the natal signature *via*, for example, the uptake of metals through adult feeding, would void any geolocation inferences (Dempster et al., 1986). Insect wings are primarily composed of chitin and proteins, and are not completely inert like vertebrate keratin. They host androconial organs (i.e., pheromone glands), sensory receptors, trachea, nerves, and have hemolymph circulating through their veins (Tsai et al., 2020). Consequently, the circulation of hemolymph could lead to some metal exchange with the rest of the insect body leading to potential modification of metal concentrations during the adult life, as has been observed for hydrogen isotope values (Lindroos et al., 2023). Additionally, exogenous bioaccumulation could contribute to the incorporation of many metals during adult life through aerosol deposition and wetting as has been observed with keratinous tissues (Hu et al., 2018, 2019). However, the potential addition of metals to insect wings after tissue formation has not been explicitly investigated.

In this study, we aimed to better characterize the incorporation mechanisms of a suite of metal and metal isotopes in insect wings over time and advance the development of metal-based tools for insect ecology. We conducted a laboratory-based diet-switching experiment to explore the environmental and dietary sources of 23 metals and metalloids, strontium isotopes (measured as $^{87}Sr/^{86}Sr$ ratios), and lead isotopes (measured as $^{208}Pb/^{206}Pb$ and $^{207}Pb/^{206}Pb$ ratios) in insect wings over an 8-week timespan. For each metal, we evaluated the effects of intrinsic factors on metal concentrations and assessed the potential sources of any bioaccumulation. We also assessed the potential for $^{87}Sr/^{86}Sr$ in insect wings to be altered by wetting. Finally, we evaluated the potential of the metal and metal isotopes for providing geolocation or pollution exposure information. By understanding the incorporation of metals and metal isotopes in insect wings over time, we will be better able to test the assumptions of geolocation using metal biomarkers and assess the metal exposure risks of insects.

2. Materials and methods

We chose for this study a representative winged insect, the monarch butterfly [*Danaus plexippus* (L.)]. The monarch butterfly is an iconic migratory insect famous for its annual, multi-generational, round-trip migration from the Oyamel fir forests of Central Mexico, through the United States, to Canada, and back. Monarchs are a well-suited species to investigate the incorporation of metal and metal isotope signals. First, they have a large geographic range with known elemental and isotopic variations meaningful for geolocation (Wieringa et al., 2020; Reich et al., 2021). Second, monarch larvae are specialist herbivores dependent on milkweed (*Asclepias* spp.). Plants are known to uptake and regulate metals in a species-specific manner; thus, this relatively high host-specificity will likely minimize potential discrepancies in metal signatures associated with differences in larval host plant species (McLean et al., 1983; Tibbett et al., 2021). Third, metal exposure is of particular concern for monarchs because milkweed is often found in disturbed habitats, such as roadsides, which often correlates with higher pollution exposure (Phillips et al., 2021). As for most insects, the incorporation and toxicology of metals in monarch butterflies are mostly unknown, although Zn has been shown to decrease larval survival under some conditions (e.g., when individuals have low access to macronutrients; Shephard et al., 2020, 2021, 2022).

To explore the incorporation of metal and metal isotopes, we first conducted a diet-switching experiment on monarch butterflies over an 8-week period. We raised larvae from eggs with controlled milkweed dietary inputs and then maintained the adults with a controlled adult diet. We measured the changes in metal concentrations and isotopes in monarch wings at weekly time intervals and compared the metal abundances found in our laboratory experiment to the range of natural metal abundances in the wings of 100 wild-caught monarch butterflies. Next, we explored the incorporation mechanisms of different metals by calculating enrichment factors to the adult diet and a proxy of mineral dust for each metal, analyzing lead isotopes in the monarch wings to assess the source of Pb bioaccumulation, and performing a wetting experiment for Sr. Finally, we measured the concentrations of 12 metals in ashed milkweed samples from across the eastern United States and assessed our ability to use soil and milkweed samples in the construction of metalscapes for monarch butterflies (Supplementary Material).

2.1. Diet-switching experiment

We conducted a diet-switching experiment in the summer of 2019 to assess the sources and preservation of metals and metalloids (hereinafter referred to collectively as metals) and metal isotope signals in monarch wings throughout the life of an adult butterfly. Eggs were collected from a single wild-caught female, allowing us to assume that all the specimens in this experiment are at least half-siblings and control for maternal effects. After collection, eggs were transferred to individual 500 ml glass rearing containers with a mesh lid and placed in a controlled environmental chamber (Biochambers Inc., model LTCB-19) held at a light to dark schedule of 12 h:12 h, light temperature of 28°C and dark temperature of 26°C, and humidity of 60%. These conditions reflect optimal conditions for monarch development (Dargent et al., 2021).

Caterpillars were fed wild common milkweed (*Asclepias syriaca* L.) leaves that were collected daily from Aug. 9–22, 2019, from a single 30 m^2 site in Ottawa, Ontario, Canada (45.41°, −75.67°). The collection site is in an urban park next to the Rideau River and is near a light rail station and bike paths. The leaves were cleaned of surface contaminates (e.g., dust) using distilled deionized (DDI) water before being fed *ad libitum* to the caterpillars. Sub-samples of the cleaned milkweed leaves were collected for analysis to check the assumption that milkweed leaves taken from the same locality will have similar elemental and isotopic signatures over the 2-week period of collection. Frass was removed from the containers daily.

After the monarchs eclosed from the chrysalises (Aug. 29–31, 2019), they were transferred to mesh butterfly cages in an indoor laboratory. Butterflies were kept two per cage, but a cloth divider was installed to minimize wing damage from collisions between individuals. The cages were misted twice a day with DDI water to maintain humidity and were given a light-to-dark schedule of about 12 h:12 h. DDI water was used to avoid additions of metals by water absorption. The temperature in the laboratory was maintained by the building's normal operations and maintenance schedule at approximately 20°C. Once per day, the adult butterflies were given a fresh serving of 50% maple syrup solution in a tube with a foam faux-flower perch and allowed to feed *ad libitum*. The adult food was renewed every day to avoid accumulation of metals from external sources (e.g., dust) in the maple syrup solution to ensure that metals sourced from the diet and exogenous aerosols could be distinguished. Because the butterflies do not always recognize the unnatural food source, individuals were also hand-fed the maple syrup for at least 1 minute every other day. The first six monarchs were sampled immediately post-eclosion (Day 0; no feeding), and two monarchs were subsequently sampled each week until up to 8 weeks post-eclosion ($n = 22$). Immediately after sampling, monarchs were placed into a freezing chamber at −18°C. Later, wings were dissected from the body and placed in glassine envelopes until elemental analysis. The time between collection and elemental or isotopic analysis ranged from a few months to 18 months.

2.1.1. Trace element analysis

Elemental analysis of monarch wings, larval diet (i.e., milkweed leaves) and adult diet (i.e., 50% maple syrup solution) was performed in two analytical runs *via* inductively coupled plasma mass spectrometry (ICP-MS; Agilent 8800 ICP-QQQ, Agilent Technologies Inc., Santa Clara, CA, United States) at the Department of Earth and Environmental Sciences, University of Ottawa. The first analytical run in February 2020 measured 23 metals in monarch wings ($n = 18$) and maple syrup ($n = 4$): aluminum (Al), arsenic (As), barium (Ba), calcium (Ca), cadmium (Cd), cobalt (Co), chromium (Cr), copper (Cu), cesium (Cs), iron (Fe), magnesium (Mg), manganese (Mn), molybdenum (Mo), sodium (Na), nickel (Ni), lead (Pb), rubidium (Rb), antimony (Sb), strontium (Sr), titanium (Ti), thallium (Tl), uranium (U), and zinc (Zn). To remove any surface contaminants (e.g., dust), a single forewing from each monarch was cleaned using pressurized nitrogen gas for about 2 min. at 10 psi (Reich et al., 2021). The monarch wings and maple syrup samples were then digested in perfluoroalkoxy alkanes (PFA) vials (Savillex, LLC., Eden Prairie, MN, United States) using 1 ml 16 M HNO_3 (double distilled TraceMetal™ Grade; Fisher Chemical, Mississauga, ON, Canada) and 0.1 ml ultraclean hydrogen peroxide (for trace analysis Grade; Sigma-Aldrich, Italy) for 12 h at 120°C. After digestion, the samples were dried on a hot plate at 90°C and then re-dissolved in 1 ml of 2% v/v HNO_3 (double distilled). A 100 µl aliquot of each solution was extracted, diluted to 2 ml 2% v/v HNO_3, and centrifuged. Calibration standards were prepared using single element certified standards (SCP Science Inc., Montreal, QC, Canada). Detection limits were conservatively estimated as three times the standard deviation of the

blanks within each run. For monarch wings, 4 measurements of As, 2 of Tl, and 8 of U were below the detection limit. Concentrations of Cd, Cs, Tl, and U were lower than the calibration range of 1.56 to 100 ppb (~200, ~800, ~900, and ~ 4,600 times lower, respectively). Metal concentrations in maple syrup were comparatively low, with all 4 As and U measures and 1 Fe measure below the detection limit. Additionally, Cd, Tl, and Pb were all well below the calibration range (~600, ~200 and ~ 200 times lower, respectively). Intra-run relative standard deviation (RSD) of the repeated standard analysis was below 3% except for Cs (RSD = 21%), Sb (RSD = 19%), Rb (RSD = 67%), and Fe (RSD = 38%).

For the second analytical run in May 2021, milkweed samples ($n = 3$) and analytical replicates of monarch wings ($n = 19$) were analyzed for 15 metals: Al, Ba, Ca, Cd, Co, Cr, Cu, Fe, Mg, Mn, Ni, Pb, Sr, Ti, and Zn. Milkweed samples were cleaned with DDI water, an ultrasonic bath (10 min.), and a MilliQ water rinse. Wing samples were dry-cleaned with pressurized nitrogen gas for 2 min. at about 10 psi for a limited, repeated elemental analysis of the monarch wings to assess if there was sample contamination of Pb during storage. For monarch tissues, a single hindwing was used for most samples. However, some samples had too low Pb concentrations and both hindwings (i.e., L2) or both hindwings and the remaining forewings were used (i.e., L11, L16, L17, L21, and L5). Samples were then digested in concentrated nitric acid (16 M; distilled TraceMetal™ Grade; Fisher Chemical, Canada) using microwave digestion (Anton Paar Multiwave 7,000, Austria): the samples were heated from ambient temperature to 250°C at a steady rate in 20 min. and then left at 250°C for 15 min. in a pressurized chamber. An aliquot of 200 µl from each sample was separated and diluted to 2 ml of 2% v/v HNO_3 (double distilled) and run on the ICP-MS. For monarch wings, 16 measurements of Co and 17 of Cd were below the detection limit; only Cd was lower than the calibration range (~155 times lower). Metal concentrations in milkweed were comparatively high, with Ca and Mg well above the calibration range (~900 and ~ 200 times higher, respectively). Intra-run RSD of the repeated standard analysis was below 3% except for Mg (RSD = 70%), Ca (RSD = 157%), and Fe (RSD = 143%).

2.1.2. Strontium isotope ratios analysis

The $^{87}Sr/^{86}Sr$ analysis was performed in two runs at the Isotope Geochemistry and Geochronology Research Center, Carleton University using a ThermoScientific™ Neptune™ high-resolution multi-collector inductively coupled plasma mass spectrometer (MC-ICP-MS; Thermo Fisher Scientific, Bremen, Germany). To prepare for the first run in February 2020, milkweed samples ($n = 3$) were cleaned using DDI water and an ultrasonic bath (10 min.), then oven-dried at 80°C before being ashed at 600°C for 4 h. to facilitate digestion. They were then digested in perfluoroalkoxy alkanes (PFA) vials (Savillex, LLC., Eden Prairie, MN, United States) using 1 ml 16 M HNO_3 (double distilled TraceMetal™ Grade; Fisher Chemical, Mississauga, ON, Canada) and 0.1 ml ultraclean hydrogen peroxide (for trace analysis Grade; Sigma-Aldrich, Italy) for 12 h. at 120°C. After digestion, the samples were dried on a hot plate at 90°C. Dried samples were re-dissolved in 1 ml of 2% v/v HNO_3 (double distilled). A 100 µl aliquot of each solution was extracted, diluted to 2 ml 2% v/v HNO_3, and the concentration of Sr was measured using the ICP-MS in October 2019. The remaining ~900 µl aliquot (90%) of sample digest was dried down and re-dissolved in 0.05 ml 6 M HNO_3. The separation of Sr was processed in 100 µl microcolumn loaded with Sr-spec Resin™ (100–150 µm; Eichrom Technologies, LLC). The matrix was rinsed out using 6 M HNO_3, and Sr was collected with 0.05 M HNO_3. After separation, eluates were dried and re-dissolved in 2 ml 2% v/v HNO_3 for $^{87}Sr/^{86}Sr$ analysis.

For the second analytical run in September 2020, the remaining aliquots (~90%) of the monarch wing ($n = 18$) and maple syrup ($n = 4$) samples run on the ICP-MS in February 2020 were used. Samples were dried down and re-dissolved in 0.5 ml 6 M HNO_3. The separation of Sr was processed in 100 µl microcolumn loaded with Sr-spec Resin™ (100–150 µm; Eichrom Technologies, LLC). The matrix was rinsed out using 6 M HNO3, and Sr was collected with 0.05 M HNO_3. The microcolumn process was repeated to ensure complete separation. After separation, the eluates were dried, and monarch wing samples were re-dissolved in 200 µl 2% v/v HNO_3 and maple syrup in 2 ml 2% v/v HNO_3 for $^{87}Sr/^{86}Sr$ analysis.

For both analytical runs, sample solutions were introduced to the MC-ICP-MS using a micro*FAST* MC single-loop system (Elemental Scientific Inc., Omaha, NE, United States). The sample introduction flow rate was 30 µl/min, and the loading volume was 200 µl for the milkweed and maple syrup and 100 µl for the monarch wing samples. The solution was introduced using a PFA nebulizer, double-pass quartz spray chamber, quartz torch, and nickel sample and skimmer cones. Isotopes ^{82}Kr, ^{83}Kr, ^{84}Sr, ^{85}Rb, ^{86}Sr, ^{87}Sr, and ^{88}Sr were simultaneously measured in L4, L3, L2, L1, C, H1, and H2 Faraday cups, respectively. Measurements of samples were made using a static multi-collector routine that consisted of one block of either 70 (milkweed and maple syrup) or 30 cycles (monarch wings) with an integration time of 4.194 s/cycle. ^{84}Sr and ^{86}Sr have isobaric interferences from ^{84}Kr and ^{86}Kr, respectively. ^{87}Sr has an isobaric interference from ^{87}Rb. The interferences of ^{84}Sr and ^{86}Sr were corrected by subtracting the amount of ^{84}Kr and ^{86}Kr corresponding to the ^{83}Kr signal. Interference of ^{87}Sr was corrected by subtracting the amount of ^{87}Rb corresponding to the ^{85}Rb signal. Instrumental mass fractionation was corrected by normalizing $^{86}Sr/^{88}Sr$ to 0.1194 using the exponential law (Moore et al., 1982). Strontium isotope compositions are reported as $^{87}Sr/^{86}Sr$ ratios. Procedural blanks were always negligible, with good reproducibility of $^{87}Sr/^{86}Sr$ for NIST SRM987 (0.710251 ± 0.000003 (1 SD), $n = 2$). Two 100 ng/g pure Sr standards were measured along with the samples as in-house standards (SrSCP: 0.70816 ± 0.00013, $n = 11$; GSC: 0.70756 ± 0.00002, $n = 4$). The long-term reproducibility of the SrSCP in-house standard is (0.70822 ± 0.00004, $n = 106$).

2.1.3. Lead isotope ratios analysis

We analyzed the lead isotope ratios ($^{208}Pb/^{206}Pb$, $^{207}Pb/^{206}Pb$) of monarch wing and milkweed samples to refine the sources of Pb in the monarch wings. The remaining aliquots (~90%) of the microwave-digested milkweed ($n = 3$) and monarch ($n = 19$) samples run on the ICP-MS in May 2021 were used. The separation of Pb was processed in polyethylene columns (Bio-Rad, Hercules, California, United States) loaded with 0.6 ml analytical grade anion exchange resin (AG 1-X8, 100–200 mesh, chloride form; Bio-Rad, Hercules, California, United States). Initial rinsing steps used 1 M HBr (OPTIMA™, Fisher Chemical, Canada) followed by the collection of the Pb fraction with ultra-clean 6 M HCl. A second pass through the column was performed to further purify Pb. After separation, the Pb eluates were dried and re-dissolved in 260 µl and 460 µl 2% v/v HNO_3, for monarch and milkweed samples, respectively (TraceMetal™ Grade; Fisher Chemical, Canada). A thallium spike (in a Tl:Pb mass ratio of 1:4) was added to each sample for mass bias correction against $^{203}Tl/^{205}Tl = 0.418922$.

The Pb isotopes analysis was performed at the Isotope Geochemistry and Geochronology Research Center, Carleton University using a Thermo Scientific™ Neptune™ high-resolution multi-collector inductively coupled plasma mass spectrometer (MC-ICP-MS; Thermo

Fisher Scientific, Bremen, Germany). Sample solutions in 2% v/v HNO_3 were aspirated using a PFA nebulizer, double-pass quartz spray chamber, quartz torch, and nickel sample and skimmer cones. Isotopes ^{202}Hg, ^{203}Tl, ^{204}Pb, ^{205}Tl, ^{206}Pb, ^{207}Pb, and ^{208}Pb were simultaneously measured in L3, L2, L1, C, H1, H2 and H3 Faraday cups, respectively. Measurements of samples were made using a static multi-collector routine that consisted of 1 block of 70 cycles for milkweed and 35–40 cycles for monarchs with an integration time of 8.389 s/cycle. Procedural blanks were negligible (<50 pg). The reported Pb isotope ratios are corrected for offsets between the analyzed and reported NBS981 (Todt et al., 1996). For a period of 12 months, average ratios and uncertainties (± SD, $n = 47$) of NBS981 bracketing samples were $^{206}Pb/^{204}Pb = 16.9310 \pm 0.0095$, $^{207}Pb/^{204}Pb = 15.4851 \pm 0.0012$, $^{208}Pb/^{204}Pb = 36.6783 \pm 0.0035$, $^{208}Pb/^{206}Pb = 2.16634 \pm 0.00011$, and $^{207}Pb/^{206}Pb = 0.91460 \pm 0.00003$.

2.1.4. Statistical analysis

To examine patterns in metal concentrations and isotopes in the monarch wings over time, and to group elements and isotopes with similar characteristics, we used multivariate multiple regression and principal component analysis (PCA). General linear models were constructed with sex, time (days), and body mass (mg) as fixed effects; multiple models were run independently because there were differences in sample size due to exclusions from the quality control process. All models were visually checked for normality, independence, and homoscedasticity of the model residuals. Body mass and sex are strongly associated (point-biserial correlation = −0.70; Supplementary Figure S3), so linear models were re-run without sex as an explanatory variable to test the sensitivity of the results to the confounding variables (Supplementary Table S3). Twenty metals were included in the PCA because of unequal sample size due to As, Tl, and U having measurements below the detection limit. All statistical analyses were performed using R (version 4.1.0; R Core Team, 2013), and a commented R markdown document has been provided (see Data Availability Statement).

2.1.5. Mobility index and enrichment factors

To explore the transfer of metals between trophic levels, we calculated the elemental mobility index for each metal between the larval diet (i.e., milkweed) and the monarchs sampled on the day of eclosion (i.e., Day 0). The mobility index was calculated as the ratio between the metal concentration in the monarch wings and the larval diet (Tigar and Hursthouse, 2016). A value greater than one indicates that the monarch wing has a higher metal concentration than its larval food and that the metal is biomagnified; whereas a value of less than one indicates that the monarch wing has lower metal concentrations than its larval food and the metal has been biodiluted.

Enrichment factors (EF) were also calculated between the adult diet and monarch wings (EF_{ms}) and between the upper continental crust (Rudnick and Gao, 2014) and monarch wings (EF_{cc}) to assess the source of metals in butterfly wings. The upper continental crust is used as a proxy for average exogenous contamination from mineral dust, which allows the EF to represent how much of a trace element is sourced endogenously (i.e., from within the organism itself) versus obtained through exogenous contamination (i.e., from the continental crust; Hu et al., 2019). We calculated the EF using calcium concentration as a normalization factor (Kabata-Pendias and Mukherjee, 2007; Equation 1). Ca is one of the major elements in the continental crust and an abundant metal in monarch wings (Supplementary Table S2); normalization to Ca makes the EF calculation less sensitive to variation between samples (Hu et al., 2019). An EF of greater than one implies that the metal is enriched in the monarch relative to the source (e.g., diet (EF_{ms}), crust (EF_{cc})), and, therefore, the source has low potential to contaminate the monarch signal. Conversely, an EF of less than one indicates that this metal in monarch wings is susceptible to contamination from that source.

$$Enrichment\ Factor_{source} = \frac{[x_{monarch}] / [Ca_{monarch}]}{[x_{source}] / [Ca_{source}]} \quad (1)$$

2.2. Wetting experiment

Because $^{87}Sr/^{86}Sr$ are currently the main metal isotopic tool used in insects, we conducted an additional experiment to refine the sources of Sr in wings and assess the potential contamination of Sr due to wetting. Submerging keratin (e.g., hair) in water can result in exogenous contamination of Sr (Hu et al., 2020), but this contamination route is untested for insect chitin. In our diet-switching experiment, the adult monarchs are not wetted, and, therefore, the Sr content and $^{87}Sr/^{86}Sr$ ratios are uncontaminated by wetting. However, in the wild, monarchs might be wetted by rain or other environmental waters, which could possibly lead to exogeneous Sr contamination *via* exchange, removal, or addition. Since butterfly wings are superhydrophobic (Pass, 2018), we hypothesized that the Sr in the wings would not be contaminated by submergence in water. We designed a simple wetting experiment to test whether exogeneous Sr could be integrated into the monarch wings when submerged in water. Two beakers of 80 ml 300 ppb Sr certified standard purchased from SCP Science Inc. (Montreal, QC, Canada) were prepared and neutralized with 60 µl 0.5 N NaOH. Two monarch butterfly wings were cleaned of surface dust using pressured nitrogen gas (10 psi for 4 min.). The wings were submerged in the beakers of solution and agitated. At designated time steps, from before the wings were submerged to 28 days after submergence, a 100 µl aliquot of the solution was removed from each beaker, diluted to 3 ml 2% v/v HNO_3 (TraceMetal™ Grade; Fisher Chemical, Canada), and centrifuged. These aliquots were then measured using the ICP-MS to monitor the change in Sr concentration of the beakers over time.

2.3. Natural metal concentrations in monarchs

To estimate the natural metal composition of wild monarch butterflies, the wings of 100 monarch butterflies from eastern North America were analyzed for a suite of 12 elements (i.e., Al, Ba, Cd, Co, Cr, Cu, Mg, Mn, Ni, Pb, Sr, Zn). The butterflies were captured in the spring of 2011 from sites in Texas, Oklahoma, and Missouri as part of a previous study (Flockhart et al., 2013). Methodological details can be found in the Supplementary Material.

3. Results

3.1. Metals classified into four categories

The concentrations of Al, As, Ba, Ca, Cd, Co, Cr, Cs, Cu, Fe, Mg, Mn, Mo, Na, Ni, Pb, Rb, Sb, Sr, Ti, Tl, U, and Zn in the wings of the

monarch butterflies, the larval diet (i.e., milkweed), and the adult diet (i.e., maple syrup) from the diet-switching experiment are reported in Supplementary Table S2. In the monarch wings, Ca was the most abundant metal (mean ± SD; 640 ± 160 ng/mg, $n = 18$) followed by Mg (290 ± 180 ng/mg, $n = 18$) and Fe (87 ± 34 ng/mg, $n = 18$). Uranium was the least abundant (0.0010 ± 0.0003 ng/mg, $n = 10$), with many samples falling below the detection limit. In the larval diet, alkaline earth metals Ca, Mg, and Sr were the most abundant (Ca: 18 ± 2 µg/mg, $n = 3$; Mg: 4.2 ± 0.3 µg/mg, $n = 3$; Sr: 190 ± 20 ng/mg, $n = 3$) and Cd was the least abundant (9.5 ± 2.2 ng/g, $n = 3$). Similarly, in the adult diet Ca (190 ± 37 ng/mg, $n = 4$) and Mg (73 ± 5, ng/mg, $n = 4$) were the most abundant and Cd the least abundant (0.4 ± 0.1 ng/g, $n = 4$).

Principal component analysis (PCA) was used to help categorize the metals in the monarch wings from the diet-switching experiment. The first principal component (PC1) explained 43.8% of the variation and was driven mainly by Al, Fe, Pb, Cr, and Cs (Figures 1A; Supplementary Figure S1A). A linear regression of PC1 with time category (i.e., early, late) and sex ($R^2 = 0.80$) detected a difference in PC1 between Week 0 and Weeks 1 to 8 ($\beta = 5.5 \pm 0.9$, 6.3, $p < 0.001$; Figure 1B), but not between the sexes ($p = 0.1$). PC2, driven by Cu, Na, Mn, Ca, and Cd (Supplementary Figure S1B), accounted for 16.1% of the variation. A linear regression with day and sex ($R^2 = 0.52$) found that PC2 trended temporally ($\beta = 0.05 \pm 0.02$, 3.5, $p = 0.003$) and differed between the sexes ($\beta = 2.3 \pm 0.6$, 3.7, $p = 0.002$), suggesting that the metals driving PC2 may be influenced by biological variables (Figure 1B).

Multivariate multiple regression found that metals in monarch wings showed distinctive associations with time (days), sex, and body mass (mg; Table 1). If metals are accumulated from endogenous or exogenous sources, we would expect a positive correlation between time and metal concentration; such associations were found for Al, Cd, Cu, Fe, Pb, Ni, and Zn. Significant negative correlations with time were found for As and Mn, suggesting that these metals are removed from the butterfly wings over time. Calcium concentrations in male monarch wings were, on average (± SE), 190 ng/mg (± 60) higher than in females (Figure 2A). Conversely, on average males had 0.04 ng/mg (± 0.01) less Co and 1.0 ng/mg (± 0.5) less Sb. Body mass was found to have a significant association with Mo ($\beta = -0.0006 \pm 0.0002$, −2.6, $p < 0.05$).

Enrichment factors and mobility indices calculated for each of the 23 metals showed distinctive patterns in the concentrations between the monarch butterfly wings and the larval diet (i.e., milkweed), the adult diet (i.e., maple syrup), and a proxy for mineral dust (i.e., continental crust). Chromium was the only metal with a mobility index greater than one indicating that it is biomagnified in monarch wings compared to milkweed (Table 1). Nickel and Zn had mobility indices close to one. The remaining elements showed low concentrations in monarch wings compared to milkweed indicating biodilution of these metals. The lowest mobility indices were found among the alkaline earth metals (i.e., Mg (0.13), Ca (0.04), Sr (0.03), and Ba (0.02)). Enrichment factors less than one suggest that the metal was susceptible to contamination from either the adult diet (EF_{ms}) or mineral dust (EF_{cc}). Of the metals that showed an increase in concentration over time, Al and Fe showed particularly low EF_{cc}, indicating that the increase in concentration could be due to additions of Al and Fe from mineral dust. Comparatively low EF_{ms} for Ni and Zn suggest that the bioaccumulation seen in these metals may be due to additions from the adult diet.

Based on the results of the PCAs, multiple multivariate regression, mobility indices, and enrichment factors, metals were separated into four categories: (1) metals affected by intrinsic factors (e.g., sex, body mass), (2) metals showing bioaccumulation likely from external sources, (3) metals showing bioaccumulation likely from dietary sources, and (4) metals without significant effects of intrinsic factors that maintain the initial metal concentration over time (Table 1; Figure 3). Metals were categorized as Category 1 if sex or mass were associated with metal concentration or there was a decrease in concentration over time. A few of these metals (i.e., Ca, Mn) were the main drivers of PC2 (Figures 1A; Supplementary Figure S1B). Metals assigned to Category 1 were As, Ca, Co, Mn, Mo, and Sb. For example, Ca was significantly more abundant in male wings than in female wings (Figure 2A), but no effect of time was detected. Category 2 metals had a positive association with time and relatively low EF_{cc}, indicating that

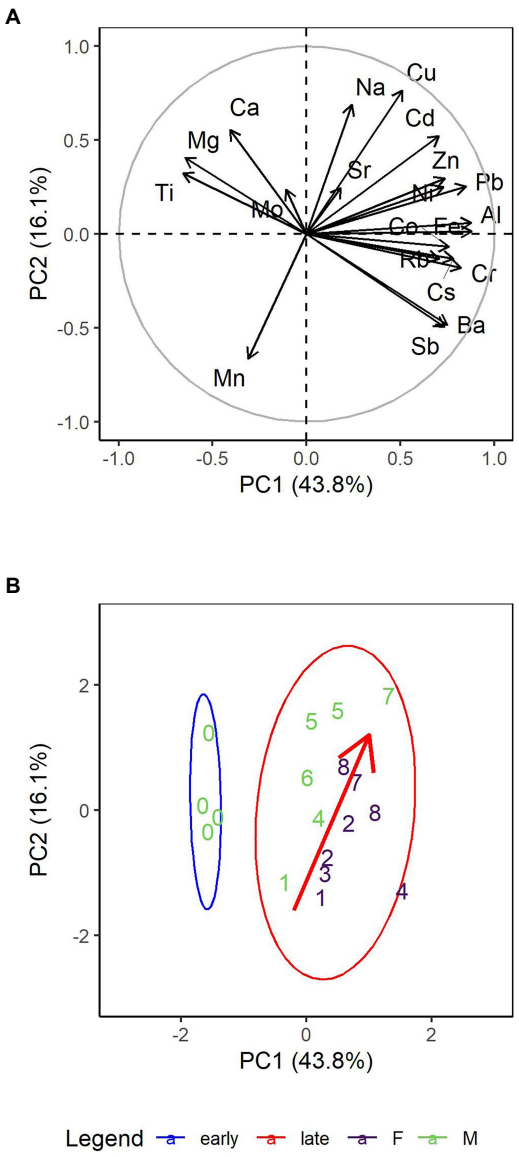

FIGURE 1
Principal components analysis biplots of 20 metals (excluding As, Tl, and U due to measurements below the detection limit) in monarch butterfly wings **(A)** Loading plot of the first two principal components for monarch wings from all weeks explaining 59.9% of the variation. **(B)** PCA score plot of monarch wings from all weeks; numbers depict the week at which the individual was sampled. There is a no overlap between the 95% data ellipses of early dates (i.e., Week 0; blue ellipse) and later dates (i.e., Weeks 1 to 8; red ellipse). There is a trend, mainly in PC2, from Week 1 to 8; a red arrow has been superimposed on the biplot to illustrate this trend. There is also grouping between female (purple) and male (green) butterflies.

TABLE 1 Metals are clustered into four categories based on their characteristics in the diet-switching experiment.

Metal	Adj. R^2	Time (days)	Sex	Body mass (mg)	MI	EF_{cc}	EF_{ms}
Category 1: intrinsic factors							
As^{TOX}	**0.60***	**−0.002 ± 0.0006, −3.1***	−0.03 ± 0.03, −1.0	0.0002 ± 0.0002, 1.2	NA	0.73	NA
Mn^{ESS}	**0.56***	**−0.03 ± 0.008, −3.9***	−0.4 ± 0.4, −0.8	0.004 ± 0.003, 1.3	0.07	0.24	0.79
Ca^{ESS}	**0.74***	0.1 ± 1.0, 0.1	**192 ± 58, 3.3***	−0.7 ± 0.4, −1.9	0.04	NA	NA
Co^{ESS}	**0.42***	0.0003 ± 0.0003, 1.0	**−0.04 ± 0.02, −2.8***	−0.0001 ± 0.0001, −1.2	0.08	0.11	1.1
Sb	**0.44***	0.004 ± 0.008, 0.5	**−1 ± 0.5, −2.2***	0.001 ± 0.003, 0.4	NA	0.0012	86
Mo^{ESS}	0.26	0.0002 ± 0.0006, 0.3	−0.04 ± 0.03, −1.1	**−0.0006 ± 0.0002, −2.6***	NA	0.13	28
Category 2: exogenous bioaccumulation							
Al^{TOX}	**0.66***	**0.3 ± 0.06, 4.6***	−2 ± 4, −0.5	0.04 ± 0.02, 1.7	0.08	0.0072	22
Cr	0.29	0.006 ± 0.003, 2.0	−0.2 ± 0.2, −1.1	0.0002 ± 0.0011, 0.15	1.42	0.45	9.2
Cd^{TOX}	**0.45***	**0.0005 ± 0.0001, 3.7***	−0.0005 ± 0.0070, −0.1	−0.00002 ± 0.00005, −0.5	0.32	7.2	12
Cu^{ESS}	**0.47***	**0.04 ± 0.01, 3.9***	0.3 ± 0.6, 0.5	−0.001 ± 0.004, −0.3	0.64	8.2	74
Fe^{ESS}	**0.56***	**1 ± 0.3, 3.2***	−29 ± 17, −1.7	−0.01 ± 0.11, −0.1	0.41	0.091	30
Pb^{TOX}	**0.76***	**0.008 ± 0.001, 6.4***	−0.02 ± 0.07, −0.2	0.0006 ± 0.0005, 1.3	0.13	0.72	85
Category 3: dietary bioaccumulation							
Ni	**0.45***	**0.02 ± 0.007, 3.5***	−0.2 ± 0.4, −0.5	−0.001 ± 0.002, −0.4	1.08	1.7	2.3
Zn^{ESS}	**0.36***	**0.3 ± 0.1, 2.8***	−4 ± 6, −0.6	−0.005 ± 0.037, −0.1	1.02	1.7	4.6
Category 4: geolocation							
Ba	**0.40***	0.02 ± 0.03, 0.8	−2 ± 2, −1.1	0.02 ± 0.01, 1.5	0.02	NA	0.20
Cs	0.21	0.00003 ± 0.00002, 1.5	−0.001 ± 0.0009, −1.1	0.0000006 ± 0.000006, 0.1	NA	0.033	0.11
Mg^{ESS}	0.16	−3 ± 2, −1.5	21 ± 118, 0.18	−0.8 ± 0.8,-1.1	0.13	0.79	1.2
Na^{ESS}	0.07	0.3 ± 0.3, 1.2	−5 ± 16, −0.3	−0.1 ± 0.1, −1.2	NA	0.11	43
Rb	0.14	0.01 ± 0.007, 2.0	−0.06 ± 0.4, −0.2	0.001 ± 0.003, 0.6	NA	0.45	0.048
Sr	−0.08	−0.006 ± 0.028, −0.2	−0.8 ± 1.5, −0.5	−0.01 ± 0.01, −1.2	0.03	0.82	0.51
Ti	0.10	−0.04 ± 0.02, −1.7	−0.08 ± 1.25, −0.07	−0.007 ± 0.008, −0.9	0.70	0.048	24
Tl	−0.006	−0.00003 ± 0.00008, −1.0	0.0006 ± 0.0012, 0.5	−0.000003 ± 0.000008, −0.4	NA	1.6	1.1
U^{TOX}	−0.37	0.000004 ± 0.000008, 0.6	0.00009 ± 0.00042, 0.2	0.000001 ± 0.000002, 0.6	NA	0.016	NA

Results of the multivariate multiple regression examining the contribution of time (days), sex, and body mass (mg) on metal concentrations of monarch wings in the diet-switching experiment are reported. Non-standardized (ng/mg) effect sizes are reported for each predictor ($\beta \pm$ SE, t-value); significant relationships are starred and in bold ($\alpha = 0.05$). The sample size is 18 for all metals except As ($n = 14$), Tl ($n = 16$), and U ($n = 10$). The mobility index (MI), enrichment factor between the monarch wings and the continental crust (EFcc), and the enrichment factor between the monarch wings and the adult diet (EFms) are also reported for each metal. Essential metals are denoted with ESS and toxic metals with TOX.

their increases in concentration over time were more likely to be sourced from mineral dust rather than from the adult diet. For instance, despite low Al levels in the maple syrup ($EF_{ms} = 22$), the concentration of Al in the monarch wings increased over time (Figure 2C). As a terrigenous metal, it is more likely that the accumulated Al is sourced from exogenous mineral dust ($EC_{cc} = 0.0072$). Some of the Category 2 elements are terrigenous metals, including Al and Fe, but others are associated with anthropogenic pollution (i.e., Cd, Cu, Cr, Pb). Several of the Category 2 metals are essential to living organisms (i.e., Cr, Cu, Fe), but others are toxic to animals even at low concentrations (i.e., Al, Cd, Pb). Category 3 metals (i.e., Ni, Zn) also had a positive association with time, but had high EF_{cc} and relatively low EF_{ms} and are therefore potentially contaminated endogenously through the adult diet. As an illustration, the monarch wings showed a two-fold accumulation of Zn over time from a concentration similar to that of the larval diet (Figure 2B). The level of this essential metal was lower in the adult diet than in the larval diet, but the EF_{ms} was relatively low (4.6), suggesting that the increase in Zn may be sourced, at least partially, from the adult diet. Finally, metals were assigned to Category 4 if they showed no significant associations with time, sex, or body mass. These metals were Ba, Cs, Mg, Na, Rb, Sr, Ti, Tl, and U.

3.2. Strontium and strontium isotope ratios

The Sr and $^{87}Sr/^{86}Sr$ of the diet-switching experiment monarch wings, larval diet, and adult diet are reported in Supplementary Table S2. Based on its characteristics, Sr was considered as Category 4 (Table 1), a metal that does not bioaccumulate and is not significantly affected by sex or body mass. The mobility index (0.03) indicated that Sr is biodiluted in the monarch wings. These low concentrations did not have significant associations with time, sex, or body mass (Table 1), although a non-significant sex-based pattern could be observed (Figure 4A).

Multiple regression of monarch wing $^{87}Sr/^{86}Sr$ was performed with predictors time (days), sex, the inverse of Sr (mg/ng), and interactions between time and sex and the inverse of Sr and sex (adj. $R^2 = 0.79$). As expected, the range of male $^{87}Sr/^{86}Sr$ matched well with the $^{87}Sr/^{86}Sr$ of the

10.3389/fevo.2023.1085903

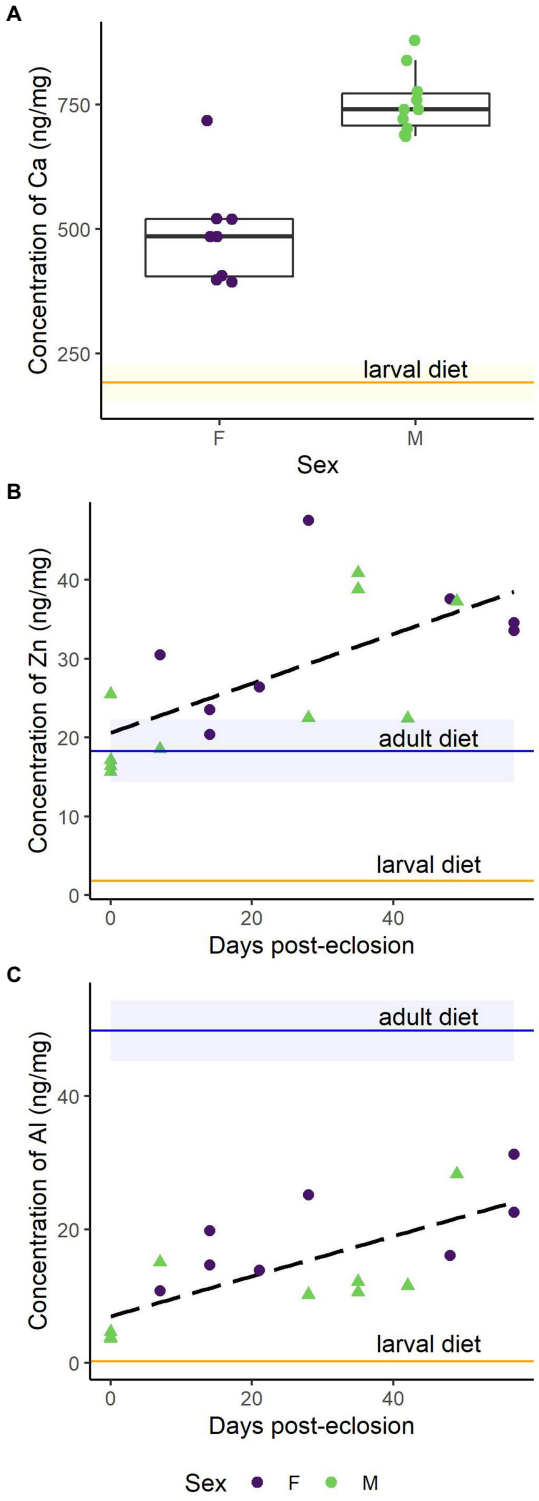

FIGURE 2
Metal concentration in monarch wings (1 ng/mg=1 ppm) from the diet-switching experiment for representative metals classified in different functional categories. Horizontal blue lines depict the mean concentration (± SD) in the larval diet, milkweed (n=3), and horizontal orange lines represent the mean concentration (± SD) in the adult diet, maple syrup (n=4). **(A)** Category 1: Boxplot of Ca concentration (ng/mg) in monarch wings by sex (RSD=4%). Sex-based differences were detected with males (green) having more Ca than females (purple). The milkweed concentration (18,500±1800ng/mg) is not shown as it far exceeds that of the monarch wings. **(B)** Category 2: The concentration of Zn (ng/mg) in monarch wings increased over the 8 weeks (RSD=1%). **(C)** Category 3: The concentration of Al (ng/mg) in monarch wings increased over the 8 weeks (RSD=2%).

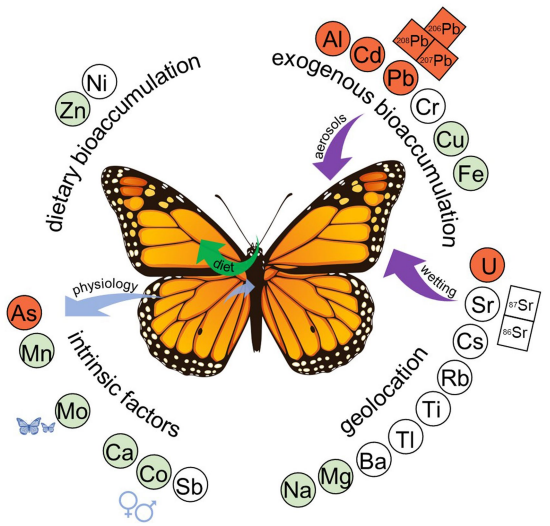

FIGURE 3
Twenty-three metals were classified into four categories based on their characteristics in the diet-switching experiment. Essential metals (green) and highly toxic metals (red) are indicated; metal isotopes are indicated by boxes. Category 1, intrinsic factors (bottom-left), includes two sub-categories: (1) metals (i.e., As, Mn) that decrease in the wing over time through unknown mechanisms (blue arrows), and (2) metals that are influenced by body mass or sex (i.e., Ca, Co, Sb, Mo). Category 2, exogenous bioaccumulation (top-right), includes metals that are, at least partly, accumulated from external sources (purple arrows), such as *via* aerosol dust (e.g., Pb and Pb isotopes; Figure 5) or under wetting conditions (e.g., Sr; Figure 4D). Category 3, dietary bioaccumulation (top-left), included metals that are likely accumulated from the adult diet (green arrow). Finally, Category 4, geolocation (bottom-right), includes metals that maintained similar concentrations over the course of the experiment and are good candidates for geolocation studies.

larval diet and did not change over time (p=0.2; Figure 4B) or with the inverse of Sr (p=0.2; Figure 4C). However, on average, the wings of the female monarchs were 0.0014 less radiogenic than the males (β=0.0014±0.0004, 3.6, p<0.01) and the $^{87}Sr/^{86}Sr$ of the female wings increased slowly over time (β=0.000010±0.000004, 2.3, p=0.03), although the lack of female monarchs sampled at Week 0 may have been biasing this result (Figure 4B). If the adult diet is responsible for the increasing $^{87}Sr/^{86}Sr$ of the female monarch wings over time, it seems unlikely that it is through accumulation, as no positive association between Sr and time was detected (p=0.8; Table 1). The $^{87}Sr/^{86}Sr$ of the female monarch wings was associated with the inverse of Sr (β=0.0037±0.0011, 3.4, p<0.01), such that females with higher concentrations of Sr had $^{87}Sr/^{86}Sr$ more disparate from those of the males and larval diet (Figure 4C). Given that radiogenic strontium isotopes do not fractionate but instead indicate sources of Sr, the principles of mixing models can be used to find missing endmembers (i.e., the $^{87}Sr/^{86}Sr$ of pure sources of Sr to the monarch wings). The intercept of regression indicated a missing endmember for the female monarchs with a less radiogenic $^{87}Sr/^{86}Sr$ of about 0.7073. Females with higher abundances of Sr in their wings tended to be those sampled earlier in the experiment; lower concentrations of Sr in the Week 8 female monarch wings aligned them with the expected $^{87}Sr/^{86}Sr$ of the larval diet (Figure 4C). Thus, the female monarchs were likely exposed to the less radiogenic Sr source either as larvae or as young adults (i.e., less than a week old).

The wetting experiment shows that exogenous contamination of Sr in butterfly wings by wetting is possible. After we submerged the monarch

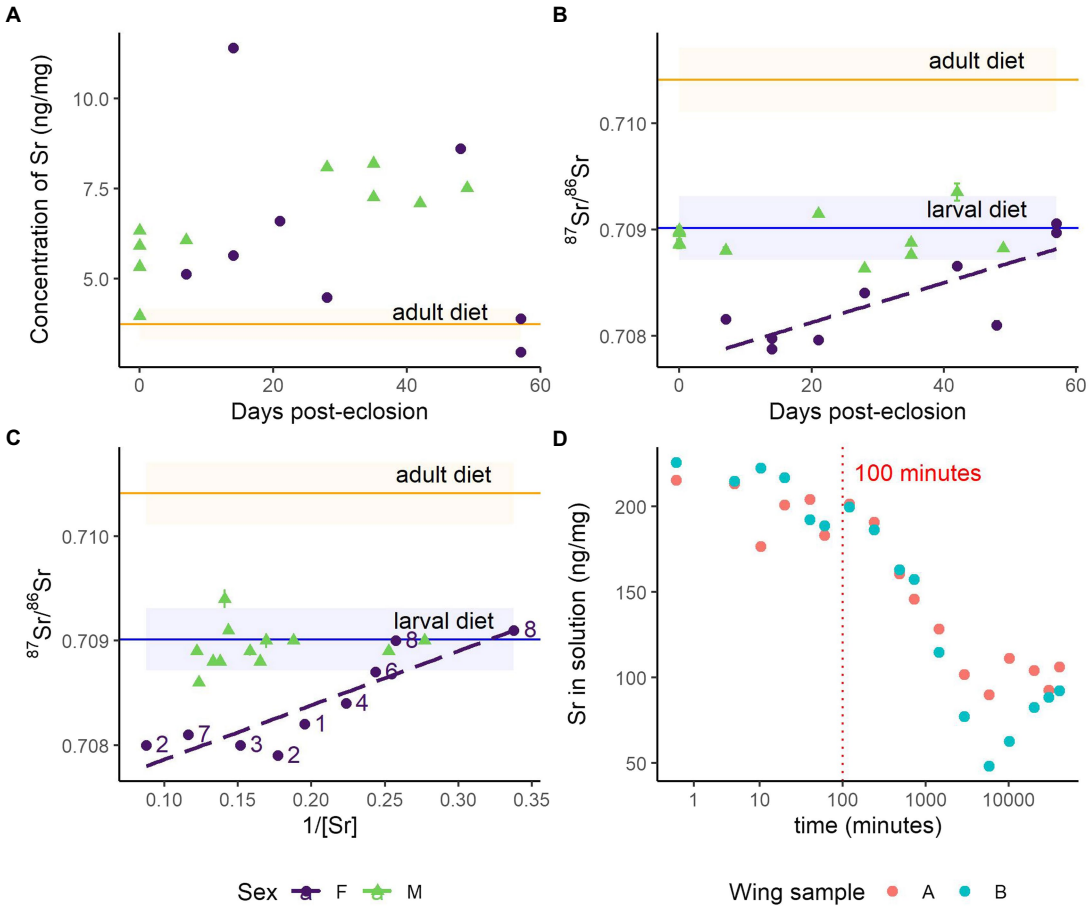

FIGURE 4
Strontium and strontium isotope ratios in monarch wings during the diet-switching and wetting experiments. Horizontal blue lines depict the mean concentration (± SD) in the larval diet, milkweed (n=3), and horizontal orange lines represent the mean concentration (± SD) in the adult diet, maple syrup (n=4). **(A)** Concentration of Sr (ng/mg) in monarch wings over 8 weeks (RSD=1%). The concentration of Sr in the larval diet is not shown as it far exceeds that of the monarchs (189±21ng/mg). **(B)** Strontium isotope ratios (± SE) in monarch wings over 8weeks; the $^{87}Sr/^{86}Sr$ ratios of the female monarch wings show a linear relationship with time. **(C)** Strontium isotope ratios (± SE) against the inverse of strontium concentration. The significant linear relationship for females is displayed; numbers depict the weeks post-eclosion that the female monarch was sampled. **(D)** Concentration of Sr (ng/mg) in solution through time during the wing wetting experiment (n=2).

wing in the aqueous solution, we detected substantial changes in the Sr concentration of the solution after 100 min. (Figure 4D). A new equilibrium was reached after about a week. Since the amount of Sr in the solution decreased over time, it is likely that the Sr accumulated in the wing.

3.3. Lead and lead isotope ratios

Lead was categorized into Category 2 because Pb concentrations in the monarch wings increased over time, likely sourced from mineral dust (Table 1; Figure 5A). Of all the toxic metals, only Pb levels in the milkweed (0.22 ± 0.06 ng/mg, n = 3) and monarch wings (0.30 ± 0.20 ng/mg, n = 18) were found to exceed the permissible limits of human food (i.e., 0.01–1 ng/mg; FAO, WHO, 2019), but Pb levels in the maple syrup (1.1 ± 0.6 ng/g, n = 4) were well below health guidelines. Lead isotope ratios showed that the larval diet matched well with regional environmental $^{208}Pb/^{206}Pb$ and $^{207}Pb/^{206}Pb$ signatures measured in snowpack (Figure 5B; Simonetti et al., 2000a,b). The early monarchs (i.e., Week 0) also matched with the larval and environmental Pb isotopes, but within a week, the Pb isotopes of the monarch wings deviated to a distinct signature with higher $^{208}Pb/^{206}Pb$ and $^{207}Pb/^{206}Pb$. Although the Pb isotope ratios were measured a year after the Pb levels, repeated measures showed that storage did not significantly change the initial Pb abundances (paired t-test: $t = -1.3$, df = 16, $p = 0.20$).

3.4. Natural metal concentrations in lab-raised and wild monarchs

In this lab-based study, we controlled the environmental conditions of the monarch caterpillars and adults, minimized conspecific interactions, reduced flight capacity, and fed the adults a non-natural and choice-restricted diet. Thus, the variation in metal concentrations in the laboratory monarch wings is expected to be different from that of wild monarch wings. These differences can clarify important processes. Comparisons with wild monarch wings show that wing concentrations were similar for Cr, Mn, and Ni (Supplementary Figure S5). Conversely, Mg, Al, Co, Cd, Ba, Pb had higher concentrations in the wild monarch wings and Cu, Zn, and Sr had lower concentrations in the wild monarchs (Supplementary Figure S5).

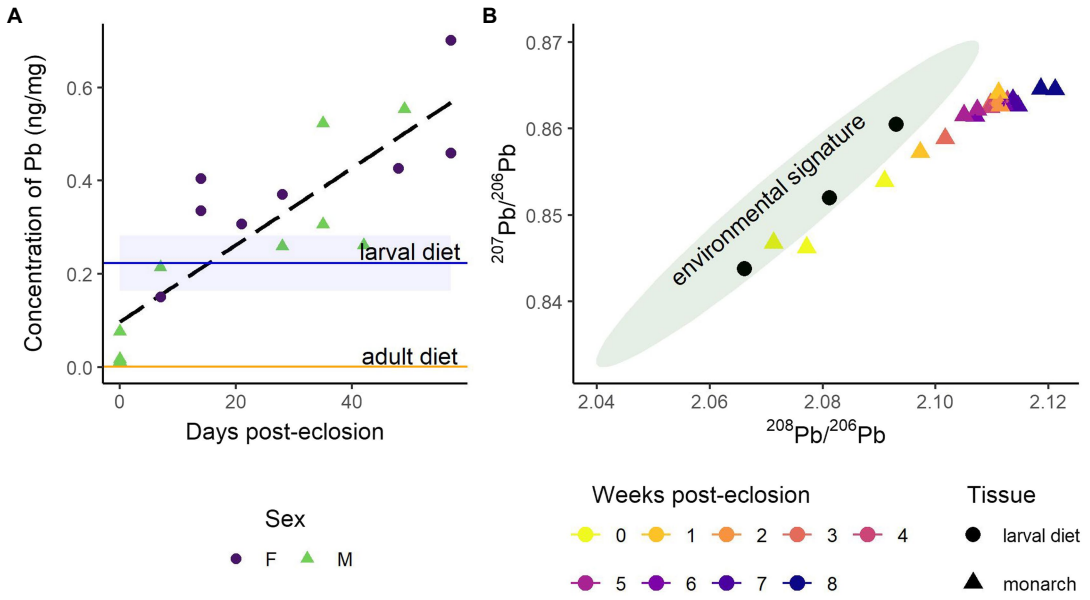

FIGURE 5
Change in lead and lead isotope ratios in monarch wings during the diet-switching experiment **(A)** Concentration of Pb (ng/mg) in monarch wings over 8 weeks (RSD=1%); the linear relationship (dashed black line) with time is for all samples. The horizontal blue line depicts the mean concentration of Pb (± SD) in the larval diet, milkweed (n=3), and the horizontal orange line represents the mean concentration of Pb (± SD) in the adult diet, maple syrup (n=4). **(B)** Biplot of $^{207}Pb/^{206}Pb$ and $^{208}Pb/^{206}Pb$ ratios. Monarch wings are depicted as triangles with colors representing the age of the butterfly in weeks; the standard error is smaller than the symbols. Measurements of the larval diet are depicted as black dots (n=3). The green 95% data ellipse shows the range of regional lead isotope ratios measured in snowpack (Simonetti et al., 2000a,b).

4. Discussion

4.1. Regulation of metals in insect wings

The 23 metals analyzed in the diet-switching experiment were classified into four categories based on whether they were influenced by intrinsic factors like sex and body mass (Category 1), bioaccumulated metals from external sources (Category 2), bioaccumulated metals from dietary sources (Category 3), or maintained the natal signature (Category 4; Figure 3). Metals classified in Category 1, including As, Mn, Mo, and Ca, showed a decreasing concentration in the wings through time or a correlation with the intrinsic characteristics of individuals. These observations suggest that the levels of these metals are regulated by the insect. Category 1 metals were grouped into two sub-categories based on their distinct trends during the experiment (Table 1). The first sub-category included As and Mn, which showed decreasing concentrations in wings throughout the adult life (Table 1), suggesting that monarchs may reallocate these metals from the wings to other parts of the body or excrete them (Tibbett et al., 2021). Manganese is an essential co-factor in many enzymes but can impact insect behavior at low doses and, like all metals, is toxic in excess (Ben-Shahar, 2018). Caterpillars of *Lymantria dispar* and *Cabera pusaria* have been shown to excrete excess Mn through frass and molting (Kula et al., 2014; Martinek et al., 2020), but adult mechanisms of excretion have not been shown and Mn homeostasis has not been studied in monarchs. Alternatively, As and Mn could be more concentrated in wing scales and decrease through time in the entire wing due to the progressive abrasion of scales as the individual ages.

The second sub-category of Category 1 included several metals (i.e., Ca, Co, Mo, Sb) that showed an influence of sex and/or body mass. However, sex and body mass were strongly correlated, with females being consistently heavier than males, making it challenging to disentangle the direct influence of mass from that of sex (Supplementary Figure S3). Molybdenum showed a negative correlation to body mass (Table 1). Molybdenum is an essential metal that acts as a co-factor for many oxidase enzymes (Dow, 2017), some of which relate to wing pigmentation (Feindt et al., 2018) and immune processes (Selvey, 2020). The decrease in Mo concentration in wings with increasing body size might be related to differential regulation of the metal relative to body size, energy reserves, or sex (Orłowski et al., 2020). Alternatively, the decrease in Mo with increasing body size could be driven by differences in surface area-to-mass ratios. Female monarchs have been noted to have thicker wings than males (Davis and Holden, 2015), leading to lower surface area-to-mass ratios in the wings. If Mo is predominantly found at the surface of the wing (e.g., pigmentation), this lower surface area-to-mass ratio could explain the pattern seen in this experiment (Kowalski et al., 1989). Similarly, we found that male monarch wings had significantly more Ca than females (Figure 2A). Notwithstanding the confounding effect of body mass, sex-based differences in Ca have also been detected in whole-body samples of butterflies (Dempster et al., 1986) and damselfly wings (Stuhr et al., 2018), suggesting that sex is the main driver of the observed differences in Ca in wings. Calcium is a known component of insect chorion (Studier, 1996; Nickles et al., 2002) and reproductive organs (Clark, 1958), and Ca has been found to be preferentially allocated to reproductive organs (Mesjasz-Przybyłowicz et al., 2014). This could explain the lower concentrations of Ca found in the wings of female monarchs, as it is possible that Ca is preferentially allocated or reallocated from the wings to reproductive organs for oogenesis. Sex-based differences in metal composition may reflect sexual dimorphism in nutritional demands, which can result in sex-specific nutritional limitations and have ecological consequences (Judd et al.,

2010; Espeset et al., 2019; Filipiak et al., 2021). Future studies could investigate the potential for sexual dimorphism in the nutritional demands of monarch butterflies in natural environments and the resultant impacts on population demography, survival, and migratory success (e.g., Snell-Rood et al., 2014).

Little is known about the pathways of metal allocation and regulation in insects. Metallomics, the study of the metal-containing biomolecules that an organism uses, aims to identify and compare metal utilization, function, evolutionary trends, and interactions (Ogra and Hirata, 2017). Of the six metals in Category 1 (Table 1), only the regulatory pathways of Ca, Co, and Mo have been well-characterized (Dow, 2017; Zhang et al., 2019), illustrating the large knowledge gap that the newly-developing field of metallomics is seeking to fill. Metal isotopes that fractionate with physiological processes can be particularly useful to advance understanding but have been under-utilized in insects thus far (but see Nitzsche et al., 2020, 2022). For example, in vertebrates, calcium isotopes have been effectively used to investigate sex-specific modifications of Ca homeostasis due to pregnancy, lactation, and egg-laying (Tacail et al., 2020). Analyzing calcium isotope ratios of different insect tissues could shed light on Ca homeostasis in insects, such as the role of calcium-storing spherites (Dow, 2017), and the sources, mechanisms, and ecological consequences of sex-based differences in Ca.

4.2. Bioaccumulation of metals in insect wings

We identified a suite of metals, including highly toxic (e.g., Al, Cd, Pb) and essential metals (e.g., Zn, Fe), that accumulated in the wings of the monarch butterflies over time (Categories 2 and 3; Table 1). Metals classified in Category 2 (i.e., Al, Cr, Cd, Cu, Fe, and Pb) increased in concentration over time in the monarch wings and had low enrichment factors between the monarch wings and continental crust (Table 1). These observations indicate that these metals were sourced, at least partially, from external sources such as mineral dust. For example, Fe and Al are highly concentrated in terrigenous dust, and previous studies on animal hair have shown that these elements were primarily sourced from exogenous sources in keratin tissues (Kempson et al., 2006; Hu et al., 2018). Our experiment minimized any accumulation of aerosol dusts in the food by replacing the food daily, thus any additions of metal from aerosols are likely incorporated exogenously. Although the initial deposition of aerosols on insects is likely superficial, the metals could become embedded in an organic matrix (i.e., epicuticular waxes; Negri et al., 2015), or, as has been shown previously for keratin, the metals could slowly penetrate deeper into the tissue when mobilized by high relative humidity or wetting (Hu et al., 2018, 2019). This pattern of diffusion is evidenced by the gradient of concentrations of these metals in keratinous tissue, from very high concentrations on the surface to low concentrations deeper in the tissue (Hu et al., 2018). In insects, high concentrations of Al in the cuticle of honeybees have also been observed, suggesting similar exogenous contamination (Shaw et al., 2018). However, given that butterfly wings are living tissue and that Fe is an essential element with known regulatory pathways (Slobodian et al., 2021), there are alternate explanations for the increase of Fe in wings through time. First, our experiment examined a single body part and therefore cannot comment on systemic metal homeostasis (Orłowski et al., 2020); Fe could be reallocated from different parts of the insect body for sequestration in response to perturbations to systemic homeostasis. Additionally, most of the accumulation of Fe in wings was observed between Week 0 and Week 1 (Figure 1B) and could be related to sclerotization and maturation processes as the wings finish forming within a few days post-eclosion (Honegger et al., 2008). Finally, Fe in wings could increase due to changes in Fe requirements over time, as has been observed in other insects (Shaw et al., 2018; Andreani et al., 2021). Finally, metamorphosis is an energetically-costly process, and the teneral butterfly could be Fe-limited, causing a short-term rapid uptake of Fe to reach a regulatory threshold within the first week in an accumulator-regulator dynamic (Tibbett et al., 2021).

Further studies could use natural metal isotopes or isotope tracing to help constrain metal sources in insect tissues, as we exemplify in this study with the use of Pb isotopes (see discussion below). Similar to Al and Fe, Pb accumulated rapidly in the monarch wings with a twentyfold increase over the 8 weeks. In parallel, we observed a temporal shift in Pb isotope ratios of the wings from a composition matching the local environment of the larval diet to a novel isotopic composition (Figure 5B). This indicated that the accumulating Pb is likely from external sources of atmospheric deposition and dust present in the laboratory air, such as from lead paint, pipes, or non-local mineral dust from a rock preparation laboratory located in the same building. Our work supports previous studies showing the contamination of insect tissues by exogenous Pb sources (e.g., Negri et al., 2015; Zhou et al., 2018). The amount of Pb in the wings of the laboratory-reared monarchs exceeded permissible limits for human food, which is between 0.01 and 1 ng/mg (FAO, WHO, 2019). Similarly, Pb in the wings of wild monarchs was also found to be above permissible limits (Supplementary Table S4) to a greater extent than the laboratory monarchs ($F(1, 116) = 24$, $p < 0.001$); our experimental results suggest that the high Pb levels accumulated in wild monarch wings are likely sourced from anthropogenic pollution encountered during their migration. Lead is toxic to insects and can cause mortality and sub-lethal effects such as reduced growth rate, body size, fecundity, and locomotor activity (Hirsch et al., 2003; Di et al., 2016; Zhou et al., 2021).

Migratory species could be at an even higher risk of adverse effects from metal exposure than non-migratory species (Seewagen, 2020). Migration is a complex behavior, and migratory insects can travel hundreds to thousands of kilometers and are potentially exposed to many sources of metal pollution along their migratory routes. However, the potential effects of toxic metals on migratory insect survival and migratory behavior are virtually unknown. Anthropogenic sources of Pb have unique Pb isotope ratios; thus, Pb and Pb isotope ratios of biological tissues could be used as indicators of environmental contamination sources (Smith et al., 2021). This principle has been applied to assess the local pollution exposure of non-migrating insects, such as honeybees (e.g., Zhou et al., 2018; Smith and Weis, 2020). We argue that Pb and Pb isotope ratios could also be used as bioindicators of pollution exposure for migratory insects. As an individual insect moves along a migratory path, it will accumulate Pb from the different atmospheric pollution sources it encounters along the way. Measuring Pb isotope ratios in migratory butterflies could provide a tool to reconstruct migratory paths and assess the exposure to pollution of individuals going through this route. This tool would be key to relating migratory success and pollution exposure and could also validate migration routes reconstructed through pollen metabarcoding (Suchan et al., 2018) and wind trajectory modeling (Otuka et al., 2005). To quantify how Pb with unique isotope ratios and concentrations are transferred to the wings from pollution sources, new laboratory studies exposing or feeding insects to isotopically-distinct Pb pollution sources

having concentrations similar to those in natural systems could be conducted. Ultimately, Pb isotopes in migratory insects could help identify key sources of pollution that are detrimental to specific species.

Metals classified in Category 3 (i.e., Ni and Zn) grouped metals which also bioaccumulated, but unlike Category 2, these metals were characterized by a relatively low enrichment factor between the monarch wings and adult diet (Table 1). Nickel is not known to be an essential element to insects. Lepidopterans show variable effects to Ni exposure, from decreased body size and fecundity to no effect (Sun et al., 2013; Kobiela and Snell-rood, 2018), suggesting that regulation mechanisms are species-specific (Tibbett et al., 2021). Nickel concentrations in the wings of monarchs in the diet-switching experiment did not significantly differ from those of wild monarchs (Supplementary Figure S5; $p = 0.4$), suggesting that concentrations may be below regulatory thresholds and thus increasing due to non-specific uptake of metal from the adult diet. Conversely, Zn was found to be lower in wild monarch wings than in the diet-switching experiment (Supplementary Figure S5; $F(1, 116) = 40$, $p < 0.001$), suggesting that the monarchs in the diet-switching experiment may have excess Zn. The high Zn in the laboratory monarch wings is unlikely to be purely a result of high Zn in the larval diet because the Zn levels in the milkweed provided in the diet-switching experiment (18 ± 4 ng/mg, $n = 3$; Supplementary Table S2) are low compared to Zn concentrations measured in wild milkweed (10–66 ng/mg, Mitchell et al., 2020). Zinc is essential for insect reproduction and immunity (Cardoso-Jaime et al., 2022), and Zn homeostasis is known to be strictly controlled in insects (Xiao and Zhou, 2016; Slobodian et al., 2021). However, excessive Zn can lead to decreased survival, growth rate, body size, and longevity (Jin et al., 2020). Although butterfly species are known to have different Zn tolerances, monarchs are sensitive to Zn under certain conditions (Shephard et al., 2022). The accumulation of Zn seen in the diet-switching experiment could reflect an upregulation of Zn metalloproteins due to environmental or physiological conditions, such as increased metabolic processes (Butt et al., 2018). Zinc isotopes have been suggested as a tool to explore the dietary sources of Zn to insects, but applications are currently hampered by the complicated pathways of Zn homeostasis and Zn fractionation in the body (Evans et al., 2017; Wanty et al., 2017; Nitzsche et al., 2020), which are poorly understood in insects compared to humans (e.g., Tanaka and Hirata, 2018).

4.3. Geolocation using metals and metal isotopes

Although metals and metal isotopes that bioaccumulate have the potential to impart geographical information, as has been proposed for Pb isotopes, they are unsuitable for provenance studies that aim to estimate the natal origins of insects. Good candidate metals for the geolocation of migratory insects are those that (1) are unaltered in the tissues of dispersing insects, (2) have predictable spatial patterns, and (3) demonstrate a strong relationship between environmental and biological signatures. Nine metals belonging to Category 4 fit the first requirement and were unaltered over time in the monarch wings: Ba, Cs, Mg, Na, Rb, Sr, Ti, Tl, and U (Table 1). For example, the alkaline earth metals Sr and Mg showed consistent concentrations in the monarch wings over time, suggesting that the natal signature is conserved. Continuous-surface geolocation using metal concentrations would require spatial models of metal variation across the landscape (i.e., metalscapes). Mapping Sr and Mg of soil samples across the eastern United States demonstrated that these metals have distinctive spatial patterns, at least in the soil (Supplementary Figure S6). However, correlations between metal concentrations in the soil and the biosphere (i.e., milkweed) were weak and non-significant (Supplementary Table S5). Previous studies have also found similarly weak correlations in both natural (Wieringa et al., 2020) and controlled laboratory conditions (Lin et al., 2021). Exploration of possible predictors of Sr and Mg concentrations in milkweed highlighted land use, milkweed species, month, and year, but not soil concentration (Supplementary Table S5). It is possible that some metal concentrations may vary at too fine a scale to be suitable for geolocation using continuous surfaces (Norris et al., 2007). Before metals can be used as geolocation biomarkers, further studies will need to improve the predictive power of spatial reference models.

Despite the apparent stability of the concentration of these metals from Category 4 through time, caution should be taken in applying these metals for insect geolocation. Of these metals, Mg and Na are essential metals and are thus expected to be regulated. Our results cannot differentiate between metals whose concentrations were unaltered in the monarch wings due to a lack of bioaccumulation and those that were held at a stable concentration through regulation for metal homeostasis. In the case of homeostasis, the metal concentration may be altered under different stressors not experienced in this experiment, such as starvation, disease, different environmental conditions, or increases in metal exposure. These stressors may alter the ability of the organism to maintain homeostasis (Hopkin, 1990) and thus disrupt the apparent larval signature. Similarly, not all sources of potential exogenous contamination were explored in this study. For example, we showed that Sr in monarch wings is susceptible to contamination or exchange after about 100 min. when submerged in Sr-concentrated aqueous solutions (Figure 4D). This supports the finding that Sr is soluble and that exogenous contamination of Sr in keratinous hair readily occurs when hair is submerged in water (Hu et al., 2018, 2020). Monarchs are behaviorally averse to submergence in water and are unlikely to be exposed to these artificial conditions in nature (i.e., full submergence in highly Sr concentrated waters). However, they are likely to be exposed to rain which usually has a low Sr concentration, except near coastal areas, but can have isotopically variable signatures (Nakano et al., 2001). Further studies will need to investigate the effect on Sr concentration and $^{87}Sr/^{86}Sr$ of wetting from rainwater with varied concentrations and isotopic signatures. As evidenced by our wetting experiment, it would take over an hour of full submersion in Sr-concentrated water to exchange Sr in the wing because the superhydrophobic property on the surface of the wings limit the exchange of metals. However, the regular or sudden wetting by rain during storms could potentially alter, accumulate, or exchange some Sr in the wings, particularly in coastal regions where Sr is more concentrated in rainwater. Consequently, future studies should investigate the susceptibility of Sr and other metals to contamination under real-world conditions, including rain, aerosols, and pollution. Raising butterflies in the wild at specific sites with known metal and metal isotope composition could help reinforce the applicability of these tools for geolocation.

We have defined a suite of metals suitable for the geolocation of monarch butterflies, but it may be inappropriate to extrapolate these findings to other organisms, including other Lepidoptera. The specialized structures that aid in metal transport can differ between

insect taxa, leading to phylogenetic-based differences in metal uptake, transfer, speciation, and segregation (Tibbett et al., 2021). This may be especially important for non-nectarivorous species because nectar contains low concentrations of metals compared to the diets of herbivores or carnivores (e.g., dragonflies). Caution should also be taken when using whole-body samples rather than a specific insect tissue with relatively low metabolic activity (Orłowski et al., 2020); it can be assumed that whole-body specimens will show greater changes over time than the wings due to greater inputs from the adult diet (Dempster et al., 1986). Even in cases where the adult insect does not feed and, thus, no dietary input is expected (e.g., eastern spruce budworm), metals which may be altered exogenously should be carefully evaluated. Ultimately, many sources of variability in metal composition need to be further explored, including the effects of host plant (Bowden et al., 1984), microbial communities (Consuegra et al., 2020), parasitism (Sures, 2004), type of metamorphosis and life-stage, reproductive status, homeostatic mechanisms, and their interactions (Tibbett et al., 2021).

Strontium isotope ratios have already been applied to the geographic assignment of monarch butterflies and other lepidopteran species and showed great promise for increasing the precision of isotope-based geographic assignment (Reich et al., 2021; Dargent et al., 2022). Here, we confirmed the assumption that the $^{87}Sr/^{86}Sr$ of monarch wings remain the same over time and continue to represent the larval signature despite adult feeding, at least in males (Figure 4B). While we showed that the Sr in wings was susceptible to exchange in extreme wetting conditions (Figure 4D), we argue that these conditions are unlikely in nature and do not question the applicability of this geolocation tracer. More surprisingly, we also observed sex-based differences in $^{87}Sr/^{86}Sr$, with females having a lower $^{87}Sr/^{86}Sr$ than both the males and their larval diet (Figures 4B,C). As $^{87}Sr/^{86}Sr$ trace the mixing of isotopically distinct sources (and not isotopic fractionation), this observation suggests that there is an unidentified source of Sr to the female monarchs. Strontium is chemically similar to Ca and is inadvertently substituted for calcium ions in the body (Capo et al., 1998). Based on our results that Ca and, to a lesser degree, Sr in wings vary by sex (Figures 2A, 4A), we argue that the difference in $^{87}Sr/^{86}Sr$ is potentially related to the preferential allocation of Ca (and thus Sr) to female reproductive organs for oogenesis, although no eggs were laid during the experiment. In this case, the $^{87}Sr/^{86}Sr$ of the wings would be determined by the milkweed $^{87}Sr/^{86}Sr$ from a discrete timestep rather than an integration of the entire larval stage. However, previous studies investigating $^{87}Sr/^{86}Sr$ in monarch wings did not detect any differences between males and females (Flockhart et al., 2015), and it is possible that our result reflects the low number of samples. Alternatively, the differences in $^{87}Sr/^{86}Sr$ between the sexes could be due to the high sensitivity of butterfly wings immediately after eclosion. The female monarchs emerged from their chrysalises 1 day earlier than the males (Supplementary Figure S4). The day that the females eclosed coincided with an observation that paint odors could be smelled in the laboratory where the adult monarchs were kept, although the laboratory itself was not painted. Many indoor paints contain high concentrations of Sr (Van Gorkum and Bouwman, 2005), as do gypsum-based mixtures (Huang, 2020), which are often applied to fill holes and sanded smooth prior to painting. High concentrations of dust from either of these substances present on the day the female monarchs eclosed from their chrysalises could have deposited on the surface of the wings, and since butterfly wings are soft and wet on the day of eclosion, it is possible that external Sr could have mobilized and penetrated the wing tissues. We suggest that future studies explore the link between sex and $^{87}Sr/^{86}Sr$ in monarch wings, and the sensitivity of metals in butterfly wings to environmental conditions on the day of eclosion.

4.4. Natural metal concentrations

The metal concentrations measured in the wings of the laboratory monarchs are unlikely to be representative of monarchs in natural environments. All the monarchs in the laboratory experiment were siblings, limiting their genetic diversity and the independence of replicates (Merritt and Bewick, 2017). Comparing the concentrations of metals found in the wings of monarchs in our laboratory study to concentrations of metals in the wings of wild monarchs, we can see that wild monarch wings had significantly higher concentrations of Mg, Al, Co, Cd, Ba, and Pb, but lower concentrations of Cu, Zn, and Sr (Supplementary Figure S5). Differences in the concentration of Category 4 metals (i.e., Mg, Ba, Sr) are likely due to different concentrations of these elements in the larval diets of the wild monarchs. Differences in the bioaccumulating metals from Categories 2 and 3 (i.e., Al, Cd, Pb, Cu, Zn) are likely due to differences in the metal concentrations of the larval diet, metal concentrations in the adult diet, environmental exposure to metals, and age of the butterflies. Of particular interest is Al, which showed much higher concentrations in the wild monarch wings, likely derived from the higher exposure to mineral dust in natural systems than in laboratory conditions. Comparisons of Zn and Na in the monarch wings with concentrations found in monarch abdomens (Shephard et al., 2021) shows that concentrations in the abdomen are approximately three times higher than in the wings. This large difference is likely due to higher allocations of essential Zn and Na to the abdomen for metabolic processes, but could also be influenced by differences in the metal concentrations of the larval diet, unabsorbed metals contained within the digestive tract of the abdomen, and differences in nutrient requirements between environments. Similar differences have been found in beetles, where abdominal samples had higher concentrations of metals than elytra and only some metals were correlated between the tissues (Orłowski et al., 2020).

5. Conclusion

This controlled diet-switching experiment demonstrated that the incorporation of metal and metal isotopes within the wing of monarch butterflies has distinct sources. Some elements (e.g., Mn, Mo, Ca) are likely incorporated from the diet but their concentrations are further modulated throughout the adult life by physiological or metabolic processes. Using those metals and their isotopes (e.g., Ca isotopes) could bring new perspectives on the distinct physiological needs and biogeochemistry of adult butterflies. Other elements are bioaccumulated from the larval and adult diet (e.g., Ni, Zn) and their concentrations keep increasing throughout the adult stage. Many metals also have increasing concentrations through time and come, at least in part, from exogenous sources including aerosols (e.g., Al, Fe, Pb). Using those metals or their isotopes (e.g., Pb) could help track the pollution exposure of individuals either locally or through their migratory travels. Finally, a few metals have concentrations that remain stable in the wing throughout the adult life (e.g., Sr, Mg). Those metals are good candidates for developing geolocation tools in population ecology studies. However, even those metals are not exempt from potential contamination as demonstrated

with the rapid exchange of Sr when wings are submerged in water. Despite these caveats, this study supported the use of $^{87}Sr/^{86}Sr$ ratios as a geolocation tool of natal origin and identified other possible geolocation tools. Finally, this study also underlined the complexity of metal incorporation processes and sources in a single insect species' tissue. The accumulation of metals absorbed or exchanged by wetting from atmospheric sources is a major incorporation mechanism for several metals in insect wings. Due to the high body surface area to volume ratio of insects and the absorbent properties of their chitinous exoskeleton, this mechanism might be a prominent contributor of metal incorporation in insect tissues with possible toxicological consequences and roles in controlling insect population dynamics.

Data availability statement

The datasets presented in this study can be found in online repositories. The names of the repository/repositories and accession number(s) can be found below: Open Science Foundation (https://doi.org/10.17605/OSF.IO/N4PVM).

Author contributions

MR conceived the idea for the study and led the writing of the manuscript. MR, FD, and HK designed the insect rearing component. MR, CB, MK, FD, and LH designed the metal and metal isotope analysis component. TF and RN collected the wild monarch and milkweed samples. MR, MK, LH, and CB analyzed the data. All authors contributed to the drafts and gave final approval for publication.

Funding

This study was funded by the New Frontiers in Research Fund (CB and GT) and Syngenta Canada, Inc. (RN). GT acknowledges funding from the grant PID2020-117739GA-I00 from MCIN/AEI/10.13039/501100011033 and the grant LINKA20399 from the CSIC iLink program. MR was supported by the Queen Elizabeth II Graduate Scholarship in Science and Technology (QEII-GSST) and an Ontario Graduate Scholarship.

Acknowledgments

We would like to thank Shuanquan Zhang for his expert guidance in operating the MC-ICP-MS at Carleton University, Joseph Spencer for running the Pb columns, Smita Mohanty for help with the ICP-MS, and Emma Brown, Daniela Quintero, and Aldo Camilo Martinez-Becerril for assisting with animal husbandry.

Conflict of interest

This study received funding from Syngenta Canada, Inc. The funder was not involved in the study design, collection, analysis, interpretation of data, the writing of this article or the decision to submit it for publication. All authors declare no other competing interests.

Publisher's note

Supplementary material

The Supplementary material for this article can be found online at: https://www.frontiersin.org/articles/10.3389/fevo.2023.1085903/full#supplementary-material

References

Anastopoulos, I., Bhatnagar, A., Bikiaris, D., and Kyzas, G. (2017). Chitin adsorbents for toxic metals: a review. *Int. J. Mol. Sci.* 18:114. doi: 10.3390/ijms18010114

Andreani, G., Ferlizza, E., Cabbri, R., Fabbri, M., Bellei, E., and Isani, G. (2021). Essential (Mg, Fe, Zn and Cu) and non-essential (Cd and Pb) elements in predatory insects (*Vespa crabro* and *Vespa velutina*): a molecular perspective. *Int. J. Mol. Sci.* 22:228. doi: 10.3390/ijms22010228

Aptekmann, A. A., Buongiorno, J., Giovannelli, D., Glamoclija, M., Ferreiro, D. U., and Bromberg, Y. (2022). Mebipred: identifying metal-binding potential in protein sequence. *Bioinformatics* 38, 3532–3540. doi: 10.1093/bioinformatics/btac358

Ben-Shahar, Y. (2018). The impact of environmental Mn exposure on insect biology. *Front. Genet.* 9, 1–7. doi: 10.3389/fgene.2018.00070

Bowden, J., Digby, P. G. N., and Sherlock, P. L. (1984). Studies of elemental composition as a biological marker in insects. I. the influence of soil type and host-plant on elemental composition of *Noctua pronuba* (Lepidoptera: Noctuidae). *Bull. Entomol. Res.* 75, 675–687. doi: 10.1017/S0007485300015947

Butt, A., Qurat-ul-Ain Rehman, K., Khan, M. X., and Hesselberg, T. (2018). Bioaccumulation of cadmium, lead, and zinc in agriculture-based insect food chains. *Environ. Monit. Assess.* 190:698. doi: 10.1007/s10661-018-7051-2

Capo, R. C., Stewart, B. W., and Chadwick, O. A. (1998). Strontium isotopes as tracers of ecosystem processes: theory and methods. *Geoderma* 82, 197–225. doi: 10.1016/S0016-7061(97)00102-X

Cardoso-Jaime, V., Broderick, N. A., and Maya-Maldonado, K. (2022). Metal ions in insect reproduction: a crosstalk between reproductive physiology and immunity. *Curr. Opin. Insect Sci.* 52:100924. doi: 10.1016/j.cois.2022.100924

Clark, E. W. (1958). A review of literature on calcium and magnesium in insects. *Ann. Entomol. Soc. Am.* 51, 142–154. doi: 10.1093/aesa/51.2.142

Consuegra, J., Grenier, T., Baa-Puyoulet, P., Rahioui, I., Akherraz, H., Gervais, H., et al. (2020). *Drosophila*-associated bacteria differentially shape the nutritional requirements of their host during juvenile growth. *PLoS Biol.* 18:e3000681. doi: 10.1371/journal.pbio.3000681

Crowley, B. E., Bataille, C. P., Haak, B. A., and Sommer, K. M. (2021). Identifying nesting grounds for juvenile migratory birds with dual isotope: an initial test using North American raptors. *Ecosphere* 12:e03765. doi: 10.1002/ecs2.3765

Dargent, F., Candau, J. N., Studens, K., Perrault, K. H., Reich, M. S., and Bataille, C. P. (2022). Characterizing eastern spruce budworm's large-scale dispersal events through flight behavior and stable isotope analyses. *BioRxiv Preprint*. doi: 10.1101/2022.10.20.513023

Dargent, F., Gilmour, S. M., Brown, E. A., Kassen, R., and Kharouba, H. M. (2021). Low prevalence of the parasite *Ophryocystis elektroscirrha* at the range edge of the Eastern North American monarch (*Danaus plexippus*) butterfly population. *Can. J. Zool.* 99, 409–413. doi: 10.1139/cjz-2020-0175

Davis, A. K., and Holden, M. T. (2015). Measuring intraspecific variation in flight-related morphology of monarch butterflies (*Danaus plexippus*): which sex has the best flying gear? *J. Insects* 2015, 1–6. doi: 10.1155/2015/591705

Dempster, J. P., Lakhani, K. H., and Coward, P. A. (1986). The use of chemical composition as a population marker in insects: a study of the brimstone butterfly. *Ecol. Entomol.* 11, 51–65. doi: 10.1111/j.1365-2311.1986.tb00279.x

Di, N., Hladun, K. R., Zhang, K., Liu, T. X., and Trumble, J. T. (2016). Laboratory bioassays on the impact of cadmium, copper and lead on the development and survival of

honeybee (*Apis mellifera* L.) larvae and foragers. *Chemosphere* 152, 530–538. doi: 10.1016/j.chemosphere.2016.03.033

Dow, J. A. (2017). The essential roles of metal ions in insect homeostasis and physiology. *Curr. Opin. Insect Sci.* 23, 43–50. doi: 10.1016/j.cois.2017.07.001

Espeset, A., Kobiela, M. E., Sikkink, K. L., Pan, T., Roy, C., and Snell-Rood, E. C. (2019). Anthropogenic increases in nutrients alter sexual selection dynamics: a case study in butterflies. *Behav. Ecol.* 30, 598–608. doi: 10.1093/beheco/arz004

Evans, R. D., Wang, W., Evans, H. E., and Georg, R. B. (2017). Variation in Zn, C, and N isotope ratios in three stream insects. *Facets* 1, 205–216. doi: 10.1139/facets-2016-0023

FAO, WHO. (2019). *Codex Alimentarius: International Food Standards*. Geneva: World Health Organization.

Fauberteau, A. E., Chartrand, M. M. G., Hu, L., St-Jean, G., and Bataille, C. P. (2021). Investigating a cold case using high-resolution multi-isotope profiles in human hair. *Forensic Chem.* 22:100300. doi: 10.1016/j.forc.2020.100300

Feindt, W., Oppenheim, S. J., DeSalle, R., Goldstein, P. Z., and Hadrys, H. (2018). Transcriptome profiling with focus on potential key genes for wing development and evolution in *Megaloprepus caerulatus*, the damselfly species with the world's largest wings. *PLoS One* 13, 1–17. doi: 10.1371/journal.pone.0189898

Filipiak, M., and Filipiak, Z. M. (2022). Application of ionomics and ecological stoichiometry in conservation biology: nutrient demand and supply in a changing environment. *Biol. Conserv.* 272:109622. doi: 10.1016/j.biocon.2022.109622

Filipiak, M., Woyciechowski, M., and Czarnoleski, M. (2021). Stoichiometric niche, nutrient partitioning and resource allocation in a solitary bee are sex-specific and phosphorous is allocated mainly to the cocoon. *Sci. Rep.* 11:652. doi: 10.1038/s41598-020-79647-7

Flockhart, D. T. T., Kyser, T. K., Chipley, D., Miller, N. G., and Norris, D. R. (2015). Experimental evidence shows no fractionation of strontium isotopes (87Sr/86Sr) among soil, plants, and herbivores: implications for tracking wildlife and forensic science. *Isot. Environ. Health Stud.* 51, 372–381. doi: 10.1080/10256016.2015.1021345

Flockhart, D. T. T., Wassenaar, L. I., Martin, T. G., Hobson, K. A., Wunder, M. B., and Norris, D. R. (2013). Tracking multi-generational colonization of the breeding grounds by monarch butterflies in Eastern North America. *Proc. R. Soc. B* 280:20131087. doi: 10.1098/rspb.2013.1087

Hirsch, H. V. B., Mercer, J., Sambaziotis, H., Huber, M., Stark, D. T., Torno-Morley, T., et al. (2003). Behavioral effects of chronic exposure to low levels of lead in Drosophila melanogaster. *Neurotoxicology* 24, 435–442. doi: 10.1016/S0161-813X(03)00021-4

Holder, P. W., Armstrong, K., Van Hale, R., Millet, M.-A., Frew, R., Clough, T. J., et al. (2014). Isotopes and trace elements as natal origin markers of *Helicoverpa armigera*-an experimental model for biosecurity pests. *PLoS One* 9:e92384. doi: 10.1371/journal.pone.0092384

Honegger, H. W., Dewey, E. M., and Ewer, J. (2008). Bursicon, the tanning hormone of insects: recent advances following the discovery of its molecular identity. *J. Comp. Physiol. A Neuroethol. Sens. Neural Behav. Physiol.* 194, 989–1005. doi: 10.1007/s00359-008-0386-3

Hopkin, S. P. (1990). Critical concentrations, pathways of detoxification and cellular ecotoxicology of metals in terrestrial arthropods. *Funct. Ecol.* 4:321. doi: 10.2307/2389593

Hu, L., Fernandez, D. P., and Cerling, T. E. (2018). Longitudinal and transverse variation of trace element concentrations in elephant and giraffe hair: implication for endogenous and exogenous contributions. *Environ. Monit. Assess.* 190:644. doi: 10.1007/s10661-018-7038-z

Hu, L., Fernandez, D. P., and Cerling, T. E. (2019). Trace element concentrations in horn: endogenous levels in keratin and susceptibility to exogenous contamination. *Chemosphere* 237:124443. doi: 10.1016/j.chemosphere.2019.124443

Hu, L., Fernandez, D. P., Cerling, T. E., and Tipple, B. J. (2020). Fast exchange of strontium between hair and ambient water: implication for isotopic analysis in provenance and forensic studies. *PLoS One* 15, e0233712–e0233714. doi: 10.1371/journal.pone.0233712

Huang, X., (2020). *Characterization of Drywall Products for Assessing Impacts Associated with End-of-life Management*. Washington, DC: U.S. Environmental Protection Agency.

Jin, P., Chen, J., Zhan, H., Huang, S., Wang, J., and Shu, Y. (2020). Accumulation and excretion of zinc and their effects on growth and food utilization of *Spodoptera litura* (Lepidoptera: Noctuidae). *Ecotoxicol. Environ. Saf.* 202:110883. doi: 10.1016/j.ecoenv.2020.110883

Joern, A., Provin, T., and Behmer, S. T. (2012). Not just the usual suspects: insect herbivore populations and communities are associated with multiple plant nutrients. *Ecology* 93, 1002–1015. doi: 10.1890/11-1142.1

Judd, T. M., Magnus, R. M., and Fasnacht, M. P. (2010). A nutritional profile of the social wasp *Polistes metricus*: differences in nutrient levels between castes and changes within castes during the annual life cycle. *J. Insect Physiol.* 56, 42–56. doi: 10.1016/j.jinsphys.2009.09.002

Kabata-Pendias, A., and Mukherjee, A. B., (2007). *Trace Elements from Soil to Human*. Springer, Berlin, Heidelberg.

Kaspari, M. (2020). The seventh macronutrient: how sodium shortfall ramifies through populations, food webs and ecosystems. *Ecol. Lett.* 23, 1153–1168. doi: 10.1111/ele.13517

Kaspari, M. (2021). The invisible hand of the periodic Table: how micronutrients shape ecology. *Annu. Rev. Ecol. Evol. Syst.* 52, 199–219. doi: 10.1146/annurev-ecolsys-012021-090118

Kempson, I. M., Skinner, W. M., and Kirkbride, K. P. (2006). Advanced analysis of metal distributions in human hair. *Environ. Sci. Technol.* 40, 3423–3428. doi: 10.1021/es052158v

Kobiela, M. E., and Snell-rood, E. C. (2018). Integrative and comparative biology nickel exposure has complex transgenerational effects in a butterfly. *Integr. Comp. Biol.* 58, 1008–1017. doi: 10.1093/icb/icy096

Kowalski, R., Davies, S. E., and Hawkes, C. (1989). Metal composition as a natural marker in anthomyiid fly *Delia radicum* (L.). *J. Chem. Ecol.* 15, 1231–1239. doi: 10.1007/BF01014825

Kula, E., Martinek, P., Chromcová, L., and Hedbávný, J. (2014). Development of *Lymantria dispar* affected by manganese in food. *Environ. Sci. Pollut. Res.* 21, 11987–11997. doi: 10.1007/s11356-014-3075-5

Lin, T., Chen, P., Chen, X., Shen, J., Zhong, S., Sun, Q., et al. (2021). Geographical classification of *Helicoverpa armigera* (Lepidoptera: Noctuidae) through mineral component analysis. *Anal. Lett.* 54, 669–683. doi: 10.1080/00032719.2020.1777560

Lin, T., Chen, X., Li, B., Chen, P., Guo, M., Zhou, X., et al. (2019). Geographical origin identification of *Spodoptera litura* (Lepidoptera: Noctuidae) based on trace element profiles using tobacco as intermedium planted on soils from five different regions. *Microchem. J.* 146, 49–55. doi: 10.1016/j.microc.2018.12.051

Lindroos, E. E., Bataille, C. P., Holder, P. W., Talavera, G., and Reich, M. S. ((2023). Temporal stability of δ^2h in insect tissues: implications for isotope-based geographic assignments. *Front. Ecol. Evol.* 11:1060836. doi: 10.3389/fevo.2023.1060836

Maret, W., (2016). *Metallomics: A Primer of Integrated Biometal Sciences*. London: Imperial College Press.

Martinek, P., Hedbávný, J., Kudláček, T., Šťasta, M., and Kula, E. (2020). Adverse responses of *Cabera pusaria* caterpillars to high dietary manganese concentration. *Entomol. Exp. Appl.* 168, 635–643. doi: 10.1111/eea.12919

McLean, J. A., Laks, P., and Shore, T. L. (1983). "Comparisons of elemental profiles of the western spruce budworm reared on three host foliages and artificial medium" in *Proceedings, Forest defoliator Host Interactions: A Comparison between Gypsy Moth and Spruce Budworms*. eds. R. L. Talerico and M. Montgomery (Broomall, PA: U.S. Department of Agriculture), 33–40.

Merritt, T. J. S., and Bewick, A. J. (2017). Genetic diversity in insect metal tolerance. *Front. Genet.* 8, 1–6. doi: 10.3389/fgene.2017.00172

Mesjasz-Przybyłowicz, J., Orłowska, E., Augustyniak, M., Nakonieczny, M., Tarnawska, M., Przybyłowicz, W., et al. (2014). Elemental distribution in reproductive and neural organs of the *Epilachna nylanderi* (Coleoptera: Coccinellidae), a phytophage of nickel hyperaccumulator *Berkheya coddii* (Asterales: Asteraceae) by micro-PIXE. *J. Insect Sci.* 14:152. doi: 10.1093/jisesa/ieu014

Mitchell, T. S., Agnew, L., Meyer, R., Sikkink, K. L., Oberhauser, K. S., Borer, E. T., et al. (2020). Traffic influences nutritional quality of roadside plants for monarch caterpillars. *Sci. Total Environ.* 724:138045. doi: 10.1016/j.scitotenv.2020.138045

Mogren, C. L., and Trumble, J. T. (2010). The impacts of metals and metalloids on insect behavior. *Entomol. Exp. Appl.* 135, 1–17. doi: 10.1111/j.1570-7458.2010.00967.x

Monchanin, C., Devaud, J. M., Barron, A. B., and Lihoreau, M. (2021). Current permissible levels of metal pollutants harm terrestrial invertebrates. *Sci. Total Environ.* 779:146398. doi: 10.1016/j.scitotenv.2021.146398

Moore, L. J., Murphy, T. J., Barnes, I. L., and Paulsen, P. J. (1982). Absolute isotopic abundance ratios and atomic weight of a reference sample of strontium. *J. Res. Natl. Bur. Stand.* 87, 1–8. doi: 10.6028/jres.087.001

Nakano, T., Jeon, S.-R., Shindo, J., Fumoto, T., Okada, N., and Shimada, J. (2001). Sr isotopic signature in plant-derived Ca in rain. *Water Air Soil Pollut.* 130, 769–774. doi: 10.1023/A:1013849905563

Negri, I., Mavris, C., Di Prisco, G., Caprio, E., and Pellecchia, M. (2015). Honey bees (*Apis mellifera*, L.) as active samplers of airborne particulate matter. *PLoS One* 10:e0132491. doi: 10.1371/journal.pone.0132491

Nessel, M. P., Konnovitch, T., Romero, G. Q., and González, A. L. (2021). Nitrogen and phosphorus enrichment cause declines in invertebrate populations: a global meta-analysis. *Biol. Rev.* 96, 2617–2637. doi: 10.1111/brv.12771

Nickles, E. P., Ghiradella, H., Bakhru, H., and Haberl, A. (2002). Egg of the Karner blue butterfly (*Lycaeides melissa samuelis*): morphology and elemental analysis. *J. Morphol.* 251, 140–148. doi: 10.1002/jmor.1079

Nitzsche, K. N., Shin, K. C., Kato, Y., Kamauchi, H., Takano, S., and Tayasu, I. (2020). Magnesium and zinc stable isotopes as a new tool to understand Mg and Zn sources in stream food webs. *Ecosphere* 11, 1–20. doi: 10.1002/ecs2.3197

Nitzsche, K. N., Wakaki, S., Yamashita, K., Shin, K. C., Kato, Y., Kamauchi, H., et al. (2022). Calcium and strontium stable isotopes reveal similar behaviors of essential Ca and nonessential Sr in stream food webs. *Ecosphere* 13, 1–19. doi: 10.1002/ecs2.3921

Norris, D. R., Lank, D. B., Pither, J., Chipley, D., Ydenberg, R. C., and Kyser, T. K. (2007). Trace element profiles as unique identifiers of western sandpiper (*Calidris mauri*) populations. *Can. J. Zool.* 85, 579–583. doi: 10.1139/Z07-024

Ogra, Y., and Hirata, T. (Eds.), (2017). *Metallomics: Recent Analytical Techniques and Applications*. Springer, Japan, Tokyo.

Orłowski, G., Mróz, L., Kadej, M., Smolis, A., Tarnawski, D., Karg, J., et al. (2020). Breaking down insect stoichiometry into chitin-based and internal elemental traits: patterns and correlates of continent-wide intraspecific variation in the largest European saproxylic beetle. *Environ. Pollut.* 262:114064. doi: 10.1016/j.envpol.2020.114064

Otuka, A., Dudhia, J., Watanabe, T., and Furuno, A. (2005). A new trajectory analysis method for migratory planthoppers, *Sogatella furcifera* (Horváth) (Homoptera: Delphacidae) and *Nilaparvata lugens* (Stål), using an advanced weather forecast model. *Agric. For. Entomol.* 7, 1–9. doi: 10.1111/j.1461-9555.2005.00236.x

Pass, G. (2018). Beyond aerodynamics: the critical roles of the circulatory and tracheal systems in maintaining insect wing functionality. *Arthropod Struct. Dev.* 47, 391–407. doi: 10.1016/j.asd.2018.05.004

Phillips, B. B., Bullock, J. M., Gaston, K. J., Hudson-Edwards, K. A., Bamford, M., Cruse, D., et al. (2021). Impacts of multiple pollutants on pollinator activity in road verges. *J. Appl. Ecol.* 58, 1017–1029. doi: 10.1111/1365-2664.13844

Prather, C. M., Laws, A. N., Cuellar, J. F., Reihart, R. W., Gawkins, K. M., and Pennings, S. C. (2018). Seeking salt: herbivorous prairie insects can be co-limited by macronutrients and sodium. *Ecol. Lett.* 21, 1467–1476. doi: 10.1111/ele.13127

R Core Team. (2013). *R: A Language and Environment for Statistical Computing*. R Foundation for Statistical Computing, Vienna, Austria.

Reich, M. S., Flockhart, D. T. T., Norris, D. R., Hu, L., and Bataille, C. P. (2021). Continuous-surface geographic assignment of migratory animals using strontium isotopes: a case study with monarch butterflies. *Methods Ecol. Evol.* 12, 2445–2457. doi: 10.1111/2041-210X.13707

Reihart, R. W., Angelos, K. P., Gawkins, K. M., Hurst, S. E., Montelongo, D. C., Laws, A. N., et al. (2021). Crazy ants craving calcium: macronutrients and micronutrients can limit and stress an invaded grassland brown food web. *Ecology* 102:e03263. doi: 10.1002/ecy.3263

Rodiouchkina, K., Rodushkin, I., Goderis, S., and Vanhaecke, F. (2022). Longitudinal isotope ratio variations in human hair and nails. *Sci. Total Environ.* 808:152059. doi: 10.1016/j.scitotenv.2021.152059

Rudnick, R. L., and Gao, S. (2014). "Composition of the continental crust" in *Treatise on Geochemistry*. eds. H. D. Holland and K. K. Turekian (Amsterdam, Netherlands: Elsevier Ltd.), 1–51.

Seewagen, C. L. (2020). The threat of global mercury pollution to bird migration: potential mechanisms and current evidence. *Ecotoxicology* 29, 1254–1267. doi: 10.1007/s10646-018-1971-z

Selvey, A. D.. (2020). *Transcriptomic Exploration of the Vanessa cardui Immune System*. University of Nevada, Reno.

Shaw, J. A., Boyd, A., House, M., Cowin, G., and Baer, B. (2018). Multi-modal imaging and analysis in the search for iron-based magnetoreceptors in the honeybee *Apis mellifera*. *R. Soc. Open Sci.* 5, 1–13. doi: 10.1098/rsos.181163

Shephard, A. M., Brown, N. S., and Snell-Rood, E. C. (2022). Anthropogenic zinc exposure increases mortality and antioxidant gene expression in monarch butterflies with low access to dietary macronutrients. *Environ. Toxicol. Chem.* 41, 1286–1296. doi: 10.1002/etc.5305

Shephard, A. M., Mitchell, T. S., Henry, S. B., Oberhauser, K. S., Kobiela, M. E., and Snell-Rood, E. C. (2020). Assessing zinc tolerance in two butterfly species: consequences for conservation in polluted environments. *Insect Conserv. Divers.* 13, 201–210. doi: 10.1111/icad.12404

Shephard, A. M., Mitchell, T. S., and Snell-rood, E. C. (2021). Monarch caterpillars are robust to combined exposure to the roadside micronutrients sodium and zinc. *Conserv. Physiol.* 9, 1–15. doi: 10.1093/conphys/coab061

Simonetti, A., Gariépy, C., and Carignan, J. (2000a). Pb and Sr isotopic evidence for sources of atmospheric heavy metals and their deposition budgets in Northeastern North America. *Geochim. Cosmochim. Acta* 64, 3439–3452. doi: 10.1016/S0016-7037(00)00446-4

Simonetti, A., Gariépy, C., and Carignan, J. (2000b). Pb and Sr isotopic compositions of snowpack from Québec, Canada: inferences on the sources and deposition budgets of atmospheric heavy metals. *Geochim. Cosmochim. Acta* 64, 5–20. doi: 10.1016/S0016-7037(99)00207-0

Slobodian, M. R., Petahtegoose, J. D., Wallis, A. L., Levesque, D. C., and Merritt, T. J. S. (2021). The effects of essential and non-essential metal toxicity in the *Drosophila melanogaster* insect model: a review. *Toxics* 9:269. doi: 10.3390/toxics9100269

Smith, K. E., and Weis, D. (2020). Evaluating spatiotemporal resolution of trace element concentrations and Pb isotopic compositions of honeybees and hive products as biomonitors for urban metal distribution. *GeoHealth* 4:e2020GH000264. doi: 10.1029/2020GH000264

Smith, K. E., Weis, D., Scott, S. R., Berg, C. J., Segal, Y., and Claeys, P. (2021). Regional and global perspectives of honey as a record of lead in the environment. *Environ. Res.* 195:110800. doi: 10.1016/j.envres.2021.110800

Snell-Rood, E. C., Espeset, A., Boser, C. J., White, W. A., and Smykalski, R. (2014). Anthropogenic changes in sodium affect neural and muscle development in butterflies. *PNAS* 111, 10221–10226. doi: 10.1073/pnas.1323607111

Studier, E. H. (1996). Composition of bodies of cave crickets (*Hadenoecus subterraneus*), their eggs, and their egg predator, *Neaphaenops tellkampfi*. *Am. Midl. Nat.* 136, 101–109. doi: 10.2307/2426635

Stuhr, S., Truong, V. K., Vongsvivut, J., Senkbeil, T., Yang, Y., Al Kobaisi, M., et al. (2018). Structure and chemical organization in Damselfly *Calopteryx haemorrhoidalis* wings: a spatially resolved FTIR and XRF analysis with synchrotron radiation. *Sci. Rep.* 8, 8413–8419. doi: 10.1038/s41598-018-26563-6

Suchan, T., Talavera, G., Sáez, L., Ronikier, M., and Vila, R. (2018). Pollen metabarcoding as a tool for tracking long-distance insect migrations. *Mol. Ecol. Resour.* 19, 149–162. doi: 10.1111/1755-0998.12948

Sun, H. X., Tang, W. C., Chen, H., Chen, W., Zhang, M., Liu, X., et al. (2013). Food utilization and growth of cutworm *Spodoptera litura* Fabricius larvae exposed to nickel, and its effect on reproductive potential. *Chemosphere* 93, 2319–2326. doi: 10.1016/j.chemosphere.2013.08.025

Sures, B. (2004). Environmental parasitology: relevancy of parasites in monitoring environmental pollution. *Trends Parasitol.* 20, 170–177. doi: 10.1016/j.pt.2004.01.014

Tacail, T., Le Houedec, S., and Skulan, J. L. (2020). New frontiers in calcium stable isotope geochemistry: perspectives in present and past vertebrate biology. *Chem. Geol.* 537:119471. doi: 10.1016/j.chemgeo.2020.119471

Tanaka, Y. K., and Hirata, T. (2018). Stable isotope composition of metal elements in biological samples as tracers for element metabolism. *Anal. Sci.* 34, 645–655. doi: 10.2116/analsci.18SBR02

Tibbett, M., Green, I., Rate, A., De Oliveira, V. H., and Whitaker, J. (2021). The transfer of trace metals in the soil-plant-arthropod system. *Sci. Total Environ.* 779:146260. doi: 10.1016/j.scitotenv.2021.146260

Tigar, B. J., and Hursthouse, A. (2016). Applying biogeochemistry to identify the geographic origins of insects-a model using *Prostephanus truncatus*. *J. Environ. Stud.* 2:9. doi: 10.13188/2471-4879.1000004

Todt, W., Cliff, R. A., Hanser, A., and Hofmann, A. W.. (1996). *Evaluation of a 202Pb–205Pb Double Spike for High - Precision Lead Isotope Analysis*. American Geophysical Union, Washington, DC, 429–437.

Tsai, C.-C., Childers, R. A., Nan Shi, N., Ren, C., Pelaez, J. N., Bernard, G. D., et al. (2020). Physical and behavioral adaptations to prevent overheating of the living wings of butterflies. *Nat. Commun.* 11, 551–514. doi: 10.1038/s41467-020-14408-8

Van Gorkum, R., and Bouwman, E. (2005). The oxidative drying of alkyd paint catalysed by metal complexes. *Coord. Chem. Rev.* 249, 1709–1728. doi: 10.1016/j.ccr.2005.02.002

Wanty, R. B., Balistrieri, L. S., Wesner, J. S., Walters, D. M., Schmidt, T. S., Stricker, C. A., et al. (2017). In vivo isotopic fractionation of zinc and biodynamic modeling yield insights into detoxification mechanisms in the mayfly *Neocloeon triangulifer*. *Sci. Total Environ.* 609, 1219–1229. doi: 10.1016/j.scitotenv.2017.07.269

Welti, E. A. R., Roeder, K. A., de Beurs, K. M., Joern, A., and Kaspari, M. (2020). Nutrient dilution and climate cycles underlie declines in a dominant insect herbivore. *Proc. Natl. Acad. Sci. U. S. A.* 117, 7271–7275. doi: 10.1073/pnas.1920012117

Wieringa, J. G., Nagel, J., Nelson, D. M., Carstens, B. C., and Gibbs, H. L. (2020). Using trace elements to identify the geographic origin of migratory bats. *PeerJ* 8, e10082–e10023. doi: 10.7717/peerj.10082

Xiao, G., and Zhou, B. (2016). What can flies tell us about zinc homeostasis? *Arch. Biochem. Biophys.* 611, 134–141. doi: 10.1016/j.abb.2016.04.016

Zhang, Y., Ying, H., and Xu, Y. (2019). Comparative genomics and metagenomics of the metallomes. *Metallomics* 11, 1026–1043. doi: 10.1039/c9mt00023b

Zhou, J., Chen, J., and Shu, Y. (2021). Lead stress affects the reproduction of *Spodoptera litura* but not by regulating the vitellogenin gene promoter. *Ecotoxicol. Environ. Saf.* 208:111581. doi: 10.1016/j.ecoenv.2020.111581

Zhou, X., Taylor, M. P., and Davies, P. J. (2018). Tracing natural and industrial contamination and lead isotopic compositions in an Australian native bee species. *Environ. Pollut.* 242, 54–62. doi: 10.1016/j.envpol.2018.06.063

frontiers | Frontiers in Ecology and Evolution

TYPE Original Research
PUBLISHED 15 February 2023
DOI 10.3389/fevo.2023.1120271

OPEN ACCESS

EDITED BY
Jose A. Masero,
University of Extremadura,
Spain

REVIEWED BY
Luis Gerardo Herrera Montalvo,
Universidad Nacional Autónoma de México,
Mexico
Erick Gonzalez Medina,
University of Extremadura,
Spain

*CORRESPONDENCE
Pablo Sabat
✉ psabat@uchile.cl

SPECIALTY SECTION
This article was submitted to
Ecophysiology,
a section of the journal
Frontiers in Ecology and Evolution

RECEIVED 09 December 2022
ACCEPTED 30 January 2023
PUBLISHED 15 February 2023

CITATION
Navarrete L, Lübcker N, Alvarez F, Nespolo R, Sanchez-Hernandez JC, Maldonado K, Sharp ZD, Whiteman JP, Newsome SD and Sabat P (2023) A multi-isotope approach reveals seasonal variation in the reliance on marine resources, production of metabolic water, and ingestion of seawater by two species of coastal passerine to maintain water balance.
Front. Ecol. Evol. 11:1120271.
doi: 10.3389/fevo.2023.1120271

A multi-isotope approach reveals seasonal variation in the reliance on marine resources, production of metabolic water, and ingestion of seawater by two species of coastal passerine to maintain water balance

Lucas Navarrete[1,2], Nico Lübcker[3], Felipe Alvarez[1,2], Roberto Nespolo[2,4,5], Juan Carlos Sanchez-Hernandez[6], Karin Maldonado[7], Zachary D. Sharp[8], John P. Whiteman[9], Seth D. Newsome[3] and Pablo Sabat[1,2]*

[1]Departamento de Ciencias Ecológicas, Facultad de Ciencias, Universidad de Chile, Santiago, Chile, [2]Center of Applied Ecology and Sustainability (CAPES), Pontificia Universidad Católica de Chile, Santiago, Chile, [3]Department of Biology, University of New Mexico, Albuquerque, NM, United States, [4]Instituto de Ciencias Ambientales y Evolutivas, Universidad Austral de Chile, Valdivia, Chile, [5]Millennium Institute for Integrative Biology (iBio), Santiago, Chile, [6]Laboratory of Ecotoxicology, University of Castilla-La Mancha, Toledo, Spain, [7]Departamento de Ciencias, Facultad de Artes Liberales, Universidad Adolfo Ibáñez, Santiago, Chile, [8]Department of Earth and Planetary Sciences, University of New Mexico, Albuquerque, NM, United States, [9]Department of Biological Sciences at Old Dominion University, Norfolk, VA, United States

Tracing how free-ranging organisms interact with their environment to maintain water balance is a difficult topic to study for logistical and methodological reasons. We use a novel combination of triple-oxygen stable isotope analyses of water extracted from plasma ($\delta^{16}O$, $\delta^{17}O$, $\delta^{18}O$) and bulk tissue carbon ($\delta^{13}C$) and nitrogen ($\delta^{15}N$) isotopes of feathers and blood to estimate the proportional contribution of marine resources, seawater, and metabolic water used by two species of unique songbirds (genus *Cinclodes*) to maintain their water balance in a seasonal coastal environment. We also assessed the physiological adjustments that these birds use to maintain their water balance. In agreement with previous work on these species, $\delta^{13}C$ and $\delta^{15}N$ data show that the coastal resident and invertivore *C. nigrofumosus* consumes a diet rich in marine resources, while the diet of migratory *C. oustaleti* shifts seasonally between marine (winter) to freshwater aquatic resources (summer). Triple-oxygen isotope analysis ($\Delta^{17}O$) of blood plasma, basal metabolic rate (BMR), and total evaporative water loss (TEWL) revealed that ~25% of the body water pool of both species originated from metabolic water, while the rest originated from a mix of seawater and fresh water. $\Delta^{17}O$ measurements suggest that the contribution of metabolic water tends to increase in summer in *C. nigrofumosus*, which is coupled with a significant increase in BMR and TEWL. The two species had similar BMR and TEWL during the austral winter when they occur sympatrically in coastal environments. We also found a positive and significant association between the use of marine resources as measured by $\delta^{13}C$ and $\delta^{15}N$ values and the estimated $\delta^{18}O$ values of ingested (pre-formed) water in both species, which indicates that Cinclodes do not directly drink seawater but rather passively ingest when consuming marine invertebrates. Finally, results obtained from physiological parameters and the isotope-based estimates of marine (food and water) resource use are consistent, supporting the use of the triple-oxygen isotopes to quantify the contribution of water sources to the total water balance of free-ranging birds.

KEYWORDS

birds, metabolic water, metabolic rates, stable isotopes, *Cinclodes*

Introduction

Bird species face both predictable and unpredictable changes in environmental conditions that impact food and water availability (Maddocks and Geiser, 2000; Landes et al., 2020). For example, an increase in ambient temperature and a decrease in the availability of freshwater affects several aspects of avian physiology including rates of energy expenditure, body mass, thermal tolerance, thermal conductance, and evaporative water loss, all of which are directly linked to a bird's ability to maintain their water balance (Carmi et al., 1993; Sabat et al., 2006a; Barceló et al., 2009; Sabat et al., 2009; Gerson and Guglielmo, 2011; Smith et al., 2017; McWhorter et al., 2018). Organisms living in seasonal environments can adjust their morphology and physiology to respond to predictable environmental changes, a phenomenon often referred to as acclimatization, a particular type of phenotypic plasticity. It is increasingly important to explore the adaptive mechanisms behind these adjustments and assess their impact on fitness because of unprecedented shifts in environmental conditions resulting from climate change, which will likely impact the amount and timing of resource availability, especially water (Şekercioğlu et al., 2012; Khaliq et al., 2014; Cooper et al., 2019; Whiteman et al., 2019; Huey and Buckley, 2022).

Deserts and other xeric habitats are among the most challenging environments for maintaining organismal water balance (Paces et al., 2021; Cabello-Vergel et al., 2022). Despite the crucial importance of water to survival, how animals deal with water scarcity has received less attention than the consequences of reduced food availability (McKechnie et al., 2016; Cooper et al., 2019; Gerson et al., 2019; Paces et al., 2021; Cabello-Vergel et al., 2022). An organism's water balance is a function of the interplay between (1) physical environment and water availability, (2) physiological and behavioral mechanisms for conserving water by reducing the total evaporative water loss (TEWL) and/or thermal conductance, and (3) the production of metabolic water (Bartholomew and Cade, 1963; MacMillen, 1990; Gerson and Guglielmo, 2011; Rutkowska et al., 2016; Albright et al., 2017). For example, some bird species respond to dehydrating conditions by increasing their rates of energy expenditure (e.g., basal metabolic rate, BMR), a response that is commonly assumed to be the cost of living in arid environments and/or regularly consuming salty water (Arad et al., 1987; Gutiérrez et al., 2011; Peña-Villalobos et al., 2013; Sabat et al., 2017). Such increases in metabolic rate could be a mechanism for water production, reducing the need for water conservation and the reliance on (pre-formed) drinking/food water (see Peña-Villalobos et al., 2013; Sabat et al., 2017). This hypothesis is supported by observations in captive rufous-collared sparrows (*Zonotrichia capensis*), in which mass loss and an increase in the mass-specific metabolic rates were associated with a higher contribution of metabolic water to the body water pool (Navarrete et al., 2021). No studies have examined this hypothesis in wild birds, and only a handful have quantified the contribution of metabolic water to the water budgets of free-ranging individuals (MacMillen, 1990; Williams and Tieleman, 2001; Giulivi and Ramsey, 2015).

Coastal deserts are especially intriguing habitats because they do not support large amounts of terrestrial productivity nor do they have significant sources of freshwater (Polis and Hurd, 1996), but can occur adjacent to very productive nearshore marine ecosystems (Fariña et al., 2008). Terrestrial animals can exploit abundant marine resources at the cost of having to deal with high salt loads (Mahoney and Jehl, 1985; Nyström and Pehrsson, 1988; Fariña et al., 2008). Salty foods can impose significant osmoregulatory challenges to songbirds (Order Passeriformes), which lack functional salt glands (Shoemaker, 1972) and have a reduced ability to concentrate urine (Goldstein and Skadhauge, 2000; Sabat, 2000). Worldwide, there are only a few passerine species (genus *Cinclodes*) capable of living in arid coastal deserts while consuming significant amounts of salty marine prey, and several of them are endemic to the central and northern coasts of Chile. Using stable isotope analyses and osmometry to study three species of *Cinclodes*, Sabat and del Río (2005) reported that the osmolality of stomach contents increased as the proportion of marine diet (assessed by stable isotope analysis) became more substantial. Typical salt concentrations in the body fluids of terrestrial and freshwater prey are 100–300 mOsm/kg (Beyenbach, 2016), whereas some coastal *Cinclodes* consume prey (e.g., mollusks and crustaceans) with salt concentrations of up to 800–1,100 mOsm/kg in their body fluids (Schmidt-Nielsen, 1997).

Here, we use multiple isotope tracers to explore seasonal variation in diet and water balance of two species of endemic, South American coastal passerines from the genus *Cinclodes* to investigate how seasonal variation in habitat use, ambient temperature, and marine resource use are related to how birds acquire (food/drinking versus metabolic) and conserve water (TEWL), expend energy (BMR), and dissipate heat (thermal conductance). *C. nigrofumosus* is year-round resident that forages on marine invertebrates in intertidal environments, while its sister species *C. oustaleti* also consumes invertebrates but migrates seasonally between dry coastal habitats and high elevation freshwater streams (Newsome et al., 2015; Rader et al., 2017; Tapia-Monsalve et al., 2018). We used carbon ($\delta^{13}C$) and nitrogen ($\delta^{15}N$) isotope analysis of feathers and blood collected during the summer and winter to characterize seasonal marine versus terrestrial resource use (Newsome et al., 2007; Martínez del Rio et al., 2009). We then used a novel methodological approach based on the measurements of the three stable isotopes of oxygen in blood plasma to measure the proportion of the body water pool that was derived from metabolic water (Whiteman et al., 2019; Passey and Levin, 2021; Sabat et al., 2021). This method utilizes natural differences in the oxygen isotope composition of preformed water versus atmospheric oxygen, which is the source of oxygen for the formation of metabolic water in the mitochondria (Whiteman et al., 2019). While several studies have focused on the physiological adjustments these species use to reduce water loss, none have identified seasonal shifts in the use of different source(s) of water (pre-formed versus metabolic) that is a critical to understanding water balance in free-ranging birds (Navarro et al., 2018; Smit et al., 2019).

We hypothesized that *C. nigrofumosus* and *C. oustaleti* used different strategies to maintain water balance due to variation in their ecological traits. We predicted that seasonal scarcity of freshwater and overall higher consumption of marine resources by *C. nigrofumosus* would result in higher osmoregulatory costs leading to elevated BMR and a corresponding increase in metabolic water production to maintain their

water balance during summer. We also expected that birds in summer would exhibit lower TEWL and higher thermal conductance to reduce water loss associated with evaporative cooling. In winter when the two species occur in sympatry along the coast, we predicted that migratory *C. oustaleti* would rely less on salty marine resources than *C. nigrofumosus* and instead consume more terrestrial invertebrates, which provide a source of less salty (food) water. By extension this would reduce the proportional contribution of metabolic water to their body water pool.

Methods

Sample collection

Wild *C. oustaleti* ($n = 11$) and *C. nigrofumosus* ($n = 9$) were collected at Bahia Mansa (32°14′22″S 71°30′54″W) on the central coast of Chile in the austral winter (June 2021) when these species occur in sympatry. We also collected seven individuals of *C. nigrofumosus* in summer (January 2022) at the same locality. This study site has a Mediterranean climate (mean annual precipitation = 396 mm) characterized by mild dry summers (mean monthly precipitation = 2 mm, T_{min} = 13°C; T_{max} = 19) and cold rainy winters (mean monthly precipitation = 85 mm; T_{min} = 7°C; T_{max} = 13) (di Castri and Hajek 1976). We observed no clear signs of reproduction (e.g., brood patch) or active molting in *C. nigrofumosus* captured during the summer. This species is not sexually dimorphic so we could not determine the sex of individuals we captured. We used mist nets and spring traps to capture birds, which were caged individually in the dark after capture to minimize stress. Biometric parameters, cloacal temperature (Tb), and blood samples were collected from each individual in the field. Blood samples were collected from the humeral vein using heparinized hematocrit capillaries. Blood was maintained in coolers (~4°C) for <2 h and then centrifuged at 10,000 rpm for 10 min to separate plasma from red blood cells. The plasma was then stored frozen until cryogenic distillation followed by oxygen isotope analysis. In addition, a subsample of whole blood was dried on two glass microscope slides and then transferred to microcentrifuge tubes and stored for $\delta^{13}C$ and $\delta^{15}N$ analysis.

Metabolic rates and total evaporative water loss

Immediately after capture, birds were transported to Algarrobo, Chile ~15 min from the capture site for captive physiological measurements. While in captivity, birds consumed mealworms and water, which were available *ad libitum*. We measured BMR (mL O_2 h^{-1}) and total evaporative water loss (TEWL) in post-absorptive (fasted for 4-h), resting birds, during their inactive period between 21:00 and 07:00 h using standard flow-through respirometry (Tapia-Monsalve et al., 2018). We removed mealworms from the cages ~4 h before BMR measurements started to ensure a post-absorptive state. Respirometry measurements for BMR were performed on up to three birds per night. Measurements were made at an ambient temperature (T_a) of 30.0 ± 0.5°C, which is within the thermoneutral zone (TNZ), using an infrared O_2-CO_2 analyzer equipped with a hygrometer (FMS, Sable Systems®). All trials were conducted in metallic metabolic chambers (volume 2,000 mL) that received air free of water and CO_2 removed *via* Drierite and CO_2 absorbent, respectively, at a flow of 800 mL/min (±1%). Inside these darkened metabolic chambers, birds perched on a wire-mesh grid that allowed excreta to fall into a tray containing mineral oil, thus trapping the water from this source. Oxygen consumption was calculated according to the equation (Lighton, 2008): $VO_2 = FR \times 60 \times (F_i O_2 - F_e O_2)/ (1 - F_i O_2)$, where FR is the flow rate in mL min^{-1}, and F_iO_2 and $F_e O_2$ are the fractional concentrations of inflow and outflow O_2 in the metabolic chamber, respectively. We calculated absolute humidity (kg/m^3) of air entering and leaving the chamber as $\rho = P/(T \times R_w)$, where P is water vapor pressure of the air in Pascal, T is the dewpoint temperature in Kelvin and R_w is the gas constant for water vapor (461.5 J/kg K, Lide, 2001). P was determined using the average value of the vapor pressure of the air entering the empty chamber during a baseline period of 15 min before and after each experiment with a dew-point hygrometer located in the FMS. TEWL was calculated as $TEWL = (V_e \times \rho_{out} - V_i \times \rho_{in})$, where TEWL is in mg/mL, ρ_{in} and ρ_{out} are the absolute humidity in kg/m^3 of the inlet air and the outlet air respectively, V_i is the flow rate of the air entering the chamber as given by the mass flow controller (800 mL min-1), and V_e is the flow of exiting air. V_e was calculated following as: $V_e = V_i - [VO_2 \times (1–RQ)] + V_{H2O}$. V_{in} and VO_2 (mL min-1) are known, and we assumed a respiratory quotient (RQ) of 0.71 (Sabat et al., 2006a,b). Output from the H_2O (kPa) analyzer, the oxygen analyzer (%), and the flow meter were digitalized using a Universal Interface II (Sable Systems, Nevada, United States) and recorded on a personal computer using EXPEDATA data acquisition software (Sable Systems, Nevada, United States). To estimate BMR and TEWL, we averaged O_2 concentrations and water vapor pressures of the excurrent air stream over a 20 min period after steady state was reached, which occurs after 3 h in *Cinclodes* (Sabat et al., 2021). We estimated the metabolic water production (MWP) using the equivalence of 0.567 mL H_2O per liter O_2 consumed (Schmidt-Nielsen, 1997) and calculated the ratio between metabolic water production and water losses (MWP/TEWL) for the 20 min period during which steady state was reached. The ratio MWP/TEWL is interpreted as the ability of birds to rely on metabolic water to maintain water balance.

To estimate wet thermal conductance (C_w), we also measured metabolic rates of birds at a T_a below the TNZ, on the day of capture, between 8:00 and 17:00 h, as described above for BMR. Because the "wet" thermal conductance is roughly constant in endotherms below thermoneutrality (Nicol and Andersen, 2007; Rezende and Bacigalupe, 2015; Andreasson et al., 2020), for simplicity and logistic restrictions we measured C_w at 15.0 ± 0.5°C. C_w was calculated as metabolic rate (MR_{15}) measured at 15°C using the equation MR/(Tb-Ta). In this case water and food was available for birds until they were placed in the metabolic chamber. Body mass was measured before the metabolic measurements using an electronic balance (± 0.1 g) and cloacal body temperature (Tb) was recorded with a thin Cole-Palmer copper-constantan thermocouple attached to a Digisense thermometer (Model 92,800–15) within a minute after the birds were removed from metabolic chamber to minimize the effect of manipulation on the temperature measurement (Nord and Folkow, 2019) We considered body temperatures of ≤36°C as hypothermic (Swanson et al., 2012) and all birds were normothermic at the end of 15°C or 30°C exposure trials. After each respirometry measurement, the birds were provided food and water *ad libitum* until their release.

$\Delta^{17}O$ analysis

To estimate the contribution of metabolic water to the body water, we used a method based on the measurement of $\Delta^{17}O$, which is the

positive or negative deviation from the tight correlation that naturally exists between values of $\delta^{17}O$ and $\delta^{18}O$ (Whiteman et al., 2019). The premise of this method is that metabolic water and drinking/food water together provide 80–99% of the body water of most animals (Bryant and Froelich, 1995; Kohn, 1996), with the remaining contribution (1–20%) resulting from condensation reactions that use bound oxygen from dietary nutrients. Here, we ignore this latter contribution and acknowledge that this induces uncertainty (Whiteman et al., 2019). Of the two other sources, metabolic water is assumed to have a $\Delta^{17}O$ value of −0.44‰ reflecting that of inhaled atmospheric oxygen (Whiteman et al., 2019; Wostbrock et al., 2020), and drinking/food water is assumed to have a $\Delta^{17}O$ value of meteoric water with a mean $\Delta^{17}O$ value of ~0.03‰ across a wide variety of potential sources (e.g., lakes, rivers, precipitation; Sharp et al., 2018). While extensive evaporation lowers the $\Delta^{17}O$ values of the remaining water (Aron et al., 2021), recent studies have suggested that in many biological applications assuming a fixed value of ~0.03‰ for meteoric water is reasonable (Whiteman et al., 2019; Sabat et al., 2021). Under this assumption, a linear mixing model can be used to calculate the proportional contribution from each source (Whiteman et al., 2019). For example, an animal body water sample with a $\Delta^{17}O$ value of −0.44‰ represents pure metabolic water and a sample with a $\Delta^{17}O$ value of 0.03‰ represents pure meteoric water. This mixing model is in the form: $\Delta^{17}O_{Body\ Water} = F_M \times (-0.44‰) + (1 - F_M) \times (0.030‰)$ where F_M represents the fractional contribution to body water from metabolic water, and (1 – Fm) represents the contribution from drinking/food water. In previous studies of captive sparrows (*Zonotrichia capensis*) and mice (*Peromyscus maniculatus*) this equation accurately predicted relative changes in $\Delta^{17}O$ based on metabolic rate and drinking water intake (Whiteman et al., 2019; Sabat et al., 2021).

We cryogenically distilled body water from blood plasma on a vacuum line. We fluorinated 1.5 µL of the distilled water with BrF5 at 450°C for 15 min under a vacuum to evolve O_2, which was purified *via* a 6 ft. × 1/8″ (1.83 m × 3.2 mm) 60/80 Mol Sieve 13X gas chromatograph (GC) column and analyzed *via* dual-inlet on a Thermo Scientific™ 253 Plus isotope ratio mass spectrometer (Sharp et al., 2018) against a working reference O_2 gas at the University of New Mexico Center for Stable Isotopes (UNM–CSI; Albuquerque). The measured values of $\delta^{17}O$ and $\delta^{18}O$ were linearized ($\delta'^{x}O = 1{,}000 \times \ln((\delta^{x}O/1000) + 1)$; x = ^{17}O or ^{18}O) and then used to calculate $\Delta'^{17}O$ ($\delta'^{17}O - (0.528 \times \delta'^{18}O)$; Whiteman et al., 2019). Deviations from the normal linear mass-dependent fractionation between $\delta'^{17}O$ and $\delta'^{18}O$ that is defined by an arbitrary reference line with a slope (λ) of 0.528, are expressed as $\Delta'^{17}O$. Samples were corrected using a one-point calibration based on intermittent measurements of an in-house standard (NM2) calibrated against VSMOW-2.

In addition to using $\Delta^{17}O$ values to understand reliance upon metabolic water, we used the combination of F_M values and $\delta^{18}O$ values of body water to calculate estimated $\delta^{18}O$ values of ingested pre-formed drinking/food water ($\delta^{18}O_{D+PF}$) with the equation $\delta^{18}O_{DFW} = (\delta^{18}O_{BW} - (F_M) \times (\delta^{18}O_{Air})) / (1\text{-}F_M)$ and assumed $\delta^{18}O_{Air}$ incorporated *via* respiration was 19.4‰ due to the fractionation that occurs during absorption of inhaled atmospheric oxygen. This fractionation depends on the efficiency of oxygen absorption (EO_2; Epstein and Zeiri, 1988). Although this efficiency was not measured in our study species, previous research suggests that an EO_2 of 0.4 is reasonable for small passerines (Clemens, 1988; Arens and Cooper, 2005), which in humans produces a fractionation of ~4.4‰ (Epstein and Zeiri, 1988). The estimated $\delta^{18}O$ of ingested water generally changes by <3‰ if you apply the plausible range of fractionation values for absorbed oxygen (2–6‰) to equation 3, which is smaller than much of the naturally-occurring variation in $\delta^{18}O$ of potential water and, therefore, unlikely to affect our conclusions

$\delta^{13}C$ and $\delta^{15}N$ analysis

We used $\delta^{13}C$ and $\delta^{15}N$ analysis to estimate the relative contribution of marine and terrestrial prey to the diet of *Cinclodes* species (Martínez del Rio et al., 2009). In general, baseline $\delta^{13}C$ and $\delta^{15}N$ values are higher in marine than terrestrial food webs (Martínez del Rio et al., 2009). For *C. nigrofumosus*, seasonal comparisons were made *via* analysis of whole blood collected in summer and winter, a tissue that integrates dietary resources assimilated during ~1–2 months prior to capture (Martínez del Rio et al., 2009). For *C. oustaleti*, seasonal comparisons were made by comparing the isotopic composition of two tissues: a primary feather (P1) reflecting dietary resources assimilated during the molting period that occurs during the austral summer in *Cinclodes* (Bertolero and Zavalaga, 2003), and blood representing the winter during which they were captured. We chose not to correct for tissue-specific discrimination between feathers and whole blood, which in a controlled experiment on passerine *Dendroica coronata* consuming a diet containing 97% insect were ~ 2.1‰ for $\delta^{13}C$ and *ca.* 0.8 ‰ for $\delta^{15}N$ (Pearson et al., 2003); these values are small in comparison to observed differences between potential marine and terrestrial food resources available at the study sites (Martínez del Rio et al., 2009).

Approximately 0.5–0.6 mg of dried whole blood or feather was weighed into tin capsules, and carbon ($\delta^{13}C$) and nitrogen ($\delta^{15}N$) isotope values were measured on a Costech 4,010 elemental analyzer coupled to a Thermo Scientific Delta V Plus isotope ratio mass spectrometer at UNM–CSI. Isotope values are reported using standard delta (δ) notation in parts per thousand or per mil (‰) as: $\delta X = (R_{sample}/R_{standard} - 1)$ where R_{sample} and $R_{standard}$ are the ratios of the heavy to light isotope of the sample (e.g., $^{15}N/^{14}N$) and the reference, respectively. The internationally accepted references are Vienna PeeDee Belemnite (VPDB) for $\delta^{13}C$ and atmospheric N_2 (AIR) for $\delta^{15}N$. Within-run precision (SD) for both $\delta^{13}C$ and $\delta^{15}N$ was estimated *via* analysis of three proteinaceous internal reference materials and measured to be ≤0.2‰ for both isotope systems.

Statistical analysis

Because body mass did not differ between seasons, after checking normality (Shapiro–Wilk) and homoscedasticity (Levene), we used a Student t-test to compare mean BMR, TEWL, MWP/TEWL, and thermal conductance between seasons. Because some isotopic data sets ($\delta^{15}N$) did not meet the assumptions of normality, we decided to use non-parametric test to compare data. A Mann–Whitney U-test was used to compare $\delta^{13}C$ and $\delta^{15}N$ values between seasons for the same tissue between species and a Wilcoxon W test to compare $\delta^{13}C$ and $\delta^{15}N$ values of feathers and blood collected from the same species to provide a seasonal comparison. To compare physiological data between species in winter we used ANCOVA with body mass as a covariate. We used a Pearson product–moment correlation matric to explore the relationship between and diet and body water $\Delta^{17}O$ using all dataset. JAMOVI software (Version 2.3., Jamovi project 2022) was used for all statistical analyses. Following Muff et al. (2021), in this paper we expressed statistical results in the language of evidence instead of the use of arbitrary value of p thresholds (e.g., $p = 0.05$). This approach translates approximate ranges of *p*-values into specific language, although the boundaries of such ranges should not be understood as hard thresholds: $p < 0.01$ as "strong evidence," $0.01 < p < 0.05$ as "moderate evidence," and $0.05 < p\ 0.10$ as "weak evidence"; for further details see Muff et al. (2021).

10.3389/fevo.2023.1120271

Results

Physiological capacities

For *C. nigrofumosus*, we found no evidence that m_b differed between seasons ($t_8 = -1.22$, $p = 0.243$; all results described here are presented in Table 1). We found strong evidence that its summer whole organism BMR was ~19% higher ($t_8 = -3.03$, $p = 0.009$), and moderate evidence that their TEWL was ~29% higher ($t_8 = -2.36$, $p = 0.034$), than winter. There was no evidence that estimated water balance at 30°C (MWP/TEWL) differed between seasons in *C. nigrofumosus* ($t_8 = 1.26$; $p = 0.230$), but wet thermal conductance increased ~18% in summer compared with winter in this species ($t_8 = -2.48$; $p = 0.026$). A linear regression of all data from both species collected in winter provided strong evidence that log BMR ($F_{1, 18} = 57.58$; $r^2 = 0.76$; $p = 0.001$) and log TEWL ($F_{1, 18} = 20.54$; $r^2 = 0.53$; $p < 0.001$) were positively correlated with log body mass. After removing the effect of body mass, there was no evidence of difference between species in whole-organismal BMR ($F_{1, 17} = 0.019$, $p = 0.89$) and TEWL ($F_{1, 17} = 1.53$, $p = 0.232$). The ratio MWP/TEWL was also similar between species ($t_8 = 0.022$; $p = 0.983$). Finally, there was strong evidence that C_w was ~46% higher in *C. nigrofumosus* than *C. oustaleti* ($t_8 = -7.08$, $p < 0.001$).

TABLE 1 Mean (±SD) physiological and biochemical variables measured in *C. nigrofumosus* captured in summer and winter and for *C. oustaleti* captured in winter.

	C. nigrofumosus		*C. oustaleti*
	Summer	*Winter*	*Winter*
n	7	9	11
Body mass (*g*)	73.67 ± 2.6	70.5 ± 6.3*	25.5 ± 1.8*
BMR (mL O_2 h^{-1})	179.6 ± 18.2[a]	145.3 ± 25.2[b]*	66.1 ± 21.2*
BMR (mL O2 h^{-1} g^{-1})	2.4 ± 0.2[a]	2.06 ± 0.3 [b]	2.6 ± 0.9
TEWL (mg H_2O h^{-1})	363.9 ± 72.3[a]	255.8 ± 102.9[b]*	113.9 ± 48.1*
TEWL (mg H_2O h^{-1} g^{-1})	5.0 ± 1.1[a]	3.7 ± 1.5[b]	4.5 ± 2.0
C_w (cal h $°C^{-1}$)	39.4 ± 6.3[a]	32.2 ± 5.3 [b]*	17.4 ± 4.0*
Tb (°C)	40.9 ± 0.3	41.3 ± 0.4	40.7 ± 0.4
MWP (mg H_2O h^{-1})	101.8 ± 10.3[a]	82.4 ± 14.3[b]*	37.5 ± 12.0*
MWP/TEWL	0.28 ± 0.07	0.32 ± 0.13	0.33 ± 0.12

Letters denote significant differences between seasons, and asterisks denote significant differences between species in winter.

Isotopic niches

There was no evidence of a difference between summer and winter $\delta^{13}C$ (Mann–Whitney U = 17, $p = 1.0$) and $\delta^{15}N$ ($U = 7.5$, $p = 0.12$) values of *C. nigrofumosus* (Table 2). In contrast, there was strong to moderate evidence that values of $\delta^{13}C$ and $\delta^{15}N$ differed between summer and winter in *C. oustaleti* as feather $\delta^{13}C$ values representing summer were 4‰ higher (Wilcoxon W = −28, $p = 0.015$) and $\delta^{15}N$ values were 13‰ higher ($W = -28$, $p = 0.05$) than isotope values for blood representing winter (Table 2). There was strong evidence that $d^{13}C$ and $d^{15}N$ values of feathers representing summer foraging differed between species (Mann–Whitney $U = 0.0$, $p < 0.001$; Table 2). There was no evidence that $\delta^{13}C$ values from blood collected in winter differed between species (Mann–Whitney $U = 11.0$, $p = 0.11$), and moderate evidence of a difference for $\delta^{15}N$ (U = 6, $p = 0.04$) (Table 2). There was no evidence that $\delta^{13}C$ values from blood collected in winter differed between species (Mann–Whitney U = 11.0, p = 0.11), and moderate evidence of a difference for $\delta^{15}N$ ($U = 6$, $p = 0.04$) (Table 2).

Metabolic and drinking/food water

There was little or no evidence that values of $\Delta^{17}O$ differed between summer and winter for *C. nigrofumosus* ($t_7 = -1.76$, $p = 0.122$, Figure 1). Using equation 2, this difference would translate to seasonal contributions from metabolic water to body water (Fm) of 24.8% in summer versus 20.7% in winter. There was no evidence that values of $\Delta^{17}O$ (and hence Fm) differed between species in winter ($t_{12} = 0.652$, $p = 0.527$) (Figure 1). There was also no evidence that the mean $\delta^{18}O$ values of plasma differed between winter and summer for *C. nigrofumosus* (−1.4 ± 0.7‰ and −1.6 ± 0.5‰ respectively; $t_7 = 0.277$, $p = 0.790$), or between *C. oustaleti* (−3.5 ± 1.1‰) and *C. nigrofumosus* (using pooled data from summer and winter: −1.5 ± 1.3‰; $t_{17} = 1.57$, $p = 0.135$). The mean estimated $\delta^{18}O$ value of the combined drinking/food water ingested by *C. nigrofumosus* did not differ between seasons (winter −6.5 ± 2.4‰, summer −8.1 ± 0.8‰; $t_7 = 1.41$, $p = 0.203$). However, we found moderate evidence that the drinking/food water ingested by *C. oustaleti* ($\delta^{18}O = -9.7 \pm 2.6$‰) was more negative than for *C. nigrofumosus* in winter (−6.5 ± 2.4‰, $t_{12} = 2.18$, $p = 0.05$) (Figure 2).

Using the whole dataset (i.e., both species and seasons), there was moderate evidence that the estimated isotopic value of drinking water

TABLE 2 Mean (±SD) $\delta^{13}C$ and $\delta^{15}N$ values of *C. nigrofumosus* and *C. oustaleti* tissues collected from a coastal locality from central Chile.

	C. nigrofumosus			*C. oustaleti*	
Tissue	Feathers	Blood		Feathers	Blood
Season	Summer (12)	Winter (5)	Summer (7)	Summer (11)	Winter (8)
$\delta^{13}C$	−13.3 ± 0.6[a]	−15.0 ± 1.5	−15.0 ± 0.8	−20.1 ± 0.7*[,b]	−16.2 ± 0.6
$\delta^{15}N$	19.1 ± 1.3[a]	17.2 ± 0.5[a]	17.8 ± 1.0	3.2 ± 0.7*[b]	16.2 ± 0.4[b]

Season (winter or summer) denotes the period of the annual life cycle reflected in each tissue. For migratory *C. oustaleti*, the isotopic composition of feathers represents dietary inputs during the (previous) summer when they forage in streams at high elevations, while blood integrates dietary information during the season of collection (winter). For resident *C. nigrofumosus*, seasonal variation in diet was assessed by comparing the isotopic composition of blood collected in winter and summer; data for feathers is shown for comparison to *C. oustaleti*. Asterisks denote differences between seasons for each tissue within species, and different letters denote differences between species for the specific season and tissue.

10.3389/fevo.2023.1120271

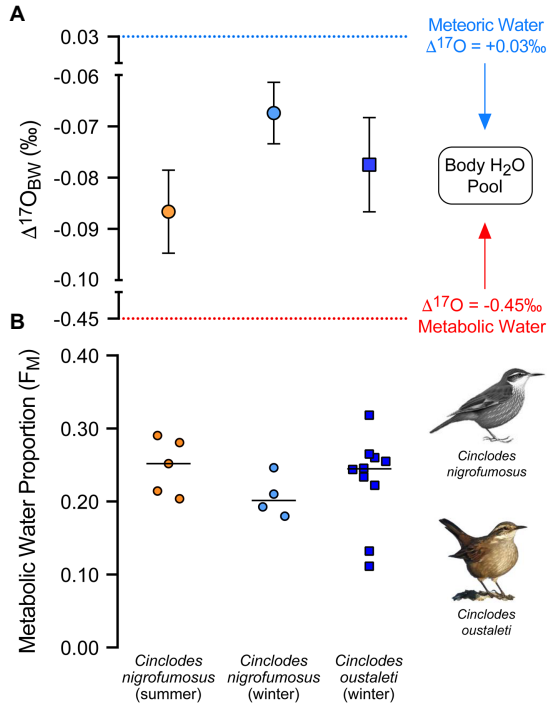

FIGURE 1
(A) Mean (±SE) $\Delta'^{17}O$ values of body water cryogenically distilled from blood plasma and **(B)** the estimated proportion of metabolic water to the total body water pool in two species of *Cinclodes* inhabiting a coastal environment in central Chile.

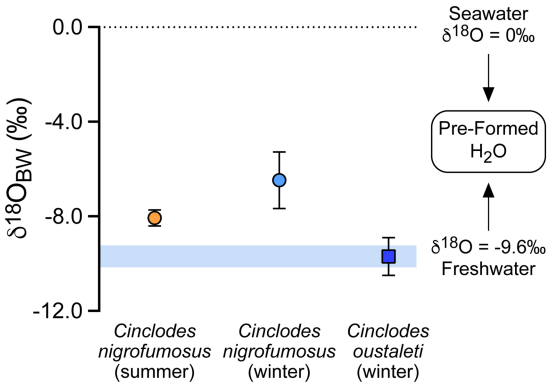

FIGURE 2
Estimated $\delta^{18}O$ values (mean±SE) of ingested pre-formed (drinking/food) water in two species of *Cinclodes* inhabiting a coastal environment in central Chile.

($\delta^{18}O_{DW}$) was different between species ($t_{17} = 2.18$, $p = 0.03$) and that $d^{18}O_{DW}$ was positively correlated with the $\delta^{13}C$ and $\delta^{15}N$ values of tissues (Supplementary Table S1 for statistical details). When data were analyzed separately for each species, there was moderate evidence that $\delta^{18}O_{DW}$ was positively correlated with blood $\delta^{15}N$ in *C. oustaleti* ($r^2 = 0.714$, $p = 0.034$) but no evidence of a relationship in *C. nigrofumosus* ($r^2 = 0.018$ $p = 0.7330$) (Figure 3). There was no evidence of a relationship between F_M and $\delta^{15}N$ in either species ($r^2 = 0.439$, $p = 0.15$ and $r^2 = 0.02$, $p = 0.73$ for *C. oustaleti* and *C. nigrofumosus* respectively). Finally, when we analyzed the whole dataset we found very strong evidence that $\Delta^{17}O$ correlated positively with $\delta^{18}O$ values of plasma ($r^2 = 0.54$, $p < 0.001$)."

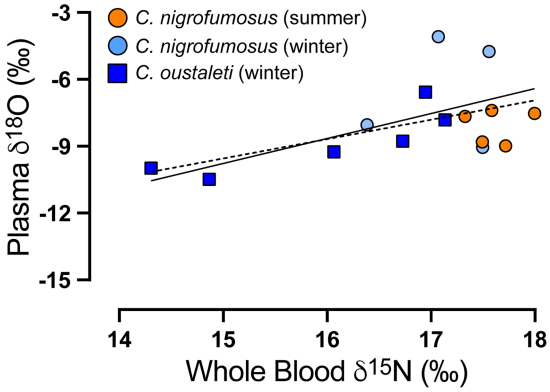

FIGURE 3
Positive and significant linear correlation between blood $\delta^{15}N$ values and the estimated $\delta^{18}O$ of ingested water based on $\Delta^{17}O$ for two species of *Cinclodes* inhabiting a coastal environment in central Chile. The dotted line represents the relationship for data pooled across both species, while the solid line represents the relationship for only *C. oustaleti*.

Discussion

The main objective of our study was to evaluate the integrated effect of seasonal variation on selected physiological and ecological traits of passerine birds living in a dry coastal environment. We explored whether the interaction between a suite of physiological variables––thermoregulation, osmoregulation, and water balance—varies seasonally in two closely related passerine species that differ in their consumption of marine versus terrestrial resources. Our results suggest that *C. nigrofumosus* and *C. oustaleti* vary in their reliance on marine resources (Table 1): $\delta^{13}C$ and $\delta^{15}N$ values of blood and feathers confirmed the coastal resident *C. nigrofumosus* consumes a diet rich in marine invertebrates, while the diet of migratory *C. oustaleti* shifts seasonally between marine (winter) and freshwater/terrestrial (summer) resources indicative of their migration from wintering in marine intertidal habitats to stream habitats at high elevations during the summer in central Chile (Martínez del Rio et al., 2009; Newsome et al., 2015; Tapia-Monsalve et al., 2018). Triple oxygen isotope analysis of blood plasma revealed that a similar proportion of the body water pool of both species originated from metabolic water, and the contribution of metabolic water tended to increase in summer in *C. nigrofumosus* in concert with increases in BMR and decreases in TEWL and C_w. In the following sections, we explore the causes and consequences of the seasonal variation in physiological variables and the contribution of different water sources to the total water balance of each species.

Physiological parameters linked to energy and water budget

In passerines, the intake of moderately salty water (~400 mOsm/kg NaCl) tends to increase urine osmolality and BMR (Peña-Villalobos et al., 2014; Sabat et al., 2017). The observed seasonal increase in BMR of *C. nigrofumosus*, however, does not appear to be associated with an increased osmotic challenge as $\delta^{13}C$ and $\delta^{15}N$ data show this species consumed a high but similar proportion of marine resources between seasons. Previous studies suggest that the osmoregulatory physiology of *Cinclodes* is influenced by both ecological (diet composition) and

environmental (climate) factors in a complex fashion (Sabat and del Río, 2005; Sabat et al., 2006a,b). For example, isotopic data for *C. nigrofumosus* from another locality in central Chile (Los Molles, 32°14'22'S 71°30'54'W) suggested a greater consumption of marine resources and an increase in plasma concentration during winter compared to summer; however, urine was more concentrated in the (hot and dry) summer than in the (cold and rainy) winter (Sabat and del Río, 2005). This pattern suggests that the effect of salt intake on osmoregulatory physiology in *C. nigrofumosus* depends on environmental temperature and availability of meteoric water. Furthermore, the mechanistic link between salt intake, energy expenditure, and the role of metabolic water in maintaining water balance is an intriguing topic that requires further attention.

Several studies have investigated seasonal changes in BMR and other measures of metabolic rate (e.g., RMR or FMR) in response to environment temperature, but results have revealed a noticeable difference in the magnitude of the response to thermal (i.e., seasonal) acclimatization (Arens and Cooper, 2005; Cavieres and Sabat, 2008; Noakes and McKechnie, 2020; Swanson et al., 2020) and the mechanisms for the global pattern of BMR acclimatization is poorly understood. It is generally believed that BMR in free-ranging birds is primarily driven by temperature, although it is possible that other abiotic and biotic factors such as photoperiod, reproduction, and body condition may be important (Daan et al., 1990; Chastel et al., 2003; Vézina and Williams, 2003; Zheng et al., 2008; McNab, 2009; Vezina and Salvante, 2010). Our results reveal considerable flexibility in the thermal physiology of *C. nigrofumosus*, as we found a ~ 20% decrease in BMR and thermal conductance and a ~ 30% decrease in TEWL in winter relative to summer, but no seasonal change in body mass. Reduced thermal conductance may enable a seasonal decline in BMR because heat is more effectively retained in winter (Speakman and Król, 2010; Rezende and Bacigalupe, 2015; Nord and Nilsson, 2019). This combination of trends suggests that the intake/storage of dietary energy and loss of heat to the environment were reduced in concert (Novoa et al., 1994; Cooper et al., 2019). Under such a scenario, the contribution of metabolic water to the body water pool would decrease. Our results contrast with the typical acclimatization response of birds from higher latitudes (McKechnie et al., 2015; Noakes and McKechnie, 2020; Swanson et al., 2022) and supports the idea that changes in BMR is not related to enhancing cold tolerance in areas where birds face milder winter minimum temperatures and more modest thermoregulatory demands.

Reproduction may also influence BMR and TEWL because behaviors such as nest building, courtship/mating, and parental care in addition to synthesizing eggs are costly and influence energy budgets (Wiersma et al., 2004; Mainwaring and Hartley, 2013; Williams, 2018). The influence of reproduction on resting rates of energy expenditure (including BMR) in free-ranging birds, however, is controversial (Nilsson, 2002; Chastel et al., 2003; Welcker et al., 2015). While seasonal increases in BMR can be explained by reproductive demands, such changes in metabolic activity may also be an adaptive response to increase metabolic water production (MacMillen, 1990; Navarrete et al., 2021). This hypothesis is consistent with results of both field- and lab-based studies that report increases in mass-specific BMR in free-ranging desert birds during the summer (Smit and McKechnie, 2010; McKechnie et al., 2015) and in captive sparrows (*Z. capensis*) who responded to water restriction by losing mass and increasing their mass-specific BMR. This hypothesis is also supported by the trend reported here showing a seasonal increase in the contribution of metabolic water to the body water pool of *C. nigrofumosus* in summer (see below). Overall, it is important to note that whole-organism metabolic rate can be affected by essentially any change in morphology or physiology, so changes in traits such as BMR can be consistent with multiple, non-exclusive mechanistic explanations.

Triple oxygen analysis: Water budget and water sources

$\Delta^{17}O$ results suggest that the contribution of metabolic water to the total water budget in *C. nigrofumosus* was slightly higher in summer (~25%) than in winter (~21%), in agreement with expectations based on differences in BMR between seasons. Both estimates are slightly lower to previously reported ^{17}O-based estimates for *C. nigrofumosus* (~28%) sampled from another locality ~200 km to the north of our field site (Sabat et al., 2021). For *C. oustaleti*, estimates of the metabolic water contribution (23%) were nearly identical to those reported for this species from the more northern locality (Sabat et al., 2021). Overall, these ^{17}O-based estimates for the importance of metabolic water in *Cinclodes* in the field agree with those based on (1) respirometry under controlled conditions in the lab, where MWP/TEWL ratios vary from 28 to 33% (Table 2), and (2) doubly-labeled water (DLW) administered to free-ranging zebra finches (*Taeniopygia guttata*), an arid-adapted passerine (Cooper et al., 2019).

Given the importance of marine resources for both species in the winter, estimated $\delta^{18}O$ values of preformed (drinking/food) water was expected to be close to that of seawater (0‰); however, mean (±SD) values were lower and significantly differed between *C. oustaleti* (−9.7 ± 2.6‰) and *C. nigrofumosus* (−6.5 ± 2.4‰). The mean $\delta^{18}O$ value for *C. oustaleti* is nearly identical to that measured in local meteoric and tap waters (−9.7 ± 0.5‰, $n = 3$). Acknowledging that the end-member $\delta^{18}O$ value for local meteoric waters is poorly constrained at present, a two-source mixing model shows that seawater contributes ~0–45% and ~ 24–66% of the total water ingested by *C. oustaleti* and *C. nigrofumosus*, respectively. These estimates differ from those obtained from a limited number of *C. oustaleti* ($n = 3$) and *C. nigrofumosus* ($n = 3$) individuals sampled at a more arid locality 200 km to the north of our study site, where ~48–100% of ingested water was sourced from seawater (Sabat et al., 2021). This difference could reflect lower terrestrial primary productivity at the more northern location, where higher consumption of marine prey would result in increased intake of seawater (Sabat et al., 2006b). Lastly, the positive correlation reported here between tissue $\delta^{15}N$ and $\delta^{18}O$ of the blood plasma (Figure 3; Supplementary Table S1) supports the hypothesis that *Cinclodes* do not directly drink seawater, but passively ingest it when consuming intertidal invertebrates (Sabat et al., 2021). Future studies that evaluate the importance of seawater in *Cinclodes* along a latitudinal gradient in aridity are crucial to establish the relative importance of ecological (resource use) and environmental (temperature and/or humidity) factors that influence water balance in this unique group of passerines.

A recent meta-analysis of field metabolic rate (FMR) and field water flux (FWF) collected from a diverse set of birds reported that seabirds had a higher FMR than terrestrial species, and granivores had a lower FMR than other functional groups (Song and Beissinger, 2020). Similarly, seabirds and terrestrial birds inhabiting regions with higher rainfall had higher FWF. Because the proportion of metabolic water in the total body water pool is dependent on both metabolic rate and water intake, both variables must be considered to understand water balance. Using data for species with both FMR and FWF data ($n = 59$) and assuming 0.567 mL of metabolic water is produced per liter O_2 consumed (Sabat et al., 2021), the average proportion of metabolic water to the body water pool for terrestrial birds and seabirds is 22 and 16%, respectively. The estimated

proportion of the total water pool derived from metabolic water for *Cinclodes* (~21–25%) is slightly higher than terrestrial birds and in the upper range for seabirds. These results suggest that *Cinclodes* is more dependent on metabolic water than other terrestrial birds but cannot solely rely on seawater to maintain water balance, which likely is the result of limitations imposed by renal function. The maximum concentrating capacity of *Cinclodes* urine rarely exceeds 100 mOsm/kg, which is the concentration of seawater (Sabat et al., 2004), while seabird salt gland secretions can be more than twice this concentration (Sabat, 2000). Finally, it is important to note that the DLW-based estimates of FMR and FWF for free-ranging birds are typically lower than those for captive birds studied in the laboratory under controlled conditions (Bartholomew and Cade, 1963; MacMillen, 1990). Overall, the 17O-based method agrees with more direct methods using DLW (field) or respirometry (lab), which confirms the usefulness of using triple oxygen isotope measurements to estimate the water balance in the field.

Potential caveats

Although our $\Delta^{17}O$-based estimates of the contribution of metabolic water to the total body water pool of *Cinclodes* are consistent with patterns in other physiological measurements (BMR, TEWL) and previous studies using other methods (DLW), it is important to recognize that Equation 2 is a simplification and includes assumptions that have not yet been fully explored. While meteoric waters collected in a wide variety of environmental contexts have a mean $\Delta^{17}O$ (±SD) value of 0.03 ± 0.02‰ (Sharp et al., 2018), a more comprehensive understanding of how $\Delta^{17}O$ values of drinking and food water available to animals in different environmental contexts is needed to refine this approach in field-based studies of water balance. For instance, extensive evaporation reduces the $\Delta'^{17}O$ values of the residual water (Aron et al., 2021; Passey and Levin, 2021), a process that could impact meteoric waters or organism body water *via* evaporative water loss in animals living in arid environments. The possibility of fractionation effects on $\Delta^{17}O$ could be captured in a flux-based model, rather than the mixing-model approach described by Equation 2. Future studies should consider these complexities and build on the nascent applications of this method (Pack et al., 2013; Whiteman et al., 2019; Sabat et al., 2021).

Conclusion

Our study revealed that the seasonal acclimatization response of *C. nigrofumosus* is not the typical response of birds from more mesic environments at higher latitudes. The higher BMR observed in summer could be associated with a higher intake of marine prey/seawater or with the energetic costs of reproduction, which may lead to an increase in the contribution of metabolic water to the body water pool. Triple oxygen isotope analysis suggests that the contribution of metabolic water is ~23% of the total water budget in both *Cinclodes* species, with a slight increase in summer relative to winter for *C. nigrofumosus*, concomitant with the observed seasonal increase in BMR. These results agree with more direct methods for estimating the proportional contribution of metabolic water to the body water pool based on DLW, confirming the usefulness of $\Delta^{17}O$ to examine the water balance of free-ranging birds. Finally, water use strategies also differed between species with seawater contributing 24–66% and 0–45% of the pre-formed water ingested by *C. nigrofumosus* and *C. oustaleti* respectively, highlighting the importance of seawater in maintaining water balance in this unique group of passerines.

Data availability statement

The raw data supporting the conclusions of this article will be made available by the authors, without undue reservation.

Ethics statement

The animal study was reviewed and approved by the animal study was reviewed and all protocols were approved by the institutional Animal Care Committee of the University of Chile (CICUA), and National Research and Development Agency (ANID).

Author contributions

PS, SN, and JW: designed research. LN, NL, FA, and PS: performed research. LN and PS: analyzed data. PS, SN, RN, JS-H, KM, ZS, NL, and JW: wrote the paper. All co-authors edited the paper. All authors contributed to the article and approved the submitted version.

Funding

This work was funded by ANID PIA/BASAL FB0002, ANID/CONICYT FONDECYT Regular Nº 1200386, and National Science Foundation grants to SN (IOS-1941903) and JW (IOS-1941853).

Acknowledgments

We thank to Andrés Sazo and its invaluable fieldwork assistance.

Conflict of interest

The authors declare that the research was conducted in the absence of any commercial or financial relationships that could be construed as a potential conflict of interest.

Publisher's note

Supplementary material

The Supplementary material for this article can be found online at: https://www.frontiersin.org/articles/10.3389/fevo.2023.1120271/full#supplementary-material

References

Albright, T. P., Mutiibwa, D., Gerson, A. R., Smith, E. K., Talbot, W. A., O'Neill, J. J., et al. (2017). Mapping evaporative water loss in desert passerines reveals an expanding threat of lethal dehydration. *Proc. Natl. Acad. Sci. U. S. A.* 114, 2283–2288. doi: 10.1073/pnas.1613625114

Andreasson, F., Nord, A., and Nilsson, J. Å. (2020). Age differences in night-time metabolic rate and body temperature in a small passerine. *J. Comp. Physiol. B* 190, 349–359. doi: 10.1007/s00360-020-01266-5

Arad, Z., Gavrieli-Levin, I., Eylath, U., and Marder, J. (1987). Effect of dehydration on cutaneous water evaporation in heat-exposed pigeons (Columba livia). *Physiol. Zool.* 60, 623–630. doi: 10.1086/physzool.60.6.30159978

Arens, J. R., and Cooper, S. J. (2005). Metabolic and ventilatory acclimatization to cold stress in house sparrows (Passer domesticus). *Physiol. Biochem. Zool.* 78, 579–589. doi: 10.1086/430235

Aron, P. G., Levin, N. E., Beverly, E. J., Huth, T. E., Passey, B. H., Pelletier, E. M., et al. (2021). Triple oxygen isotopes in the water cycle. *Chem. Geol.* 565:120026. doi: 10.1016/j.chemgeo.2020.120026

Barceló, G., Salinas, J., Cavieres, G., Canals, M., and Sabat, P. (2009). Thermal history can affect the short-term thermal acclimation of basal metabolic rate in the passerine Zonotrichia capensis. *J. Therm. Biol.* 34, 415–419. doi: 10.1016/j.jtherbio.2009.06.008

Bartholomew, G. A., and Cade, T. J. (1963). The water economy of land birds. *Auk* 80, 504–539. doi: 10.2307/4082856

Bertolero, A., and Zavalaga, C. (2003). Observaciones sobre la biometría y la muda del Churrete Marisquero (Cinclodes taczanowskii) en Punta San Juan, costa sur del Perú. *Ornitol. Neotrop.* 14, 469–475.

Beyenbach, K. W. (2016). The plasticity of extracellular fluid homeostasis in insects. *J. Exp. Biol.* 219, 2596–2607. doi: 10.1242/jeb.129650

Bryant, D. J., and Froelich, P. N. (1995). A model of oxygen isotope fractionation in body water of large mammals. *Geochim. Cosmochim. Acta* 59, 4523–4537. doi: 10.1016/0016-7037(95)00250-4

Cabello-Vergel, J., González-Medina, E., Parejo, M., Abad-Gómez, J. M., Playà-Montmany, N., Patón, D., et al. (2022). Heat tolerance limits of Mediterranean songbirds and their current and future vulnerabilities to temperature extremes. *J. Exp. Biol.* 225:jeb244848. doi: 10.1242/jeb.244848

Carmi, N., Pinshow, B., Horowitz, M., and Bernstein, M. H. (1993). Birds conserve plasma volume during thermal and flight-incurred dehydration. *Physiol. Zool.* 66, 829–846. doi: 10.1086/physzool.66.5.30163826

Cavieres, G., and Sabat, P. (2008). Geographic variation in the response to thermal acclimation in rufous-collared sparrows: are physiological flexibility and environmental heterogeneity correlated? *Funct. Ecol.* 22, 509–515. doi: 10.1111/j.1365-2435.2008.01382.x

Chastel, O., Lacroix, A., and Kersten, M. (2003). Pre-breeding energy requirements: thyroid hormone, metabolism and the timing of reproduction in house sparrows *Passer domesticus*. *J. Avian Biol.* 34, 298–306. doi: 10.1034/j.1600-048X.2003.02528.x

Clemens, D. T. (1988). Ventilation and oxygen consumption in rosy finches and house finches at sea level and high altitude. *J. Comp. Physiol. B* 158, 57–66. doi: 10.1007/BF00692729

Cooper, C. E., Withers, P. C., Hurley, L. L., and Griffith, S. C. (2019). The field metabolic rate, water turnover, and feeding and drinking behavior of a small Avian Desert Granivore during a summer heatwave. *Front. Physiol.* 10:1405. doi: 10.3389/fphys.2019.01405

Daan, S., Masman, D., and Groenewold, A. (1990). Avian basal metabolic rates: their association with body composition and energy expenditure in nature. *Am. J. Physiol. Regul. Integr. Comp. Physiol.* 259, R333–R340. doi: 10.1152/ajpregu.1990.259.2.R333

Di Castri, F., and Hajek, E. (1976). *Bioclimatología de Chile*. (Santiago, Chile: Universidad Católica de Chile.

Epstein, S., and Zeiri, L. (1988). Oxygen and carbon isotopic compositions of gases respired by humans. *Proc. Natl. Acad. Sci.* 85, 1727–1731. doi: 10.1073/pnas.85.6.1727

Fariña, J. M., Palma, A. T., and Ojeda, F. P. (2008). "Subtidal kelp associated communities off the temperate Chilean coast" in *Food Webs Trophic Dynamics of Marine Benthic Ecosystems*, eds. G. M. Branch and T. R. McClanahan (New York, USA: Oxford University Press),79–102.

Gerson, A. R., and Guglielmo, C. G. (2011). House sparrows (Passer domesticus) increase protein catabolism in response to water restriction. *Am. J. Physiol. Regul. Integr. Comp. Physiol.* 300, R925–R930. doi: 10.1152/ajpregu.00701.2010

Gerson, A. R., McKechnie, A. E., Smit, B., Whitfield, M. C., Smith, E. K., and Talbot, W. A. (2019). The functional significance of facultative hyperthermia varies with body size and phylogeny in birds. *Funct. Ecol.* 33, 597–607. doi: 10.1111/1365-2435.13274

Giulivi, C., and Ramsey, J. (2015). On fuel choice and water balance during migratory bird flights. *Int. Biol. Rev.* 2015:58. doi: 10.18103/ibr.v0i1.58

Goldstein, D. L., and Skadhauge, E. (2000). "Renal and Extrarenal regulation of body fluid composition" in *Sturkie's Avian Physiology* ed. G. C. Whittow (Amsterdam: Elsevier), 265–297.

Gutiérrez, J. S., Masero, J. A., Abad-Gómez, J. M., Villegas, A., and Sánchez-Guzmán, J. M. (2011). Understanding the energetic costs of living in saline environments: effects of salinity on basal metabolic rate, body mass and daily energy consumption of a long-distance migratory shorebird. *J. Exp. Biol.* 214, 829–835. doi: 10.1242/jeb.048223

Huey, R. B., and Buckley, L. B. (2022). Designing a seasonal acclimation study presents challenges and opportunities. *Integr. Organ. Biol.* 4:obac016. doi: 10.1093/iob/obac016

Khaliq, I., Hof, C., Prinzinger, R., Böhning-Gaese, K., and Pfenninger, M. (2014). Global variation in thermal tolerances and vulnerability of endotherms to climate change. *Proc. Royal Soc. B: Biol. Sci.* 281:20141097. doi: 10.1098/rspb.2014.1097

Kohn, M. J. (1996). Predicting animal $\delta^{18}O$: accounting for diet and physiological adaptation. *Geochim. Cosmochim. Acta* 60, 4811–4829. doi: 10.1016/S0016-7037(96)00240-2

Landes, J., Pavard, S., Henry, P. Y., and Terrien, J. (2020). Flexibility is costly: hidden physiological damage from seasonal phenotypic transitions in heterothermic species. *Front. Phys.* 11:985. doi: 10.3389/fphys.2020.00985

Lide, D. R. (2001). *CRC Handbook of Chemistry and Physics*. Boca Raton: CRC press.

Lighton, J. R. B. (2008). Measuring Metabolic Rates: A Manual for Scientists. New York, NY: Oxford University Press.

MacMillen, R. E. (1990). Water economy of Granivorous birds: a predictive model. *Condor* 92:379. doi: 10.2307/1368235

Maddocks, T. A., and Geiser, F. (2000). Seasonal variations in thermal energetics of Australian silvereyes (Zosterops lateralis). *J. Zool.* 252, 327–333. doi: 10.1111/j.1469-7998.2000.tb00627.x

Mahoney, S. A., and Jehl, J. R. (1985). Adaptations of migratory shorebirds to highly saline and alkaline lakes: Wilson's phalarope and American avocet. *Condor* 87, 520–527. doi: 10.2307/1367950

Mainwaring, M. C., and Hartley, I. R. (2013). The energetic costs of nest building in birds. *Avian Biol. Res.* 6, 12–17. doi: 10.3184/175815512X13528994072997

Martínez del Rio, C., Sabat, P., Anderson-Sprecher, R., and Gonzalez, S. P. (2009). Dietary and isotopic specialization: the isotopic niche of three Cinclodes ovenbirds. *Oecologia* 161, 149–159. doi: 10.1007/s00442-009-1357-2

McKechnie, A. E., Noakes, M. J., and Smit, B. (2015). Global patterns of seasonal acclimatization in avian resting metabolic rates. *J. Ornithol.* 156, 367–376. doi: 10.1007/s10336-015-1186-5

McKechnie, A. E., Whitfield, M. C., Smit, B., Gerson, A. R., Smith, E. K., Talbot, W. A., et al. (2016). Avian thermoregulation in the heat: efficient evaporative cooling allows for extreme heat tolerance in four southern hemisphere columbids. *J. Exp. Biol.* 219, 2145–2155. doi: 10.1242/jeb.138776

McNab, B. K. (2009). Ecological factors affect the level and scaling of avian BMR. *Comp. Biochem. Physiol. Part A: Mol. Integr. Physiol.* 152, 22–45. doi: 10.1016/j.cbpa.2008.08.021

McWhorter, T. J., Gerson, A. R., Talbot, W. A., Smith, E. K., McKechnie, A. E., and Wolf, B. O. (2018). Avian thermoregulation in the heat: evaporative cooling capacity and thermal tolerance in two Australian parrots. *J. Exp. Biol.* 221:jeb168930. doi: 10.1242/jeb.168930

Muff, S., Nilsen, E. B., O'Hara, R. B., and Nater, C. R. (2021). Rewriting results sections in the language of evidence. *Trends Ecol. Evol.* 37, 203–210. doi: 10.1016/j.tree.2021.10.009

Navarrete, L., Bozinovic, F., Peña-Villalobos, I., Contreras-Ramos, C., Sanchez-Hernandez, J. C., Newsome, S. D., et al. (2021). Integrative physiological responses to acute dehydration in the rufous-collared sparrow: metabolic, enzymatic, and oxidative traits. *Front. Ecol. Evol.* 9:767280. doi: 10.3389/fevo.2021.767280

Navarro, R. A., Meijer, H. A. J., Underhill, L. G., and Mullers, R. H. E. (2018). Extreme water efficiency of cape gannet Morus capensis chicks as an adaptation to water scarcity and heat stress in the breeding colony. *Mar. Freshw. Behav. Physiol.* 51, 30–43. doi: 10.1080/10236244.2018.1442176

Newsome, S. D., Martínez del Rio, C., Bearhop, S., and Phillips, D. L. (2007). A niche for isotopic ecology. *Front. Ecol. Environ.* 5, 429–436. doi: 10.1890/1540-9295(2007)5[429:ANFIE]2.0.CO;2

Newsome, S. D., Sabat, P., Wolf, N., Rader, J. A., Del Rio, C. M., and Peters, D. P. C. (2015). Multi-tissue δ^2H analysis reveals altitudinal migration and tissue-specific discrimination patterns in Cinclodes. *Ecosphre.* 6:art213. doi: 10.1890/ES15-00086.1

Nicol, S. C., and Andersen, N. A. (2007). Cooling rates and body temperature regulation of hibernating echidnas *(Tachyglossus aculeatus)*. *J. Exp. Biol.* 210, 586–592. doi: 10.1242/jeb.02701

Nilsson, J. Å. (2002). Metabolic consequences of hard work. *Proc. R. Soc. Lond. B Biol. Sci.* 269, 1735–1739. doi: 10.1098/rspb.2002.2071

Noakes, M. J., and McKechnie, A. E. (2020). Phenotypic flexibility of metabolic rate and evaporative water loss does not vary across a climatic gradient in an Afrotropical passerine bird. *J. Exp. Biol.* 223:jeb220137. doi: 10.1242/jeb.220137

Nord, A., and Folkow, L. P. (2019). Ambient temperature effects on stress-induced hyperthermia in Svalbard ptarmigan. *Biol. Open* 8:bio043497. doi: 10.1242/bio.043497

Nord, A., and Nilsson, J. Å. (2019). Heat dissipation rate constrains reproductive investment in a wild bird. *Funct. Ecol.* 33, 250–259. doi: 10.1111/1365-2435.13243

Novoa, F. F., Bozinovic, F., and Rosenmann, M. (1994). Seasonal changes of thermal conductance in Zonotrichia capensis (Emberizidae), from Central Chile: the role of plumage. *Comp. Biochem. Physiol. Part A: Mol. Integr. Physiol.* 107, 297–300. doi: 10.1016/0300-9629(94)90384-0

Nyström, K. K., and Pehrsson, O. (1988). Salinity as a constraint affecting food and habitat choice of mussel-feeding diving ducks. *Ibis* 130, 94–110. doi: 10.1111/j.1474-919X.1988.tb00960.x

Paces, B., Waringer, B. M., Domer, A., Burns, D., Zvik, Y., Wojciechowski, M. S., et al. (2021). Evaporative water loss and stopover behavior in three passerine bird species during autumn migration. *Front. Ecol. Evol.* 9:704676. doi: 10.3389/fevo.2021.704676

Pack, A., Gehler, A., and Süssenberger, A. (2013). Exploring the usability of isotopically anomalous oxygen in bones and teeth as paleo-CO2-barometer. *Geochim. Cosmochim. Acta* 102, 306–317. doi: 10.1016/j.gca.2012.10.017

Passey, B. H., and Levin, N. E. (2021). Triple oxygen isotopes in meteoric waters, carbonates, and biological apatites: implications for continental paleoclimate reconstruction. *Rev. Mineral. Geochem.* 86, 429–462. doi: 10.2138/rmg.2021.86.13

Pearson, S. F., Levey, D. J., Greenberg, C. H., and Martínez del Rio, C. (2003). Effects of elemental composition on the incorporation of dietary nitrogen and carbon isotopic signatures in an omnivorous songbird. *Oecol.* 135, 516–523. doi: 10.1007/s00442-003-1221-8

Peña-Villalobos, I., Nuñez-Villegas, M., Bozinovic, F., and Sabat, P. (2014). Metabolic enzymes in seasonally acclimatized and cold acclimated rufous-collared sparrow inhabiting a Chilean Mediterranean environment. *Curr. Zool.* 60, 338–350. doi: 10.1093/czoolo/60.3.338

Peña-Villalobos, I., Valdés-Ferranty, F., and Sabat, P. (2013). Osmoregulatory and metabolic costs of salt excretion in the rufous-collared sparrow *Zonotrichia capensis*. *Comp. Biochem. physiol., Mol. Part A; Integr. Physiol.* 164, 314–318. doi: 10.1016/j.cbpa.2012.10.027

Polis, G. A., and Hurd, S. D. (1996). Linking marine and terrestrial food webs: allochthonous input from the ocean supports high secondary productivity on small islands and coastal land communities. *Am. Nat.* 147, 396–423. doi: 10.1086/285858

Rader, J. A., Newsome, S. D., Sabat, P., Chesser, R. T., Dillon, M. E., and Martínez del Rio, C. (2017). Isotopic niches support the resource breadth hypothesis. *J. Anim. Ecol.* 86, 405–413. doi: 10.1111/1365-2656.12629

Rezende, E. L., and Bacigalupe, L. D. (2015). Thermoregulation in endotherms: physiological principles and ecological consequences. *J. Comp. Physiol. B* 185, 709–727. doi: 10.1007/s00360-015-0909-5

Rutkowska, J., Sadowska, E. T., Cichon, M., and Bauchinger, U. (2016). Increased fat catabolism sustains water balance during fasting in zebra finches. *J. Exp. Biol.* 219, 2623–2628. doi: 10.1242/jeb.138966

Sabat, P. (2000). Birds in marine and saline environments: living in dry habitats. *Rev. Chil. Hist. Nat.* 73, 401–410. doi: 10.4067/s0716-078x2000000300004

Sabat, P., Cavieres, G., Veloso, C., and Canals, M. (2006b). Water and energy economy of an omnivorous bird: population differences in the rufous-collared sparrow (Zonotrichia capensis). *Comp. Biochem. Physiol. Part A: Mol. Integr. Physiol.* 144, 485–490. doi: 10.1016/j.cbpa.2006.04.016

Sabat, P., and del Río, C. M. (2005). Seasonal changes in the use of marine food resources by Cinclodes nigrofumosus (Furnariidae, Aves): Carbon isotopes and osmoregulatory physiology. *Rev. Chil. Hist. Nat.* 78, 253–260. doi: 10.4067/S0716-078X2005000200009

Sabat, P., Gonzalez-Vejares, S., and Maldonado, K. (2009). Diet and habitat aridity affect osmoregulatory physiology: an intraspecific field study along environmental gradients in the rufous-collared sparrow. *Comp. Biochem. Physiol. Part A: Mol. Integr. Physiol.* 152, 322–326. doi: 10.1016/j.cbpa.2008.11.003

Sabat, P., Maldonado, K., Canals, M., and Del Rio, C. M. (2006a). Osmoregulation and adaptive radiation in the ovenbird genus Cinclodes (Passeriformes: Furnariidae). *Funct. Ecol.* 20, 799–805. doi: 10.1111/j.1365-2435.2006.01176.x

Sabat, P., Maldonado, K., Rivera-Hutinel, A., and Farfan, G. (2004). Coping with salt without salt glands: osmoregulatory plasticity in three species of coastal songbirds (ovenbirds) of the genus Cinclodes (Passeriformes: Furnariidae). *J. Comp. Physiol. B* 174, 415–420. doi: 10.1007/s00360-004-0428-2

Sabat, P., Narváez, C., Peña-Villalobos, I., Contreras, C., Maldonado, K., Sanchez-Hernandez, J. C., et al. (2017). Coping with saltwater habitats: metabolic and oxidative responses to salt intake in the rufous-collared sparrow. *Front. Physiol.* 8, 1–11. doi: 10.3389/fphys.2017.00654

Sabat, P., Newsome, S. D., Pinochet, S., Nespolo, R., Sanchez-Hernandez, J. C., Maldonado, K., et al. (2021). Triple oxygen isotope measurements (Δ'17O) of body water reflect water intake, metabolism, and δ18O of ingested water in passerines. *Front. Physiol.* 12:710026. doi: 10.3389/fphys.2021.710026

Schmidt-Nielsen, K. (1997). *Animal Physiology: Adaptation and Environment*. New York, NY: Cambridge University Press.

Şekercioğlu, Ç. H., Primack, R. B., and Wormworth, J. (2012). The effects of climate change on tropical birds. *Biol. Conserv.* 148, 1–18. doi: 10.1016/j.biocon.2011.10.019

Sharp, Z. D., Wostbrock, J. A. G., and Pack, A. (2018). Mass-dependent triple oxygen isotope variations in terrestrial materials. *Geochem. Perspect. Lett* 7, 27–31. doi: 10.7185/geochemlet.1815

Shoemaker, V. (1972). "Osmoregulation and excretion in birds" in *Avian Biology*. eds. D. S. Farner, J. King and K. Parkes (New York: Academic Press), 527–574.

Smit, B., and McKechnie, A. E. (2010). Avian seasonal metabolic variation in a subtropical desert: basal metabolic rates are lower in winter than in summer. *Funct. Ecol.* 24, 330–339. doi: 10.1111/j.1365-2435.2009.01646.x

Smit, B., Woodborne, S., Wolf, B. O., and McKechnie, A. E. (2019). Differences in the use of surface water resources by desert birds are revealed using isotopic tracers. *Auk* 136:uky005. doi: 10.1093/auk/uky005

Smith, E. K., O'Neill, J. J., Gerson, A. R., McKechnie, A. E., and Wolf, B. O. (2017). Avian thermoregulation in the heat: resting metabolism, evaporative cooling and heat tolerance in Sonoran Desert songbirds. *J. Exp. Biol.* 220, 3290–3300. doi: 10.1242/jeb.161141

Song, S., and Beissinger, S. R. (2020). Environmental and ecological correlates of avian field metabolic rate and water flux. *Funct. Ecol.* 34, 811–821. doi: 10.1111/1365-2435.13526

Speakman, J. R., and Król, E. (2010). Maximal heat dissipation capacity and hyperthermia risk: neglected key factors in the ecology of endotherms. *J. Anim. Ecol.* 79, 726–746. doi: 10.1111/j.1365-2656.2010.01689.x

Swanson, D. L., Thomas, N. E., Liknes, E. T., and Cooper, S. J. (2012). Intraspecific correlations of basal and maximal metabolic rates in birds and the aerobic capacity model for the evolution of endothermy. *PLoS ONE.* 7: e34271. doi: 10.1371/journal.pone.0034271

Swanson, D. L., Agin, T. J., Zhang, Y., Oboikovitz, P., and DuBay, S. (2020). Metabolic flexibility in response to within-season temperature variability in house sparrows. *Integr. Org. Biol.* 2:obaa039. doi: 10.1093/iob/obaa039

Swanson, D. L., Zhang, Y., and Jimenez, A. G. (2022). Skeletal muscle and metabolic flexibility in response to changing energy demands in wild birds. *Front. Physiol.* 13:13. doi: 10.3389/fphys.2022.961392

Tapia-Monsalve, R., Seth, M., Juan, D. N., Hernandez, C. S., Bozinovic, F., Nespolo, R., et al. (2018). Terrestrial birds in coastal environments: metabolic rate and oxidative status varies with the use of marine resources. *Oecol.* 188, 65–73. doi: 10.1007/s00442-018-4181-8

The jamovi project (2022). jamovi. (Version 2.3) [Computer Software]. Available at: https://www.jamovi.org. (Accessed January 10, 2023).

Vezina, F., and Salvante, K. G. (2010). Behavioral and physiological flexibility are used by birds to manage energy and support investment in the early stages of reproduction. *Curr. Zool.* 56, 767–792. doi: 10.1093/czoolo/56.6.767

Vézina, F., and Williams, T. D. (2003). Plasticity in body composition in breeding birds: what drives the metabolic costs of egg production? *Physiol. Biochem. Zool.* 76, 716–730. doi: 10.1086/376425

Welcker, J., Speakman, J. R., Elliott, K. H., Hatch, S. A., and Kitaysky, A. S. (2015). Resting and daily energy expenditures during reproduction are adjusted in opposite directions in free-living birds. *Funct. Ecol.* 29, 250–258. doi: 10.1111/1365-2435.12321

Whiteman, J. P., Sharp, Z. D., Gerson, A. R., and Newsome, S. D. (2019). Relating Δ17O values of animal body water to exogenous water inputs and metabolism. *BioSci.* 69, 658–668. doi: 10.1093/biosci/biz055

Wiersma, P., Selman, C., Speakman, J. R., and Verhulst, S. (2004). Birds sacrifice oxidative protection for reproduction. *Proc. R. Soc. Lond. B Biol. Sci.* 271, S360–S363. doi: 10.1098/rsbl.2004.0171

Williams, T. D. (2018). Physiology, activity and costs of parental care in birds. *J. Exp. Biol.* 221:jeb169433. doi: 10.1242/jeb.169433

Williams, J. B., and Tieleman, B. I. (2001). "Physiological ecology and behavior of desert birds" in *Current Ornithology* (Boston, MA: Springer)

Wostbrock, J. A. G., Cano, E. J., and Sharp, Z. D. (2020). An internally consistent triple oxygen isotope calibration of standards for silicates, carbonates and air relative to VSMOW2 and SLAP2. *Chem. Geol.* 533:119432. doi: 10.1016/j.chemgeo.2019.119432

Zheng, W. H., Li, M., Liu, J. S., and Shao, S. L. (2008). Seasonal acclimatization of metabolism in Eurasian tree sparrows (Passer montanus). *Comp. Biochem. Physiol. Part A: Mol. Integr. Physiol.* 151, 519–525. doi: 10.1016/j.cbpa.2008.07.009

frontiers | Frontiers in Ecology and Evolution

TYPE Original Research
PUBLISHED 23 February 2023
DOI 10.3389/fevo.2023.1050582

OPEN ACCESS

EDITED BY
Seth Newsome,
University of New Mexico,
United States

REVIEWED BY
Kyung-Hoon Shin,
Hanyang University,
Republic of Korea
Irena Raselli,
Université de Fribourg,
Switzerland

*CORRESPONDENCE
Matthew D. Ramirez
✉ ramirezmd@uncw.edu

SPECIALTY SECTION
This article was submitted to Ecophysiology, a section of the journal Frontiers in Ecology and Evolution

RECEIVED 21 September 2022
ACCEPTED 11 January 2023
PUBLISHED 23 February 2023

CITATION
Ramirez MD, Avens L, Meylan AB, Shaver DJ, Stahl AR, Meylan PA, Clark JM, Howell LN, Stacy BA, Teas WG and McMahon KW (2023) Dietary plasticity linked to divergent growth trajectories in a critically endangered sea turtle. *Front. Ecol. Evol.* 11:1050582. doi: 10.3389/fevo.2023.1050582

Dietary plasticity linked to divergent growth trajectories in a critically endangered sea turtle

Matthew D. Ramirez[1]*, Larisa Avens[2], Anne B. Meylan[3,4], Donna J. Shaver[5], Angela R. Stahl[1], Peter A. Meylan[4,6], Jamie M. Clark[2,7], Lyndsey N. Howell[8], Brian A. Stacy[9], Wendy G. Teas[10] and Kelton W. McMahon[1]

[1]Graduate School of Oceanography, University of Rhode Island, Narragansett, RI, United States, [2]National Marine Fisheries Service, Southeast Fisheries Science Center, NOAA Beaufort Laboratory, Beaufort, NC, United States, [3]Florida Fish and Wildlife Conservation Commission, Fish and Wildlife Research Institute, Saint Petersburg, FL, United States, [4]Smithsonian Tropical Research Institute, Panama City, Panama, [5]National Park Service, Padre Island National Seashore, Corpus Christi, TX, United States, [6]Eckerd College, Natural Sciences Collegium, Saint Petersburg, FL, United States, [7]Cooperative Institute for Marine and Atmospheric Studies, University of Miami, Miami, FL, United States, [8]National Marine Fisheries Service, Office of Protected Resources, NOAA Pascagoula Laboratory, Pascagoula, MS, United States, [9]National Oceanic and Atmospheric Administration, National Marine Fisheries Service, Office of Protected Resources at University of Florida, Gainesville, FL, United States, [10]National Marine Fisheries Service, Southeast Fisheries Science Center, Miami, FL, United States

Foraging habitat selection and diet quality are key factors that influence individual fitness and meta-population dynamics through effects on demographic rates. There is growing evidence that sea turtles exhibit regional differences in somatic growth linked to alternative dispersal patterns during the oceanic life stage. Yet, the role of habitat quality and diet in shaping somatic growth rates is poorly understood. Here, we evaluate whether diet variation is linked to regional growth variation in hawksbill sea turtles (*Eretmochelys imbricata*), which grow significantly slower in Texas, United States versus Florida, United States, through novel integrations of skeletal growth, gastrointestinal content (GI), and bulk tissue and amino acid (AA)-specific stable nitrogen ($\delta^{15}N$) and carbon ($\delta^{13}C$) isotope analyses. We also used AA $\delta^{15}N$ ΣV values (heterotrophic bacterial re-synthesis index) and $\delta^{13}C$ essential AA ($\delta^{13}C_{EAA}$) fingerprinting to test assumptions about the energy sources fueling hawksbill food webs regionally. GI content analyses, framed within a global synthesis of hawksbill dietary plasticity, revealed that relatively fast-growing hawksbills stranded in Florida conformed with assumptions of extensive spongivory for this species. In contrast, relatively slow-growing hawksbills stranded in Texas consumed considerable amounts of non-sponge invertebrate prey and appear to forage higher in the food web as indicated by isotopic niche metrics and higher AA $\delta^{15}N$-based trophic position estimates internally indexed to baseline nitrogen isotope variation. However, regional differences in estimated trophic position may also be driven by unique isotope dynamics of sponge food webs. AA $\delta^{15}N$ ΣV values and $\delta^{13}C_{EAA}$ fingerprinting indicated minimal bacterial re-synthesis of organic matter ($\Sigma V<2$) and that eukaryotic microalgae were the primary energy source supporting hawksbill food webs. These findings run contrary to assumptions that hawksbill diets predominantly comprise high microbial abundance sponges expected to primarily derive energy from bacterial symbionts. Our findings suggest alternative foraging patterns could underlie regional variation in hawksbill growth rates, as divergence from typical sponge prey might correspond with increased energy expenditure and reduced foraging success or diet quality. As a result, differential dispersal patterns may infer substantial individual and population fitness costs and represent a previously unrecognized challenge to the persistence and recovery of this critically endangered species.

KEYWORDS

amino acid, carbon isotope fingerprinting, compound-specific isotope analysis, *Eretmochelys imbricata*, trophic position, somatic growth, spongivory, sponge (porifera)

1. Introduction

The distribution and abundance of food resources are key factors determining habitat quality and shaping animal populations through effects on demographic rates (Dias, 1996; Sutherland, 1997). As a result, within spatially heterogenous environments, mobile species are theoretically expected to distribute themselves in relation to preferred food resources so as to maximize individual fitness (Fretwell and Lucas, 1969). However, many organisms occupy suboptimal habitats for a variety of reasons that vary spatiotemporally, including a lack of complete knowledge of resource distribution, threat level (e.g., predator abundance, excessive human activity), inability to select (e.g., passive dispersers) or unwillingness to emigrate to (e.g., high site fidelity) high-quality habitats, or perceptual errors that decouple settlement cues from patterns of habitat quality (e.g., ecological traps; Swearer et al., 2021). As a result, many organisms occupy suboptimal habitats where demographic rates are reduced from theoretical maxima. Within widely distributed species, such as sea turtles, this may result in the partitioning of individuals into subpopulations with divergent demographic trajectories (Heinrichs et al., 2016), where regional population persistence requires demographic surpluses in high-quality habitats to outweigh deficits accumulated in low-quality habitats (Dias, 1996). Dispersal and foraging habitat selection are thus important processes shaping individual fitness and meta-population dynamics.

Recent research suggests that hawksbill sea turtles (*Eretmochelys imbricata*) have divergent demographic trajectories linked to differential oceanic stage dispersal patterns that can result in transport to suboptimal habitats with insufficient food resources for growth (Avens et al., 2021). Like most cheloniid sea turtles, the hawksbill sea turtle has a complex life cycle that begins with a dispersive-oceanic stage characterized by epipelagic foraging and ends with recruitment to coastal habitats and benthic foraging (Meylan et al., 2011). This life cycle likely includes several shifts between benthic developmental foraging habitats before final settlement in adult foraging sites. Importantly, ocean currents are believed to be a primary source of variation in the composition of benthic developmental foraging aggregations *via* passive dispersal (Bowen et al., 2007; Blumenthal et al., 2009). The quantity and quality of food resources in these early stages will determine somatic growth rates and thereby influence predation risk (Scharf et al., 2000; Salmon and Scholl, 2014), making prey distribution and abundance primary drivers of habitat quality for sea turtles during the juvenile life stage. Notably, juvenile hawksbills stranded in Texas were recently found to grow markedly slower than hawksbills stranded in Florida (Avens et al., 2021). Complementary bulk tissue stable nitrogen isotope ($\delta^{15}N$) analyses revealed that turtles stranded in Texas having substantially higher bone $\delta^{15}N$ values than turtles stranded in Florida (Avens et al., 2021), suggesting this regional variation in growth may be linked to differences in diet. However, mechanistic drivers of this somatic growth variation have yet to be identified.

Characterizing variation in hawksbill diet is critical to evaluating drivers of divergent demographic trajectories within United States waters. However, few data have been published in the literature despite United States hawksbill diets being known to Sea Turtle Stranding and Salvage Network personnel as early as 1981 (Supplementary Table S1). Globally, neritic stage hawksbills were once described as indiscriminate feeders (Carr and Stancyk, 1975), but subsequent studies revealed a high importance of sponges in hawksbill diets globally (e.g., Meylan, 1988; Carrión-Cortez et al., 2013; Von Brandis et al., 2014; see Supplementary material for detailed review). In Florida, digestive tract contents of four stranded pelagic-sized hawksbills suggested linkage to the surface-pelagic drift community; buccal samples from two subadults encountered on coral reefs consisted of sponge (Meylan, 1984; Meylan and Redlow, 2006). Additionally, Wood et al. (2017) found sponges were the only prey consumed during 141 min of video behavioral observations taken on coral reefs. Yet several other prey items, particularly tunicates, corallimorpharians, zoanthids, and algae have also been identified as important additional food sources (Mayor et al., 1997; León and Bjorndal, 2002; Bell, 2013; Carrión-Cortez et al., 2013), demonstrating potential for dietary plasticity for this species. In contrast to Florida hawksbills, the diets of hawksbills in Texas waters have yet to be characterized, despite oceanic and small neritic juveniles having been documented there since at least 1972 (Amos, 1989). United States waters, particularly Texas and Florida, provide important developmental habitats for this critically endangered species (Meylan and Redlow, 2006; Wood et al., 2013; Gorham et al., 2014), creating the need to better understand their trophic dynamics in this region, particularly in relation to demographic variation (Avens et al., 2021).

Gastrointestinal (GI) content studies have traditionally been the primary tools used to characterize sea turtle trophic ecology globally (Bjorndal, 1997). However, applications of other methods have grown in the last two decades (reviewed by Jones and Seminoff, 2013), including stable isotope analysis, which provides valuable metrics of foraging niche breadth (Newsome et al., 2007). More recently, compound-specific stable isotope analysis of amino acids (CSIA-AA) has significantly advanced the study of energy flow within food webs by unlocking unique metabolic information contained within individual amino acids to reveal how organisms acquire, modify, and allocate resources (McMahon and Newsome, 2019). For example, because the $\delta^{15}N$ values of certain classes of amino acids do ('trophic' amino acids) or do not ('source' amino acids) change appreciably with trophic transfer (McClelland and Montoya, 2002), amino acid $\delta^{15}N$ values can be used to estimate consumer trophic positions (TP) that are internally indexed to those nitrogen isotope baselines (Chikaraishi et al., 2009). This is particularly useful to the study of hawksbill dietary plasticity, and that of other widely distributed species, because it allows for the assessment of whether geographic variation in consumer bulk tissue $\delta^{15}N$ values reflects variation in trophic ecology, foraging across habitats with isotopically distinct baselines, or both (e.g., Matthews and Ferguson, 2014; Lorrain et al., 2015). Specifically, higher trophic positions for hawksbills in Texas relative to Florida would suggest they have altered foraging patterns that may be influencing their growth rates.

Stable carbon isotope analysis of essential amino acids ($\delta^{13}C_{EAA}$) has emerged as a powerful technique for understanding carbon flow through food webs. This is because: (1) different primary producers have

unique multivariate differences in their $\delta^{13}C_{EAA}$ values (i.e., $\delta^{13}C_{EAA}$'fingerprints') owed to the diversity of biochemical pathways they use to synthesize amino acids (Larsen et al., 2013), and (2) $\delta^{13}C_{EAA}$ values pass through the food web relatively unaltered because most animals have lost the ability to synthesize essential amino acids *de novo* and must obtain them directly from their diet (McMahon et al., 2010). As a result, $\delta^{13}C_{EAA}$ fingerprinting greatly improves the identification of taxon-specific production sources, for example between bacteria and eukaryotic microalgae supporting focal food webs (e.g., Arthur et al., 2014; McMahon et al., 2016). This is particularly relevant for reconstructing foraging patterns of consumers that prey on sponges, which exhibit a wide breadth of feeding strategies. In contrast to classical assumptions that sponges are principally heterotrophic filter feeders on eukaryotic microalgae, there is growing recognition that many sponges can obtain a high proportion of their energy *via* routing of microbially-processed dissolved organic matter to sponge tissues (de Goeij et al., 2008; Rix et al., 2020). High microbial abundance (HMA) sponges, whose holobionts are among the most microbially diverse environments on Earth (Hentschel et al., 2006), can derive up to ~60% of their heterotrophic diet from their bacterial symbionts (Rix et al., 2020). In contrast, low microbial abundance (LMA) sponges, which contain 2–4 orders of magnitude fewer microbes (Hentschel et al., 2006), obtain <1% of their diet from their bacterial symbionts (Rix et al., 2020; Hudspith et al., 2021). Given that eukaryotic microalgae and macroalgae are the main sources of particulate and dissolved organic matter in marine environments (Volkham and Tanoue, 2002) and have $\delta^{13}C_{EAA}$ fingerprints distinct from bacteria (Larsen et al., 2013), $\delta^{13}C_{EAA}$ fingerprinting provides a potential tool for differentiating consumption of HMA vs. LMA sponges. For example, recent CSIA-AA analyses of HMA sponges observed a significant contribution of bacterially derived carbon and nitrogen (Macartney et al., 2020; Shih et al., 2020). This process provides a quantifiable metric of diet in sponge predators, which appear to display selectivity for palatable, chemically undefended sponges that are also typically classified as HMA sponges (Pawlik et al., 2018). A complementary approach quantifying variance in trophic amino acid $\delta^{15}N$ values relative to expected primary producer patterns, a metric termed ΣV (McCarthy et al., 2007), also serves as a valuable proxy of bacterial re-synthesis to assess the degree to which bacterial production supports consumer food webs.

Here, we integrate GI content, bulk tissue stable isotope analysis, and amino acid $\delta^{15}N$ and $\delta^{13}C$ analyses to evaluate whether trophic plasticity is linked to regional growth variation in neritic stage hawksbill sea turtles. First, we collated quantitative and qualitative GI content data from stranded hawksbills, including novel analyses of turtles stranded in Texas, as well as Sea Turtle Stranding and Salvage Network records to assess whether diet composition varied regionally. We then performed complementary bulk tissue $\delta^{15}N$ and $\delta^{13}C$ and amino acid-specific $\delta^{15}N$ analyses of stranded hawksbill bone tissue to determine whether trophic niches and trophic positions differed between neritic stage turtles stranded in Florida vs. Texas. Lastly, we used $\delta^{13}C_{EAA}$ fingerprinting and ΣV values to evaluate the contribution of bacterially derived energy to hawksbill food webs as a metric of sponge foraging dynamics. We hypothesize that the regional variation in bulk $\delta^{15}N$ values observed by Avens et al. (2021) reflects regional differences in trophic dynamics that are associated with divergent demographic rates for hawksbills inhabiting United States waters. We hypothesize that Florida-stranded turtles follow the typical pattern of primary sponge consumption and that their food webs are principally supported by bacterially derived energy as would be expected for HMA sponge consumers. In contrast, we hypothesize the relatively high $\delta^{15}N$ values observed by Avens et al. (2021) for hawksbills in Texas reflect expanded trophic niches with turtles foraging at higher trophic levels in a food web supported by pelagic production sources (e.g., eukaryotic microalgae) rather than bacterially supported sponges. Consumption of atypical diets may be caused by reduced foraging success or prey availability, which in turn may influence turtle condition and somatic growth. Collectively, this work explores how trophic plasticity linked to differential dispersal patterns may influence sea turtle demographic rates.

2. Materials and methods

2.1. Sample collection and skeletochronology

Hawksbill front flippers and GI tracts were opportunistically collected through the United States Sea Turtle Stranding and Salvage Network from turtles that died along the coasts of Florida (FL; 1981–2018) and Texas (TX; 1983–2008; Supplementary Figure S1). Stranding date, location, and sex (male, female, unknown) were recorded, as well as either straightline (SCL) or curved (CCL) carapace length (nuchal notch to pygal notch, $SCL_{n\text{-}n}$, $CCL_{n\text{-}n}$, or nuchal notch to posterior tip, $SCL_{n\text{-}t}$, $CCL_{n\text{-}t}$). All body size measurements were converted to $SCL_{n\text{-}t}$ (hereafter SCL) following Bjorndal et al. (2016); Supplementary Table S1. Samples were either stored frozen (flippers, GI tracts) or preserved in ethanol (GI contents) until further processing. Although humeri and GI tracts were analyzed across the full spectrum of stranded turtles (i.e., post-hatchling to adult), analyses herein focus primarily on the neritic life stage.

All humeri sampled herein ($n = 71$ stranded turtles) were previously analyzed in Avens et al. (2021) following standard skeletochronology methods (Avens and Snover, 2013). Briefly, this included excising humeri from flippers; decalcifying, thin-sectioning, and staining bone cross-sections; and identifying and measuring the lines of arrested growth (LAGs; i.e., annual growth layers). The visible LAGs in the histologically processed skeletochronology sections were used to guide growth increment-specific sampling for stable isotope analyses.

For turtles that retained the first-year growth mark, or "annulus," age at death was determined directly from LAG counts, adjusted to the nearest 0.25 year based on stranding date relative to mean population hatch date (September). For turtles whose annulus was not visible, the number of LAGs lost to bone resorption were estimated using correction factors developed based on the relationship between LAG number and diameter from known age individuals (Parham and Zug, 1997). Estimated number of LAGs lost to resorption were then added to the visible number of LAGs to estimate age at death. Final age estimates were used to back-assign age estimates to all visible LAGs within each humerus sample.

To estimate somatic growth rates, we first estimated SCL for each visible LAG using an allometric equation that integrates the humerus section diameter (HSD): SCL relationship for processed humeri with the body proportional hypothesis back-calculation technique that accounts for individual variability in the HSD and SCL relationship (Francis, 1990). Annual somatic growth rates were then calculated by taking the difference between SCL estimates of successive LAGs. Growth rates were binned into 10 cm SCL size classes to facilitate comparison with the published literature.

2.2. Diet composition

We characterized hawksbill diet composition using two primary data sources: (1) examination of dead, stranded turtle GI contents (FL: $n = 36$, TX: $n = 56$), and (2) necropsy reports containing GI content observations (FL: $n = 18$, TX: $n = 6$). These data were compiled from multiple independent research endeavors over multiple decades that used varied sampling criteria (e.g., stomach only, partial GI tract, etc). As a result, we used a variety of qualitative and quantitative metrics to evaluate GI content data herein, each of which has its advantages and disadvantages (Esteban et al., 2020).

All GI contents were first visually examined to provide basic summaries of major dietary components. These data were used to estimate the percent frequency of occurrence of prey items for 10 general prey groups: sponge, annelid, cnidarian, crustacean, fish, mollusc, tunicate, other animal matter, plant/algae, and debris (natural and anthropogenic). We acknowledge percent frequency of occurrence provides an imperfect view of diet composition that can overemphasize infrequently consumed prey taxa. However, we necessarily include this consistent metric because this is still a standard metric reported in GI content studies and more detailed diet composition data were not collected for most Florida-stranded turtles nor recorded in necropsy reports. In contrast, for most Texas hawksbill GI tracts ($n = 52$ of 62), prey items were also identified to the lowest possible taxonomic level, dried, and weighed to estimate the percent dry weight of individual prey items.

Hawksbills were divided into life stages based on their GI contents, with those whose contents were primarily pelagic (e.g., *Sargassum*, floating species) or benthic (e.g., sponge, other benthic invertebrates, macroalgae/seagrass) prey assigned to the *oceanic* and *neritic* life stage, respectively. If GI contents contained both pelagic and benthic prey turtles were classified as *intermediate*. Turtles with minimal or ambiguous GI contents (e.g., small fish and crabs) were classified as *unknown*. For both qualitative and quantitative analyses, GI content data were evaluated relative to both SCL and mass (kg), which was estimated using the power function regression provided by Diez and van Dam (2002) instead of being measured to reduce error associated with frozen, damaged stranded animals. Metadata for stranded turtles sampled for GI contents, including diet descriptions, are presented in Supplementary Table S1.

To evaluate United States hawksbill diets within a broader context, we also performed a comprehensive literature review of global hawksbill diet composition data. We specifically targeted studies that reported diet composition as either percent dry or wet weight, collected *via* gastric lavage or stranded turtle GI content analysis only. Using standard search methods (e.g., Scopus, Google Scholar) in combination with a review of the International Sea Turtle Symposium conference proceedings, we identified nine studies that met criteria for inclusion in this data synthesis, including seven from the Caribbean, one from the eastern Pacific Ocean, and one from the western Indian Ocean. Four additional studies that reported percent weight data were excluded from comparisons because quantitative data could not be extracted from the manuscript, GI content weights were unusually low, or only fecal matter was analyzed (see Supplementary material). Data collated from these nine studies were used to calculate a weighted mean percent weight of prey taxa consumed by hawksbills across studies. This necessarily included integration of both wet and dry wet data. To evaluate patterns of sponge consumption, whenever possible, sponge taxa were subsequently classified as HMA or LMA sponges based on best available information from the literature.

2.3. Stable isotope analysis

We used a computer-guided micromill (ESI New Wave Research) to collect ~1.6 mg of bone dust from 11 Texas -stranded hawksbills ($n = 20$ growth layers) and 14 Florida-stranded hawksbills ($n = 47$ growth layers). Only humerus growth layers reflective of the neritic life stage were sampled (e.g., $\geq$ 1.75 years; Avens et al., 2021). Between one and seven growth layers were sampled from individual turtles (mean ± SD = 2.7 ± 1.8). Bone dust was analyzed for bulk $\delta^{15}N$ and $\delta^{13}C$ values *via* continuous-flow isotope-ratio mass spectrometry at Oregon State University, Corvallis, OR, United States. Analytical precision was 0.09‰ for $\delta^{15}N$ and 0.07‰ for $\delta^{13}C$ values. Following Ramirez et al. (2020), we corrected bulk $\delta^{13}C$ values for the Suess effect by standardizing all data to the year 2016 using a linear correction of −0.025 ‰ per year. Bulk $\delta^{13}C$ values were not corrected to account for carbonate-derived carbon due to the lack of a hawksbill-specific correction factor and because we did not use the bulk $\delta^{13}C$ data to estimate diet composition. Bulk $\delta^{13}C$ values were also not corrected for lipid content because tissue C:N ratios (%C divided by %N) were below 3.5, characteristic of unaltered protein with low lipid content (Post et al., 2007). Bulk SIA data presented herein were previously analyzed in Avens et al. (2021).

For a subset of 17 turtles (FL: $n = 11$, TX: $n = 6$), we analyzed turtle bone collagen tissue *via* CSIA-AA. We used a computer-guided micromill to isolate an approximately 5 mm x 2 mm x 1 mm section of bone, taken from the growth layer deposited in the final growth year of life to reflect most recent foraging to stranding, which was then decalcified in 0.5 N HCl at room temperature for 20–24 h. Isolated bone collagen was rinsed three times with Milli-Q water, air dried for 48–72 h, and then analyzed *via* CSIA-AA at the University of Rhode Island, Narragansett, Rhode Island, United States, following protocols modified from Brault et al. (2019) (see Supplementary material).

We analyzed the $\delta^{15}N$ and $\delta^{13}C$ values of 12 amino acids: alanine (Ala), glycine (Gly), threonine (Thr), serine (Ser), valine (Val), leucine (Leu), isoleucine (Ile), proline (Pro), aspartic acid (Asp), glutamic acid (Glu), phenylalanine (Phe), and lysine (Lys). Acid hydrolysis converts glutamine (Gln) and asparagine (Asn) into Glu and Asp, respectively, resulting in the measurement of combined Gln + Glu (hereafter referred to as Glx) and Asn + Asp (hereafter referred to as Asx). Hydroxyproline (Hpro) likely co-eluted with Pro given its high abundance in collagen, however, there are no isotopic difference between these amino acids because Hpro is a post-translationally modified variant of Pro (O'Connell and Collins, 2018). For $\delta^{15}N$ analyses, we assigned Glx, Asx, Ala, Leu, Ile, Pro, and Val as trophic amino acids, and Phe and Lys as source amino acids. Gly, Ser, and Thr were kept as separate groups due to a lack of consensus on their classification (McMahon and McCarthy, 2016). For $\delta^{13}C$ analyses, we assigned Thr, Val, Leu, Ile, Phe, and Lys as essential amino acids ($\delta^{13}C_{EAA}$) and all other amino acids as non-essential amino acids ($\delta^{13}C_{NEAA}$).

2.4. Data analysis

We used generalized additive models to evaluate regional variation in somatic growth rates for neritic stage turtles (i.e., ages >2). First, we implemented a set of simplified generalized additive models to

characterize region-specific growth patterns that included only the outermost, 'terminal' growth rate for each turtle. We then implemented a second set of generalized additive mixed models that included the full growth dataset (i.e., each turtles' full growth history). Generalized additive (mixed) models included either SCL or age as a fixed effect, an identity link, a quasi-likelihood error function, and turtle-specific random effects (mixed models only) and were implemented using the "*mgcv*" and "*nlme*" packages (Wood, 2006; Pinheiro et al., 2017). SCL and age exhibit high concurvity in sea turtles and were thus necessarily separated into different models.

Bulk $\delta^{15}N$ and $\delta^{13}C$ data were used in combination with the R package '*SIBER*' (Stable Isotope Bayesian Ellipses in R; Jackson et al., 2011) to compare isotopic niche widths of hawksbills that stranded in south Florida (sFL: Florida Keys to Biscayne Bay, FL), west Florida (wFL: Fort Myers to Tampa, FL), and Texas (TX: Aransas Bay to US/Mexico border). For the stable isotope analyses, data for turtles from south Florida and west Florida were evaluated separately to examine the potential effects of foraging habitat availability on diet composition—Florida's coral reefs are primarily concentrated in the Florida Keys and along the southeastern coastline but hawksbills also occur in western Florida up to Tampa Bay (Meylan and Redlow, 2006). The *SIBER* technique uses the univariate bulk $\delta^{13}C$ and $\delta^{15}N$ data to calculate bivariate ellipses, termed Standard Ellipse Areas, for each group, which account for *c.* 40% of those data and are corrected for sample sizes, serve as proxies for the isotopic niche of each group of turtles. Bayesian Standard Ellipse Areas were used to estimate uncertainty in region-specific isotopic niches.

Hawksbill trophic positions (TP) were calculated in multiple ways (see Supplementary material). First, we calculated region-specific TP_{bulk} using bulk tissue isotope values intergated into a Bayesian isotope mixing model using the R package "*tRophicPosition*" (Quezada-Romegialli et al., 2018). Here, we estimated population-level TP_{bulk} using both particulate organic matter and seagrass as $\delta^{15}N_{baseline}$. We calculated TP_{bulk} using both general consumer diet-collagen trophic discrimination factor value of 3.2 ± 1.0 ‰ (Schoeninger and DeNiro, 1984) as well as a green sea turtle-specific trophic discrimination factor of 5.1 ± 1.1 ‰ (Turner Tomaszewicz et al., 2017). We also calculated TP using the TP_{CSIA} equation, both using the classic pairing of Glx and Phe $\delta^{15}N$ values (e.g., Chikaraishi et al., 2009) as well as the weighted mean $\delta^{15}N$ values of multiple trophic (Ala, Val, Leu, Ile, Pro, and Glx) and source (Phe, Lys) amino acids (Nielsen et al., 2015). In both instances, amino acid-specific β values were derived from Ramirez et al. (2021) (Glx–Phe = 3.3 ± 1.8 ‰; Avg TrAA–Avg SrAA = 2.7 ± 3.0 ‰). Amino acid-specific trophic discrimination factor values were derived from Lemons et al. (2020) (Glx–Phe = 4.0 ± 0.5 ‰; Avg TrAA–Avg SrAA = 4.8 ± 0.7 ‰). Errors were propagated using the "propagate" package in R (Spiess, 2018) using the aforementioned β and trophic discrimination factor value uncertainties and the error estimates resulting from triplicate sample injections for each amino acid for each hawksbill sea turtle.

Following Larsen et al. (2013), we used an amino acid $\delta^{13}C$ fingerprinting approach to identify the primary production sources fueling hawksbill food webs. We used published $\delta^{13}C_{EAA}$ data for Thr, Val, Leu, Ile, and Phe from the three most likely primary producers supporting hawksbill food webs, prokaryotic bacteria, macroalgae, and eukaryotic microalgae (Larsen et al., 2013; McMahon et al., 2016; Stahl, 2021). We also used Caribbean HMA sponge $\delta^{13}C_{EAA}$ data from Macartney et al. (2020) for comparison with the hawksbill data. Although the sponge taxa sampled in Macartney et al. (2020) are not known to be consumed by hawksbills, they are included for reference because they are the only sponge $\delta^{13}C_{EAA}$ data reported in the literature. We explicitly assume their $\delta^{13}C_{EAA}$ patterns reflect a typical HMA sponge, although further study is needed. Hawksbill, sponge, and primary producer $\delta^{13}C_{EAA}$ data were normalized to their individual means to facilitate comparison of $\delta^{13}C_{EAA}$ patterns among groups (e.g., Larsen et al., 2015; Stahl, 2021). We then performed a linear discriminant analysis on the normalized $\delta^{13}C_{EAA}$ values to separate primary producer groups and used leave-one-out cross-validation to predict group membership for hawksbill sea turtles and sponges (Larsen et al., 2013).

Lastly, we calculated Σ*V* values (McCarthy et al., 2007), a proxy of bacterial re-synthesis and translocation of bacterial amino acids, to further assess whether energy sources fueling hawksbill food webs were derived from bacterial or eukaryotic sources. Σ*V* was calculated as the average deviation in the $\delta^{15}N$ values of the trophic amino acids Ala, Asx, Glx, Ile, Leu, and Pro (Eq. 3):

$$\Sigma V = 1/n\,\Sigma Abs\left(X_{AA}\right) \quad (1)$$

Where *X* of each trophic amino acid = [$\delta^{15}N_{AA}$ – AVG $\delta^{15}N_{AA}$ (Ala, Asx, Glx, Ile, Leu, and Pro)] and n = the total number of $\delta^{15}N_{AA}$ used in the calculation. Σ*V* values <1 reflect algal sources whereas Σ*V* values ≥2 indicate predominantly bacterial re-synthesis of organic matter (McCarthy et al., 2007). All statistical tests were carried out using the statistical software program R version 4.1.1 (R Core Team, 2021).

3. Results

3.1. Somatic growth rate variation

As observed by Avens et al. (2021), somatic growth rates were markedly lower for neritic stage hawksbills stranded in Texas relative to hawksbills stranded in Florida across all size classes (Table 1). Growth responses were similar between generalized additive models that included only the final, "terminal" growth rate for each individual and mixed models that included full multi-year growth records across all sampled turtle (Figure 1; Table 2). Growth responses were generally similar between models that included SCL or age as a fixed effect, showing the typical pattern of declining growth rate with increasing SCL and age (Figure 1; Supplementary Figure S2).

3.2. Gastrointestinal content analyses

GI content data were examined from 116 stranded hawksbills that ranged in size from 5.2 to 82.5 cm SCL (mean ± SD: 22.6 ± 17.4 cm; Supplementary Table S3; Supplementary Figure 3). Florida hawksbills for which GI contents were examined ranged from 7.0 to 82.5 cm SCL at stranding, whereas Texas hawksbills ranged from 5.2 to 36.8 cm SCL at stranding. Of the 116 stranded turtles with GI contents, 53 had an unknown cause of death due to lack of evaluation or lack of external abnormalities, 43 experienced sudden death (e.g., trauma, cold-stunning, possible forced submergence), 17 likely died because of health-related issues (e.g., underweight, infections, accumulated epibiota), and 3 had evidence of both trauma and health issues.

Based on GI contents, we classified 39 turtles to the neritic life stage (FL: *n* = 28, TX: *n* = 11), 57 turtles to the oceanic life stage (FL: *n* = 24, TX: *n* = 33), 9 turtles as in-between oceanic and neritic life stages (i.e.,

TABLE 1 Size class-specific somatic growth rates for hawksbill sea turtles stranded in Texas and Florida.

Size class (cm SCL)	Florida (n=35 turtles)					Texas (n=36 turtles)				
	n	Mean	SD	Min	Max	n	Mean	SD	Min	Max
<19.9	23	8.8	4.3	2.1	15.3	45	8.3	4.6	0.8	16.7
20–29.9	18	6.1	2.8	1.2	13.5	36	4	3	0.2	11.2
30–39.9	23	5.7	3.2	0.4	11.2	7	3.5	2.3	0.4	6.9
40–49.9	32	4	2.2	0.1	8.8	6	3.8	1.7	2	6.1
50–59.9	27	3.6	1.6	0	5.7	8	2.6	2.8	0.4	8.8
60–69.9	13	3.2	1.9	1	7.7	8	2.1	2.3	0.2	6.6
70–79.9	3	2.7	1.4	1.1	3.9	14	0.8	0.9	0.1	2.7
>80	–	–	–	–	–	2	0.2	0.2	0	0.3

SCL, straightline carapace length (notch-to-tip); n = number of growth rates.

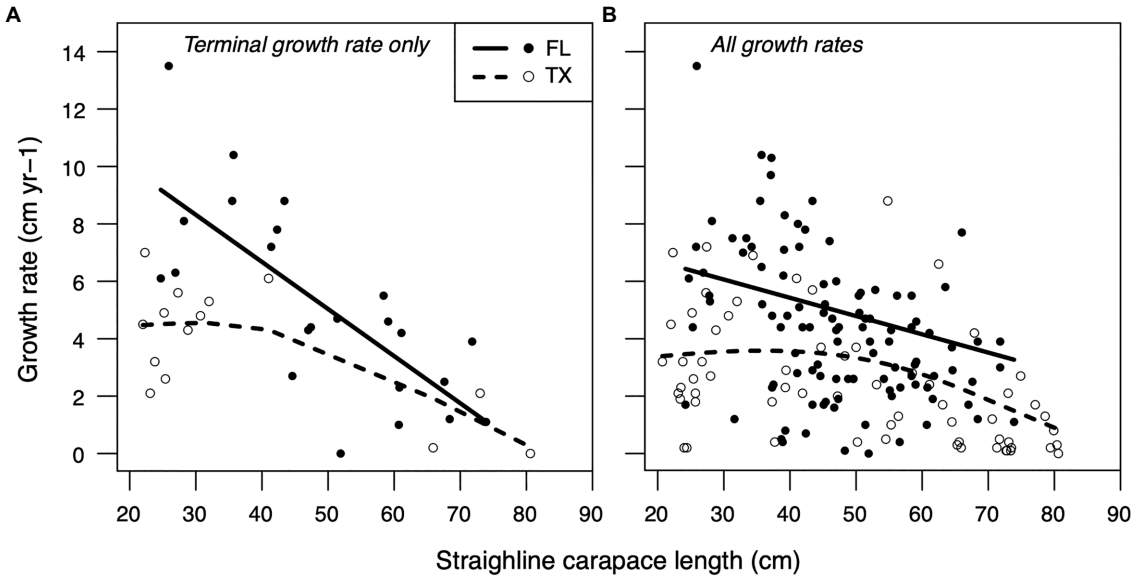

FIGURE 1
Generalized additive (mixed) model smoothing spline fits characterizing relationships between neritic stage growth rates (ages >2yr) and straightline carapace length for hawksbills stranded in Florida (FL; solid lines, closed points) and Texas (TX; dashed lines, open points). Region-specific models were implemented using **(A)** only the final 'terminal' growth rate for each turtle or **(B)** the full growth dataset that included multi-year growth records for each turtle.

intermediate; FL: n = 1, TX: n = 8), and 11 turtles whose diet could not be assigned to either life stages as *unknown* (Supplementary Figure S4). GI content results for turtles classified as *oceanic*, *intermediate*, and *unknown* are reported in the Supplementary material. Plastic was observed in the GI contents of 49% of all turtles examined in this study (57/116, FL: 24/54, TX: 33/62), including 75% (43/57) of oceanic stage turtles and 15% (6/39) of all neritic stage turtles.

For neritic stage hawksbills, sponges were the dominant prey observed in GI contents of turtles stranded in Florida (27 of 28 turtles; up to 4 L volume), whereas a mix of sponge and non-sponge prey were observed in Texas-stranded turtle GI contents (Figure 2A; Supplementary Tables S1, S2). Sponge diet was taxonomically classified for five of the 28 Florida-stranded turtles and primarily included the HMA sponges *Geodia* sp., *Chondrilla nucula*, and *Chondrosia* sp. and the LMA sponge *Placospongia* sp., which are among the most commonly observed sponge prey for hawksbills in the Caribbean (Meylan, 1988; Supplementary Table S5). Also recorded among FL-stranded turtle diets were hydroids (mostly attached to sponges) and benthic tunicates (2/28 individuals); the GI tract of one 27.7 cm SCL hawksbill contained ~1 L of the sessile, solitary tunicate *Molgula* sp., and little else other than a blade of *Thalassia* sp. seagrass.

Sponges were also frequently observed in the GI contents of neritic stage hawksbills stranded in Texas (8/11 individuals). However, for turtles where percent dry weight data were collected (n = 8), cnidarians (e.g., sea pens and anemones) contributed the greatest proportion of dietary dry weight (44.0%) followed by sponges (30.3%), molluscs (19.4%), and debris (3.6%; Supplementary Table S3). Based on percent dry weight, sponges comprised the dominant prey item for only four of eight Texas-stranded turtles (Figure 2B). The other sampled turtles had GI contents dominated by unidentified molluscs (n = 2) or cnidarians (sea pens, unidentified anemone; n = 2; Figure 2B). The three Texas-stranded turtles where GI contents were only qualitatively evaluated had diets dominated by the tunicate *cf. Styela plicata* (n = 2) or a *Hypnea* sp (n = 1), with lesser amounts of sponge and a variety of other prey items

TABLE 2 Summary of statistical output for generalized additive (mixed) models used to evaluate the influence of straightline carapace length (SCL, notch-to-tip) and age on region-specific growth rates for hawksbill sea turtles.

Model	n	Adj. R^2	AIC	Smooth terms			
				Variable	Edf	F	Prob (F)
(A) Restricted growth dataset ($n = 1$ per turtle)							
FL: Growth ~ SCL	23	0.53	108	SCL	1	25.7	<0.001
FL: Growth ~ Age	23	0.62	108	Age	1.8	23	<0.001
TX: Growth ~ SCL	14	0.48	58	SCL	1.7	5.8	0.014
TX: Growth ~ Age	14	0.55	58	Age	1	18.2	0.001
(B) Full growth dataset ($n \geq 1$ per turtle)							
FL: Growth ~ SCL	106	0.15	473	SCL	1	10.1	0.002
FL: Growth ~ Age	106	0.29	471	Age	2.7	9.9	<0.001
TX: Growth ~ SCL	63	0.23	265	SCL	1.9	3.5	0.025
TX: Growth ~ Age	63	0.25	265	Age	1	22.5	<0.001

Growth rates were back-calculated using skeletochronology. Only growth rates reflective of the neritic life stage (age > 2 year) were included in the models. Separate models were implemented using **(A)** only the final 'terminal' growth rate for each turtle or **(B)** the full growth dataset that included multi-year growth records for each turtle. FL, Florida; TX, Texas.

(see Supplementary Table S1). Texas hawksbill GI content dry weights were 1.25 to 29.14 g (mean ± SD: 9.45 ± 9.62 g). Importantly, only one of the 11 Texas-stranded and three of the 28 Florida-stranded neritic stage hawksbills died of apparent health-related issues (Supplementary Table S1), with the vast majority experiencing sudden or unknown causes of death. No Texas-stranded turtles >40 cm SCL were examined for this study, which strand infrequently in Texas. With the exception of two male hawksbills that stranded in Florida (82.0 and 82.5 cm SCL) all of the benthic-stage hawksbills represented in this diet analysis were likely immature based on size and data recorded on the necropsy reports.

Our literature review of hawksbill diet studies ($n = 10$, including Texas data herein) yielded 231 neritic stage turtles with GI contents evaluated as percent dry or wet weight. Methodologies included examination of GI contents of dead turtles and esophageal lavage and gastric lavage of living, captured turtles with study-specific sample sizes ranging from 5 to 54 turtles. For these turtles, the weighted mean percent mass of sponges observed in the GI contents was 61.8% (0.4–95.7% for individual studies) followed by cnidarians (27.4%, 0.0–94.0%), algae/plant (7.3%, 0.0–84.4%), and tunicates (1.6%, 0.0–32.5%; Table 3; Supplementary Table S4). Within individual studies, molluscs, arthropods, other animals, and debris (natural and anthropogenic) have generally constituted <5% of dietary weight. Across eight studies that classified sponge prey taxonomically, HMA and LMA sponges averaged 44.8% (0.4–67.4%) and 11.3% (0.2–30%) of total dietary weight, respectively (Table 3; Supplementary Table S4). 6.5% (0.00–76.1%) of sponge dietary weight could not be classified as HMA/LMA because the sponge prey were not taxonomically classified in the diet or they were classified but lacked HMA/LMA designations in literature. Twenty-seven sponge genera representing 11 sponge orders were observed in hawksbill GI contents across studies, with the genera *Chondrilla* and *Geodia* the most frequently observed and generally the greatest percent weight within individual studies (Supplementary Table S4). Note that although we have included results from studies using various methodologies in Supplementary Table S4, we urge caution in interpretation as to the equivalence of results. Esteban et al. (2020) noted small sample size and potential selective retention of larger items by esophageal papillae in the lavage method and reported on nontrivial differences in results using different methodologies at the same study site for green sea turtles (*Chelonia mydas*). In Supplementary Table S4, we note the pattern of greater predominance in sponges in studies involving examination of GI contents of dead turtles as compared to either gastric or esophageal lavage.

3.3. Isotopic metrics of trophic dynamics

Humeri sampled for stable isotopes were collected from 25 stranded hawksbill sea turtles (Supplementary Figure S1), which ranged in size from 24.0 to 68.1 cm SCL (mean ± SD: 40.1 ± 12.2 cm). Region-specific isotopic niche widths varied among turtles that stranded in south Florida ($n = 34$), west Florida ($n = 13$), and Texas ($n = 20$; Figure 3). Median Bayesian Standard Ellipse Area values (and 95% credible intervals) were largest for turtles in west Florida (8.4 ‰^{2}, 4.3–13.9 ‰^{2}) followed by south Florida (4.6 ‰^{2}, 3.2–6.4 ‰^{2}) then Texas turtles (2.7 ‰^{2}, 1.6–4.1 ‰^{2}). Hawksbills stranded in Texas had significantly higher $\delta^{15}N$ values relative to hawksbills stranded in Florida for all amino acids except Threonine, where they were lower (Supplementary Figure S5). Amino acid $\delta^{13}C$ values were generally similar among stranding regions (Supplementary Figure S5).

We observed strong regional variability in TP estimates derived through both bulk stable isotope analysis and CSIA-AA (Figure 4; Supplementary Table S6). Median posterior TP_{bulk} estimates were higher for Texas-stranded turtles (2.7–4.1) relative to turtles stranded in west Florida (2.3–3.1) and south Florida (2.0–3.0; Supplementary Table S6) and those patterns held for TP_{CSIA} estimates as well (TX: 3.1–3.4, wFL: 2.0–2.6, sFL: 1.7–2.4; Supplementary Table S6). Pairwise comparisons of posterior distributions showed that there was generally a > 95% probability that Texas-stranded hawksbills had TP_{bulk} estimates greater than south Florida- and west Florida-stranded hawksbills (Supplementary Table S7). There was also a 66 to 91% probability that west Florida hawksbills had TP_{bulk} estimates greater than or equal to south Florida hawksbills (Supplementary Table S7). Texas hawksbills were estimated to forage 0.5 to 1.5 TPs higher than south Florida hawksbills, whereas west Florida hawksbills were estimated to forage 0.1 to 0.4 TPs higher than south Florida hawksbills (Figure 4; Supplementary Table S6).

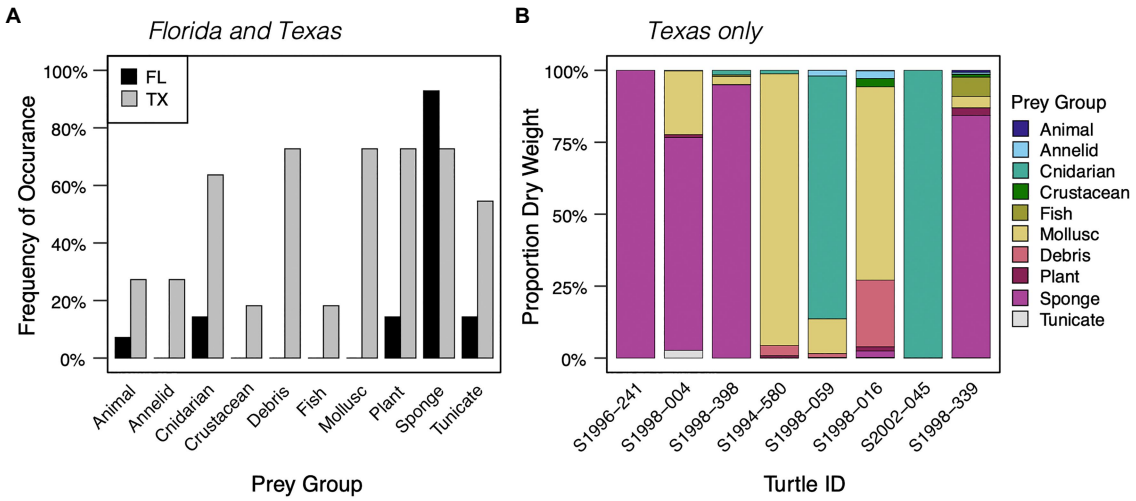

FIGURE 2
(A) Frequency of occurrence of prey items in diets of small neritic stage hawksbills (< 40cm SCL) stranded along the coasts of Florida (FL, *n*=14, 27.6±5.6cm SCL) and Texas (TX, *n*=11, 27.0±6.4cm SCL). **(B)** Percent dry weight of prey items for 8 neritic stage hawksbills (12.8–36.8cm SCL) stranded in Texas only. Neritic stage was assessed based on presence of benthic resources in GI contents.

TABLE 3 Mean percent weight of all prey taxa recorded in hawksbill sea turtle gastrointestinal contents in this study and globally (*n*=10 including this study).

Taxonomic classification	This study, TX neritic (*n*=8)	All studies, weighted mean (*n*=231)
Sponge	30.3	61.8
HMA	–	44.8
LMA	–	11.3
Unknown	30.3*	6.5
Cnidarian	44.0	27.4
Algae/Plant	0.4	7.3
Tunicate	0.2	1.6
Mollusc	19.4	0.7
Arthropod	0.5	0.1
Misc. animal	1.7	0.0
Debris	3.6	0.7
Unidentified	–	0.2

Data for this study are percent dry weights, whereas data synthesized from the literature include both percent dry and wet weights. HMA, high microbial abundance; LMA,low microbial abundance; Unknown, unknown HMA/LMA status due to either conflicting HMA/LMA designation in the literature or (*) lack of taxonomic classification within the diet study (e.g., herein). See Supplementary Table S4 for study-specific data used to calculate the weighted mean percent weight across studies.

The linear discriminant analysis used to assess the likely carbon sources supporting hawksbill food webs had reclassification success rates of 100, 88, and 89% for prokaryotic bacteria, macroalgae, and eukaryotic microalgae, respectively. The first linear discriminant (LD_1) explained 88% of the overall variation between groups (Supplementary Table S8), with the essential amino acids Ile, Leu, and Val most important for separating the three primary producer groups. The linear discriminant analysis classified all of the hawksbill turtles with eukaryotic microalgae, with >62% probability for all turtles and >90% probability for 14 of 17 (82%) turtles (Figure 5; Supplementary Table S9). All HMA sponge data from Macartney et al. (2020) were classified with prokaryotic bacteria (Figure 5; Supplementary Table S9).

ΣV values ranged between 1.1 and 2.0 for hawksbill turtles (Supplementary Table S9). Mean ΣV was the lowest for south Florida-stranded turtles (1.3, range = 1.1–1.6) and highest for west Florida-stranded turtles (1.7, range 1.5–1.9). Texas-stranded turtle ΣV values were the most variable of the three groups (1.2–2.0).

4. Discussion

Through integration of traditional gastrointestinal content analysis and advanced molecular isotope techniques, we show hawksbill sea turtles have regionally distinct diets that likely contribute to observed regional differences in somatic growth rates. Hawksbills in Texas foraged at higher trophic levels on varied invertebrate prey, whereas hawksbills in Florida had a sponge-dominated diet. Hawksbills in both regions foraged within eukaryotic-microalgal dominated food webs, which contrasts with expectations that hawksbills in Florida consume primarily microbially supported HMA sponges. Collectively, these results provide important context for understanding regional growth variation in hawksbills and suggest that divergence from typical sponge prey may be associated with increased energy expenditure, reduced foraging success, or nutritional stress. These results indicate that western North Atlantic hawksbills have multiple initial ontogenetic and demographic trajectories that are linked to differential dispersal patterns and associated prey fields.

4.1. Regionally variable hawksbill diets

Our analyses represent the first insights into hawksbill foraging ecology in Texas waters where this critically endangered species exhibits significantly reduced growth rates compared to hawksbills in Florida and the Caribbean. Prior to the current synthesis, the only GI content data recorded for hawksbills in Texas comprised marine

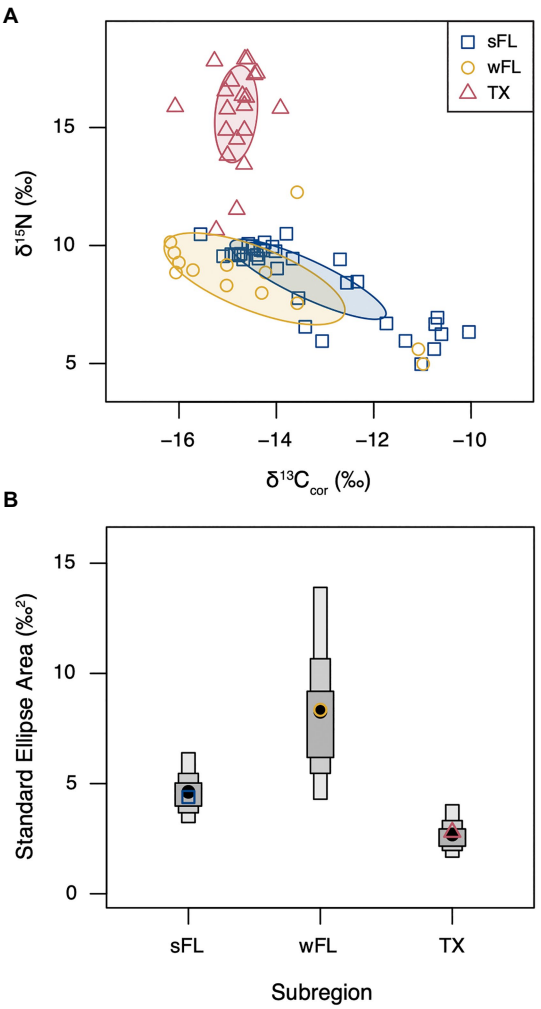

FIGURE 3
(A) Stable carbon ($\delta^{13}C_{cor}$) and nitrogen ($\delta^{15}N$) isotope values for neritic stage hawksbill sea turtle humerus bone growth layers by stranding region. Solid lines and shaded areas represent Standard Ellipse Areas corrected for sample size (SEAc). $\delta^{13}C_{cor}$ values were corrected for the Suess Effect. **(B)** Bayesian Standard Ellipse Areas (SEA-B), where filled black circles represent the median SEA-B value, grey boxes represent the 50, 75, and 95% credible intervals, and open colored shapes represent the mean SEAc values from panel A. south Florida (sFL, blue, *n*=34, 17.4–64.8cm SCL): stranding location from Florida Keys to Biscayne Bay, FL; west Florida (wFL, gold, *n*=13, 28.2–58.4cm SCL): stranding locations from Fort Myers to Tampa, FL; Texas (TX, red, *n*=20, 21.8–41.0cm SCL): stranding locations from Aransas Bay to Mexico border.

debris content for a single stranded turtle (Plotkin and Amos, 1988). Though a limited sample size ($n = 11$), our neritic stage hawksbill data for turtles stranded in Texas clearly demonstrate much larger contributions of non-sponge invertebrate prey relative to turtles in Florida, both based on percent frequency of occurrence and percent dry weight and after restricting percent frequency of occurrence comparisons to similarly sized neritic stage turtles (< 40 cm SCL; Figure 2A). This observation of higher dietary diversity for Texas-stranded hawksbills is further supported by our isotopic analyses of different stranded turtles that suggest Texas hawksbills forage 0.5 to 1.5 TPs higher in the food web than Florida conspecifics. Our Texas hawksbill $\delta^{13}C_{EAA}$ fingerprints, which overlap eukaryotic microalgae, also align with expectations of foraging in diverse food webs supported by pelagic production sources. Importantly, our stable isotope data reflect multiple years of prey consumption and energy assimilation following the oceanic-to-neritic habitat shift and are thus buffered from temporal biases associated with GI content analysis. Although other studies have reported significant hawksbill dietary plasticity (e.g., León and Bjorndal, 2002; Rincon-Diaz et al., 2011), Texas-stranded hawksbill diets may be uniquely diverse, including significant contributions of sponges, molluscs, cnidarians, crustaceans, and possibly shrimp and fish presumably consumed as fisheries discards. The consumption of this broader range of energy sources would be expected to yield increased mean foraging trophic level relative to a sponge-dominated diet, as observed herein. Importantly, our observation of regional differences in dietary breadth among similarly sized neritic stage juveniles <40 cm SCL suggests that Texas hawksbill dietary plasticity may not be due to general patterns of post-pelagic turtles foraging on more diverse prey before shifting to spongivory, which has been proposed to explain consumption of non-sponge prey in this species (Bjorndal, 1997; van Dam and Diez, 1997; Bjorndal and Bolten, 2010). This pattern of regional diet plasticity follows recent findings for Kemp's ridley sea turtles (*Lepidochelys kempii*) that also appear to forager at higher trophic levels in Texas than elsewhere in the Gulf of Mexico and United States Atlantic Coast (Ramirez et al., 2020). Expanded study of sea turtle diets and habitat use in Texas coastal waters are needed, including additional direct comparisons of GI contents and tissue stable isotope values, to further characterize the causes and consequences of this dietary plasticity.

Primary sponge consumption for hawksbills in Florida observed herein extends our limited understanding of hawksbill trophic ecology in United States tropical waters. To date, only three studies have detailed hawksbill foraging aggregations and behaviors in the U.S., all conducted within south Florida and suggestive of high importance of sponges to hawksbill diets. In-water studies of hawksbills at an offshore reef tract in Palm Beach County observed long-term residency and high site fidelity within coral reef hard-bottom habitats (Wood et al., 2013), where turtles targeted primarily sponges for consumption (Meylan, 1984; Wood et al., 2017). Within the Florida Keys, hawksbills primarily associated with rock rubble jetty structures extensively colonized with sponges and hard and soft corals (Gorham et al., 2014). In our study, we observed sponges in the GI contents of >80% of neritic stage hawksbills stranded in Florida, with infrequent observations of other prey items. As primary consumers, sponges would be expected to have TPs of ~2, yielding a TP of ~3 for their consumers. Our median TP_{bulk} estimates of 2.6 to 3.1 based on a trophic discrimination factor of 3.2 ‰ for hawksbills in Florida most closely align with this assumption. The lone hawksbill sampled for both GI contents and stable isotopes in our study, a turtle stranded near St. Petersburg, FL, had GI contents packed with ~4 liters of sponges (*Chondrosia* sp. and *Geodia* sp.) and TP_{bulk} estimates of ~3.5. Mean TP_{CSIA} estimates for Florida (1.7–2.6) were surprisingly low for a secondary consumer. In a recent application of CSIA-AA to a deep-sea food web, Hanz et al. (2022) observed TP_{CSIA} estimates of 2–2.5 for LMA sponges and 1.3 for HMA sponges, akin to a primary producer (TP = 1). These results, combined with those herein, demonstrate that it may be uniquely challenging to estimate TP_{CSIA} for sponge predators and calculate exact TP_{CSIA} differences between hawksbills in Florida and Texas because the isotope dynamics of sponges are not well understood. Specifically, it appears there may be an invisible stable nitrogen isotope trophic transfer for HMA sponge predators, as seen with heterotrophic protists (Gutiérrez-Rodríguez et al., 2014), which warrants further

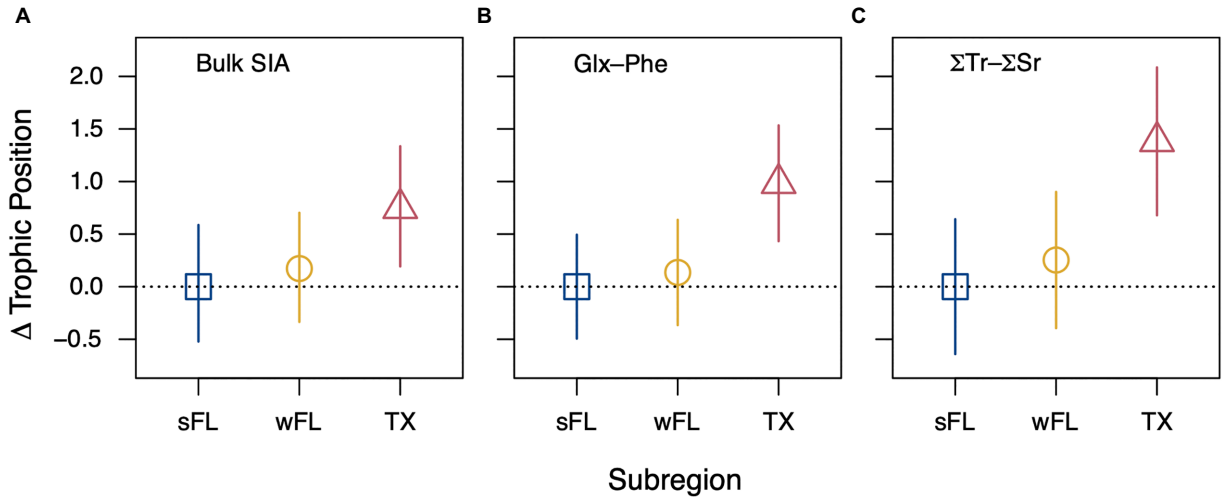

FIGURE 4
Relative difference in neritic stage hawksbill sea turtle trophic position estimates among stranding regions (within panels) calculated using three different trophic position equations (between panels). **(A)** Difference in median posterior trophic position estimates among regions with 95% credible intervals generated through Bayesian analysis of bulk $\delta^{15}N$ data (south Florida, sFL: *n*=34, 17.4–64.8cm SCL; west Florida, wFL: *n*=13, 28.2–58.4cm SCL; Texas, TX: *n*=20, 21.8–41.0cm SCL). **(B,C)** Difference in CSIA-AA derived trophic position estimates among regions using **(B)** Glx and Phe only or **(C)** the weighted mean of multiple trophic (Ala, Val, Leu, Ile, Pro, and Glx) and source (Phe, Lys) amino acids (sFL: *n*=6, 24.7–54.1cm SCL; wFL: *n*=5, 35.6–58.4cm SCL; TX: *n*=6, 25.2–41.0cm SCL). Amino acid-specific trophic discrimination factors and β values were taken from Lemons et al. (2020) and Ramirez et al. (2021), respectively.

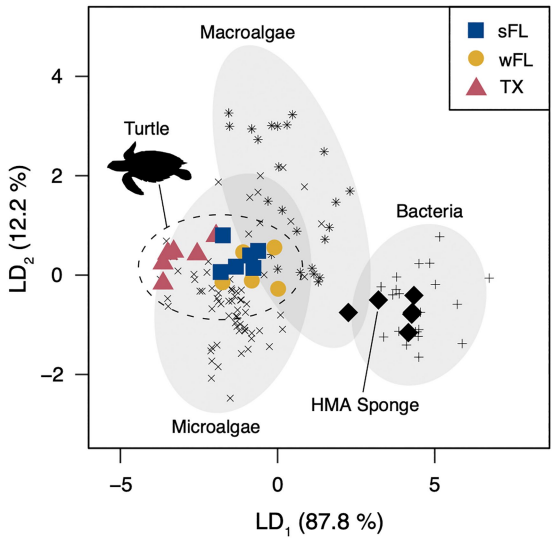

FIGURE 5
Linear discriminant analysis of the normalized $\delta^{13}C_{EAA}$ values (Thr, Val, Leu, Ile, and Phe) for stranded hawksbill sea turtles (sFL=south Florida, *n*=6; wFL=west Florida, *n*=5; TX=Texas, *n*=6), Caribbean HMA sponges (*n*=6), and three source end members: prokaryotic bacteria (plus symbol, *n*=20), macroalgae (asterisk symbol, *n*=24), and eukaryotic microalgae (cross symbol, *n*=71). Dashed lines represent 95% confidence ellipses around each source group. Sponge data taken from Macartney et al. (2020). Source end member data taken from Larsen et al. (2013), McMahon et al. (2016), and Stahl (2021).

investigation to refine application of these techniques in sponge food webs.

While our study supports previous work highlighting the importance of sponges to the diet of hawksbill sea turtles in Florida, our $\delta^{13}C_{EAA}$ fingerprinting analyses suggest that Florida hawksbill foraging patterns may be more complex than previously assumed. GI content studies, including Florida GI content data herein, demonstrate that hawksbills have clear preferences for a narrow range of sponges from the orders *Chondrillida* and *Tetractinellida*, particularly HMA sponges of the genera *Chondrilla* and *Geodia* (Meylan, 1988; Von Brandis et al., 2014; Pawlik et al., 2018; Supplementary Table S5). HMA sponges host dense communities of microbial symbionts that can contribute up to ~60% of their heterotrophic diet (Rix et al., 2020). As a result, HMA sponges, and by proxy their consumers, would be expected to have $\delta^{13}C_{EAA}$ fingerprints similar to prokaryotic bacteria (Macartney et al., 2020; Figure 5). In contrast, LMA sponges, which derive 99% of their energy through filter feeding, should have $\delta^{13}C_{EAA}$ fingerprints similar to eukaryotic microalgae or macroalgae (Rix et al., 2020; Hudspith et al., 2021). Our linear discriminant analysis suggested that eukaryotic microalgae were the primary carbon source at the base of Florida hawksbill food webs. This conclusion is further supported by our observation of ΣV values <2 for hawksbills, particularly those from south Florida (1.1–1.6), which indicates minimal bacterial re-synthesis of organic matter. For comparison, the HMA sponge *M. grandis* exhibited an ΣV value of 3.0 (Shih et al., 2020), which fits expectations of significant contributions of primarily microbially derived energy.

Our finding that microalgae are the primary production source at the base of Florida hawksbill food webs does not agree well with observed taxonomic patterns of spongivory in hawksbill sea turtles or other consumers. Specifically, our results suggest that (1) hawksbills in Florida derive a greater proportion of energy from LMA sponges or other invertebrate prey than previously thought and/or (2) current understanding of sponge nutritional ecology and isotope dynamics is incomplete. Interestingly, our synthesis of GI content studies revealed that, on average globally, hawksbill diet composition comprises ~11% LMA sponges and ~38% non-sponge prey, with the remainder being HMA sponges. As a result, on average, ~ 49% of hawksbill diets may consist of prey from food chains where eukaryotic algae would likely

be the primary basal energy source. From a mass balance perspective, a scenario where diets comprise 50% HMA sponges (60/40 bacterial/algal $\delta^{13}C_{EAA}$ fingerprint) and 50% LMA sponge or other invertebrate (100% algal $\delta^{13}C_{EAA}$ fingerprint) would yield consumer $\delta^{13}C_{EAA}$ fingerprints heavily skewed toward algae, as observed herein for Florida hawksbills. Our results may thus indicate that over annual time scales, Florida hawksbills assimilate energy from non-trivial amounts of LMA sponges and other invertebrates—either through active or passive consumption—that facilitates transfer of substantial algal-derived energy to their tissues. Alternatively, it is possible that HMA sponges consumed by Florida hawksbills derive less energy from their bacterial symbiont than has been suggested for HMA sponges studied to date. In the first study of sponge amino acid isotope dynamics, Shih et al. (2020) demonstrated that HMA sponges may derive amino acids primarily from direct transfer from microbial symbionts to sponge host tissue, similar to patterns observed in scleractinian corals and their endosymbionts (Rädecker et al., 2015). However, scientists have only recently begun quantifying microbial symbiont contribution to heterotrophy in sponges (Rix et al., 2020; Hudspith et al., 2021), exclusively in species not consumed by hawksbills. HMA/LMA status has also not been directly assessed at the species level for the vast majority of sponges known to be consumed by hawksbills, requiring HMA/LMA designations herein to be primarily based on genus level classification. Additionally, like corals (e.g., Fox et al., 2019; Wall et al., 2021), it is possible that mechanisms of sponge energy acquisition (microbial transfer vs. heterotrophic feeding) vary under different environmental conditions. There is thus a pressing need to further study the trophic and isotope dynamics of sponge species commonly consumed by predators so that we can better characterize energy flow and food web dynamics in these systems and predict system responses to environmental change.

4.2. Drivers of hawksbill sea turtle trophic plasticity

Regionally variable diets of hawksbill sea turtles within United States coastal waters aligns with a growing body of evidence that their foraging behaviors are more complex than classically considered and that gross habitat type may influence hawksbill dietary choices (e.g., León and Bjorndal, 2002; Bell, 2013). For example, sponge consumption is high on coral reefs and other hard bottom habitats, which are generally considered one of the primary foraging habitats for hawksbills in tropical waters globally because they are favorable to sponge growth (e.g., Limpus, 1992; Diez and van Dam, 2002; Houghton et al., 2003; Meylan and Redlow, 2006). Within Florida's coastal waters, hawksbill occurrence aligns closely with the extent of the Florida Reef Tract and other hard-bottom communities in the southeastern Gulf of Mexico, Florida Keys, and along the southeastern coast of Florida, particularly in association with sponges or sponge gardens (Meylan and Redlow, 2006; Wood et al., 2013; Gorham et al., 2014). However, around the world hawksbills also forage in other hard bottom habitats where sponges can be found, although at lower abundances, such as seagrass beds and even mangrove-fringed estuaries (in the Eastern Pacific; Bjorndal and Bolten, 2010; Gaos et al., 2012). In the Eastern Pacific, where hawksbills associate with rocky reefs, mangrove estuaries, and fjord-like embayments, tunicates and algae/plants comprise a non-trivial component of hawksbill diet in addition to sponges (Carrión-Cortez et al., 2013; Martínez-Estévez et al., 2022). Much like the Eastern Pacific, Texas coastal waters generally lack coral reefs with the exception of those occurring >100 km from the Texas coastline in the Flower Garden Banks National Marine Sanctuary (Schmahl et al., 2008). Instead, Texas coastal waters are broadly characterized by open soft bottom bays, seagrass beds, oyster reefs, hypersaline lagoons, and mangrove estuaries, each of which support prey assemblages distinct from coral reefs (and each other) and likely explain the relatively broad Texas-stranded turtle diets observed herein. Hawksbills in Texas have also been observed along rock jetties and shipping channels (D. Shaver, *pers. comm.*), habitats that promote omnivory in otherwise herbivorous green sea turtles (Howell and Shaver, 2021).

Beyond gross habitat type, temperature may also contribute to regional hawksbill diet variation in United States waters. A rich body of research has shown that abiotic factors can disproportionately influence organismal behavior at cool range edges reviewed in Paquette and Hargreaves (2021). For example, at higher latitudes, animal matter features prominently in the diets of herbivorous green turtles (Esteban et al., 2020), suggesting that temperature may be an important driver of trophic plasticity in sea turtles towards higher trophic levels, as observed for the Texas hawksbills in this study. Texas coastal waters experience much stronger seasonal shifts in temperature (16–30°C) than south Florida (22–30°C). As the most tropical of the seven sea turtle species, hawksbills are maladapted to cooler environmental conditions and may be unable to forage consistently during winter periods in Texas, which may impact growth and survival rates. Herein, eight of the 11 neritic stage turtles from Texas stranded in boreal winter months (December to March). However, sponges were the dominant prey taxa for two of these turtles as well as 11 neritic stage turtles stranded during the winter near Tampa, Florida, which also experiences seasonal temperature fluctuations. As a result, the extent to which temperature influences hawksbill diets relative to habitat type warrants further investigation.

Hawksbill dietary plasticity may also be driven by interactions between prey availability and selectivity. Even within coral reef habitats, hawksbills display complex dietary preferences. In a number of cases, hawksbills have been observed consuming prey at rates disproportionate to their abundance in the environment, including both specific sponge species (e.g., *Spirastrella coccinea, Myriastra kalitetilla*: León and Bjorndal, 2002; *Melophlus ruber*; Berube et al., 2012) as well as non-sponge prey such as the corallimorph *Ricordea florida* (León and Bjorndal, 2002; Rincon-Diaz et al., 2011), zoanthids (Mayor et al., 1997), and algae (Bell, 2013). Additionally, video behavioral observations show hawksbills spend considerable time investigating and biting—but not chewing—individual prey items (Dunbar et al., 2008; Wood et al., 2017), which suggests prey selectivity. However, in other cases, local abundance is thought to explain relatively high consumption rates of certain sponge (e.g., *Chondrilla nucula*: León and Bjorndal, 2002) and non-sponge (e.g., algae *Lobophora variegata*: Rincon-Diaz et al., 2011; zoanthids: Mayor et al., 1997) prey. Herein, the diets of individual neritic stage turtles stranded in Texas tended to be dominated by single prey types (Figure 2B). The extent to which these patterns reflect selective, opportunistic, or desperation feeding warrants further investigation as inferences herein are necessarily limited due to small samples sizes and biases of GI content analysis to recently consumed prey. However, the general agreement of the GI content and stable isotope data, the latter which reflect annual foraging, suggest these diverse diets are more likely reflective of foraging habitat than individual stranding condition. Furthermore, for sponge-eating hawksbills, the presence/absence of chemical defenses likely plays a key role in sponge selectivity given the overrepresentation of palatable, chemically undefended sponge taxa in hawksbill diets (Pawlik et al., 2018). However, palatability as a driver of

sponge prey selectivity has yet to be directly evaluated and warrants further investigation, particularly with respect to potetnial LMA sponge consumption by hawksbills in Florida.

Ultimately, hawksbill trophic plasticity in United States waters is likely driven primarily by gross habitat type, which dictates the breadth of resources available to individual turtles. Coastal Texas's turbid, temperate waters and lack of tropical coral reefs and hard bottom habitats likely restrict the extent of suitable habitat needed for hawksbill prey sponges to thrive. As a result, there may be insufficient sponge density in Texas waters to support exclusive sponge consumption by hawksbills over annual time scales, necessitating consumption of a broad range of prey to meet metabolic demands. Expanded study of hawksbill foraging patterns and prey fields in Florida and Texas are needed, including longitudinal studies of individual foraging patterns through *in-situ* sampling or sequential isotopic analyses of accretionary tissues (Vander Zanden et al., 2010; *sensu* Turner Tomaszewicz et al., 2016), to further refine drivers of dietary plasticity and their demographic consequences.

4.3. Implications of alternative demographic trajectories

Our multi-metric study of hawksbill dietary plasticity offers unique insight into the relationship between resource use and demography, suggesting that dietary plasticity in hawksbill turtles may contribute to regional somatic growth variation and thus come with substantial individual and population fitness costs both in the Wider Caribbean Region and globally. Notably, the relatively slow growth rates for small (30–40 cm: 3.5 cm yr^{-1}) and large (50–70 cm: 2.1–2.6 cm yr^{-1}; Table 1) neritic stage hawksbills stranded in Texas are similar to those reported for hawksbills from other regions where consumption of non-sponge prey is common, including the Eastern Pacific (30–40 cm: 3.1–3.6 cm yr^{-1}, 40–50 cm: 1.3–3.2 cm yr^{-1}; Llamas et al., 2017), Great Barrier Reef (50–70 cm: 1.9–2.5 cm yr^{-1}; Bell and Pike, 2012), and Northern Territory, Australia (50–60 cm: 2.4 cm yr^{-1}; Limpus, 1992; Whiting and Guinea, 1998). This is in stark contrast with hawksbill growth rates in Florida and the Caribbean that can average 5–9 cm yr^{-1} for small neritic juveniles (30–40 cm) and 3–6 cm yr^{-1} for large neritic juveniles (50–70 cm; reviewed in Avens et al., 2021). However, in the Bahamas, hawksbills inhabiting what are considered suboptimal seagrass habitats have similar growth rates to hawksbills in Florida and other Caribbean locations (Bjorndal and Bolten, 2010), illustrating that perceived habitat quality alone may be insufficient in explaining demographic variation. Somatic growth patterns are influenced by complex interactions between genetic and environmental (physical and biological) factors resulting in variable manifestation of phenotypic traits such as prey preferences, timing of ontogenetic diet shifts, and metabolism (e.g., Yamahira and Conover, 2002; Bourret et al., 2016). Consumption of diets atypical for a given life stage can result in imbalance of macronutrients, element ratios, and essential micronutrients that in turn affect physiological processes determining the extent of energy resources devoted to maintenance and somatic growth (e.g., Lukas et al., 2011; Canosa and Bertucci, 2020). For example, if hawksbills forage on non-sponge prey because of low foraging success or low sponge availability, this may increase foraging time and energy expenditure and lead to nutritional imbalances that impact growth rates. Variability in individual and population performance in suboptimal habitats and at range limits may ultimately lead to diverse population outcomes and represent a new challenge to the persistence and recovery of this critically endangered species. Our work will hopefully stimulate new lines of research into hawksbill foraging behavior in relation to prey availability, habitat features, and demography to further constrain the mechanistic drivers of divergent hawksbill population dynamics. For example, expanded CSIA-AA sampling to all hawksbill turtle bone growth layers coupled with growth increment-specific hormone analyses (Fleming et al., 2018) would greatly expand understanding of links between foraging trophic level, nutritional stress, and somatic growth.

Ultimately, Texas coastal waters may represent a sink habitat for some hawksbills belonging to certain populations in the western North Atlantic Ocean, which may have important implications for regional population dynamics. Juvenile hawksbills captured or stranded in United States waters disproportionately originate from rookeries on the Yucatán Peninsula (TX: 85–93%, FL: 56–75%; Bowen et al., 2007; Blumenthal et al., 2009; Wood et al., 2013; Gorham et al., 2014), which hosts multiple, genetically distinct rookeries (Labastida-Estrada et al., 2019). Connectivity of these Mexican rookeries to foraging grounds in Texas and Florida, combined with its limited genetic connectivity with other rookeries in the Caribbean (Blumenthal et al., 2009), make their conservation uniquely important to species persistence and recovery in the greater west Atlantic (Meylan, 1999). This is especially true as an unknown fraction of juveniles from these rookeries disperse to suboptimal habitats in Texas (Bowen et al., 2007) where somatic growth rates are reduced, which may have negative effects on population fitness through reduced survival rates, reproductive rates, or delayed maturity (Avens et al., 2021). This may ultimately be an example of a marine ecological trap (Swearer et al., 2021), with some hawksbills mistakenly preferring habitats where their fitness is reduced. However, unlike green sea turtles in Bermuda, which may be temporarily trapped within degrading habitats due to life history constraints (Meylan et al., 2022), hawksbills in Texas are presumably capable of migrating along the coastline to more suitable foraging habitat in Mexico or Florida, which may explain why few hawksbills >40 cm SCL are observed in Texas coastal waters (Amos, 1989; Shaver, 1998; Meylan and Redlow, 2006). Further assessment of whether the absence of these larger hawksbills reflects reduced survival or emigration, as well as study of sea turtle settlement cues, would greatly advance our understanding of fitness-related consequences of this regional growth variability. The regionally specific dietary plasticity results from our study, coupled with future work to quantify the proportion of hawksbills that disperse from the Yucatán rookery to different foraging grounds, would greatly improve modeling efforts to predict differential population trajectories in the region within a meta-population theory framework (Grimm et al., 2003).

Data availability statement

The original contributions presented in the study are publicly available. This data can be found here: https://doi.org/10.5061/dryad.xgxd254kt.

Ethics statement

Ethical review and approval was not required for the animal study because study was conducted on dead, stranded animals, which does not require IACUC approval. Research was authorized by USFWS ESA

permit number TE-676379-5 issued to the National Marine Fisheries Service's Southeast Fisheries Science Center.

Author contributions

MR, LA, AM, and KM conceived the study. MR, LA, and JC collected and analyzed the growth data. MR, AM, DS, PM, WT, LH, and BS collected and analyzed the GI content data. MR, AS, and KM collected and analyzed the stable isotope data. MR, AM, and KM led the writing of the manuscript. All authors contributed to manuscript revision and gave final approval for publication.

Funding

MR was supported by the NSF Postdoctoral Research Fellowship in Biology under grant number 1907144. Funding for the CSIA-AA portion of this work was provided through URI Foundation support to KM.

Acknowledgments

We are grateful to members of the National Sea Turtle Stranding and Salvage Network who collected the samples and necropsy data that made this study possible, especially participants in Florida and Texas, in particular to A. F. Amos, A. Foley, P. Plotkin, B. Schroeder, and J. Walker. In addition, we are grateful to S. Pomponi and J. Rudloe for their assistance with identification of forage items recovered during necropsy. We also thank L. R. Goshe assistance with skeletochronological analyses. Research was authorized by USFWS ESA permit number TE-676379-5 issued to the National Marine Fisheries Service's Southeast Fisheries Science Center.

Conflict of interest

The authors declare that the research was conducted in the absence of any commercial or financial relationships that could be construed as a potential conflict of interest.

Publisher's note

Supplementary material

The Supplementary material for this article can be found online at: https://www.frontiersin.org/articles/10.3389/fevo.2023.1050582/full#supplementary-material

References

Amos, A. F. (1989). "The occurrence of hawksbills Eretmochelys imbricata along the Texas coast" in *Proceedings of the Ninth Annual Workshop on Sea Turtle Conservation and Biology*, eds. S. A. Eckert, K. L. Eckert and T. H. Richardson. NOAA Technical Memorandum NMFS-SWFSC-54, 9–11.

Arthur, K. E., Kelez, S., Larsen, T., Choy, C. A., and Popp, B. N. (2014). Tracing the biosynthetic source of essential amino acids in marine turtles using $\delta^{13}C$ fingerprints. *Ecology* 95, 1285–1293. doi: 10.1890/13-0263.1

Avens, L., Ramirez, M., Goshe, L., Clark, J., Meylan, A., Teas, W., et al. (2021). Hawksbill Sea turtle life-stage durations, somatic growth patterns, and age at maturation. *Endang. Species Res.* 45, 127–145. doi: 10.3354/esr01123

Avens, L., and Snover, M. L. (2013). "Age and age estimation in sea turtles," in *The biology of sea turtles*. eds. J. Wyneken, K. J. Lohmann and J. A. Musick (Boca Raton, FL: CRC Press), 97–134.

Bell, I. (2013). Algivory in hawksbill turtles: *Eretmochelys imbricata* food selection within a foraging area on the northern great barrier reef. *Mar. Ecol.* 34, 43–55. doi: 10.1111/j.1439-0485.2012.00522.x

Bell, I., and Pike, D. (2012). Somatic growth rates of hawksbill turtles *Eretmochelys imbricata* in a northern great barrier reef foraging area. *Mar. Ecol. Prog. Ser.* 446, 275–283. doi: 10.3354/meps09481

Berube, M. D., Dunbar, S. G., Rützler, K., and Hayes, W. K. (2012). Home range and foraging ecology of juvenile hawksbill sea turtles (*Eretmochelys imbricata*) on inshore reefs of Honduras. *Chelonian Conserv. Biol.* 11, 33–43. doi: 10.2744/CCB-0898.1

Bjorndal, K. A. (1997). "Foraging ecology and nutrition of sea turtles," in *The biology of sea turtles*. eds. P. L. Lutz and J. A. Musick (Boca Raton, FL: CRC Press), 199–231.

Bjorndal, K. A., and Bolten, A. B. (2010). Hawksbill Sea turtles in seagrass pastures: success in a peripheral habitat. *Mar. Biol.* 157, 135–145. doi: 10.1007/s00227-009-1304-0

Bjorndal, K. A., Chaloupka, M., Saba, V. S., Diez, C. E., van Dam, R. P., Krueger, B. H., et al. (2016). Somatic growth dynamics of West Atlantic hawksbill sea turtles: a spatio-temporal perspective. *Ecosphere* 7:e01279. doi: 10.1002/ecs2.1279

Blumenthal, J. M., Abreu-Grobois, F. A., Austin, T. J., Broderick, A. C., Bruford, M. W., Coyne, M. S., et al. (2009). Turtle groups or turtle soup: dispersal patterns of hawksbill turtles in the Caribbean. *Mol. Ecol.* 18, 4841–4853. doi: 10.1111/j.1365-294X.2009.04403.x

Bourret, S. L., Caudill, C. C., and Keefer, M. L. (2016). Diversity of juvenile Chinook salmon life history pathways. *Rev. Fish. Biol. Fish.* 26, 375–403. doi: 10.1007/s11160-016-9432-3

Bowen, B. W., Grant, W. S., Hillis-Starr, Z., Shaver, D. J., Bjorndal, K. A., Bolten, A. B., et al. (2007). Mixed-stock analysis reveals the migrations of juvenile hawksbill turtles (*Eretmochelys imbricata*) in the Caribbean Sea. *Mol. Ecol.* 16, 49–60. doi: 10.1111/j.1365-294X.2006.03096.x

Brault, E., Koch, P., Costa, D., McCarthy, M., Hückstädt, L., Goetz, K., et al. (2019). Trophic position and foraging ecology of Ross, Weddell, and crabeater seals revealed by compound-specific isotope analysis. *Mar. Ecol. Prog. Ser.* 611, 1–18. doi: 10.3354/meps12856

Canosa, L. F., and Bertucci, J. I. (2020). Nutrient regulation of somatic growth in teleost fish. The interaction between somatic growth, feeding and metabolism. *Mol. Cell. Endocrinol.* 518:111029. doi: 10.1016/j.mce.2020.111029

Carr, A., and Stancyk, S. (1975). Observations on the ecology and survival outlook of the hawksbill turtle. *Biol. Conserv.* 8, 161–172. doi: 10.1016/0006-3207(75)90060-9

Carrión-Cortez, J., Canales-Cerro, C., Arauz, R., and Riosmena-Rodríguez, R. (2013). Habitat use and diet of juvenile eastern Pacific hawksbill turtles (*Eretmochelys imbricata*) in the North Pacific coast of Costa Rica. *Chelonian Conserv. Biol.* 12, 235–245. doi: 10.2744/CCB-1024.1

Chikaraishi, Y., Ogawa, N. O., Kashiyama, Y., Takano, Y., Suga, H., Tomitani, A., et al. (2009). Determination of aquatic food-web structure based on compound-specific nitrogen isotopic composition of amino acids. *Limnol. Oceanogr. Methods* 7, 740–750. doi: 10.4319/lom.2009.7.740

de Goeij, J. M., Moodley, L., Houtekamer, M., Carballeira, N. M., and van Duyl, F. C. (2008). Tracing 13C-enriched dissolved and particulate organic carbon in the bacteria-containing coral reef sponge *Halisarca caerulea*: evidence for DOM-feeding. *Limnol. Oceanogr.* 53, 1376–1386. doi: 10.4319/lo.2008.53.4.1376

Dias, P. C. (1996). Sources and sinks in population biology. *Trends Ecol. Evol.* 11, 326–330. doi: 10.1016/0169-5347(96)10037-9

Diez, C., and van Dam, R. (2002). Habitat effect on hawksbill turtle growth rates on feeding grounds at Mona and Monito Islands, Puerto Rico. *Mar. Ecol. Prog. Ser.* 234, 301–309. doi: 10.3354/meps234301

Dunbar, S. G., Salinas, L., and Stevenson, L. (2008). In-water observations of recently released juvenile hawksbills (*Eretmochelys imbricata*). *Mar. Turt. Newsl.* 121, 5–9.

Esteban, N., Mortimer, J. A., Stokes, H. J., Laloë, J.-O., Unsworth, R. K. F., and Hays, G. C. (2020). A global review of green turtle diet: sea surface temperature as a potential driver of omnivory levels. *Mar. Biol.* 167:183. doi: 10.1007/s00227-020-03786-8

Fleming, A. H., Kellar, N. M., Allen, C. D., and Kurle, C. M. (2018). The utility of combining stable isotope and hormone analyses for marine megafauna research. *Front. Mar. Sci.* 5:338. doi: 10.3389/fmars.2018.00338

Fox, M. D., Elliott Smith, E. A., Smith, J. E., and Newsome, S. D. (2019). Trophic plasticity in a common reef-building coral: insights from $\delta^{13}C$ analysis of essential amino acids. *Funct. Ecol.* 33, 2203–2214. doi: 10.1111/1365-2435.13441

Francis, R. (1990). Back-calculation of fish length: a critical review. *J. Fish Biol.* 36, 883–902. doi: 10.1111/j.1095-8649.1990.tb05636.x

Fretwell, S. D., and Lucas, H. L. (1969). On territorial behavior and other factors influencing habitat distribution in birds. *Acta Biotheor.* 19, 16–36. doi: 10.1007/BF01601953

Gaos, A. R., Lewison, R. L., Yañez, I. L., Wallace, B. P., Liles, M. J., Nichols, W. J., et al. (2012). Shifting the life-history paradigm: discovery of novel habitat use by hawksbill turtles. *Biol. Lett.* 8, 54–56. doi: 10.1098/rsbl.2011.0603

Gorham, J. C., Clark, D. R., Bresette, M. J., Bagley, D. A., Keske, C. L., Traxler, S. L., et al. (2014). Characterization of a subtropical hawksbill sea turtle (*Eretmochelys imbricata*) assemblage utilizing shallow water natural and artificial habitats in the Florida keys. *PLoS One* 9:e114171. doi: 10.1371/journal.pone.0114171

Grimm, V., Reise, K., and Strasser, M. (2003). Marine meta-populations: a useful concept? *Helgol. Mar. Res.* 56, 222–228. doi: 10.1007/s10152-002-0121-3

Gutiérrez-Rodríguez, A., Décima, M., Popp, B. N., and Landry, M. R. (2014). Isotopic invisibility of protozoan trophic steps in marine food webs. *Limnol. Oceanogr.* 59, 1590–1598. doi: 10.4319/lo.2014.59.5.1590

Hanz, U., Riekenberg, P., de Kluijver, A., van der Meer, M., Middelburg, J. J., de Goeij, J. M., et al. (2022). The important role of sponges in carbon and nitrogen cycling in a deep-sea biological hotspot. *Funct. Ecol.* 36, 2188–2199. doi: 10.1111/1365-2435.14117

Heinrichs, J. A., Lawler, J. J., and Schumaker, N. H. (2016). Intrinsic and extrinsic drivers of source–sink dynamics. *Ecol. Evol.* 6, 892–904. doi: 10.1002/ece3.2029

Hentschel, U., Usher, K. M., and Taylor, M. W. (2006). Marine sponges as microbial fermenters: marine sponges as microbial fermenters. *FEMS Microbiol. Ecol.* 55, 167–177. doi: 10.1111/j.1574-6941.2005.00046.x

Houghton, J. D. R., Callow, M. J., and Hays, G. C. (2003). Habitat utilization by juvenile hawksbill turtles (*Eretmochelys imbricata*, Linnaeus, 1766) around a shallow water coral reef. *J. Nat. Hist.* 37, 1269–1280. doi: 10.1080/00222930110104276

Howell, L. N., and Shaver, D. J. (2021). Foraging habits of green sea turtles (*Chelonia mydas*) in the northwestern Gulf of Mexico. *Front. Mar. Sci.* 8:658368. doi: 10.3389/fmars.2021.658368

Hudspith, M., van der Sprong, J., Rix, L., Víg, D., Schoorl, J., and de Goeij, J. (2021). Quantifying sponge host and microbial symbiont contribution to dissolved organic matter uptake through cell separation. *Mar. Ecol. Prog. Ser.* 670, 1–13. doi: 10.3354/meps13789

Jackson, A. L., Inger, R., Parnell, A. C., and Bearhop, S. (2011). Comparing isotopic niche widths among and within communities: SIBER – stable isotope Bayesian ellipses in R. *J. Anim. Ecol.* 80, 595–602. doi: 10.1111/j.1365-2656.2011.01806.x

Jones, T. T., and Seminoff, J. A. (2013). "Feeding biology: advances from field-based observations, physiological studies, and molecular techniques," in *The biology of sea turtles*. eds. J. Wyneken, K. J. Lohmann and J. A. Musick (Boca Raton, FL: CRC Press), 211–247.

Labastida-Estrada, E., Machkour-M'Rabet, S., Díaz-Jaimes, P., Cedeño-Vázquez, J. R., and Hénaut, Y. (2019). Genetic structure, origin, and connectivity between nesting and foraging areas of hawksbill turtles of the Yucatan peninsula: a study for conservation and management. *Aquat. Conserv.* 29, 211–222. doi: 10.1002/aqc.2999

Larsen, T., Bach, L. T., Salvatteci, R., Wang, Y. V., Andersen, N., Ventura, M., et al. (2015). Assessing the potential of amino acid ^{13}C patterns as a carbon source tracer in marine sediments: effects of algal growth conditions and sedimentary diagenesis. *Biogeosciences* 12, 4979–4992. doi: 10.5194/bg-12-4979-2015

Larsen, T., Ventura, M., Andersen, N., O'Brien, D. M., Piatkowski, U., and McCarthy, M. D. (2013). Tracing carbon sources through aquatic and terrestrial food webs using amino acid stable isotope fingerprinting. *PLoS One* 8:e73441. doi: 10.1371/journal.pone.0073441

Lemons, G. E., Lewison, R. L., Seminoff, J. A., Coppenrath, C. M., and Popp, B. N. (2020). Nitrogen isotope fractionation of amino acids from a controlled study on the green turtle (*Chelonia mydas*): expanding beyond Glx/Phe for trophic position. *Mar. Biol.* 167:149. doi: 10.1007/s00227-020-03745-3

León, Y. M., and Bjorndal, K. A. (2002). Selective feeding in the hawksbill turtle, an important predator in coral reef ecosystems. *Mar. Ecol. Prog. Ser.* 245, 249–258. doi: 10.3354/meps245249

Limpus, C. J. (1992). The hawksbill turtle, *Eretmochelys imbricata*, in Queensland: population structure within a southern great barrier reef feeding ground. *Wildl. Res.* 19, 489–506. doi: 10.1071/WR9920489

Llamas, I., Flores, E., Abrego, M., Seminoff, J., Hart, C., Pena, B., et al. (2017). Distribution, size range and growth rates of hawksbill turtles at a major foraging ground in the eastern Pacific Ocean. *lajar* 45, 597–605. doi: 10.3856/vol45-issue3-fulltext-9

Lorrain, A., Graham, B. S., Popp, B. N., Allain, V., Olson, R. J., Hunt, B. P. V., et al. (2015). Nitrogen isotopic baselines and implications for estimating foraging habitat and trophic position of yellowfin tuna in the Indian and Pacific oceans. *Deep-Sea Res. II Top. Stud. Oceanogr.* 113, 188–198. doi: 10.1016/j.dsr2.2014.02.003

Lukas, M., Sperfeld, E., and Wacker, A. (2011). Growth rate hypothesis does not apply across co-limiting conditions: cholesterol limitation affects phosphorus homoeostasis of an aquatic herbivore: Co-limitation affects consumer's stoichiometry. *Funct. Ecol.* 25, 1206–1214. doi: 10.1111/j.1365-2435.2011.01876.x

Macartney, K. J., Slattery, M., and Lesser, M. P. (2020). Trophic ecology of Caribbean sponges in the mesophotic zone. *Limnol. Oceanogr.* 66, 1113–1124. doi: 10.1002/lno.11668

Martínez-Estévez, L., Steller, D. L., Zilliacus, K. M., Cuevas Amador, J. P., Amador, F. C., Szuta, D., et al. (2022). Foraging ecology of critically endangered eastern Pacific hawksbill sea turtles (*Eretmochelys imbricata*) in the Gulf of California, Mexico. *Mar. Environ. Res.* 174:105532. doi: 10.1016/j.marenvres.2021.105532

Matthews, C. J. D., and Ferguson, S. H. (2014). Spatial segregation and similar trophic-level diet among eastern Canadian Arctic/north-West Atlantic killer whales inferred from bulk and compound specific isotopic analysis. *J. Mar. Biol. Ass.* 94, 1343–1355. doi: 10.1017/S0025315413001379

Mayor, P. A., Phillips, B., and Hillis-Starr, Z.-M. (1997). Results of the stomach content analysis on the juvenile hawksbill turtles of Buck Island reef National Monument, USVI in Proceedings of the Seventeenth Annual Symposium on Sea Turtle Biology and Conservation, eds. S. P. Epperly and J. Braun, NOAA Technical Memorandum NMFS -SEFSC-415, 244–247.

McCarthy, M. D., Benner, R., Lee, C., and Fogel, M. L. (2007). Amino acid nitrogen isotopic fractionation patterns as indicators of heterotrophy in plankton, particulate, and dissolved organic matter. *Geochim. Cosmochim. Acta* 71, 4727–4744. doi: 10.1016/j.gca.2007.06.061

McClelland, J. W., and Montoya, J. P. (2002). Trophic relationships and the nitrogen isotopic composition of amino acids in plankton. *Ecology* 83, 2173–2180. doi: 10.1890/0012-9658(2002)083[2173:TRATNI]2.0.CO;2

McMahon, K. W., Fogel, M. L., Elsdon, T. S., and Thorrold, S. R. (2010). Carbon isotope fractionation of amino acids in fish muscle reflects biosynthesis and isotopic routing from dietary protein. *J. Anim. Ecol.* 79, 1132–1141. doi: 10.1111/j.1365-2656.2010.01722.x

McMahon, K. W., and McCarthy, M. D. (2016). Embracing variability in amino acid $\delta^{15}N$ fractionation: mechanisms, implications, and applications for trophic ecology. *Ecosphere* 7:e01511. doi: 10.1002/ecs2.1511

McMahon, K. W., and Newsome, S. D. (2019). "Amino acid isotope analysis: a new frontier in studies of animal migration and foraging ecology," in *Tracking animal migration with stable isotopes*. eds. K. A. Hobson and L. I. Wassenaar (London, UK: Academic Press), 173–190. doi: 10.1016/B978-0-12-814723-8.00007-6

McMahon, K. W., Thorrold, S. R., Houghton, L. A., and Berumen, M. L. (2016). Tracing carbon flow through coral reef food webs using a compound-specific stable isotope approach. *Oecologia* 180, 809–821. doi: 10.1007/s00442-015-3475-3

Meylan, A. B. (1984). *Feeding ecology of the hawksbill turtle (Eretmochelys imbricata): Spongivory as a feeding niche in the coral reef community*. University of Florida, 128.

Meylan, A. (1988). Spongivory in hawksbill turtles: a diet of glass. *Science* 239, 393–395. doi: 10.1126/science.239.4838.393

Meylan, A. B. (1999). Status of the hawksbill turtle (*Eretmochelys imbricata*) in the Caribbean region. *Chelonian Conserv. Biol.* 3:8.

Meylan, P. A., Hardy, R. F., Gray, J. A., and Meylan, A. B. (2022). A half-century of demographic changes in a green turtle (*Chelonia mydas*) foraging aggregation during an era of seagrass decline. *Mar. Biol.* 169:74. doi: 10.1007/s00227-022-04056-5

Meylan, P. A., Meylan, A. B., and Gray, J. A. (2011). The ecology and migrations of sea turtles 8. Tests of the developmental habitat hypothesis. *Bull. Am. Mus. Nat. Hist.* 357, 1–70. doi: 10.1206/357.1

Meylan, A., and Redlow, A. (2006). *Eretmochelys imbricata* - hawksbill turtle. *Chelonian Res. Monogr.* 3, 105–127.

Newsome, S. D., Martinez del Rio, C., Bearhop, S., and Phillips, D. L. (2007). A niche for isotopic ecology. *Front. Ecol. Environ.* 5, 429–436. doi: 10.1890/060150.1

Nielsen, J. M., Popp, B. N., and Winder, M. (2015). Meta-analysis of amino acid stable nitrogen isotope ratios for estimating trophic position in marine organisms. *Oecologia* 178, 631–642. doi: 10.1007/s00442-015-3305-7

O'Connell, T. C., and Collins, M. J. (2018). Comment on ecological niche of Neanderthals from spy cave revealed by nitrogen isotopes of individual amino acids in collagen. *J. Hum. Evol.* 117, 53–55. doi: 10.1016/j.jhevol.2017.05.006

Paquette, A., and Hargreaves, A. L. (2021). Biotic interactions are more often important at species' warm versus cool range edges. *Ecol. Lett.* 24, 2427–2438. doi: 10.1111/ele.13864

Parham, J. F., and Zug, G. R. (1997). Age and growth of loggerhead sea turtles (*Caretta caretta*) of coastal Georgia: an assessment of skeletochronological age-estimates. *Bull. Mar. Sci.* 61, 287–304.

Pawlik, J. R., Loh, T.-L., and McMurray, S. E. (2018). A review of bottom-up vs. top-down control of sponges on Caribbean fore-reefs: what's old, what's new, and future directions. *PeerJ* 6:e4343. doi: 10.7717/peerj.4343

Pinheiro, J., Bates, D., DebRoy, S., and Sarkar, D.R Core Team (2017). Nlme: linear and nonlinera mixed effects models. *R Package* 3, 1–131.

Plotkin, P. T., and Amos, A. F. (1988). *Entanglement and ingestion of marine debris by sea turtles stranded along the South Texas coast* in Proceedings of the eighth annual workshop on sea turtle conservation and biology, ed. B. A. Schroeder, NOAA Technical Memorandum NMFS -SEFSC-214, 79–82.

Post, D. M., Layman, C. A., Arrington, D. A., Takimoto, G., Quattrochi, J., and Montaña, C. G. (2007). Getting to the fat of the matter: models, methods and assumptions for dealing with lipids in stable isotope analyses. *Oecologia* 152, 179–189. doi: 10.1007/s00442-006-0630-x

Quezada-Romegialli, C., Jackson, A. L., Hayden, B., Kahilainen, K. K., Lopes, C., and Harrod, C. (2018). Trophic position, an R package for the Bayesian estimation of trophic position from consumer stable isotope ratios. *Methods Ecol. Evol.* 9, 1592–1599. doi: 10.1111/2041-210X.13009

R Core Team (2021). *R: A language and environment for statistical computing*. R Foundation for Statistical Computing, Vienna, Austria.

Rädecker, N., Pogoreutz, C., Voolstra, C. R., Wiedenmann, J., and Wild, C. (2015). Nitrogen cycling in corals: the key to understanding holobiont functioning? *Trends Microbiol.* 23, 490–497. doi: 10.1016/j.tim.2015.03.008

Ramirez, M. D., Avens, L., Goshe, L. R., Snover, M. L., Cook, M., and Heppell, S. S. (2020). Regional variation in Kemp's ridley sea turtle diet composition and its potential relationship with somatic growth. *Front. Mar. Sci.* 7:253. doi: 10.3389/fmars.2020.00253

Ramirez, M. D., Besser, A. C., Newsome, S. D., and McMahon, K. W. (2021). Meta-analysis of primary producer amino acid δ^{15}N values and their influence on trophic position estimation. *Methods Ecol. Evol.* 12, 1750–1767. doi: 10.1111/2041-210X.13678

Rincon-Diaz, M. P., Diez, C. E., Van Dam, R. P., and Sabat, A. M. (2011). Foraging selectivity of the hawksbill sea turtle (*Eretmochelys imbricata*) in the Culebra archipelago, Puerto Rico. *J. Herpetol.* 45, 277–282. doi: 10.1670/10-120.1

Rix, L., Ribes, M., Coma, R., Jahn, M. T., de Goeij, J. M., van Oevelen, D., et al. (2020). Heterotrophy in the earliest gut: a single-cell view of heterotrophic carbon and nitrogen assimilation in sponge-microbe symbioses. *ISME J.* 14, 2554–2567. doi: 10.1038/s41396-020-0706-3

Salmon, M., and Scholl, J. (2014). Allometric growth in juvenile marine turtles: possible role as an antipredator adaptation. *Zoology* 117, 131–138. doi: 10.1016/j.zool.2013.11.004

Scharf, F., Juanes, F., and Rountree, R. (2000). Predator size-prey size relationships of marine fish predators: interspecific variation and effects of ontogeny and body size on trophic-niche breadth. *Mar. Ecol. Prog. Ser.* 208, 229–248. doi: 10.3354/meps208229

Schmahl, G. P., Hickerson, E. L., and Precht, W. F. (2008). "Biology and ecology of coral reefs and coral communities in the flower garden banks region, northwestern Gulf of Mexico" in *Coral reefs of the United States*. eds. B. M. Riegl and R. E. Dodge (Dordrecht: Springer Netherlands), 221–261. doi: 10.1007/978-1-4020-6847-8_6

Schoeninger, M. J., and DeNiro, M. J. (1984). Nitrogen and carbon isotopic composition of bone collagen from marine and terrestrial animals. *Geochim. Cosmochim. Acta* 48, 625–639. doi: 10.1016/0016-7037(84)90091-7

Shaver, D. J. (1998). "Sea turtle strandings along the Texas coast, 1980-1994," in *Characteristics and causes of Texas marine strandings*. ed. R. Zimmerman NOAA Technical Memorandum NMFS 143, 57–72.

Shih, J. L., Selph, K. E., Wall, C. B., Wallsgrove, N. J., Lesser, M. P., and Popp, B. N. (2020). Trophic ecology of the tropical Pacific sponge *Mycale grandis* inferred from amino acid compound-specific isotopic analyses. *Microb. Ecol.* 79, 495–510. doi: 10.1007/s00248-019-01410-x

Spiess, A.-N. (2018). Propagate: propagation of uncertainty. *R Package* 1.0–6. Available at: https://CRAN.R-project.org/package=propagate.

Stahl, A. (2021). Identifying novel isotopic tracers of marine primary producers to study food web carbon cycles. University of Rhode Island. 94. Available at: https://digitalcommons.uri.edu/theses/1936/.

Sutherland, W. J. (1997). *From individual behaviour to population ecology*. Oxford: Oxford University Press Available at: https://www.journals.uchicago.edu/doi/10.1086/419724 (Accessed July 26, 2022)..

Swearer, S. E., Morris, R. L., Barrett, L. T., Sievers, M., Dempster, T., and Hale, R. (2021). An overview of ecological traps in marine ecosystems. *Front. Ecol. Environ.* 19, 234–242. doi: 10.1002/fee.2322

Turner Tomaszewicz, C. N., Seminoff, J. A., Avens, L., and Kurle, C. M. (2016). Methods for sampling sequential annual bone growth layers for stable isotope analysis. *Methods Ecol. Evol.* 7, 556–564. doi: 10.1111/2041-210X.12522

Turner Tomaszewicz, C. N., Seminoff, J. A., Price, M., and Kurle, C. M. (2017). Stable isotope discrimination factors and between-tissue isotope comparisons for bone and skin from captive and wild green sea turtles (*Chelonia mydas*). *Rapid Commun. Mass Spectrom.* 31, 1903–1914. doi: 10.1002/rcm.7974

van Dam, R. P., and Diez, C. E. (1997). *Predation by hawksbill turtles on sponges at Mona Island, Puerto Rico* in Proceedings of the 8th International Coral Reef Symposium, eds. H. A. Lessios and I. G. Macintyre. Smithsonian Tropical Research Institute, 1421–1426.

Vander Zanden, H. B., Bjorndal, K. A., Reich, K. J., and Bolten, A. B. (2010). Individual specialists in a generalist population: results from a long-term stable isotope series. *Biol. Lett.* 6, 711–714. doi: 10.1098/rsbl.2010.0124

Volkham, J. K., and Tanoue, E. (2002). Chemical and biological studies of particulate organic matter in the ocean. *Curr. Biol.* 7, R126–R279. doi: 10.1016/S0960-9822(97)70976-X

Von Brandis, R. G., Mortimer, J. A., Reilly, B. K., van Soest, R. W. M., and Branch, G. M. (2014). Diet composition of hawksbill turtles (*Eretmochelys imbricata*) in the Republic of Seychelles. *Western Indian Ocean J. Mar. Sci.* 13, 81–91.

Wall, C. B., Wallsgrove, N. J., Gates, R. D., and Popp, B. N. (2021). Amino acid δ^{13}C and δ^{15}N analyses reveal distinct species-specific patterns of trophic plasticity in a marine symbiosis. *Limnol. Oceanogr.* 66, 2033–2050. doi: 10.1002/lno.11742

Whiting, S. D., and Guinea, M. L. (1998). *A large population of slow growing hawksbills: preliminary results from a wild foraging population in fog bay, Northern Territory* in Proceedings of the seventeenth annual symposium on sea turtle biology and conservation. Miami, FL: NOAA Tech Memo NMFS–SEFSC-415, 104–107.

Wood, S. N. (2006). *Generalized additive models: An introduction with R*. Boca Raton, FL: Chapman and Hall/CRC, doi: 10.1201/9781420010404.

Wood, L. D., Hardy, R., Meylan, P. A., and Meylan, A. B. (2013). Characterization of a hawksbill turtle (*Eretmochelys imbricata*) foraging aggregation in a high-latitude reef community in southeastern Florida, United States. *Herpetol. Conserv. Biol.* 8, 258–275.

Wood, L. D., Milton, S. L., and Maple, T. L. (2017). Foraging behavior of wild hawksbill turtles (*Eretmochelys imbricata*) in Palm Beach County, Florida, United States. *Chelonian Conserv. Biol.* 16, 70–75. doi: 10.2744/CCB-1242.1

Yamahira, K., and Conover, D. O. (2002). Intra- vs. interspecific latitudinal variation in growth: adaptation to temperature or seasonality? *Ecology* 83, 1252–1262. doi: 10.1890/0012-9658(2002)083[1252:IVILVI]2.0.CO;2

frontiers | Frontiers in Ecology and Evolution

TYPE Original Research
PUBLISHED 16 March 2023
DOI 10.3389/fevo.2023.1060982

OPEN ACCESS

EDITED BY
Seth Newsome,
University of New Mexico,
United States

REVIEWED BY
Ramiro Barberena,
CONICET Mendoza,
Argentina
John Whiteman,
Old Dominion University,
United States

*CORRESPONDENCE
Felipe Dargent
✉ fdargent@uottawa.ca;
✉ felipe.dargent@mail.mcgill.ca
Clement Pierre Bataille
✉ cbataill@uottawa.ca

SPECIALTY SECTION
This article was submitted to Ecophysiology, a section of the journal Frontiers in Ecology and Evolution

RECEIVED 04 October 2022
ACCEPTED 21 February 2023
PUBLISHED 16 March 2023

CITATION
Dargent F, Candau J-N, Studens K, Perrault KH, Reich MS and Bataille CP (2023) Characterizing eastern spruce budworm's large-scale dispersal events through flight behavior and stable isotope analyses.
Front. Ecol. Evol. 11:1060982.
doi: 10.3389/fevo.2023.1060982

Characterizing eastern spruce budworm's large-scale dispersal events through flight behavior and stable isotope analyses

Felipe Dargent[1,2]*, Jean-Noël Candau[1], Kala Studens[2], Kerry H. Perrault[2], Megan S. Reich[3] and Clement Pierre Bataille[1,3]*

[1]Advanced Research Complex Building, Department of Earth and Environmental Sciences, University of Ottawa, Ottawa, ON, Canada, [2]Great Lakes Forestry Centre, Canadian Forest Service, Natural Resources Canada, Sault Ste. Marie, ON, Canada, [3]Department of Biology, University of Ottawa, Ottawa, ON, Canada

Eastern spruce budworm moth (*Choristoneura fumiferana* (Clem.)) mass outbreaks have widespread economic and ecological consequences. A key explanation for the large-scale spread and synchronization of these outbreaks is the long-distance dispersal (up to 450km) of moths from hotspots (high-density populations) to lower-density areas. These events have proved difficult to monitor because dispersal flights occur only a few times a year, have no consistent routes, and commonly used tracking methods (e.g., population genetics, mark-recapture, radio telemetry) are inadequate for this system. Confirming immigration and distinguishing between local and immigrant individuals are crucial steps in identifying the physical and ecological drivers of moth dispersal. Here, we test whether isotopes of hydrogen (i.e., delta notation: δ^2H) and strontium (i.e., strontium isotope ratios: $^{87}Sr/^{86}Sr$), known to independently vary in space in a predictable manner, can be used to show that an immigration event occurred and to distinguish between local and immigrant adult spruce budworm moths. We used an automated pheromone trap system to collect individuals at six different sites in eastern Canada within and outside the current outbreak area of budworm moths. We first use moth flight behavior and time of capture, currently the best available tool, to determine putative local vs. immigrant status, and then evaluate whether individual $^{87}Sr/^{86}Sr$ and δ^2H differ between putative classes. At two sites, we detect immigrant individuals that differ significantly from putative locals and thus confirm immigration has occurred. Saliently, sites where putative locals were sampled before the occurrence of potential immigration events (~10 days) showed the strongest differences between immigrant individuals' and local $^{87}Sr/^{86}Sr$ and δ^2H values. Sites where the collection of putative locals was close in time (hours) or following an immigration event (days) had a less-clear distinction between putative immigrants and locals, and showed signs of mixing between these two groups. We speculate that recent immigration could have led to the misclassification of immigrants as putative locals. $^{87}Sr/^{86}Sr$ and δ^2H data generally support the adequacy of current approaches using capture-time to detect immigration events, and provide enhanced resolution to distinguish between local and immigrant individuals and to confirm an immigration event. We discuss the broader implication of adding isotopes to the toolkit to monitor spruce budworm dispersal and suggest next steps in implementing these tools.

KEYWORDS

δ^2H, $^{87}Sr/^{86}Sr$, hydrogen isotope, spruce budworm moth, strontium isotope ratios, geolocation, dispersal, nominal geographic assignment

Introduction

The eastern spruce budworm (*Choristoneura fumiferana* (Clem.)) is the most pervasive native pest of the North American boreal forest (Maclean, 2016). Large-scale outbreaks in eastern Canada occur in 30 to 40-year cycles (Jardon et al., 2003) and have severe ecological and socioeconomic consequences (Chang et al., 2012; Maclean, 2016). Spruce budworm larvae preferentially feed on new foliage of balsam fir (*Abies balsamea* (Mill.)) and spruces (*Picea* sp.). Outbreaks can lead to high-density populations ($>17\times10^6$ large larvae per hectare) (Ludwig et al., 1978) which defoliate extensive areas of forest (e.g., approximately 52 million hectares in 1975) (Sleep et al., 2009). Multi-annual defoliation leads to high average tree mortalities (e.g., 85% in balsam fir stands), and growth reduction (e.g., of up to 90%), over extensive areas of forest (Maclean, 1980). In turn, this impacts forest regeneration and succession dynamics (Bouchard et al., 2007), increases CO_2 emissions (Dymond et al., 2010; Maclean, 2019) and the likelihood of forest fires (James et al., 2017), and costs hundreds of millions of dollars in revenue loss and mitigation efforts (Natural Resources Canada, 2021).

Recent observations of the dynamics of rising budworm populations support a theory that attributed the rapid spread, extensive coverage, and widespread synchronization of spruce budworm outbreaks to dispersal events from high-density (i.e., outbreak) areas to low-density ones (Stedinger, 1984; Régnière et al., 2019a). At low-density sites, budworm population size is controlled by larvae mortality when failing to find food, and by predator and parasitoid-induced mortality, so that a limited number of adults contributes to the next generation (Stedinger, 1984). Immigrant arrivals can facilitate the transition to an outbreak density through the large influx of gravid moths causing a rapid population increase that, in turn, reduces stochasticity in larval survival caused during foliage searching, and cannot be suppressed by local enemies (Stedinger, 1984). Despite continuous research on this system for more than 50 years (Royama et al., 2017) and progress in control strategies (Maclean, 2019), gaps in our understanding of dispersal patterns and drivers make outbreaks a major challenge to predict and manage (Johns et al., 2019).

Understanding spruce budworm dispersal is challenging because dispersal events are irregular (Greenbank et al., 1980). Unlike classic roundtrip migrations or seasonal migrations that involve large numbers of actively-flying insects following the same routes every year [e.g., Monarch butterflies (Urquhart and Urquhart, 1978, 1979), Painted Ladies (Menchetti et al., 2019), Bogong moths (Warrant et al., 2016)], spruce budworm moths are mostly passive fliers and use wind currents for long-distance transport (Greenbank et al., 1980; Boulanger et al., 2017). Spruce budworm larvae have limited mobility and stay in the same tree, or adjacent ones, to their site of eclosion (Sanders, 1991), but adults may disperse large distances. After pupation, and for the 10- to 15-day life span of adult moths (Morris and Miller, 1954; Rhainds and Heard, 2015), whenever there is no rain and temperatures are above 14°C (Sanders et al., 1978; Greenbank et al., 1980), individuals will fly upward at dusk. These vertical flights can go up to an altitude of 400 m, with most individuals concentrated between 150 m and 300 m, and last for a few hours, after which the moths settle below canopy level for the rest of the day (Greenbank et al., 1980). During vertical flying, dispersal events may occur when moths are carried away by wind currents, and in some instances, hundreds of thousands of individuals can be transported hundreds of kilometers away by this process (Greenbank et al., 1980). These wind-facilitated dispersal events are relatively infrequent, occurring a few times per source site each year, are directional, which means that simple modeling approaches that assume an isomorphic radiation outside of a source area are inadequate, and could simultaneously involve large extents of forest as source and arrival locations. Such processes, in turn, make it challenging to predict the source of take-off, the direction of travel, or the landing area of dispersal flights. Additionally, this complex dispersal limits the viability of tracking approaches such as tagging [note that this approach is useful for monitoring local movement, i.e., distances below 100 m (e.g., Sanders, 1983)] while the small size of this insect makes radio telemetry unfeasible. Finally, the lack of genetic structure across Eastern Canada's local "subpopulations" (Lumley et al., 2020) makes genetic-based monitoring approaches unviable. Consequently, there is currently no efficient tool to monitor spruce budworm dispersal, hampering our understanding of processes and conditions driving mass take-off and landing, and ultimately limiting our ability to predict and manage the spread of outbreaks (Johns et al., 2019).

To improve monitoring of spruce budworm dispersal, a network of 22–30 automated traps has been deployed by the Federal and Provincial governments of Canada (Canadian Forest Service and the provinces of Quebec, Nova Scotia, and Newfoundland and Labrador) across Eastern Canada since 2018. This network is strategically set up to sample populations within outbreak areas and at the margins of the spruce budworm distribution, where density ought to be low but susceptible to the spread of the outbreak (Figure 1). These traps gather information that can be used to distinguish between local activity and immigration events (see Materials and Methods). Crucially, local individuals are expected to fly around dusk (Greenbank et al., 1980), thus, captures occurring between 17:00 to 23:00 are interpreted as potential locals. Captures between 23:00 and 05:00 are interpreted as putative immigrants, as immigrant individuals are expected to have some delay between their local-flying time and the time at which they land in a non-local patch after being carried away by winds. To enhance the accuracy of this approach, other lines of evidence are considered when trying to determine the migration status of moths, these include (1) local phenology, which informs if conditions are adequate for adults to be present in the area; (2) temperature and wind patterns at the time of capture, which informs whether moths are likely to have been flying at a given site and the potential trajectory of travel; and (3) radar data, which can detect when large numbers of moths disperse. Although this multifaceted approach improves the detection of dispersal events, it has some potentially important limitations. On the one hand, short-distance migrants could arrive a few hours after their vertical flight and before the 23:00 cut-off point, which would lead to mixing between presumed locals and short-distance immigrants. On the other hand, after an immigration event, previous-day immigrants would initiate their vertical flight behavior around dusk, and therefore, captures between 17:00 and 23:00 may be composed of a mixture of locals and immigrants. One way in which the accuracy of these methods can be validated, and lead to improved detection of immigration events, is by looking at the isotopic signals of captured individuals.

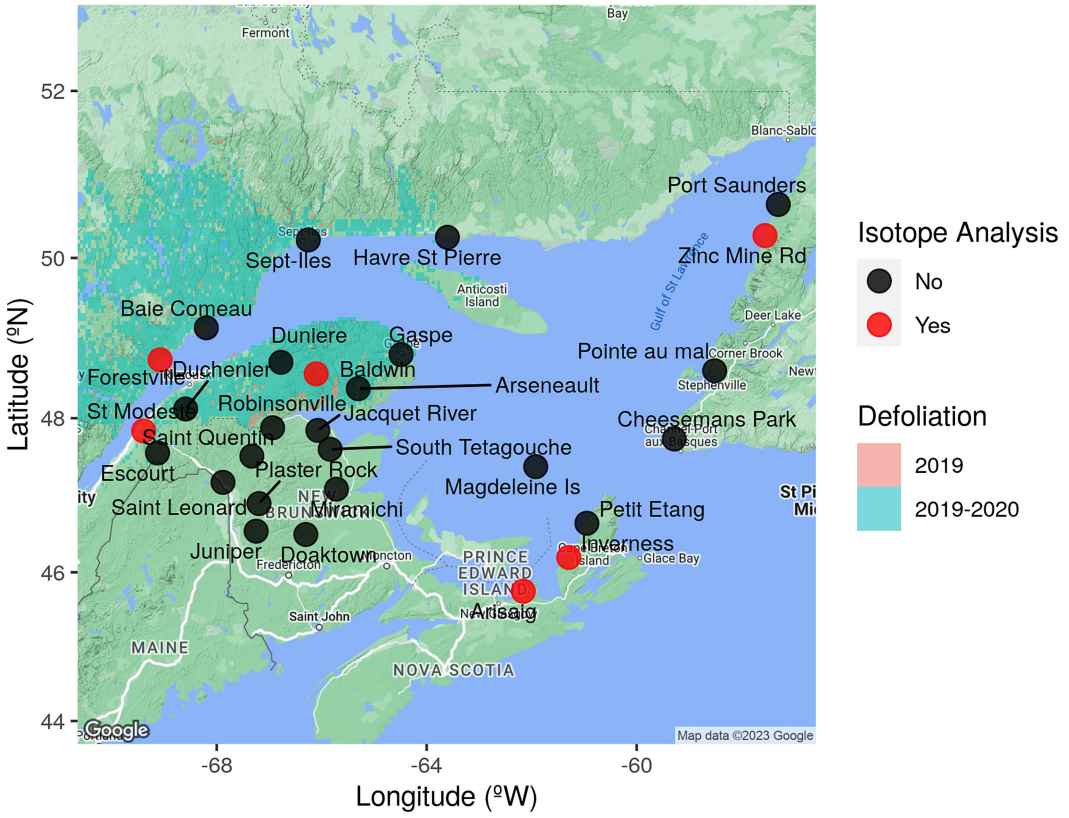

FIGURE 1
Trap location and eastern spruce budworm defoliation area. Map of eastern Canada with location of automatic traps in the network (black points), traps used in this study (red points) and the 2019 and 2020 spruce budworm area of defoliation, which is used as a proxy for population density and extent of the outbreak in a given year.

Isotopes of hydrogen (referred to using the delta notation or δ^2H values) and strontium (referred to using the ratio of ^{87}Sr to ^{86}Sr or ^{87}Sr/^{86}Sr) are intrinsic markers of geographic origin because they reflect where an organism developed, and thus can identify whether an individual grew up in the area where it was captured (Wassenaar and Hobson, 1998; Hobson et al., 1999; Flockhart et al., 2015). Local isotopic signals are integrated into an organism through the process of tissue development. As an organism grows and forms new tissue, hydrogen and strontium isotopes are incorporated into its body from the local food and water they consumed (Bowen et al., 2005; Bataille et al., 2020). Studies on migratory insects (Flockhart et al., 2015; Reich et al., 2023, this issue; Lindroos et al., 2023, this issue), demonstrate that tissues with low metabolic activity (e.g., wings) will carry and preserve the isotopic signal of the location at which the insect fed on the local vegetation (Lindroos et al., 2023, this issue). As spruce budworm moths do not feed during their short adult life (i.e., 10–15 days), it is likely that wings and other tissues preserve the isotopic signature of the spruce or balsam fir needles the larval stages fed on. Hydrogen isotopes are used in insect population ecology because of the predictable relationship between chitinous wings, which have low metabolic activity (Lindroos et al., 2023, this issue), and precipitation δ^2H values (Hobson, 2019). The δ^2H values in precipitation vary predictably in space and time with the hydrological cycle—in particular through the influence of evaporation and precipitation processes which, in turn, leads to the differential concentration of heavy relative to light hydrogen in local water (i.e., fractionation) (Bowen and Revenaugh, 2003; Bowen et al., 2005). δ^2H values variation in organisms follows those of precipitation but also includes a predictable contribution of physical and metabolic processes that segregate light vs. heavy isotopes further (Bowen and West, 2019). The ^{87}Sr/^{86}Sr ratio is another tool with strong potential to complement hydrogen isotopes for ecological provenance studies (Bataille et al., 2020). ^{87}Sr/^{86}Sr ratios in ecosystems usually vary at higher spatial resolution than δ^2H values following the chemical composition and age of surface geology, are stable through time, and are corrected for metabolic-induced fractionation (Bataille et al., 2020). As such, ^{87}Sr/^{86}Sr ratios vary independently from δ^2H values and have a strong potential to provide more specific geolocation (Bataille et al., 2020). Recent progress in analytical methods has allowed the successful application of ^{87}Sr/^{86}Sr ratios in wings to track the migration of other Lepidoptera (Reich et al., 2021). However, spruce budworms are small insects and their wings are too small for a precise ^{87}Sr/^{86}Sr analysis. While Sr concentrations and ^{87}Sr/^{86}Sr ratios in the wings of migratory insects have been shown to reflect the larval diet and local soils, it is possible that some strontium might cycle through insect bodies (Reich et al., 2023, this issue). However, for spruce budworm, adults do not feed which means that there is no addition of dietary Sr during the adult stage. Additionally, spruce budworm moths live for approximately 10 days following emergence (Greenbank et al., 1980) and up to 4 days after immigration (Rhainds

et al., 2022) limiting the possibility of Sr intake from locations different from the larval stage site. Consequently, it is likely that the $^{87}Sr/^{86}Sr$ ratios in short-lived spruce budworm reflect the larval stage and can be applied for geolocation.

Eastern Canada is an excellent location to apply insect isotope geolocation techniques. The climate of eastern Canada is varied with strong precipitation and temperature gradients going from the coast to more in-land locations leading to large δ^2H value variations across the breeding range of eastern spruce budworm. Similarly, the geology of Eastern Canada is one of the most varied in the world with Paleozoic carbonate units juxtaposed with Precambrian cratons and Grenville orogeny lithologies (Canada and Wheeler, 1996) leading to large $^{87}Sr/^{86}Sr$ ratios variability across the breeding range of eastern spruce budworms. Consequently, these geolocation tools are highly applicable across this study area. Combining hydrogen and strontium isotopes have shown great promise in increasing the specificity of geographic assignments of animals (Reich et al., 2021). Dual hydrogen-strontium isotope geolocation has a high potential to facilitate the identification of local vs. immigrant insects (i.e., nominal assignment) as well as estimating the location of origin of immigrant individuals (i.e., continuous geographic assignment) (Wunder, 2010; Ma et al., 2020; Magozzi et al., 2021). As a first step toward modeling the dispersal dynamics of spruce budworm, we test the applicability of δ^2H values and $^{87}Sr/^{86}Sr$ ratios as tools to evaluate whether immigration events have occurred at a given site, and distinguish between local and migrant individuals of eastern spruce budworm moths in six automated trap sites across the current outbreak and potential expansion distribution of the species (Figure 1). These automated trap sites are chosen based on the current spread of the spruce budworm outbreak. Three of our sites are in locations undergoing outbreak dynamics and thus have high population densities (Forestville, St. Modeste and Baldwin in Quebec, sampled in 2019), and the three other sites are in areas susceptible to the spread of an outbreak but remained at endemic levels with low-density populations at the time of sampling (Arisaig and Inverness in Nova Scotia 2020, and Zinc Mine in Newfoundland in 2019). First, we use a subset of individuals captured at these sites, presumed to be locals, and individuals following an immigration event that are presumed to be immigrants. We hypothesize that selected individuals will differ in their δ^2H values and $^{87}Sr/^{86}Sr$ ratios given that locals and immigrants likely fed and formed their tissues in different localities of eastern Canada. Second, we discuss currently used flight-behavior approaches to determine the origin of individuals, contrast them to isotopic approaches, and make suggestions for better understanding dispersal of spruce budworm moths.

Materials and methods

Determining local vs. immigrant individuals through flight behavior, phenology, and atmospheric modeling

Our automatic trap network uses automatic pheromone traps (Trapview+ model; EFOS d.o.o., Slovenia). Each trap has a synthetic pheromone lure that attracts male spruce budworm moths which then fall onto a roll of sticky paper. Four times a day at approximately 05:00, 11:00, 17:00, and 23:00 the trap cameras take a picture of the moths on the sticky roll and upload the image to a server *via* a cell phone network connection. The images are available in real-time and the sticky paper can be rolled remotely if it has a high number of moths attached. Moth numbers are automatically estimated by the Trapview software (EFOS d.o.o., Slovenia), new captures are distinguished from previously present moths, and records are then validated by CFS personnel to confirm proper species identification. At the end of the flight season, the full roll is recovered and stored under laboratory conditions. A sticky roll can be later unrolled and the chronology of moths captured on the paper can be established so moths captured at a specified date and time (i.e., between 05:00–11:00, 11:00–17:00, 17:00–23:00, and 23:00–05:00) can be recovered for isotope analysis (Supplementary Figure 1).

Moths are presumed as local or immigrant based on their flight behavior and the time of capture. Individuals captured between 17:00 and 23:00 are assumed to be locals, because spruce budworm moths tend to initiate their flight activity around dusk (Greenbank et al., 1980; Régnière et al., 2019b). Moths captured between 23:00 and 05:00, past the time of local flight activity, are assumed to be immigrants that were carried by winds and were transported to the trap location. Although rare, captures between 05:00 and 11:00 are interpreted as possible long-distant immigrants, and captures between 11:00 and 17:00 are interpreted as early locals. These interpretations are then validated by cross-referencing with the location phenology (https://burps.budworm.ca) to determine if adults are expected in the area at a given date and local temperature, as spruce budworm moths are unlikely to fly in cold temperatures (i.e., below 13°C for males and 17.5°C for females) (Sanders et al., 1978; Greenbank et al., 1980). Furthermore, capture numbers are also interpreted relative to recent day captures and activity across the approximately 30 traps in the network (Figure 1). Thus, high numbers of captures, even before 23:00, preceded and followed by days with much lower captures, are marked as a potential immigration event. Potential immigrants are then confirmed by looking at wind patterns during the time of capture, cross-referenced with areas where phenology indicates adults are present, and trajectory models are generated to evaluate potential sources of immigration (Stein et al., 2015; HYSPLIT, v.4.8[1]). Furthermore, on average at a given location, spruce budworm adult emergence occurs for a period of 2 weeks and local moth activity lasts 3 weeks, yet the influx of immigrants that remain active following dispersal can extend the duration of activity at any given site (Greenbank et al., 1980). Overlaps in immigration events and local emergence affect the reliability of the interpretation of captures around dusk, as surviving immigrants—which can live for about 4 days (Rhainds et al., 2022)—can be misidentified as locals without any additional tools for discrimination.

We selected three sites within the active defoliation area of the current spruce budworm outbreak which have high population densities. These sites had the highest capture rates of the 2019 flight season: Forestville (48.738°N, −69.07783°W), St. Modeste (47.83683°N, −69.39133°W), and Baldwin (48.562°N, −66.1055°W) (Figure 1). The other sites were outside the current outbreak area and are mostly experiencing endemic (low-density) spruce budworm population dynamics, but are predicted to

1 https://www.ready.noaa.gov/HYSPLIT.php

be potential zones of future outbreak expansion. These sites had an overall low number of captures throughout the flight season: Zinc Mine Rd. (50.273°N, −57.555°W), Arisaig (45.75°N, −62.16°W), and Inverness (46.196°N, −61.294°W) (Figure 1). Once a group of moths that was captured at a specific date and time block (e.g., 17:00–23:00) had been identified as putative locals or putative immigrants, by the methods described above, we haphazardly subsampled about three putative locals and five putative immigrants per site for isotope analyses.

Hydrogen isotope composition analysis

Before measuring δ^2H values in spruce budworm wings, we cleaned the wings in a 2:1 v/v chloroform:methanol solution in three successive washes for 30 min, at least 3 h, and 15 min respectively, to remove glue (from the sticky roll), lipids, dust, and contaminants that could impact the δ^2H values of the samples. The chloroform:methanol wash effectively removed these contaminants (Supplementary Figure 2). The wings were then air dried in a class-100 fume hood and stored in a glass vial. For each individual, we sampled 0.10 to 0.15 mg of wing tissues packed into silver capsules. The δ^2H values of the non-exchangeable hydrogen of butterfly wings were determined at the Jan Veizer Stable Isotope Laboratory using the comparative equilibration (CE) approach similar to Wassenaar and Hobson (1998). We initially used the dual-vapor equilibration (DVE) approach (n = 12 samples) following Meier-Augenstein et al. (2011), but given the larger amount of wing material (approximately 0.3 mg) required for this method, most moths did not have enough wing mass, and we chose to continue the assays using the CE method (n = 41) (see Supplementary Table 3 for a sample by population breakdown). To ensure consistency between δ^2H values of the non-exchangeable hydrogen of butterfly wings using different analytical approaches (Magozzi et al., 2021), we corrected DVE δ^2H values with the following formula $y = 0.8432x - 10.43$ ($R^2 = 0.9923$, $n = 9$) obtained from wing-tissue analyzed using both the DVE and CE methods. We performed hydrogen isotopic measurements on H_2 gas derived from high-temperature (1,400°C) flash pyrolysis (TCEA, Thermo, Germany) of 0.15 ± 0.015 mg of wing subsamples, along with keratin standards: Caribou Hoof Standard (CBS; δ^2H = −157.0 ± 0.9 ‰), Kudo Horn Standard (KHS; δ^2H = −35.3 ± 1.1‰) (Soto et al., 2017), USGS42 hair (δ^2H = −72.9 ± 2.2 ‰), USGS43 hair (δ^2H = −44.4 ± 2.0 ‰) (Coplen and Qi, 2012), and two internal standards made of chitin material: ground and homogenized spongy moths (*Lymantria dispar,* Linnaeus, 1758) (δ^2H = −64 ± 0.8‰) and Alfa Aesar chitin (δ^2H = −22 ± 1.2‰). The resultant separated H_2 flowed to a Conflow IV (Thermo, Germany) interfaced to a Delta V Plus IRMS (Thermo, Germany) for δ^2H analysis. The USGS42 hair sample was calibrated with a three-point calibration curve to the reference materials (i.e., CBS, KHS, and USGS43), while USGS42 and the two chitin internal standards were used as quality checks. The measured δ^2H values for USGS42 (−72.5 ± 1.6‰, $n = 4$), spongy moths (−63.67 ± 0.52‰, $n = 6$), and Alfa Aesar chitin (−19.25 ± 0.96‰, $n = 4$) were within the reported value and uncertainty. The analytical precision of these measurements is based on the reproducibility of USGS42 and the chitin internal standards, and is better than ±2‰. All δ^2H measurements are reported following the international scale VSMOW-SLAP.

Strontium isotope ratio analysis

To remove the glue and other potential contaminants deposited on samples, we cleaned abdomen, thorax, and head tissue in a 2:1 chloroform:methanol solution in three successive washes for 30 min, 3 h, and 15 min, respectively, (Supplementary Figure 2). Samples were air dried in a class-100 fume hood and stored in glassine envelopes. Samples were then digested in concentrated nitric acid (16 M; distilled TraceMetal™ Grade; Fisher Chemical, Canada) for 15 min at 250°C using Microwave digestion (Organic High setting—Anton Paar Multiwave 7,000, Austria). After digestion, the vials were limpid suggesting complete digestion. After drying the sample, 1 ml 6 M HNO_3 was added to each vial and then transferred to a 7 ml Savillex PTFE vial. An aliquot of 50 µL of the solution from each Savillex vial was pipetted to Labcon MetalFree™ centrifuge tubes and diluted with 2 ml of 2% v/v HNO_3. Sr concentration analysis was performed by Inductively Coupled Plasma Mass Spectrometry (ICP-MS) (Agilent 8800 triple quadrupole mass spectrometer) at the Department of Earth and Environmental Sciences, University of Ottawa. Calibration standards were prepared using single element certified standards purchased from SCP Science (Montreal, Canada).

The remaining ∼1 ml aliquot of the sample in the 7 ml Savillex PTFE vial was dried down and re-dissolved in 1 ml 6 M HNO_3. The separation of Sr was processed in 100 µL microcolumns loaded with Sr-spec ResinTM (100–150 µm; Eichrom Technologies, LLC). The matrix was rinsed out using 6 M HNO_3. The Sr was collected with 0.05 M HNO_3. After separation, the eluates were dried and re-dissolved in 200 µL 2% v/v HNO_3 for $^{87}Sr/^{86}Sr$ analysis. The $^{87}Sr/^{86}Sr$ analysis was performed at the Pacific Centre for Isotopic and Geochemical Research using a Nu-Plasma II high-resolution multi-collector inductively coupled plasma mass spectrometer (MC-ICP-MS; Nu Instruments) coupled to a desolvating nebulizer (Aridus IITM, CETAC Technologies). The interference of ^{87}Sr was corrected by subtracting the amount of ^{87}Rb corresponding to the ^{85}Rb signal. Interferences of 84Sr and 86Sr were corrected by subtracting the amount of 84Kr and 86Kr corresponding to the 83Kr signal. Instrumental mass fractionation was corrected by normalizing $^{86}Sr/^{88}Sr$ to 0.1194 using the exponential law. Strontium isotope compositions are reported as $^{87}Sr/^{86}Sr$ ratios. The reproducibility of the $^{87}Sr/^{86}Sr$ measurement for 5 ppb NIST SRM987 is 0.71025 ± 0.00009 (1 SD, n = 138) and for 1.4 ppb NIST SRM987 0.71019 ± 0.00011 (1 SD, n = 48). As Lepidoptera cuticle is made of chitin, we also used one chitin internal standard, 5 ppb Alfa Aesar chitin 0.713959 ± 0.00009 (1SD, n = 3).

Statistical analyses

Since spruce budworm larvae have limited mobility, local individuals ought to have formed their tissues within the same location under a limited area. Thus, we expect putative local individuals captured at a given site to have similar δ^2H values and $^{87}Sr/^{86}Sr$ ratios to each other. Furthermore, we expect isotope variation among these putative locals to have limited variation. At a given site,

δ^2H values usually fit a normal distribution (Hobson et al., 1999) whereas $^{87}Sr/^{86}Sr$ ratios can fit either a normal or lognormal distribution depending on the geological context (Bataille et al., 2020). Here, we assume a normal distribution for both isotopes at the site of collection. Unlike locals, immigrants arriving at a site may have heterogeneous origins -i.e., can originate in different sites across a broad spatial extent- and thus we expect them to have different isotopic values among themselves. Heterogeneous origins can also lead to non-normal distributions of values, and therefore, we chose not to treat putative immigrants at a given capture site as if they were part of a homogeneous group. For these reasons, at each site and for each isotopic system, we performed a non-traditional equivalent to a t-test on individual putative immigrants -instead of the group of immigrants as a whole- and compared them to the local population mean and standard deviation, as a way to determine whether they were true immigrants. This test uses a t-statistic to obtain a value of p (see derivation in Supplementary Materials 4). The test statistic we derive is equivalent to that of a two-sample t-test under the assumption of equal variances; however in our case, we are not rejecting the hypothesis that the means are equal but that both the means and the variances are equal. Thus, rejecting the null hypothesis in our case is either rejecting the hypothesis that the means are equal or that the variances are equal (we do not have enough information to know which, though it does not matter in our case).

We further explored whether the isotopic composition of spruce budworm can be used to detect an immigration event by discriminating between locals and immigrants using the combined information from dual hydrogen and strontium isotopes. Due to the uncertainty in the classification of observed individuals into local vs. immigrant groups, traditional methods for testing differences between groups (such as t-tests) have reduced power. While a t-test exists under uncertain group membership conditions (Bauer et al., 2021), this test relies on quantifying the group membership probability, and assumes equal variances and normality for both groups. We do not expect the variance of the local and immigrant groups to be the same, and since the immigrant group could have several different geographic origins, we cannot assume that the distributions of observed values for the immigrant groups are normal. With these violations of the typical assumptions required for comparing groups, along with the additional issue of uncertain group membership, we decided to examine robust estimates of location and scale for the assumed local groups in each location. By using a median to represent location and a scaled median absolute deviation (Rousseeuw and Croux, 1993) to represent scale, we anchor the estimates to central points in the group; ideally, these points are the most likely to actually belong to that group. We were unable to use robust estimates for the correlation between δ^2H and $^{87}Sr/^{86}Sr$, due to very small sample sizes of single observations with both measurements. We created bivariate normal ellipses to discriminate the local population signal from immigrant individuals. To this end, the median values for δ^2H and $^{87}Sr/^{86}Sr$ were calculated across all putative local observations for each site, and these values were used as the location parameters. The median absolute deviations of these observations were also calculated, and scaled to use as estimates for sigma, the marginal standard deviations. To draw the ellipses, 100 points were sampled from bivariate normal distributions parameterized by these values along with the estimates of correlation, and the ggplot function stat_ellipse() was applied (package tidyverse Wickham et al., 2019). Only ellipses for putative local groups were generated since we do not assume that the values of our variables of interest in the immigrant groups are normally distributed. It is important to note that these plots are mainly for exploration and comparison, and are not used as a formal test or indication of group membership.

All analyses were performed using R 4.0.3 (R Core Team, 2020). We used the ggplot2 (Wickham, 2016) package for figures and the rgdal (Bivand et al., 2022) and raster (Hijmans, 2020) packages for spatial analyses.

Results

Trap capture over flight season

The frequency and number of captures in our automated trap network varied by site, in a manner consistent with expected population densities. Traps outside the spruce budworm outbreak area had in general a lower number of captures, reflective of lower density populations (i.e., Arisaig and Inverness, but less so at Zinc Mine), whereas sites within the current outbreak zone had a high number of daily captures, as expected for high-density populations (i.e., Forestville, St. Modeste and Baldwin) (Figure 2). At Arisaig and Inverness (Nova Scotia – Figures 2A,B), we sampled for putative locals early during the flight season (i.e., when adults are present in the area), at a time point which ought to reflect local activity because capture numbers are initially low and increase through the days, environmental conditions matched expected adult emergence phenology for that latitude, and no immigration events were detected on the days before or immediately following sampling. At these two sites, immigration events on the 23rd of July 2020 were confirmed by radar and the event occurred about 10 days after local activity had ceased at Arisaig, and at least 2 weeks after the time-point we sampled for locals. Despite our expectation of immigrants arriving overnight (after 23:00), these putative immigrants arrived between 17:00 and 23:00. At Zinc Mine (Newfoundland–Figure 2C) we sampled putative locals from captures on the 30th of July between 19:00 to 23:00, and captures from the 31st July between 07:00 to 19:00 and 19:00 to 23:00, whereas putative immigrants were identified through radar images showing a large dispersal event and sampled from a capture between 19:00 and 23:00 on 3rd August 2019. Capture times were different from other sites to have a better resolution of potential immigrants arriving from the mainland. Additionally, some mixing between putative locals and immigrants is likely to have occurred since on the night of July 30th an immigration event, confirmed by light traps and radar, was detected at this site.

At St. Modeste and Baldwin (Quebec), putative immigrants were captured between 23:00 and 05:00 following dispersal events confirmed by radar (St. Modeste- 19th–20th July 2019, Baldwin-26th–27th July 2019), and putative locals were sampled from captures between 17:00 and 23:00 the same night (i.e., July 19th at St. Modeste and July 26th at Baldwin) (Figures 2E,F). It is possible that dawn captures could be a mix of true local individuals flying close to dusk and early arriving immigrants. Additionally, although no radar-confirmed immigration events were detected previously at these two sites, high and sudden peaks on 14th and 15th July at St. Modeste, and the 23rd July at Baldwin, are suggestive of an earlier immigration event

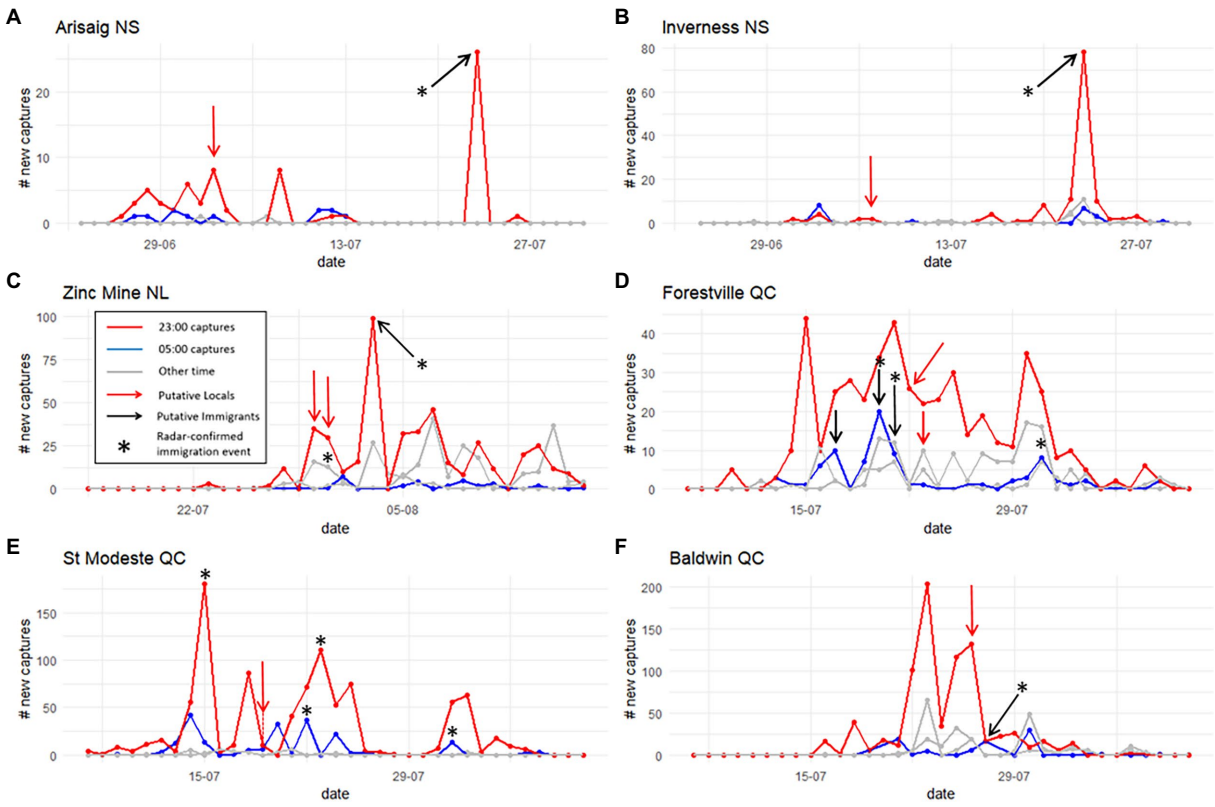

FIGURE 2
Number of eastern spruce budworm moths caught at each site on a given date and time. Each panel represents the flight season (June to August) captures of a given trap **(A–F)**. Moths collected between 17:00 and 23:00 (red line) are often assumed to be putative locals, whereas moths captured between 23:00 and 05:00 (blue line) are generally interpreted as putative immigrants. Captures between 5:00 and 17:00 (gray lines) are more difficult to interpret and could be composed of late-arriving immigrants or early-flying locals. Arrows indicate time of sampling of local individuals (red arrows) and immigrant individuals (black arrows) for isotope analyses.

before our sample collection. At Forestville (Quebec - Figure 2D) we sampled putative immigrants from captures between 23:00 and 05:00 on the nights of 16th to the 17th July 2019 and 2 nights later on 19th to 20th of July. The peaks of July 17th and 20th at dawn are suggestive of an immigration event, and on July 20th, we also have radar confirmation of a mass flight reaching this area. We sampled putative locals from captures between 17:00 and 23:00 on the 22nd July 2019.

Hydrogen isotope composition differences between local and immigrant spruce budworm

The δ^2H values of putative immigrant individuals were different from that of the putative local group mean in Arisaig (Figure 3). At sites like Arisaig and Inverness, which are on the margins of the spruce budworm distribution, and where putative locals were collected much earlier than any suspected immigration event, all putative immigrants were far away from the local population and had lower δ^2H values than putative locals (Arisaig, Figure 3A) or show values suggestive of possible, albeit non-significant, distant origin (Inverness, Figure 3B). At other sites, apparent differences in δ^2H values were not significant. Individuals seem to diverge, non-significantly, from the local population δ^2H values at Forestville (Figure 3D) and St. Modeste (Figure 3E) but not at the remaining populations (3C, 3F). The Forestville and St. Modeste putative immigrants (not significantly different) had lower or higher δ^2H values than the average local population. None of the putative immigrants at Zinc Mine or Baldwin had δ^2H values that were significantly different from those of the putative local population values (Figures 3C,F).

$^{87}Sr/^{86}Sr$ differences between local and immigrant spruce budworm

When comparing individual immigrants to the mean local population value, we found that $^{87}Sr/^{86}Sr$ ratios of putative immigrant individuals differed significantly in two of the six populations (Figure 4), consistent with δ^2H value results. As with δ^2H values, Arisaig and Inverness showed putative immigrants having significantly different $^{87}Sr/^{86}Sr$ ratios than those of the putative locals. At Arisaig, immigrants developed in locations which have higher $^{87}Sr/^{86}Sr$ ratios (Figure 4A), whereas at Inverness, immigrants arrived from sites with both higher and lower $^{87}Sr/^{86}Sr$ ratios (Figure 4B). Zinc Mine, on the other hand, did not show significant differences in the $^{87}Sr/^{86}Sr$ ratios of putative immigrant individuals and those of putative locals (Figure 4C). At St. Modeste and Baldwin, where putative immigrants

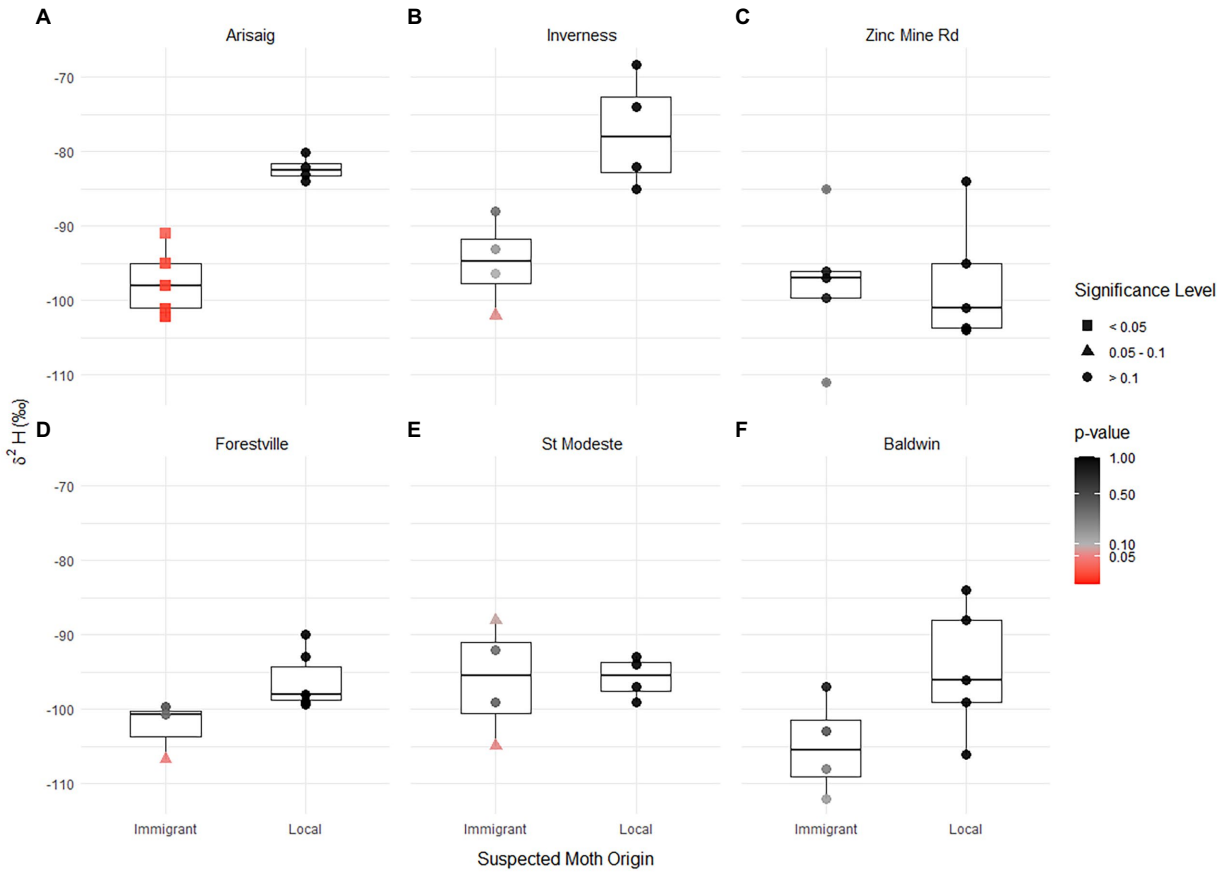

FIGURE 3
Box and whisker plot of δ^2H values for immigrant and local spruce budworm individuals by sampling site (population, **A–F**). Points represent individual samples. Putative local individuals are colored black, immigrant individual symbols represent whether they significantly differ from locals (squares; *t*-test; value of $p<0.05$), were not significantly circle (black; *t*-test; value of $p>0.1$) or were marginally non-significant (triangles; *t*-test; $0.1>$value of $p>0.05$).

were sampled immediately following the sampling of putative locals (23:00 to 05:00 and 17:00 to 23:00, respectively), the $^{87}Sr/^{86}Sr$ ratios of putative immigrants did not differ significantly from that of putative locals (Figures 4E,F), despite the strontium isotope ratio of these putative immigrants spanning a broad range of values suggesting different origins from putative locals, and a marginally non-significant $^{87}Sr/^{86}Sr$ ratio for a putative immigrant in Baldwin. At Forestville, where immigration events had occurred five and two days before we sampled for local individuals, we found no difference between putative immigrant individuals and the putative local $^{87}Sr/^{86}Sr$ ratios. Yet the range of putative local values is extreme in comparison with the isotope variation present in other putative local groups (from 0.71147 to 0.71440—Figure 4D).

Dual hydrogen and strontium isotopes among local populations and immigrant individuals

Overall, in most instances, putative immigrants can be confirmed as true immigrant individuals since they do not fall in the same range of combined δ^2H and $^{87}Sr/^{86}Sr$ values as locals (i.e., they fall out of the ellipses which are centered in the median value for both isotopes for putative locals–Figure 5). In particular, at Arisaig (Figure 5A) and Inverness (Figure 5B) all putative immigrants fall outside of the local confidence interval, showing that they developed at a site with different isotopic composition. Zinc Mine showed limited divergence among putative locals and immigrants, and our interpretations were limited by the scarcity of individuals we were able to sample for both δ^2H values and $^{87}Sr/^{86}Sr$ ratios, which did not allow us to create bivariate normal ellipses for this site. At St. Modeste (Figure 5E) and Baldwin (Figure 5F) some putative immigrants fall outside the ellipses whereas others are mixed with the putative local group and cannot be differentiated from putative locals, a result that is consistent with the single isotope data. The putative locals at Baldwin have a broad range of values for both δ^2H values and $^{87}Sr/^{86}Sr$ ratios, a range of values unlikely for true locals. Forestville shows another interesting pattern, where several immigrants can be detected, but where putative locals also have more extreme values than immigrants (Figure 5D).

Discussion

The eastern spruce budworm is the most severe pest of the boreal forest and causes millions of dollars in lost revenue to the Canadian economy during outbreak periods (Maclean, 2019). A key component

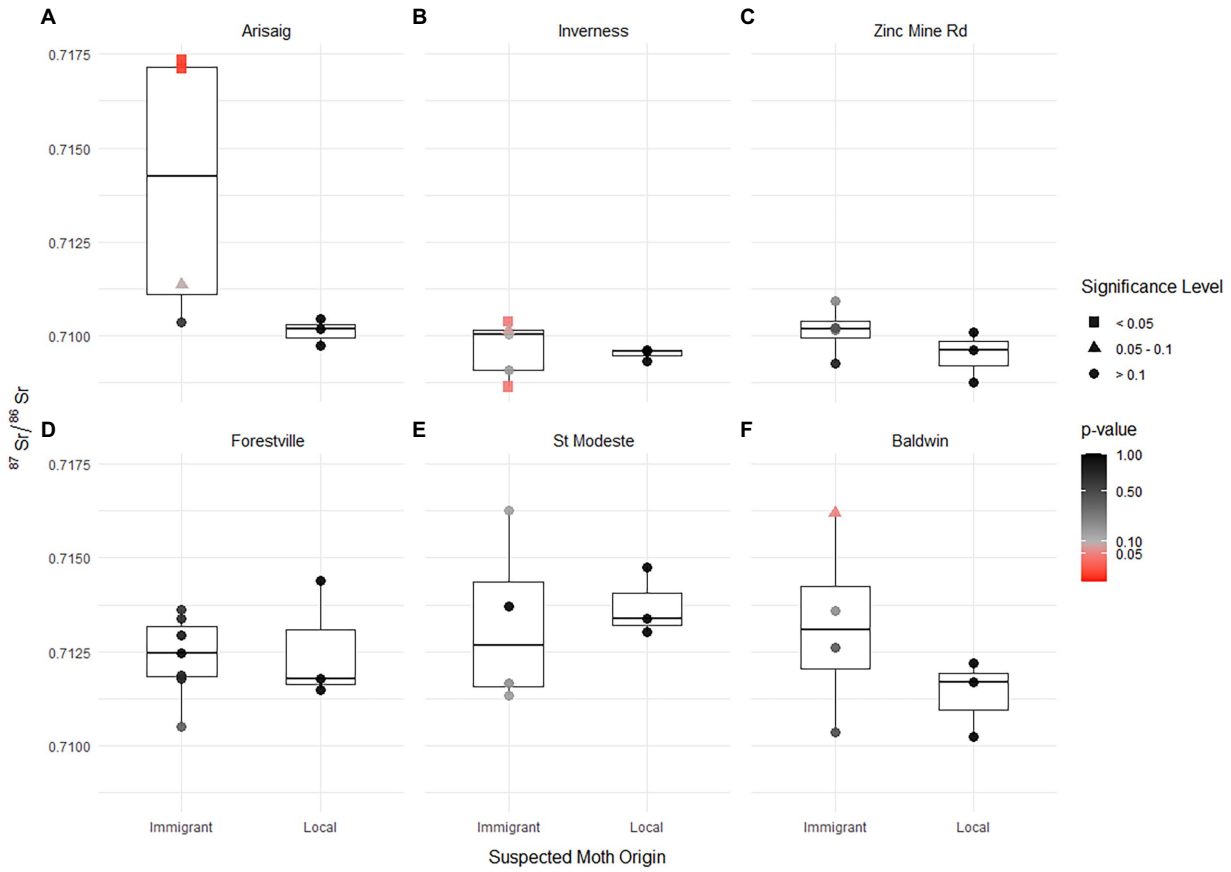

FIGURE 4
Box and whisker plot of $^{87}Sr/^{86}Sr$ ratios for immigrant and local spruce budworm individuals by sampling site (population, **A–F**). Local individuals are colored black, immigrant individual symbols represent whether they significantly differ from locals (squares; *t*-test; value of $p < 0.05$), were not significantly different (circles; *t*-test; value of $p > 0.1$) or were marginally non-significant (triangles; *t*-test; 0.105>value of $p > 0.05$<=0.1).

of outbreak dynamics and spread is dispersal from areas of high spruce budworm density (i.e., areas undergoing an outbreak) to areas of low density [i.e., undergoing endemic dynamics where spruce budworm populations numbers are kept down through low larval survival rates while foliage searching and through the action of predators and parasitoids (Stedinger, 1984)]. Spruce budworm moth dispersal has been challenging to monitor and manage, despite major improvements in the understanding of the ecology and pest control strategies of the species (Johns et al., 2019; Maclean, 2019). In this study, we use hydrogen and strontium isotopes to improve an approach currently used to determine migration events, which combines a network of automated traps that record the date and time of capture in discrete blocks, and evidence of local activity and dispersal from radar data, weather patterns and phenological records (see Materials and Methods).

We found that both δ^2H values and $^{87}Sr/^{86}Sr$ ratios, individually and when combined, allow to discriminate between putative locals and immigrants (i.e., putative immigrants confirmed to be distinct from the local population isotopic values). The isotope data generally supports the current classification approach based on time of capture (and other lines of evidence), particularly for identifying immigrants, and thus confirm that immigration events did occur by providing evidence that non-local spruce budworm are present at a given site. Among all the putative immigrants analyzed, at least one individual per site shows independent isotope data that differed significantly from that of putative local populations in two out of six populations (Figures 3, 4) and for five of the six populations when comparing dual-isotope signals (Figure 5). Yet, in some instances, the flight behavior and isotope methods do not support each other in identifying locals vs. immigrants. In particular, when immigration events occurred before the collection of putative locals (e.g., up to approximately 1 week, e.g., Forestville, QC and Zinc Mine, NL) or when putative locals were collected immediately before an immigration event (e.g., Baldwin and St. Modeste, QC), the overlapping activity between locals and immigrants may lead to misclassification of trap captures when it is only based on behavior (Figure 2). Our approach using combined δ^2H values and $^{87}Sr/^{86}Sr$ ratios enhances the resolution of the above methods and allows to distinguish between spruce budworm that completed their larval cycle at the site of capture (i.e., locals) vs. individuals from sites that differed in their isotopic composition (i.e., confirmed immigrants) (Figure 5). In particular, our novel isotopic tool allows to identify instances of potential misclassification and to make inferences about mixing of locals and immigrants in the population. Thus, δ^2H values and $^{87}Sr/^{86}Sr$ ratios are an effective tool to confirm whether an immigration event has occurred at a given site and, with larger sample sizes, could also help determine the relative composition of locals and immigrants in a given site.

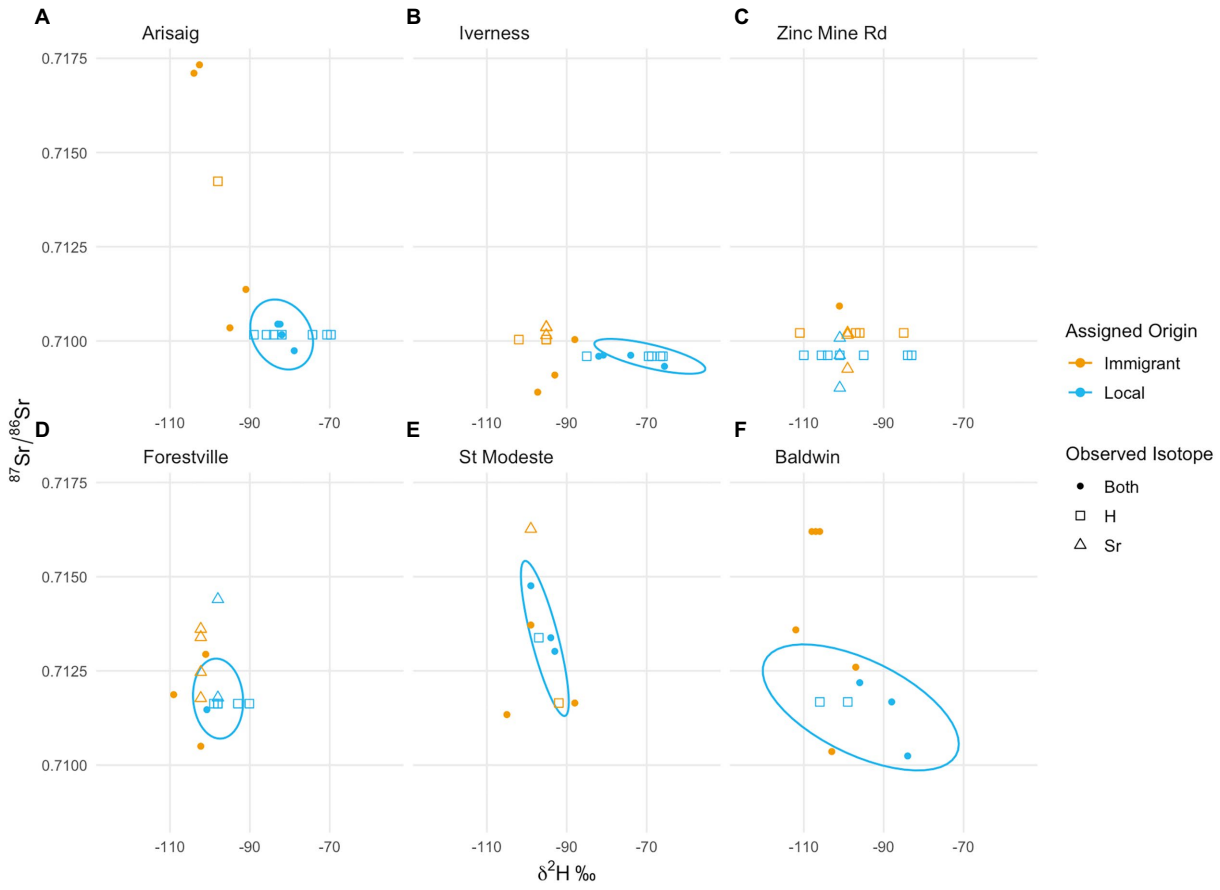

FIGURE 5
Dual isotope trait-space plot showing local population values (ellipse) and individual immigrants by site. Individuals with both a δ^2H values and $^{87}Sr/^{86}Sr$ ratios are represented by filled symbols, individuals with only one isotope system measured are plotted at the median value of the isotope that was not measured. Points are segregated by putative immigrant/local status (δ^2H-only values=squares, $^{87}Sr/^{86}Sr$-only ratios=triangles). Ellipses are bivariate normal, centered in the media value of both isotope systems and used to visually discriminate between the local signal and immigrants. Zinc Mine only had one individual with dual isotope data, and we could not parametrize an ellipse. Each panel **(A–F)** represents an independent sampling site/trap location.

The confidence with which putative immigrants and locals were successfully identified based on capture-time and flight behavior differed among sites, and reflected the nuances of local activity and immigration history at the sites of capture (Figure 2). Arisaig and Inverness (Nova Scotia) are located outside the range of the current spruce budworm outbreak and have low, endemic, population densities (i.e., comparatively low trap capture numbers) and experience less frequent immigration events (Figure 1). At these sites, only one immigration event was detected during the 2020 season and occurred several days (~10 days) after the peak activity of the local population (Figures 2A,B). The timing of the immigration event, close to dusk rather than after 23:00, suggests that these immigrants may have originated relatively close to (i.e., not hundreds of kilometers away) the capture sites, but the differences in δ^2H values, in a few instances over 20‰, suggests that these individuals might have come from inland areas further north and away from the coast (Figures 3A,B). The $^{87}Sr/^{86}Sr$ ratios are generally higher and corroborate that the immigrants did originate in a site different from the capture (local) site. The higher $^{87}Sr/^{86}Sr$ ratios of immigrants at Arisaig (up to 0.717) support a northern origin on the Precambrian North American craton in Quebec, whereas the variable $^{87}Sr/^{86}Sr$ ratios of immigrants at Inverness suggest a more regional origin with $^{87}Sr/^{86}Sr$ ratios typical of the geologically younger Maritimes (Figures 3A,B). At both sites, dual isotope plots show clear discrimination among immigrant individuals and local values (Figures 5A,B). Furthermore, immigrants at both sites show a broad range of isotopic values, suggesting that they do not come from a single area but instead have different geographical origins covering a likely broad spatial extent consistent with a large dispersal event. The remainder of the sites we sampled reveal a more complex pattern of immigrant and local distributions, highlighting some of the limitations of the flight-behavior approach at high spatial resolutions, and underscoring the value of using isotopes to study spruce budworm dispersal.

Using δ^2H values and $^{87}Sr/^{86}Sr$ ratios showed that several putative immigrants were indeed immigrants, that is, these individuals had significantly distinct δ^2H values and $^{87}Sr/^{86}Sr$ ratios from the putative local populations (Figures 3,5). This demonstrates that the combined approaches used to detect immigration (e.g., flight-behavior and timing, radar, phenology, weather) are an effective tool to confirm whether an immigration event has occurred at a given area. Yet, our results also showed a few instances of putative local values falling well

outside the range of expected local isotopic variation (e.g., Figures 3C,F, 4D), and several instances of putative immigrants not being different from putative local values.

The first set of unusual outcomes points to likely misclassification of immigrants as putative locals. For example, the δ^2H value of the putative local at Zinc Mine with a value of −84‰ (Figure 3C) and the putative local at Forestville with an $^{87}Sr/^{86}Sr$ ratio of 0.71440 (Figure 4D) place them as outliers and is well beyond the expectation of local variation that corresponds to a 20 km radius of variation in δ^2H values from precipitation or in bioavailable $^{87}Sr/^{86}Sr$ ratios (Supplementary Table 5). One possible explanation for this potential misclassification is that following immigration to a given site, surviving immigrants then behave as locals on subsequent days, and lead to the mixing of immigrant and local individuals, an issue that is detected by our isotope tools but which current approaches, including population genetics (e.g., Lumley et al., 2020), have been unable to address.

Putative immigrant individuals that were not significantly isotopically distinct from local groups can be interpreted in several ways. First, they could be 'true' locals that were flying during the arrival of immigrants and thus are misclassified individuals. Although local flying activity and the likelihood of encountering the traps are expected to be highest around dusk (Greenbank et al., 1980), it is not known whether the influx of large numbers of immigrants and the likely spike in pheromones from arriving females, could influence local male activity and induce them to become active. Second, given that in our analyses immigrants are defined by comparison to putative locals, limited sample sizes of local individuals and misclassifications - which increase the estimate of the population variance - likely decrease our ability to detect 'true' immigrants. For example, removing the outlier putative local from Forestville (i.e., the individual with an $^{87}Sr/^{86}Sr$ ratio of 0.71440) changes the putative local mean (± sd) and decreases the standard deviation from 0.71255 (±0.00161) to 0.71163 (±0.00023), making the difference between putative immigrants and locals more conspicuous. Increasing sample size and quality of local individuals (i.e., collections before the arrival of immigrants) will improve the precision of immigrant identification—as is shown by assays in Arisaig and Inverness. Third, individuals that were not significantly different could still be immigrants, but which had originated at sites that have similar isotopic signatures to the local site or had traveled only a short distance. While both δ^2H values and $^{87}Sr/^{86}Sr$ ratios are redundant independently (Bowen et al., 2005; Bataille et al., 2020), the redundancy decreases substantially when combining these isotope tools because of their independent patterns and scales of variation (Wunder, 2010). Globally, δ^2H varies continuously at large spatial scales, with decreasing values as latitude increases and increasing distance away from coastal regions (Bowen and Revenaugh, 2003), and thus non-significant differences in δ^2H values could be expected for short-distance migrants coming from climatically similar regions. $^{87}Sr/^{86}Sr$ ratios vary at a high spatial resolution, reflecting the age and composition of local geology, and thus, even short-distance travelers could show significant divergence in their $^{87}Sr/^{86}Sr$ ratios. However, $^{87}Sr/^{86}Sr$ ratios are highly redundant at regional to global scale (Bataille et al., 2020). Therefore, similar dual hydrogen and strontium isotopes between locals and immigrants is unlikely.

We expected, based on their patterns and scales of variation, that local individuals would show limited variance in both δ^2H values and especially $^{87}Sr/^{86}Sr$ ratios, since they originate in the same location and are expected to have limited dispersal (Sanders, 1983), relative to immigrant individuals that can have more spatially heterogeneous origins. We indeed find that, overall, $^{87}Sr/^{86}Sr$ ratios tended to show smaller variance among locals than immigrant individuals (in particular when we consider potential misclassification of putative locals–e.g. Forestville, QC) (Figure 4). With the exception of Arisaig, we did not detect this same trend in δ^2H variance which is likely related to the low scale and continuous variation of this isotope. However, this observation of similar variance between immigrants and locals also underlines the relatively large δ^2H variance of local individuals (SD = Arisaig: 1.66‰, Inverness: 7.6‰, Zinc Mine: 8.38‰, Forestville: 3.82‰, St. Modeste: 2.75‰, Baldwin: 8.76‰) well beyond the analytical uncertainty (<2‰). Typical sources of variation in local δ^2H values, such as seasonal shifts in precipitation and evaporation, adult feeding, and the formation of new tissue, are unlikely to be relevant to this species. Spruce budworm are short-lived and all individuals at any site have their life-history synchronized, with the emergence of adults—a reflection of developmental rates—occurring within a two-week period (Kucera, 1980; Sanders, 1985). Additionally, spruce budworm does not feed as adults and we sampled wings for δ^2H analysis, which have low metabolic activity (Lindroos et al., 2023, this issue), making seasonal variation in precipitation δ^2H values unlikely to cause variation in the local moth values. Diet-induced variations at a given site are possible, as local spruce budworm could feed on different trees with distinct water sources (e.g., precipitation, groundwater, lake, river) depending on their rooting depth and position on the landscape. If the local landscape has multiple isotopically distinct reservoirs, this could add further heterogeneity to the δ^2H values that get integrated into spruce and balsam fir needles and then transferred to spruce budworm, further increasing local δ^2H value variance. Even within one single tree, there are several layers of needles grown at different years which might have δ^2H differences. While spruce budworms are known to feed preferentially on fresh needles they can switch to older needles if they emerge too early in the spring to access young needles or when younger needles are not available (Régnière and Nealis, 2008). In any case, our data support the work of Hobson et al. (1999); Hobson (2019) who found that the δ^2H values of locally raised monarch butterflies had a standard deviation of approximately 4.5‰ within any given site. Other studies that have analyzed known-origin Lepidoptera also report large intra-site standard deviation, sometimes >5‰ (e.g., Brattström et al., 2008; Satterfield et al., 2018). When considered together, our isotope results suggest that local moth individuals move further than the 100 m suggested by Sanders (1983). Isotope data rather suggest local mobility in the scale of kilometers but precisely determining the range and drivers of local spruce budworm movements requires further investigation.

Our findings have fundamental and applied implications. First, we provide an independent validation that the combined use of automated traps, radar monitoring, phenology, and weather data is effective at detecting immigration events in spruce budworm, while underscoring the complementarity of using isotopes to validate and enhance the resolution of this trap network. Second, the difficulty in confirming immigration events in spruce budworm means that current approaches to management rely heavily on widespread winter monitoring of larvae at sites with endemic population dynamics, to detect early immigration-driven population increases and to control

population growth before it shifts to an outbreak stage (Early Intervention Strategy - Johns et al., 2019; Maclean, 2019). Although this approach is proving to be effective (Maclean et al., 2019), it is also expensive. The combined use of automated traps and isotopes provides a more targeted approach to confirm immigration events, estimate the relative proportion to which they contribute to the local adult population—a proxy for the following year's reproductive output and population density—and allow cost-effective decision-making of where to invest in subsequent larval monitoring and eradication strategies. Finally, we confirmed that dual hydrogen-strontium isotopic tools can be applied for the geolocation of low-mass insect species with wing material for hydrogen isotope analysis below 150 μg (~ two wings) and body mass for strontium isotopes below 3 mg. We also confirmed that combined δ^2H values and ^{87}Sr/^{86}Sr ratios have enough discriminatory power to investigate the dispersal of these small insect species over small spatial scales (i.e., <100 km). To better understand dispersal dynamics in this system, our next step is to complete analyses on known-origin samples, which will considerably reduce variance around the local population mean, develop spruce budworm moth-calibrated δ^2H and ^{87}Sr/^{86}Sr isoscapes for Eastern Canada, and then perform dual continuous isotope assignment of immigrant moths and reconstruct their origin and dispersal trajectory. The development of these isotope tools to study non-migratory wind-assisted dispersal behavior of small winged insects will open new research avenues to investigate the mobility of many Boreal pest species (e.g., emerald ash borer, mountain pine beetle, spongy moth and Asian long-horned beetle). Dual isotope geolocation can help ascertain if the pest in question has been in a particular region for a long period (i.e., locally reared pest) or if it has recently arrived (i.e., long-distance migrants or invasives). It can also help identify their dispersal routes. Cumulatively, this information is key to develop more efficient early-eradication strategies (e.g., containment and spraying efforts) and to improve the cost-effectiveness and sustainability of forest management decisions by industry and government practitioners.

Data availability statement

The raw data supporting the conclusions of this article can be found in the Supplementary material.

Author contributions

FD, J-NC, and CB: conceived and designed the project. FD, J-NC, KP, and MR: collected data. FD, J-NC, KS, and CB: analyzed the data. J-NC and CB: contributed reagents/materials/analysis tools. FD: wrote the first draft with input from coauthors. FD, J-NC, KS, KP, MR, and CB: revised and edited the manuscript. All authors contributed to the article and approved the submitted version.

Funding

This study was funded through Healthy Forest Partnership Early Intervention Strategy against Spruce Budworm Phase II Contribution Program awarded to the Invasive Species Centre by Natural Resources Canada. BCP also received funding from the University of Ottawa start-up fund, and NSERC Discovery Grant. MR was supported by the Queen Elizabeth II Graduate Scholarship in Science and Technology (QEII-GSST) and Ontario Graduate Scholarship.

Acknowledgments

The authors would like to thank our colleagues who helped collect samples at NRCan CFS [Emily Owens, Rob Johns, Gaetan Leclair, and Jeff Fidgen] and in the provinces [Pierre Therrien and Jean-Jacques Bertrand (Quebec MFFP), Dan Lavigne and Troy Rideout (Newfoundland FIA)], Kerry Klassen and Paul Middlestead at the Jan Veizer laboratory for developing the low-mass hydrogen analyses, and Lihai Hu and Smita Mohanty for help with ICP-MS and strontium analyses.

Conflict of interest

The authors declare that the research was conducted in the absence of any commercial or financial relationships that could be construed as a potential conflict of interest.

Publisher's note

Supplementary material

The Supplementary material for this article can be found online at: https://www.frontiersin.org/articles/10.3389/fevo.2023.1060982/full#supplementary-material

References

Bataille, C. P., Crowley, B. E., Wooller, M. J., and Bowen, G. J. (2020). Advances in global bioavailable strontium isoscapes. *Palaeogeogr. Palaeoclimatol. Palaeoecol.* 555:109849. doi: 10.1016/j.palaeo.2020.109849

Bauer, T. A., Folster, A., Braun, T., and Oertzen, T. V. (2021). A group comparison test under uncertain group membership. *Psychometrika* 86, 920–937. doi: 10.1007/s11336-021-09794-x

Bivand, R., Keitt, T., Rowlingson, B., Pebesma, E., Sumner, M., Hijmans, R., et al. (2022). Package 'rgdal' (R package version 1.5–32). Available at: https://CRAN.R-project.org/package=rgdal.

Bouchard, M., Kneeshaw, D., and Messier, C. (2007). Forest dynamics following spruce budworm outbreaks in the northern and southern mixedwoods of Central Quebec. *Can. J. For. Res.* 37, 763–772. doi: 10.1139/X06-278

Boulanger, Y., Fabry, F., Kilambi, A., Pureswaran, D. S., Sturtevant, B. R., and Saint-Amant, R. (2017). The use of weather surveillance radar and high-resolution three dimensional weather data to monitor a spruce budworm mass exodus flight. *Agric. For. Meteorol.* 234-235, 127–135. doi: 10.1016/j.agrformet.2016.12.018

Bowen, G. J., and Revenaugh, J. (2003). Interpolating the isotopic composition of modern meteoric precipitation. *Water Resour. Res.* 39, 1–13. doi: 10.1029/2003WR002086

Bowen, G. J., Wassenaar, L. I., and Hobson, K. A. (2005). Global application of stable hydrogen and oxygen isotopes to wildlife forensics. *Oecologia* 143, 337–348. doi: 10.1007/s00442-004-1813-y

Bowen, G. J., and West, J. B. (2019). "Isoscapes for terrestrial migration research" in *Tracking animal migration with stable isotopes* (Amsterdam: Elsevier), 53–84.

Brattström, O., Wassenaar, L. I., Hobson, K. A., and Åkesson, S. (2008). Placing butterflies on the map – testing regional geographical resolution of three stable isotopes in Sweden using the monophagus peacock Inachis io. *Ecography* 31, 490–498. doi: 10.1111/j.0906-7590.2008.05267.x

Canada, G.S.O., and Wheeler, J. (1996). Geological map of Canada: Carte Géologique Du Canada. Geological survey of Canada.

Chang, W.-Y., Lantz, V. A., Hennigar, C. R., and Maclean, D. A. (2012). Economic impacts of forest pests: a case study of spruce budworm outbreaks and control in New Brunswick, Canada. *Can. J. For. Res.* 42, 490–505. doi: 10.1139/x11-190

Coplen, T. B., and Qi, H. (2012). USGS42 and USGS43: Human-hair stable hydrogen and oxygen isotopic reference materials and analytical methods for forensic science and implications for published measurement results. *Forensic Sci. Int.* 214, 135–141.

Dymond, C. C., Neilson, E. T., Stinson, G., Porter, K., Maclean, D. A., Gray, D. R., et al. (2010). Future spruce budworm outbreak may create a carbon source in eastern Canadian forests. *Ecosystems* 13, 917–931. doi: 10.1007/s10021-010-9364-z

Flockhart, D. T. T., Kyser, T. K., Chipley, D., Miller, N. G., and Norris, D. R. (2015). Experimental evidence shows no fractionation of strontium isotopes (87Sr/86Sr) among soil, plants, and herbivores: implications for tracking wildlife and forensic science. *Isot. Environ. Health Stud.* 51, 372–381. doi: 10.1080/10256016.2015.1021345

Greenbank, D. O., Schaefer, G. W., and Rainey, R. C. (1980). Spruce budworm (Lepidoptera: Tortricidae) moth flight and dispersal: new understanding from canopy observations, radar, and aircraft. *Memo. Entomol. Soc. Canada* 112, 1–49. doi: 10.4039/entm112110fv

Hijmans, R. (2020). Raster: Geographic data analysis and modeling (R package version 3.3–13). Available at: https://CRAN.R-project.org/package=raster

Hobson, K. A., Wassenaar, L. I., and Taylor, O. R. (1999). Stable isotopes (δD and δ13C) are geographic indicators of natal origins of monarch butterflies in eastern North America. *Oecologia* 120, 397–404.

Hobson, K. A. (2019). "Application of isotopic methods to tracking animal movements" in *Tracking animal migration with stable isotopes* (Amsterdam: Elsevier), 85–115.

James, P. M. A., Robert, L.-E., Wotton, B. M., Martell, D. L., and Fleming, R. A. (2017). Lagged cumulative spruce budworm defoliation affects the risk of fire ignition in Ontario, Canada. *Ecol. Appl.* 27, 532–544. doi: 10.1002/eap.1463

Jardon, Y., Morin, H., and Dutilleul, P. (2003). Périodicité et synchronisme des épidémies de la tordeuse des bourgeons de l'épinette au Québec. *Can. J. For. Res.* 33, 1947–1961. doi: 10.1139/x03-108

Johns, R. C., Bowden, J. J., Carleton, D. R., Cooke, B. J., Edwards, S., Emilson, E. J., et al. (2019). A conceptual framework for the spruce budworm early intervention strategy: can outbreaks be stopped? *Forests* 10:910. doi: 10.3390/f10100910

Kucera, D. R. (1980). *Spruce budworm in the eastern United States*. Washington: US Department of Agriculture Forest Service.

Lindroos, E. E., Bataille, C. P., Holder, P. W., Talavera, G., and Reich, M. S. (2023). Temporal stability of δ2H in insect tissues: Implications for isotope-based geographic assignments. *Front. Ecol. Evol.* 11.

Ludwig, D., Jones, D. D., and Holling, C. S. (1978). Qualitative analysis of insect outbreak systems: the spruce budworm and forest. *J. Anim. Ecol.* 47, 315–332. doi: 10.2307/3939

Lumley, L. M., Pouliot, E., Laroche, J., Boyle, B., Brunet, B. M. T., Levesque, R. C., et al. (2020). Continent-wide population genomic structure and phylogeography of North America's most destructive conifer defoliator, the spruce budworm (*Choristoneura fumiferana*). *Ecol. Evol.* 10, 914–927. doi: 10.1002/ece3.5950

Ma, C., Vander Zanden, H. B., Wunder, M. B., and Bowen, G. J. (2020). assignR: an r package for isotope-based geographic assignment. *Methods Ecol. Evol.* 11, 996–1001. doi: 10.1111/2041-210X.13426

Maclean, D. A. (1980). Vulnerability of fir-spruce stands during uncontrolled spruce budworm outbreaks: a review and discussion. *For. Chron.* 56, 213–221. doi: 10.5558/tfc56213-5

Maclean, D. A. (2016). Impacts of insect outbreaks on tree mortality, productivity, and stand development. *Can. Entomol.* 148, S138–S159. doi: 10.4039/tce.2015.24

Maclean, D. A. (2019). Protection strategy against spruce budworm. *Forests* 10:1137. doi: 10.3390/f10121137

Maclean, D. A., Amirault, P., Amos-Binks, L., Carleton, D., Hennigar, C., Johns, R., et al. (2019). Positive results of an early intervention strategy to suppress a spruce budworm outbreak after five years of trials. *Forests* 10:448. doi: 10.3390/f10050448

Magozzi, S., Bataille, C. P., Hobson, K. A., Wunder, M. B., Howa, J. D., Contina, A., et al. (2021). Calibration chain transformation improves the comparability of organic hydrogen and oxygen stable isotope data. *Methods Ecol. Evol.* 12, 732–747. doi: 10.1111/2041-210X.13556

Meier-Augenstein, W., Chartrand, M. M. G., Kemp, H. F., and St-Jean, G. (2011). An inter-laboratory comparative study into sample preparation for both reproducible and repeatable forensic 2H isotope analysis of human hair by continuous flow isotope ratio mass spectrometry. *Rapid Commun. Mass Spectrom.* 25, 3331–3338. doi: 10.1002/rcm.5235

Menchetti, M., Guéguen, M., and Talavera, G. (2019). Spatio-temporal ecological niche modelling of multigenerational insect migrations. *Proc. R. Soc. B* 286:20191583. doi: 10.1098/rspb.2019.1583

Morris, R., and Miller, C. (1954). The development of life tables for the spruce budworm. *Can. J. Zool.* 32, 283–301. doi: 10.1139/z54-027

Natural Resources Canada (2021). The state of Canada's forests: Annual report 2020.).

Régnière, J., Cooke, B. J., Béchard, A., Dupont, A., and Therrien, P. (2019a). Dynamics and management of rising outbreak spruce budworm populations. *Forests* 10:748. doi: 10.3390/f10090748

Régnière, J., Garcia, M., and Saint-Amant, R. (2019b). Modeling migratory flight in the spruce budworm: circadian rhythm. *Forests* 10:877. doi: 10.3390/f10100877

Régnière, J., and Nealis, V. G. (2008). The fine-scale population dynamics of spruce budworm: survival of early instars related to forest condition. *Ecol. Entomol.* 33, 362–373. doi: 10.1111/j.1365-2311.2007.00977.x

Reich, M. S., Flockhart, D. T. T., Norris, D. R., Hu, L., and Bataille, C. P. (2021). Continuous-surface geographic assignment of migratory animals using strontium isotopes: a case study with monarch butterflies. *Methods Ecol. Evol.* 12, 2445–2457. doi: 10.1111/2041-210X.13707

Reich, M. S., Kindra, M., Dargent, F., Hu, L., Flockhart, D. T. T., Norris, D. R., et al. (2023). Metals and metal isotopes incorporation in insect wings: Implications for geolocation and pollution exposure. *Front. Ecol. Evol.* 11.

Rhainds, M., and Heard, S. B. (2015). Sampling procedures and adult sex ratios in spruce budworm. *Entomol. Exp. Appl.* 154, 91–101. doi: 10.1111/eea.12257

Rhainds, M., Lavigne, D., Boulanger, Y., Demerchant, I., Delisle, J., Motty, J., et al. (2022). I know it when I see it: incidence, timing and intensity of immigration in spruce budworm. *Agric. For. Entomol.* 24, 152–166. doi: 10.1111/afe.12479

Rousseeuw, P. J., and Croux, C. (1993). Alternatives to the median absolute deviation. *J. Am. Stat. Assoc.* 88, 1273–1283. doi: 10.1080/01621459.1993.10476408

Royama, T., Eveleigh, E. S., Morin, J. R. B., Pollock, S. J., Mccarthy, P. C., Mcdougall, G. A., et al. (2017). Mechanisms underlying spruce budworm outbreak processes as elucidated by a 14-year study in New Brunswick, Canada. *Ecol. Monogr.* 87, 600–631. doi: 10.1002/ecm.1270

Sanders, C. (1985). Recent advances in spruce budworms research, in: CANUSA spruce budworms research symposium (1984: Bangor, Me.): Canadian Forestry Service [distributor]).

Sanders, C. (1991). "Biology of north American spruce budworms" in *Tortricid pests, their biology, Natural enemies and control*. eds. L. Van Der Geest and H. Evenhuis (The Netherlands: Elsevier Science Publishers BV)

Sanders, C. J. (1983). Local dispersal of male spruce budworm (Lepidoptera: Tortricidae) moths determined by mark, release, and recapture. *Can. Entomol.* 115, 1065–1070. doi: 10.4039/Ent1151065-9

Sanders, C. J., Wallace, D. R., and Lucuik, G. S. (1978). Flight activity of female eastern spruce budworm (Lepidoptera: Tortricidae) at constant temperatures in the laboratory. *Can. Entomol.* 110, 627–632. doi: 10.4039/Ent110627-6

Satterfield, D. A., Maerz, J. C., Hunter, M. D., Flockhart, D. T. T., Hobson, K. A., Norris, D. R., et al. (2018). Migratory monarchs that encounter resident monarchs show life-history differences and higher rates of parasite infection. *Ecol. Lett.* 21, 1670–1680. doi: 10.1111/ele.13144

Sleep, D. J. H., Drever, M. C., and Szuba, K. J. (2009). Potential role of spruce budworm in range-wide decline of Canada warbler. *J. Wildl. Manag.* 73, 546–555. doi: 10.2193/2008-216

Soto, D. X, Koehler, G., Wassenaar, L. I., and Hobson, K. A. (2017). Re-evaluation of the hydrogen stable isotopic composition of keratin calibration standards for wildlife and forensic science applications. *Rapid Commun. Mass Spectrom.* 31, 1193–1203.

Stedinger, J. R. (1984). A spruce budworm-forest model and its implications for suppression programs. *For. Sci.* 30, 597–615.

Stein, A., Ngan, F., Draxler, R., and Chai, T. (2015). Potential use of transport and dispersion model ensembles for forecasting applications. *Weather Forecast.* 30, 639–655. doi: 10.1175/WAF-D-14-00153.1

R Core Team. (2020). R: A language and environment for statistical computing. R foundation for statistical computing, Vienna, Austria: R Core Team.

Urquhart, F. A., and Urquhart, N. R. (1978). Autumnal migration routes of the eastern population of the monarch butterfly (Danaus p. plexippus L.; Danaidae; Lepidoptera) in

North America to the overwintering site in the Neovolcanic plateau of Mexico. *Can. J. Zool.* 56, 1759–1764. doi: 10.1139/z78-240

Urquhart, F. A., and Urquhart, N. R. (1979). Vernal migration of the monarch butterfly (*Danaus p. plexippus*, Lepidoptera: Danaidae) in North America from the overwintering site in the neo-volcanic plateau of Mexico. *Can. Entomol.* 111, 15–18. doi: 10.4039/Ent11115-1

Warrant, E., Frost, B., Green, K., Mouritsen, H., Dreyer, D., Adden, A., et al. (2016). The Australian Bogong moth *Agrotis infusa*: a long-distance nocturnal navigator. *Front. Behav. Neurosci.* 10:77. doi: 10.3389/fnbeh.2016.00077

Wassenaar, L. I., and Hobson, K. A. (1998). Natal origins of migratory monarch butterflies at wintering colonies in Mexico: new isotopic evidence. *Proc. Natl. Acad. Sci. U. S. A.* 95, 15436–15439. doi: 10.1073/pnas.95.26.15436

Wickham, H. (2016). *ggplot2: Elegant graphics for data analysis*. London: Springer.

Wickham, H., Averick, M., Bryan, J., Chang, W., Mcgowan, L. D. A., François, R., et al. (2019). Welcome to the Tidyverse. *J. Open Sour. Softw.* 4:1686. doi: 10.21105/joss.01686

Wunder, M. B. (2010). "Using isoscapes to model probability surfaces for determining geographic origins" in *Isoscapes* (London: Springer), 251–270.

frontiers | Frontiers in Ecology and Evolution

TYPE Original Research
PUBLISHED 17 March 2023
DOI 10.3389/fevo.2023.1086616

OPEN ACCESS

EDITED BY
Todd Jason McWhorter,
University of Adelaide,
Australia

REVIEWED BY
Michał Filipiak,
Jagiellonian University,
Poland
Mario Diaz,
Spanish National Research Council (CSIC),
Spain

*CORRESPONDENCE
Çağan H. Şekercioğlu
✉ c.s@utah.edu

SPECIALTY SECTION
This article was submitted to Ecophysiology, a section of the journal Frontiers in Ecology and Evolution

RECEIVED 01 November 2022
ACCEPTED 21 February 2023
PUBLISHED 17 March 2023

CITATION
Şekercioğlu ÇH, Fullwood MJ, Cerling TE, Brenes FO, Daily GC, Ehrlich PR, Chamberlain P and Newsome SD (2023) Using stable isotopes to measure the dietary responses of Costa Rican forest birds to agricultural countryside.
Front. Ecol. Evol. 11:1086616.
doi: 10.3389/fevo.2023.1086616

Using stable isotopes to measure the dietary responses of Costa Rican forest birds to agricultural countryside

Çağan H. Şekercioğlu[1,2,3,4]*, Melissa J. Fullwood[5], Thure E. Cerling[1,6], Federico Oviedo Brenes[7], Gretchen C. Daily[2], Paul R. Ehrlich[2], Page Chamberlain[8] and Seth D. Newsome[9]

[1]School of Biological Sciences, University of Utah, Salt Lake City, UT, United States, [2]Center for Conservation Biology, Department of Biology, Stanford University, Stanford, CA, United States, [3]Department of Molecular Biology and Genetics, Koç University, Sarıyer, Istanbul, Türkiye, [4]KuzeyDoğa Society, Kars, Türkiye, [5]Cancer Science Institute of Singapore, National University of Singapore, Singapore, Singapore, [6]Department of Geology, Geophysics College of Mines and Earth Sciences, University of Utah, Salt Lake City, UT, United States, [7]300m Norte de la Escuela de Buena Vista, Barva, Heredia, Costa Rica, [8]Department of Geological Sciences, Doerr School of Sustainability, Stanford University, Stanford, CA, United States, [9]Department of Biology, University of New Mexico, Albuquerque, NM, United States

How human modification of native habitats changes the feeding patterns and nutritional ecology of tropical birds is critical to conserving avian biodiversity, but tropical bird diets are laborious to investigate using the traditional methods of diet analysis. Stable isotope analysis provides a cost-effective and efficient proxy to identify general foraging patterns, especially when dietary shifts spanning multiple trophic levels have occurred due to ecosystem disturbance or transformation. To characterize the diets of forest bird species that persist in tropical agricultural countryside, we compared feather carbon ($\delta^{13}C$) and nitrogen ($\delta^{15}N$) isotope values of four species caught and radio-tracked in a 270 hectare forest reserve, smaller forest remnants (including mature forest, secondary forest, and riparian strips), and coffee plantations in mid-elevation (*ca.* 800–1,400m) southern Costa Rica. Bird habitat choice had a significant effect on diet composition as revealed by $\delta^{13}C$ and $\delta^{15}N$ values. Three of the four species studied showed evidence of significantly reduced consumption of invertebrates in coffee plantations, with the isotope values of two species (*Tangara icterocephala* and *Mionectes oleaginous*) indicating, by comparison, nearly a doubling of invertebrate consumption in forest remnants. Our results suggest that coffee plantations are deficient in invertebrates preferred by forest generalist birds that forage in both native forest remnants and coffee plantations. In this region, typical of mountainous American tropics, small forest remnants and a larger forest reserve provide critical dietary resources for native forest birds that utilize the agricultural countryside.

KEYWORDS

ornithology, avian ecology, conservation biology, tropical biology, ecosystem services, deforestation, neotropics, stable isotope ecology

Introduction

Forests worldwide are being reduced to biologically-impoverished remnants (Laurance and Bierregaard, 1997) embedded in agricultural countryside (Daily et al., 2001; Şekercioğlu et al., 2019) – croplands, pasture, gardens, open second growth, and a scattering of forest fragments, riparian strips, and remnant trees. Even though human-dominated areas are the preferred

habitat of fewer than 1% of the world's ~11,000 avian species (Şekercioğlu et al., 2004), about a third make some use of such habitats (Şekercioğlu et al., 2007), including many temperate-tropical migratory birds (Blount et al., 2021) that are increasingly threatened with extinction (Horns and Şekercioğlu, 2018). Tropical agricultural countryside can even favor generalist species by providing them with additional food resources (Clough et al., 2011; Fahrig et al., 2011). Given the high rate of tropical deforestation, the extent and ecological qualities of deforested countryside will determine whether some forest species can persist in the absence of large, intact forest patches.

Nitrogen is an essential component of protein synthesis but is found in limited quantities in most ecosystems (White, 1993). Compared to tropical fruits, which average ~5% dry mass as protein (Bosque and Pacheco, 2000), invertebrates have substantially higher protein content (~60% of dry mass; Bell, 1990) and are key sources of nitrogen for most tropical bird species.

A limitation of protein-rich food sources could have large-scale effects on avian communities because the relative level of protein intake has important impacts on bird growth and reproduction (Izhaki, 1998; Gill et al., 2019). Proteins are critical in many cellular processes, and the growth, development and consequently the fitness of organisms may be limited by a deficiency of nitrogen in their dietary resources. The underappreciated research frameworks of ecological stoichiometry and ionomics address how such changes in the environmental nutritional supply affect the ecophysiology, behavior, health, and fitness of individuals, influencing their ecological interactions, population functioning and conservation biology (Kaspari, 2021; Filipiak and Filipiak, 2022).

Stoichiometric mismatch between metabolic demands and nutritional supply can be especially critical for juveniles (Filipiak and Filipiak, 2022). For example, even for bird species that predominantly eat fruits as adults, invertebrates are preferentially caught by adults and fed to offspring during critical periods of growth and development (Izhaki, 1998), enabling chicks to rapidly fledge in an environment full of nest predators, with some exceptions in granivorous birds (Díaz, 1996). Some tropical forest birds time their breeding with increased insect availability (Hau et al., 2000). Declines in protein sources can thus lead to reduced growth rates, increased chick mortality, declines in population recruitment, and other limitations on the growth rate and overall size of a bird population.

We used stable isotope analysis (SIA) to test the hypothesis that the breeding season diets of native forest birds that continue to persist in and adjacent to coffee plantations in southern Costa Rica are deficient in nitrogen (protein) in coffee plantations when compared to their diets in native forest remnants. Because birds have higher energy and protein needs during reproduction (Klasing, 1998) and songbirds tend to consume more arthropods during this period (Izhaki, 1998), we conducted our study to coincide with the main breeding season of our study species between March and June. By examining the carbon ($\delta^{13}C$) and nitrogen ($\delta^{15}N$) isotope values of feathers ($n = 170$) collected from four resident bird species, we tested the hypothesis that individual birds foraging in southern Costa Rican human-modified habitats dominated by coffee plantations consume fewer invertebrates in comparison to individuals of the same species foraging in native forest vegetation. We also collected and analyzed samples of common sources of food (fruits and invertebrates) consumed by our focal bird species (Şekercioğlu et al., 2007). We sampled birds and dietary items from two primary habitats, partially shaded coffee plantations and forest remnants that include primary forest, secondary forest, and riparian strips; hereafter referred to as "coffee" and "non-coffee" habitats, respectively. We also used radiotelemetry data to assess the overall habitat use of each individual bird and to understand the level of use of coffee versus non-coffee habitats. A total of 49 individuals from three species were intensively radio-tracked and their habitat use patterns were documented in detail (Şekercioğlu et al., 2007), which allowed for a unique coupling of isotopically derived dietary information with information on individual movement patterns.

Based on *a priori* knowledge of the birds' habitat and dietary preferences, we hypothesized that there would be significant isotopic differences among bird species related to their degree of insectivory, which would mirror those recorded from field observations (Şekercioğlu et al., 2007). Coffee plantations in our study area have depauperate invertebrate communities (Goehring et al., 2002; Ricketts et al., 2002), so we also predicted that birds that spend a greater amount of time in these areas should consume fewer invertebrates than do the birds spending more time in forest remnants. The unique coupling of extensive radio-tracking data with isotopically derived dietary information on resource use and assimilation provides a rare perspective on the potential effects of landscape modification on the nutrient uptake of a tropical bird community. This is one of the few ornithological studies that combines radio tracking and SIA to address a critical conservation issue for tropical avian species.

Materials and methods

Study site

Our study area in southern Costa Rica (Figure 1), near the Las Cruces Biological Station, is a formerly forested region now dominated by coffee plantations (~50% of land cover), cattle pastures (~20%), and other human-modified environments (~10%). In these agricultural areas, large quantities of chemicals in the form of fungicides, pesticides, and fertilizers are applied on coffee plantations, and the regulations restricting the use of pesticides are not adequately enforced (Stiles and Skutch, 1989). Thus, the conversion of forests to agricultural countryside may not only reduce the abundance of invertebrates *via* decreases in vegetation structure and botanical diversity, but the elimination of invertebrates with pesticides can lead to the poisoning of birds and other non-target species while directly decreasing the amount of protein available to the resident bird species. Previous studies at our study site found significant decreases in the numbers of invertebrates such as Blatteria, Coleoptera, Diptera, Lepidoptera, and Orthoptera in coffee plantations in comparison to the forest remnants (Goehring et al., 2002; Ricketts et al., 2002). These insect orders are major components of local bird diets (Şekercioğlu, 2002) and such reductions could result in nitrogen limitation for birds that spend a considerable amount of their time foraging in coffee plantations.

Study species

Catharus aurantiirostris (Orange-billed Nightingale-thrush, hereafter *Catharus*) is a species with low forest dependence and

10.3389/fevo.2023.1086616

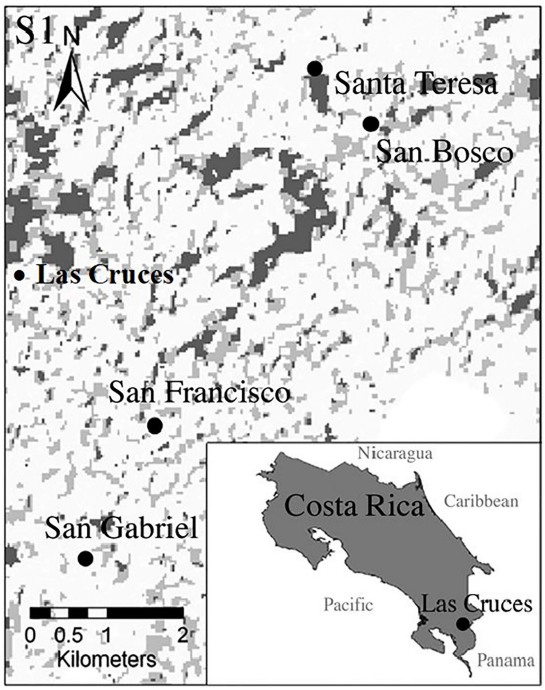

FIGURE 1
Map of the study area. Dark gray represents arboreal cover (forest fragments, riparian strips, and remnant trees), gray represents second growth with few trees, and white represents human-dominated habitats (pastures, coffee plantations, other agriculture, and towns).

prefers forest edge, second growth, thickets, plantations, and gardens (Stiles and Skutch, 1989). *Tangara icterocephala* (Silver-throated Tanager, hereafter *Tangara*) has intermediate forest dependence and is a common species of forest canopy, forest edge and agricultural habitats in the study area. *Tangara* was the most common seed disperser visiting *Miconia* trees (a major food source analyzed in this study) isolated in the pastures surrounding the intact Las Cruces forest (Luck and Daily, 2003). *Turdus assimilis* (White-throated Thrush, hereafter *Turdus*) is most often found in moist forests, but also enters bordering thickets, riparian corridors, second growth and isolated fruiting trees, especially outside the breeding season (Stiles and Skutch, 1989). Finally, *Mionectes oleaginous* (Ochre-bellied Flycatcher, hereafter *Mionectes*) is most often found in the lower levels of humid forest, secondary growth, and clearings (Stiles and Skutch, 1989). *Mionectes* was the only species that was not radio-tracked. All four species are regularly found in forest and open countryside, feed on fruits and invertebrates, and are likely to be important dispersers of forest plants into non-forested areas. *Catharus* is mostly insectivorous, whereas the others are mostly frugivorous (Stiles and Skutch, 1989; Şekercioğlu et al., 2007).

We analyzed a subset of feathers from 170 individuals of these four bird species (Table 1). The feathers were part of a collection of contour and tail feathers from over 6,000 individuals of 211 Costa Rican bird species obtained during a long-term bird banding and radio telemetry study centered around the Las Cruces Biological Station in the Coto Brus canton of southern Costa Rica (Şekercioğlu et al., 2002, 2007, 2015, 2019).

Radio tracking

For three of these four species, we collected extensive radiotelemetry data on 49 individuals (Şekercioğlu et al., 2007). We used radiotelemetry data to assess the habitat use of each individual bird, especially the use of forest habitats (the mostly intact primary forest of the Las Cruces Forest Reserve, small forest remnants, and riparian strips) versus agricultural habitats (mostly coffee plantations). Various studies have shown that radio tags have minimal to no impact on bird physiology and behavior (Kenward, 2001; Wells et al., 2003), and the radio tags in this study had no observable effects on our study species (Şekercioğlu et al., 2007).

From the average radio-tracked individual, we collected ≥55 Global Positioning System (GPS) points during more than 45 h of radio-tracking distributed across 11 days. To assess the level of confidence we could place on bird capture locations for understanding habitat use, we analyzed the fit between 97 capture site data points, each of which describes the location where an individual bird was caught, and each bird's radio tracking locations, which give detailed information on habitat use by the same individual bird. For each bird, we calculated the ratio of the number of telemetry data points collected in coffee plantations to all telemetry data points. To assess whether the capture location of the bird could predict the habitat where the bird spent most of its time according to radiotelemetry, the vegetation cover of the study area was classified as "coffee" versus "non-coffee," each of which had ~50% cover based on extensive vegetation surveys (Şekercioğlu et al., 2007).

If an individual bird spent more than 50% of its time in coffee plantations, we interpreted it as a preference for that habitat type and vice versa for non-coffee areas. We divided the number of times capture data and radio-tracking data assigned an individual to the same habitat (coffee or non-coffee) by the total number of radio-tracked birds. A *z*-test was performed to see if this was significantly different than the 50% value that would be expected by chance alone. We expected the fit between the capture locations and the corresponding telemetry data points to be better than that expected by chance alone. As the coffee and non-coffee areas each represent ~50% of the study site, the expected agreement rate due to chance alone was ~50%.

For the purposes of the isotope mixing models and statistical analyses, percent agricultural use was calculated for each bird by dividing the number of telemetry points from agricultural habitats by the total number of telemetry points. An index value of 34% or less was arbitrarily taken to indicate light use of agricultural countryside, between 34 and 67% moderate use, and above 67%, heavy use. For birds that were not radio-tracked, capture data was used instead, and 0% was assigned to a bird captured in a non-coffee site, while 100% was assigned to a bird captured in a coffee site. We also calculated the percent of each bird's home range that was covered by trees and used linear regression to analyze the relationship between percent tree cover and the isotopic composition of each bird's feathers.

We assumed that the location of each bird during the time of feather formation (and reflected in its isotopic signatures) corresponds to the location in which the bird was caught or to the locations in which the bird spent most of its time as revealed by radio tracking studies. In addition, we assumed that a bird's diet during the period of feather formation is representative of its typical diet. This might not

be true because feather formation requires high amounts of protein and thus, during this time, birds may be preferentially consuming more protein (Earle and Clarke, 1991; Wolf et al., 2003). Nevertheless, even if an individual does modify its foraging behavior to consume more protein during the molting/re-growth period, a bird impoverished in protein post-formation was likely even more nutrient impoverished during feather formation.

Stable isotopes as avian dietary proxies

SIA has yielded important insights into the life history, ecology, migration, and evolution of birds (Hobson and Clark, 1992; Chamberlain et al., 1997; Hobson, 1999a; Rubenstein et al., 2002; Smith et al., 2002; Hobson and Bairlein, 2003; Pain et al., 2004). Specifically, carbon ($\delta^{13}C$) and nitrogen ($\delta^{15}N$) isotope analyses of bird tissues have been used to investigate trophic relationships (Hobson, 1999b; Kelly, 2000; Herrera et al., 2003) and to characterize avian diet composition (Mizutani et al., 1990; Thompson et al., 1995; Thompson and Furness, 1995; Bearhop et al., 1999; Hocking and Reimchen, 2002). The use of SIA to analyze diet has several advantages. Traditionally, the examination of regurgitates, feces, and pellets, and other laborious means have been necessary to study avian diets (Rosenberg and Cooper, 1990; Şekercioğlu et al., 2002). These techniques provide a snapshot of dietary information and typically represent food ingested over a few days prior to capture. These techniques are also highly invasive, may create intolerable levels of stress for study subjects, and can even lead to mortality (Poulin et al., 1994). Isotopic analysis of feathers, easily collected during any study that involves mist netting (Smith et al., 2002), removes the need for the laborious and invasive processes involved in obtaining regurgitates and feces, and provides direct insights into the diet of an individual bird recorded in its feathers during the period of feather growth (Mizutani et al., 1990).

Finally, quantitative estimates of dietary sources can sometimes be made with SIA by applying trophic discrimination factors to consumer tissue isotope values to account for isotopic sorting during metabolic and biosynthetic processes, and then using mixing models designed to calculate the relative proportion of dietary sources in consumer diets (Phillips and Koch, 2002; Phillips and Gregg, 2003; Parnell, 2019). In most cases, consumers are enriched in the rare heavy isotope (^{13}C or ^{15}N) relative to their diets by ~1–2‰ for $\delta^{13}C$ and 3–5‰ for $\delta^{15}N$ for each increase in trophic level (Kelly, 2000; Caut et al., 2009).

Fruit and invertebrate samples

We conducted SIA of commonly consumed fruit and invertebrate samples from the sites where the birds were captured. We sampled the fruits of *Miconia trinervia* (family Melastomataceae; hereafter *Miconia*), a regular food resource of all the study species and a plant that is commonly found in natural and human-dominated habitats in the study area. We also collected the fruits of *Cecropia* spp. (family Cecropiaceae; hereafter *Cecropia*), also fruits commonly consumed by our study species. For invertebrates, we sampled predaceous arachnids (spiders) and grazing Orthoptera (grasshoppers), which represent two trophic levels and are two of the four invertebrate groups (others include Coleoptera and Formicidae) that are most frequently encountered in the diet samples of birds from our study area we collected *via* regurgitation (Şekercioğlu et al., 2002). We collected and analyzed 4–25 samples of each dietary item from coffee and non-coffee areas to compare the isotopic differences between these treatments.

Stable isotope analyses

Bird tail feathers were prepared for isotope analysis by washing in a 2:1 chloroform/methanol mixture to remove surface contaminants, followed by drying for at least 8 h in a fume hood to remove solvents (Kelly, 2000). Fruits and invertebrates were freeze-dried and homogenized using a mortar and pestle. Dried samples of feathers (0.5 mg) and potential food items (invertebrates: ~0.5 mg; fruits: ~5.0 mg) were sealed in tin capsules, and $\delta^{13}C$ or $\delta^{15}N$ values were measured using a Costech elemental analyzer interfaced with a Finnegan Delta Plus gas source mass spectrometer in the Department of Geological and Environmental Sciences at Stanford University (Palo Alto, CA). Results are expressed as δ values, $\delta^{13}C$ or δ^{15} $N = 1{,}000\ [(R_{sample}/R_{standard}) - 1]$, where R_{sample} and $R_{standard}$ are the $^{13}C/^{12}C$ or $^{15}N/^{14}N$ ratios of the sample and standard, respectively; units are expressed as parts per thousand or per mil (‰). The standards are Vienna-Pee Dee Belemnite limestone (V-PDB) for carbon and atmospheric N_2 for nitrogen. Repeated within-run measurements of a gelatin standard yielded an average standard deviation of <0.2‰ for both $\delta^{13}C$ and $\delta^{15}N$ values. Duplicate isotopic measurements were performed on ~20% of all unknown samples and yielded an absolute difference of 0.2‰ for both $\delta^{13}C$ and $\delta^{15}N$ values. We also measured the weight percent carbon and nitrogen concentrations of all samples, which are presented as nitrogen concentrations and C/N ratios in Table 1.

An analysis of variance (ANOVA) with a Tukey-HSD *post hoc* comparison test was used to test for significance among groups (bird species or prey types), which was assessed at an α-value of 0.05. In addition, we used a Bayesian concentration-dependent mixing model, Stable Isotope Mixing Models in R (simmr; Parnell, 2019), to estimate the relative contribution of four prey types to the diet of each bird species. Based on the results of a controlled feeding experiment on an omnivorous passerine (Pearson et al., 2003), we varied $\delta^{13}C$ and $\delta^{15}N$ trophic discrimination factors (TDF) among prey types to account for the differences in assimilation due to prey protein (nitrogen) content. For $\delta^{13}C$, we applied mean (±SD) TDFs of 3.0 ± 0.5‰ for invertebrates (spiders and grasshoppers) and 2.0 ± 0.5‰ for fruits (Cecropia and Miconia). For $\delta^{15}N$, we applied mean (±SD) TDFs of 3.5 ± 0.5‰ for invertebrates (spiders and grasshoppers) and 3.0 ± 0.5‰ for fruits (Cecropia and Miconia). The model also included elemental concentration data and we used mean weight percent [C] and [N] for each prey type reported in Table 1. Gelman diagnostics for all model runs produced values of one, indicating model convergence. We used a two-tailed t-test to assess the significant differences in prey contributions between habitats within species, and significance was assessed using an α-value of 0.05. The dietary percentages presented in Table 2 represent the mean source contributions (SD in parentheses) of all individuals within a species versus habitat type based on telemetry data or capture location (coffee versus non-coffee).

10.3389/fevo.2023.1086616

TABLE 1 Mean (±SD) $\delta^{13}C$ and $\delta^{15}N$ values and the sample sizes of tail feathers of four bird species and potential food sources collected in coffee and non-coffee habitats.

	Coffee					Non-coffee					
Species/prey type	*n*	$\delta^{13}C$	$\delta^{15}N$	[N]	C/N	*n*	$\delta^{13}C$	$\delta^{15}N$	[N]	C/N	Forest dependence
Catharus aurantiirostris	28	−23.9 ± 1.5	8.3 ± 1.3	–	–	35	−24.1 ± 0.8	7.8 ± 1.0	–	–	Low
Turdus assimilis	5	−23.5 ± 0.5	6.7 ± 0.7	–	–	33	−24.4 ± 0.7	6.6 ± 1.1	–	–	High
Tangara icterocephala	15	−23.7 ± 0.8	5.6 ± 1.1	–	–	19	−24.0 ± 0.4	4.5 ± 1.2	–	–	Medium
Mionectes oleaginous	5	−23.3 ± 0.5	7.8 ± 1.4	–	–	31	−23.0 ± 1.4	6.6 ± 1.4	–	–	Medium
Spiders	7	−23.1 ± 1.7	8.9 ± 1.6	12.6 ± 0.4	3.9 ± 0.3	9	−24.8 ± 0.6	5.8 ± 1.1	11.6 ± 1.1	4.2 ± 0.4	–
Grasshoppers	20	−26.3 ± 2.8	3.9 ± 2.8	11.1 ± 1.4	4.2 ± 0.2	22	−26.5 ± 2.6	4.1 ± 1.5	10.7 ± 0.5	4.3 ± 0.4	–
Miconia Fruits	4	−27.0 ± 0.7	1.3 ± 1.7	1.9 ± 0.3	23.3 ± 4.7	33	−28.2 ± 1.4	0.5 ± 1.0	1.9 ± 0.3	24.7 ± 4.5	–
Cecropia Fruits	8	−26.7 ± 1.3	4.2 ± 0.9	1.9 ± 0.4	25.0 ± 4.6	10	−26.9 ± 0.9	4.4 ± 1.6	2.0 ± 0.3	23.4 ± 3.6	–

Mean (±SD) weight percent nitrogen [N] concentration and [C]/[N] ratios are also provided for potential food sources. Estimates of forest dependence are from Şekercioğlu et al. (2007, 2019).

TABLE 2 Mean (±SD) contributions of potential prey to the diets of four bird species collected in coffee and non-coffee habitats.

Species	Habitat	Spiders	Grasshoppers	*Miconia*	*Cecropia*
Catharus	Coffee (*28*)	11.5 ± 3.2***	17.7 ± 8.0	35.3 ± 20.1*	35.6 ± 21.8
	Non-coffee (*35*)	25.8 ± 5.8	19.2 ± 5.4	24.7 ± 12.2	30.4 ± 17.0
Turdus	Coffee (*5*)	9.8 ± 6.5	20.5 ± 13.5	42.4 ± 21.6*	27.3 ± 19.5
	Non-coffee (*33*)	8.4 ± 3.9	21.8 ± 5.2	28.1 ± 11.1	41.8 ± 15.4
Tangara	Coffee (*15*)	3.1 ± 2.1***	12.7 ± 10.6	70.8 ± 18.5***	13.3 ± 12.2***
	Non-coffee (*19*)	22.9 ± 11.3	15.9 ± 9.0	28.5 ± 20.8	32.7 ± 15.3
Mionectes	Coffee (*5*)	16.1 ± 7.6*	23.2 ± 12.8***	33.3 ± 18.0***	27.4 ± 18.0
	Non-coffee (*31*)	22.8 ± 6.0	52.6 ± 7.8	11.5 ± 7.0	13.1 ± 8.3

The numbers in italics next to the habitat designations denote the number of individuals captured in each habitat. Results of two-tailed t-tests of prey contributions between habitats within species are indicated by superscripts; $p < 0.001$***, $p < 0.01$**, $p < 0.05$*.

Results

Habitat use

The agreement between 97 capture site data points and telemetry data points was 68%. This was significantly higher ($z = 3.70$; $p = 0.0002$) than would be expected based on chance alone, meaning that the capture location was a good predictor of the habitat use of an individual bird over time. Hence, capture location data were used in data analyses for birds that were not radio-tracked. We also calculated the average percent (±SD) agricultural use of radio-tracked birds to determine the extent of use of agricultural countryside. Percent agricultural use was 14% (±5.9%) for Mionectes, 22% (±5.0%) for Turdus, 33% (±4.9%) for Catharus, and 34% (±6.9%) for Tangara, indicating that these species made relatively low use of the agricultural countryside. Percent agricultural use for Mionectes was calculated using only the capture locations since this species was not radio-tracked.

Foraging observations

Each species differed from the other two in its resource use (Figure 2), based on the proportion of foraging observations on the resources that each species was observed to exploit (all $\chi^2 > 120$; all $p < 0.001$; Figure 2). *Catharus* (Figure 2), although observed to forage on 14 plant taxa, foraged predominantly on invertebrates, either directly or on substrates (i.e., soil, rotting fruit) where invertebrates are commonly found. *Turdus* (Figure 2) and *Tangara* (Figure 2) were more frugivorous and foraged on 71 and 45 plant taxa, respectively. Fruits of *Cecropia peltata*, *Ficus* spp., and *Syzygium malacanse* were favorite dietary items for both species.

Isotopic composition of dietary sources

There were significant differences between $\delta^{15}N$ values, $\delta^{13}C$ values, and weight percent carbon:nitrogen (C/N) concentrations among potential food sources (Tukey HSD, $p < 0.01$; Table 1; Figure 3). Spiders collected within coffee habitats had significantly higher $\delta^{15}N$ values than any other food source (Figure 3). Miconia fruits collected in non-coffee habitats had significantly lower $\delta^{15}N$ values than any other food source. $\delta^{15}N$ and $\delta^{13}C$ values of Cecropia fruits were not statistically distinguishable from those of grasshoppers in either habitat. For both habitats, spiders had significantly higher values than did grasshoppers, but only grasshoppers collected in non-coffee habitats had significantly higher $\delta^{15}N$ values than non-coffee Miconia

10.3389/fevo.2023.1086616

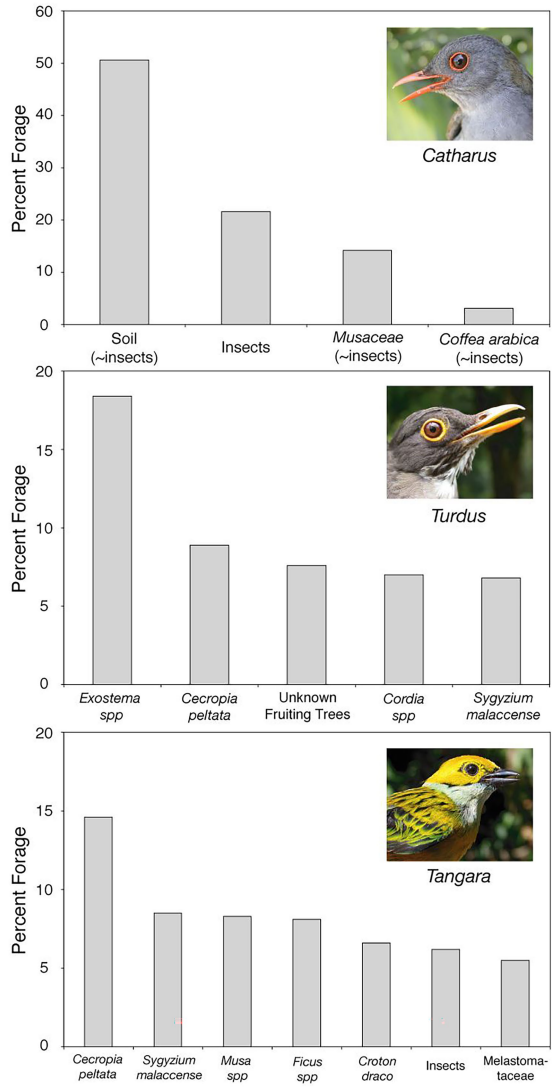

FIGURE 2
The relative percentage of foraging observations on common food resources (each type comprising >5% of all total foraging observations for three of the four bird species examined in this study). No foraging data were collected for *Mionectes*. Data are from Şekercioğlu et al., 2007.

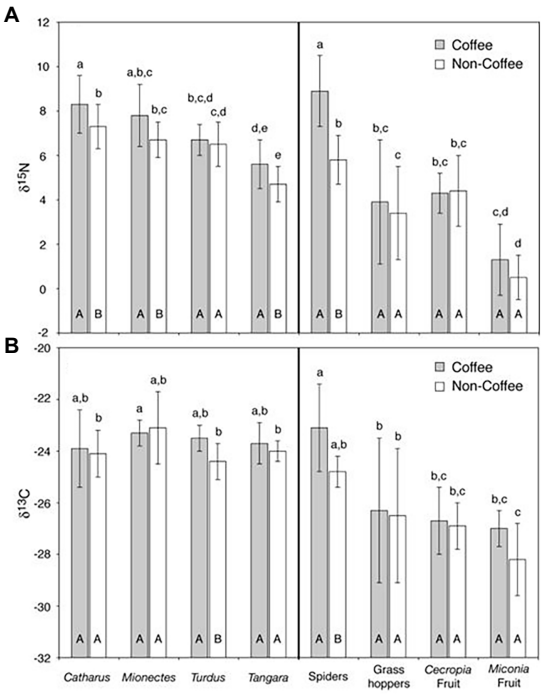

FIGURE 3
Mean $\delta^{15}N$ **(A)** and $\delta^{13}C$ **(B)** values of the four bird species and common dietary resources collected in coffee versus forested non-coffee habitats. Error bars denote one standard deviation from the mean. Refer to Table 1 for the sample sizes. Lowercase letters signify results of a one-way ANOVA comparing mean values among prey types and uppercase letters signify ANOVA results for the comparisons of a single prey type between habitats.

fruits. $\delta^{15}N$ values of grasshoppers were indistinguishable from $\delta^{15}N$ values of Miconia fruits in coffee plantations. Lastly, spiders collected in coffee habitat had significantly higher $\delta^{15}N$ values than spiders from non-coffee habitats.

Like $\delta^{15}N$ results, spiders collected within coffee habitats also had significantly higher $\delta^{13}C$ values than any other food source (Figure 3), with the only exception being spiders collected from non-coffee habitats. The $\delta^{13}C$ composition of grasshoppers collected in coffee or non-coffee habitats was indistinguishable from that of *Cecropia* fruits. The mean $\delta^{13}C$ value of *Cecropia* fruits from either habitat was indistinguishable from that of *Miconia* fruits. However, *Miconia* fruits collected from non-coffee habitats had significantly lower $\delta^{13}C$ values than grasshoppers from either habitat. Lastly, within-type comparisons of food sources collected in coffee versus non-coffee habitats showed no significant differences in $\delta^{13}C$ values except for spiders, which (like $\delta^{15}N$) had higher $\delta^{13}C$ values in coffee versus non-coffee habitats (Figure 3B).

Grasshoppers had significantly higher variance in $\delta^{13}C$ and $\delta^{15}N$ values than any other food source type (Table 1; Figure 3). There were no differences in the concentrations of carbon [C] and nitrogen [N] between samples of particular food types collected in coffee versus non-coffee habitats (Table 1). Invertebrates (spiders and grasshoppers) had significantly higher [N] than fruits, resulting in significant differences in C/N ratios between these two general types of food (Table 1).

Isotopic composition of bird feathers

We measured the $\delta^{13}C$ and $\delta^{15}N$ values of feathers collected from 63 *Catharus*, 38 *Turdus*, 34 *Tangara*, and 36 *Mionectes* individuals (Table 1). At the species level, sex, wingspan, and body mass did not have significant effects on $\delta^{13}C$ and $\delta^{15}N$ values (ANOVA, $p > 0.05$). For intraspecific comparisons (uppercase letters, Figure 3), the location of capture had a significant effect on feather $\delta^{15}N$ values for *Catharus, Mionectes,* and *Tangara*, where individuals captured in coffee habitats had significantly higher $\delta^{15}N$ values than individuals from non-coffee habitats (Figure 3; ANOVA). For $\delta^{13}C$, intraspecific comparisons showed significant effects of habitat for only one species. *Turdus* individuals captured in coffee plantations had significantly higher $\delta^{13}C$ values than those caught in non-coffee habitats (Figure 3).

10.3389/fevo.2023.1086616

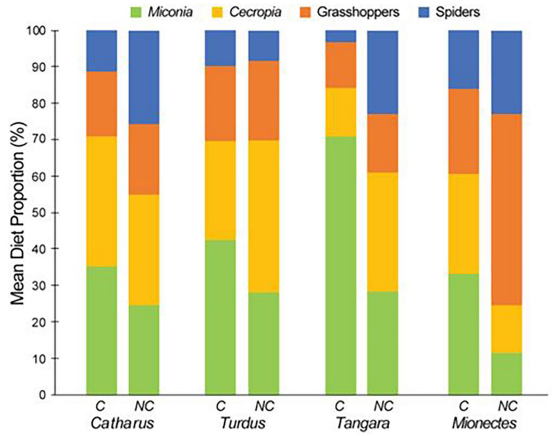

FIGURE 4
Mean diet proportions of potential prey types consumed by the four bird species in coffee (C) and forested non-coffee (NC) habitats.

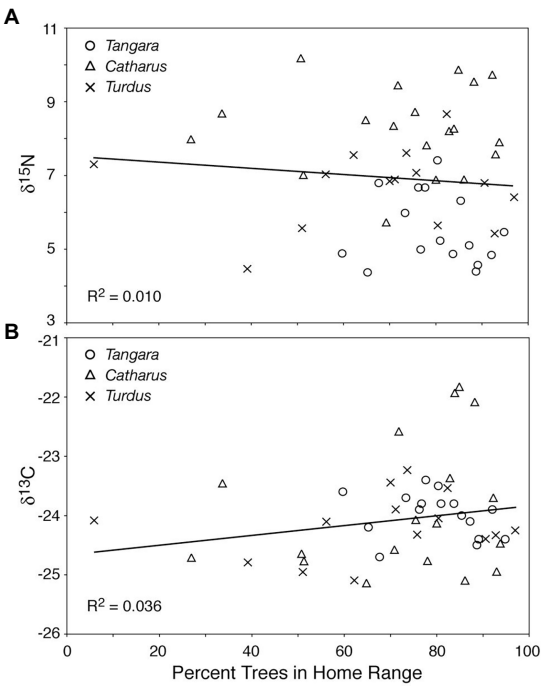

FIGURE 5
Effect of percent tree cover in radio-tracked birds' home ranges on the nitrogen **(A)** and carbon **(B)** isotopic composition of bird feathers. Regression statistics for the entire bird community (rather than single species) are provided because bivariate analyses of isotopic composition versus percent tree cover for each species were similar (r^2 <0.10; p >0.05 for both δ^{13}C and δ^{15}N).

Interspecific ANOVA comparisons (lower case letters, Figure 3) show significant differences in mean δ^{15}N but not mean δ^{13}C values among species. *Catharus* and *Mionectes* have significantly higher δ^{15}N values than do *Tangara*. Furthermore, *Turdus* captured in non-coffee habitats have significantly lower δ^{15}N values than *Catharus* captured in either habitat type. Likewise, *Tangara* captured in non-coffee habitats have lower δ^{15}N values than *Turdus* caught in either habitat type.

Results of the δ^{13}C and δ^{15}N concentration-dependent mixing model are presented in Table 2. Consumption of invertebrates was higher in forested versus coffee habitats for three of the four focal bird species (Figure 4). Specifically, the mean contribution of spiders to the diets of *Catharus*, *Tangara*, and *Mionectes* was higher in forested versus coffee habitats. The mean contribution of grasshoppers to the diet of *Mionectes* was higher in forested versus coffee habitats. Conversely, the consumption of *Miconia* fruits was higher in coffee versus forested habitats for all four bird species, but the consumption of *Cecropia* fruits by *Tangara* was higher in forested versus coffee habitats. These results mostly confirm our hypotheses. All species except *Turdus* consume substantially more invertebrates in forested non-coffee habitats than they do in coffee plantations, with *Tangara* and *Mionectes* consuming nearly double the invertebrates in forest remnants than they do in coffee plantations (Figure 4). Patterns among species are similar; overall, *Mionectes* has the highest invertebrate consumption and *Turdus* and *Tangara* have the lowest (Figure 4).

Of the 170 individual birds sampled for isotopes, 19 *Catharus*, 16 *Tangara*, and 14 *Turdus* were radio-tracked. The percentage of trees in their home ranges had no significant effect (r^2 <0.10; p >0.05 for both isotope systems) on feather δ^{13}N (Figure 5A) or δ^{13}C values (Figure 5B) for any of the species that were radio-tracked.

Discussion

Our results indicate that three of the four bird species examined in this study fed on fewer invertebrates in coffee plantations than in forested habitats comprised mostly of forest remnants as well as riparian strips and a larger (270 ha) forest reserve. In the mosaic of habitat types in our study area, extensive coffee plantations and other human-modified habitats have a significant negative effect on the diet composition of the four frugivore-insectivore bird species we examined in this study. Individual birds that were captured in coffee plantations, or known (*via* radiotelemetry data) to spend a considerable portion of time in coffee plantations, may be able to make up for some of their resulting deficiency in invertebrates because their mobility allows them to move among coffee plantations and the surrounding forest remnants, including primary forests, small forest fragments, secondary forest, and/or riparian strips adjacent to coffee-dominated habitat. This explanation is supported by our radio-tracking data, which showed that *Tangara* and *Turdus* were highly mobile and remained in coffee plantations for relatively short periods of time in comparison to the amount of time spent in forest remnants (Şekercioğlu et al., 2007). Moreover, we were able to capture a greater number of *Tangara* and *Turdus* individuals in non-coffee habitats versus coffee plantations in comparison to *Catharus*. Of the species radio tracked, *Tangara* and *Turdus* have significantly larger home ranges than *Catharus*. Average home range estimates for *Tangara* range from ~16–22 ha and between ~30–70 ha for *Turdus* (Şekercioğlu et al., 2007), but only ~1.7–3.6 ha for *Catharus*, depending on whether minimum convex polygon versus kernel densities were used to calculate home range size. This suggests that highly mobile birds that can rapidly move between forest remnants in agricultural countryside may have greater access to nitrogen-rich foods (invertebrates), but less mobile species such as *Catharus* may be stuck between paying a high

energetic cost by constantly moving between forest remnants or getting less invertebrate protein in coffee plantations.

Catharus has relatively low forest dependence compared to most other forest birds in the region (Stiles, 1985), and its natural preference for forest gaps, edges, and second growth has resulted in its successful adaptation to coffee plantations (Şekercioğlu et al., 2007). Most other insectivorous birds in the region are more forest dependent (e.g., *Lophotriccus pileatus, Platyrinchus mystaceus, Thamnophilus bridgesi*) and generally avoid the nonforest matrix dominated by coffee plantations (Şekercioğlu, 2002; Şekercioğlu et al., 2015, 2019). Future tracking and dietary studies should focus on these species, although capturing sufficient numbers of more forest-dependent species in coffee plantations will remain a challenge.

While our isotopic results show differences in the percentages of invertebrates consumed among species, all the species examined are generalist omnivores and likely have broader dietary tolerances than do the more specialist species. In comparison to many tropical forest insectivore specialists that are particularly sensitive to habitat disturbance and fragmentation and are rarely found outside forested areas (Şekercioğlu and Sodhi, 2007; Sherry et al., 2020), the relatively mobile and omnivorous bird species we examined here are more capable of using the agricultural countryside effectively to obtain the protein they require. Nonetheless, our results show that even these more adaptable species consume substantially fewer invertebrates in coffee plantations than they do in forest remnants.

Intraspecific comparisons showed that capture habitat sometimes had a significant effect on $\delta^{15}N$ values. This effect appears to be mainly driven by the differences in spider $\delta^{15}N$ values (Figure 3) and not in the differences in the proportion of dietary items consumed in different habitats. We do not know why spiders captured in coffee plantations have significantly higher $\delta^{15}N$ values than do the spiders in non-coffee habitats. However, it is unlikely to be due to the influence of anthropogenic nitrogenous inputs (e.g., fertilizers, atmospheric deposition) in agricultural areas because other dietary items (grasshoppers, *Cecropia*, and *Miconia*) at lower trophic levels collected in coffee plantations do not have significantly higher $\delta^{15}N$ values than those collected in forested habitats. Spiders are generalist insectivores (Sanders and Platner, 2007) and could forage at multiple trophic levels, so the observed differences in mean $\delta^{15}N$ values could relate to the differences in their diet composition in coffee versus forested habitats.

Our results indicate significant differences in diet composition among species that agree with these birds' foraging preferences based on our observational evidence (Şekercioğlu et al., 2007). These results mostly confirm our hypotheses. All species except *Turdus* consume substantially more invertebrates in forested non-coffee habitats than they do in coffee plantations, with *Tangara* and *Mionectes* consuming nearly double the invertebrates in forest remnants than they do in coffee plantations (Figure 4). Patterns among species are similar; overall, *Mionectes* has the highest invertebrate consumption and *Turdus* and *Tangara* have the lowest (Figure 4).

One limitation of our study was that we were only able to analyze four food sources that likely represent a small subset of possible resources consumed by these bird species, especially in southern Costa Rica's very diverse tropical habitats. Although *Cecropia* and *Miconia* fruits are consumed by these species regularly, and spiders and grasshoppers make up two of the top four invertebrate types eaten by these species in our study area (Şekercioğlu et al., 2002), these generalist bird species likely feed on a wide range of fruits and invertebrates in this diverse landscape mosaic. When dealing with omnivorous species inhabiting diverse ecosystems, it is sometimes difficult to isotopically characterize all potential food sources. Thus, we designed our sampling protocol to capture potential items representative of three trophic levels, including primary producers (fruits), primary consumers (grasshoppers), and secondary consumers (spiders) to specifically evaluate the relative proportion of nitrogen-rich (invertebrates) versus nitrogen-poor (fruits) resources in individual bird diets.

The second potential source of error in our analyses is associated with the precision of our habitat use classifications for individual birds that were not radio-tracked, especially in relation to the timing of feather formation in the species examined. While our statistical analysis suggests that the location of capture is a dependable indicator of individual habitat use, the high mobility of some species may bias our coffee versus non-coffee classification scheme if all individuals (within a species) are utilizing habitats in equal proportion to the average habitat use reflected in the radio-tracking data (Şekercioğlu et al., 2007). A comparison of habitat use data derived from radiotelemetry, however, suggests a considerable amount of variance in the types of habitats utilized and the home range sizes of individual birds. For instance, some *Catharus* and *Turdus* individuals spend a lot of time in agricultural areas even though average habitat use at the species level suggests low use of this habitat type in comparison to forested habitats (Figure 5). Furthermore, just how persistent individual movement patterns are over the course of feather growth remains unresolved. For individuals that were radio-tracked, each bird was followed for an average of 45 h distributed across an average of 11 days. We must consider the possibility that the temporal persistence of individual habitat preferences is shorter than the average duration of feather growth. For the four resident tropical forest bird species examined, feather molt and regrowth occur from June to September, which coincides with the wet season in southern Costa Rica. The radiotelemetry data and the dietary samples for isotopic analysis were collected during the months of March–June. If the individual habitat preferences, as recorded in the radio-tracking data, are more ephemeral than the duration of time required to regrow tail feathers during the molting period, than it is possible that the telemetric and isotopic data do not correlate in time (as seen in Figure 5).

Conclusion

Our results indicate that coffee plantations in southern Costa Rica may be deficient in the invertebrates preferred by generalist birds that use both forest remnants and coffee plantations. Forest remnants surrounding coffee plantations in our study area provide important dietary resources for native forest birds that utilize the agricultural countryside. At least three of the four species examined in this study may be obtaining most of their food from forest remnants and spending time in coffee plantations only while moving between remnants. This interpretation is supported by our extensive radio-tracking data (Şekercioğlu et al., 2007), which showed that most of these same forest species have persisted in agricultural landscapes by being highly mobile foragers that feed on dozens of different native plant and invertebrate species scattered in small forest remnants.

Landscape context is increasingly shown to be of paramount importance for biodiversity conservation in human-dominated, agricultural landscapes (Kati and Şekercioğlu, 2006; Concepción et al., 2008; Şekercioğlu, 2009; Martin et al., 2019; Meier et al., 2022) and our findings support this. Conservation strategies should focus on increasing the connectivity of forest remnants – intact forest, secondary growth, riparian strips – in tropical agricultural countryside, and it is urgent to prioritize the conservation and regeneration of forest remnants in increasingly human-dominated agricultural areas that continue to replace the world's most biodiverse tropical forests.

Data availability statement

The raw data supporting the conclusions of this article will be made available by the authors, without undue reservation.

Ethics statement

The animal study was reviewed and approved by Stanford University IACUC.

Author contributions

ÇŞ developed the idea for the paper, conceptualized and designed the study, with support from SN, PC, GD, and PE. GD, PE, and ÇŞ acquired funding and resources for the field work. ÇŞ and FB conducted the field work and collected the radio tracking data, feather and diet samples. ÇŞ analyzed the radio tracking and habitat use data. MF conducted isotopic analyses on the diet and feather samples, with help from SN and PC. PC provided the mass spectrometer and other resources for isotopic analyses. ÇŞ, MF, and SN and led the writing of the manuscript. PC, TC, GD, and PE reviewed the manuscript and provided intellectual insights. All authors contributed to the article and approved the submitted version.

Funding

We are grateful to H. Bing, P. Bing, T. Brokaw, Center for Latin American Studies, W. Loewenstern, Koret Foundation, Moore Family Foundation, National Geographic Society (grants #7730-04 and #8411-08), Wildlife Conservation Society, Winslow Foundation, and the Carnegie Institution for Science for providing financial support.

Acknowledgments

We thank the Costa Rican government (MINAE) and the Organization for Tropical Studies for allowing us to work at the Las Cruces Biological Research Station.

Conflict of interest

The authors declare that the research was conducted in the absence of any commercial or financial relationships that could be construed as a potential conflict of interest.

Publisher's note

References

Bearhop, S., Thompson, D. R., Waldron, S., Russell, I. C., Alexander, G., and Furness, R. W. (1999). Stable isotopes indicate the extent of freshwater feeding by cormorants (*Phalacrocorax carbo*) shot at island fisheries in England. *J. Appl. Ecol.* 36, 75–84. doi: 10.1046/j.1365-2664.1999.00378.x

Bell, G. P. (1990). Birds and mammals on an insect diet: a primer on diet composition analysis in relation to ecological energetics. *Stud. Avian Biol.* 13, 416–422.

Blount, D., Horns, J. J., Kittelberger, K., Neate-Clegg, M. H. C., and Şekercioğlu, Ç. H. (2021). Avian use of agricultural areas as migration stopover sites: a review of crop management practices and ecological correlates. *Front. Ecol. Evol.* 9:e664764. doi: 10.3389/fevo.2021.650641

Bosque, C., and Pacheco, M. A. (2000). Dietary nitrogen as a limiting nutrient in frugivorous birds. *Rev. Chil. Hist. Nat.* 73, 441–450. doi: 10.4067/S0716-078X2000000300007

Caut, S., Angulo, E., and Courchamp, F. (2009). Variation in discrimination factors ($\Delta^{15}N$ and $\Delta^{13}C$): the effect of diet isotopic values and applications for diet reconstruction. *J. Appl. Ecol.* 46, 443–453. doi: 10.1111/j.1365-2664.2009.01620.x

Chamberlain, C. P., Blum, J. D., Holmes, R. T., Feng, X., Sherry, T. W., and Graves, G. R. (1997). The use of isotope tracers for identifying populations of migratory birds. *Oecologia* 109, 132–141. doi: 10.1007/s004420050067

Clough, Y., Barkmann, J., Juhrbandt, J., Kessler, M., Wanger, T. C., Anshary, A., et al. (2011). Combining high biodiversity with high yields in tropical agroforests. *Proc. Natl. Acad. Sci.* 108, 8311–8316. doi: 10.1073/pnas.1016799108

Concepción, E. D., Díaz, M., and Baquero, R. A. (2008). Effects of landscape complexity on the ecological effectiveness of Agri-environment schemes. *Landsc. Ecol.* 23, 135–148. doi: 10.1007/s10980-007-9150-2

Daily, G. C., Ehrlich, P. R., and Sanchez-Azofeifa, G. A. (2001). Countryside biogeography: use of human-dominated habitats by the avifauna of southern Costa Rica. *Ecol. Appl.* 11, 1–13. doi: 10.1890/1051-0761(2001)011[0001:CBUOHD]2.0.CO;2

Díaz, M. (1996). Food choice by seed-eating birds in relation to seed chemistry. *Comp. Biochem. Physiol. A Physiol.* 113, 239–246. doi: 10.1016/0300-9629(95)02093-4

Earle, K. E., and Clarke, N. R. (1991). The nutrition of the budgerigar (*Melopsittacus-undulatus*). *J. Nutr.* 121, S186–S192. doi: 10.1093/jn/121.suppl_11.S186

Fahrig, L., Baudry, J., Brotons, L., Burel, F. G., Crist, T. O., Fuller, R. J., et al. (2011). Functional landscape heterogeneity and animal biodiversity in agricultural landscapes. *Ecol. Lett.* 14, 101–112. doi: 10.1111/j.1461-0248.2010.01559.x

Filipiak, M., and Filipiak, Z. M. (2022). Application of ionomics and ecological stoichiometry in conservation biology: nutrient demand and supply in a changing environment. *Biol. Conserv.* 272:e109622:109622. doi: 10.1016/j.biocon.2022.109622

Gill, F. B., Prum, R. O., and Robinson, S. K. (2019). *Ornithology*, *4th* (New York: W.H. Freeman, Macmillan Learning).

Goehring, D. M., Daily, G. C., and Şekercioğlu, Ç. H. (2002). Distribution of ground-dwelling arthropods in tropical countryside habitats. *J. Insect Conserv.* 6, 83–91. doi: 10.1023/A:1020905307244

Hau, M., Wikelski, M., and Wingfield, J. C. (2000). Visual and nutritional food cues fine-tune timing of reproduction in a neotropical rainforest bird. *J. Exp. Zool.* 286, 494–504. doi: 10.1002/(SICI)1097-010X(20000401)286:5<494::AID-JEZ7>3.0.CO;2-3

Herrera, L. G., Hobson, K. A., Rodríguez, M., and Hernandez, P. (2003). Trophic partitioning in tropical rainforest birds: insights from stable isotope analysis. *Oecologia* 136, 439–444. doi: 10.1007/s00442-003-1293-5

Hobson, K. A. (1999a). Tracing origins and migrations of wildlife using stable isotopes: a review. *Oecologia* 120, 314–326. doi: 10.1007/s004420050865

Hobson, K. A. (1999b). Stable-carbon and nitrogen isotope ratios of songbird feathers grown in two terrestrial biomes: implications for evaluating trophic relationships and breeding origins. *Condor* 101, 799–805. doi: 10.2307/1370067

Hobson, K. A., and Bairlein, F. (2003). Isotopic fractionation and turnover in captive garden warblers (*Sylvia borin*): implications for delineating dietary and migratory associations in wild passerines. *Can. J. Zool.* 81, 1630–1635. doi: 10.1139/z03-140

Hobson, K. A., and Clark, R. G. (1992). Assessing avian diets using stable isotopes II: factors influencing diet-tissue fractionation. *Condor* 94, 189–197. doi: 10.2307/1368808

Hocking, M. D., and Reimchen, T. E. (2002). Salmon-derived nitrogen in terrestrial invertebrates from coniferous forests of the Pacific northwest. *BMC Ecol.* 2:4. doi: 10.1186/1472-6785-2-4

Horns, J. J., and Şekercioğlu, Ç. H. (2018). Conservation of migratory species. *Curr. Biol.* 28, R980–R983. doi: 10.1016/j.cub.2018.06.032

Izhaki, I. (1998). Essential amino acid composition of fleshy fruits versus maintenance requirements of passerine birds. *J. Chem. Ecol.* 24, 1333–1345. doi: 10.1023/A:1021274716062

Kaspari, M. (2021). The invisible hand of the periodic table: how micronutrients shape ecology. *Annu. Rev. Ecol. Evol. Syst.* 52, 199–219. doi: 10.1146/annurev-ecolsys-012021-090118

Kati, V., and Şekercioğlu, Ç. H. (2006). Diversity, ecological structure, and conservation of the land bird community of Dadia reserve, Greece. *Divers. Distrib.* 12, 620–629. doi: 10.1111/j.1366-9516.2006.00288.x

Kelly, J. F. (2000). Stable isotopes of carbon and nitrogen in the study of avian and mammalian trophic ecology. *Can. J. Zool.* 78, 1–27. doi: 10.1139/z99-165

Kenward, R. E. (2001). *A Manual for Wildlife Radio Tagging*. (London: Academic Press).

Klasing, K. C. (1998). *Comparative Avian Nutrition* (Wallingford, UK: CAB International).

Laurance, W. F., and Bierregaard, R. O. (1997). *Tropical Forest Remnants: Ecology, Management, and Conservation of Fragmented Communities* (Chicago: University of Chicago Press).

Luck, G. W., and Daily, G. C. (2003). Tropical countryside bird assemblages: richness, composition, and foraging differ by landscape context. *Ecol. Appl.* 13, 235–247. doi: 10.1890/1051-0761(2003)013[0235:TCBARC]2.0.CO;2

Martin, E. A., Dainese, M., Clough, Y., Báldi, A., Bommarco, R., Gagic, V., et al. (2019). The interplay of landscape composition and configuration: new pathways to manage functional biodiversity and agroecosystem services across Europe. *Ecol. Lett.* 22, 1083–1094. doi: 10.1111/ele.13265

Meier, E. S., Lüscher, G., and Knop, E. (2022). Disentangling direct and indirect drivers of farmland biodiversity at landscape scale. *Ecol. Lett.* 25, 2422–2434. doi: 10.1111/ele.14104

Mizutani, H., Fukuda, M., and Wada, E. (1990). Carbon isotope ratio of feathers reveals feeding behavior of cormorants. *Auk* 107, 400–403. doi: 10.2307/4087626

Pain, D. J., Green, R. E., Gieing, B., Kozulin, A., Poluda, A., Ottosson, U., et al. (2004). Using stable isotopes to investigate migratory connectivity of the globally threatened aquatic warbler *Acrocephalus paludicola*. *Oecologia* 138, 168–174. doi: 10.1007/s00442-003-1416-z

Parnell, A. (2019). Simmr: A Stable Isotope Mixing Model. R package version 0.4.6.9000. Available at: https://CRAN.R-project.org/package=simmr (Accessed January 11, 2023).

Pearson, S. F., Levey, D. J., Greenberg, C. H., and Martinez del Rio, C. (2003). Effects of elemental composition on the incorporation of dietary nitrogen and carbon isotopic signatures in an omnivorous songbird. *Oecologia* 135, 516–523. doi: 10.1007/s00442-003-1221-8

Phillips, D. L., and Gregg, J. W. (2003). Source partitioning using stable isotopes: coping with too many sources. *Oecologia* 136, 261–269. doi: 10.1007/s00442-003-1218-3

Phillips, D. L., and Koch, P. L. (2002). Incorporating concentration dependence in stable isotopes: a critique. *Oecologia* 130, 114–125. doi: 10.1007/s004420100786

Poulin, B., Lefebvre, G., and McNeil, R. (1994). Effect and efficiency of tartar emetic in determining the diet of tropical land birds. *Condor* 96, 98–104. doi: 10.2307/1369067

Ricketts, T. H., Daily, G. C., and Ehrlich, P. R. (2002). Does butterfly diversity predict moth diversity? Testing a popular indicator taxon at local scales. *Biol. Conserv.* 103, 361–370. doi: 10.1016/S0006-3207(01)00147-1

Rosenberg, K. V., and Cooper, R. J. (1990). Approaches to avian diet analysis. *Stud. Avian Biol.* 13, 80–90.

Rubenstein, D. R., Chamberlain, C. P., Holmes, R. T., Ayres, M. P., Waldbauer, J. R., Graves, G. R., et al. (2002). Linking breeding and wintering ranges of a migratory songbird using stable isotopes. *Science* 295, 1062–1065. doi: 10.1126/science.1067124

Sanders, D., and Platner, C. (2007). Intraguild interactions between spiders and ants and top-down control in a grassland food web. *Oecologia* 150, 611–624. doi: 10.1007/s00442-006-0538-5

Şekercioğlu, Ç. H. (2002). Forest fragmentation hits insectivorous birds hard. *Dir. Sci.* 1, 62–64. doi: 10.1100/tsw.2002.190

Şekercioğlu, Ç. H. (2009). Tropical conservation: riparian corridors connect fragmented forest populations. *Curr. Biol.* 19, R210–R213. doi: 10.1016/j.cub.2009.01.006

Şekercioğlu, Ç. H., Daily, G. C., and Ehrlich, P. R. (2004). Ecosystem consequences of bird declines. *Proc. Natl. Acad. Sci.* 101, 18042–18047. doi: 10.1073/pnas.0408049101

Şekercioğlu, Ç. H., Ehrlich, P. R., Daily, G. C., Aygen, D., Goehring, D., and Sandi, R. F. (2002). Disappearance of insectivorous birds from tropical forest fragments. *Proc. Natl. Acad. Sci.* 99, 263–267. doi: 10.1073/pnas.012616199

Şekercioğlu, Ç. H., Loarie, S., Oviedo-Brenes, F., Daily, G. C., and Ehrlich, P. R. (2007). Persistence of forest birds in tropical countryside. *Conserv. Biol.* 21, 482–494. doi: 10.1111/j.1523-1739.2007.00655.x

Şekercioğlu, Ç. H., Loarie, S., Oviedo-Brenes, F., Mendenhall, C. D., Daily, G. C., and Ehrlich, P. R. (2015). Tropical countryside riparian corridors provide critical habitat and connectivity for seed-dispersing forest birds in a fragmented landscape. *J. Ornithol.* 156, 343–353. doi: 10.1007/s10336-015-1299-x

Şekercioğlu, Ç. H., Mendenhall, C. D., Oviedo-Brenes, F., Horns, J. J., Ehrlich, P. R., and Daily, G. C. (2019). Long-term declines in bird populations in tropical agricultural countryside. *Proc. Natl. Acad. Sci.* 116, 9903–9912. doi: 10.1073/pnas.1802732116

Şekercioğlu, Ç. H., and Sodhi, N. S. (2007). Conservation biology: predicting birds' responses to forest fragmentation. *Curr. Biol.* 17, R838–R840. doi: 10.1016/j.cub.2007.07.037

Sherry, T. W., Kent, C. M., Sánchez, N. V., and Şekercioğlu, Ç. H. (2020). Insectivorous birds in the Neotropics: ecological radiations, specialization, and coexistence in species-rich communities. *Auk* 137:ukaa049. doi: 10.1093/auk/ukaa049

Smith, T. B., Marra, P. P., Webster, M. S., Lovette, I., Gibbs, H. L., Holmes, R. T., et al. (2002). A call for feather sampling. *Auk* 20, 218–221. doi: 10.2307/4090162

Stiles, F. G. (1985). "Conservation of forest birds in Costa Rica: problems and perspectives" in *Conservation of Tropical Forest Birds*. eds. A. W. Diamond and T. E. Lovejoy (Cambridge, UK: International Council for Bird Preservation), 141–170.

Stiles, F. G., and Skutch, A. F. (1989). *A Guide to the Birds of Costa Rica* (New York: Cornell University Press).

Thompson, D. R., and Furness, R. W. (1995). Stable isotope of carbon and nitrogen in feathers indicate seasonal dietary shifts in northern fulmars. *Auk* 112, 493–498. doi: 10.2307/4088739

Thompson, D. R., Furness, R. W., and Lewis, S. A. (1995). Diets and long-term changes in $\delta^{15}N$ and $\delta^{13}C$ values in northern fulmars (*Fulmarus glacialis*) from two Northeast Atlantic colonies. *Mar. Ecol. Prog. Ser.* 125, 3–11. doi: 10.3354/meps125003

Wells, K. M. S., Washburn, B. E., Millspaugh, J. J., Ryan, M. R., and Hubbard, M. W. (2003). Effects of radio-transmitters on fecal glucocorticoid levels in captive dickcissels. *Condor* 105, 805–810. doi: 10.1093/condor/105.4.805

White, T. C. R. (1993). *The Inadequate Environment: Nitrogen and the Abundance of Animals* (Heidelberg, Springer Berlin).

Wolf, P., Rabehl, N., and Kamphues, J. (2003). Investigations on feathering, feather growth and potential influences of nutrient supply on feathers' regrowth in small pet birds (canaries, budgerigars and lovebirds). *J. Anim. Physiol. Anim. Nutr.* 87, 134–141. doi: 10.1046/j.1439-0396.2003.00426.x

frontiers | Frontiers in Ecology and Evolution

TYPE Original Research
PUBLISHED 31 March 2023
DOI 10.3389/fevo.2023.1055534

OPEN ACCESS

EDITED BY
Bing Chen,
Hebei University,
China

REVIEWED BY
Maya L. Evenden,
University of Alberta,
Canada
Wei Guo,
Institute of Zoology (CAS),
China

*CORRESPONDENCE
Libesha Anparasan
lanparas@uwo.ca

†These authors have contributed equally to this work

SPECIALTY SECTION
This article was submitted to Ecophysiology, a section of the journal Frontiers in Ecology and Evolution

RECEIVED 27 September 2022
ACCEPTED 16 February 2023
PUBLISHED 31 March 2023

CITATION
Anparasan L, Hobson KA and McNeil JN (2023) Effect of rearing conditions on fatty acid allocation during flight in nectivorous lepidopteran *Mythimna unipuncta*. *Front. Ecol. Evol.* 11:1055534. doi: 10.3389/fevo.2023.1055534

Effect of rearing conditions on fatty acid allocation during flight in nectivorous lepidopteran *Mythimna unipuncta*

Libesha Anparasan[1*†], Keith A. Hobson[1,2†] and Jeremy N. McNeil[1†]

[1]Department of Biology, University of Western Ontario, London, ON, Canada, [2]Environment and Climate Change Canada, Saskatoon, SK, Canada

Insect species that are nectivorous as adults acquire essential fatty acids almost exclusively from host plants during larval development. Thus, as essential fatty acids are important for a number of different biological processes, adult allocation of this limited resource may result in important trade-offs. Most lepidopteran species that migrate do so as sexually immature adults, so essential fatty acids used for migratory flight would not be available for subsequent reproduction. Using the true armyworm, *Mythimna unipuncta,* as a model system we analyzed fat body samples to test the hypothesis that environmental cues would influence the use of essential fatty acids during migratory flight. We used diets manipulated isotopically to trace origins and use of stored lipids and used chromatographic analyses to determine fatty acid composition. In the first experiments, 5-day old moths that had been reared in summer or fall (migratory) conditions and were force flown for different lengths of time (0–6h) after which samples of the fat body were analyzed. Rearing conditions did not affect fatty acid loading however patterns of use during flight differed with essential fatty acids being conserved under fall but not summer conditions. As migratory flight can take several days, we repeated the experiment when 5-day old moths were flown for 8h each day for up to 5 days. Some moths were provided access to sugar water after each flight while others were only given water or only given sugar water once. When sugar water was readily or sporadically available, moths reared under fall conditions conserved their essential fatty acids indicating that the environmental cues responsible for the onset of migratory flight result in physiological changes that modify lipid use. However, when moths had only water, the essential fatty acids were not conserved, highlighting the importance of nectar availability at stopovers for the conservation essential fatty acids during migration. Isotopic analysis of the moth fat body indicated a large contribution of adult-derived diet to lipids used as fuel. The implications of using isotopic approaches to other flight studies and future research on differential resource allocation in winged monomorphic migratory insects are discussed. Summary statement: Isotopic tracing methods and gas chromatography were used to demonstrate that environmental cues can impact patterns of fatty acid use in true armyworm moths. In particular, essential fatty acids are conserved during migratory flight. However, availability of adult food sources will determine the degree to which essential fatty acids are conserved.

KEYWORDS

true armyworm, essential fatty acids, migration, carbon-13, trade off

1. Introduction

Diapause or seasonal migration in response to proximal cues indicating impending habitat deterioration, such as declining temperature, photoperiod, and host plant quality, are key components in the life history of many temperate insect species (Dingle, 1972, 2014; Saunders, 1987; Dixon et al., 1993). Whether entering a dormant state locally or emigrating to more favorable habitats, there is a need to acquire the appropriate energy reserves, as the failure to do so could result in death or a significant decline in the subsequent reproductive success of survivors.

Acquiring the appropriate energy reserves, predominantly in the form of lipids, is often associated with periods of hyperphagia (Beenakkers, 1969; Schneider and Dorn, 1994; McCue et al., 2015). The subsequent allocation of lipids during diapause or migration is important as they are also used for hormone synthesis, neuronal development, membrane integrity, defensive secretions, and reproduction (Stanley-Samuelson et al., 1988). Certain fatty acids (FAs) are considered as nonessential (NFAs) as they can be synthesized by the adult insect from other macronutrients, and so could be replaced through feeding post diapause or migration. However, others cannot be synthesized and are considered essential (EFAs) as they must be obtained directly from the diet. Thus, any EFAs used during diapause or migration that cannot be replaced could have negative consequences.

In the case of migratory Lepidoptera, the onset of migration is typically initiated by adults in reproductive diapause (Johnson, 1963; Dingle, 2014) and any subsequent replacement of lipids used during migration would have to be synthesized from nectar (i.e., carbohydrate) sources. However, as nectar only contains trace amounts of FAs (Nicolson and Thornburg, 2007; Krenn, 2010), the majority of EFA acquisition by Lepidoptera occurs during larval development. Thus, any EFAs used during migration would not be replaced. Previous studies on Lepidoptera have shown that EFAs are not conserved during flight under summer condition (Murata and Tojo, 2002; Sakamoto et al., 2004) but in their study comparing solitary and gregarious desert locusts (*Schistocerca gregaria*) (thus non migratory and migratory), Schneider and Dorn (1994) raised the possibility that EFAs may be conserved during migratory flight. If this were the case in migratory Lepidoptera, the conservation of EFAs during migratory flight would limit any negative post migration effects on reproduction. Therefore, we tested the hypothesis that the physiological changes in response to the environmental cues that induce the onset of migration would also influence the use of EFAs during flight. We predicted that adults reared under fall conditions would conserve EFAs while those under summer conditions would not.

We used the true armyworm, *Mythimna unipuncta*, a sporadic agricultural pest as a model system as it is a seasonal migrant (Guppy, 1961; Fields and McNeil, 1984; Hobson et al., 2018). Furthermore, previous research has shown that individuals reared under fall conditions have significant physiological differences than those reared under summer conditions, affecting sexual maturation, pheromone communication and lipid accumulation (Turgeon and McNeil, 1983; Delisle and McNeil, 1987; Cusson and McNeil, 1989). We reared insects under several different ecological conditions and then determined the fat body lipid content of newly emerged adults and 5-day old adults using gas chromatography and isotopically ($\delta^{13}C$) distinct larval and adult diets. In addition, moths were force flown for different lengths of time to determine if rearing conditions, flight duration and resource availability play a role in influencing fatty acid use during flight.

2. Methods

2.1. Insect colony

All individuals used were from a colony established using adults collected from light and pheromone traps (a minimum of 30 males and 30 females captured during the 2022 spring immigrant flight period) at the Environmental Sciences Western (ESW) Field Station (43.07°N, 81.34°W). The colony was maintained at 25°C, 16:8D, 70 ± 5% RH, with larvae being reared individually on a (C3: $\delta^{13}C$: ~−25.2‰) pinto bean diet (Shorey and Hale, 1965) while adults were provided an *ad lib* supply of 25% (C4: $\delta^{13}C$:~−12.2‰) cane sugar and tap water solution. The adults used for all experiments had not been in rearing for more than two generations.

Depending on the specific experiment, the larvae used were reared under the same laboratory conditions as the colony, or in an insectary under natural conditions in June/July and August/September, subsequently referred to as summer and fall conditions, respectively.

2.2. General protocol for fat body lipid extraction and chromatographic analysis

At the end of each experiment, adults were weighed (to nearest mg, Supplementary A1) and stored at −80°C until fat body tissue was analyzed. In all experiments, fat body tissue was excised (5–10 mg) and the lipids extracted in a 2:1 chloroform:methanol solution (Folch et al., 1957) containing 0.01% butylated hydroxytoluene. If they were used for GC analyses the extraction was performed under N_2 flow to reduce oxidation of FAs. Twenty µL of an internal standard reference, *margaric acid* (17:0, 3 mg/mL), was added. One milliliter of 0.25% KCl was added to the sample to separate out aqueous solutes. The FAs were then converted into fatty acid methyl esters by adding 200 µL of 0.5 M methanolic hydrogen chloride and reacting at 90°C for 30 min. The solution was then reduced to dryness under nitrogen, resuspended in hexane and 100 µL samples subsequently analyzed using gas chromatography. Analyses were performed using a gas chromatography/flame ionization detector (Agilent Technologies® 6890 N G1530N, Santa Clara, United States) equipped with a DB23 column (Agilent DB23 122-2332, Santa Clara, United States). The injector temperature was 250°C and the flame ionization detector temperature was at 280°C. During each run, a 100 µL dichloromethane control was also included. The retention times of PUFA standards (Supelco® PUFA and 37 component) were averaged to create a library of known fatty acid peaks. The distinct and clear peaks of each sample chromatograph were compared to the known retention times to

Abbreviations: FA, fatty acid; EFA, essential fatty acid; NFA, nonessential fatty acid; TAW, true armyworm; OL, oleic acid; PA, palmitic acid; ST, stearic acid; LA, linoleic acid; ALA, alpha linolenic acid; AKH, Adipokinetic hormone; JH, juvenile hormone.

identify fatty acids. This, combined with the known concentration of the internal standard were used to calculate the concentration of each fatty acid (nmol/mL). When required separate fat body samples were used for isotopic analysis (see below).

2.3. General protocol for flight assays

The scales on the dorsal surface of the thorax were removed and a 3 cm piece of clear plastic tubing (2 mm diameter) was attached using EVO–STIK (Stafford, United Kingdom) instant contact adhesive. Each moth was then suspended from a copper wire placed perpendicular to flight apparatus base *via* the thoracic tether and force flown for the required period of time (Figure 1). If a moth stopped flying its back legs were gently touched with a camel hair brush but if the individual did not resume flight after three such stimulations it was not included in subsequent analyses.

2.4. Protocols of specific experiments

To test that the majority of lipid present in the fat body of mature individuals is acquired from adult resources, we reared cohorts under lab, summer, and fall conditions. Under each rearing condition 20 individuals (10 of each sex) were sacrificed at emergence and an equal number fed sugar water *ad lib* were sacrificed after 5 days. The fat body $\delta^{13}C$ values of newly emerged individuals would reflect only the C3 larval diet while those of 5-day old individuals would also include the contribution from the C4 sugar water diet.

For $\delta^{13}C$ analyses 0.91–0.99 mg of frozen lipid (see above) were placed into tin capsules (8×5 mm) and crushed. All prepared samples were shipped *via* expedited courier to the Cornell Isotope Laboratory (COIL, Ithaca, NY, United States) where isotopic measurements were performed. Here, crushed capsules were combusted at 1,000°C in a Carlo-Erba NC2500 Elemental Analyzer (Carlo Erba, Italy) and CO_2 gas transferred *via* a ConFlo IV (Thermo Scientific, Bremen Germany) device to a Delta V Advantage Isotope Ratio Mass Spectrometer (Thermo Scientific, Bremen Germany). Data were normalized using internal calibrated lab standards (Cayuga brown trout: −25.58‰ and corn: −13.02‰); instrument linearity was assessed using in-house methionine (−27.2‰) and ground deer hair (−20.1‰) standards. All values are reported in standard delta (δ) notation relative to the Vienna Pee Dee Belemnite (VPDB) standard in parts per 1000 (‰).

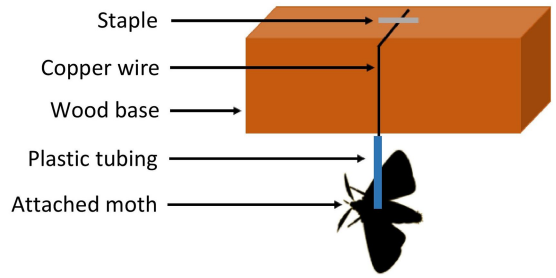

FIGURE 1
Set up used for forced flight experiments of tethered true armyworm moths. A video is provided as Supplementary Video S1.

Measurement error based on within-run standards was estimated as ±0.1‰.

If lipids used during flight were principally of adult (C4) origin, then one would predict that as they were metabolized the $\delta^{13}C$ values in the fat body would change, becoming closer and closer to the C3 larval diet value as a function of flight duration. To determine if this was the case, 10 five-day old adults (5 of each sex) were reared under either natural summer or fall conditions, then force flown for 0, 1, 4, or 6 h, after which time lipids were extracted from fat body tissue and prepared for $\delta^{13}C$ isotopic analysis, as in the previous experiment.

Using the samples prepared for GC analyses, described above, we quantified the relative concentrations of specific FAs in fat body samples from the same individuals as the two previous experiments. We selected the NFAs oleic (OL), palmitic (PA), and stearic acid (ST), as they are found in high levels in Lepidoptera (Subramanyam and Cutkomp, 1987; Canavoso et al., 2001) and the EFAs alpha-linolenic acid (ALA) and linoleic acid (LA) as they cannot be *de novo* synthesized by Lepidopterans but are essential for adults, particularly for reproduction (Canavoso et al., 2001).

In light of the differences observed in EFA use between the summer- and fall-reared insects, and the fact that migratory flight generally occurs over more than one night, we conducted additional experiments using a cohort of 120 fall-reared individuals that were fed sugar water *ad lib* for 5 days. Then 20 (10 of each sex) were sacrificed without being flown, while the remaining 100 were flown for 8 h, after which 10 (5 of each sex) were sacrificed and fat body samples taken. A subset of 40 moths were flown 8h/day and fed sugar water ad lib after each flight period, with a subsample (five of each sex) sacrificed after 1, 2, 3, or 4 days. The same protocol was repeated with 40 moths only provided *ad lib* water after each flight. In addition, a subset of 20 moths receiving only water were provided sugar water ad lib once, after the third day of flight. Fat body samples were analysed, as described above, to determine the changes in relative FA concentrations as a function of the number of flight periods and the availability of adult resources.

2.5. Statistical analysis

All statistical tests (ANOVA, Tukey's post-hoc analysis, unpaired *t*-tests) were performed using R Studio (Version 3.4.2 (2017-09-28)). ANOVA and Tukey's post-hoc analysis were used to compare specific FA levels and $\delta^{13}C$ values of the fat body (dependent variable) across different ages, rearing conditions and flight durations (independent variables). Unpaired *t*-tests were used to determine specific differences in FA patterns or $\delta^{13}C$ values of the fat body between sexes. Normality of data was confirmed using Skew (−1 to +1) and Kurtosis (−4 to +4) analyses.

3. Results

While the $\delta^{13}C$ values of the fat body from newly emerged adults reflected the C3 larval diet, after 5 days of *ad lib* feeding, the $\delta^{13}C$ values increased regardless of rearing conditions (ANOVA, df, 5,112, $F = 936.3$, $p < 0.001$), and clearly reflected the addition of lipids derived from the C4 adult diet (Figure 2). In both age groups there were no

differences in $\delta^{13}C$ values of the fat body due to rearing conditions (Tukey HSD, Day 0 fall versus summer: $p = 0.21$, Day 0 fall versus lab: $p = 0.99$, Day 0 summer versus lab: $p = 0.47$, Day 5 fall versus summer: $p = 0.93$, Day 5 fall versus lab: $p = 0.14$, Day 5 summer versus lab: $p = 0.17$) or sex (ANOVA, df, 1,112, $F = 0.631$, $p = 0.425$). The concentration of total FAs increased significantly from day 0 to day 5 in non-flown adults across all rearing conditions (Table 1; ANOVA, df, 5,119, $F = 27.72$, $p < 0.0001$). This was due to the marked changes in the NFAs (Table 1; ANOVA, df, 5,119, $F_{PA} = 27.45$, $F_{OL} = 26.52$ $F_{ST} = 8.74$, $p < 0.001$), but there were no significant differences in FA concentrations between the three rearing conditions at either age (Tukey HSD, Day 0 fall versus summer: $p = 0.99$, Day 0 fall versus lab: $p = 1.0$, Day 0 summer versus lab: $p = 1.0$, Day 5 fall versus summer: $p = 0.69$, Day 5 fall versus lab: $p = 0.25$, Day 5 summer versus lab: $p = 0.97$). In contrast, while the concentration of the two EFAs did not differ between rearing conditions within any age group, both declined with age (Table 1; ANOVA, df, 5,119, $F_{LA} = 16.72$, $F_{ALA} = 21.48$, $p < 0.001$).

There was a significant decline in the lipid $\delta^{13}C$ values of 5-day old individuals as a function of flight duration under both rearing conditions, although the patterns differed. For moths reared under summer conditions, an overall decline was only significant after 6 h (Figure 3A; ANOVA, df, 3,49, $F = 21.24$, $p < 0.05$, Tukey HSD, $p < 0.05$) and was more pronounced in females than males (Supplementary A2; Unpaired t-test, $t = 9.15$, df = 1,19, $p < 0.05$). For fall moths a significant change was observed after 4 h (Figure 3B; ANOVA, df, 3,49, $F = 21.634$, $p < 0.05$, Tukey HSD, $p < 0.05$), and, as with summer moths, the change was more evident in females than males (Supplementary A3; Unpaired t-test, $t_4 = 3.84$, $t_6 = 4.72$ df = 1,19, $p < 0.05$).

The total concentration of FAs declined as a function of flight duration in both summer (Table 2; ANOVA, df, 3,49, $F = 10.321$, $p < 0.001$, Tukey HSD, $p < 0.05$) and fall (Table 3; ANOVA, df, 3,49, $F = 10.261$, $p < 0.001$, Tukey HSD, $p < 0.05$) reared 5-day old moths. In summer moths, the decline in NFA was due to decreases in the concentrations of PA and OA, and both EFAs (Table 2; ANOVA, df, 3,49, $F_{PA} = 8.414$ $F_{OL} = 6.301$ $F_{LA} = 5.706$ $F_{ALA} = 4.910$; $p < 0.05$, Tukey HSD, $p < 0.05$, for all). In all cases, the significant declines in FA concentration were observed after 4 h of sustained flight (Tukey HSD, $p < 0.05$). In fall-reared moths a significant decline in total FAs was detected after 6 h of sustained flight (Tukey HSD, $p < 0.05$), due to lower levels of all three NFA but with no change in the concentration of the two EFAs (Table 3; ANOVA, df, 3,49, $F_{PA} = 10.331$, $F_{ST} = 7.654$, $F_{OL} = 9.864$, $p < 0.01$, Tukey HSD, $p < 0.05$; $F_{LA} = 0.671$, $F_{ALA} = 1.802$ $P_{LA} = 0.67$, $P_{ALA} = 0.31$).

During multiple days of flight, the concentration of total FAs increased after the first day of flight and remained stable when fall moths were fed *ad lib*. This was due to an increase in OL, as the concentrations of the other NFAs and EFAs did not change significantly (Figures 4A, 5A; ANOVA, df, 5,69, $F_{PA} = 0.957$, $F_{ST} = 0.965$, $F_{LA} = 0.512$ $F_{ALA} = 0.487$, $P_{PA} = 0.42$, $P_{ST} = 0.41$ $P_{LA} = 0.49$ $P_{ALA} = 0.51$; $F_{total} = 4.759$, $F_{OL} = 5.704$; $p < 0.05$). In contrast, when moths were only provided water during the rest periods there was an overall decline in the total concentration of FAs. This was due to lower levels of all NFAs and EFAs, with most significant differences being observed after 4 days of forced flight (Figures 4B, 5B; ANOVA, df, 5,69 $F = 4.751$, $F_{PA} = 6.847$, $F_{ST} = 2.533$, $F_{OL} = 5.147$, $F_{LA} = 3.716$ $F_{ALA} = 4.446$, $p < 0.05$). However, if moths were provided *ad lib* sugar water after the third night of flight, the levels of total FAs remained stable on days 8 and 9 (Figures 4C, 5C; ANOVA, df, 2,29 $F = 1.727$, $p = 0.33$).

4. Discussion

Anparasan et al. (2021) reported that non-flown TAW moths accumulated stored lipids under summer conditions and our current results show this occurs regardless of rearing conditions. This is driven by a rapid accumulation of adult-diet derived NFAs, reflected in the rapid rise in PA and OL (approximately three times the amount found at emergence; Table 1) and the change in $\delta^{13}C$ values of the fat body (Figure 2). Concentrations of the EFAs declined slightly between 0 and 5 days in non-flown individuals under all rearing conditions (Table 1) but probably for different

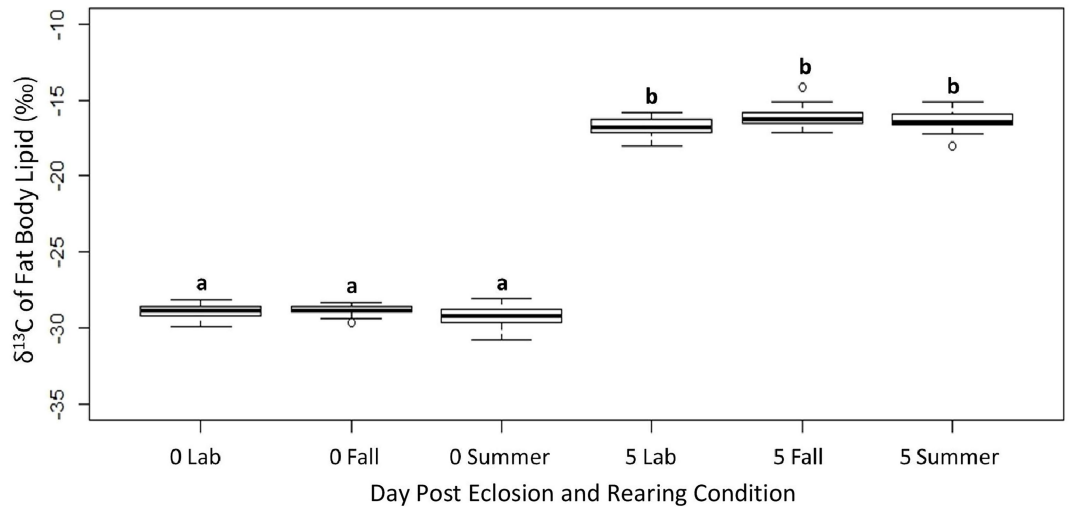

FIGURE 2
The $\delta^{13}C$ values of the fat body from non-flown true armyworm adults fed sugar water *ad lib* as a function of age and rearing conditions. Significant differences are indicated by different letters (Tukey's HSD, $p < 0.05$). $N = 20$ per sample group.

TABLE 1 Concentration of specific essential and non-essential fatty acids in the fat body of non-flown true armyworm adults as a function of age and rearing conditions.

Fatty acid	Lab day 0 (μmol/mL)	Fall day 0 (μmol/mL)	Summer day 0 (μmol/mL)	Lab day 5 (μmol/mL)	Fall day 5 (μmol/mL)	Summer day 5 (μmol/mL)
Palmitic	$39.5 \pm 2.5^{(a)}$	$39.2 \pm 2.2^{(a)}$	$38.9 \pm 3.4^{(a)}$	$86.6 \pm 4.7^{(b)}$	$108.1 \pm 6.4^{(b)}$	$84.1 \pm 5.8^{(b)}$
Stearic	$3.1 \pm 0.5^{(a)}$	$3.5 \pm 0.2^{(a)}$	$4.7 \pm 0.6^{(a)}$	$7.9 \pm 0.6^{(b)}$	$8.8 \pm 0.3^{(b)}$	$8.4 \pm 0.9^{(b)}$
Oleic	$58.5 \pm 3.3^{(a)}$	$54.1 \pm 3.2^{(a)}$	$58.1 \pm 4.6^{(a)}$	$153.7 \pm 12.5^{(b)}$	$170.9 \pm 11.2^{(b)}$	$159.9 \pm 10.8^{(b)}$
Linoleic	$5.0 \pm 0.2^{(a)}$	$5.4 \pm 0.4^{(a)}$	$5.3 \pm 0.3^{(a)}$	$3.9 \pm 0.4^{(b)}$	$4.5 \pm 0.2^{(b)}$	$3.8 \pm 0.5^{(b)}$
Alpha linolenic	$1.8 \pm 0.1^{(a)}$	$2.0 \pm 0.2^{(a)}$	$1.9 \pm 0.2^{(a)}$	$1.6 \pm 0.1^{(b)}$	$1.5 \pm 0.1^{(b)}$	$1.5 \pm 0.1^{(b)}$
Total FA	$107.7 \pm 8.1^{(a)}$	$112.7 \pm 5.1^{(a)}$	$118.8 \pm 8.4^{(a)}$	$259.0 \pm 18.1^{(b)}$	$300.3 \pm 18.6^{(b)}$	$266.8 \pm 17.4^{(b)}$

Letter differences indicate statistically significant differences within each row for individual and total fatty acids (Tukey's HSD, $p < 0.05$). $N = 20$ per sample group.

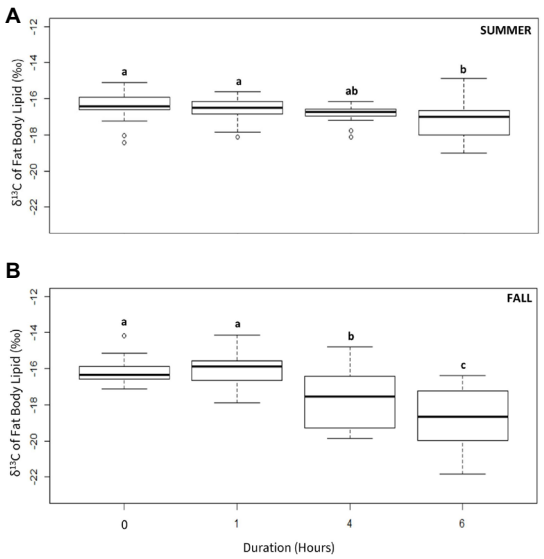

FIGURE 3
$\delta^{13}C$ values of the fat body from 5-day old true armyworm moths after different periods of force flight when reared under **(A)** summer or **(B)** fall conditions. Letters indicate statistically significant differences in isotopic values as a function of flight time (Tukey's HSD, $p < 0.05$). $N = 10$ per sample group ($N = 20$ in Day 5 no flight).

reasons. Under summer conditions, most males and females are sexually mature at 5 days post emergence (Delisle and McNeil, 1987; Cusson and McNeil, 1989; Dumont and McNeil, 1992) and thus some EFAs would be incorporated in different components of the reproductive systems, as reported in other Lepidoptera (Martin, 1969; Arrese and Soulages, 2010). In contrast, under fall conditions that initiate migratory behavior, adults take several weeks to become sexually mature (Delisle and McNeil, 1987; Cusson and McNeil, 1989; Dumont and McNeil, 1992). There is little or no development of the reproductive systems on day five under fall conditions, however as EFAs LA and ALA are found at high levels in the thorax muscles of other migratory insects (e.g., Turunen, 1974) the observed decline may be the result of their incorporation in flight muscle.

The decline in the NFAs OL and PA, as well as the $\delta^{13}C$ value of the fat body, as a function of flight duration in 5-day old moths supports the idea that adult-derived FAs are preferentially used by the true armyworm to fuel flight, as reported for other insects (Schneider and Dorn, 1994; Wang and Ouyang, 1995; Murata and Tojo, 2002; Sakamoto et al., 2004; Levin et al., 2017). Furthermore, the fact that following flight the levels of LA and ALA in the fat body decline in moths reared under summer conditions but not in those reared under fall conditions (Tables 2, 3) support our hypothesis of differential FA allocation under different environmental conditions. As these EFAs are important for reproduction (Martin, 1969; Arrese and Soulages, 2010), the fact that they are conserved under the environmental conditions stimulating the onset of migration would ensure more are available once a suitable habitat is located and could reduce the costs of migration on future reproductive success.

The difference in the time taken to see a significant decline in FAs in summer- and fall-reared 5 day-old moths as a function of flight duration (Tables 2, 3; Figure 3) may reflect physiological differences related to fuel-use efficiency arising from differences in the physiology of the two seasonal morphs. These could include different levels of muscle FA binding proteins (Haunerland, 1997) and/or increased levels of and responsiveness to lipophorin molecules (Chino et al., 1992). Furthermore, insects reared under migratory conditions may have more developed flight muscles (Boggs, 2009) and/or differential wing loading (Roff and Fairbairn, 1991). The decline in the LA and ALA in the fat body of force-flown moths reared under summer conditions may be the result of their mobilization to flight muscles (see above). Under both rearing conditions, it took at least 4 h of forced flight to detect any significant decline in lipid levels and this was likely related to the initial phase of flight being fueled by carbohydrates, as reported in another migratory noctuid, *Agrotis ipsilon* (Sappington et al., 1995). The release of lipids from the fat body of the armyworm is modulated by adipokinetic hormone (AKH) and previous work has shown that it takes about an hour of forced flight for lipid levels to stabilize in the haemolymph (Orchard et al., 1991), a pattern also reported in the tobacco hornworm (*Manduca sexta*; Arrese and Wells, 1997).

As noted, the reduction in the EFAs in summer- but not fall-reared moths supports our hypothesis that physiological changes in response to environmental cues associated with onset of migratory behavior help conserve EFAs during migration. Schneider and Dorn (1994) suggested this may be the case in gregarious migratory locusts and proposed several possible mechanisms to explain such an adaptation. One included the involvement of juvenile hormone (JH), as higher titers may reduce fat body lipid storage in locusts. Previous research on the

TABLE 2 Change in the concentration of essential and nonessential fatty acids in the fat body of 5-day old true armyworm moths as a function of flight duration under summer conditions.

Flight	Palmitic (μmol/mL)	Stearic (μmol/mL)	Oleic (μmol/mL)	Linoleic (μmol/mL)	Alpha Linolenic (μmol/mL)	Total FA (μmol/mL)
No flight	84.1 ± 5.8$^{(a)}$	8.4 ± 0.9$^{(a)}$	159.9 ± 10.8$^{(a)}$	3.8 ± 0.5$^{(a)}$	1.5 ± 0.1$^{(a)}$	266.8 ± 17.4$^{(a)}$
1 h flight	85.9 ± 3.5$^{(a)}$	8.4 ± 0.5$^{(a)}$	142.6 ± 8.1$^{(a)}$	3.4 ± 0.2$^{(a)}$	1.3 ± 0.1$^{(a)}$	243.4 ± 11.1$^{(a)}$
4 h flight	74.2 ± 2.2$^{(b)}$	7.8 ± 0.3$^{(a)}$	110.9 ± 6.3$^{(b)}$	2.8 ± 0.1$^{(b)}$	1.1 ± 0.05$^{(b)}$	204.7 ± 9.01$^{(b)}$
6 h flight	68.3 ± 2.6$^{(c)}$	7.7 ± 0.2$^{(a)}$	86.7 ± 2.5$^{(c)}$	2.4 ± 0.1$^{(c)}$	1.1 ± 0.06$^{(b)}$	170.1 ± 4.8$^{(c)}$

Letters indicate statistically significant differences within the column for each fatty acid (Tukey's HSD, $p < 0.05$). $N = 10$ per sample group ($N = 20$ in no flight).

TABLE 3 Change in the concentration of essential and nonessential fatty acids in the fat body of 5- day old true armyworm moths as a function of flight duration under fall conditions.

Flight	Palmitic (μmol/mL)	Stearic (μmol/mL)	Oleic (μmol/mL)	Linoleic (μmol/mL)	Alpha Linolenic (μmol/mL)	Total FA (μmol/mL)
No flight	108.1 ± 6.4$^{(a)}$	8.8 ± 0.3$^{(a)}$	170.9 ± 11.2$^{(a)}$	4.5 ± 0.2$^{(a)}$	1.5 ± 0.1$^{(a)}$	300.3 ± 18.6$^{(a)}$
1 h flight	105.1 ± 3.5$^{(a)}$	9.2 ± 0.8$^{(a)}$	155.3 ± 5.9$^{(ab)}$	4.4 ± 0.5$^{(a)}$	1.6 ± 0.1$^{(a)}$	291.3 ± 8.4$^{(a)}$
4 h flight	108.9 ± 3.3$^{(a)}$	8.8 ± 0.2$^{(a)}$	154.0 ± 2.5$^{(b)}$	4.8 ± 0.3$^{(a)}$	1.6 ± 0.1$^{(a)}$	288.5 ± 6.6$^{(a)}$
6 h flight	97.0 ± 1.4$^{(b)}$	8.3 ± 0.2$^{(b)}$	138.5 ± 3.0$^{(c)}$	4.5 ± 0.4$^{(a)}$	1.6 ± 0.1$^{(a)}$	254.9 ± 4.8$^{(b)}$

Letters indicate statistically significant differences within the column for each fatty acid (Tukey's HSD, $p < 0.05$). $N = 10$ per sample group ($N = 20$ in no flight).

armyworm has shown that there are lower JH titers in moths reared under fall conditions resulting in the delayed development of the reproductive organs, as well as the production of, and response to, the female sex pheromone (Delisle and McNeil, 1987; Cusson and McNeil, 1989; Dumont and McNeil, 1992). However, additional research is required to determine if JH plays a role in the conservation of EFAs during migration.

The results obtained when fall-reared moths were flown for 8h/day on five consecutive days indicate that the EFAs are conserved over the entire period as long as moths have access to suitable resources. Interestingly, for 5-day-old moths flown for only 8h there was sharp decline in OL levels compared with those of non-flown individuals of the same age, while the post flight concentration on subsequent days were similar to the non-flown controls. This is undoubtedly due to adults increasing the amount of resources consumed following forced flight, possibly the result of increased levels of JH, which can affect feeding behaviour (Rankin, 1991; Dingle and Winchell, 1997). Min et al. (2004) reported a post flight increase in JH titers for migratory grasshoppers, and Cusson et al. (1990) reported increased JH production when TAW adults experienced an increase in ambient temperature. Thus, if increasing body temperature following flight resulted in higher JH levels and led to higher consumption of resources, it would result in greater changes in levels of OL compared with the other FAs, as it is one of the most readily used fuel sources in insects (Schneider and Dorn, 1994; Wang and Ouyang, 1995; Tomcala et al., 2010).

In the absence of such resources, the concentration of EFAs in the fat body decline significantly. However, when water fed moths were provided one *ad lib* meal of sugar water after 3 days of flight they only used NFAs when force flown for two additional days. This shows they only used EFAs when there was no other option and underlines the importance of nectar availability at stopover sites during the migratory process, as any shortages could significantly impact individual reproductive success and whether populations subsequently reach pest densities. Nectar availability could vary significantly at different sites along the migratory path due to different environmental conditions. For example, extreme weather events associated with climate change could not only affect the density of available flowers but also the quantity and quality of nectar (Takkis et al., 2018; Descamps et al., 2021). Furthermore, under hot, dry conditions the viscosity of nectar will increase and armyworm moths are less effective at acquiring resources when nectar concentrations are high (Pivnick and McNeil, 1985).

We have shown that if adults have access to nectar resources during migration, they are able to conserve the EFAs found in the fat body. However, if some are utilized to sustain flight there is potential for negative impacts on future reproduction as EFAs are a substantial component to the eggs of many lepidopterans (Martin, 1969; Forte et al., 2002) and thus a decline in the availability of these FAs can reduce the number of viable offspring. This possibility needs further investigation but when quantifying such potential impacts, one also needs to consider other EFA sources that adults might access following migration For example, bark beetles, break down their flight muscles post migration in response to an increase in JH titers (Borden and Slater, 1968; Sahota and Farris, 1980) and these authors have suggested that these resources are invested in reproduction. As noted above there is a significant increase in JH associated with the onset of reproduction in the true armyworm, and it is possible that this change in titer may stimulate post migratory release of EFA resources from flight muscle. However, unlike bark beetles which do not resume flight after colonizing a tree host, the armyworm and other lepidopterans need functional flight muscles for foraging and reproduction throughout adult life, thus obtaining resources through flight muscle degradation may be limited. Secondly, females of some migratory species are polyandrous (Torres-Vila et al., 2004) and thus obtaining several spermatophores from repeated mating could offer them an alternative source of resources. Both eggs and female somatic tissue contain male-derived resources (Boggs and Gilbert, 1979; Boggs, 1981; Wiklund et al., 1993), and males of some migratory species transfer JH at the time of mating (e.g., Park et al., 1998). As *M. unipuncta* is polyandrous, the spermatophores are potential nutrient sources (Marshall and McNeil, 1989) and repeated mating increases female reproductive output (Svärd and McNeil, 1994), so the potential importance of male derived EFAs merits further attention.

In addition to JH, various analogs of AKH have been shown to mobilize FAs differentially which may also be a mechanism by which resource limited TAW moths are allocating FAs. The migratory morph of *Locusta migratoria* expresses high levels of AKH II which mobilizes more OL and saturated fatty acids compared to other analogs (Tomcala et al., 2010). TAW moths may produce similar AKH analogs and merits investigation as the previous study on AKH in TAW did

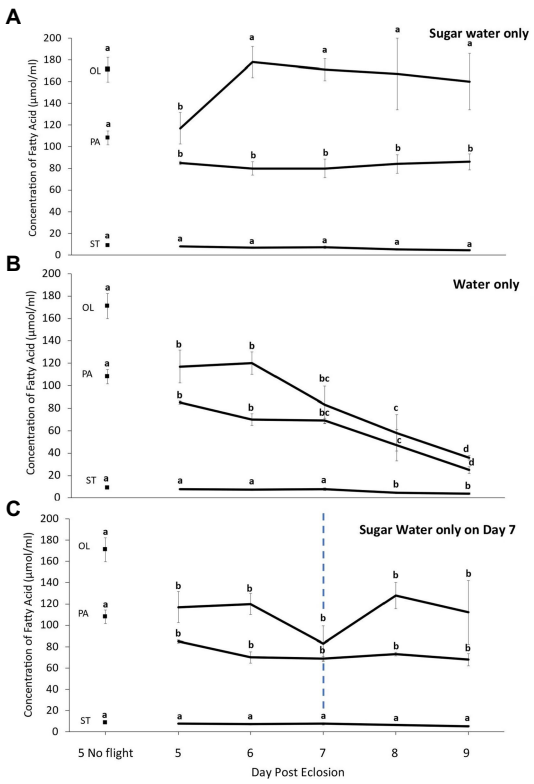

FIGURE 4
Change in the concentration of non-essential [palmitic (PA), oleic (OL) and stearic (ST)] fatty acids in fat body of true armyworm moths reared under fall conditions as a function of the number of 8-h flight periods when fed **(A)** sugar water *ad lib* daily, **(B)** provided water only, or **(C)** provided water on all days except at the end of Day 7 when they were provided sugar water *ad lib* during the rest period. The two values for Day 5 represent samples taken from un-flown moths prior to the flight period and from moths after 8h of flight. In the other days samples were taken at the end of the flight period. Letters indicate statistically significant differences in each category of fatty acid (Tukey's HSD, p <0.05). N =10 per sample group (N =20 in Day 5 no flight).

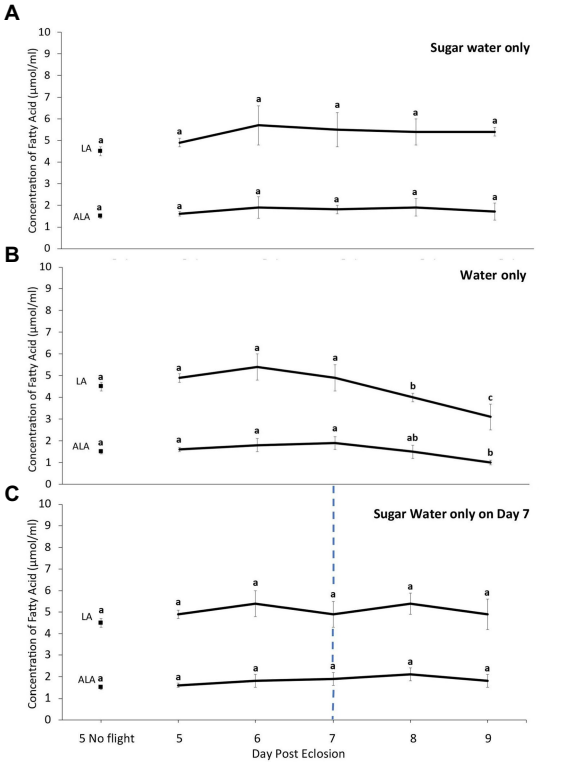

FIGURE 5
Change in the concentration of essential [linoleic (LA) and alpha linolenic (ALA)] fatty acids in the fat body of true armyworm moths reared under fall conditions as a function of the number of 8-h flight periods when fed **(A)** sugar water *ad lib* daily, **(B)** provided water only, or **(C)** provided water on all days except at the end of the flight period on Day 7 when they were provided sugar water *ad lib* during the rest period. The two values for Day 5 represent samples taken from un-flown moths prior to the flight period and from moths after 8h of flight. In the other days samples were taken at the end of the flight period. Letters indicate statistically significant differences in each category of fatty acid (Tukey's HSD, p <0.05). N =10 per sample group (N =20 in Day 5 no flight).

not explore the possible role of different AKH analogs (Orchard et al., 1991).

Our study demonstrates the power of using bulk isotopic tracing to examine the evolution of lipid allocation in migrant insects, particularly for insects such as the TAW where larval and adult diets are distinct. The use of carbon isoscapes, especially a compound-specific approach using $\delta^{13}C$ in individual EFAs and NFAs (Whiteman et al., 2019; Pilecky et al., 2022) would allow for a greater understanding about nectaring stopover sites and sources of vital nutrients for migrant species in the wild. In fact, using a similar design setup to this experiment, tracing of isotopically labeled EFAs and NFAs could be used (as seen in studies on amino acids, e.g., Levin et al., 2017) to determine the fate, isotopic changes and confirmed source of FAs from the fat body, as well as the subsequent allocation to reproduction after flight. Clearly, future research will need to address all of these possibilities as this will not only contribute to our understanding of basic flight energetics but also how energy use would affect the population of migrants whether they are pests or ones, like the monarch butterfly (*Danaus plexippus*), that we wish to protect.

Data availability statement

The raw data supporting the conclusions of this article will be made available by the authors, without undue reservation.

Author contributions

LA, KH, and JM developed the protocols and wrote the manuscript, with LA performing the experiments. All authors contributed to the article and approved the submitted version.

Funding

LA was supported through a graduate stipend from the University of Western Ontario and the Queen Elizabeth II Graduate Scholarships in Science and Technology. This research was funded by Natural Science and Engineering Research Council of Canada (NSERC) Discovery grants to KH (#2017-04430) and JM (#2020-07203).

Acknowledgments

We thank (i) Blanca X. Mora-Alvarez and Erna Leclair for assistance in the lab, (ii) the Cornell University Stable Isotope Laboratory at Cornell University, Ithaca NY for stable isotope analyses, and (iii) C. Guglielmo for the use of the gas chromatography/flame ionization detector.

Conflict of interest

The authors declare that the research was conducted in the absence of any commercial or financial relationships that could be construed as a potential conflict of interest.

Publisher's note

All claims expressed in this article are solely those of the authors and do not necessarily represent those of their affiliated organizations, or those of the publisher, the editors and the reviewers. Any product that may be evaluated in this article, or claim that may be made by its manufacturer, is not guaranteed or endorsed by the publisher.

Supplementary material

The Supplementary material for this article can be found online at: https://www.frontiersin.org/articles/10.3389/fevo.2023.1055534/full#supplementary-material

References

Anparasan, L., McNeil, J. N., and Hobson, K. A. (2021). Tracing sources of carbon and hydrogen to stored lipids in the migratory moth, *Mythimna unipuncta*, using stable isotopes (δ^2H, δ^{13}C). *Physiol. Entomol.* 46, 45–51. doi: 10.1111/phen.12343

Arrese, E. L., and Soulages, J. L. (2010). Insect fat body: energy, metabolism, and regulation. *Annu. Rev. Entomol.* 55, 207–225. doi: 10.1146/annurev-ento-112408-085356

Arrese, E. L., and Wells, M. A. (1997). Adipokinetic hormone-induced lipolysis in the fat body of an insect, *Manduca sexta*: synthesis of sn-1,2-diacylglycerols. *J. Lipid Res.* 38, 68–76. doi: 10.1016/S0022-2275(20)37276-X

Beenakkers, A. M. T. (1969). Carbohydrate and fat as a fuel for insect flight. A comparative study. *J. Insect Physiol.* 15, 353–361. doi: 10.1016/0022-1910(69)90281-9

Boggs, C. L. (1981). Selection pressures affecting male nutrient investment at mating in heliconine butterflies. *Evolution* 35, 931–940. doi: 10.1111/j.1558-5646.1981.tb04959.x

Boggs, C. L. (2009). Understanding insect life histories and senescence through a resource allocation lens. *Funct. Ecol.* 23, 27–37. doi: 10.1111/j.1365-2435.2009.01527.x

Boggs, C. L., and Gilbert, L. E. (1979). Male contribution to egg production in butterflies: evidence for transfer of nutrients at mating. *Science* 206, 83–84. doi: 10.1126/science.206.4414.83

Borden, J. H., and Slater, C. E. (1968). Induction of flight muscle degeneration by synthetic juvenile hormone in *Ips confusus* (Coleoptera: Scolytidae). *Z. Vergl. Physiol.* 61, 366–368. doi: 10.1007/BF00428009

Canavoso, L. E., Jouni, Z. E., Karnas, K. J., Pennington, J. E., and Wells, M. A. (2001). Fat metabolism in insects. *Annu. Rev. Nutr.* 21, 23–46. doi: 10.1146/annurev.nutr.21.1.23

Chino, H., Lum, P. Y., Nagao, E., and Hiraoka, T. (1992). The molecular and metabolic essentials for long-distance flight in insects. *J. Comp. Physiol. B.* 162, 101–106. doi: 10.1007/BF00398334

Cusson, M., and McNeil, J. N. (1989). Ovarian development in female armyworms, *Pseudaletia unipuncta*: its relationship with pheromone release activities. *Can. J. Zool.* 67, 1380–1385. doi: 10.1139/z89-196

Cusson, M., McNeil, J. N., and Tobe, S. (1990). In vitro biosynthesis of juvenile hormone by corpora allata of Pseudaletia unipuncta virgin females as a function of age, environmental conditions, calling behaviour and ovarian development. *J. Insect Physiol.* 33, 139–146. doi: 10.1016/0022-1910(90)90185-I

Delisle, J., and McNeil, J. N. (1987). Calling behaviour and pheromone titre of the true armyworm *Pseudaletia unipuncta* (haw.) (Lepidoptera: Noctuidae) under different temperature and photoperiodic conditions. *J. Insect Physiol.* 33, 315–324. doi: 10.1016/0022-1910(87)90119-3

Descamps, C., Quinet, M., and Jacquemart, A. (2021). Climate change–induced stress reduce quantity and alter composition of nectar and pollen from a bee-pollinated species (*Borago officinalis*, Boraginaceae). *Front. Plant Sci.* 12:755843. doi: 10.3389/fpls.2021.755843

Dingle, H. (1972). Migration strategies of insects. *Science* 175, 1327–1335. doi: 10.1126/science.175.4028.1327

Dingle, H. (2014). *Migration: the biology of life on the move, 2nd ed.*, Oxford, UK: Oxford University Press, 13–23.

Dingle, H., and Winchell, R. (1997). Juvenile hormone as a mediator of plasticity in insect life histories. Arch. *Insect Biochem. Physiol.* 35, 359–373. doi: 10.1002/(SICI)1520-6327(1997)35:4<359::AID- ARCH2>3.0.CO;2-N

Dixon, A. F. G., Horth, S., and Kindlmann, P. (1993). Migration in insects: cost and strategies. *J. Anim. Ecol.* 62, 182–190. doi: 10.2307/5492

Dumont, S., and McNeil, J. N. (1992). Responsiveness of *Pseudaletia unipuncta* (Lepidoptera: Noctuidae) males, maintained as adults under different temperature and photoperiodic conditions, to female sex pheromone. *J. Chem. Ecol.* 18, 1797–1807. doi: 10.1007/BF02751104

Fields, P. G., and McNeil, J. N. (1984). The overwintering potential of true armyworm *Pseudaletia unipuncta* (Lepidoptera: Noctuidae) populations in Quebec. *Can. Entomol.* 116, 1647–1652. doi: 10.4039/Ent1161647-12

Folch, J., Lees, M., and Stanley, G. H. S. (1957). A simple method for the isolation and purification of total lipids from animal tissues. *J. Biol. Chem.* 226, 497–509. doi: 10.1016/S0021-9258(18)64849-5

Forte, S. N., Ferrero, A. A., and Alonso, T. S. (2002). Content and composition of phosphoglycerols and neutral lipids at different developmental stages of the eggs of the codling moth, *Cydia pomonella* (Lepidoptera: Tortricidae). *Arch. Insect Biochem. Physiol.* 50, 121–130. doi: 10.1002/arch.10036

Guppy, J. C. (1961). Life history and behavior of the armyworm, *Pseudaletia unipuncta* (Haw.) (Lepidoptera: Noctuidae), in eastern Canada. *Can. Entomol.* 93, 1141–1153. doi: 10.4039/Ent931141-12

Haunerland, N. H. (1997). Transport and utilization in insect flight muscles. *Comp. Biochem. Physiol. B* 117, 475–482. doi: 10.1016/S0305-0491(97)00185-5

Hobson, K. A., Doward, K., Kardynal, K. J., and McNeil, J. N. (2018). Inferring origins of migrating insects using isoscapes: a case study using the true armyworm, *Mythimna unipuncta*, in North America. *Ecol. Entomol.* 43, 332–341. doi: 10.1111/een.12505

Johnson, C. G. (1963). Physiological factors in insect migration by flight. *Nature* 198, 423–427. doi: 10.1038/198423a0

Krenn, H. W. (2010). Feeding mechanisms of adult lepidoptera: structure, function, and evolution of the mouthparts. *Annu. Rev. Entomol.* 55, 307–327. doi: 10.1146/annurev-ento-112408-085338

Levin, E., McCue, M. D., and Davidowitz, G. (2017). More than just sugar: allocation of nectar amino acids and fatty acids in a lepidopteran. *Proc. Royal Soc. B-Biol. Sci.* 284, 2016–2126. doi: 10.1098/rspb.2016.2126

Marshall, L. D., and McNeil, J. N. (1989). Spermatophore mass as an estimate of male nutrient investment: a closer look in *Pseudaletia unipuncta* (Haworth) (Lepidoptera: Noctuidae). *Funct. Ecol.* 3, 605–612. doi: 10.1098/rspb.2016.2126

Martin, J. S. (1969). Lipid composition of fat body and its contribution to the maturing oöcytes in *Pyrrhocoris apterus*. *J. Insect Physiol.* 15, 1025–1045. doi: 10.1016/0022-1910(69)90142-5

McCue, M. D., Guzman, R. M., Passement, C. A., and Davidowitz, G. (2015). How and when do insects rely on endogenous protein and lipid resources during lethal bouts of starvation? A new application for ^{13}C-breath testing. *PLoS One* 10:e0140053. doi: 10.1371/journal.pone.0140053

Min, K. J., Jones, N., Borst, D. W., and Rankin, M. A. (2004). Increased juvenile hormone levels after long-duration flight in the grasshopper, *Melanoplus sanguinipes*. *J. Insect. Physiol.* 50, 531–537. doi: 10.1016/j.jinsphys.2004.03.009

Murata, M., and Tojo, S. (2002). Utilization of lipid for flight and reproduction in *Spodoptera litura* (Lepidoptera: Noctuidae). *Eur. J. Entomol.* 99, 221–224. doi: 10.14411/eje.2002.031

Nicolson, S. W., and Thornburg, R. W. (2007). *Nectaries and nectar*. The Netherlands: Springer, 215–265.

Orchard, I., Cusson, M., and McNeil, J. N. (1991). Adipokinetic hormone of the armyworm, *Pseudaletia unipuncta*, immunohistochemistry, amino acid analysis, quantification and bioassay. *Physiol. Entomol.* 16, 439–445. doi: 10.1111/j.1365-3032.1991.tb00583.x

Park, Y. I., Shu, S., Ramaswamy, S. B., and Srinivasan, A. (1998). Mating in *Heliothis virescens*: transfer of juvenile hormone during copulation by male to female and

stimulation of biosynthesis of endogenous juvenile hormone. *Arch. Insect Biochem. Physiol.* 38, 100–107. doi: 10.1002/(SICI)1520-6327(1998)38:2<100::AID-ARCH6>3.0.CO;2-X

Pilecky, M., Kämmer, S. K., Mathieu-Resuge, M., Wassenaar, L. I., Taipale, S. J., Martin-Creuzburg, D., et al. (2022). Hydrogen isotopes (δ^2H) of polyunsaturated fatty acids track bioconversion by zooplankton. *Funct. Ecol.* 36, 538–549. doi: 10.1111/1365-2435.13981

Pivnick, K. A., and McNeil, J. N. (1985). Effects of nectar concentrations on butterfly feeding: measured feeding rates for *Thymelicus lineola* (Lepidoptera:Hesperiidae) and a general feeding model for adult Lepidoptera. *Oecologia* 66, 226–237. doi: 10.1007/BF00379859

Rankin, M. A. (1991). Endocrine effects on migration. *Am. Zool.* 31, 217–230. doi: 10.1093/icb/31.1.217

Roff, D. A., and Fairbairn, D. J. (1991). Wing dimorphisms and the evolution of migratory polymorphisms among the Insecta. *Am. Zool.* 31, 243–251. doi: 10.1093/icb/31.1.243

Sahota, T. S., and Farris, S. H. (1980). Inhibition of flight muscle degeneration by precocene II in the spruce bark beetle, *Dendroctonus rufipennis* (Kirby) (Coleoptera: Scolytidae). *Can. J. Zool.* 58, 378–381. doi: 10.1139/z80-048

Sakamoto, R., Murata, M., and Tojo, S. (2004). Effects of larval diets on flight capacity and flight fuel in adults of the common cutworm, *Spodoptera litura* (Lepidoptera: Noctuidae). *Appl. Entomol. Zool.* 39, 133–138. doi: 10.1303/aez.2004.133

Sappington, T. W., Fescemyer, H. W., and Showers, W. B. (1995). Lipid and carbohydrate utilization during flight of the migratory moth, *Agrotis ipsilon* (Lepidoptera: Noctuidae). *Arch. Insect Biochem. Physiol.* 29, 397–414. doi: 10.1002/arch.940290407

Saunders, D. S. (1987). Photoperiodism and the hormonal control of insect diapause. *Sci. Prog.* 71, 51–69.

Schneider, M., and Dorn, A. (1994). Lipid storage and mobilization by flight in relation to phase and age of *Schistocerca gregaria* females. *Insect Biochem. Mol. Biol.* 24, 883–889. doi: 10.1016/0965-1748(94)90017-5

Shorey, H. H., and Hale, R. L. (1965). Mass-rearing of the larvae of nine noctuid species on a simple artificial medium. *J. Econ. Entomol.* 58, 522–524. doi: 10.1093/jee/58.3.522

Stanley-Samuelson, D. W., Jurenka, R. A., Cripps, C., Blomquist, G. J., and Renobales, M. (1988). Fatty acids in insects: composition, metabolism, and biological significance. *Arch. Insect Biochem. Physiol.* 9:1. doi: 10.1002/arch.940090102

Subramanyam, B., and Cutkomp, L. K. (1987). Total lipid and fatty acid composition in male and female larvae of Indian-meal moth and almond moth (Lepidoptera: Pyralidae). *Gt. Lakes Entomol.* 20:10.

Svärd, L., and McNeil, J. N. (1994). Female benefit, male risk: polyandry in the true armyworm *Pseudaletia unipuncta*. *Behav. Ecol. Sociobiol.* 35, 319–326. doi: 10.1007/BF00184421

Takkis, K., Tscheulin, T., and Petanidou, T. (2018). Differential effects of climate warming on the nectar secretion of early- and late-flowering Mediterranean plants. *Front. Plant Sci.* 9:874. doi: 10.3389/fpls.2018.00874

Tomcala, A., Bártů, I., Simek, P., and Kodrík, D. (2010). Locust adipokinetic hormones mobilize diacylglycerols selectively. *Comp. Biochem. Physiol.* 156, 26–32. doi: 10.1016/j.cbpb.2010.01.015

Torres-Vila, L. M., Rodrguez-Molina, M. C., and Jennions, M. D. (2004). Polyandry and fecundity in the Lepidoptera: can methodological and conceptual approaches bias outcomes? *Behav. Ecol. Sociobiol.* 55, 315–324. doi: 10.1007/s00265-003-0712-2

Turgeon, J., and McNeil, J. N. (1983). Modifications in the calling behaviour of *Pseudaletia unipuncta* (Lepidoptera: Noctuidae), induced by temperature conditions during pupal and adult development. *Can. Entomol.* 115, 1015–1022. doi: 10.4039/Ent1151015-8

Turunen, S. (1974). Metabolism and function of fatty acids in a phytophagous lepidopteran. *Ann. Zool. Fenn.* 11, 170–184.

Wang, Z., and Ouyang, Y. (1995). Flight activity and fatty acid utilization in *Mythimna separata* (Walker) moths. *Insect Sci.* 2, 370–376. doi: 10.1111/j.1744-7917.1995.tb00061.x

Whiteman, J. P., Elliott-Smith, E. A., Besser, A. C., and Newsome, S. D. (2019). A guide to using compound-specific stable isotope analysis to study the fates of molecules in organisms and ecosystems. *Diversity* 11:8. doi: 10.3390/d11010008

Wiklund, C., Kaitala, A., Lindfors, V., and Abenius, J. (1993). Polyandry and its effect on female reproduction in the green-veined white butterfly (*Pieris napi* L.). *Behav. Ecol. Sociobiol.* 33, 25–33. doi: 10.1007/BF00164343

frontiers | Frontiers in Ecology and Evolution

TYPE Original Research
PUBLISHED 17 April 2023
DOI 10.3389/fevo.2023.1082226

OPEN ACCESS

EDITED BY
Keith Alan Hobson,
Western University,
Canada

REVIEWED BY
Kevin John Kardynal,
Environment and Climate Change Canada (ECCC),
Canada
Steven Goodman,
Field Museum of Natural History,
United States

*CORRESPONDENCE
Elizabeth Yohannes
✉ elizabeth.yohannes@vogelwarte.ch

†PRESENT ADDRESS
Elizabeth Yohannes,
Swiss Ornithological Institute,
Migration Uni, Sempach,
Switzerland

‡These authors share first authorship

SPECIALTY SECTION
This article was submitted to Ecophysiology, a section of the journal Frontiers in Ecology and Evolution

RECEIVED 28 October 2022
ACCEPTED 13 March 2023
PUBLISHED 17 April 2023

CITATION
Yohannes E, Berthoud J-L and Woog F (2023) Trait based niche differentiation in tetrakas (Bernieridae) endemic to Madagascar: A multi-isotope approach.
Front. Ecol. Evol. 11:1082226.
doi: 10.3389/fevo.2023.1082226

Trait based niche differentiation in tetrakas (Bernieridae) endemic to Madagascar: A multi-isotope approach

Elizabeth Yohannes[1,2*†‡], Jean-Louis Berthoud[3‡] and Friederike Woog[4]

[1]Institute of Limnology, University of Konstanz, Konstanz, Germany, [2]Swiss Ornithological Institute, Sempach, Switzerland, [3]Faubourg de l'Hôpital 58, Neuchâtel, Switzerland, [4]Staatliches Museum für Naturkunde Stuttgart (SMNS), Stuttgart, Germany

Introduction: Tropical rainforest species interact with each other and their environment over a wide range of spatiotemporal scales. However, our understanding of resource partitioning and the mechanisms of avian species coexistence is largely restricted to subjective visual observations or acoustic monitoring. Therefore, the relative magnitudes of interspecific and intraspecific differences in resource use have remained difficult to quantify, particularly regarding different diets and habitat use. The eastern rainforest belt of Madagascar is inhabited by several species of insectivorous tetrakas belonging to an endemic bird family of Madagascar (Bernieridae). These species occupy similar habitats in the forest understory and are morphologically similar but because of likely differences (e.g., in foraging behaviors) we expect their foraging niches to be segregated allowing coexistence.

Methods: We examined the niche differentiation of four of these species: the Grey-crowned Tetraka (*Xanthomixis cinereiceps*), Long-billed Tetraka (*Bernieria madagascariensis*), Spectacled Tetraka (*Xanthomixis zosterops*), and White-throated Oxylabes (*Oxylabes madagascariensis*) in the Maromizaha rainforest in eastern Madagascar combining morphometry with stable carbon, nitrogen, and sulfur isotope ratios ($\delta^{13}C$, $\delta^{15}N$, and $\delta^{34}S$) from feathers.

Results: We show considerable variation in isotopic niche positions, niche breadth and interspecific niche overlap. In two species, the Long-billed Tetraka and Spectacled Tetraka, we found an indication of sex-specific niche space, with males exhibiting a larger isotopic niche-area relative to females. Morphological traits of five species (including the Wedge-tailed Tetraka, *Hartertula flavoviridis*) coupled with stable isotope data provided explanations of patterns of niche overlap and isotopic position.

Discussion: The observed isotopic niche differences may be explained by differences in resource acquisition strategies that might be associated with specific morphological traits and spatial distribution. This may play an important role in niche differentiation among coexisting and phylogenetically closely related species.

KEYWORDS

Bernieridae, morphometry, ecological niche, stable isotopes, stable carbon (δ13C), stable nitrogen (δ15N) isotope, stable sulfur isotope, Madagascar

Introduction

Despite the coexistence of phylogenetically closely related and morphologically similar species, niche theory suggests that a complete niche overlap may evolutionarily be unlikely (e.g., Hutchinson, 1957; Hardin, 1960). Coexisting species evolved varying forms of resource

utilization, such as niche partitioning or niche differentiation (Levins, 1968; MacArthur, 1972), which have been widely used to explain coexistence patterns in community assemblages (Schoener, 1974; Giller, 1984; Ross, 1986). Coexistence may occur due to segregation of specific resources (also known as resource partitioning) or through spatiotemporal variation in resource use (Pianka, 1974; Schoener, 1974; Ross, 1986). In tropical forest bird assemblages, partitioning of dietary resources is one of the fundamental mechanisms of niche separation (e.g., Frith, 1984; Symes and Woodborne, 2010; Mansor and Ramli, 2017; Mansor et al., 2022). In line with the competitive exclusion principle (Hardin, 1960) if any species with identical niches or ecological roles compete, one will drive the other to extinction. By implication, multiple species cannot occupy the same exact niche in one habitat and coexist in a stable manner. Consequently, when these species differentiate their niches, they tend to reduce competition, and promote coexistence. This niche differentiation can be achieved through different mechanisms, which includes consuming various dietary items or partitioning of the environment, such as using different vertical strata of the tropical rainforest (Thiel et al., 2021).

The family of tetrakas (Bernieridae) consists of mostly greenish to yellowish songbirds, all of which are endemic to Madagascar. Some resemble typical warblers (Sylviidae), others are bulbul-like (Pycnotidae), and some did not appear to fit in any systematic group (Cibois et al., 1999, 2001). Their systematic relationship was resolved by the genetic studies of Cibois et al. (2010), which referred to them as a separate family, the Bernieridae. Under current taxonomy, they represent an adaptive radiation of 13 species in eight genera (Reddy et al., 2022; Safford et al., 2022). Some show extensive interspecific resemblance but also intraspecific cryptic diversity (Bickford et al., 2007; Block, 2012; Safford and Hawkins, 2013; Block et al., 2015; Reddy et al., 2022).

The adaptive radiation of tetrakas has been at a relatively continuous diversification rate (Block, 2012) since its estimated dispersal to Madagascar between 9–17 MY (Cibois et al., 2001) or 19.2–25.2 MY ago (Beresford et al., 2005). These range estimates are approximately the same as that for the better known adaptive radiation of a Malagasy bird family, the vangas (Vangidae) (Jønsson et al., 2012; Reddy et al., 2012). Contrary to the vangas, the adaptive radiation of the tetrakas does not appear to have resulted in such a large range of morphological variations and feeding behaviors. Present knowledge of the tetrakas describes all of them as almost exclusively insectivorous (Goodman and Parrillo, 1997; Raherilalao and Goodman, 2011; Block, 2012; Hawkins et al., 2015; Faliarivola et al., 2020). Using their slender bills, their feeding behaviors are relatively homogenous, mostly gleaning insects, probably also using flutter-chase or even flush-pursue strategies (Remsen and Robinson, 1990) when participating in mixed-species foraging flocks (Eguchi et al., 1993; Sridhar et al., 2009). Eleven species are understory or even ground-dwelling in relatively pristine or even exclusively in primary forests, while the Rand's Warbler (*Randia pseudozosterops*) and Cryptic Warbler (*Cryptosylvicola randrianasoloi*) can be found in the canopy (Goodman et al., 1996; Raherilalao and Goodman, 2011; Hawkins et al., 2015).

In the eastern tropical rainforests of Madagascar, up to eight species of tetraka can be found living sympatrically. Since they share dense habitats or the high canopy, they can be very difficult to observe. Previously, some information relating to the ecological niche and microhabitats of these species has been described (Raherilalao and Goodman, 2011; Safford and Hawkins, 2013). However, the mechanisms behind the successful sympatry of these phylogenetically closely related species have yet to be explained in detail. A species' ecological space, which is often linked to diet, substrate use and foraging behavior can be indirectly approximated by the morphological space filled by each species (Jønsson et al., 2012) and may be visible in their isotopic signatures (Procházka et al., 2010; Yohannes and Woog, 2020).

Stable isotopes have been employed effectively as a tool to determine the origin of dietary nutrient sources for various taxonomic groups (Kelly, 2000). The stable isotopes in feathers can reveal the dietary sources of birds by providing information on the habitat use and nutrient intake during feather growth, which occurs during molt. These isotopes can indicate whether the birds consumed plant matter, such as fruits or seeds, or invertebrate-based diets, such as insects or spiders or both. The stable isotope ratios, particularly nitrogen ($\delta^{15}N$), can provide insight into the trophic level of the prey and thus the bird, as ($\delta^{15}N$) values tend to increase at higher trophic levels (Inger and Bearhop, 2008). Stable nitrogen isotopes undergo an increase ranging from 2 to 4‰ in heavy isotope enrichment with each trophic level and can therefore serve as a tool to determine dietary shifts and trophic positions (Inger and Bearhop, 2008). Stable carbon isotopes can be used to distinguish between plants that use either C_3, C_4 or CAM modes of photosynthesis, since the C_4 and CAM pathways lead to lower carbon fractionation than C_3 photosynthesis (Karasov and Martínez del Rio, 2007). Carbon isotopes can thus be used to reconstruct habitat use regarding C_3, C_4 and CAM plants and therefore, the diet preferences of the study species (Hobson, 1999). Changes in $\delta^{13}C$ due to consumer tissue-diet fractionation range from 1 to 2‰. Furthermore, there is a discernible difference in the stable isotope ratios of plants growing in different vertical strata within closed canopy forests, as seen in carbon ($\delta^{13}C$) values. This phenomenon is commonly referred to as the canopy effect (van der Merwe and Medina, 1991), whereby vertical gradients in sunlight penetration, humidity, water source and photosynthetic processes regulate the stable isotope values. Consistently, this produces ^{13}C-depleted plant values from ground to canopy; the most positive values are usually at the upper vertical portion. Canopy effects on avian studies (understorey or ground-dwelling birds) have been measured as height from the ground, rather than estimating or measuring the vertical distance from the canopy (e.g., Rajaonarivelo et al., 2020, 2021; Lowry et al., 2021).

Compared with carbon and nitrogen isotopes, stable sulfur isotopes have been used less frequently, and their potential as tracers in biochemical and physiological studies are only beginning to be realized. Mechanisms and accompanying minor or null isotope fractionations involved during the uptake and assimilation of sulfur compounds by animals can be utilized as bioindicators of the foraging niche (Richards et al., 2003; Arneson and MacAvoy, 2005; Florin et al., 2011), to distinguish the origin of dietary sources (e.g., Lott et al., 2003) and to track movement and habitat use (e.g., Date et al., 2022). Sulfur plays an essential role in the synthesis of key metabolic intermediates. For example, the metabolism of sulfur-containing amino acids, methionine and cysteine are essential to protein synthesis in birds (Griffith, 1987). For optimal growth and survival of individuals, the diet must provide these two amino acids and sulfur-containing vitamins, such as thiamine and biotin (Brosnan and Brosnan, 2006). Variations in $\delta^{34}S$ values on a small geographic scale

are described as local soil sulfate variability. It can significantly influence the plants that grow in these soils and is expressed in the animal tissues (e.g., insects, birds) that feed on them. The fractionation of sulfur isotopes in increasing food chains is comparatively low (McCutchan et al., 2003). Consequently, a wide range of feather $\delta^{34}S$ values indicate variable input of sulfur-containing amino acids from a range of consumed dietary sources or recycled body proteins during molt.

In tetrakas, only qualitative descriptions of their feeding habits and diets have been published so far, but information on the stable isotopes in their feathers or prey have not yet been assessed. As a first step, to explore their niche differentiation that may be related to their diet or to the strata they use in the forest, we used a multi-elemental approach analyzing feather isotopes combined with morphometric measurements. We aim to link multi-isotope results toward canopy stratigraphy and avian feeding niches in a rainforest ecosystem and to construct isotopic food web relations among the species dwelling in the same ecosystem. To uncover this diversification and niche segregation, we use a combination of morphometry and multi-element stable isotope analyses of body feathers ($\delta^{13}C$, $\delta^{15}N$, and $\delta^{34}S$) that can be linked to a variety of microhabitats and prey. For keratinous tissues that are metabolically inert following synthesis (e.g., feather), their isotopic values are "fixed" specifically representing the time over which the feather was grown (Hobson, 1999). We hypothesize that niche partitioning and dietary resource segregation may explain the sympatry of insectivorous tetrakas in the Maromizaha rainforest in eastern Madagascar. Specifically, we compare five species of Tetraka: the Grey-crowned Tetraka (*Xanthomixis cinereiceps*), Long-billed Tetraka (*Bernieria madagascariensis*), Spectacled Tetraka (*Xanthomixis zosterops*), White-throated Oxylabes (*Oxylabes madagascariensis*), and Wedge-tailed Tetraka (*Hartertula flavoviridis*) and explore niche partitioning patterns and the mechanism of coexistence between them. In two sexually dimorphic species (Long-billed Tetraka and Spectacled Tetraka), we investigate the effect of sex on isotopic niches. We examine whether morphological trait-based niche differentiation was evident. The degree of isotopic niche overlap was expected to reflect the extent of interspecific feeding competition between these co-occurring species.

Methods

Study site

The Maromizaha rainforest (18°56′49′S, 48°27′33′E, Figure 1) is an officially protected area located approximately 150 km east of the capital Antananarivo in the commune of Andasibe, district of Moramanga, Madagascar. It is an area of approximately 1,881 ha, and is characterized by mountainous terrain ranging from 751 to 1,250 m in altitude with many small streams and is part of the Ankeniheny-Zahamena forest corridor. At the edges, along the central valley and along the "route nationale," approximately 600 ha have been deforested to obtain firewood and to create agricultural areas. Bird capture sites were located in five different habitats between 1,005 and 1,110 m altitude: a pristine mountain ridge, a mostly undisturbed river site, a mountain saddle, a plantation of vegetables and fruits surrounded by forest and a degraded open savannah near a quarry (Woog et al., 2006; Yohannes and Woog, 2020).

Study species

Tetrakas exhibit a range of morphological traits, including variation in bill shapes, wing, tail, and tarsus lengths (Safford and Hawkins, 2013). Wings are mostly short and rounded, the tail of medium length and somewhat graduated. While all study species can be found in undisturbed forests, some may also forage in secondary forest habitats (Benjara et al., 2021). Long-billed Tetrakas are found in both wet and dry habitats throughout Madagascar, except for the central mountain range and the Southwest. Tetrakas feed on invertebrates, typically captured from the substrate, and may form either single or mixed species flocks, often containing previous offspring (Raherilalao and Goodman, 2011). They are considered as resident species (Raherilalao and Goodman, 2011; Safford and Hawkins, 2013). Expressed as the percentage of individuals recaptured between years of all ringed birds per species, tetrakas showed high site fidelity (recapture percentage at the original ringing site between years (2003–2016): Grey-crowned Tetraka 9.7%, Long-billed Tetraka 25.5%, Spectacled Tetraka 15.4%, Wedge-tailed Tetraka 30% and White-throated Oxylabes 8.3%; Woog et al., 2018). Safford and Hawkins (2013) provide a description of the known habitat uses and feeding behavior, as summarized in Table 1.

Bird capture, morphometry and sampling

Between 2003 and 2018, birds were caught in mist nets during field seasons lasting about a month between September and January. This period represents the southern spring and coincides with the breeding season for many species. For the identification and ageing of the birds, Morris and Hawkins (1998) and Sinclair and Langrand (2013) were used. Birds were caught and ringed with aluminum rings from SAFRING to enable individual identification in the future. All measurements were taken by FW following Eck et al. (2011) and included wing (maximum chord), 3rd (outermost) primary, Kipp measure (outermost secondary to tip of wing), tip of outermost primary to longest primary, minimum tarsus (metatarsal bone), tail, bill to skull, bill length, height, and width from distal edge of nostril, weight, breeding and molting status. Up to five flank feathers from underneath the wing and a tail feather were collected for stable isotope analyses. For molecular sexing, a blood sample was taken from the brachial vein and placed in a DNA buffer (Wink, 2006) before the birds were released back into the wild.

There is no published information about the molting periods of this bird family. During our study, the onset of molt appeared to start after the young fledged. Body molt for all tetraka species started in November and lasted into January, after which no data was collected and was synchronous for males and females. Wing molt started in November and December, except for the Long-billed Tetraka, where no wing molt was observed in this period. Currently, there is no information available regarding post-juvenile molt in tetrakas, which may occur in January or February, coinciding with the cyclone season. Because of high site fidelity during breeding and molt and a presumed minor variation of habitat use throughout the year, a reduced temporal effect on feather isotope values, as well as a limited variation between sexes was assumed. To test for these effects, flank and tail feathers (which could be molted at different times of the year) were tested for significant differences in the stable isotope ratio

FIGURE 1
Map of Madagascar and the approximate location of the Maromizaha rainforest (indicated by a black square symbol).

values. Following the absence of differences (Paired *t*-test, $p > 0.05$), the focus was put on flank feather samples, as they provided the larger sample size. The current approach has limitations as more data are needed on molt in these birds, and repeated feather sampling throughout the annual cycle.

Capture height

Regular mist-nets were used to capture the birds. By design, they had five pockets measuring 50 cm each, reaching from the ground to 2.5 m in height. High nets were built using two superposed nets and reached from the ground to 5 m in height. Ten height classes were marked out between 1 and 5 m height above the ground, representing the pocket in which the birds were caught. The pocket (referred here as capture height) was noted for each individual at capture. A Chi-square test of independence was performed between the Long-billed Tetraka and the four other species. All captures above the height of class 4 were pooled, and the repartition of captures of Long-billed Tetraka was tested against the other species. The canopy height was variable and reached higher than the mist-nets in most cases, but capturing birds at greater heights was technically not feasible. Therefore, all capture height data reported in this study refer to birds caught within the mist-nets, at heights between 0 and 5 m. This approach is commonly used on research in habitat usage by ground-dwelling or understory birds (e.g., Rajaonarivelo et al., 2020, 2021; Lowry et al., 2021), but its drawback is the lack of information it provides regarding birds inhabiting the strata above the nets.

Feather stable isotope measurements

In the laboratory, the flank feather samples were prepared by washing each individual sample in a 3:1 solution of chloroform and methanol for 24 h, followed by a thorough rinse with distilled water and drying to ensure the purity of the samples. Samples of *ca.* 1 mg were pre-weighed in tin cups and combusted using a vario MICRO cube elemental analyzer (Elementar, Analysensysteme GmbH, Germany). Simultaneous resultant CO_2, N_2 and SO_2 gases were introduced into a Micromass Isoprime isotope ratio mass spectrometer (Isoprime Ltd., United Kingdom) *via* a continuous flow-through inlet system. Sample $^{13}C/^{12}C$, $^{15}N/^{14}N$, and $^{34}S/^{32}S$ ratios are expressed in the delta ($\delta^{13}C$, $\delta^{15}N$, and $\delta^{34}S$) notation in parts per thousand (‰) relative to the following standards: the Vienna Pee Dee Belemnite (VPDB) for C, atmospheric N_2 for nitrogen, and sulphanilamide-calibrated and traceable to NBS-127 (barium sulfate) for S. Stable isotope ratios were obtained using the equation:

$\delta^X(‰) = 1{,}000 \times (R_{sample}/R_{standard} - 1)$, where X is ^{13}C, ^{15}N or ^{34}S and R is $^{13}C/^{12}C$, $^{15}N/^{14}N$ or $^{34}S/^{32}S$. Internal laboratory standards indicate

TABLE 1 Summary of the known habitat and foraging behaviors of the study species.

Species	Abbreviations	Habitat and foraging behavior	References
Grey-crowned Tetraka (*Xanthomixis cinereiceps*)	GRECTE	Gleans in dense undergrowth on ground, small shrubs, mossy trunks, large branches, excavating litter and investigating holes.	Thompson and Evans (1991), Evans et al. (1992), and Goodman et al. (2000)
Long-billed Tetraka (*Bernieria madagascariensis*)	LOBITE	Forages in dense lower and middle strata with tall trees, 1–20 m above the ground, sometimes in tree-tops. Gleans from branches and leaves, also clinging to vertical trunks where it searches crevices and epiphytes for insect prey in shallow cavities, fallen trees, bases of palm fronds and under leaves on the ground. Occasionally catch flying prey in mid-air, foraging in diverse habitats.	Hino (1998)
Spectacled Tetraka (*Xanthomixis zosterops*)	SPECTE	Gleans through low vegetation, on creepers, ferns, branches, and on low trunks, 0.5–5 m above the ground.	Safford and Hawkins (2013)
White-throated Oxylabes (*Oxylabes madagascariensis*)	WITOXY	Low understory, mostly terrestrial or in shrubs under 1 m from the ground. Moves on the ground or through dense low vegetation, below fallen trees and in bush tangles, taking small insects from the undersides of leaves and small stems and may dig through leaf litter.	Safford and Hawkins (2013)
Wedge-tailed Tetrakas (*Hartertula flavoviridis*)	WEDJTE	Middle and lower strata, about 1–5 m from the ground, hopping along branches, gleaning from leaves, and actively searching foliage, epiphytes, bark and catching prey by snatching or probing.	Benson et al. (1976), Langrand (1990), and Hawkins et al. (1998)

that our measurement errors (SD) were ± 0.15‰, 0.03‰ and 0.05‰ for $\delta^{15}N$, $\delta^{13}C$, and $\delta^{34}S$, respectively.

Molecular and morphological based sexing

Blood samples ($n = 118$) were collected in the field. DNA was extracted using the DNeasy Blood and Tissue Kit (QIAGEN, Hilden, Germany), following the manufacturer's protocol (Çakmak et al., 2017). PCRs using the primer pair CHD1F/CHD1R (Lee et al., 2010) were conducted with the kit HotStarTaq Plus DNA Polymerase (QIAGEN, Hilden, Germany), following the standard protocol. The resulting PCR products were separated by electrophoresis on a 2% agarose gel containing 1 µl GelRed® Nucleic Acid Gel Stain (BIOTIUM, Fremont, United States) for 40 min at 100 V in a standard Tris-borate-EDTA buffer. The primer pair yielded only one band for both sexes, but after separation by electrophoresis, a characteristic difference in fragment size was evident. For the birds for which blood samples could not be collected, sexing was conducted using plumage characteristics and presence/absence of a brood patch in females or the shape of the cloacal protuberance for males (Redfern et al., 2001). Samples of individuals which were sexed both in the field and using the molecular approach ($n = 42$) showed a concordance of more than 90%. Molecular sexing of tetrakas was not as straightforward as expected and is subject to further research.

Morphometric data analyses

All data analyses were performed in R V. 4.2.1 and RStudio V. 2022.7.1.554 (R Core Team, 2022; RStudio Team, 2022). Some morphological variables within one anatomical feature (i.e., wing or beak) were strongly correlated. As a result, the following measurements for morphometric analyses were selected: (1) wing length: maximum chord, (2) tarsus: metatarsal bone, (3) bill width: bill width at distal edge of nostril, and (4) bill length: bill to skull. Preliminary and descriptive analyses were performed on the data using different packages in R (Wickham, 2016; Dowle and Srinivasan, 2021; Wickham et al., 2022), before checking for multivariate normality using an Energy test (Rizzo and Szekely, 2022), as well as Mardia's test (Fletcher, 2022). Homoscedasticity was tested with Levene's test (Fox and Weisberg, 2019) and the homogeneity of variance–covariance matrices was tested using Box's *M* test (da Silva, 2021). ANOVAs were performed for each variable, and the species were sorted into statistically significant groups using Tukey's Honestly Significant Differences (HSD) post-hoc tests (Bryan, 2017; Wickham et al., 2019; de Mendiburu, 2021; Iannone et al., 2022). In each case, the normal distribution of the residuals was verified by a Shapiro–Wilk test. The significance of the disparity between males and females was tested for each variable and for each species using Welch's *t*-tests.

Quadratic discriminant analysis (QDA) and Linear discriminant analysis (LDA) were used for classification and graphical representation. The log-transformed values of the four morphological variables, which were also scaled for the LDA (Legendre and Legendre, 2012), were used as the response variable and because of sample size restrictions, only the species were taken as the supervised grouping variable (Sievert, 2020). Both analyses (LDA and QDA) were applied to investigate the morphological classification and categorization of individuals into their respective groups using a leave-one-out cross-validation (also known as jack-knifed validation) method (Venables and Ripley, 2002). To infer the difference between the sexes, the sexes were subsequently displayed in the graphical

representation. For each species, the results of the QDA were sorted by sex and the species assignment accuracy was explored.

Stable isotope data analyses

This part of the analysis was performed for only four species since stable isotope values were not available for Wedge-tailed Tetrakas. Analysis of variance (ANOVA) and Student's *t*-tests were employed to test for differences in stable isotope values between sites for each species and for each element separately (ANOVA and *T*-test, $p > 0.05$). Since there were no statistically significant differences, samples from all sites were pooled. Species-specific trophic niche width was calculated using metrics that include the total convex hull area (TA) occupied by all individuals of each species in the $\delta^{15}N/\delta^{13}C$ and $\delta^{34}S/\delta^{13}C$ biplots (Layman et al., 2007). As described by Jackson et al. (2011), standard ellipse areas (SEA) with a correction for small sample sizes (SEAc) were used. This technique relies on a Bayesian method that accounts for data uncertainty and permits isotopic community metrics comparison between groups implemented through stable isotope Bayesian ellipses (Jackson et al., 2011) using 40% overlap analysis. To estimate the extent of overlap between the isotopic niches of a given species pair, triple isotopic nestedness based on convex hulls was calculated using scaled isotope data following the scale function described by Cucherousset and Villéger (2015). Convex hulls for the species and sexes were computed, and pairs of isotopes were graphically depicted (Wickham, 2016; Habel et al., 2022).

Isotopic overlap metrics [isotopic similarity (ISim) and nestedness (Ines)] were calculated following Villéger et al. (2011, 2013) and Cucherousset and Villéger (2015) using the isotopic richness (convex hull volume) of two species (pairwise species comparisons) and the volume of isotopic space they shared (i.e., intersection volume). Isotopic niche has typically been characterized through carbon and nitrogen ratios, limiting the modeling approaches to two dimensions (Layman et al., 2007). Yet, other stable isotopes (e.g., $\delta^{34}S$) can provide additional power to resolve questions associated with variations in resource use and simultaneously enhance the dimensions to three elements (3D). An analogous methodology was used, which incorporated variation across three dimensions, comparing all three stable isotopes at the same time to estimate the significant features of a species isotopic space. ISim is the ratio between the volume of the intersection and the volume of the union of the two groups of organisms in the stable isotope space. ISim ranges from 0 in cases where organisms fill totally different parts to 1 when the species fill the same portion of the isotopic space. It is multi-dimensional and unitless but could nonetheless be influenced by the differences in size of the convex hull area of the species considered. Ines was also applied as a complementary index. It represents the ratio between the volume of the intersection and the minimal volume filled by the species.

Morphometry combined with stable isotope data

After checking for normal distribution for each group and variable, a Pearson correlation coefficient table was calculated for the log-transformed morphometric variables and for the stable isotope values. A principal component analysis (PCA) was performed on the scaled data as an unsupervised dimension reduction method. Then, it was possible to check which combinations of variables were most relevant to resolving the ecological space of the species and sexes. The variation along the first two principal components (PC1 and PC2) was presented as a biplot, showing the best possible spread of the data points along these axes (Borcard et al., 2011), and the species and sexes were also displayed graphically.

Results

Between 2003 and 2018, a total of 205 tetrakas were caught and measured at five different sites (mountain ridge: $n = 13$, river valley: $n = 99$, mountain saddle: $n = 67$, plantation: $n = 25$, dry savannah: $n = 1$). Tetrakas were abundant in almost all habitats, except for the highly degraded dry savannah. All species were most abundant in the river valley and were captured predominantly in the lower pockets of the nets: 0.01–0.5 m ($n = 29$); 0.51–1.0 m ($n = 63$); 1.01–1.5 m ($n = 57$); 1.51–2.0 m ($n = 29$); 2.01–2.5 m ($n = 14$); 2.51–3.0 m ($n = 4$); 3.01–3.5 m ($n = 0$); 3.51–4.0 m ($n = 2$); 4.01–4.5 m ($n = 5$); and 4.51–5.0 m ($n = 2$) (Figure 2). White-throated Oxylabes and Wedge-tailed Tetrakas were consistently captured at the lower pockets, most often between 0.5 and 1 m (68% of total captures). In contrast, Long-billed Tetrakas were captured at higher net heights (capture heights 5 to 10, above 2 m) more often than the other species (Figure 2). Chi-Square test of independence: $\chi^2 = 12.57$, df = 4, $p = 0.014$, for a total of 205 captures; Grey-crowned Tetraka: $n = 32$, Long-billed Tetraka: $n = 65$, Spectacled Tetraka: $n = 71$, Wedge-tailed Tetraka: $n = 12$, White-throated Oxylabes: $n = 25$).

Morphometrics

The five species of tetraka differed morphologically from one another and sexual dimorphism of varying degrees was apparent (Figures 3A–D; Table 2; Supplementary Table S1). Grey-crowned and Spectacled Tetrakas were morphologically similar regarding their tarsi and wing lengths, but regarding bill length, the Grey-crowned Tetraka was closer to the Wedge-tailed Tetraka, whereas the Spectacled Tetraka was more similar to the White-throated Oxylabes. Very strong sexual dimorphism was apparent in Long-billed Tetrakas, where males had much longer tarsi, wings and bills than females. To a lesser extent, this was also the case for White-throated Oxylabes. Spectacled Tetraka females also had shorter wings and bills than males, while for the Grey-crowned Tetraka this was only the case for wing length. Contrastingly, bill width was very similar for both sexes in all species and was therefore not a good predictor of sexual dimorphism. Wedge-tailed Tetrakas exhibited smaller values for all measurements. Therefore, the Wedge-tailed Tetraka was excluded from the subsequent analyses that aimed at differentiating species of very similar morphology.

The two supervised classification analyses of the four morphometrically closest species (LDA and QDA) showed an overlap between Grey-crowned and Spectacled Tetrakas (as well as female Long-billed Tetrakas to a lesser degree; Figure 4; Table 3; Supplementary Tables S2, S3). White-throated Oxylabes remained separated, implying the morphological distinctiveness of the species. A strong diffused clustering of the male and female Long-billed Tetrakas was apparent, even without taking sex into account in the analysis (Figure 4), illustrating the sexual dimorphism. In all species except for White-throated Oxylabes, females had a lower species assignment accuracy, but this was particularly evident for Grey-crowned and

Spectacled Tetrakas (Table 3). Nonetheless, our models using only four morphometric measurements were very robust toward classifying each species, accordingly, indicating a strong segregation in the morphological space (Supplementary Table S3). The QDA showed a higher prediction accuracy than the LDA (96.24%, versus 93.98%).

Stable isotopes

The stable isotope ratios in flank feathers from the four species of tetraka showed a wide variation [ranges (‰): $\delta^{13}C$: −26.30 to −23.26; $\delta^{15}N$: 5.11 to 10.29; $\delta^{34}S$: 16.18 to 18.79] even between males and females of the same species (Figure 5). Overall, Long-billed Tetrakas had higher values of $\delta^{13}C$ than all the other species. On the other hand, ground-dwelling species like the White-throated Oxylabes and the Spectacled Tetraka showed much lower $\delta^{13}C$ values and higher $\delta^{15}N$ values, whereas $\delta^{15}N$ values in Long-billed Tetraka feathers were lower on average. Male and female Spectacled Tetrakas showed a considerable overlap in their $\delta^{15}N$ isotopic values.

A comparison of the $\delta^{34}S$ data between the four species showed a different trend. On average, White-throated Oxylabes exhibited higher values compared to other ground dwelling species, among these, Grey-crowned Tetrakas had the lowest values. In both species, the males exhibited a much larger $\delta^{34}S$ niche than the females. Altogether, Grey-crowned Tetrakas had the smallest spread and the least overlap with the other four tetraka species. Pairwise comparison of species flank feather stable isotope similarity and nestedness using three elements ($\delta^{13}C$, $\delta^{15}N$, and $\delta^{34}S$) showed low isotopic similarity and nestedness (Table 4). Nonetheless, Spectacled Tetrakas and White-throated Oxylabes had a 62% overlap, while Grey-crowned and Spectacled Tetrakas shared 19% of the three-element isotopic niche area. Long-billed and Spectacled Tetrakas had the highest values of total isotopic area and SEAc (Supplementary Table S4).

Morphometry combined with stable isotope data

Wing and bill length were strongly (positively) correlated with higher $\delta^{13}C$ values, while being negatively correlated with $\delta^{15}N$ values to a lesser extent (Supplementary Table S5).

$\delta^{34}S$ values seemed to be very similarly positively correlated with both bill dimensions. This can also be seen in the loading and eigenvectors of the PCA (Figure 6 and Supplementary Table S6), in which $\delta^{15}N$ stands out by itself. $\delta^{13}C$ and wing length, and $\delta^{34}S$ and bill width are very closely linked, respectively, and of similar relative importance in the first two principal axes, while bill length is linked with both in both axes. Having the smallest eigenvectors in the first two principal axes, tarsus length does not seem to be a useful variable for segregation of the groups at first. But in PC3, which represents about 13% of the variance, its eigenvector is by far the highest, indicating its relative importance in the multidimensional scale. Supplementary Figures S1A,B shows variation of isotope values by species and sex groups.

Discussion

The five tetraka species studied herein, all members of a bird family endemic to Madagascar and representing an adaptive radiation, showed considerable differences in morphological characters, exhibited varying degrees of sexual dimorphism, and had low isotopic similarity and limited isotopic niche overlap. The observed trait-based niche differentiation in tetrakas leads to the assumption that at Maromizaha, each of the five species (and individuals within the species) might consume a subset of the resources locally available, a phenomenon which could be described as species diet specialization in relation to morphology. Such differentiation might play a pivotal role in the diversification, adaptation and speciation in tropical birds. It is possible that these species have overlapping diets acquired from different strata of the forest canopy. This could explain why there is dietary variation among these tropical birds, with differences in the utilization of vertical forest strata playing a critical role in establishing unique niches (Frith, 1984).

Long-billed Tetrakas were the most widely distributed, surprisingly even using a dry quarry outside the forest, whereas all other taxa were restricted to native forest with little degradation. Within the forest, most tetraka species were caught in the lower strata below 2 m and very rarely above 2.5 m, with only Long-billed Tetrakas regularly using higher forest strata. Long-billed Tetrakas seem to have a larger ecological niche, as they have been observed to venture beyond the forest and utilize higher strata, which is different from the behavior of other tetraka species investigated in this study. Additionally, the morphological differentiation of this species is more pronounced than anticipated, particularly with regards to their tarsus, wings, and bill length. Each of these measures has been attributed to specialization regarding avian feeding ecology and behavior. For instance, differences in bill morphology point toward how species or sexes within a species specialize in the prey they feed on (Leisler and Winkler, 1985, 1991), shorter wings may facilitate moving through dense undergrowth (Winkler and Leisler, 1985; Forstmeier et al., 2001), whilst more robust tarsi enable birds to have a stronger grip on vegetation and substrate such as branches (Winkler, 1988; Leisler et al., 1989) and may provide insight into the types of perching substrates used by the birds. Males were often larger than females and this was most striking in the Long-billed Tetraka, where males had 7% longer tarsi, 18% longer wings and impressively 28% longer bills than females. The other tetraka species also showed sexual size dimorphism in multiple morphological measures, including the wing, tarsus, and beak, which point toward possible resource partitioning between sexes.

Regarding stable isotopes, there were only slight differences in $\delta^{15}N$, as expected by a comparison between insectivorous taxa, however, species occurring closer to the ground had higher $\delta^{15}N$ values, indicating that their prey may be higher up in the food chain. Spiders, for example, should have higher $\delta^{15}N$ values as they prey on arthropods and are abundant in leaf litter (Nyffeler, 1999). However, elevated $\delta^{15}N$ values may indicate not only trophic level but also the patterns of nitrogen cycling in the ecosystem. Different habitats can have varying levels of nitrogen availability and cycling rates, which can affect the $\delta^{15}N$ values of organisms living in those habitats (Craine et al., 2009).

Comparison of the $\delta^{34}S$ data between the four species shows an overall similar trend, with higher values of $\delta^{34}S$ for the ground-dwelling White-throated Oxylabes, but interestingly also for the Long-billed Tetrakas, which uses higher strata more often than the other species. This may indicate differences in protein sources and sulfur-containing amino acids in diet such as cysteine and methionine (Brosnan and Brosnan, 2006), the two principal sulfur-containing building blocks of proteins. However, additional research is necessary to confirm this hypothesis, for example, through the

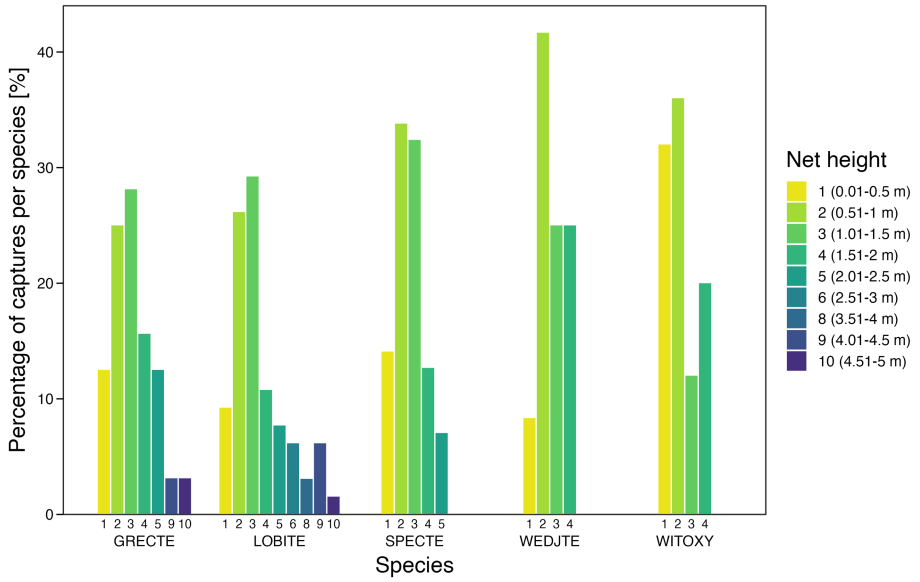

FIGURE 2
Percentage of captured individuals per species at each capture height. Number of captures at each height class (1–10 for each species respectively): GRECTE (4, 8, 9, 5, 4, 0, 0, 0, 1, 1), LOBITE (6, 17, 19, 7, 5, 4, 0, 2, 4, 1), SPECTE (10, 24, 23, 9, 5, 0, 0, 0, 0, 0), WEDJTE (1, 5, 3, 3, 0, 0, 0, 0, 0, 0), WITOXY (8, 9, 3, 5, 0, 0, 0, 0, 0, 0). For species abbreviations, see Table 1.

study of protein and amino acid specific stable isotopes found in insect prey.

The canopy effect describes vertical variation in $\delta^{13}C$ within plants throughout the forest canopy (van der Merwe and Medina, 1991). Long-billed Tetrakas had the highest $\delta^{13}C$ values, which may be due to their use of higher strata in the canopy. Significant variation in $\delta^{13}C$ in response to height in combination with light availability and tree species was expected, as leaves in lower strata of the forest tend to exhibit lower $\delta^{13}C$ values compared to those in higher strata. While this vertical isotopic variation was not tested using plant leaves and insect consumers, the effect was expected to be directly reflected in the $\delta^{13}C$ of avian insect diet in the forest. Based on the triple elemental dissimilarity in the four tetraka species, we argue that some prey taxa were commonly consumed by one species and not others. Alternatively, the tetraka species might be preying on different taxa at the same trophic level. The correlations between wing and bill length and $\delta^{13}C$ and $\delta^{15}N$ values provides evidence that individual tetrakas may segregate into different habitat structures based on a combination of their physical characteristics and food preferences. Potential ecological factors that may contribute to this habitat segregation may include differences in microhabitat preference.

Thus, marginal nestedness in isotopic niche space indicates that the species use unique resources, enhancing their ability to avoid competition and the means for niche partitioning. We are aware that assumed dietary segregation was not assessed concurrently with resource abundance, which is likely to influence the degree of partitioning (Holmes et al., 1986). More data is needed on this.

The observation of incomplete niche overlap and distinct isotopic signatures can be interpreted as evidence for the absence of strong competitive interactions between the organisms in question. Yet, the enhanced dissimilarities in isotope values could parsimoniously be explained by species foraging non-opportunistically as specialists, targeting specific prey items. Nevertheless, since there is a lack of detailed information on the diet and insect species involved, this assumption remains uncertain. The presence of differences and dissimilarities in these sympatric species appears to be essential to species coexistence, at least during the molting season. Insofar the presence of resource partitioning is not expected to lead to exclusion in a resource-rich system. Yet, if prey is scarce and resources are depleted, particularly during the dry season, it can skew the resource utilization pattern if molting coincides with this period. Overall, the isotopic distributions are consistent with well-known stable isotope distribution patterns along vertical strata in forest ecosystems (Van der Merwe and Medina, 1991), supporting the prediction that similar endemic species partitioned their resources and habitat use in a complex manner.

Tetrakas varied in their morphology and isotopic niches, which could be described as ecological specializations, presumably necessary for coexistence. Some species showed a certain level of overlap in resource use, with modest resource specialization. The nature of this resource segregation, coupled with the data on morphological traits, provided evidence that birds occupy different niches to avoid dietary competition. In groups with high resource overlap with complementary distinct specializations, it is often understood that coexistence is explained as species being imperfect generalists with "own" resources available to individuals or species (Sánchez-de León et al., 2014). In fact, this might be linked to morphological traits. Elsewhere, this pattern is referred to as Liem's Paradox, where species show foraging specializations that permit resource access to unique prey items but still exhibit high niche overlap (Liem, 1980; Bandl et al., 2015; Golcher-Benavides and Wagner, 2019). This might well be the case for the Spectacled Tetraka and its potential competitor, the White-throated Oxylabes, since they had an overlap of about 62% in the three dietary elements.

While the capture height data in this study is only qualitative and cannot be statistically linked to the isotope data, it can provide

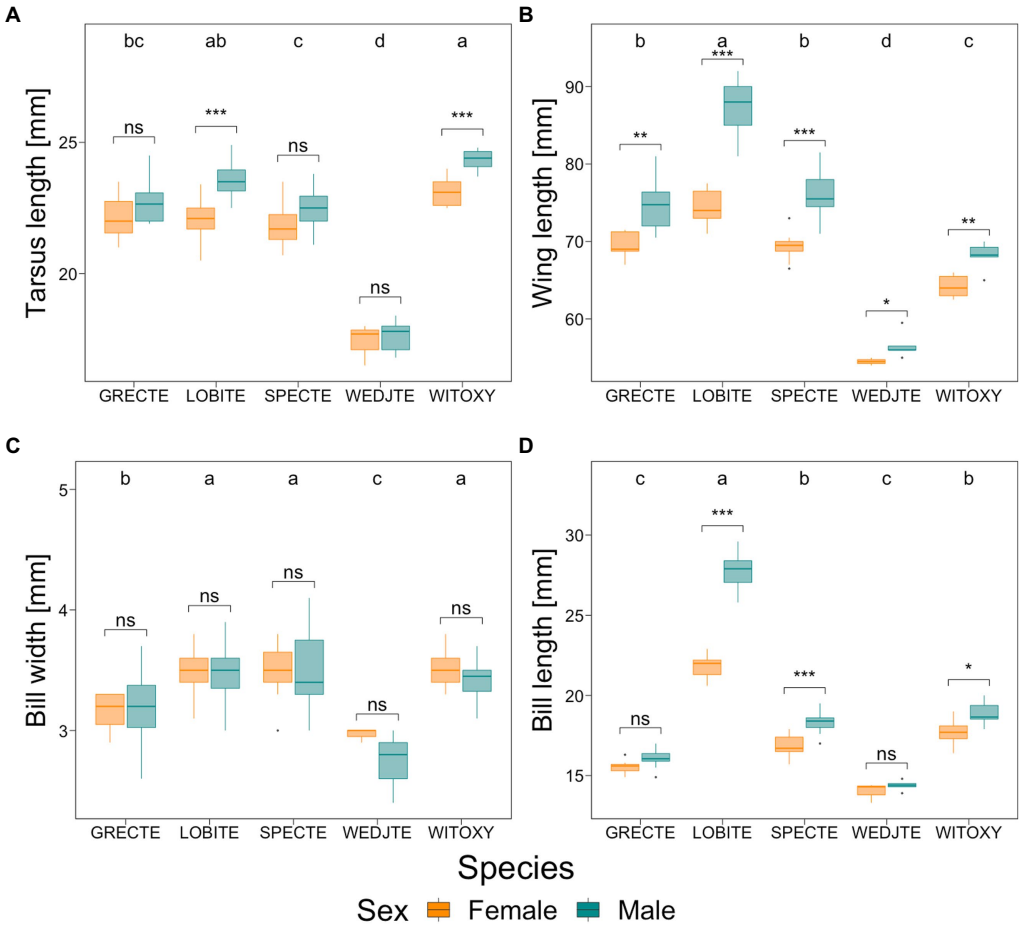

FIGURE 3
Tarsus length **(A)**, wing length **(B)**, bill width **(C)** and bill length (bill to skull) **(D)** of males (green) and females (orange) in five species of tetrakas. Brackets indicate differences between males and females calculated using Welch's *T*-tests (Table 2). Significance levels: <0.001=***; <0.01=**; <0.05=*; ≥0.05=ns. Sample sizes: GRECTE: females (*f*)=7, males (*m*)=10; LOBITE: *f*=21, *m*=23; SPECTE: *f*=11, *m*=19; WEDJTE: *f*=3, *m*=5; WITOXY: *f*=9, *m*=6. The classification into groups through one-way ANOVAs and Tukey's HSD tests are indicated as a–d (Supplementary Table S1). For species abbreviations, see Table 1.

TABLE 2 Sexual dimorphism (%) in four morphological variables and results of pairwise Welsh's *T*-tests of these measures between males and females.

	GRECTE		LOBITE		SPECTE		WEDJTE		WITOXY	
Variables	[%]	*T*-test	[%]	*T*-test	[%]	*T*-test	[%]	*T*-test	[%]	*T*-test
Tarsus length	2.54	$T_{11.87}=1.24$ ns	6.87	$T_{41.98}=7.53$***	2.93	$T_{20.68}=2.08$ ns	1.26	$T_{3.67}=0.40$ ns	5.04	$T_{12.76}=4.55$***
Wing length	7.26	$T_{13.76}=3.90$**	17.50	$T_{40.27}=16.33$***	9.68	$T_{27.51}=8.32$ ***	3.85	$T_{5.02}=2.57$*	6.33	$T_{8.83}=4.81$**
Bill width	1.04	$T_{14.08}=0.28$ ns	0.57	$T_{41.51}=0.30$ ns	0.41	$T_{27.13}=0.14$ ns	−7.64	$T_{4.72}=-2.01$ ns	−2.38	$T_{8.56}=-0.86$ ns
Bill to skull	3.26	$T_{14.45}=1.99$ ns	28.03	$T_{36.05}=24.17$***	8.62	$T_{18.95}=5.98$***	2.71	$T_{2.71}=1.00$ ns	6.29	$T_{11.48}=2.65$ *

Positive values indicate cases where males are larger than females. For species abbreviations, see Table 1. Significance levels: <0.001 = ***; <0.01 = **; <0.05 = *; ≥0.05 = ns.

additional insight into the strata that the birds utilized, along with observations from previously published studies on foraging heights. Evidently, tetrakas enhance the likelihood of coexistence by dividing foraging spaces at a microhabitat level and not necessarily resources partitioning *per se* (e.g., Schoener, 1974). These results complement the concept of species utilizing resources that other competitors could not, presumably due to morphological or behavioral constraints (e.g., Robinson and Wilson, 1998; Sánchez-de León et al., 2014). It could well be expected that this may lead to a coexistence mechanism in the tetraka species, generating sex-based morphometric and isotopic niche differentiation within the larger niche space (Wilson, 2010).

In Madagascar, when not breeding, insectivorous birds of different sizes, taxonomic groups and dietary preferences are known to form mixed-species flocks (Rand, 1936), which are characterized by two or more individuals moving together to forage, profiting (1) from the disturbance created by the other members of the flock, i.e., by flushing up insects and (2) from increased vigilance with increasing flock size

10.3389/fevo.2023.1082226

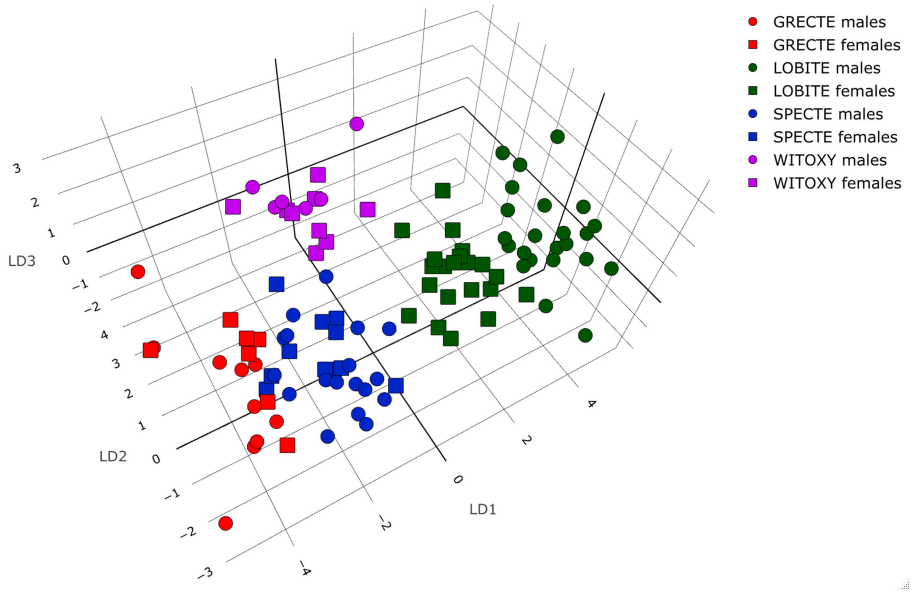

FIGURE 4
Linear discriminant analysis (LDA) showing clustering by length of tarsus and wing, bill width and bill length of the four morphologically closest species. Assignment accuracy per analysis (%) is shown in Supplementary Table S3. For species abbreviations, see Table 1.

TABLE 3 Individual assignment accuracy (%) of the Quadratic Discriminant Analysis of (*n*=205) into each supervised grouping variable (namely the species in this analysis), which was sorted by sex and species.

	GRECTE	LOBITE	SPECTE	WITOXY
Assignment accuracy into each species (%) and sex				
GRECTE				
f	75.14	0	24.86	0
m	85.50	0	14.50	0
LOBITE				
f	0	98.62	1.38	0
m	0	100	0	0
SPECTE				
f	12.91	0.36	86.09	0.45
m	0.84	1.74	97.42	0
WITOXY				
f	0	2.00	0.22	97.78
m	0	7.83	0	92.17

f, female; *m*, male. For species abbreviations, see Table 1.

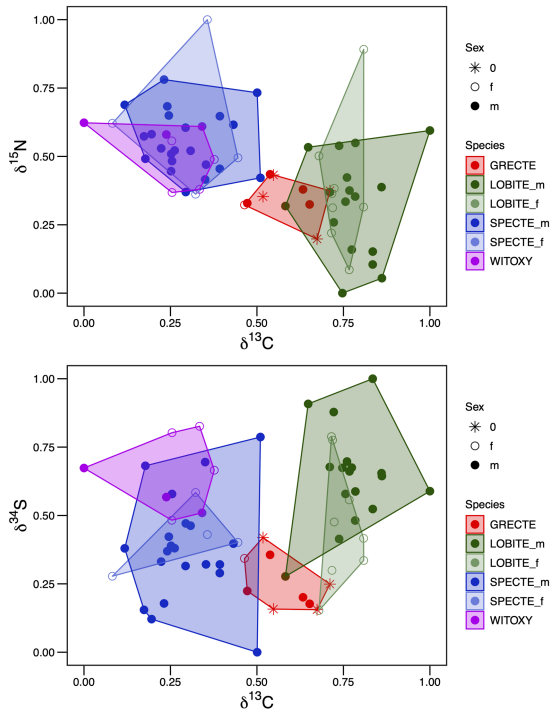

FIGURE 5
Scaled flank feather stable isotope results ($\delta^{13}C$, $\delta^{15}N$, and $\delta^{34}S$) showing isotopic niche of four Tetraka species. *f*=female, *m*=male, 0=sex unidentified. For species abbreviations, see Table 1.

to detect predators. Most tetraka species are known to take part in such flocks (Safford and Hawkins, 2013). This highly specialized cooperative behavior, coupled with the dissimilarities in their respective morphometric and isotopic spaces, could be an indication of their shared sympatric coevolutionary history. We assume that the co-adaptation of these species is based on niche differentiation, rather than outcompeting one another. This theory needs to be corroborated by detailed foraging studies and more precise data on the diet and habitat use of the tetrakas, including more species.

Morphological differences between the sexes were also reflected in their isotopic niches. The female isotopic niche was only part of the male niche in at least two species, the Long-billed and the Spectacled Tetraka. Males of at least two species (Long-billed and Spectacled Tetraka) appear to have extended niches, interestingly, away from the isotopic niches of the other taxa, which suggests that this leads to a reduction in competition for food but more data is needed. Long-billed and Spectacled Tetrakas had

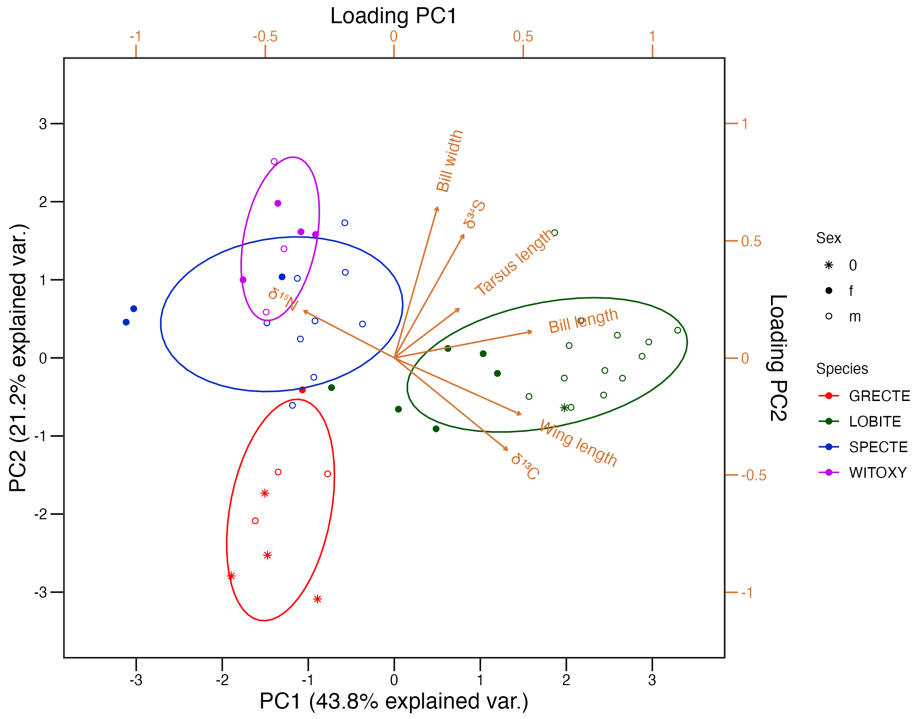

FIGURE 6
Principal component analysis biplot of the morphological and stable isotope data. Species and sexes were not included in the analysis and only displayed for graphical analysis purposes. Correlation values are given in Supplementary Table S5. The proportion of variation explained by each PCA axis, and the relative importance of each variable are given in Supplementary Table S6. *f*=female, *m*=male, 0=sex unidentified. For species abbreviations, see Table 1.

TABLE 4 Pairwise comparison of species flank feather isotopic overlap metrics (based on convex hull volume) in three dimensions ($\delta^{13}C$, $\delta^{15}N$, and $\delta^{34}S$).

Species	Isotopic similarity (ISim)	Isotopic nestedness (%) (Inest)
GRECTE ~ LOBITE	0.004	5.0
GRECTE ~ SPECTE	0.003	19.0
GRECTE ~ WITOXY	0.000	0.0
LOBITE ~ SPECTE	0.014	3.7
LOBITE ~ WITOXY	0.000	0.0
SPECTE ~ WITOXY	0.070	62.0

Isotopic similarity (ISim) is the ratio between the shared volume and the union volume of the convex hulls (Figure 5). Isotopic nestedness (INest) is the ratio between the shared and unshared convex hull volume between two species. For species abbreviations, see Table 1.

a wide range of $\delta^{34}S$ values implying a diverse sulfur containing dietary origins. Male Long-billed Tetrakas had heavier bills and it is very likely they prey on larger insects relative to females, presumably contributing to trophic niche extension in males. Thus, it could be argued that species dietary selection plays an important role in micro-habitat partitioning (vertical spatial distribution) and toward avoiding competition and therefore modulating the patterns of spatial use and coexistence between the sexes. Moreover, these data complement the assumption that niche overlaps and intraspecific competition might be minimized by increased specialization enforced through sexual dimorphism (e.g., Pyke et al., 1977). These and additional assumptions described here are solely based on morphology and isotope values obtained during the feather growing season. To validate this, repeated and long-term empirical data as well as evidence for the differences in prey items taken by individuals of the same species are essential (Roughgarden, 1972; Bolnick et al., 2002; Bolnik et al., 2007). Furthermore, stable isotope composition of the different species of insect prey needs to be studied in the different forest strata across different seasons and habitats. Morphometric data are crucial for the description of a species' niche. Detailed assessment of diet and foraging behaviors are required to infer the sources of differences in morphometry. Identifying which ecological and evolutionary factors are the most important drivers of species specialization is pivotal in understanding how these ecological variations are promoted and sustained.

Conclusion

We report considerable variation in isotopic niche positions, niche breadth and interspecific niche overlap in tetraka species that exhibit a close phylogenetic relationship. Morphological traits coupled with potential dietary groups and micro-habitat trends provided explanations of patterns of isotopic niche areas and positions. We conclude that dietary segregation may be based on specialized foraging strata and species "spatial-resource" specialization. The measurable differences found among these related species could be considered stratified resource use along the vertical canopy gradient, indicating habitat-based structural niches in tetrakas that might assist in reducing interspecific competition. These results refine knowledge of the species and their ecology. Even minor differences in the degree of species specialization among related taxa may have important implications for trophic structure. While disentangling these causes and differences is beyond the scope of this study, these results offer insights into the evolution of differential resource

utilization through comparison of both phenotype and ecological aspects of endemic species in a tropical rainforest community. Finally, our results emphasize the efficacy of these proposed coexistence mechanisms through spatial segregation and therefore variation in nutrient acquisition. Future studies should examine the role of coexistence as a flexible strategy in complex, multi-species communities with phylogenetically closely related species. Studies that do not focus on a species' sex groups may miss important ecological relationships, such as differences in resource use between sex groups. More detailed mechanisms can be elucidated by conducting further studies with larger sample sizes per species and sex group in multiple tetraka species across a wider geographic scale. Additionally, information on the isotopic signatures of plants and invertebrates in their habitats would be useful in interpreting the findings further.

Data availability statement

The raw data supporting the conclusions of this article will be made available by the authors, without undue reservation.

Author contributions

J-LB, EY, and FW conceived and designed this study and prepared and edited the manuscript. FW collected the samples in the field and took all the measurements. EY performed the stable isotope analyses at the Stable Isotope Lab of the University of Konstanz. J-LB performed the laboratory work for molecular sexing at the Natural History Museum Stuttgart. J-LB and EY performed the morphological and stable isotope data analyses. All authors have read and agreed to the published version of the manuscript.

Funding

This project was supported by funding by the "Ausschuss für Forschungsfragen" from the University of Konstanz.

Acknowledgments

We are indebted to the Malagasy authorities for granting all the relevant research and export permits (available upon request) and to the Groupe d'Étude et de Recherche sur les Primates de Madagascar (GERP), namely Jonah Ratsimbazafy and Rose Marie Randrianarison, for letting us work at Maromizaha. Hajanirina Rakotomanana, Daniel Rakotondravony, and Zafimahery Rakotomalala at the Department of Animal Biology, University of Antananarivo supported us throughout the field study. We thank Jean-Robert Lekamisi, Lova Tahiry Rasolondraibe, Onja Randriamalala, Nicola Lillich, Pia Reufsteck and all the other assistants for their help in the field. We thank Wolfgang Kornberger and Claudia Greis for the assistance in the stable isotope lab. We are especially grateful to Jonah Ulmer for language editing and for commenting on earlier drafts of the manuscript. We thank Karl-Otto Rothhaupt for all the support. Finally, we thank the three reviewers for their valuable comments and suggestions that helped to improve the manuscript. All field research, collection of bird samples (specimens released after sampling) and their export was approved by the Madagascan Ministère de l'Environnement, des Eaux et des Forêts (Direction des Eaux et Forêts, DEF) now la Direction de la Préservation de la Biodiversité, under the following permits: 10 September 2003 (No. 0182 et 0184/MINENVEF/SG/DGEF/DPB/SCBLF); 19 October 2004 (No. 234/MINENVEF/SG/DGEF/DPB/SCBLF/RECH); 4 November 2005 (No. 262 et 261/MINENVEF/SG/DGEF/DPB/SCBLF/RECH); 21 November 2006 (No. 275 et 276/MINENVEF/SG/DGEF/DPB/SCBLF/RECH); 4 December 2007 (No. 0296/07/MEEFT/SG/DGEF/ DPSAP/SSE); 19 November 2010 (No. 335/10/MEF/SG/ DGF/DCB.SAP/SCB; renewal of No. 296/07); 8 November 2012 (No. 284/12/MEF/SG/DGF/DCB.SAP/SCB); 7 October 2014 (No. 265/14/MEEF/SG/DGF/DCB.SAP/ScB); 11 October 2016 (No. 204/16/MEEF/SG/DGF/DCB.SAP/ScB.Re); 13 November 2018 (No. 279/18/MEEF/SG/DGF/DCB.SAP/ScB.Re).

Conflict of interest

The authors declare that the research was conducted in the absence of any commercial or financial relationships that could be construed as a potential conflict of interest.

Publisher's note

All claims expressed in this article are solely those of the authors and do not necessarily represent those of their affiliated organizations, or those of the publisher, the editors and the reviewers. Any product that may be evaluated in this article, or claim that may be made by its manufacturer, is not guaranteed or endorsed by the publisher.

Supplementary material

The Supplementary material for this article can be found online at: https://www.frontiersin.org/articles/10.3389/fevo.2023.1082226/full#supplementary-material

References

Arneson, L. S., and MacAvoy, S. E. (2005). Carbon, nitrogen, and sulfur diet-tissue discrimination in mouse tissues. *Can. J. Res Section D Zool. Sci.* 83, 989–995. doi: 10.1139/z05-083

Bandl, S. J., Williams, D. R., and Bellwood, D. R. (2015). Exploring the nature of ecological specialization in a coral reef fish community: morphology, diet and foraging microhabitat use. *Proc. R. Soc. B* 282:1147. doi: 10.1098/rspb.2015.1147

Benjara, A., de Roland, L. A. R., Rakotondratsima, M., and Thorstrom, R. (2021). Effects of tropical rainforest fragmentation on bird species: a case study from the Bemanevika protected area, northwestern Madagascar. *Ostrich* 92, 257–269. doi: 10.2989/00306525.2021.2005704

Benson, C. W., Colebrook-Robjent, J. F. R., and Williams, A. (1976). Contribution à l'ornithologie de Madagascar. *Oiseau Rev. Franç. Ornithol.* 46, 103–386.

Beresford, P., Barker, F. K., Ryan, P. G., and Crowe, T. M. (2005). African endemics span the tree of songbirds (Passeri): molecular systematics of several evolutionary "enigmas". *Proc. Royal Soc. B.* 272, 849–858. doi: 10.1098/rspb.2004.2997

Bickford, D., Lohman, D. J., Sodhi, S. N., Ng, K. L. P., Meier, R., Winker, K., et al. (2007). Cryptic species as a window on diversity and conservation. *Trends Ecol. Evol.* 22, 148–155. doi: 10.1016/j.tree.2006.11.004

Block, N. L. (2012). Cryptic diversity and phylogeography in the Bernieridae, an endemic Malagasy passerine radiation. The University of Chicago. Dissertations Publishing.

Block, N. L., Goodman, S. M., Hackett, S. J., Bates, J. M., and Raherilalao, M. J. (2015). Potential merger of ancient lineages in a passerine bird discovered based on evidence from host-specific ectoparasites. *Ecol. Evol.* 5, 3743–3755. doi: 10.1002/ece3.1639

Bolnick, D. I., Yang, L. H., Fordyce, J. A., Davis, J. M., and Svanbäck, R. (2002). Measuring individual-level resource specialization. *Ecology*. 83, 2936–2941.

Bolnik, D. I., Svanback, R., Araujo, M., and Persson, L. (2007). Comparative support for the niche variation hypothesis that more generalized populations also are more heterogeneous. *Proc. Nat. Acad. Sci.* 104, 10075–10079.

Borcard, D., Gillet, F., and Legendre, P. (2011). *Numerical ecology with R*. New York: Springer-Verlag.

Brosnan, T. G., and Brosnan, E. M. (2006). The Sulphur-containing amino acids: an overview. *J. Nutr.* 136, S1636–S1640. doi: 10.1093/jn/136.6.1636S

Bryan, J. (2017). *gapminder: Data from Gapminder. R package version 0.3.0*. Available at https://CRAN.R-project.org/package=gapminder

Çakmak, E., Akın Pekşen, Ç., and Bilgin, C. C. (2017). Comparison of three different primer sets for sexing birds. *J. Vet. Diagn. Investig.* 29, 59–63. doi: 10.1177/1040638716675197

Cibois, A., David, N., Gregory, S. M. S., and Pasquet, E. (2010). Bernieridae (Aves: Passeriformes): a family-group name for the Malagasy sylvioid radiation. *Zootaxa* 2554:65. doi: 10.11646/zootaxa.2554.1.6

Cibois, A., Pasquet, E., and Schulenberg, T. S. (1999). Molecular systematics of the Malagasy babblers (Passeriformes: Timaliidae) and warblers (Passeriformes: Sylviidae), based on cytochrome b and 16S rRNA sequences. *Mol. Phyl. Evol.* 13, 581–595. doi: 10.1006/mpev.1999.0684

Cibois, A., Slikas, B., Schulenberg, T. S., and Pasquet, E. (2001). An endemic radiation of Malagasy songbirds is revealed by mitochondrial DNA sequence data. *Evolution* 55, 1198–1206. doi: 10.1111/j.0014-3820.2001.tb00639.x

Craine, J. M., Elmore, A. J., Aidar, M. P. M., Bustamante, M., Dawson, T. E., Hobbie, E. A., et al. (2009). Global patterns of foliar nitrogen isotopes and their relationships with climate, mycorrhizal fungi, foliar nutrient concentrations, and nitrogen availability. *New Phytol.* 183, 980–992. doi: 10.1111/j.1469-8137.2009.02917.x

Cucherousset, J., and Villéger, S. (2015). Quantifying the multiple facets of isotopic diversity: new metrics for stable isotope ecology. *Ecol. Indic.* 56, 152–160. doi: 10.1016/j.ecolind.2015.03.032

da Silva, A. R. (2021). *Biotools: Tools for biometry and applied statistics in agricultural science. R package version*, vol. 4, 2. Available at https://cran.r-project.org/package=biotools

Date, Y., Managave, S., Jathar, G., Khot, R., and Hobson, K. A. (2022). Stable Sulphur isotope ($\delta^{34}S$) ratios in bird feathers from India indicate strong segregation between the Himalaya and Gangetic plain, and the rest of India. *Isot. Environ. Health Stud.* 58, 327–339. doi: 10.1080/10256016.2022.2113995

de Mendiburu, F. (2021). *Agricolae: statistical procedures for agricultural research. R package version*, vol. 1, 3–5. Available at http://CRAN.R-project.org/package=agricolae

Dowle, M., and Srinivasan, A. (2021). *Data.Table: Extension of 'data.Frame'. R package version 1.14.2.* Available at https://CRAN.R-project.org/package=data.table

Eck, S., Fiebig, J., Fiedler, W., Heynen, I., Nicolai, B., Töpfer, T., et al. (2011). *Measuring Birds-Vögel vermessen*. Radolfzell: Deutsche Ornithologen-Gesellschaft.

Eguchi, K., Yamagishi, S., and Randorianasolo, V. (1993). The composition and foraging behaviour of mixed-species flocks of forest-living birds in Madagascar. *Ibis* 135, 91–96. doi: 10.1111/j.1474-919X.1993.tb02814.x

Evans, M. I., Duckworth, J. W., Hawkins, A. F. A., Safford, R. J., Sheldon, B. C., and Wilkinson, R. J. (1992). Key bird species of Marojejy strict nature reserve. *Bird Conserv. Int.* 2, 201–220. doi: 10.1017/S0959270900002446

Faliarivola, M. L., Raherilalao, M. J., Andrianarimisa, A., and Goodman, S. M. (2020). The diet of Malagasy dry forest understory birds based on faecal samples. *Ostrich* 91, 35–44. doi: 10.2989/00306525.2019.1661309

Fletcher, T.D. (2022). QuantPsyc: Quantitative psychology tools. R package version. Available at: https://CRAN.R-project.org/package=QuantPsyc

Florin, S. T., Felicetti, L. A., and Robbins, C. T. (2011). The biological basis for understanding and predicting dietary-induced variation in nitrogen and sulphur isotope ratio discrimination. *Funct. Ecol.* 25, 519–526. doi: 10.1111/j.1365-2435.2010.01799.x

Forstmeier, W., Bourski, O. V., and Leisler, B. (2001). Habitat choice in *Phylloscopus* warblers: the role of morphology, phylogeny and competition. *Oecologia* 128, 566–576. doi: 10.1007/s004420100678

Fox, J., and Weisberg, S. (2019). *An {R} companion to applied regression, 3rd*. Thousand Oaks CA: Sage

Frith, D. W. (1984). Foraging ecology of birds in an upland tropical rainforest in North Queensland. *Aust. Wildlife Res.* 11, 325–347. doi: 10.1071/WR9840325

Giller, P. S. (1984). *Community structure and the niche*. London: Chapman and Hall

Golcher-Benavides, J., and Wagner, C. E. (2019). Playing out Liem's paradox: opportunistic Piscivory across Lake Tanganyikan cichlids. *Am. Nat.* 194, 260–267. doi: 10.1086/704169

Goodman, S. M., Langrand, O., and Whitney, B. M. (1996). A new genus and species of passerine from the eastern rainforest of Madagascar. *Ibis* 138, 153–159. doi: 10.1111/j.1474-919X.1996.tb04322.x

Goodman, S. M., and Parrillo, P. (1997). A study of the diets of malagasy birds based on stomach contents. *Ostrich* 68, 104–123. doi: 10.1080/00306525.1997.9639723

Goodman, S., Tello, J., and Langrand, O. (2000). Patterns of morphological and molecular variation in *Acrocephalus newtoni* on Madagascar. *Ostrich* 71, 367–370. doi: 10.1080/00306525.2000.9639832

Griffith, O. W. (1987). Mammalian sulfur amino acid metabolism: an overview. *Methods Enzymol.* 143, 366–376. doi: 10.1016/0076-6879(87)43065-6

Habel, K., Grasman, R., Gramacy, R., Mozharovskyi, P., and Sterratt, D. (2022). *Geometry: Mesh generation and surface tessellation*. Available at https://CRAN.R-project.org/package=geometry

Hardin, G. (1960). The competitive exclusion principle. *Science* 131, 1292–1297. doi: 10.1126/science.131.3409.1292

Hawkins, F., Safford, R., and Skerrett, A. (2015). *Birds of Madagascar and the Indian Ocean Islands*. London, UK: Christopher Helm.

Hawkins, A. F. A., Thiollay, J.-M., and Goodman, S. M. (1998). The birds of the reserve Spéciale d'Anjanaharibe-Sud Madagascar. *Fieldiana. Zoology* 90, 93–127.

Hino, T. (1998). Mutualistic and commensal organization of avian mixed-species foraging flocks in a forest of western Madagascar. *J. Avian Biol.* 29, 17–24. doi: 10.2307/3677336

Hobson, K. (1999). Tracing origins and migration of wildlife using stable isotopes: a review. *Oecologia* 120, 314–326. doi: 10.1007/s004420050865

Holmes, R. T., Sherry, T. W., and Sturges, F. W. (1986). Bird community dynamics in a temperate deciduous forest: long-term trends at Hubbard brook. *Ecol. Monogr.* 56, 201–220. doi: 10.2307/2937074

Hutchinson, G. E. (1957). Concluding remarks. Cold spring harbor symposia on quant. *Biol.* 22, 415–427. doi: 10.1101/SQB.1957.022.01.039

Iannone, R., Cheng, J., Schloerke, B., and Hughe, E. (2022). *Gt: Easily create presentation-ready display tables. R package version 0.7.0* Available at https://CRAN.R-project.org/package=gt

Inger, R., and Bearhop, S. (2008). Application of stable isotope analyses to avian ecology. *Ibis* 150, 447–461. doi: 10.1111/j.1474-919X.2008.00839.x

Jackson, A. L., Inger, R., Parnell, A. C., and Bearhop, S. (2011). Comparing isotopic niche widths among and within communities: SIBER–stable stable isotope Bayesian ellipses in R. *J. Anim. Ecol.* 80, 595–602. doi: 10.1111/j.1365-2656.2011.01806.x

Jønsson, K. A., Fabre, P.-H., Fritz, A. S., Etienne, R. S., Ricklefs, R. E., Jørgensen, T. B., et al. (2012). Ecological and evolutionary determinants for the adaptive radiation of the Madagascan vangas. *Proc. Nat. Acad. Sci.* 109, 6620–6625. doi: 10.1073/pnas.1115835109

Karasov, W. H., and Martínez del Rio, C. (2007). *Physiological ecology. How animals process energy, nutrients, and toxins*. Princeton and Oxford: Princeton University Press. 741

Kelly, J. F. (2000). Stable isotopes of carbon and nitrogen in the study of avian and mammalian trophic ecology. *Can. J. Zool.* 78, 1–27. doi: 10.1139/z99-165

Langrand, O. (1990). *Guide to the birds of Madagascar*. New Haven, USA: Yale University Press.

Layman, C. A., Arrington, D. A., Montana, C. G., and Post, D. M. (2007). Can stable isotope ratios provide for community-wide measures of trophic structure? *Ecology* 88, 42–48. doi: 10.1890/0012-9658(2007)88[42:CSIRPF]2.0.CO;2

Lee, J. C. I., Tsai, L. C., Hwa, P. Y., Chan, C. L., Huang, A., Chin, S. C., et al. (2010). A novel strategy for avian species and gender identification using the CHD gene. *Mol. Cell. Probes* 24, 27–31. doi: 10.1016/j.mcp.2009.08.003

Legendre, P., and Legendre, L. (2012). *Numerical Ecology*. Oxford: Elsevier.

Leisler, B., Ley, H. W., and Winkler, H. (1989). Habitat, behaviour and morphology of *Acrocephalus warblers*: an integrated analysis. *Ornis Scand.* 20, 181–186. doi: 10.2307/3676911

Leisler, B., and Winkler, H. (1985). Ecomorphology. *Curr. Ornithol.* 2, 155–186. doi: 10.1007/978-1-4613-2385-3_5

Leisler, B., and Winkler, H. (1991). Ergebnisse und Konzepte ökomorphologischer Untersuchungen an Vögeln. *J. Ornithol.* 132, 373–425. doi: 10.1007/BF01640381

Levins, R. (1968). *Evolution in changing environments*. Princeton University Press. Princeton, New Jersey

Liem, K. F. (1980). Adaptive significance of intra-and interspecific differences in the feeding repertoires of cichlid fishes. *Integr. Comp. Biol.* 20, 295–314. doi: 10.1093/icb/20.1.295

Lott, C. A., Meehan, T. D., and Heath, J. A. (2003). Estimating the latitudinal origins of migratory birds using hydrogen and sulfur stable isotopes in feathers: influence of marine prey base. *Oecologia* 134, 505–510. doi: 10.1007/s00442-002-1153-8

Lowry, B. E., Wittig, R. M., Pittermann, J., and Oelze, V. M. (2021). Stratigraphy of stable isotope ratios and leaf structure within an African rainforest canopy with implications for primate isotope ecology. *Sci. Rep.* 11:14222. doi: 10.1038/s41598-021-93589-8

MacArthur, R. H. (1972). "Coexistence of species" in *Challenging biological problems*. ed. A. J. Behnke (Oxford: Oxford Univ. Press), 253–259.

Mansor, M. S., and Ramli, R. (2017). Foraging niche segregation in Malaysian babblers (family: Timaliidae). *PLoS One* 12:e0172836. doi: 10.1371/journal.pone.0172836

Mansor, M. S., Rozali, F. Z., Davies, S., Nor, S. M., and Ramli, R. (2022). High-throughput sequencing reveals dietary segregation in Malaysian babblers. *Curr. Zool.* 68, 381–389. doi: 10.1093/cz/zoab074

McCutchan, J. H. Jr., Lewis, W. M. Jr., Kendall, C., and McGrath, C. C. (2003). Variation in trophic shift for stable isotopic ratios of carbon, nitrogen, and sulfur. *Oikos* 102, 378–390. doi: 10.1034/j.1600-0706.2003.12098.x

Morris, P., and Hawkins, F. (1998). *Birds of Madagascar: A photographic guide*. Robertsbridge, East Sussex: Pica Press.

Nyffeler, M. (1999). Prey selection of spiders in the field. *J. Arachnol.* 27, 317–324.

Pianka, E. R. (1974). Niche overlap and diffuse competition. *Proc. Natl. Acad. Sci. U. S. A.* 71, 2141–2145. doi: 10.1073/pnas.71.5.2141

Procházka, P., Reif, J., Hořák, D., Klvaňa, P., Lee, R. W., and Yohannes, E. (2010). Using stable isotopes to trace resource acquisition and trophic position in four Afrotropical birds with different diets. *Ostrich* 81, 273–275. doi: 10.2989/00306525.2010.519889

Pyke, G. H., Pulliam, H. R., and Charnov, E. L. (1977). Optimal foraging: a selective review of theory and tests. *Q. Rev. Biol.* 52, 137–154. doi: 10.1086/409852

R Core Team (2022). R: A language and environment for statistical computing. R Foundation for Statistical Computing, Vienna, Austria. Available at: https://www.R-project.org/

Raherilalao, M. J., and Goodman, S. M. (2011). *Histoire naturelle des familles et sous-familles endémiques d'oiseaux de Madagascar*. Antananarivo: Association Vahatra.

Rajaonarivelo, J. A., Andrianarimisa, A., Raherilalao, M. J., and Goodman, S. (2020). Vertical distribution and daily patterns of birds in the dry deciduous forests of central western Madagascar. *Tropical Zool.* 33, 36–52. doi: 10.4081/tz.2020.66

Rajaonarivelo, J. A., Raherilalao, M. J., Andrianarimisa, A., and Goodman, S. M. (2021). Seasonal variation in the vertical distribution of birds in the dry deciduous forest of central western Madagascar. *Wilson J. Ornithol.* 133, 258–265. doi: 10.1676/20-00088

Rand, A. L. (1936). The distribution and habits of Madagascar birds. *Bull. Am. Mus. Nat. Hist.* 72, 143–499.

Reddy, S., Driskell, A., Rabosky, D. L., Hackett, S. J., and Schulenberg, T. S. (2012). Diversification and the adaptive radiation of the vangas of Madagascar. *Proc. R. Soc. B Biol. Sciences* 279, 2062–2071. doi: 10.1098/rspb.2011.2380

Reddy, S., Schulenberg, T. S., and Block, N. (2022). "Passeriformes: Bernieriedae, Tetrakas" in *The new natural history of Madagascar*. ed. S. Goodman (Princeton and Oxford: Princeton University Press)

Redfern, C. P. F., Clark, J. A., Wilson, A., Gough, S., and Robertson, D. (2001). *Ringers' manual*. Thetford: British Trust for Ornithology.

Remsen, J. V., and Robinson, S. K. A. (1990). Classification scheme for foraging behavior of birds in terrestrial habitats. *Stud. Avian Biol.* 13, 144–160.

Richards, M. P., Fuller, B. T., Sponheimer, M., Robinson, T., and Ayliffe, L. (2003). Sulphur isotopes in paleodietary studies: a review and results from a controlled feeding experiment. *Int. J. Osteoarchaeol.* 13, 37–45. doi: 10.1002/oa.654

Rizzo, M., and Szekely, G. (2022). Energy: E-statistics: Multivariate inference via the energy of data. R package version. Available at: https://CRAN.R-project.org/package=energy

Robinson, B. W., and Wilson, D. S. (1998). Optimal foraging, specialization and a solution to Liem's paradox. *Am. Nat.* 151, 223–235. doi: 10.1086/286113

Ross, S. T. (1986). Resource partitioning in fish assemblages: a review of field studies. *Copeia* 352–388. doi: 10.2307/1444996

Roughgarden, J. (1972). Evolution of niche width. *The American Naturalist* 106, 683–718.

RStudio Team (2022). *RStudio: Integrated development environment for R*. Boston, MA: RStudio PBC.

Safford, R. J., Goodman, S. M., Raherilalao, M. J., and Hawkins, A. F. A. (2022). "Introduction to the 676 birds" in *The new natural history of Madagascar*. ed. S. Goodman, pp. 677, 1553 –1602.

Safford, R., and Hawkins, F. (2013). *The birds of Africa: Volume VIII: The Malagasy region: Madagascar, Seychelles, Comoros, Mascarenes*. London, UK: Christopher Helm

Sánchez-de León, Y., Lugo-Pérez, J., Wise, D. H., Jastrow, J. D., and González-Meler, M. A. (2014). Aggregate formation and carbon sequestration by earthworms in soil from a temperate forest exposed to elevated atmospheric CO_2: a microcosm experiment. *Soil Biol. Biochem.* 68, 223–230. doi: 10.1016/j.soilbio.2013.09.023

Schoener, T. W. (1974). Resource partitioning in ecological communities. *Science* 185, 27–39. doi: 10.1126/science.185.4145.27

Sievert, C. (2020). *Interactive web-based data visualization with R, plotly, and shiny* Chapman and Hall/CRC Florida.

Sinclair, I., and Langrand, O. (2013). *Birds of the Indian Ocean Islands: Madagascar, Mauritius, Reunion, Rodrigues, Seychelles and the Comoros*. Cape Town: Struik Publishers. 184

Sridhar, H., Beauchamp, G., and Shanker, K. (2009). Why do birds participate in mixed- species foraging flocks? A large-scale synthesis. *Anim. Behav.* 78, 337–347. doi: 10.1016/j.anbehav.2009.05.008

Symes, C. T., and Woodborne, S. M. (2010). Trophic level delineation and resource partitioning in a south African afromontane forest bird community using carbon and nitrogen stable isotopes. *Afr. J. Ecol.* 48, 984–993. doi: 10.1111/j.1365-2028.2009.01201.x

Thiel, S., Tschapka, M., Heymann, E. W., and Heer, K. (2021). Vertical stratification of seed- dispersing vertebrate communities and their interactions with plants in tropical forests. *Biol. Rev.* 96, 454–469. doi: 10.1111/brv.12664

Thompson, P. M., and Evans, M. I. (1991). *The birds of Ambatovaky. Madagascar*. London: Madagascar Environmental Research Group.

Van der Merwe, N. J., and Medina, E. (1991). The canopy effect, carbon isotope ratios and food webs in Amazonia. *J. Archaeol. Sci.* 18, 249–259. doi: 10.1016/0305-4403(91)90064-V

Venables, W. N., and Ripley, B. D. (2002). *Modern applied statistics with S. 4th*. New York: Springer

Villéger, S., Novack-Gottshall, P. M., and Mouillot, D. (2011). The multidimensionality of the niche reveals functional diversity changes in benthic marine biotas across geological time. *Ecology Letters*. 14, 561–568.

Villéger, S., Grenouillet, G., and Brosse, S. (2013). Decomposing functional β-diversity reveals that low functional β-diversity is driven by low functional turnover in European fish assemblages. *Global Ecology and Biogeography*. 22, 671–681.

Wickham, H. (2016). *ggplot2: Elegant graphics for data analysis*. New York: Springer-Verlag

Wickham, H., Averick, M., Bryan, J., Chang, W., McGowan, L. D., François, R., et al. (2019). Welcome to the tidyverse. *J. Open Source Softw.* 4:1686. doi: 10.21105/joss.01686

Wickham, H., François, R., Henry, L., and Müller, K. (2022). Dplyr: A grammar of data manipulation. R package version 1.0.10. Available at https://cran.r-project.org/package=dplyr

Wilson, R. P. (2010). Resource partitioning and niche hypervolume overlap in free-living Pygoscelid penguins. *Funct. Ecol.* 24, 646–657. doi: 10.1111/j.1365-2435.2009.01654.x

Wink, M. (2006). Use of DNA markers to study bird migration. *J. Ornithol.* 147, 234–244. doi: 10.1007/s10336-006-0065-5

Winkler, H. (1988). An examination of concepts and methods in ecomorphology. *ACTA XIX Proc. Int. Ornithol. Congr.* 19, 2246–2253.

Winkler, H., and Leisler, B. (1985). "Morphological aspects of habitat selection in birds" in *Habitat selection in birds*. ed. M. L. Cody (London: Academic Press), 415–434.

Woog, F., Ramanitra, N., and Rasamison, S. (2006). Effects of deforestation on eastern Malagasy bird communities. In Proceedings of the German-Malagasy research cooperation in life and earth sciences, Eds. C. Schweitzer, S. Brandt, O. Ramilijaona, H. Rakotomalala, M. Razanahoera and D. Ackermannet al. Concept Verlag, Berlin, 203–214.

Woog, F., Ramanitra, N., Rasamison, A. S., and Tahiry, R. L. (2018). Longevity in some Malagasy rainforest passerines. *Ostrich* 89, 281–286. doi: 10.2989/00306525.2018.1502693

Yohannes, E., and Woog, F. (2020). A multi-isotope and morphometric analysis to uncover ecological niche divergence in two endemic island birds from Madagascar: the dark and common Newtonia (Vangidae). *J. Ornithol.* 161, 137–147. doi: 10.1007/s10336-019-01702-6

frontiers | Frontiers in Ecology and Evolution

TYPE Original Research
PUBLISHED 01 June 2023
DOI 10.3389/fevo.2023.1053535

OPEN ACCESS

EDITED BY
Carlos Freitas,
Federal University of Amazonas, Brazil

REVIEWED BY
Jamerson Aguiar-Santos,
Federal University of Maranhão, Brazil
Raniere Garcez Costa Sousa,
Federal University of Rondônia, Brazil

*CORRESPONDENCE
André C. Pereira
✉ rancoper@gmail.com

RECEIVED 25 September 2022
ACCEPTED 05 May 2023
PUBLISHED 01 June 2023

CITATION
Pereira AC, Mancuso CJ, Newsome SD, Nardoto GB and Colli GR (2023) Agricultural input modifies trophic niche and basal energy source of a top predator across human-modified landscapes. *Front. Ecol. Evol.* 11:1053535. doi: 10.3389/fevo.2023.1053535

Agricultural input modifies trophic niche and basal energy source of a top predator across human-modified landscapes

André C. Pereira[1,2]*, Christy J. Mancuso[3], Seth D. Newsome[3], Gabriela B. Nardoto[2] and Guarino R. Colli[1]

[1]Departamento de Zoología, Instituto de Ciências Biológicas, Universidade de Brasília, Brasília, Brazil, [2]Departamento de Ecología, Instituto de Ciências Biológicas, Universidade de Brasília, Brasília, Brazil, [3]Department of Biology, University of New Mexico, Albuquerque, NM, United States

Land-use conversion and resulting habitat fragmentation can affect the source(s) of primary productivity that fuels food webs and alter their structure in ways that leads to biodiversity loss. We investigated the effects of landscape modification on food webs in the Araguaia River floodplain in central Brazil using the top predator, and indicator species *Caiman crocodilus* (Crocodilia, Alligatoridae). We measured carbon (δ^{13}C) and nitrogen (δ^{15}N) isotope values of three tissues with different isotopic incorporation rates to evaluate spatial and temporal changes in caiman isotopic niche width with hierarchical Bayesian models that accounted for habitat use, intraspecific trait variation (sex and body size), and landscape attributes (composition and configuration). We also measured δ^{13}C values of essential amino acids to assess if different primary producers are fueling aquatic food webs in natural and anthropogenic areas. Spatial analysis showed that caiman in agricultural areas had larger isotopic niche widths, which likely reflects some use of terrestrial resources in environments dominated by C_4 plants. Patterns in δ^{13}C values among essential amino acids were clearly different between natural and anthropogenic habitats. Overall, our findings suggest that caimans can persist in heterogeneous landscapes fueled by natural and agricultural energy sources of energy, which has implications for effectively managing such landscapes to maximize biodiversity.

KEYWORDS

Araguaia floodplain, compound-specific stable isotope analysis, crocodilian, essential amino acids, hierarchical Bayesian modeling, pasture, spatial analysis

1. Introduction

Agribusiness requires extensive areas to meet human global food demand, compromising natural biodiversity and ecosystem processes (Phalan et al., 2013; Laurance et al., 2014). Floodplains provide fertile soils and water for agricultural activities but suffer intense habitat degradation and loss that impact terrestrial and aquatic ecosystems (Allan, 2004; Best, 2018). These changes occur in wetland ecosystems characterized by high complexity, productivity, and functionality that support unique and rich biodiversity and provide ecosystem goods and services (Millennium Ecosystem Assessment, 2005; Maltby and Baker, 2009). The middle Araguaia River floodplain in central Brazil, a region rich in

natural communities and ecosystem processes, faces rapid conversion of native vegetation and waterbody management (pumping irrigation and damming) to supply agricultural demand and development primarily for soybean and rice production and livestock (Hunke et al., 2014; Companhia Nacional de Abastecimento [CONAB], 2015; Oliveira et al., 2015; Garcia et al., 2017; Araújo et al., 2019). Efforts to adopt sustainable practices in land and water management play an essential role in the ecological integrity of floodplain ecosystems like the Araguaia River, contributing to the conservation of biodiversity and ecosystem processes and reducing the negative impacts of anthropogenic alterations (Laurance et al., 2014; Leal et al., 2020).

Biodiversity patterns and food web dynamics are affected by the complexities of landscape modification (in the dimensions of extension, composition, and configuration) owing to the loss and fragmentation of natural habitats and alteration in the matrix of unsuitable habitats (Fischer and Lindenmayer, 2007; Haddad et al., 2015; Liao et al., 2017b). Landscape attributes, such as habitat configuration, size, and quality are determinants of population distribution and dynamics, and variation in these factors can even cause the local extinction of populations (Fahrig, 2003; Ewers and Didham, 2006). Matrix quality and type also play pivotal roles in population dynamics through factors such as permeability, hostility, disturbance, and resource availability (Quesnelle et al., 2015). However, matrix quality varies spatially and temporally for biodiversity (Driscoll et al., 2013). Because matrix and habitat quality are perceived at the species level, species traits (e.g., dispersal ability, habitat specialization, trophic level, and feeding behavior) are critically important for their persistence in fragmented landscapes (Ewers and Didham, 2006). Landscape simplification acts as an ecological filter and drives biotic homogenization of biodiversity abundance and richness, where restriction to habitat and resource availability favors species with ecological plasticity, whereas sensitive and specialist species are eliminated (Newbold et al., 2015; Le Provost et al., 2020). Such changes severely affect ecological processes such as productivity, functioning, stability, resilience, and resistance (Scheffer et al., 2001; Duffy et al., 2007; Hooper et al., 2012).

Stable isotope analysis (SIA) of consumer tissues offers an integrated analytical assessment of biochemical cycles, food web dynamics, and trophic niche information for organisms (Newsome et al., 2007; Crawford et al., 2008). Carbon isotope ($\delta^{13}C$) analysis can trace the basal carbon source(s) that fuel food webs while nitrogen isotope ($\delta^{15}N$) analysis is typically used to estimate trophic position and food chain length owing to predictable isotopic enrichment with each trophic transfer (Ben-David and Flaherty, 2012). An organism's isotopic niche—a bidimensional δ-space (Newsome et al., 2007)—can be used as a proxy for niche variation related to ecological traits (e.g., body size and sex) that lead to differences in resource exploitation, ecosystem or habitat use, and trophic position (Marques et al., 2013; Nifong et al., 2015). In addition, SIA can reveal ecological responses to anthropogenic disturbances. For example, agricultural matrices (pastures or croplands) alter the nutrient dynamics and proportions of natural C_3 autochthonous production and C_4 allochthonous subsidies in aquatic food webs (Martinelli et al., 2007; Carvalho et al., 2015; Bentivoglio et al., 2016; Parreira de Castro et al., 2016). SIA can help link landscape modification with alterations in trophic dynamics that result in trophic downgrading, niche collapse, low niche redundancy, high niche overlap, homogenization of energy flow, and niche shifts (Layman et al., 2007; Resasco et al., 2017; Magioli et al., 2019; Price et al., 2019; Burdon et al., 2020).

Furthermore, spatial extension mediates the spatial heterogeneity of stable isotope ratios in ecosystems, including under small-scale and human influence (Zambrano et al., 2010; Doi et al., 2013; Merlo-Galeazzi and Zambrano, 2014) that can directly affect the isotopic niche (Ceia et al., 2014; Reddin et al., 2018). In general, landscape attributes are neglected in spatial food web models to elucidate the functioning mechanisms, especially in ongoing landscape modification worldwide (Pillai et al., 2011; Liao et al., 2017a). Ignoring spatial isotopic variability could lead to misinterpretation and potentially mask the impacts of anthropogenic disturbances. For example, SIA-based assessments of the impacts of anthropogenic disturbances in aquatic ecosystems often make inferences from categorical or disturbance gradient designs using dispersal-limited top predators, such as fishes (Carvalho et al., 2015; Price et al., 2019; Burdon et al., 2020). Such approaches are inappropriate for top predators in wetland ecosystems, which are often large-bodied and highly mobile species that utilize a generalist feeding behavior. For example, crocodilians explore all waterbody habitats and have population dynamics according to landscape attributes, exerting ecological influence on aquatic and adjacent terrestrial food webs (Somaweera et al., 2020). Thus, spatial analysis and landscape-level patterns (amount, composition, configuration of habitats, and matrix types) can integrate SIA data from top predators to provide critical information and context about spatial ecological processes in the floodplains (Wang et al., 2014; Riva and Nielsen, 2020).

Additionally, the limitations of studies using only bulk tissue SIA can make it challenging to identify the type(s) of primary production fueling aquatic or terrestrial food webs (Finlay and Kendall, 2008; Boecklen et al., 2011; Zaia Alves et al., 2017). The primary limitation is that algal-derived aquatic and plant-derived terrestrial primary producers often show overlap in their $\delta^{13}C$ composition (Whiteman et al., 2019). An emerging alternative approach is measuring the $\delta^{13}C$ values of essential amino acids. Plants and algae have distinct patterns in essential amino acid $\delta^{13}C$ values ($\delta^{13}C_{EAA}$) due to differences in the way(s) each producer type synthesizes these compounds (Larsen et al., 2009, 2013; Besser et al., 2022). Most eukaryotic consumers cannot synthesize essential amino acids *de novo* and must route these compounds directly from the protein in their food, leading to minimal isotope alteration of essential amino acids as they are passed up the food chain (McMahon et al., 2015; Whiteman et al., 2019; Manlick and Newsome, 2022). Applying this approach to top consumers can identify the basal source(s) of energy that fuels the food webs they rely on and examine potential human-induced shifts in energy sources (Thorp and Bowes, 2016; Bowes et al., 2019), especially in landscapes heavily influenced by agriculture.

Here, we combined landscape attributes, species intraspecific traits, and isotope-based estimates of the trophic ecology of *Caiman crocodilus* (spectacled caiman) to investigate the anthropogenic impacts of landscape modification on the food webs of the Araguaia floodplain using a spatially explicit approach. *Caiman crocodilus*

(Crocodylia, Aligatoridae) is an indicator species and a model organism for detecting and monitoring environmental impacts in the Araguaia floodplain owing to its high detectability and seasonal and ontogenetic movements across a variety of terrestrial and aquatic habitats (Rosenblatt et al., 2013; Somaweera et al., 2020; Pereira and Colli, 2022). We assessed (1) the effects of intraspecific traits of sex, ontogeny, and habitat use based on the $\delta^{13}C$ and $\delta^{15}N$ isotopes values of *C. crocodilus* tissues; (2) the influence of landscape attributes (land-use composition and wetland configuration) on the isotopic niche of *C. crocodilus*; and (3) the influence of crop-derived (rice and soybean) energy on the food webs utilized by *C. crocodilus* in human-modified environments.

2. Materials and methods

2.1. Study area

We conducted this study in the middle Araguaia River floodplain (**Figure 1**). The region is in a highly dynamic and complex Cerrado–Amazonia transitional zone in central Brazil (Marques E. Q. et al., 2020). The pronounced tropical wet-dry climate influences the flooding regime: the discharge increases from November to April (wet season) when the flood pulse can span approximately 88,000 km^2 of surface area at maximum flood level and interconnects several waterbodies, and decreases during June and September (dry season), when waterbodies represent only 3.3% (2,930 km^2) of the coverage area (Irion et al., 2016). The floodplain's high spatial and temporal heterogeneity supports a rich and abundant biota, with many endemic and endangered species, sheltered in several protected areas and indigenous lands, including Bananal Island, RAMSAR site no. 624 (Ramsar Convention [RAMSAR], 2002). These protected areas are crucial in limiting the advance of fragmentation and land-use conversion (Carranza et al., 2014; Garcia et al., 2017).

However, this region is under sustained pressure from agricultural development funded by international and state programs because of the favorable topography and hydrology that has turned the floodplain into one of Brazil's leading producers of irrigated rice (Fragoso et al., 2013; Companhia Nacional de Abastecimento [CONAB], 2015). The production is based on irrigated systems, where crops are cultivated according to the hydrological regime: rice in the wet season alternates with other crops (e.g., soybeans, beans, and watermelon) in the dry season (Oliveira et al., 2015). Similar to the entire Cerrado biome (Hunke et al., 2014; Dias et al., 2016), the Araguaia River Basin suffers sustained pressure from agricultural activities that have reduced native vegetation to less than 50% in the Upper Araguaia River (Ferreira et al., 2008; Coe et al., 2011) and changed the hydrogeomorphological dynamics owing to water damming, pumping, sedimentation, silting, erosion, and contamination (Latrubesse et al., 2009; Coe et al., 2011; Oliveira et al., 2015). A 26% reduction in native vegetation coverage was recorded between 1975 and 2013 in the middle Araguaia River floodplain, mainly driven by the expansion of pasturelands (Garcia et al., 2017). Currently, the land use pattern of the Cerrado is changing slowly from extensification to intensification of agricultural activities; however, pastureland coverage remains high (Dias et al., 2016).

2.2. Study design

We conducted fieldwork between July and September (dry season) in the years 2016 and 2018 in seven localities in five municipalities of Tocantins State (**Figure 1**), namely Bananal, Canguçu, Cristalândia, Cooperformoso, Coopergran, Xavante, and Lagoa (sampled in 2016). We sampled caimans in natural and anthropogenic habitats distributed across 32 sites under distinct land-use regimes, including inside and outside protected areas. Natural habitats include rivers and lakes derived from natural geomorphological processes in the Araguaia floodplain (Irion et al., 2016). Rivers comprise small and sizeable lotic water body tributaries of the Araguaia River, characterized by a sinuous water topology and natural riparian vegetation. Lakes include the small (0.5–5 ha) and large (>5 ha) lentic water bodies of diverse forms with riparian vegetation, but also large reservoirs created to supply water for agricultural activities. We defined anthropogenic habitats as waterbodies constructed for human activities within an agricultural matrix, such as artificial ponds (restricted to shallow waterbodies of <0.5 ha in area, created by soil excavation for livestock watering or fish farms and maintained by water complementation) and agricultural irrigation ditches—channelized drainages of permanent water flow inside agricultural fields—5–20 m wide and 0.5–2 m deep, with networks in a linear planform and right angles with vegetated or bare bank slopes (Davies et al., 2008; Herzon and Helenius, 2008; Biggs et al., 2016).

Migration and movement studies of South American crocodilians indicate a maximum movement distance of 20 km over 1–5 years (Gorzula, 1978; Ouboter and Nanhoe, 1988; Campos et al., 2006). Therefore, the sampling localities were at least 20 km apart, and sites within each locality were as far apart as possible. Therefore, we created circular buffer areas of 500 m, 1 km, and 3 km centered at each capture point to calculate the landscape metrics for the characterization, assessment, and measurement of human-modified landscapes. Based on home range studies, we considered buffer zones as a utilization area of caimans, which estimated ranges between 0.048 and 3.5 km^2 (Ouboter and Nanhoe, 1988; Campos et al., 2006; Caut et al., 2019; Marques T. S. et al., 2020).

We assessed human land-use composition and wetland configuration through landscape metrics based on circular buffers of 500 m, 1 km, and 3 km centered at each animal in the site. First, we obtained land use/cover rasters from the MapBiomas Project (collection 4, 2016 and 2018).[1] We grouped MapBiomas land-use classes into five categories: waterbody, forest, savanna (savanna, grassland, non-forest natural formation, and other non-forest natural formations), pasture (pasture and other non-vegetated areas), agriculture (annual and perennial crops), and urban (urban infrastructure). To improve water coverage assessment, we incorporated a hydrographic raster from a vector database acquired from Secretaria do Meio Ambiente e Recursos Hídricos of the

1 http://mapbiomas.org

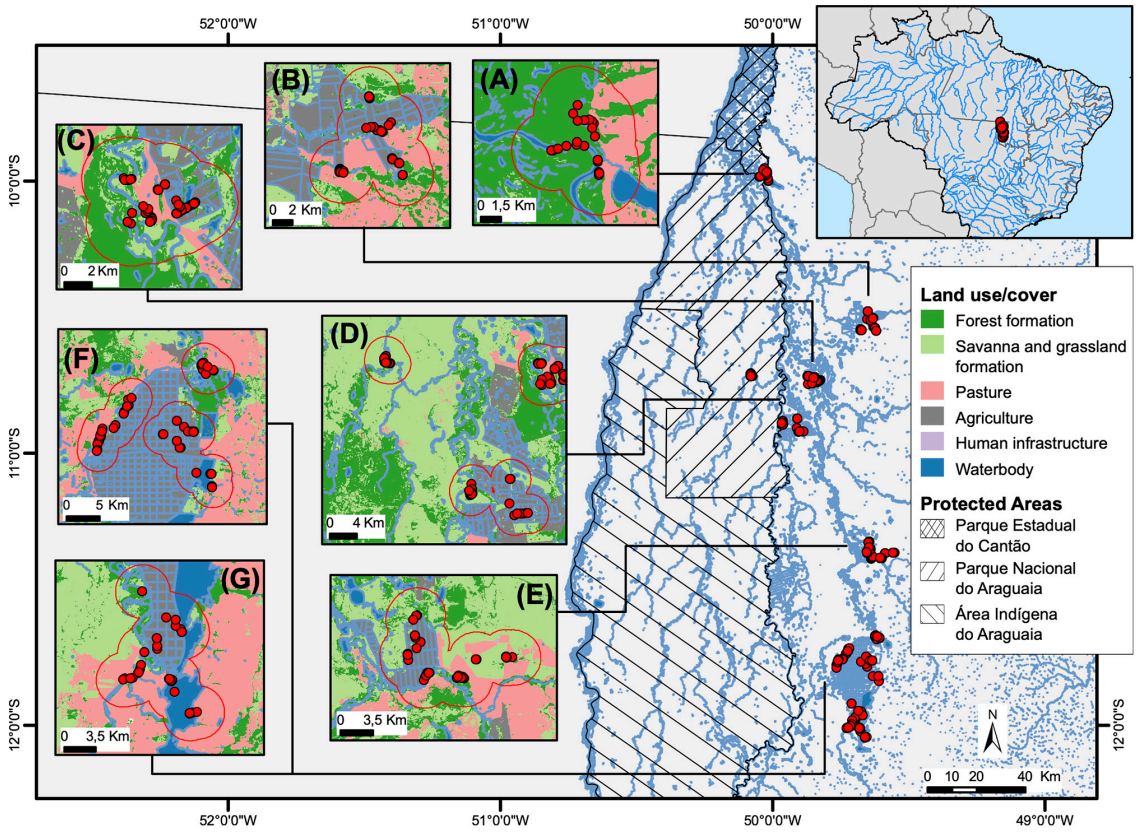

FIGURE 1
Location of seven sampling landscapes in the middle Araguaia River floodplain, Central Brazil: **(A)** Canguçu; **(B)** Cristalândia; **(C)** Lagoa; **(D)** Bananal; **(E)** Xavante; **(F)** Coopergran; **(G)** Cooperformoso. Inset boxes ordered from North to South. Land use classification, hydrograph, and protected areas in the region are denoted. Red points represent the position of captured caimans in each sampling site. Red lines indicate the maximum spatial region that include a 3 km buffer for landscape attributes estimates. The 3 km buffers were merged when they overlapped.

State of Tocantins.[2] Furthermore, we improved land use owing to differences between the supervised coverage in situ and the MapBiomas raster, reclassifying and redefining the topology guided by Landsat 8 satellite images for the same sampling period in 2016 and 2018 obtained from the Instituto Nacional de Pesquisas Espaciais–INPE (Brazilian Space Agency)[3] using QGIS, version 3.12 (QGIS Development Team, 2020).

Second, we calculated the landscape metrics at the class and landscape levels for each buffer using the R package LANDSCAPEMETRICS (Hesselbarth et al., 2019). The landscape division index (LDI) was selected at the landscape level. At the class level, the metrics included only the proportion of classes (PCLASS) for all categories to describe the landscape composition. In contrast, the metrics at the patch level were restricted to water coverage to estimate wetland configuration: mean Euclidean nearest-neighbor distance (ENN), largest patch index (LPI), patch cohesion index (COHESION), and mean patch area (MPA). Such landscape metrics reflect the aspects of proportion, isolation, patch dominance, aggregation, physical connectivity, and landscape fragmentation (McGarigal and Marks, 1995; Jaeger, 2000).

Third, we minimized multicollinearity among landscape metrics using the variance inflation factor with a maximum of 4 in the R package USDM (Naimi et al., 2014), resulting in the retention of 14 metrics with a maximum correlation of r = 0.67 among them (**Supplementary Table 1**). We then calculated the mean values of landscape metrics at each site, applied a log (x + 1) transformation, and standardized the values around the mean with one standard deviation for posterior analyses.

2.3. Caiman sampling

We sampled each locality only once, staying between 4 and 7 days to perform captures, where we visited the sampled sites up to four times. We captured 275 caimans with sampling effort per site ranging from 6 to 14 animals and a sex ratio (male:female) of 2:1 (**Supplementary Table 2**). We captured caimans through nocturnal spotlight surveys with locking cable snares or by hand after locating the animals by eye reflection, with subsequent physical restraint of mouth and limbs with ropes and adhesive tape (Fitzgerald, 2012; Brien and Manolis, 2016). We recorded the snout-vent length (SVL; with a 0.1 cm precision tape), body mass (with 5, 10, or 50 kg spring scales, Scale Macro Line, Pesola Präzisionswaagen AG®, Schindellegi, Switzerland), and sex, determined by cloacal examination and palpation of the penis (Reed and Tucker, 2012).

2 https://semarh.to.gov.br/car/base-vetorial-digital-tematica-do-car/
3 http://www.inpe.br/

In addition, we individually marked *C. crocodilus* by notching tail scutes as a standardized numerical code and released them at the exact capture location after handling (Plummer and Ferner, 2012). We conducted this study under permits SISBIO #13324-6 and #57940-3 (issued by Instituto Chico Mendes de Conservação da Biodiversidade), FUNAI #08620.005147/2018-38 (Fundação Nacional do Índio), and CEUA-UnB #94/2017 (Comissão de Ética no Uso de Animais da Universidade de Brasília).

2.4. Bulk tissue $\delta^{13}C$ and $\delta^{15}N$ analysis

We collected claw (~5 mm fragments), tail muscle (1 g), and whole blood (~3 mL) samples from the captured animals for SIA (Beaupre et al., 2004; Fleming and Fontenot, 2015). Blood samples were obtained from the dorsal cervical sinus with a blood collection kit using 21G × 1" needles (25 × 8 mm) coupled to a 4 mL BD Vacutainer® with lithium heparin anticoagulant, which showed no significant isotopic effect on plasma and red blood cell samples within 3 h (Kim and Koch, 2012). Blood samples were then centrifuged at 1,370 g for 60 s (OMEGA, Laborline®, São Paulo, Brazil) to separate and collect the plasma samples. In the field, we stored claw samples in plastic, while other tissue samples were stored at -80°C in a cryogenic liquid nitrogen container until preparation in the laboratory.

In the laboratory, claw and muscle samples were cleaned, and lipids were extracted with a 2:1 ratio of chloroform:methanol solvent solution for three washes for 2 h each (Post et al., 2007). Samples were then dried at 50°C and ground into a homogenous powder. Plasma tissue samples were freeze-dried for 24 h (Mod. E-C MicroModulyo, E-C Apparatus®) and stored at 20°C. Additionally, we collected and prepared crop samples with seeds from the Coopergran locality (rice: $n = 10$; soybean: $n = 10$). The samples were dried in an oven (60°C for 48 h) and ground into a homogenous powder. Finally, we weighed approximately 1–2 mg of each caiman sample and 2.0–2.5 mg of each crop sample and placed them into a 3 × 5 mm tin capsules for $\delta^{13}C$ and $\delta^{15}N$ analysis.

Carbon ($\delta^{13}C$) and nitrogen ($\delta^{15}N$) isotope values were determined by combustion using a Carlo Erba, CHN-1100 elemental analyzer coupled with a Thermo Finnigan Delta Plus isotope ratio mass spectrometer at the Laboratory of Isotope Ecology of the "Centro de Energia Nuclear na Agricultura" (CENA/Universidade de São Paulo), Piracicaba, São Paulo, Brazil. Based on the internationally recognized standard, the results were expressed in delta notation (δ) in parts per thousand (‰). The following equation was used:

$$\delta^{13}C \text{ or } \delta^{15}N = \left[\frac{R_{sample} - R_{standard}}{R_{standard}}\right] \times 1000$$

where R_{sample} and $R_{standard}$ represent the heavy and light isotope molar ratios ($^{13}C/^{12}C$ or $^{15}N/^{14}N$) of the sample and standard, respectively. The internationally accepted standards for $\delta^{13}C$ and $\delta^{15}N$ analysis is Vienna Pee Dee Belemnite (Vienna PDB; $^{13}C/^{12}C$ ratio = 0.01118) and atmospheric nitrogen ($^{15}N/^{14}N$ ratio = 0.0036765), respectively. Internal reference materials (USGS-42 and sugarcane leaves) were routinely interspersed with unknown samples. The mean within-run analytical precision for the internal reference materials was 0.2‰ for both $\delta^{13}C$ and $\delta^{15}N$.

We also measured each sample's weight percent carbon:nitrogen concentrations (C:N). Most samples had mean (±SD) C:N values within acceptable limits in plasma (3.3 ± 0.2), muscle (3.3 ± 1.9), and claw (2.9 ± 0.1) (Post et al., 2007), indicating little presence of lipids. However, 17 muscle samples had C:N values >4.0, suggesting a high lipid content (Post et al., 2007; Logan et al., 2008). To address this problem, we imputed the $\delta^{13}C$ values of these samples using the procedures described below in the *Data Analysis* subsection (Penone et al., 2014). We did not consider using lipid correction equations because such equations are species- and tissue-specific (Logan et al., 2008) and are not currently available for crocodilian tissues.

We evaluated resource use at multiple temporal and spatial scales using tissues with different isotopic incorporation rates that integrate diet over different periods (Crawford et al., 2008; Ben-David and Flaherty, 2012). Based on the tissue-specific isotopic incorporation rates available from a congener crocodilian species (*Caiman latirostris*), we assumed that plasma provides a relatively short timescale (~90 days), muscle reflects an intermediate timescale (130–190 days), and claws represent a relatively long timescale integrating >1 year of ecological information (Caut, 2013; Marques et al., 2014; Vander Zanden et al., 2015).

2.5. Essential amino acid (AA_{ESS}) $\delta^{13}C$ analysis

We randomly selected muscle samples from 40 caimans for essential amino acid (AA_{ESS}) $\delta^{13}C$ analysis. These samples were collected in both natural (lakes and river) and anthropogenic (ponds and ditches) habitats from four localities: 10 individuals from lakes (five from Canguçu and five from Bananal), 10 individuals from rivers (five from Canguçu and five from Bananal), 10 individuals from ponds (five from Coopergran and five from Cooperformoso), and 10 individuals from ditches (five from Coopergran and five from Cooperformoso). Descriptions of selected caiman populations are in **Supplementary Table 3**. Muscle samples were prepared for amino acid $\delta^{13}C$ analysis at the University of New Mexico Center for Stable Isotopes (Albuquerque, NM). A ~3–4 mg of lipid-extracted muscle sample was hydrolyzed to constituent amino acids in 1 ml of 6N HCl at 110°C for 20 h; tubes were flushed with N_2 gas before sealing to prevent oxidation during hydrolysis. Amino acids were subsequently derivatized with 2-isopropanol and trifluoracetic acid (Silfer et al., 1991) and analyzed in duplicate to assess accuracy and precision. $\delta^{13}C$ measurements were made on a Thermo Scientific Delta Plus IRMS (Bremen, Germany) after samples were separated on a 60 m BPX5 column (SGE Analytical Science, Ringwood, Victoria, Australia) in a Thermo Scientific Trace 1310 gas chromatograph (GC, Bremen, Germany) and underwent combustion to CO_2 in a ceramic reactor set at 1,000°C in a Thermo Scientific IsoLink II (Bremen, Germany).

For amino acid $\delta^{13}C$ measurements, we used a mixture of commercially available powdered amino acids (Sigma Aldrich, St. Louis, MO, USA) as a reference material derivatized and analyzed alongside each batch of unknown samples. All reference materials and unknown samples were processed and analyzed simultaneously with the same reagents and subject to the same protocols. $\delta^{13}C$

values for each underivatized amino acid were previously measured with a Costech 4,010 elemental analyzer coupled to a Thermo Scientific Delta V Plus IRMS (Breman, Germany). Like bulk tissue results, amino acid isotope data are reported using the standard δ-notation using the Vienna Pee Dee Belemnite (V-PDB) scale. We measured δ^{13}C values of six essential amino acids including threonine (Thr), valine (Val), leucine (Leu), isoleucine (Ile), phenylalanine (Phe), tyrosine (Tyr), and lysine (Lys). The average within-run standard deviation of δ^{13}C values of the in-house amino acid reference material ranged from 0.2‰ (isoleucine) to 0.6‰ (lysine); mean analytical precision across all six AA_{ESS} was 0.4‰. We describe in **Supplementary Appendix A** the preparation and measurement procedures used for the AA_{ESS} δ^{13}C analysis (Whiteman et al., 2019).

2.6. Data analysis

We treated the missing values (δ^{13}C and δ^{15}N from eight individuals for muscle sample; n = 16) and δ^{13}C values for muscle samples with a C:N ratio > 4 (n = 17), representing 0.02% of all data (n = 1650), through imputation using the R package missForest (Stekhoven and Buühlmann, 2012). Imputation is a viable solution when missing data can introduce bias and lead to incorrect conclusions owing to the masking of biological patterns (Penone et al., 2014). missForest is a non-parametric method that relies on random forest algorithms to predict missing values (Stekhoven and Buühlmann, 2012). Performance is assessed using the normalized root mean squared error (NRMSE), where excellent performance leads to a value close to 0 (Stekhoven and Buühlmann, 2012). In our case, the NRMSE was 0.03%.

We estimated isotopic niche widths through the Bayesian standard ellipse area metric (SEA_B; in ‰^{2}) using the R package SIBER with its default settings (Jackson et al., 2011). SEA_B estimates were quantified at the site level for each tissue type. We also selected landscape metrics relevant to isotopic niche width using the R package Boruta (Kursa and Rudnicki, 2010), a random forest-based selection method that identifies *all-relevant variables*. We used a *ntree* of 2,000, *maxRuns* of 2,000, and the default settings for the other parameters. We retained the landscape attributes with mean and normalized importance values above zero (*meanImp* and *normImp* > 0), obtained through the function *attStats* (**Supplementary Tables 2, 4**).

We implemented a hierarchical Bayesian approach to model the spatial variation in the (i) isotopic composition (δ^{13}C and δ^{15}N) under the effects of intraspecific traits of sex, ontogeny, and habitat and (ii) the isotopic niche width of *C. crocodilus* under the effects of land-use composition and wetland configuration across landscapes in the Araguaia floodplain. Spatial hierarchical Bayesian models were structured through stochastic partial differential equations (SPDE) combined with the integrated nested Laplace approximation (INLA) algorithm using the R package R-INLA (Rue et al., 2009; Lindgren et al., 2011); thus, this approach accounted for the spatial dependency between sampling sites and the effects of selected predictors. We created models separately for each tissue, where the response variables were δ^{13}C, δ^{15}N, and isotopic niche width. The predictors were SVL, sex, habitat, and their interactions (for δ^{13}C and δ^{15}N models) or landscape attributes (for the isotopic niche width model). We applied backward stepwise procedures to INLA to obtain the best model using the *INLAstep* function in the R package INLAutils (Redding et al., 2017). We standardized the SVL around the mean with one standard deviation and applied an orthogonal contrast to categorical matrices using the *model.matrix* function.

For each model, we evaluated the performance of different mesh designs based on deviance information (DIC) and Watanabe-Akaike information (WAIC) criteria (Wang et al., 2018). We created five mesh designs using constrained refined Delaunay triangulation based on individual positions for the δ^{13}C and δ^{15}N models or sampling site locations for the isotopic niche width model by varying the sizes of triangles within and outside the sampled area (**Supplementary Figure 1**), attempting to minimize any boundary effects (Lindgren and Rue, 2015). Details about the models, representation of the spatial random fields, and descriptions of the posterior estimates of hyperparameters from the spatial hierarchical Bayesian approach are provided in **Supplementary Appendix B**.

We investigated differences in patterns of measured AA_{ESS} δ^{13}C values (or fingerprints) of caiman collected across habitats or localities. We performed linear discriminant analysis (LDA) using the R package MASS (Venables and Ripley, 2002) to discriminate between habitats or localities. We applied and examined the reclassification error rates using the leave-one-out cross-validation approach (Larsen et al., 2013). In LDA, we plotted the 95% confidence interval ellipses for each habitat or location, and the dataset was not standardized. All statistical tests were performed using R, version 3.6.1 (R Development Core Team, 2021).

3. Results

3.1. δ^{13}C and δ^{15}N models

The hierarchical Bayesian approach demonstrated that the mesh design performed differently in the δ^{13}C and δ^{15}N models as indicated by DIC and WAIC (**Supplementary Tables 5, 6**). The spatial structure of mesh 1 was the best for all tissues in δ^{13}C models, whereas mesh 1 (plasma and claw) and 5 (muscle) were the best for the δ^{15}N models. The isotopic models had similar random fields among tissues, with reduced spatial uncertainty in the regions of the sampled points (**Supplementary Figures 2, 3**).

The spatial distribution of δ^{13}C and δ^{15}N values differed among tissues, i.e., the time window (**Figures 2A, B**). The predicted spatial distribution of δ^{13}C showed the lowest value in plasma and the highest in claw. In contrast, the predicted spatial distribution of δ^{15}N values showed little difference (~0.5‰) among the tissues. The Xavante, Cooperformoso, and Coopergran localities had higher δ^{13}C and δ^{15}N values than other areas (**Figures 2A, B** and **Supplementary Figures 4A, B**).

In the δ^{13}C models, only habitat affected δ^{13}C in the plasma model (short timescale), with ponds having higher values than other habitats (**Table 1**). Models for muscle (intermediate timescale) and claw (long timescale) showed similar results, with significant effects of habitat, SVL, and habitat: sex: SVL interaction; muscle and claw collected in ponds had higher δ^{13}C values while ditches had lower δ^{13}C values in comparison to other habitats. SVL

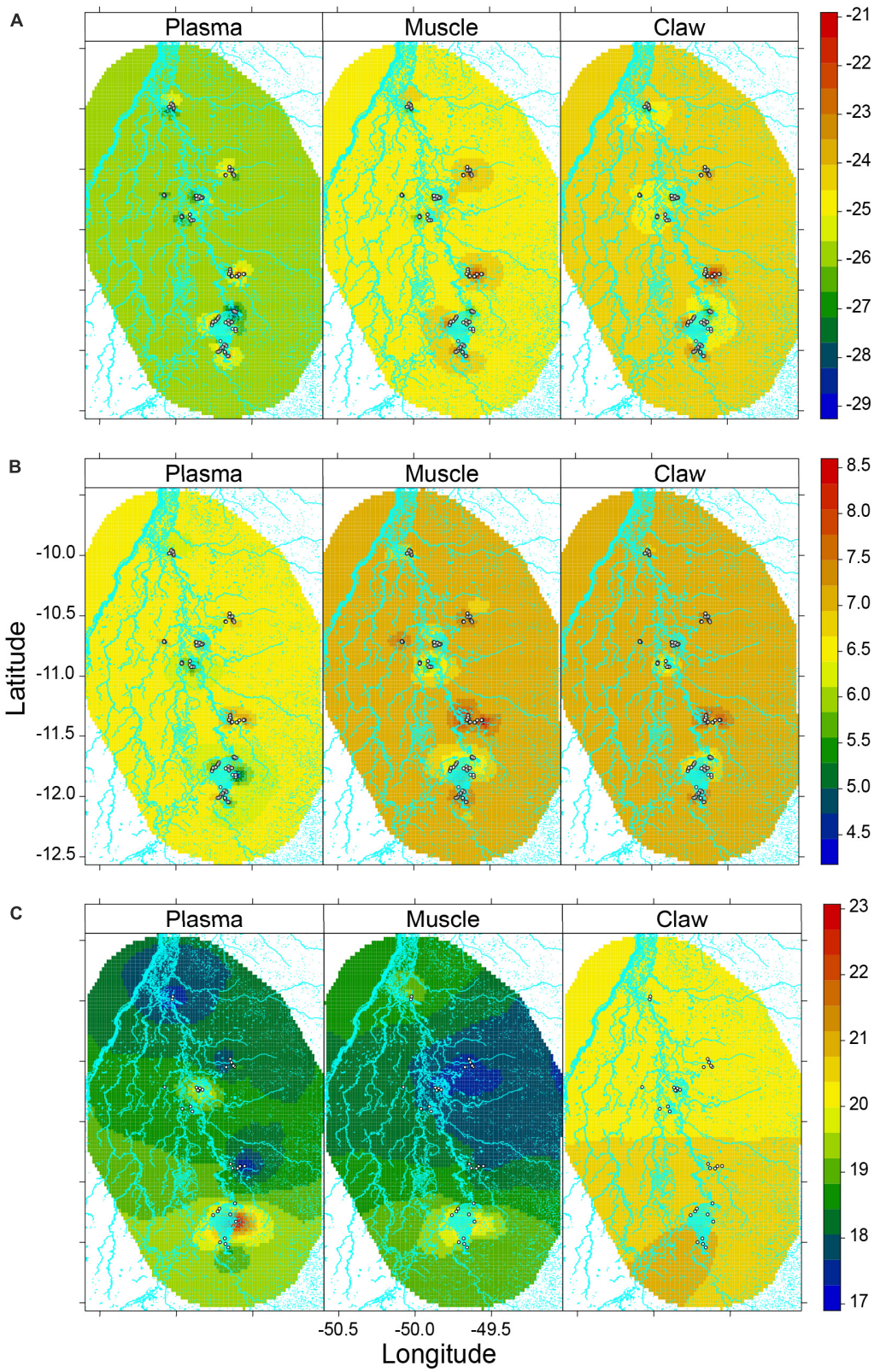

FIGURE 2
Predicted values from spatial hierarchical Bayesian best models for **(A)** δ^{13}C, **(B)** δ^{15}N, **(C)** isotopic niche width of *Caiman crocodilus* according to tissue across landscapes in the Araguaia floodplain. Hydrograph was depicted in light blue color in the frames and white points represent each sampled caiman **(A,B)** or sampling sites **(C)**. The colors indicate levels of mean δ^{13}C (‰), δ^{15}N (‰), isotopic niche width (‰^{2}) according to the associated legend. High values in bulk tissue δ^{13}C and δ^{15}N are related to anthropogenic habitats (e.g., irrigation systems) while surrounding natural habitats have lower values creating a spatial isotopic variability at landscape scales. Additionally, larger caiman isotopic niche widths were concentrated in the largest agricultural irrigation system and related to a greater proportion of pasture coverage. Some human-modified landscapes had similar niche widths as natural landscapes in the Araguaia floodplain, suggesting the same intensity of resource use in these populations across the landscape.

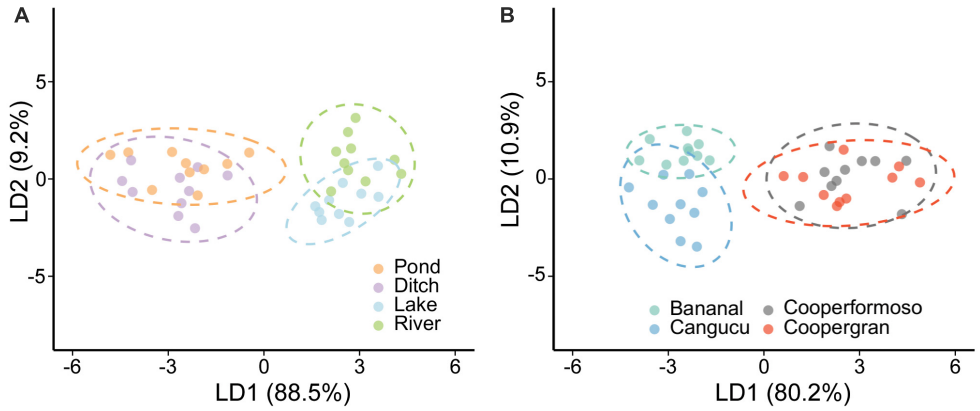

FIGURE 3
Multivariate discrimination based on AA_{ESS} $\delta^{13}C$ values of *Caiman crocodilus* according to habitat **(A)** and locality **(B)**. Ellipses indicate the 95% confidence interval region for classified groups of *C. crocodilus*. There is a distinction in basal carbon sources fueling food webs in natural versus anthropogenic habitats utilized by caiman, indicating an anthropogenic influence on energy and nutrient flow.

negatively affected muscle and claw $\delta^{13}C$ values, indicating that larger males positively influence the SVL–$\delta^{13}C$ relationship.

In the $\delta^{15}N$ models, only habitat significantly affected plasma $\delta^{15}N$ values, with ponds having lower values than other habitats (Table 2). Muscle $\delta^{15}N$ differed among habitats, with lakes having lower values than other habitats. Furthermore, habitat and sex influenced the SVL–$\delta^{15}N$ relationship, in which males in the ditch showed that $\delta^{15}N$ values decreased with SVL while in the pond, males showed that $\delta^{15}N$ values increased with SVL. Finally, claw $\delta^{15}N$ was affected by the SVL–$\delta^{15}N$ relationship owing to the habitat effect of the ditch, showing a negative trend. The same SVL–$\delta^{15}N$ relationship in the ditch differed according to sex, with males having a negative effect.

3.2. Effect of land use composition and wetland configuration on caiman isotopic niche width

We found similar DIC and WAIC values among mesh designs within each tissue model, suggesting that the structures had similar spatial dependencies in the hierarchical Bayesian approach for isotopic niche width (Supplementary Table 7). However, we selected the mesh structure with the lowest DIC and WAIC values: mesh 2 for plasma, mesh 5 for muscle, and mesh 1 for the claw. The spatial random fields of caiman isotopic niche widths varied according to tissue type (Supplementary Figures 2C, 3C). Plasma and claw random fields had low spatial dependence and reduced uncertainty across the Araguaia floodplain, whereas the muscle random field had high dependence and uncertainty, especially in the north and south of the study area.

The Boruta and INLA stepwise selection procedures retained only the proportion of pasture coverage and the fragmentation index for models of isotopic niche width (Table 3). The proportion of pasture coverage in the 500 m buffer affected the caiman isotopic niche width, with a positive effect in the plasma. The remaining predictors in their respective tissue models did not affect the caiman isotopic niche widths. The predicted isotopic niche width showed spatial variability across sites with a large range in plasma, intermediate range in muscle, and small range in claw (Figure 2C and Supplementary Figure 4C). Plasma isotopic niche widths were remarkably high in the Cooperformoso and Coopergran regions. For muscle, the central region of the study area had small isotopic niche widths, whereas the Cooperformoso and Coopergran regions maintained high values. Overall, the spatial distribution of isotopic niche width in the claws was higher than in other tissues, but it was distributed homogeneously across the Araguaia floodplain.

3.3. Essential amino acid (AA_{ESS}) $\delta^{13}C$ analysis

Linear discriminant analysis showed that essential amino acid (AA_{ESS}) $\delta^{13}C$ patterns differed among habitats with an overall successful reclassification rate of 65%. Successful reclassification was 50% for ponds, 60% for ditches, 70% for lakes, and 80% for rivers (Supplementary Appendix C). The linear discriminant axes explained 88% (LD1) and 9% (LD2) of the overall variation among habitats, and the most informative coefficients were phenylalanine, leucine, and lysine $\delta^{13}C$ values. The LDA results showed a clear distinction between caiman sampled in natural (rivers and lakes) versus anthropogenic (ponds and ditches) habitats (Figure 3A).

Linear discriminant analysis also showed that AA_{ESS} $\delta^{13}C$ patterns differed among localities (Figure 3B), with an overall correct reclassification rate of 85%. Successful reclassification varied between localities: Canguçu (70%), Coopergran (80%), Cooperformoso (90%), and Bananal (100%) (Supplementary Appendix D). LD1 and LD2 explained 80 and 10% of the variation, respectively, and the most informative coefficients were for phenylalanine, leucine, and lysine $\delta^{13}C$ values.

4. Discussion

We showed that human-induced landscape modifications affect wetland food webs in the Araguaia floodplain. Analysis of spatial

TABLE 1 Posterior estimates (mean, SD, and 95% credibility interval) from spatial hierarchical Bayesian best models relating sex, snout-vent length (SVL), and habitat effects to δ^{13}C values of *Caiman crocodilus* across landscapes in the Araguaia floodplain.

Tissue	Parameter	Mean	SD	$Q_{0.025}$	$Q_{0.975}$
Plasma	Intercept	−25.764	0.413	−26.609	−24.960
	Ditch	−0.174	0.336	−0.840	0.484
	Lake	−0.377	0.334	−1.039	0.274
	Pond	**1.200**	**0.361**	**0.498**	**1.915**
	Male	−0.103	0.115	−0.330	0.122
	SVL	−0.282	0.150	−0.576	0.012
	Ditch:Male	−0.027	0.169	−0.359	0.305
	Lake:Male	0.191	0.174	−0.150	0.532
	Ditch:SVL	−0.315	0.200	−0.708	0.078
	Male:SVL	−0.260	0.144	−0.544	0.023
	Ditch:Male:SVL	−0.216	0.200	−0.608	0.175
	Pond:Male:SVL	0.265	0.187	−0.102	0.632
Muscle	Intercept	−24.616	0.401	−25.446	−23.841
	Ditch	**−0.725**	**0.318**	**−1.354**	**−0.102**
	Lake	0.417	0.332	−0.241	1.066
	Pond	**0.851**	**0.341**	**0.187**	**1.530**
	SVL	**−0.451**	**0.149**	**−0.744**	**0.158**
	Ditch:Male	−0.170	0.185	−0.534	0.194
	Lake:Male	0.398	0.223	−0.040	0.835
	Pond:Male	−0.183	0.217	−0.609	0.243
	Ditch:SVL	−0.208	0.216	−0.632	0.216
	Lake:SVL	0.340	0.261	−0.174	0.853
	Male:SVL	−0.142	0.144	−0.425	0.142
	Ditch:Male:SVL	−0.381	0.213	−0.800	0.038
	Lake:Male:SVL	**0.642**	**0.273**	**0.104**	**1.178**
	Pond:Male:SVL	0.111	0.222	−0.325	0.547
Claw	Intercept	−24.483	0.400	−25.301	−23.697
	Ditch	**−0.759**	**0.312**	**−1.376**	**−0.145**
	Lake	0.380	0.327	−0.270	1.017
	Pond	**0.983**	**0.342**	**0.319**	**1.664**
	SVL	**−0.463**	**0.149**	**−0.757**	**−0.170**
	Ditch:Male	−0.147	0.185	−0.511	0.218
	Lake:Male	0.301	0.226	−0.142	0.744
	Pond:Male	−0.098	0.221	−0.531	0.335
	Ditch:SVL	−0.374	0.219	−0.805	0.057
	Lake:SVL	0.480	0.275	−0.062	1.020
	Pond:SVL	0.243	0.254	−0.257	0.742
	Male:SVL	−0.200	0.146	−0.488	0.087
	Ditch:Male:SVL	−0.402	0.214	−0.822	0.017
	Lake:Male:SVL	**0.680**	**0.277**	**0.135**	**1.224**
	Pond:Male:SVL	0.294	0.256	-0.209	0.797

Bold values indicate parameters significantly different from zero.

TABLE 2 Posterior estimates (mean, SD, and 95% credibility interval) from spatial hierarchical Bayesian best models relating sex, snout-vent length (SVL), and habitat effects to δ^{15}N values of *Caiman crocodilus* across landscapes in the Araguaia floodplain.

Tissue	Parameter	Mean	SD	$Q_{0.025}$	$Q_{0.975}$
Plasma	Intercept	6.400	0.218	5.960	6.837
	Ditch	0.273	0.143	−0.011	0.550
	Pond	**−0.537**	**0.152**	**−0.834**	**−0.236**
	SVL	0.080	0.068	−0.053	0.213
	Ditch:Male	−0.046	0.081	−0.206	0.114
	Pond:Male	0.105	0.093	−0.078	0.287
	Ditch:SVL	−0.154	0.100	−0.349	0.042
	Lake:SVL	0.096	0.109	−0.118	0.310
	Pond:SVL	0.215	0.116	−0.012	0.442
	Male:SVL	0.061	0.067	−0.071	0.192
	Ditch:Male:SVL	−0.182	0.098	−0.374	0.009
	Lake:Male:SVL	0.132	0.117	−0.096	0.362
	Pond:Male:SVL	0.219	0.116	−0.009	0.446
Muscle	Intercept	7.024	0.197	6.632	7.417
	Ditch	0.228	0.118	−0.005	0.458
	Lake	**−0.252**	**0.121**	**−0.489**	**−0.012**
	Pond	−0.214	0.122	−0.454	0.025
	Male	−0.053	0.052	−0.156	0.050
	SVL	0.040	0.053	−0.064	0.143
	Ditch:Male	−0.135	0.085	−0.302	0.031
	Lake:Male	0.152	0.101	−0.046	0.349
	Pond:Male	0.047	0.100	−0.150	0.244
	Ditch:SVL	**−0.293**	**0.094**	**−0.478**	**−0.108**
	Lake:SVL	0.181	0.127	−0.068	0.431
	Pond:SVL	**0.329**	**0.114**	**0.104**	**0.554**
	Ditch:Male:SVL	**−0.194**	**0.090**	**−0.370**	**−0.017**
	Lake:Male:SVL	0.132	0.126	−0.116	0.380
	Pond:Male:SVL	**0.262**	**0.116**	**0.034**	**0.490**
Claw	Intercept	7.062	0.182	6.695	7.421
	Ditch	0.119	0.147	−0.172	0.408
	Pond	−0.305	0.160	−0.620	0.008
	Male	−0.032	0.061	−0.151	0.087
	SVL	0.095	0.061	−0.025	0.214
	Ditch:Male	−0.104	0.096	−0.293	0.083
	Lake:Male	0.160	0.113	−0.062	0.382
	Pond:Male	0.026	0.112	−0.196	0.246
	Ditch:SVL	**−0.279**	**0.107**	**−0.490**	**−0.069**
	Lake:SVL	0.246	0.144	−0.036	0.528
	Pond:SVL	0.237	0.129	−0.016	0.489
	Ditch:Male:SVL	**−0.315**	**0.101**	**−0.514**	**−0.117**
	Lake:Male:SVL	0.224	0.138	−0.047	0.496
	Pond:Male:SVL	0.258	0.131	0.000	0.514

Bold values indicate parameters significantly different from zero.

isotopic patterns showed that high values of $\delta^{13}C$ and $\delta^{15}N$ values, as well as large isotopic niche widths of *Caiman crocodilus* were associated with agricultural areas. Pasture coverage was the principal landscape feature that affected caiman niche width, with changes resulting from land-use conversion, habitat alteration, and fragmentation. Moreover, AA_{ESS} $\delta^{13}C$ analysis revealed that natural and anthropogenic habitats differed in basal carbon sources, indicating that crop-derived energy contributed to fuel caiman food webs in anthropogenic habitats.

TABLE 3 Posterior estimates (mean, SD, and 95% credibility interval) from spatial hierarchical Bayesian best models relating Boruta-selected landscape attributes to isotopic niche width (SEA_B) of *Caiman crocodilus* across landscapes in the Araguaia floodplain.

Tissue	Parameter	Mean	SD	$Q_{0.025}$	$Q_{0.975}$
Plasma	Intercept	17.966	7.972	−3.315	33.467
	PCLASS (Pasture) 0.5-B	**11.54**	**5.199**	**1.236**	**21.759**
	PCLASS (Pasture) 3-B	−3.205	5.234	−13.511	7.144
Muscle	Intercept	16.833	10.301	−12.355	36.336
	PCLASS (Pasture) 3-B	4.413	2.682	−0.94	9.669
	LDI 3-B	0.724	2.68	−4.523	6.074
Claw	Intercept	19.395	7.557	−1.691	33.682
	PCLASS (Pasture) 3-B	4.478	2.424	−0.323	9.254

Bold values indicate parameters significantly different from zero. Buffers zones for landscape metrics include 0.5-B for 500 m buffer, 1-B for 1 km buffer, and 3-B for 3 km buffer.

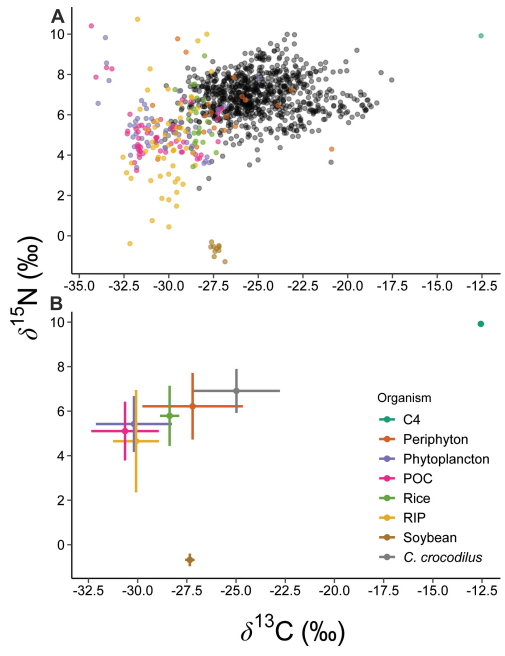

FIGURE 4
$\delta^{13}C$ and $\delta^{15}N$ values **(A)** and associated means ± SD **(B)** of basal sources in the Araguaia River Basin, crop samples (rice and soybean), and all caiman samples collected in our study. Remarkable isotopic variability in the bulk $\delta^{13}C$ and $\delta^{15}N$ occurs in basal sources, including with agricultural samples and caimans. Basal source isotopic data for primary producers is from Zaia Alves et al. (2017) and includes periphyton, phytoplankton, particulate organic carbon (POC), C_4 terrestrial grass, and C_3 riparian vegetation.

Crocodilians are highly mobile top predators with opportunistic and generalist foraging strategies (Magnusson et al., 1987; Da Silveira and Magnusson, 1999; Somaweera et al., 2020). The diet varies with ontogeny, i.e., hatchlings feed primarily on aquatic and terrestrial invertebrates, whereas adults feed on vertebrates and fishes; flood pulse, with invertebrates predominating in the wet season and fishes in the dry season (Magnusson et al., 1987; Thorbjarnarson, 1993, 1997; Da Silveira and Magnusson, 1999); and sex, with mature females using different habitats and consumed resources during the nesting period for mature females (Barão-Nóbrega et al., 2016). Moreover, crocodilians can participate in aquatic and terrestrial food webs according to prey preferences and habitat use. Sympatric Amazonian crocodilians (*Paleosuchus trigonatus*, *P. palpebrosus*, *Melanosuchus niger*, and *Caiman crocodilus*) exhibit interspecific niche divergences based on the energy source, with more autochthonous sources in the floodplains over allochthonous inputs in the headwaters (Villamarín et al., 2017). We show that habitat, sex, and ontogeny regulate the strength and dynamics of their trophic interactions (Rosenblatt et al., 2013; Somaweera et al., 2020). Crocodilian studies show niche divergence through ontogenetic variation along stable isotopes or in the isotopic niches, which relates to reduced intraspecific competition (Radloff et al., 2012; Marques et al., 2013; Nifong et al., 2015; Caut et al., 2019). A previous study in the Araguaia region indicated that sex-related ontogenetic shifts drive isotopic niche partitioning in *Caiman crocodilus* that occupy similar habitats (Pereira et al., 2018). Such variations can be mediated by density-dependent mechanisms (such as social hierarchy and sexual dimorphism or nutritional and physiological requirements) to impose differences in the isotopic values, and niche segregation at the habitat and microhabitat level (Marques et al., 2013; Caut et al., 2019).

We observed marked landscape-scale spatial heterogeneity in $\delta^{13}C$ and $\delta^{15}N$ values of caimans from the Araguaia River floodplain. This variation is likely driven by spatial variation in the sources of primary production—aquatic versus terrestrial or natural versus agricultural across distinct habitats— and thus, to ecological processes and conditions across distinct habitats (Finlay and Kendall, 2008; Boecklen et al., 2011; Zaia Alves et al., 2017). Similar patterns in isotope variation across small spatial scales have been reported in artificial and natural freshwater ecosystems (Zambrano et al., 2010; Doi et al., 2013; Merlo-Galeazzi and Zambrano, 2014). Additionally, we found that caiman trophic niche width was influenced by pasture coverage in the Araguaia region, with high values clustered in the most extensive irrigation systems such as the Cooperformoso and Coopergran areas. The conversion of the floodplain to pasture changes the photosynthetic type of terrestrial production from C_3 trees/shrubs to C_4 grasses and alters soil hydro-physical properties that maximize the susceptibility of aquatic ecosystems to pasture inputs through erosion, sedimentation, and leaching processes, including a reduction in riparian vegetation (Latrubesse et al., 2009; Coe et al., 2011; Hunke et al., 2014). While (C_4) grass fragments can enter the aquatic ecosystem and increase the $\delta^{13}C$ composition of dissolved inorganic carbon and particulate organic matter at the base of aquatic food webs (Martinelli et al., 2007), such resources are not easily assimilated by aquatic consumers, who instead favor higher quality autochthonous (algae) or allochthonous (C_3 terrestrial)

resources (Wantzen et al., 2010; Thorp and Bowes, 2016). C_4-derived carbon from pasture or savanna can be introduced into caiman tissues by consuming insectivorous-omnivorous fishes or terrestrial invertebrate or vertebrate grazer prey (Wantzen et al., 2010). Our results show that caimans that use artificial ponds are highly susceptible to that allochthonous subsidy (Jardine et al., 2017).

Basal autochthonous (particulate organic matter and algae) and allochthonous (C_3 and C_4 plants) resources that fuel aquatic food webs adjacent to pasturelands can have highly variable $\delta^{13}C$ and $\delta^{15}N$ values, which can be identified and monitored via analysis of consumer tissues (García et al., 2017). Thus, variation in the proportion of pasture coverage can drive considerable alterations in basal resources, feeding behaviors, and isotopic niche sizes of consumers. Large-scale conversion of wetlands to pasture can be an irreversible change (in the sense of intangible recovery of the previous state), disrupting ecological processes that define food web structure and function (Fischer and Lindenmayer, 2007; Tscharntke et al., 2012; Haddad et al., 2015). The relevant association of the fragmentation index with the caiman isotopic niche suggests a chronic effect of landscape modification and habitat disturbance on terrestrial and aquatic food webs through land-use conversion, expanding an agricultural matrix over natural vegetation. Overall, the Cerrado biome suffers from a historical and constant pressure of pasturelands and cropland expansion (Barretto et al., 2013; Dias et al., 2016), including in the Araguaia River Basin (Ferreira et al., 2008; Coe et al., 2011; Garcia et al., 2017). The favorable climate, topography, and soil physical properties in the Araguaia floodplain linked to government incentives through technological, mechanical, and financial support have converged this region into an agricultural frontier (Fragoso et al., 2013; Phalan et al., 2013; Araújo et al., 2019). Although future agribusiness expansion can be reduced by agriculture intensification and new protected areas (Barretto et al., 2013; Carranza et al., 2014; Dias et al., 2016; Garcia et al., 2017), areas of natural vegetation will still be fragmented and converted to pasturelands or croplands, with species in the Cerrado facing a considerable challenge to persist (Strassburg et al., 2017; Lemes et al., 2019).

Bulk tissue stable isotope analysis shows high isotopic variability and overlap of $\delta^{13}C$ values between aquatic (algal) primary producers and the most common crops harvested in agricultural matrices (soybean and rice) in the Araguaia River floodplain, **Figure 4** (Zaia Alves et al., 2017). However, essential amino acid $\delta^{13}C$ data identified a clear distinction in basal carbon sources fueling food webs in natural versus anthropogenic habitats utilized by caiman, indicating an anthropogenic influence on energy and nutrient flow. We hypothesize that the distinct AA_{ESS} $\delta^{13}C$ fingerprints between habitats or localities is driven by the incorporation of carbon from (C_3) crops (soybeans and rice) which could have distinct AA_{ESS} $\delta^{13}C$ fingerprints in comparison to natural (C_3) vegetation. We acknowledge that this hypothesis has not been rigorously tested. Alternatively, a recent study shows that C_3 and C_4 plants have distinct AA_{ESS} $\delta^{13}C$ fingerprints (Besser et al., 2022), so the patterns shown in **Figure 3** could be primarily driven by greater incorporation of C_4 resources caiman diets in anthropogenic habitats, ponds and ditches (Pereira et al., 2018; Pereira and Colli, 2022). Unfortunately, we cannot currently discriminate between these two explanations because AA_{ESS} $\delta^{13}C$ data are unavailable for local primary producers.

5. Conclusion

The spatially explicit Bayesian models approach employed here helps explore the relationship between landscape attributes and species responses that consider intraspecific variations and avoid dichotomic/categorical landscape evaluations (e.g., Resasco et al., 2017; Magioli et al., 2019) that do not reflect spatial variations and mechanisms that moderate the landscape use by organisms (Tscharntke et al., 2012; Wang et al., 2014; Riva and Nielsen, 2020). Landscape configuration drives food web structure and trophic interactions (Rooney et al., 2008; Pillai et al., 2011; Liao et al., 2017b). Realistic ecological responses to landscape alteration arise from considering species traits (e.g., trophic level, feeding behavior, body size, and dispersal ability) and species-oriented habitat perception (Ewers and Didham, 2006). These traits interact with landscape characteristics modeling species' sensitivity and tolerance in the face of disturbance and determining the persistence in human-modified landscapes (Villard et al., 2014).

Our findings support evidence that a mixture of natural and anthropogenic (agricultural) energy can support top predators in highly modified landscapes in the Araguaia River floodplain. However, previous studies found that changes in trophic structure occur and energy channels can be lost in anthropic landscapes, making it unfeasible for a food web to support top predators in the long term (Layman et al., 2007; Liao et al., 2017b), triggering a trophic cascade with pronounced impacts on ecosystem resilience and resistance to disturbances (Scheffer et al., 2001; Duffy et al., 2007; Hooper et al., 2012). Our results show that the diversification of energy pathways (or channels) may stabilize the structure of food webs in some human modified environments. The fragmentation threshold for species extinction depends on community and landscape contexts (Villard et al., 2014; Liao et al., 2017a). Understanding the potential of anthropogenic landscapes to support biodiversity and ecological and conservation values relies on evaluating the key attributes of species, food webs, and ecosystem processes in the spatial context of landscape properties (Rooney et al., 2008). Our results emphasize that landscape modification can be reflected in the trophic niche of a semi-aquatic top predator, and provides new insights into how landscape fragmentation affects food web dynamics in a human-modified floodplain. These results enhance our understanding and contributing critical information to environmental policies, conservation planning, and land use management.

Data availability statement

The raw data supporting the conclusions of this article will be made available by the authors, without undue reservation.

Ethics statement

This animal study was reviewed and approved by SISBIO #13324-6 and #57940-3 (issued by Instituto Chico Mendes de

Conservação da Biodiversidade), FUNAI #08620.005147/2018-38 (Fundação Nacional do Índio), and CEUA-UnB #94/2017 (Comissão de Ética no Uso de Animais da Universidade de Brasília).

Author contributions

AP conceived the ideas together with GN and GC and designed the study. AP conducted fieldwork. AP, CM, and SN conducted laboratory analyzes of compound specific stable isotopes. AP and GC analyzed the data with help from SN. AP, GN, CM, and SN interpreted isotopic results. AP wrote the manuscript. All authors contributed to the drafts and gave final approval for publication.

Funding

This study received funding from Coordenação de Aperfeiçoamento de Pessoal de Nível Superior–CAPES (http://www.capes.gov.br), Finance Code: 001, Ph.D.; Programa de Doutorado Sanduíche no Exterior (PDSE)—CAPES, Process Number: 88881.357613/2019-01; Coordenação de Aperfeiçoamento de Pessoal de Nível Superior (CAPES), Edital CAPES 25/2014—Pró-Forenses, Project Number: 23038.006832/2014-11; Conselho Nacional de Desenvolvimento Científico e Tecnológico–CNPq (http://www.cnpq.br), Award Number: 140284/2018-4; The Rufford Foundation (https://www.rufford.org), Award Number: 23971-1; Programa de Pós-Graduação em Ecologia da Universidade de Brasília; Fundação de Apoio à Pesquisa do Distrito Federal (FAPDF), and the USAID's PEER program under cooperative agreement AID-OAA-A-11-00012. The funders had no role in the study design, data collection, analysis, decision to publish, or manuscript preparation.

Acknowledgments

We thank all landowners and Conservation Units managers for permission and for being supportive during the development of fieldwork. We thank members of the SD, GN, and GC labs for significant comments, support, tips, and help during fieldwork, especially Bruno Araújo and Humberto Nappo. AP recognizes that Figure 1 was previously published in Pereira and Colli (2022).

Conflict of interest

The authors declare that the research was conducted in the absence of any commercial or financial relationships that could be construed as a potential conflict of interest.

Publisher's note

Supplementary material

The Supplementary Material for this article can be found online at: https://www.frontiersin.org/articles/10.3389/fevo.2023.1053535/full#supplementary-material

References

Allan, J. D. (2004). Landscapes and riverscapes: The influence of land use on stream ecosystems. *Annu. Rev. Ecol. Evol. Syst.* 35, 257–284. doi: 10.1146/annurev.ecolsys.35.120202.110122

Araújo, M. L. S. D., Sano, E. E., Bolfe, ÉL., Santos, J. R. N., dos Santos, J. S., and Silva, F. B. (2019). Spatiotemporal dynamics of soybean crop in the Matopiba region, Brazil (1990–2015). *Land Use Policy* 80, 57–67. doi: 10.1016/j.landusepol.2018.09.040

Barão-Nóbrega, J. A. L., Marioni, B., Dutra-Araújo, D., Botero-Arias, R., Nogueira, A. J. A., Magnusson, W. E., et al. (2016). Nest attendance influences the diet of nesting female spectacled caiman (*Caiman crocodilus*) in Central Amazonia, Brazil. *Herpetol. J.* 26, 65–71.

Barretto, A. G., Berndes, G., Sparovek, G., and Wirsenius, S. (2013). Agricultural intensification in Brazil and its effects on land-use patterns: An analysis of the 1975-2006 period. *Glob. Chang. Biol.* 19, 1804–1815. doi: 10.1111/gcb.12174

Beaupre, S. J., Jacobson, E. R., Lillywhite, H. B., and Zamudio, K. (2004). *Guidelines for use of live amphibians and reptiles in field and laboratory research*. Norman: Herpetological Animal Care and Use Committee of the American Society of Ichthyologists and Herpetologist.

Ben-David, M., and Flaherty, E. A. (2012). Stable isotopes in mammalian research: A beginner's guide. *J. Mammal.* 93, 312–328. doi: 10.1644/11-mamm-s-166.1

Bentivoglio, F., Calizza, E., Rossi, D., Carlino, P., Careddu, G., Rossi, L., et al. (2016). Site-scale isotopic variations along a river course help localize drainage basin influence on river food webs. *Hydrobiologia* 770, 257–272. doi: 10.1007/s10750-015-2597-2

Besser, A. C., Elliott Smith, E. A., and Newsome, S. D. (2022). Assessing the potential of amino acid δ^{13}C and δ^{15}N analysis in terrestrial and freshwater ecosystems. *J. Ecol.* 110, 935–950. doi: 10.1111/1365-2745.13853

Best, J. (2018). Anthropogenic stresses on the world's big rivers. *Nat. Geosci.* 12, 7–21. doi: 10.1038/s41561-018-0262-x

Biggs, J., von Fumetti, S., and Kelly-Quinn, M. (2016). The importance of small waterbodies for biodiversity and ecosystem services: Implications for policy makers. *Hydrobiologia* 793, 3–39. doi: 10.1007/s10750-016-3007-0

Boecklen, W. J., Yarnes, C. T., Cook, B. A., and James, A. C. (2011). On the use of stable isotopes in trophic ecology. *Annu. Rev. Ecol. Evol. Syst.* 42, 411–440. doi: 10.1146/annurev-ecolsys-102209-144726

Bowes, R. E., Thorp, J. H., and Delong, M. D. (2019). Reweaving river food webs through time. *Freshw. Biol.* 65, 390–402. doi: 10.1111/fwb.13432

Brien, M., and Manolis, C. (2016). "Crocodilians," in *Reptile ecology and conservation*, ed. C. K. Dodd (Oxford: Oxford University Press), 211–224.

Burdon, F. J., McIntosh, A. R., and Harding, J. (2020). Mechanisms of trophic niche compression: Evidence from landscape disturbance. *J. Anim. Ecol.* 89, 730–744. doi: 10.1111/1365-2656.13142

Campos, Z., Coutinho, M., Mourão, G., Bayliss, P., and Magnusson, W. E. (2006). Long distance movements by *Caiman crocodilus yacare*: Implications for management of the species in the Brazilian Pantanal. *Herpetol. J.* 16, 123–132.

Carranza, T., Balmford, A., Kapos, V., and Manica, A. (2014). Protected area effectiveness in reducing conversion in a rapidly vanishing ecosystem: The Brazilian Cerrado. *Conserv. Lett.* 7, 216–223. doi: 10.1111/conl.12049

Carvalho, D. R., Castro, D., Callisto, M., Moreira, M. Z., and Pompeu, P. S. (2015). Isotopic variation in five species of stream fishes under the influence of different land uses. *J. Fish Biol.* 87, 559–578. doi: 10.1111/jfb.12734

Caut, S. (2013). Isotope incorporation in broad-snouted caimans (crocodilians). *Biol. Open* 2, 629–634. doi: 10.1242/bio.20134945

Caut, S., Francois, V., Bacques, M., Guiral, D., Lemaire, J., Lepoint, G., et al. (2019). The dark side of the black caiman: Shedding light on species dietary ecology and movement in Agami Pond. French Guiana. *PLoS One* 14:e0217239. doi: 10.1371/journal.pone.0217239

Ceia, F. R., Paiva, V. H., Garthe, S., Marques, J. C., and Ramos, J. A. (2014). Can variations in the spatial distribution at sea and isotopic niche width be associated with consistency in the isotopic niche of a pelagic seabird species? *Mar. Biol.* 161, 1861–1872. doi: 10.1007/s00227-014-2468-9

Coe, M. T., Latrubesse, E. M., Ferreira, M. E., and Amsler, M. L. (2011). The effects of deforestation and climate variability on the streamflow of the Araguaia River, Brazil. *Biogeochemistry* 105, 119–131. doi: 10.1007/s10533-011-9582-2

Companhia Nacional de Abastecimento [CONAB] (2015). *A cultura do arroz*. Brasília: Companhia Nacional de Abastecimento.

Crawford, K., McDonald, R. A., and Bearhop, S. (2008). Applications of stable isotope techniques to the ecology of mammals. *Mamm. Rev.* 38, 87–107. doi: 10.1111/j.1365-2907.2008.00120.x

Da Silveira, R., and Magnusson, W. E. (1999). Diets of spectacled and black caiman in the Anavilhanas Archipelago, Central Amazonia, Brazil. *J. Herpetol.* 33, 181–192. doi: 10.2307/1565713

Davies, B. R., Biggs, J., Williams, P. J., Lee, J. T., and Thompson, S. (2008). A comparison of the catchment sizes of rivers, streams, ponds, ditches and lakes: Implications for protecting aquatic biodiversity in an agricultural landscape. *Hydrobiologia* 597, 7–17. doi: 10.1007/s10750-007-9227-6

Dias, L. C. P., Pimenta, F. M., Santos, A. B., Costa, M. H., and Ladle, R. J. (2016). Patterns of land use, extensification, and intensification of Brazilian agriculture. *Glob. Chang. Biol.* 22, 2887–2903. doi: 10.1111/gcb.13314

Doi, H., Zuykova, E. I., Shikano, S., Kikuchi, E., Ota, H., Yurlova, N. I., et al. (2013). Isotopic evidence for the spatial heterogeneity of the planktonic food webs in the transition zone between river and lake ecosystems. *PeerJ* 1:e222. doi: 10.7717/peerj.222

Driscoll, D. A., Banks, S. C., Barton, P. S., Lindenmayer, D. B., and Smith, A. L. (2013). Conceptual domain of the matrix in fragmented landscapes. *Trends Ecol. Evol.* 28, 605–613. doi: 10.1016/j.tree.2013.06.010

Duffy, J. E., Cardinale, B. J., France, K. E., McIntyre, P. B., Thébault, E., and Loreau, M. (2007). The functional role of biodiversity in ecosystems: Incorporating trophic complexity. *Ecol. Lett.* 10, 522–538. doi: 10.1111/j.1461-0248.2007.01037.x

Ewers, R. M., and Didham, R. K. (2006). Confounding factors in the detection of species responses to habitat fragmentation. *Biol. Rev.* 81, 117–142. doi: 10.1017/S1464793105006949

Fahrig, L. (2003). Effects of habitat fragmentation on biodiversity. *Annu. Rev. Ecol. Evol. Syst.* 34, 487–515. doi: 10.1146/annurev.ecolsys.34.011802.132419

Ferreira, M. E., Ferreira, L. G., Latrubesse, E. M., and Miziara, F. (2008). "High resolution remote sensing based quantification of the remnant vegetation cover in the Araguaia River Basin, Central Brazil," in *IGARSS 2008 - IEEE International Geoscience and Remote Sensing Symposium*, (Piscataway: Institute of Electrical and Electronics Engineers), 739–741.

Finlay, J. C., and Kendall, C. (2008). "Stable isotope tracing of temporal and spatial variability in organic matter sources to freshwater ecosystems," in *Stable isotopes in ecology and environmental science*, 2nd Edn, eds R. Michener and K. Lajtha (Oxford: Blackwell Publishing Ltd), 283–333.

Fischer, J., and Lindenmayer, D. B. (2007). Landscape modification and habitat fragmentation: A synthesis. *Glob. Ecol. Biogeogr.* 16, 265–280. doi: 10.1111/j.1466-8238.2007.00287.x

Fitzgerald, L. A. (2012). "Finding and capturing reptiles," in *Reptile biodiversity: Standard methods for inventory and monitoring*, 1st Edn, eds R. W. McDiarmid, M. S. Foster, C. Guyer, J. W. Gibbons, and N. Chernoff (London: University of California Press), 77–80.

Fleming, G. J., and Fontenot, D. K. (2015). "Crocodilians (crocodiles, alligators, caiman, gharial)," in *Fowler's zoo and wild animal medicine*, eds R. E. Miller and M. E. Fowler (St. Louis: Elsevier Inc), 38–49.

Fragoso, D. B., Cardoso, E. A., Souza, E. R., and Ferreira, C. M. (2013). *Caracterização e diagnóstico da cadeia produtiva do arroz no Estado do Tocantins*. Brasília: Embrapa Arroz e Feijão.

Garcia, A. S., Sawakuchi, H. O., Ferreira, M. E., and Ballester, M. V. R. (2017). Landscape changes in a neotropical forest-savanna ecotone zone in central Brazil: The role of protected areas in the maintenance of native vegetation. *J. Environ. Manag.* 187, 16–23. doi: 10.1016/j.jenvman.2016.11.010

García, L., Cross, W. F., Pardo, I., and Richardson, J. S. (2017). Effects of landuse intensification on stream basal resources and invertebrate communities. *Freshw. Sci.* 36, 609–625. doi: 10.1086/693457

Gorzula, S. J. (1978). An ecological study of *Caiman crocodilus crocodilus* inhabiting savanna lagoons in the Venezuelan Guayana. *Oecologia* 35, 21–34. doi: 10.1007/bf00345539

Haddad, N. M., Brudvig, L. A., Clobert, J., Davies, K. F., Gonzalez, A., Holt, R. D., et al. (2015). Habitat fragmentation and its lasting impact on Earth's ecosystems. *Sci. Adv.* 1:e1500052. doi: 10.1126/sciadv.1500052

Herzon, I., and Helenius, J. (2008). Agricultural drainage ditches, their biological importance and functioning. *Biol. Conserv.* 141, 1171–1183. doi: 10.1016/j.biocon.2008.03.005

Hesselbarth, M. H. K., Sciaini, M., With, K. A., Wiegand, K., and Nowosad, J. (2019). landscapemetrics: An open-source R tool to calculate landscape metrics. *Ecography* 42, 1648–1657. doi: 10.1111/ecog.04617

Hooper, D. U., Adair, E. C., Cardinale, B. J., Byrnes, J. E., Hungate, B. A., Matulich, K. L., et al. (2012). A global synthesis reveals biodiversity loss as a major driver of ecosystem change. *Nature* 486, 105–108. doi: 10.1038/nature11118

Hunke, P., Mueller, E. N., Schroeder, B., and Zeilhofer, P. (2014). The Brazilian Cerrado: Assessment of water and soil degradation in catchments under intensive agricultural use. *Ecohydrology* 8, 1154–1180. doi: 10.1002/eco.1573

Irion, G., Nunes, G. M., Nunes-da-Cunha, C., de Arruda, E. C., Santos-Tambelini, M., Dias, A. P., et al. (2016). Araguaia River floodplain: Size, age, and mineral composition of a large tropical savanna wetland. *Wetlands* 36, 945–956. doi: 10.1007/s13157-016-0807-y

Jackson, A. L., Inger, R., Parnell, A. C., and Bearhop, S. (2011). Comparing isotopic niche widths among and within communities: SIBER - Stable Isotope Bayesian Ellipses in R. *J. Anim. Ecol.* 80, 595–602. doi: 10.1111/j.1365-2656.2011.01806.x

Jaeger, J. A. G. (2000). Landscape division, splitting index, and effective mesh size: New measures of landscape fragmentation. *Landsc. Ecol.* 15, 115–130. doi: 10.1023/A:1008129329289

Jardine, T. D., Rayner, T. S., Pettit, N. E., Valdez, D., Ward, D. P., Lindner, G., et al. (2017). Body size drives allochthony in food webs of tropical rivers. *Oecologia* 183, 505–517. doi: 10.1007/s00442-016-3786-z

Kim, S. L., and Koch, P. L. (2012). Methods to collect, preserve, and prepare elasmobranch tissues for stable isotope analysis. *Environ. Biol. Fishes* 95, 53–63. doi: 10.1007/s10641-011-9860-9

Kursa, M. B., and Rudnicki, W. R. (2010). Feature selection with the Boruta package. *J. Stat. Softw.* 36, 1–13. doi: 10.18637/jss.v036.i11

Larsen, T., Taylor, D. L., Leigh, M. B., and O'Brien, D. M. (2009). Stable isotope fingerprinting: A novel method for identifying plant, fungal, or bacterial origins of amino acids. *Ecology* 90, 3526–3535. doi: 10.1890/08-1695.1

Larsen, T., Ventura, M., Andersen, N., O'Brien, D. M., Piatkowski, U., and McCarthy, M. D. (2013). Tracing carbon sources through aquatic and terrestrial food webs using amino acid stable isotope fingerprinting. *PLoS One* 8:e73441. doi: 10.1371/journal.pone.0073441

Latrubesse, E. M., Amsler, M. L., de Morais, R. P., and Aquino, S. (2009). The geomorphologic response of a large pristine alluvial river to tremendous deforestation in the South American tropics: The case of the Araguaia River. *Geomorphology* 113, 239–252. doi: 10.1016/j.geomorph.2009.03.014

Laurance, W. F., Sayer, J., and Cassman, K. G. (2014). Agricultural expansion and its impacts on tropical nature. *Trends Ecol. Evol.* 29, 107–116. doi: 10.1016/j.tree.2013.12.001

Layman, C. A., Quattrochi, J. P., Peyer, C. M., Allgeier, J. E., and Suding, K. (2007). Niche width collapse in a resilient top predator following ecosystem fragmentation. *Ecol. Lett.* 10, 937–944. doi: 10.1111/j.1461-0248.2007.01087.x

Le Provost, G., Badenhausser, I., Le Bagousse-Pinguet, Y., Clough, Y., Henckel, L., Violle, C., et al. (2020). Land-use history impacts functional diversity across multiple trophic groups. *Proc. Natl. Acad. Sci. U.S.A.* 117, 1573–1579. doi: 10.1073/pnas.1910023117

Leal, C. G., Lennox, G. D., Ferraz, S. F. B., Ferreira, J., Gardner, T. A., Thomson, J. R., et al. (2020). Integrated terrestrial-freshwater planning doubles conservation of tropical aquatic species. *Science* 370, 117–121. doi: 10.1126/science.aba7580

Lemes, L., de Andrade, A. F. A., and Loyola, R. (2019). Spatial priorities for agricultural development in the Brazilian Cerrado: May economy and conservation coexist? *Biodivers. Conserv.* 29, 1683–1700. doi: 10.1007/s10531-019-01719-6

Liao, J., Bearup, D., and Blasius, B. (2017b). Food web persistence in fragmented landscapes. *Proc. R. Soc. B-Biol. Sci.* 284:1859. doi: 10.1098/rspb.2017.0350

Liao, J., Bearup, D., and Blasius, B. (2017a). Diverse responses of species to landscape fragmentation in a simple food chain. *J. Anim. Ecol.* 86, 1169–1178. doi: 10.1111/1365-2656.12702

Lindgren, F., and Rue, H. (2015). Bayesian spatial modelling with R-INLA. *J. Stat. Softw.* 63:25. doi: 10.18637/jss.v063.i19

Lindgren, F., Rue, H., and Lindström, J. (2011). An explicit link between Gaussian fields and Gaussian Markov random fields: The stochastic partial differential equation approach. *J. R. Stat. Soc. Ser. B* 73, 423–498. doi: 10.1111/j.1467-9868.2011.00777.x

Logan, J. M., Jardine, T. D., Miller, T. J., Bunn, S. E., Cunjak, R. A., and Lutcavage, M. E. (2008). Lipid corrections in carbon and nitrogen stable isotope analyses: Comparison of chemical extraction and modelling methods. *J. Anim. Ecol.* 77, 838–846. doi: 10.1111/j.1365-2656.2008.01394.x

Magioli, M., Moreira, M. Z., Fonseca, R. C. B., Ribeiro, M. C., Rodrigues, M. G., and Ferraz, K. (2019). Human-modified landscapes alter mammal resource and habitat use and trophic structure. *Proc. Natl. Acad. Sci. U.S.A.* 116, 18466–18472. doi: 10.1073/pnas.1904384116

Magnusson, W. E., Da Silva, E. V., and Lima, A. P. (1987). Diets of Amazonian crocodilians. *J. Herpetol.* 21, 85–95. doi: 10.2307/1564468

Maltby, E., and Baker, T. (2009). *The wetland handbook*. Oxford: Wiley-Blackwell.

Manlick, P. J., and Newsome, S. D. (2022). Stable isotope fingerprinting traces essential amino acid assimilation and multichannel feeding in a vertebrate consumer. *Methods Ecol. Evol.* 13, 1819–1830. doi: 10.1111/2041-210X.13903

Marques, E. Q., Marimon-Junior, B. H., Marimon, B. S., Matricardi, E. A. T., Mews, H. A., and Colli, G. R. (2020). Redefining the cerrado-amazonia transition: Implications for conservation. *Biodivers. Conserv.* 29, 1501–1517. doi: 10.1007/s10531-019-01720-z

Marques, T. S., Bassetti, L. A. B., Lara, N. R. F., Portelinha, T. C. G., Piña, C. I., and Verdade, L. M. (2020). Home range and movement pattern of the broad-snouted caiman (*Caiman latirostris*) in a silviculture dominated landscape. *South Am. J. Herpetol.* 16, 16–25. doi: 10.2994/sajh-d-18-00052.1

Marques, T. S., Bassetti, L. A. B., Lara, N. R. F., Araujo, M. S., Piña, C. I., Camargo, P. B., et al. (2014). Isotopic discrimination factors (Δ^{15}N and Δ^{13}C) between tissues and diet of the broad-snouted caiman (*Caiman latirostris*). *J. Herpetol.* 48, 332–337. doi: 10.1670/12-274

Marques, T. S., Lara, N. R. F., Bassetti, L. A. B., Piña, C. I., Camargo, P. B., and Verdade, L. M. (2013). Intraspecific isotopic niche variation in broad-snouted caiman (*Caiman latirostris*). *Isot. Environ. Health Stud.* 49, 325–335. doi: 10.1080/10256016.2013.835309

Martinelli, L. A., Ometto, J. P. H. B., Ishida, F. Y., Domingues, T. F., Nardoto, G. B., Oliveira, R. S., et al. (2007). "The use of carbon and nitrogen stable isotopes to track effects of land-use changes in the Brazilian Amazon region," in *Terrestrial ecology*, eds T. E. Dawson and R. T. W. Siegwolf (New York, NY: Elsevier), 301–318.

McGarigal, K., and Marks, B. J. (1995). "FRAGSTATS: Spatial pattern analysis program for quantifying landscape structure," in *USDA Forest Service General Technical Report PNW-GTR-351*, ed. U.S. Department of Agriculture, Forest Service, Pacific Northwest Research Station (Portland, OR: U.S. Department of Agriculture, Forest Service, Pacific Northwest Research Station).

McMahon, K. W., Polito, M. J., Abel, S., McCarthy, M. D., and Thorrold, S. R. (2015). Carbon and nitrogen isotope fractionation of amino acids in an avian marine predator, the gentoo penguin (*Pygoscelis papua*). *Ecol. Evol.* 5, 1278–1290. doi: 10.1002/ece3.1437

Merlo-Galeazzi, A., and Zambrano, L. (2014). The effect of land use on isotope signatures of the detritus pathway in an urban wetland system. *Wetlands* 34, 1183–1190. doi: 10.1007/s13157-014-0577-3

Millennium Ecosystem Assessment (2005). *Ecosystems and human well-being: Wetlands and water synthesis*. Washington, DC: World Resources Institute.

Naimi, B., Hamm, N. A. S., Groen, T. A., Skidmore, A. K., and Toxopeus, A. G. (2014). Where is positional uncertainty a problem for species distribution modelling? *Ecography* 37, 191–203. doi: 10.1111/j.1600-0587.2013.00205.x

Newbold, T., Hudson, L. N., Hill, S. L., Contu, S., Lysenko, I., Senior, R. A., et al. (2015). Global effects of land use on local terrestrial biodiversity. *Nature* 520, 45–50. doi: 10.1038/nature14324

Newsome, S. D., Martínez del Rio, C., Bearhop, S., and Phillips, D. L. (2007). A niche for isotopic ecology. *Front. Ecol. Environ.* 5, 429–436. doi: 10.1890/060150.1

Nifong, J. C., Layman, C. A., and Silliman, B. R. (2015). Size, sex and individual-level behaviour drive intrapopulation variation in cross-ecosystem foraging of a top-predator. *J. Anim. Ecol.* 84, 35–48. doi: 10.1111/1365-2656.12306

Oliveira, T. A., Viola, M. R., Mello, C. R., Giongo, M., and Coelho, G. (2015). Natural vulnerability of water resources in the Formoso River Basin, Northern Brazil. *Afr. J. Agric. Res.* 10, 1107–1114. doi: 10.5897/ajar2014.9370

Ouboter, P. E., and Nanhoe, L. M. R. (1988). Habitat selection and migration of *Caiman crocodilus crocodilus* in a swamp and swamp-forest habitat in northern Suriname. *J. Herpetol.* 22, 283–294. doi: 10.2307/1564151

Parreira de Castro, D. M., Reis de Carvalho, D., Pompeu, P. D. S., Moreira, M. Z., Nardoto, G. B., and Callisto, M. (2016). Land use influences niche size and the assimilation of resources by benthic macroinvertebrates in tropical headwater streams. *PLoS One* 11:e0150527. doi: 10.1371/journal.pone.0150527

Penone, C., Davidson, A. D., Shoemaker, K. T., Di Marco, M., Rondinini, C., Brooks, T. M., et al. (2014). Imputation of missing data in life-history trait datasets: Which approach performs the best? *Methods Ecol. Evol.* 5, 961–970. doi: 10.1111/2041-210x.12232

Pereira, A. C., and Colli, G. R. (2022). Landscape features affect caiman body condition in the middle Araguaia River floodplain. *Anim. Conserv*. doi: 10.1111/acv.12841

Pereira, A. C., Nardoto, G. B., and Colli, G. R. (2018). "Intraspecific variation and spatial-temporal differences in the isotopic niche of Caiman crocodilus (spectacled caiman) in an agricultural landscape," in *Proceedings of the 25th working meeting of the IUCN-SSC Crocodile Specialist Group convened at Santa Fe, Argentina* (Gland: IUCN), 72.

Phalan, B., Bertzky, M., Butchart, S. H., Donald, P. F., Scharlemann, J. P., Stattersfield, A. J., et al. (2013). Crop expansion and conservation priorities in tropical countries. *PLoS One* 8:e51759. doi: 10.1371/journal.pone.0051759

Pillai, P., Gonzalez, A., and Loreau, M. (2011). Metacommunity theory explains the emergence of food web complexity. *Proc. Natl. Acad. Sci. U.S.A.* 108, 19293–19298. doi: 10.1073/pnas.1106235108

Plummer, M. V., and Ferner, J. W. (2012). "Marking reptiles," in *Reptile biodiversity: Standard methods for inventory and monitoring*, 1st Edn, eds R. W. McDiarmid, M. S. Foster, C. Guyer, J. W. Gibbons, and N. Chernoff (Berkeley, CA: University of California Press), 143–150.

Post, D. M., Layman, C. A., Arrington, D. A., Takimoto, G., Quattrochi, J., and Montaña, C. G. (2007). Getting to the fat of the matter: Models, methods and assumptions for dealing with lipids in stable isotope analyses. *Oecologia* 152, 179–189. doi: 10.1007/s00442-006-0630-x

Price, E. L., Sertic Peric, M., Romero, G. Q., and Kratina, P. (2019). Land use alters trophic redundancy and resource flow through stream food webs. *J. Anim. Ecol.* 88, 677–689. doi: 10.1111/1365-2656.12955

QGIS Development Team (2020). *QGIS Geographic Information System". 3*, 12 Edn. Chicago, IL: Open Source Geospatial Foundation Project.

Quesnelle, P. E., Lindsay, K. E., and Fahrig, L. (2015). Relative effects of landscape-scale wetland amount and landscape matrix quality on wetland vertebrates: A meta-analysis. *Ecol. Appl.* 25, 812–825. doi: 10.1890/14-0362.1

R Development Core Team (2021). *R: A language and environment for statistical computing*, 4.1.0 Edn. Vienna: R Foundation for Statistical Computing.

Radloff, F. G., Hobson, K. A., and Leslie, A. J. (2012). Characterising ontogenetic niche shifts in Nile crocodile using stable isotope (δ^{13}C, δ^{15}N) analyses of scute keratin. *Isot. Environ. Health Stud.* 48, 439–456. doi: 10.1080/10256016.2012.667808

Ramsar Convention [RAMSAR] (2002). *Ramsar sites information service - Ilha do Bananal no. 624*. Gland: Ramsar Convention.

Reddin, C. J., Bothwell, J. H., O'Connor, N. E., Harrod, C., and Briones, M. J. (2018). The effects of spatial scale and isoscape on consumer isotopic niche width. *Funct. Ecol.* 32, 904–915. doi: 10.1111/1365-2435.13026

Redding, D. W., Lucas, T. C. D., Blackburn, T. M., and Jones, K. E. (2017). Evaluating Bayesian spatial methods for modelling species distributions with clumped and restricted occurrence data. *PLoS One* 12:e0187602. doi: 10.1371/journal.pone.0187602

Reed, R. N., and Tucker, A. D. (2012). "Determining age, sex, and reproductive condition," in *Reptile biodiversity: Standard methods for inventory and monitoring*, eds R. W. McDiarmid, M. S. Foster, C. Guyer, J. W. Gibbons, and N. Chernoff (Berkeley,CA: University of California Press), 151–163.

Resasco, J., Tuff, K. T., Cunningham, S. A., Melbourne, B. A., Hicks, A. L., Newsome, S. D., et al. (2017). Generalist predator's niche shifts reveal ecosystem changes in an experimentally fragmented landscape. *Ecogrjaphy* 41, 1209–1219. doi: 10.1111/ecog.03476

Riva, F., and Nielsen, S. E. (2020). Six key steps for functional landscape analyses of habitat change. *Landsc. Ecol.* 35, 1495–1504. doi: 10.1007/s10980-020-01048-y

Rooney, N., McCann, K. S., and Moore, J. C. (2008). A landscape theory for food web architecture. *Ecol. Lett.* 11, 867–881. doi: 10.1111/j.1461-0248.2008.01193.x

Rosenblatt, A. E., Heithaus, M. R., Mather, M. E., Matich, P., Nifong, J. C., Ripple, W. J., et al. (2013). The roles of large top predators in coastal ecosystems: New insights from long-term ecological research. *Oceanography* 26, 156–167. doi: 10.5670/oceanog.2013.59

Rue, H., Martino, S., and Chopin, N. (2009). Approximate Bayesian inference for latent Gaussian models by using integrated nested Laplace approximations. *J. R. Stat. Soc. Ser. B* 71, 319–392. doi: 10.1111/j.1467-9868.2008.00700.x

Scheffer, M., Carpenter, S., Foley, J. A., Folke, C., and Walker, B. (2001). Catastrophic shifts in ecosystems. *Nature* 413, 591–596.

Silfer, J. A., Engel, M. H., Macko, S. A., and Jumeau, E. J. (1991). Stable carbon isotope analysis of amino acid enantiomers by conventional isotope ratio mass spectrometry and combined gas chromatography/isotope ratio mass spectrometry. *Anal. Chem.* 63, 370–374. doi: 10.1021/ac00004a014

Somaweera, R., Nifong, J., Rosenblatt, A., Brien, M. L., Combrink, X., Elsey, R. M., et al. (2020). The ecological importance of crocodylians: Towards evidence-based justification for their conservation. *Biol. Rev.* 95, 936–959. doi: 10.1111/brv.12594

Stekhoven, D. J., and Buühlmann, P. (2012). MissForest – non-parametric missing value imputation for mixed-type data. *Bioinformatics* 28, 112–118. doi: 10.1093/bioinformatics/btr597

Strassburg, B. B. N., Brooks, T., Feltran-Barbieri, R., Iribarrem, A., Crouzeilles, R., Loyola, R., et al. (2017). Moment of truth for the Cerrado hotspot. *Nat. Ecol. Evol.* 1, 1–3. doi: 10.1038/s41559-017-0099

Thorbjarnarson, J. (1997). Are crocodilian sex ratios female biased? The data are equivocal. *Copeia* 1997, 451–455. doi: 10.2307/1447771

Thorbjarnarson, J. B. (1993). Diet of the spectacled caiman (*Caiman crocodilus*) in the central Venezuelan Llanos. *Herpetologica* 49, 108–117.

Thorp, J. H., and Bowes, R. E. (2016). Carbon sources in riverine food webs: New evidence from amino acid isotope techniques. *Ecosystems* 20, 1029–1041.

Tscharntke, T., Tylianakis, J. M., Rand, T. A., Didham, R. K., Fahrig, L., Batary, P., et al. (2012). Landscape moderation of biodiversity patterns and processes - eight hypotheses. *Biol. Rev.* 87, 661–685. doi: 10.1111/j.1469-185X.2011.00216.x

Vander Zanden, M. J., Clayton, M. K., Moody, E. K., Solomon, C. T., and Weidel, B. C. (2015). Stable isotope turnover and half-life in animal tissues: A literature synthesis. *PLoS One* 10:e0116182. doi: 10.1371/journal.pone.0116182

Venables, W. N., and Ripley, B. D. (2002). *Modern applied statistics with S*. New York, NY: Springer.

Villamarín, F., Jardine, T. D., Bunn, S. E., Marioni, B., and Magnusson, W. E. (2017). Opportunistic top predators partition food resources in a tropical freshwater ecosystem. *Freshw. Biol.* 62, 1389–1400. doi: 10.1111/fwb.12952

Villard, M.-A., Metzger, J. P., and Saura, S. (2014). Beyond the fragmentation debate: A conceptual model to predict when habitat configuration really matters. *J. Appl. Ecol.* 51, 309–318. doi: 10.1111/1365-2664.12190

Wang, X., Blanchet, F. G., and Koper, N. (2014). Measuring habitat fragmentation: An evaluation of landscape pattern metrics. *Methods Ecol. Evol.* 5, 634–646. doi: 10.1111/2041-210X.12198

Wang, X., Yue, Y. R., and Faraway, J. J. (2018). *Bayesian regression modeling with INLA*. New York, NY: CRC Press.

Wantzen, K. M., Fellerhoff, C., and Voss, M. (2010). "Stable isotope ecology of the food webs of the Pantanal," in *The Pantanal: Ecology, biodiversity and sustainable management of a large neotropical seasonal wetland*, eds W. Junk, C. J. Silva, and C. Nunes da Cunha (Sofia: Pensoft Publishers), 597–616.

Whiteman, J. P., Smith, E. A. E., Besser, A. C., and Newsome, S. D. (2019). A guide to using compound-specific stable isotope analysis to study the fates of molecules in organisms and ecosystems. *Diversity* 11:18. doi: 10.3390/d11010008

Zaia Alves, G. H., Hoeinghaus, D. J., Manetta, G. I., and Benedito, E. (2017). Dry season limnological conditions and basin geology exhibit complex relationships with delta C-13 and delta N-15 of carbon sources in four Neotropical floodplains. *PLoS One* 12:e0174499. doi: 10.1371/journal.pone.0174499

Zambrano, L., Valiente, E., and Vander Zanden, M. J. (2010). Stable isotope variation of a highly heterogeneous shallow freshwater system. *Hydrobiologia* 646, 327–336. doi: 10.1007/s10750-010-0182-2

frontiers | Frontiers in Ecology and Evolution

TYPE Original Research
PUBLISHED 13 June 2023
DOI 10.3389/fevo.2023.1161105

OPEN ACCESS

EDITED BY
Keith Alan Hobson,
Western University, Canada

REVIEWED BY
Steven Y. Litvin,
Monterey Bay Aquarium Research Institute (MBARI), United States
John Whiteman,
Old Dominion University, United States

*CORRESPONDENCE
Clive N. Trueman
✉ trueman@soton.ac.uk

RECEIVED 07 February 2023
ACCEPTED 17 May 2023
PUBLISHED 13 June 2023

CITATION
Jones J, Hunter E, Hambach B, Wilding M and Trueman CN (2023) Individual variation in field metabolic rates of wild living fish have phenotypic and ontogenetic underpinnings: insights from stable isotope compositions of otoliths.
Front. Ecol. Evol. 11:1161105.
doi: 10.3389/fevo.2023.1161105

Individual variation in field metabolic rates of wild living fish have phenotypic and ontogenetic underpinnings: insights from stable isotope compositions of otoliths

Joseph Jones[1], Ewan Hunter[2,3], Bastian Hambach[1], Megan Wilding[1] and Clive N. Trueman[1]*

[1]School of Ocean and Earth Science, University of Southampton, Southampton, United Kingdom, [2]Centre for Environment, Fisheries and Aquaculture Science (CEFAS), Lowestoft, United Kingdom, [3]Agri-Food and BioSciences Institute (AFBI), Belfast, United Kingdom

Introduction: Individual metabolism has been identified as a key variable for predicting responses of individuals and populations to climate change, particularly for aquatic ectotherms such as fishes. Predictions of organism standard metabolic rate (SMR), and the thermal sensitivity of metabolic rate are typically based on allometric scaling rules and respirometry-based measures of respiratory potential under laboratory conditions. The relevance of laboratory-based measurement and theoretical allometric rules to predict performance of free-ranging animals in complex natural settings has been questioned, but determining time averaged metabolic rate in wild aquatic animals is challenging.

Methods: Here we draw on stable isotope compositions of aragonite in fish otoliths to estimate time averaged experienced temperature and expressed field metabolic rate (FMR) simultaneously and retrospectively at an individual level. We apply the otolith FMR proxy to a population of European plaice (*Pleuronectes platessa*) from the North Sea during a period of rapid warming between the 1980s to the mid-2000s, sampling otolith tissue grown in both juvenile and adult stages.

Results: Among-individual variations in realized mass-specific FMR were large and independent of temperature and scaled positively with body size in adult life stages, contradicting simplistic assumptions that FMR follows scaling relationships inferred for standard metabolic rates (SMR). In the same individuals, FMR in the first summer of life co-varied positively with temperature.

Discussion: We find strong evidence for the presence of consistent metabolic phenotypes within the sampled population, as FMR in the first year of life was the strongest single predictor for among individual variation in FMR at the point of sampling. Nonetheless, best fitting models explained only 20% of the observed variation, pointing to large among-individual variation in FMR that is unexplained by body mass, temperature or metabolic phenotype. Stable isotope-derived estimates of field metabolic rate have great potential

to expand our understanding of ecophysiology in general and especially mechanisms underpinning the relationships between animal performance and changing environmental and ecological conditions.

KEYWORDS

ecophysiology, metabolic theory, biomineral, fisheries, carbon isotope ($\delta^{13}C$)

1. Introduction

The physiological performance of wild fishes reflects the interaction between the individual phenotype and the availability of resources (Killen et al., 2016; Metcalfe et al., 2016; Duncan et al., 2020). Population growth, size and distribution (and consequently fisheries production) depends on the energetic efficiency with which individuals can acquire and assimilate the available resources (Andersen, 2018). In a changing climate, fish production also depends on the ability of a population to either adapt their physiology to changing conditions or migrate toward more favorable habitats (Dulvy et al., 2008; Perry et al., 2011; Violle et al., 2012; Blowes et al., 2019). The relationship between fish physiology and environmental conditions is inherently complex, drawing on multiple interactive internal and external processes, which are difficult to simulate under laboratory conditions (Jutfelt, 2020; Lindmark et al., 2022). Consequently, attempts to produce field-relevant predictions of how fish performance will respond to environmental change has been a contentiously debated topic within the field of fisheries sciences for several decades (Mieszkowska et al., 2009; Albouy et al., 2013; Halsey et al., 2018; Pauly, 2021).

External water temperature is one of the most commonly measured environmental drivers in fish ecophysiology (Deutsch et al., 2015; Andersen, 2018; Pauly, 2021). The internal body temperature of ectothermic fishes closely matches ambient water temperature, and therefore influences fish physiology directly (Schulte et al., 2011), and through the inverse relationship between temperature and oxygen solubility (Pörtner et al., 2017). Changes in water temperature may produce complex physiological responses, including behavioral changes (e.g., long-distance- or local migratory responses), changes in feeding intensity, activity levels or physiological effects such as metabolic responses or changes to allocation of energy resources (Rijnsdorp, 1990; Murawski, 1993; MacKenzie et al., 2011; Little et al., 2020; McKenzie et al., 2021). Responses are likely to vary depending on the magnitude and rate of experienced temperature variation relative to the long term climate average in the population's home range (Schulte et al., 2011; Jutfelt, 2020), and are likely to vary locally, e.g., based on the availability of resources (Vinton and Vasseur, 2022). From a physiological perspective, metabolic effects of temperature have received the most attention in terms of attempting to explain fish distributions and predict changes to fish production and distributions under future ocean conditions (Cheung et al., 2013; Petrik et al., 2020; Deutsch et al., 2022).

Metabolic rate represents the sum of all energetic activity in an organism, and is a useful trait as a proxy for whole animal performance (Andersen, 2018). Whole-organism metabolic rate is the combination of the rates of energy-consuming chemical reactions (enzyme-mediated oxidation of food resources), and in ectotherms is directly influenced by the external temperature. At temperatures below an individual's thermal optimum, metabolism is thought to be limited by the thermodynamics of enzyme kinetic reactions (Ern, 2019). Above the thermal optimum metabolic rates decline with increasing temperature due to either declining performance of enzyme proteins due to structural effects associated with denaturing limiting enzymatic reaction rate (Schulte, 2015; Ern, 2019), or due to limitations on the capacity to acquire, process and distribute resources, especially oxygen, through the body. Thermal response curves for metabolism can be determined under laboratory conditions, and used to infer likely physiological responses to external temperatures, and thus predict spatial distributions of populations (Lamine et al., 2010; Rutterford et al., 2015). Predictions of fish responses to temperature change based on laboratory-determined metabolic performance curves may not however, be directly applicable to *in situ* fish communities. The realized thermal sensitivity of fish physiological performance in wild conditions reflects a combination of direct thermodynamic effects on reaction rates, limitations to performance from capacity to supply oxygen and nutrients, and behavioral energetic trade-offs, all moderated through the phenotypic and genotypic adaptive capacity of the population (Skelly et al., 2007; Hofmann and Todgham, 2010; Healy and Schulte, 2012; Norin et al., 2014; Holt and Jørgensen, 2015).

Teleost fish also typically increase body size over orders of magnitude during growth, with strong selection pressure acting to maximize growth in early life, but less in later life. Changes in energy allocation across life stages could potentially induce ontogenetic differences in the thermal sensitivity of field metabolic rate across life history stages in an individual fish (Andersen, 2018; Dahlke et al., 2020). Laboratory studies have suggested higher thermal sensitivity for metabolic rates in early juvenile life stages of fishes (Dahlke et al., 2020), potentially linked to observed reduction in thermal tolerance limits associated with increased activity (Deutsch et al., 2020). To better understand population dynamics, and improve predictions of the responses of wild fish populations under rising seawater temperatures, we need to understand how *in-situ* energy use varies with temperature and with life stage. Specifically, we need to identify if field metabolic rate (FMR), the energetic response of the entire organism to the physical and ecological environment) varies with temperature in a similar manner to laboratory-based measurements of metabolic rate, as predictive models use respiratory potential data to estimate biogeography.

1.1. Stable isotope based estimation of field metabolic rate

Field metabolic rate is arguably the most ecologically relevant measure of energy consumption (Speakman, 1999; Pontzer et al., 2021), but has proven challenging to estimate especially in aquatic organisms (Payne et al., 2016; Treberg et al., 2016). Where direct calorimetry is impractical, metabolic rate is typically inferred from the rate of consumption of oxygen or of production of carbon dioxide, both of which can be traced via isotopic labeling of oxygen and hydrogen (Speakman, 1998) or carbon (Welch et al., 2016; Urca et al., 2021). Where natural isotope compositions of metabolic and environmental sources differ either for oxygen or carbon, there is potential to infer rates of oxidation of dietary substrates (and production of carbon dioxide) from isotope markers expressed in tissues. Drawing on natural isotope markers has the advantage that no prior intervention is needed, and all individuals are effectively labeled naturally. Here we apply an emerging method for deriving simultaneous estimates of experienced temperature and expressed field metabolic rate from the stable isotope composition of carbon and oxygen in otolith aragonite (Chung et al., 2019a,b; Martino et al., 2020).

Oxygen in otolith aragonite is deposited at, or close to, isotopic equilibrium with the ambient water, with a temperature-dependent fractionation such that the temperature of otolith precipitation can be estimated from knowledge of the isotopic compositions of the ambient water and the otolith (Campana and Thorrold, 2001). Carbon in otolith aragonite is not in isotopic equilibrium with the surrounding dissolved inorganic carbon (DIC) (Kalish, 1991; Gauldie, 1996; Solomon et al., 2006) . Rather, carbon in the blood is a mixture of carbon derived from dissolved inorganic carbonate and carbon released from respiration of food. The stable isotope composition of these sources is very different: seawater carbon ($\delta^{13}C_{sw}$) values typically range between c.1 and −7% globally, while respiratory carbon ($\delta^{13}C_{resp}$) values generally vary between c. −10 to −25% in marine fishes. Otolith carbonate biomineral is formed from a mixture of these sources of HCO_3^- ions transported from blood into the biomineralising medium (endolymph fluid within the inner ear sacculus). The isotopic composition of inorganic carbon in blood, the endolymph fluid and otolith aragonite mineral is a weighted average of the relative contribution of respiratory carbon and seawater dissolved carbon (McConnaughey et al., 1997; Schwarcz et al., 1998; Solomon et al., 2006; Tohse and Mugiya, 2008). Critically, blood carbonate levels must be regulated to maintain optimum pH, therefore as the rate of respiration of food sources increases, the relative proportion of respiratory carbon in blood increases (Chung et al., 2019a). The proportion of respiratory carbon in otolith aragonite (otolith C_{resp}) can be determined from isotopic mass balance given estimates of the isotopic composition of diet and seawater carbon sources, providing a proxy measure of FMR averaged over the timeframe of otolith growth (Weidman and Millner, 2000; Jamieson et al., 2004; Trueman et al., 2013; Sinnatamby et al., 2015; Trueman et al., 2016).

The relationship between C_{resp} values and oxygen consumption rates can be estimated in laboratory experiments, using temperature to manipulate metabolic rates (Chung et al., 2019b; Martino et al., 2020). Experiments to date suggest an exponential limited relationship between C_{resp} values and oxygen consumption rates (Chung et al., 2019a; Martino et al., 2020) however, it is likely that the non-linear portion of the relationship (at high induced metabolic rates) is influenced by experimental artifacts associated with metabolic demands other than SMR contributing to oxygen consumption at high temperatures (Alewijnse, 2022). Many studies have demonstrated relationships between $\delta^{13}C$ values of otoliths and relative metabolic rates (Kalish, 1991; Weidman and Millner, 2000; Sherwood and Rose, 2003; Nelson et al., 2011; Trueman et al., 2013; Sinnatamby et al., 2015; Alewijnse et al., 2021; Smoliński et al., 2021; Sakamoto et al., 2022), but to date, few studies have explored individual-level variations in expressed field metabolic rates within a single population. In this study we use otolith isotope-derived estimates of field metabolic rate to quantify the relationship between experienced temperature and expressed field metabolic rate across life stages in a single population of free-roaming wild fish.

The European plaice *Pleuronectes platessa* (henceforth, plaice) is an abundant north east Atlantic flatfish which supports an extensive fishery throughout the North Sea and surrounding areas. The fishery has existed in some form for hundreds of years, and has been commercially monitored from the 1800s. Otoliths are routinely removed from North Sea plaice for age and growth studies, and the UK fisheries laboratory CEFAS have maintained an otolith archive with (incomplete) sampling dating to the early 1900s. Due to their commercial value, plaice have been well-studied (Engelhard et al., 2011; Rutterford et al., 2023), with annual fisheries surveys [ICES, (Datras: Survey descriptions, accessed 2023)] estimating mortality and stock spawning biomass. Extensive data on plaice biology, behavior and population structure within the North Sea coupled with the availability of otolith archives, make North Sea plaice attractive as a model species.

2. Materials and methods

2.1. Sample selection

Plaice otoliths were obtained from archived otolith collections held in the CEFAS fisheries otolith archive. Plaice were sampled from research fishery cruises conducted as part of ICES co-ordinated bottom trawling surveys in the North Sea. Otolith selection was designed to capture seasonal variations and potential differences between years with warm and cold mean water temperatures. Fish sampled were caught in each of four fishing monthly quarters and from North Sea ICES areas IVB and IVC (**Figure 1A**). Otoliths were selected from survey years with high sample coverage (**Table 1**). To minimize age-dependent metabolic variability and sample fish with a relatively high growth rate and therefore larger volumes of otolith available for sampling, sample selection targeted individuals assessed to have been spawned 4 years prior to capture. All otoliths were pre-aged by CEFAS otolith readers.

Annual average water temperature in the North Sea experienced a significant period of warming within ICES areas IVB and IVC between 1980 and 2010 (Núñez-Riboni and Akimova, 2015), otoliths were therefore selected from years reflecting colder (pre 1990) and warmer (post 1990) periods as well as periods with relatively high and low plaice abundance. The full list of ICES

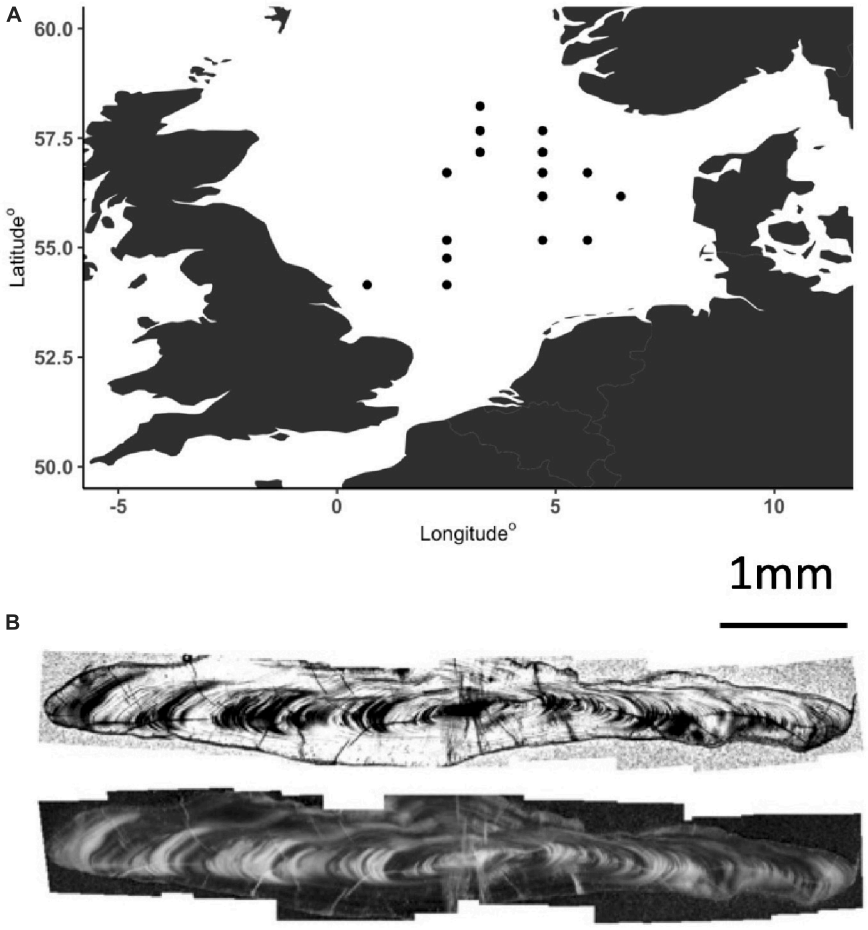

FIGURE 1
(A) Sample capture locations for fish. **(B)** Longitudinal section through a plaice otolith viewed with transmitted light and the same image with enhanced contrast.

TABLE 1 Numbers of sampled male and female plaice assigned to sub-group A and used for subsequent analyses.

Year	Males	Females
1985	13	10
1986	9	7
1987	6	18
1990	13	12
1993	12	18
1995	6	5
1997	6	18
1998	14	27
1999	14	22
2001	4	6
2002	10	19
Total	**107**	**162**

rectangles sampled and individual distribution across each quarter is provided within the **Supplementary Material**. The sample years selected were 1984, 1985, 1986, 1987, 1990 1993, 1995, 1997, 1998, 1999, 2001, and 2002. In total, 558 individual otolith samples were selected and analyzed, this sample suite was restricted to fish inhabiting high salinity waters (see below).

2.2. Sample preparation

The otolith preparation protocol followed previous work (Shephard et al., 2007; Chung et al., 2019b; Alewijnse et al., 2021). Otolith sampling was designed to provide sufficient powder while averaging over the smallest time interval possible, targeting the regions of fastest growth of the otolith. Initially otoliths were cleaned with fresh water to remove any residual tissue, and fixed to an epoxy (Struers EopFix resin) mount with the proximal (sulcus) surface uppermost. The external otolith surface area representing the most recent period of aragonite deposition was then sampled using a Dremel 4,000 rotary engraving tool, with straight sided, cylindrical diamond-encrusted dental bits. Milling aimed to remove a target mass of c.50 μg of aragonite powder. Following external edge sampling, a subset of 101 otoliths were sectioned to approximately 20 micron thickness at the University of Southampton Rock Preparation and Thin-Sectioning Laboratories (National Oceanography Centre, UK). Otolith sections were used

to visually estimate the depth of external milling and therefore the time period of sampled otolith growth over which FMR and temperature is integrated, and to provide access to the first year of growth for analyses of FMR and temperature during juvenile life stages (**Figure 1B**). Otolith growth representing the second half of the first year of life was sampled using an ESI New Wave Micromill either by milling trenches or from multiple drill holes. The time integrated period for juvenile otolith sampling was kept to a minimum, estimated from otolith growth analyses to represent a maximum period of a month.

2.3. Mass spectrometry

The stable isotope compositions of carbon and oxygen in otolith aragonite were measured at the Stable Isotope Ratio Mass Spectrometry (SIRMS) Laboratory (University of Southampton, National Oceanography Centre, Southampton, UK), with a Kiel IV Carbonate Device coupled with a MAT253 isotope ratio mass spectrometer (both Thermo Fisher Scientific, Bremen, Germany). Approximately 20–70 μg of aragonite powder was accurately weighed into borosilicate glass reaction vessels prior to evolution of CO_2 through reaction with 106% phosphoric acid at a constant 70°C temperature. The calibration standards used were NBS 19 and NBS 18 (IAEA, Vienna, Austria), as well as a quality control GS1 (Internal Carrara marble standard produced by the SIRMS laboratory). Results are reported as $\delta^{13}C$ and $\delta^{18}O$ values in permille (‰) units relative to Vienna Pee Dee Belemnite. Accuracy and precision determined from long-term analyses of internal carbonate standards of known composition is 0.02% for both $\delta^{13}C$ and $\delta^{18}O$ values in otolith aragonite. Standard deviations of repeated measures of $\delta^{13}C$ and $\delta^{18}O$ values in internal standards in each run contributing to the results discussed here are presented in the **Supplementary Materials**.

2.4. Estimation of the proportion of metabolic carbon in otolith aragonite

We estimated the proportion of respiratory carbon in otolith aragonite (C_{resp}) from a two-component mixing model (Chung et al., 2019a):

$$C_{resp} = (\delta^{13}C_{oto} - \delta^{13}C_{DIC})/(\delta^{13}C_{diet} - \delta^{13}C_{DIC}) + \in_{total} \quad (1)$$

where $\delta^{13}C_{oto}$ represents the $\delta^{13}C$ value of the sampled otolith aragonite, $\delta^{13}C_{DIC}$ represents the $\delta^{13}C$ value of dissolved inorganic carbon in seawater, and $\delta^{13}C$ values $\delta^{13}C_{diet}$ represents the $\delta^{13}C$ value of individual diet (Chung et al., 2019a). δ_{total} is the total isotopic fractionation from DIC and diet to blood, blood to endolymph and endolymph to otolith (Solomon et al., 2006). The absolute value of δ_{total} may vary among species (Solomon et al., 2006; Tohse and Mugiya, 2008; Nelson et al., 2011; Smoliński et al., 2021), and requires further laboratory experimentation to calculate. Within this study, we assume that δ_{total} does not vary systematically among individuals of the same species and is set to 0 (Solomon et al., 2006; Chung et al., 2019a). $\delta^{13}C_{diet}$ values were estimated based on 72 individual plaice within a compilation of stable isotope data from fishes from the North Sea (Jennings and Cogan, 2015), with data from plaice ranging from −19.4 to −14.5%, averaging −16.8%.

$\delta^{13}C_{DIC}$ values across the North Sea are relatively positive compared to average seawater (Burt et al., 2016), likely reflecting intense photosynthetic production. We drew on these data to estimate a median likely $\delta^{13}C_{DIC}$ value of c. 1% and applied an uncertainty (standard deviation) of 0.25% to this value. We estimated uncertainty associated with mass balance solutions for C_{resp} values (equation 1) from 100 Monte Carlo resampling rounds with applied uncertainties and resulting parameter uncertainty estimates presented in **Table 2**.

2.5. Estimating oxygen consumption rates

To assist with comparisons with alternative measures of metabolic rate, the C_{resp} expression was converted into oxygen consumption rate based on the linear form of a statistical relationship between measured oxygen consumption associated with resting (fed) metabolic rate and C_{resp} values in juvenile cod (Chung et al., 2019a).

$$\text{Mass} - \text{specific oxygen consumption rate } (mgO_2\ Kg^{-1}hr^{-1})$$

$$= (C_{resp} - 0.041 \pm 0.00102/9.71^{*}10^{-4} \pm 9.57^{*}10^{-5} \quad (2)$$

This experimental calibration above is based on the observed relationship between C_{resp} and resting metabolic rate in 80 individual cod assigned to 4 experimental temperatures.

2.6. Estimating experienced temperature

Time averaged experienced temperature was reconstructed using a species-specific otolith isotope temperature equation (Geffen, 2012):

$$\delta^{18}O_{c-}\delta^{18}O_w = 3.72 - 0.19T(°C) \quad (3)$$

$\delta^{18}O$ values of ambient sea water ($\delta^{18}O_w$) vary largely according to salinity, as freshwater inputs have lower $\delta^{18}O_w$ values than seawater. In the North Sea salinity varies considerably in space and time, complicating the use of oxygen isotope thermometry (see below. $\delta^{18}O_w$ values of the ambient sea water were initially estimated from LeGrande and Schmidt (2006), with model outputs presented in **Figure 2**. The location (and therefore expected $\delta^{18}O_w$ values) experienced by individuals in the first year of life are unknown, but the sampled population spawns in the central North Sea, with juveniles unlikely to experience the relatively low salinity conditions seen in the extreme south-eastern North Sea. To infer experienced temperatures during juvenile life stages we assume a $\delta^{18}O_w$ value of 0.1% ± 0.2% (**Table 2**).

TABLE 2 Parameter values, uncertainties and sources employed in Monte Carlo resampling to estimate uncertainties in inferred temperatures and C_{resp} values.

Parameter	Value (range)	Uncertainty (std dev)	95% Confidence	References
$\delta^{18}O_w$	0.01–0.294%	0.1%	0.4%	LeGrande and Schmidt, 2006
$\delta^{18}O_{oto}$	0.01–3.3%	0.025%	0.1%	UoS SIRMS laboratory
$\delta^{13}C_{diet}$	−16.8% (−19.4 to −14.5)	0.25%	1%	Jennings and Cogan, 2015
$\delta^{13}C_{DIC}$	1%	0.25%	1%	Burt et al., 2016
$\delta^{13}C_{oto}$	−2.9–0.47%	0.1%	0.4%	UoS SIRMS laboratory, Rooker et al., 2008
Thermometry slope	−0.19	0.004	0.019	Geffen, 2012
Thermometry intercept	3.72	0.03	0.24	Geffen, 2012

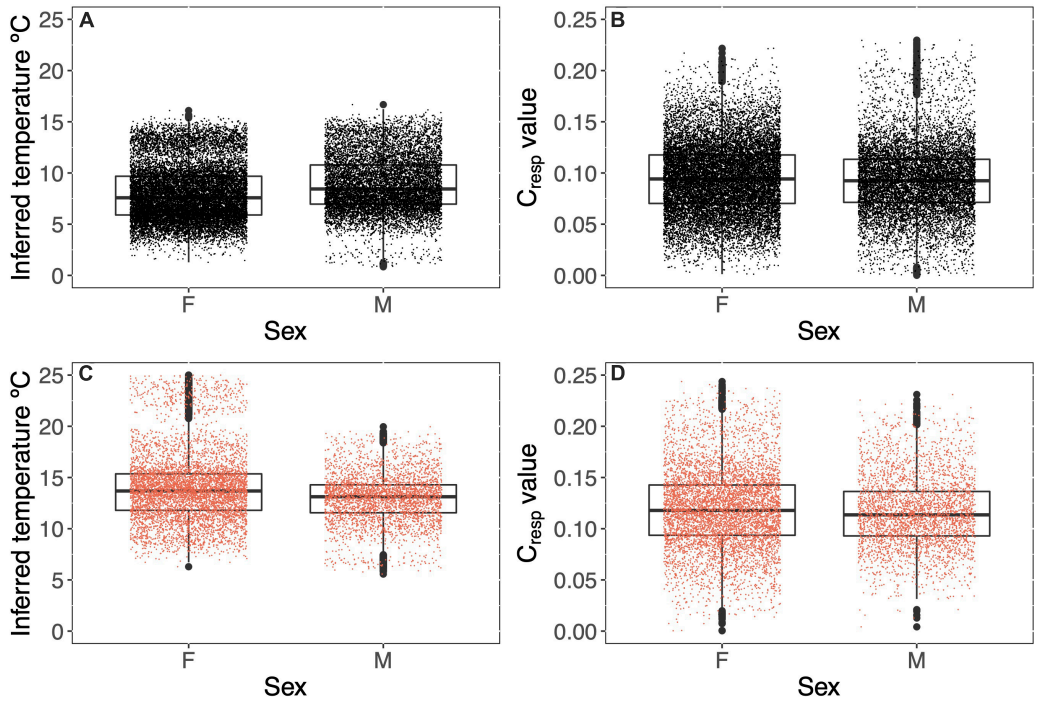

FIGURE 2
Otolith-inferred temperatures **(A,C)** and C_{resp} values **(B,D)** experienced by sampled plaice at the point of capture as adults (**A,B**, black points) and during the first summer of life (**C,D**, red points). Points represent Monte Carlo resampling of the 281 **(A,B)** and 95 **(C,D)** otoliths.

2.7. Restricting analyses to avoid fish from low salinity waters

Plaice in the North Sea are divided into three groups based primarily on summer feeding locations, and the three groups experience differing and variable salinity environments, resulting in characteristic combinations of $\delta^{18}O_{oto}$ values and water temperature (Darnaude et al., 2014). Of the three identified groups, group (A) experiences the least variable water conditions with fluctuations in $\delta^{18}O_w$ values limited to less than 1.5‰ (reflecting salinities between 34.5 and 36%). We therefore aimed to target individuals from group A for subsequent analyses and developed a sample selection pipeline as follows based on information in Darnaude et al. (2014): Individuals captured north of 56°N are likely to belong to group A, and are therefore included, however, individuals from populations B or C could potentially have recently moved north of 56°N. We therefore excluded data from any fish captured N of 56°N which expressed reconstructed temperatures values (>14°C), as this would imply recent movement from waters with low salinity and/or low $\delta^{18}O_w$ values. Similarly, population A fish recently moving south of 56°N would be expected to express anomalously high $\delta^{18}O_{oto}$ values, reflecting cold and saline water. We therefore included individuals caught at latitudes lower than 56°N, but with $\delta^{18}O_{oto}$ values in excess of 2.3% (Darnaude et al., 2014).

2.8. Statistical treatment of data

The relationship between oxygen consumption, experienced temperature (as inferred from $\delta^{18}O$ data), weight, sex and year of sampling was investigated using linear mixed effects modeling. Sex

and year were treated as random effects. All continuous variables were z-scored prior to modeling. REML structure was applied to all linear mixed effects models. The potential influence of within-individual metabolic phenotype was explored by adding oxygen consumption at year 1 as an additional fixed effect. Linear mixed effects models were performed in R using the "lme4" package and models were compared using AIC values.

3. Results

A total of 95% confidence intervals in estimates of experienced temperature and C_{resp} values were calculated as 4× the mean standard deviation over the 100 Monte Carlo resampled values drawing on estimates of uncertainty in source values expressed in Table 2. Uncertainties were estimated for individuals identified as belonging to population A. Estimated 95% confidence intervals were 2.4°C for experienced temperature and 0.05 in C_{resp} values (translating to an 95% confidence interval in individual oxygen consumption rates of 57 $mgO_2^{-1}Kg^{-1}hr^{-1}$).

We successfully recovered stable isotope data from 459 individual fish. From the overall sampled population, 269 fish were assigned to population A with known sex. The distribution of samples throughout sexes and years is presented in Table 1. From these, 101 fish were selected at random, sectioned and sampled to recover $\delta^{18}O$ and $\delta^{13}C$ values representing growth in the first summer of life, resulting in data successfully recovered from 95 individuals.

3.1. Estimating the time integration window

The time period integrated during milling will vary according to seasonal changes in otolith growth rate, and was estimated from thin sectioned otoliths. Where the sampled zone was clearly visible within thin section as a trench, the time period over which isotopic values are averaged was estimated to the nearest month based on the relative depth of sampled trench and distance from the intact edge of the otolith to the last annulus. Average estimated sampling duration by month of capture ranged between 1 and 2.3 months with longer time integration periods in winter months. Sampling of otolith growth during the first year of life targeted the first translucent band (representing the first summer of life). The time integration period for first year sampling is estimated to be 1 month.

3.2. Experienced temperature

Time averaged experienced temperature reconstructed from $\delta^{18}O$ values of the otolith outer edge ranged between 1.38 to 17.29°C with an average of 8.02°C (Figures 2A, C and Table 3). These values are consistent with previous estimates of experienced temperature for North Sea plaice ranging between 4 and 14°C over the annual cycle (Darnaude et al., 2014). We found no significant difference in experienced temperature between sexes (Kruskal–Wallis $t = 0.4$).

The time integrated experienced temperature during the second half of the first year of life of 95 individuals ranged between 5.8 and 26°C with an average of 14°C (+−3.2). These temperatures are comparable to sea surface temperatures seen in the Wadden Sea and German Bight, which typically range between 2 and 20°C (Núñez-Riboni and Akimova, 2015). We saw no difference in experienced temperature between sexes (Kruskal–Wallis p-value of 0.481) or among years (Kruskal–Wallis p-value of 0.48).

3.3. C_{resp} values

Adult C_{resp} values range between 0.03 and 0.22, with an average of 0.12. There is no significant difference between adult C_{resp} values by sex with a Kruskal–Wallis p-value of 0.481, or between sample years, with a Kruskal–Wallis p-value of 0.134. These C_{resp} values are consistent with data from other pleuronectiformes (Alewijnse, 2022), suggesting relatively low field metabolic rates for this order compared to other sampled teleosts when body mass and temperature are controlled.

Inferred mass-specific oxygen consumption rates ranged between 0 and 203 $mgO_2^{-1}Kg^{-1}hr^{-1}$, averaging 54 $mgO_2^{-1}Kg^{-1}hr^{-1}$ (Figures 2B, D and Table 3). Estimated oxygen consumption rates inferred within this study are similar to standard metabolic rates based on laboratory respirometry, and are therefore lower than expected. However, we are unsure of the appropriate parameters used to convert C_{resp} values to oxygen consumption for plaice without prior experimentation, therefore we are drawing on calibration parameters derived for Atlantic cod. Oxygen consumption rates in plaice measured via respirometry in laboratory conditions range between 13 and 202 $mgO_2^{-1}Kg^{-1}hr^{-1}$over comparable temperatures (5–20°C) and body masses (27–632 g) as the samples presented within this study (data compiled from Fish base).

C_{resp} values expressed during the first year of life in individuals from sub-population A range between 0 and 0.25 with an average of 0.1. There is no expressed significant difference in C_{resp} values between sexes during juvenile life stages (Kruskal–Wallis p-value = 0.481). When comparing years there is a significant difference, with a Kruskal–Wallis p-value of 0.0161, and years with warmer average temperatures resulting in higher C_{resp} averages for juvenile populations.

3.4. Relationship between FMR (C_{resp} values), body mass, and experienced temperature

Mass-specific basal (standard) metabolic rate is expected to decrease with body mass and to increase with temperature. We drew on linear mixed effects models to assess the potential effect of temperature and body mass on expressed field metabolic rates. The full model structure used to explore variations in adult oxygen consumption rate was:

$$\log_{10}\text{oxygen consumption} \sim \log_{10}\text{temperature} + \log_{10}\text{mass} + (1|\text{sex}) + (1|\text{year}) \quad (4)$$

The retrospective nature of otolith analyses allows us to test for a potential effect of individual metabolic phenotype. We included oxygen consumption in the first year as an additional explanatory variable and compared the two model performance using AIC scores:

$$\log_{10}\text{Oxygen consumption} \sim \log_{10}\text{temperature} + \log_{10}\text{mass} + \log_{10}\text{oxygen consumption at year 0} + (1|\text{sex}) + (1|\text{year}) \quad (5)$$

The model with FMR in the first year of life included as a fixed effect performed better (AIC −5,505 compared to −4,260). We estimated the goodness of fit drawing on marginal and conditional R^2 values (Nakagawa and Schielzeth, 2013), as implemented in the MuMIn package (Bartoń, 2023). The full model explained approximately 20% of the total among-individual variance in FMR, with fixed effects accounting for 11% of the total variance. By contrast, the model without FMR in the first year of life explained 12% of the total variation in among individual FMR, and fixed effects accounted for only 4% of variance. A summary of model outputs is provided in **Tables 4**, **5**. We further explored the relationship between FMR at year 0 and FMR at year 4 by comparing residuals from the relationships between FMR and temperature (age 0) and body mass (Age 3–6). Residuals were positively correlated, and variation in temperature-corrected FMR at age 0 explained c. 20% of the expressed variation in among mass-corrected FMR at age 3–6 (**Figure 3**).

To visualize the relationship between the fixed effects and oxygen consumption rates at capture, we used the best fitting model to predict oxygen consumption rates as a function of fixed and random parameters (**Figure 4**). At the point of sampling (median age 4), temperature has a non-significant influence on inferred FMR, body mass has a positive influence, but FMR in the first year of life has the strongest positive covariance with among-individual variation in FMR in later life stages. The relationship between temperature and oxygen consumption rate also varies between the two time points of sampling (for the same individual fish), temperature having a stronger positive influence on FMR in early life stages (**Figure 5**).

4. Discussion

We used a new indirect respirometry approach to retrospectively infer field metabolic rates from the otoliths of wild living plaice, and explored the thermal sensitivity of FMR across life stages between and within individuals. The experienced temperatures and FMR estimates from otolith stable isotope compositions are comparable to those expected for plaice in the North Sea based on archival tag data and laboratory respirometry, adding confidence to a growing literature deriving ecophysiological information about wild ranging fishes based on the stable isotope composition of incrementally-grown otolith aragonite (Jamieson et al., 2004; Shephard et al., 2007; Sinnatamby et al., 2015; Alewijnse et al., 2021; Chung et al., 2021; Smoliński et al., 2021; Sakamoto et al., 2022).

In our dataset of 281 wild roaming adult plaice, C_{resp} values varied by 2–5× among individuals. Individual body mass varied between approximately 200 and 800 g, and experienced temperatures varied over 12 degrees. Body size and temperature contributed to the regression models best describing variance in inferred FMR, but the associated coefficients are small compared to those expected based on allometric scaling or metabolic theory, and compared to co-variances between body mass and FMR seen in other studies employing otolith $\delta^{13}C$ values (Shephard et al., 2007; Trueman et al., 2016; Chung et al., 2019a,b; Alewijnse, 2022). Uncertainties around $\delta^{13}C$ values of carbon sources likely account for some of the unexplained variance in inferred FMR values, but we suggest that energy consuming processes independent of body size and temperature also contribute strongly to variation in individual-level FMR in wild ranging adult plaice in the North Sea. Plaice are known to make use of environmental transport (selective tidal stream transport) which may reduce energy costs associated with directed movement (Metcalfe et al., 1990, 2006). Variations in the degree to which activity costs are reduced via tidal stream transport may contribute greatly to the high among-individual variation, and relatively low absolute FMR values recorded in plaice. Seasonal variations in energy allocation may influence observed relationships between body mass, temperature and FMR. Additionally, among-individual variations in feeding intensity (including specific dynamic action), and reproductive investment likely elicit large variations in energy expenditure, and for fishes operating within their aerobic scope, body size and temperature may be poor predictors for daily energy expenditure (Neubauer and Andersen, 2019).

In the first year of life, experienced temperature positively co-varied with FMR. Age 0 fish are under strong selective pressure to partition all available energy into somatic growth, potentially with fewer behavioral energetic trade-offs. Consequently external temperature is likely to be a more reliable predictor of fish performance in early life stages, provided fish are operating within their aerobic scope. Distributions of plaice in the North Sea have changed significantly over the 90 year period for which fishery catch and effort data are available, with a marked shift toward more northerly and deeper (i.e., cooler) waters (Dulvy et al., 2008; Engelhard et al., 2011) with distribution shifts more closely correlated with climate drivers than with fishery effects. In 1989, in an attempt to rebuild falling plaice populations, the main distribution area for undersized plaice in the North Sea was closed to large fishing vessels (a region along the continental coast of the south eastern North Sea termed the "Plaice Box"). However, in the intervening time, the distribution of small plaice changed, leading to inferences that previous coastal nursery areas have become unsuitable for juvenile plaice (van Keeken et al., 2007). Our results imply a greater thermal sensitivity for metabolic rate in plaice in the first year of life, compared to later life stages, potentially supporting suggestions that conditions in the first year of life are particularly important for the distribution of juvenile plaice and subsequent recruitment rates.

4.1. Phenotypic effects (metabolic phenotypes)

Individual variation has been used to measure population stability in previous studies, as a high degree of phenotypic

TABLE 3 Summary statistics for estimated experienced temperatures, C_{resp} values and inferred oxygen consumption rates for plaice otoliths sampled to reflect conditions at the point of capture and in the first year of life.

	Temperature (°C)	Temperature first year (°C)	C_{resp} value	C_{resp} value first year	O_2 consumption rate ($mgO_2Kg^{-1}hr^{-1}$)	O_2 consumption rate first year ($mgO_2Kg^{-1}hr^{-1}$)
Mean	8	14	0.94	0.11	54	79
Std. dev.	2.8	3.2	0.03	0.04	36	39
Max.	17	26	0.24	0.25	203	215
Min.	0.2	5.8	0	0	−76	−46
95% CI	2.4	2.4	0.06	0.06	58	58
n	281	95	281	95	281	95

95% confidence intervals represent the Monte-Carlo estimated combined uncertainty on individual values estimated from uncertainty in equation parameters as detailed in Table 2.

TABLE 4 Model fits for linear mixed effects model. Marginal (combined) and conditional (fixed) R^2 values (Nakagawa and Schielzeth, 2013) were determined using the MuMIn package (Bartoń, 2023).

Model	AIC	R^2 fixed effects	R^2 combined model
$\log_{10}$ oxygen consumption~ $\log_{10}$ temperature + $\log_{10}$ mass + (1|sex) + (1 year)	−4,258	0.04	0.12
$\log_{10}$ Oxygen consumption~ $\log_{10}$ temperature + $\log_{10}$ mass + $\log_{10}$ oxygen consumption at year 0 + (1|sex) + (1 year)	−5,461	0.11	0.19
$\log_{10}$ oxygen consumption at year 0~ $\log_{10}$ temperature at year 0 + (1|sex) + (1 year)	–	0.05	0.21

TABLE 5 Parameter terms from the best fitting mixed effects model (Equation 5), Parameter effects visualized in Figure 3.

Variable	Coefficient	Std. error	P-value	Effect type	Random effect
Intercept	1.91	0.03	< 0.001	Fixed	
Log_{10} Temperature	0.00	0.002	0.03	Fixed	
Log_{10} Body mass	0.04	0.002	< 0.001	Fixed	
Log_{10} Oxygen consumption in year 1	0.05	0.002	< 0.001	Fixed	
	0.05			Random	Year
	0.01			Random	Sex
	0.18			Random	Residual

variation increases the population's capacity to absorb environmental instability (Nussey et al., 2007; Rutterford et al., 2015). Drawing on the otoliths incremental growth, we explored the potential for phenotypic effects at the population level by assessing the extent to which among-individual variation in FMR expression at year 4 was related to variation in FMR in the first year of life for the same individuals. We also tested for an individual level effects (the relationship between temperature-corrected FMR at age 0 and mass corrected FMR at age 3–6). In our sub-sample of 95 fish for which we obtained estimates of FMR in the first year of life and at capture, FMR in the first year of life explained more of the variation in adult FMR than either body size or temperature, accounting for c.20% of the variation in mass-corrected FMR at age 3–6. These data imply a major role for individual phenotypic variability in energy use in wild plaice. However, individual energy use did not covary with body size, so we did not see a clear lifetime growth advantage related to relatively high sustained individual-level FMR.

Ontogenetically-persistent among-individual variation in metabolic rate could arise through genetic differences, or could reflect canalization of energy metabolism traits based on conditions experienced in early life stages. Previous studies have demonstrated the existence of metabolic phenotypes through controlled selective breeding under laboratory conditions, where individuals of elevated or suppressed energetic demand are selected to reproduce (Metcalfe et al., 2016; Jutfelt, 2020; Wootton et al., 2021); here we infer similar persistent phenotypic metabolic traits expressed within wild populations. Diversity in metabolic phenotypic expression could be a measure of the resilience of the population to environmental instability. Populations where individual level energetic demand is closely centered around the population level mean are thought to be more vulnerable to extrinsic variability. With increased individual level deviance there is a greater chance that a section of a population will survive and be better suited to environmental re-structuring, therefore the population is more stable. Our sampled population lies toward the warm edge of the range of plaice. We were not able to assess whether sub-groups of plaice (or plaice at cold or mid- range edges) express a similar degree of phenotypic variation in energy use.

4.2. Applicability of these findings

External temperature, either directly through its effect on enzyme efficiency or indirectly via effects on resource supply/demand ratios appears to play a critical role in

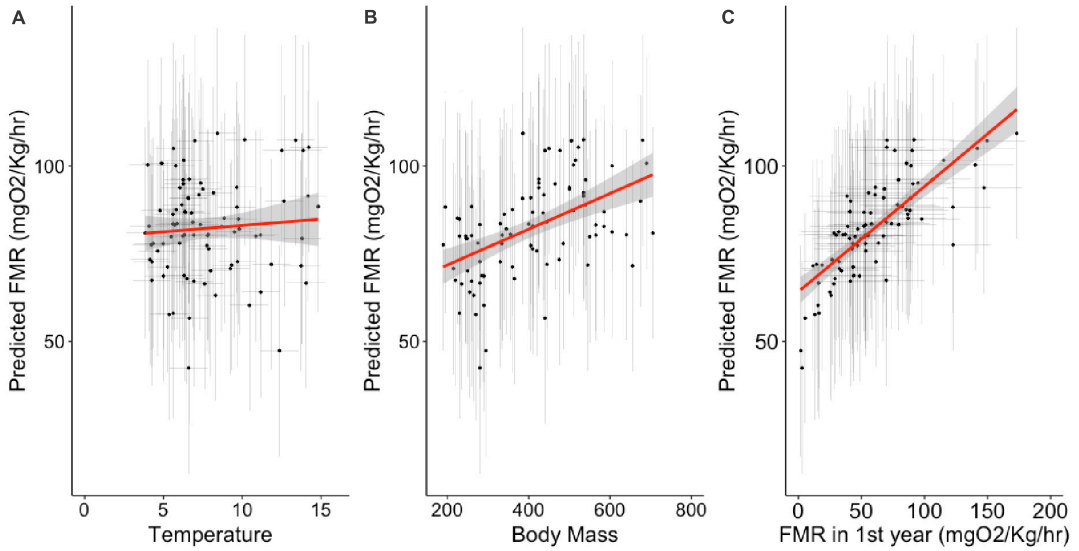

FIGURE 3
Relationship between fixed effects of temperature **(A)**, body mass **(B)**, and FMR during the first year of life **(C)** and oxygen consumption rates in the best fitting mixed effects model (Equation 5); model fit is described in **Table 4** and best fitting parameters given in **Table 5**. Error bars represent 95% confidence intervals around individual estimates calculated from Monte Carlo resampling.

defining limits of species persistence (Deutsch et al., 2015). Consequently laboratory derived measures of physiologically limiting temperatures may be effective at constraining species ranges in current and future conditions. However, within an organism's optimal thermal range, the relationship between external temperature and physiological performance is much less clear. In laboratory conditions, physiological performance typically describes a thermal performance curve displaying an optimum temperature at which either physiological performance or aerobic scope is maximized. Such optimal temperatures (or preferred temperatures slightly below optimal temperatures) have been suggested as predictors for species' core ranges (Pörtner, 2021). However, the thermal sensitivity of physiological performance in the laboratory does not fully describe the range of behavioral and ecological responses to changes in temperature (and associated physiological trade-offs) observed in natural conditions. Critically the thermal sensitivity of physiological performance in wild conditions may differ markedly from laboratory observation due to either buffering or exaggerating local environmental and ecological contexts. It has been suggested that field physiological data is needed to improve our understanding of realized responses of populations to climate change, hence the need to measure metabolic responses in wild populations (Jager and Zimmer, 2012; Nisbet et al., 2012). Further, as populations respond to change over multi-generational time scales, the role of phenotypic diversity in modulating population sensitivity to external environmental drivers is important to quantify (Violle et al., 2012; Metcalfe et al., 2016; Jutfelt, 2020).

4.3. Limitations

Drawing ecophysiological inferences from biochemical proxy data in field-derived samples has obvious value in terms of recording the external temperature experienced by individual fish, and the individual-level metabolic response. But natural sampling creates a number of limitations. Firstly, to reconstruct experienced temperature, we are forced to make assumptions about the isotopic composition of the external water. In full salinity marine conditions, estimates of $\delta^{18}O_w$ values can be drawn relatively robustly from existing data. However, in coastal areas or restricted basins with fluctuating river water input, confidence in assumed $\delta^{18}O_w$ values, and associated experienced temperatures is reduced. In the current study we limited our analyses to plaice assumed to restrict movements within regions of the North Sea with relatively stable $\delta^{18}O_w$ values, at least over the time integration window. However, for retrospective analyses of juveniles, we have no direct knowledge of the location of individuals, which may inhabit lower salinity coastal waters, and consequently estimates of experienced temperature are more uncertain. Nonetheless, our inferred temperatures lie within the temperatures expected to be experienced by plaice within the North Sea.

Estimates of FMR based on otolith $\delta^{13}C$ values are subject to similar assumptions around the isotopic compositions of carbon sources (diet and DIC) and the calibration between the proportion of respiratory carbon in the otolith and oxygen consumption rates. The overall proportion of metabolic (diet) carbon in otolith aragonite is typically between 10 and 30% except for high metabolic fish such as tuna (Kalish, 1991; Sherwood and Rose, 2003; Chung et al., 2019a; Alewijnse, 2022), so estimates of C_{resp} values are relatively insensitive to variations in diet $\delta^{13}C$ values. As no soft tissues for the individuals sampled from otolith archives were available, we drew on compilations of $\delta^{13}C$ values for plaice sampled from the North Sea to estimate likely diet $\delta^{13}C$ values. Plaice otolith $\delta^{13}C$ values varied between 0.5 and −2.9‰. Applying the medians of estimated likely ranges of $\delta^{13}C$ values for DIC and diet to mixing models, c.4% of otolith carbon derives from diet. Therefore variations in diet $\delta^{13}C$ values have relatively

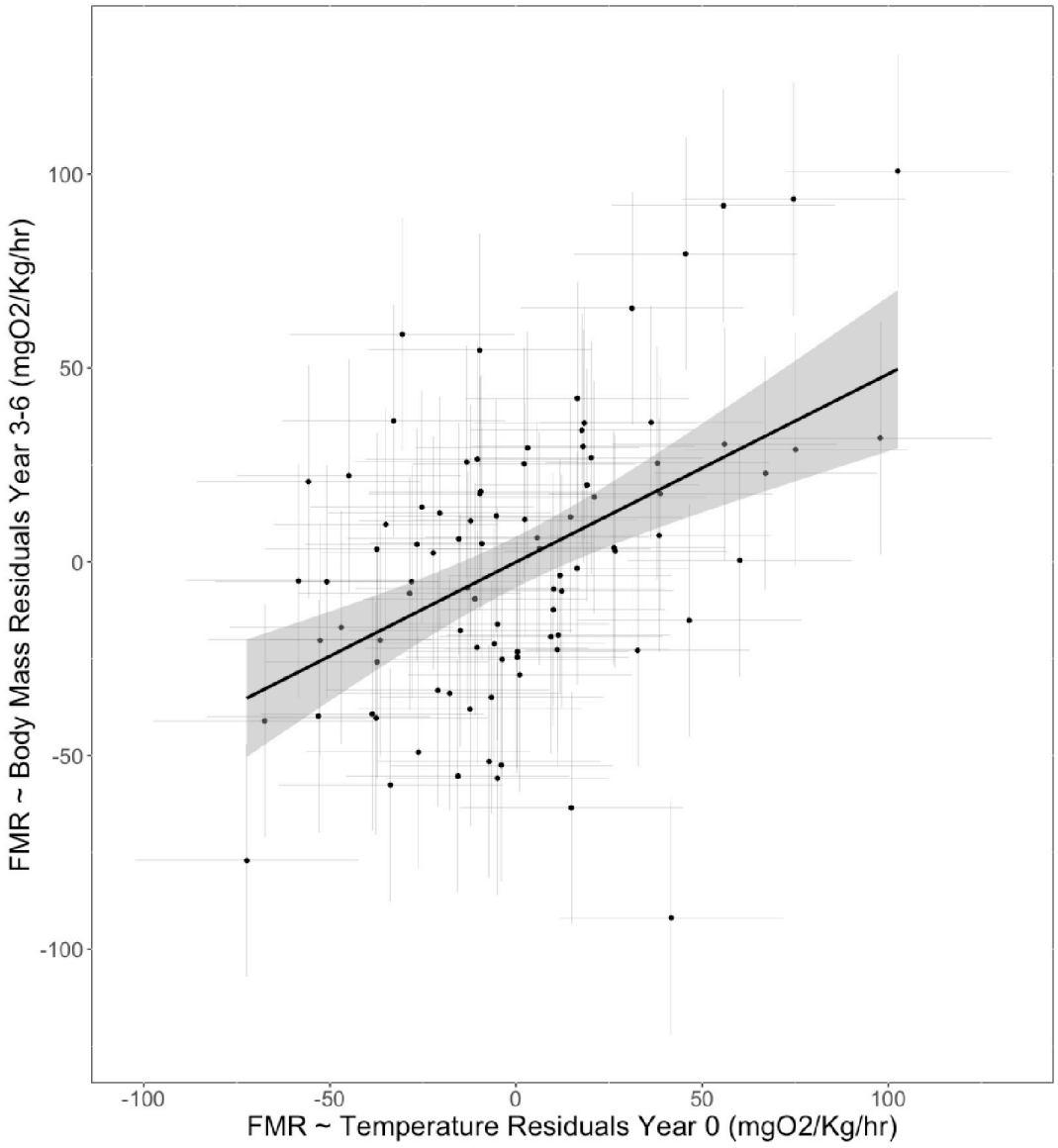

FIGURE 4
Relationship between residuals of linear mixed effects models between otolith-inferred FMR and experienced temperature for otolith aragonite grown during the first year of life and FMR and body mass for otolith aragonite formed immediately prior to sampling (3–6 year of life).

minor effects – for instance, holding DIC and otolith $\delta^{13}C$ values constant and varying potential $\delta^{13}C$ diet values across the whole 5‰ range reported in Jennings and Cogan (2015) results in a range in C_{resp} values of 0.02, which is considerably lower than the 95% confidence range we apply to each individual inferred C_{resp} value. Inferred C_{resp} values are much more sensitive to variations in $\delta^{13}C$ values of DIC, and we drew on a single dataset of spatially averaged $\delta^{13}C$ values of DIC (Burt et al., 2016). It is likely that we did not capture true variations in $\delta^{13}C_{DIC}$ values, as we were unable to directly recover potentially large local scale spatial and seasonal variability in $\delta^{13}C_{DIC}$ values, which probably accounts for some of the unexplained variation in inferred FMR values. We attempted to quantify the effect of uncertainty in water $\delta^{18}O$ and carbon source $\delta^{13}C$ values with a Monte Carlo resampling approach. Undoubtedly, having matched measurements of the isotopic composition of carbon sources and their spatial and temporal variability will reduce uncertainty in estimates of metabolic rates derived from carbonate biominerals and allow identification of more subtle ecological or environmental drivers of variation. However, such matched values are unlikely to be available for historic, archived otolith samples.

The calibration between C_{resp} values and oxygen consumption rates is based on cod. As long as this calibration is statistical rather than mechanistic there is a valid criticism that species-specific calibration terms could apply – i.e., that different species maintain different proportions of respiratory carbon in blood for a given rate of oxygen consumption. Species-specific variations in optimum blood carbonate concentrations could potentially contribute to relatively low estimates of apparent oxygen consumption rates in plaice. However, we feel it is unlikely that the slope of the calibration term will vary systematically across species given the stoichiometric relationship between oxygen consumption and carbon production

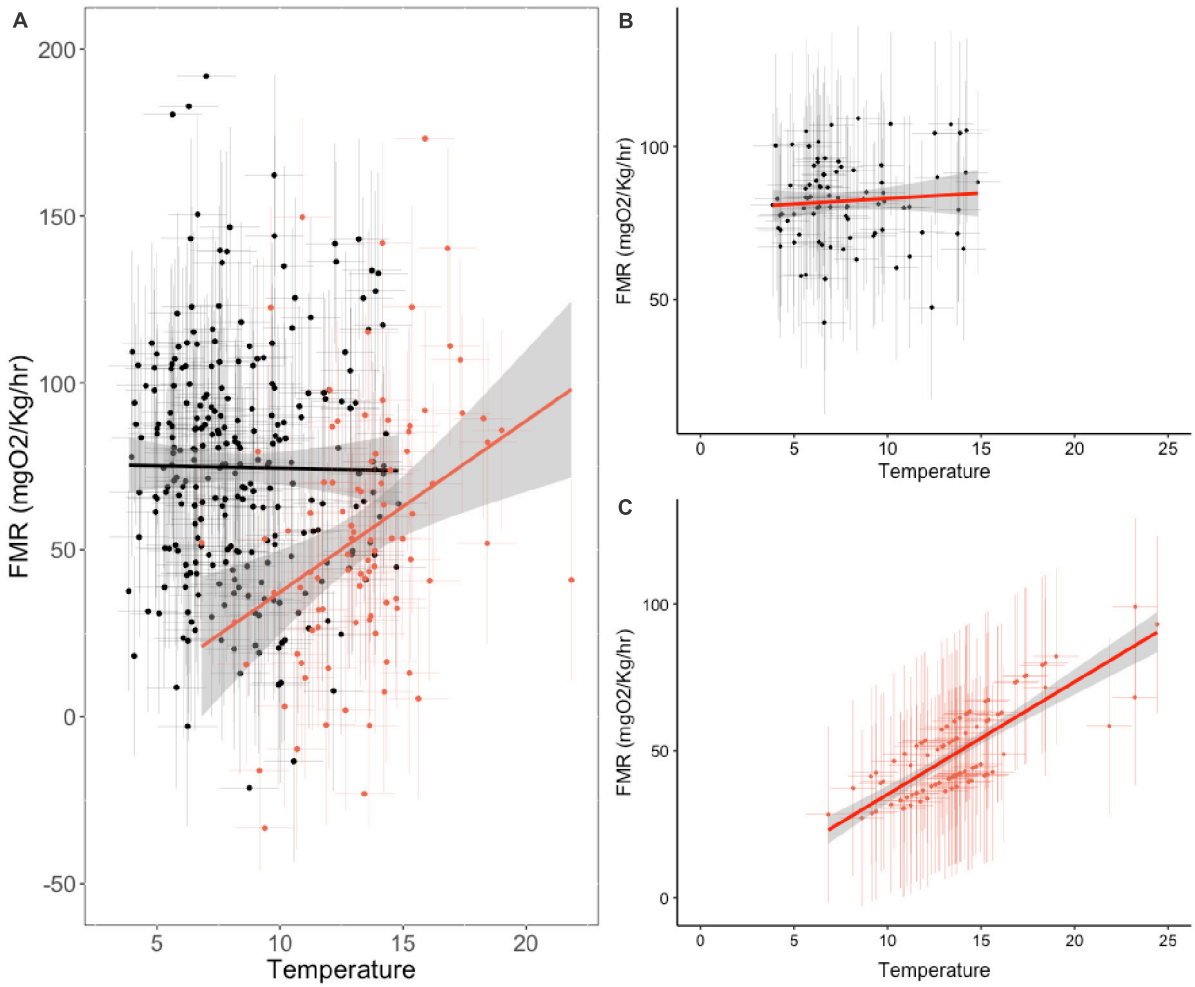

FIGURE 5
Thermal sensitivity of field metabolic rate across life stages of wild living plaice. **(A)** Isotope-inferred temperature and oxygen consumption rates at capture (year 3–6, black) and in the first year of life (red). **(B,C)** Partial effects of temperature on oxygen consumption rates as predicted from best fitting linear mixed effects models (i.e., accounting for random effects of sex and year of sampling, and fixed effect of mass at capture) at age 3–6 **(B)** and in the first summer of life **(C)**. Error bars represent 95% confidence intervals on individual estimates calculated from Monte Carlo resampling.

through respiration. Increasing oxygen consumption rates (and therefore increasing production of respiratory CO_2) must increase the proportion of respiratory carbon in blood–as long as blood carbonate concentrations are physiologically regulated. Most marine teleost fishes regulate chronic blood bicarbonate levels to common levels to maintain pH balance. Therefore we expect a relatively common relationship between C_{resp} values and oxygen consumption rates and we do not expect this relationship to be strongly or systematically influenced by body mass age.

While acknowledging the limitations stated above, the stable isotope composition of carbonate biominerals, and fish otoliths in particular, offer unique insights into individual-level temperature preference and energy use in free-ranging, wild fishes. Natural tags have the advantage that large numbers of individuals can be analyzed, recording among-individual variation. Furthermore, the relative ease of sampling and individual-level of analysis can provide insights specific to the local ecological context and draw on a specific population adapted over multiple generations to the fluctuating environmental conditions experienced– these aspects of ecophysiology are difficult to account for in laboratory contexts. Finally, the incremental nature of many carbonate biominerals also allows recovery of metabolic information over the lifespan of the individual (while recognizing that uncertainty regarding reference isotopic compositions of carbon and oxygen sources increases with increasing time intervals between capture and growth of the sampled portion of the biomineral).

Consequently, otolith stable isotope analyses compliment ecophysiological information obtained from laboratory experimentation, telemetry and tagging. Together, these approaches can refine estimates of population responses to climate change at spatial scales relevant to fisheries and ecosystem managers.

Data availability statement

The original contributions presented in this study are included in the article/Supplementary material, further inquiries can be directed to the corresponding authors.

Ethics statement

The animal study was reviewed and approved by the University of Southampton Research Ethics.

Author contributions

CT, EH, and JJ conceived and designed the project and drafted the manuscript, with contributions from MW and BH. JJ, MW, and BH conducted the analyses. JJ and CT analyzed the data. All authors contributed to the article and approved the submitted version.

Funding

This work was funded from NERC Case award NE/P009700/1.

Acknowledgments

We would like to thank all skippers, crew and scientists involved in the ICES IBTS survey, and all CEFAS staff involved in collection, processing and curation of historic otolith samples and associated metadata.

Conflict of interest

The authors declare that the research was conducted in the absence of any commercial or financial relationships that could be construed as a potential conflict of interest.

Publisher's note

Supplementary material

The Supplementary Material for this article can be found online at: https://www.frontiersin.org/articles/10.3389/fevo.2023.1161105/full#supplementary-material

References

Albouy, C., Guilhaumon, F., Leprieur, F., Lasram, F. B. R., Somot, S., Aznar, R., et al. (2013). Projected climate change and the changing biogeography of coastal Mediterranean fishes. *J. Biogeogr.* 40, 534–547. doi: 10.1111/jbi.12013

Alewijnse, S. R. (2022). *Macroecological study of otolith-derived field metabolic rates of marine fishes. Ph.D.* Southampton: University of Southampton.

Alewijnse, S. R., Stowasser, G., Saunders, R., Belcher, A., Crimmen, O., Cooper, N., et al. (2021). Otolith-derived field metabolic rates of myctophids (Family Myctophidae) from the Scotia Sea (Southern Ocean). *Mar. Ecol. Progr. Ser.* 675, 113–131. doi: 10.3354/meps13827

Andersen, K. H. (2018). *Fish ecology, evolution, and exploitation*. Princeton, NJ: Princeton University Press.

Bartoń, K. (2023). *_MuMIn: Multi-Model Inference*. R package version 1.47.5. Available online at: https://CRAN.R-project.org/package=MuMIn

Blowes, S., Supp, S., Antão, L., Bates, A., Bruelheide, H., Chase, J., et al. (2019). The geography of biodiversity change in marine and terrestrial assemblages. *Science* 366, 339–345. doi: 10.1126/science.aaw1620

Burt, W. J., Thomas, H., Hagens, M., Pätsch, J., Clargo, N. M., Salt, L. A., et al. (2016). Carbon sources in the North Sea evaluated by means of radium and stable carbon isotope tracers. *Limnol. Oceanogr.* 61, 666–683. doi: 10.1002/lno.10243

Campana, S. E., and Thorrold, S. R. (2001). Otoliths, increments, and elements: Keys to a comprehensive understanding of fish populations? *Can. J. Fish. Aquat. Sci.* 58, 30–38. doi: 10.1139/f00-177

Cheung, W. W. L., Sarmiento, J. L., Dunne, J., Frölicher, T. L., Lam, V. W. Y., Palomares, M. L. D., et al. (2013). Shrinking of fishes exacerbates impacts of global ocean changes on marine ecosystems. *Nat. Clim. Change* 3, 254–258. doi: 10.1038/nclimate1691

Chung, M.-T., Jørgensen, K.-E. M., Trueman, C. N., Knutsen, H., Jorde, P. E., and Grønkjær, P. (2021). First measurements of field metabolic rate in wild juvenile fishes show strong thermal sensitivity but variations between sympatric ecotypes. *Oikos* 130, 287–299. doi: 10.1111/oik.07647

Chung, M.-T., Trueman, C., Godiksen, J., Holmstrup, M., and Grønkjær, P. (2019a). Field metabolic rates of teleost fishes are recorded in otolith carbonate. *Commun. Biol.* 2:24. doi: 10.1038/s42003-018-0266-5

Chung, M.-T., Trueman, C. N., Godiksen, J. A., and Grønkjær, P. (2019b). Otolith δ13C values as a metabolic proxy: Approaches and mechanical underpinnings. *Mar. Freshw. Res.* 70:1747. doi: 10.1071/mf18317

Dahlke, F., Wohlrab, S., Butzin, M., and Pörtner, H. (2020). Thermal bottlenecks in the life cycle define climate vulnerability of fish. *Science* 369, 65–70. doi: 10.1126/science.aaz3658

Darnaude, A., Sturrock, A., Trueman, C., Mouillot, D., Eimf, Campana, E., et al. (2014). Listening in on the past: What can ctolith δ18O values really tell us about the environmental history of fishes? *PLoS One* 9:e108539. doi: 10.1371/journal.pone.0108539

Deutsch, C., Ferrel, A., Seibel, B., Pörtner, H., and Huey, R. (2015). Climate change tightens a metabolic constraint on marine habitats. *Science* 348, 1132–1135. doi: 10.1126/science.aaa1605

Deutsch, C., Penn, J. L., and Seibel, B. (2020). Metabolic trait diversity shapes marine biogeography. *Nature* 585, 557–562. doi: 10.1038/s41586-020-2721-y

Deutsch, C., Penn, J., Verberk, W. E., Inomura, K., Endress, M., and Payne, J. (2022). Impact of warming on aquatic body sizes explained by metabolic scaling from microbes to macrofauna. *Proc. Nat. Acad. Sci. U.S.A.* 119:e2201345119. doi: 10.1073/pnas.2201345119

Dulvy, N. K., Rogers, S. I, Jennings, S., Stelzenmüller, V., Dye, S. R., and Skjoldal, H. R. (2008). Climate change and deepening of the North Sea fish assemblage: A biotic indicator of warming seas. *J. Appl. Ecol.* 45, 1029–1039. doi: 10.1111/j.1365-2664.2008.01488.x

Duncan, M. I., James, N. C., Potts, W. M., and Bates, A. E. (2020). Different drivers, common mechanism; the distribution of a reef fish is restricted by local-scale oxygen and temperature constraints on aerobic metabolism. *Conserv. Physiol.* 8:coaa090. doi: 10.1093/conphys/coaa090

Engelhard, G. H., Pinnegar, J. K., Kell, L. T., and Rijnsdorp, A. D. (2011). Nine decades of North Sea sole and plaice distribution. *ICES J. Mar. Sci.* 68, 1090–1104. doi: 10.1093/icesjms/fsr031

Ern, R. (2019). A mechanistic oxygen- and temperature-limited metabolic niche framework. *Philos. Trans. R. Soc. Lond. B Biol. Sci.* 374:20180540. doi: 10.1098/rstb.2018.0540

Gauldie, R. W. (1996). Biological factors controlling the carbon isotope record in fish otoliths: Principles and evidence. *Comp. Biochem. Physiol. B* 115, 201–208. doi: 10.1016/0305-0491(96)00077-6

Geffen, A. J. (2012). Otolith oxygen and carbon stable isotopes in wild and laboratory-reared plaice (*Pleuronectes platessa*). *Environ. Biol. Fishes* 95, 419–430. doi: 10.1007/s10641-012-0033-2

Halsey, L. G., Killen, S. S., Clark, T. D., and Norin, T. (2018). Exploring key issues of aerobic scope interpretation in ectotherms: Absolute versus factorial. *Rev. Fish Biol. Fish.* 28, 405–415. doi: 10.1007/s11160-018-9516-3

Healy, T. M., and Schulte, P. M. (2012). Thermal acclimation is not necessary to maintain a wide thermal breadth of aerobic scope in the common killifish (*Fundulus heteroclitus*). *Physiol. Biochem. Zool.* 85, 107–119. doi: 10.1086/664584

Hofmann, G. E., and Todgham, A. E. (2010). Living in the now: Physiological mechanisms to tolerate a rapidly changing environment. *Annu. Rev. Physiol.* 72, 127–145. doi: 10.1146/annurev-physiol-021909-135900

Holt, R. E., and Jørgensen, C. (2015). Climate change in fish: Effects of respiratory constraints on optimal life history and behaviour. *Biol. Lett.* 11:20141032. doi: 10.1098/rsbl.2014.1032

Jager, T., and Zimmer, E. I. (2012). Simplified Dynamic Energy Budget model for analysing ecotoxicity data. *Ecol. Model.* 225, 74–81. doi: 10.1016/j.ecolmodel.2011.11.012

Jamieson, R. E., Schwarcz, H. P., and Brattey, J. (2004). Carbon isotopic records from the otoliths of Atlantic cod (*Gadus morhua*) from eastern Newfoundland, Canada. *Fish. Res.* 68, 83–97. doi: 10.1016/j.fishres.2004.02.009

Jennings, S., and Cogan, S. M. (2015). Nitrogen and carbon stable isotope variation in northeast Atlantic fishes and squids. *Ecology* 96, 2568–2568. doi: 10.1890/15-0299.1

Jutfelt, F. (2020). Metabolic adaptation to warm water in fish. *Funct. Ecol.* 34, 1138–1141. doi: 10.1111/1365-2435.13558

Kalish, J. M. (1991). 13 C and 18 O isotopic disequilibria in fish otoliths: Metabolic and kinetic effects. *Mar. Ecol. Progr. Ser.* 75, 191–203.

Killen, S., Glazier, D., Rezende, E., Clark, T., Atkinson, D., Willener, A. T., et al. (2016). Ecological influences and morphological correlates of resting and maximal metabolic rates across teleost fish species. *Am. Nat.* 187, 592–606. doi: 10.1086/685893

Lamine, E., Schickele, A., Guidetti, P., Allemand, D., Hilmi, N., and Raybaud, V. (2010). Large-scale redistribution of maximum fisheries catch potential in the global ocean under climate change. *Global Change Biol.* 16, 24–35. doi: 10.1111/j.1365-2486.2009.01995.x

LeGrande, A. N., and Schmidt, G. A. (2006). Global gridded data set of the oxygen isotopic composition in seawater. *Geophys. Res. Lett.* 33:L12604. doi: 10.1029/2006gl026011

Lindmark, M., Audzijonyte, A., Blanchard, J. L., and Gårdmark, A. (2022). Temperature impacts on fish physiology and resource abundance lead to faster growth but smaller fish sizes and yields under warming. *Global Change Biol.* 28, 6239–6253. doi: 10.1111/gcb.16341

Little, A. G., Loughland, I., and Seebacher, F. (2020). What do warming waters mean for fish physiology and fisheries? *J. Fish Biol.* 97, 328–340. doi: 10.1111/jfb.14402

MacKenzie, K., Palmer, M., Moore, A., Ibbotson, A., Beaumont, W. C., Poulter, D. S., et al. (2011). Locations of marine animals revealed by carbon isotopes. *Sci. Rep.* 1:21. doi: 10.1038/srep00021

Martino, J. C., Doubleday, Z., Chung, M., and Gillanders, B. (2020). Experimental support towards a metabolic proxy in fish using otolith carbon isotopes. *J. Exp. Biol.* 223:jeb217091. doi: 10.1242/jeb.217091

McConnaughey, T. A., Burdett, J., Whelan, J. F., and Paull, C. K. (1997). Carbon isotopes in biological carbonates: Respiration and photosynthesis. *Geochim. Cosmochim. Acta.* 61, 611–622.

McKenzie, D. J., Geffroy, B., and Farrell, A. P. (2021). Effects of global warming on fishes and fisheries. *J. Fish Biol.* 98, 1489–1492. doi: 10.1111/jfb.14762

Metcalfe, J. D., Arnold, G. P., and Webb, P. W. (1990). The energetics of migration by selective tidal stream transport: An analysis for plaice tracked in the southern North Sea. *J. Mar. Biol. Assoc. U.K.* 70, 149–162. doi: 10.1017/S0025315400034275

Metcalfe, J. D., Hunter, E., and Buckley, A. A. (2006). The migratory behaviour of North Sea plaice: Currents, clocks and clues. *Mar. Freshw. Behav. Physiol.* 39, 25–36. doi: 10.1080/10236240600563404

Metcalfe, N. B., Van Leeuwen, T. E., and Killen, S. S. (2016). Does individual variation in metabolic phenotype predict fish behaviour and performance? *J. Fish Biol.* 88, 298–321. doi: 10.1111/jfb.12699

Mieszkowska, N., Genner, M., Hawkins, S., and Sims, D. (2009). Chapter 3. Effects of climate change and commercial fishing on atlantic cod *Gadus morhua*. *Adv. Mar. Biol.* 56, 213–273. doi: 10.1016/S0065-2881(09)56003-8

Murawski, S. A. (1993). Climate change and marine fish distributions: Forecasting from historical analogy. *Trans. Am. Fish. Soc.* 122, 647–658.

Nakagawa, S., and Schielzeth, H. (2013). A general and simple method for obtaining R2 from generalized linear mixed-effects models. *Meth. Ecol. Evol.* 4, 133–142. doi: 10.1111/j.2041-210x.2012.00261.x

Nelson, J., Hanson, C., Koenig, C., and Chanton, J. (2011). Influence of diet on stable carbon isotope composition in otoliths of juvenile red drum *Sciaenops ocellatus*. *Aquat. Biol.* 13, 89–95. doi: 10.3354/ab00354

Neubauer, P., and Andersen, K. H. (2019). Thermal performance of fish is explained by an interplay between physiology, behaviour and ecology. *Cons. Physiol.* 7:coz025. doi: 10.1093/conphys/coz025

Nisbet, R., Jusup, M., Klanjscek, T., and Pecquerie, L. (2012). Integrating dynamic energy budget (DEB) theory with traditional bioenergetic models. *J. Exp. Biol.* 215, 892–902. doi: 10.1242/jeb.059675

Norin, T., Malte, H., and Clark, T. D. (2014). Aerobic scope does not predict the performance of a tropical eurythermal fish at elevated temperatures. *J. Exp. Biol.* 217, 244–251. doi: 10.1242/jeb.089755

Núñez-Riboni, I., and Akimova, A. (2015). Monthly maps of optimally interpolated in situ hydrography in the North Sea from 1948 to 2013. *J. Mar. Sys.* 151, 15–34. doi: 10.1016/j.jmarsys.2015.06.003

Nussey, D. H., Wilson, A. J., and Brommer, J. E. (2007). The evolutionary ecology of individual phenotypic plasticity in wild populations. *J. Evol. Biol.* 20, 831–844. doi: 10.1111/j.1420-9101.2007.01300.x

Pauly, D. (2021). The gill-oxygen limitation theory (GOLT) and its critics. *Sci. Adv.* 7:eabc6050. doi: 10.1126/sciadv.abc6050

Payne, N. L., Smith, J., van der Meulen, D., Taylor, M., Watanabe, Y., Takahashi, A., et al. (2016). Temperature dependence of fish performance in the wild: Links with species biogeography and physiological thermal tolerance. *Funct. Ecol.* 30, 903–912. doi: 10.1111/1365-2435.12618

Perry, C., Salter, M., Harborne, A., Crowley, S. F., Jelks, H., and Wilson, R. (2011). Fish as major carbonate mud producers and missing components of the tropical carbonate factory. *Proc. Natl. Acad. Sci. U.S.A.* 108, 3865–3869. doi: 10.1073/pnas.1015895108

Petrik, C., Stock, C., Andersen, K., van Denderen, P., and Watson, J. (2020). Large pelagic fish are most sensitive to climate change despite pelagification of ocean food webs. *Front. Mar. Sci.* 7:588482. doi: 10.3389/fmars.2020.588482

Pontzer, H., Yamada, Y., Sagayama, H., Ainslie, P., Andersen, L., Anderson, L., et al. (2021). Daily energy expenditure through the human life course. *Science* 373, 808–812.

Pörtner, H. O., Bock, C., and Mark, F. C. (2017). Oxygen- and capacity-limited thermal tolerance: Bridging ecology and physiology. *J. Exp. Biol.* 220, 2685–2696. doi: 10.1242/jeb.134585

Pörtner, H.-O. (2021). Climate impacts on organisms, ecosystems and human societies: Integrating OCLTT into a wider context. *J. Exp. Biol.* 224(Pt Suppl 1):jeb238360. doi: 10.1242/jeb.238360

Rijnsdorp, A. D. (1990). The mechanism of energy allocation over reproduction and somatic growth in female North Sea plaice, *Pleuronectes platessa* L. *Neth. J. Sea Res.* 25, 279–289. doi: 10.1016/0077-7579(90)90027-E

Rooker, J. R., Secor, D., DeMetrio, G., Kaufman, A., Belmonte Ríos, A., and Ticina, V. (2008). Evidence of trans-Atlantic movement and natal homing of bluefin tuna from stable isotopes in otoliths. *Mar. Ecol. Progr. Ser.* 368, 231–239. doi: 10.3354/meps07602

Rutterford, L. A., Genner, M. G., Engelhard, G. H., Simpson, S. D., and Hunter, E. (2023). Fishing impacts on age-structure may conceal environmental drivers of body-size in exploited fish populations. *ICES J. Mar. Sci.* 80, 848–860. doi: 10.1093/icesjms/fsad014

Rutterford, L. A., Simpson, S. D., Jennings, S., Johnson, M. P., Blanchard, J. L., Schön, P. J., et al. (2015). Future fish distributions constrained by depth in warming seas. *Nat. Clim. Change* 5, 569–573. doi: 10.1038/nclimate2607

Sakamoto, T., Takahashi, M., Chung, M., Rykaczewski, R., Komatsu, K., Shirai, K., et al. (2022). Contrasting life-history responses to climate variability in eastern and western North Pacific sardine populations. *Nat. Commun.* 13:5298. doi: 10.1038/s41467-022-33019-z

Schulte, P. M. (2015). The effects of temperature on aerobic metabolism: Towards a mechanistic understanding of the responses of ectotherms to a changing environment. *J. Exp. Biol.* 218, 1856–1866. doi: 10.1242/jeb.118851

Schulte, P. M., Healy, T. M., and Fangue, N. A. (2011). Thermal performance curves, phenotypic plasticity, and the time scales of temperature exposure. *Integr. Comp. Biol.* 51, 691–702. doi: 10.1093/icb/icr097

Schwarcz, H. P., Gao, Y., Browne, D., Knyf, M., and Brand, U. (1998). Stable carbon isotope variations in otoliths of Atlantic cod (*Gadus morhua*). *Can. J. Fish. Aquat. Sci.* 55, 1798–1806. doi: 10.1139/f98-053

Shephard, S., Trueman, C., Rickaby, R., and Rogan, E. (2007). Juvenile life history of NE Atlantic orange roughy from otolith stable isotopes. *Deep Sea Res.* 54, 1221–1230. doi: 10.1016/j.dsr.2007.05.007

Sherwood, G. D., and Rose, G. A. (2003). Influence of swimming form on otolith delta 13C in marine fish. *Mar. Ecol. Progr. Ser.* 258, 283–289.

Sinnatamby, R. N., Brian Dempson, J., Reist, J. D., and Power, M. (2015). Latitudinal variation in growth and otolith-inferred field metabolic rates of Canadian young-of-the-year Arctic charr. *Ecol. Freshw. Fish.* 24, 478–488. doi: 10.1111/eff.12166

Skelly, D. K., Joseph, L., Possingham, H., Freidenburg, L., Farrugia, T., Kinnison, M., et al. (2007). Evolutionary responses to climate change. *Conserv. Biol.* 21, 1353–1355. doi: 10.1111/j.1523-1739.2007.00764.x

Smoliński, S., Denechaud, C., von Leesen, G., Geffen, A., Grønkjær, P., Godiksen, J., et al. (2021). Differences in metabolic rate between two Atlantic cod (*Gadus morhua*) populations estimated with carbon isotopic composition in otoliths. *PLoS One* 16:e0248711. doi: 10.1371/journal.pone.0248711

Solomon, C. T., Weber, P., Cech, J. Jr., LIngram, B., Conrad, M., Machavaram, M., et al. (2006). Experimental determination of the sources of otolith carbon and associated isotopic fractionation. *Can. J. Fish. Aquat. Sci.* 63, 79–89. doi: 10.1139/f05-200

Speakman, J. R. (1998). The history and theory of the doubly labeled water technique. *Am. J. Clin. Nutr.* 68, 932S–938S. doi: 10.1093/ajcn/68.4.932S

Speakman, J. R. (1999). "The cost of living: Field metabolic rates of small mammals," in *Advances in ecological research*, eds A. H. Fitter and D. G. Raffaelli (Cambridge, MA: Academic Press), 177–297. doi: 10.1016/S0065-2504(08)60019-7

Tohse, H., and Mugiya, Y. (2008). Sources of otolith carbonate: Experimental determination of carbon incorporation rates from water and metabolic CO2, and their diel variations. *Aquat. Biol.* 1, 259–268. doi: 10.3354/ab00029

Treberg, J., Killen, S., MacCormack, T., Lamarre, S., and Enders, E. (2016). Estimates of metabolic rate and major constituents of metabolic demand in fishes under field conditions: Methods, proxies, and new perspectives. *Comp. Biochem. Physiol. A Mol. Integr. Physiol.* 202, 10–22. doi: 10.1016/j.cbpa.2016.04.022

Trueman, C. N., Chung, M.-T., and Shores, D. (2016). Ecogeochemistry potential in deep time biodiversity illustrated using a modern deep-water case study. *Philos. Trans. R. Soc. Lond. B Biol. Sci.* 371:20150223. doi: 10.1098/rstb.2015.0223

Trueman, C. N., Rickaby, R. E. M., and Shephard, S. (2013). Thermal, trophic and metabolic life histories of inaccessible fishes revealed from stable-isotope analyses: A case study using orange roughy *Hoplostethus atlanticus*: *Hoplostethus atlanticus* life history. *J. Fish Biol.* 83, 1613–1636. doi: 10.1111/jfb.12267

Urca, T., Levin, E., and Ribak, G. (2021). Insect flight metabolic rate revealed by bolus injection of the stable isotope 13C. *Proc. Biol. Sci.* 288:20211082. doi: 10.1098/rspb.2021.1082

van Keeken, O. A., van Hoppe, M., Grift, R. E., and Rijnsdorp, A. D. (2007). Changes in the spatial distribution of North Sea plaice (*Pleuronectes platessa*) and implications for fisheries management. *J. Sea Res.* 57, 187–197. doi: 10.1016/j.seares.2006.09.002

Vinton, A. C., and Vasseur, D. A. (2022). Resource limitation determines realized thermal performance of consumers in trophodynamic models. *Ecology Letters* 25, 2142–2155. doi: 10.1111/ele.14086

Violle, C., Enquist, B., McGill, B., Jiang, L., Albert, C. H., Hulshof, C., et al. (2012). The return of the variance: Intraspecific variability in community ecology. *Trends Ecol. Evol.* 27, 244–252. doi: 10.1016/j.tree.2011.11.014

Weidman, C. R., and Millner, R. (2000). High-resolution stable isotope records from North Atlantic cod. *Fish. Res.* 46, 327–342. doi: 10.1016/S0165-7836(00)00157-0

Welch, K., Péronnet, F., Hatch, K., Voigt, C. C., and McCue, M. D. (2016). Carbon stable-isotope tracking in breath for comparative studies of fuel use. *Ann. N. Y. Acad. Sci.* 1365, 15–32. doi: 10.1111/nyas.12737

Wootton, H. F., Audzijonyte, A., and Morrongiello, J. (2021). Multigenerational exposure to warming and fishing causes recruitment collapse, but size diversity and periodic cooling can aid recovery. *Proc. Natl. Acad. Sci. U.S.A.* 118:7. doi: 10.1073/pnas.2100300118

frontiers | Frontiers in Ecology and Evolution

TYPE Original Research
PUBLISHED 01 August 2023
DOI 10.3389/fevo.2023.1139441

OPEN ACCESS

EDITED BY
Yixin Zhang,
Soochow University, China

REVIEWED BY
Graeme Clive Hays,
Deakin University, Australia
Kristen Marie Hart,
United States Department of the Interior,
United States

*CORRESPONDENCE
Mathew A. Vanderklift
mat.vanderklift@csiro.au

RECEIVED 07 January 2023
ACCEPTED 12 June 2023
PUBLISHED 01 August 2023

CITATION
Vanderklift MA, Pillans RD, Rochester W, Stubbs JL, Skrzypek G, Tucker AD and Whiting SD (2023) Ontogenetic changes in green turtle (*Chelonia mydas*) diet and home range in a tropical lagoon. *Front. Ecol. Evol.* 11:1139441. doi: 10.3389/fevo.2023.1139441

Ontogenetic changes in green turtle (*Chelonia mydas*) diet and home range in a tropical lagoon

Mathew A. Vanderklift[1]*, Richard D. Pillans[2], Wayne Rochester[2], Jessica L. Stubbs[3], Grzegorz Skrzypek[3], Anton D. Tucker[4] and Scott D. Whiting[4]

[1]CSIRO Environment, Indian Ocean Marine Research Centre, Crawley, WA, Australia, [2]CSIRO Environment, Biosciences Precinct, St. Lucia, QLD, Australia, [3]School of Biological Sciences, The University of Western Australia, Crawley, WA, Australia, [4]Marine Science Program, Department of Biodiversity, Conservation and Attractions, Kensington, WA, Australia

Ontogenetic changes in habitat and diet are widespread among marine species. Most species of sea turtles are characterized by extreme ontogenetic changes in habitat use and diet, with large changes occurring in early developmental stages (e.g., neonates to juveniles). Changes can continue even after recruitment to shallow coastal habitats. In places where substantial transitions in habitat occur across short distances, it is possible that the distances of developmental movements from one habitat to another could be short. We investigated ontogenetic changes in home range size, home range location and diet of *Chelonia mydas* in a tropical coastal lagoon in north-western Australia by combining acoustic telemetry with stable isotope analysis. There was a substantial (but nonlinear) increase in home-range size (kernel utilization distribution: KUD) with length, and an increase in the average distance of the center of home ranges from shore with length: larger turtles tended to occupy larger areas further from the shore. These patterns were accompanied by complex nonlinear changes in δ^{13}C, δ^{15}N and δ^{34}S of red blood cells and nails; changes were rapid from 36 cm (the length of the smallest individual captured) to 50 cm, before reversing more gradually with increasing size. δ^{15}N and δ^{34}S (but not δ^{13}C) of red blood cells and nails increased monotonically with KUD and distance from shore. Seagrass was likely an important food for all sizes, macroalgae was potentially important for small (< 60 cm CCL) individuals, and the proportion of scyphozoan jellyfish in diet increased monotonically with size. The combination of acoustic telemetry and stable isotope analysis revealed ontogenetic shifts in use of space and diet across short distances in a tropical coastal lagoon.

KEYWORDS

stable isotope, home range, mixing model, Ningaloo, seagrass, macroalgae, jellyfish

1 Introduction

Ontogenetic changes in habitat use and diet are widespread among marine species (Snover, 2008). They frequently include changes in habitat type and location, combined with changes in diet. Such changes can be understood in the context of optimizing a trade-off between growth and mortality (Werner and Gilliam, 1984). Effective management (whether for conservation, harvest, or other purposes) of species that change habitat type and location as they grow needs to account for ontogenetic changes in the types and magnitudes of the threats that they face. For example, body size can be an important predictor of the risk of predation (although evidence for this is equivocal: Preisser and Orrock, 2012), and so management might need to accommodate ontogenetic changes in probability of natural and human-induced mortality.

Most species of sea turtles are characterized by extreme ontogenetic changes in habitat and diet (Bolten, 2003). Young individuals of most species occupy oceanic areas far from mainland coasts, moving to shallower coastal habitats as they attain a certain size. The green sea turtle *Chelonia mydas* adheres to this pattern: after hatching, neonates swim immediately offshore and spend years in oceanic habitats, travelling up to thousands of kilometers (Hays and Scott, 2013) before moving to shallow coastal habitats. The size at which this occurs varies among populations (Musick and Limpus, 1996). After they recruit to shallow coastal habitats, juvenile *C. mydas* in some places remain resident until maturity. In other places, there are further movements to different habitats as they mature (Musick and Limpus, 1996). The distances of these movements away from developmental habitat can be large, up to hundreds of kilometers (e.g., Chambault et al., 2018; Doherty et al., 2020). However, in places where substantial transitions in habitat occur across short distances, it is possible that distances of developmental shifts to different habitats could also be short.

Coincident with ontogenetic habitat shifts, *C. mydas* also changes its diet. The diet of juveniles inhabiting oceanic habitats is probably primarily carnivorous (e.g., Reich et al., 2007; Turner Tomaszewicz et al., 2018). Once they have recruited to shallow coastal habitats, they are primarily herbivorous, although there is ample evidence that many individuals are omnivorous (indeed, this might be the norm: Seminoff et al., 2021). Most studies indicate that the switch to herbivory is maintained as they mature into adults, but Arthur et al. (2008) found that δ^{15}N (an indicator of trophic level) of sexually-mature individuals was slightly higher than that of immature individuals.

Diet is fundamental to energetics, which in turn determines growth and reproduction, so changes to diets of individuals could manifest as population-level demographic changes through altering egg production (Stubbs et al., 2020). One of the most widely used tools to understand diet of sea turtles is stable isotope analysis. Investigations of patterns in stable isotope composition with size have yielded trends that suggest changes in diet extend for decades after juveniles recruit to shallow coastal habitats (e.g., Arthur et al., 2008; Burgett et al., 2018; Roche et al., 2021). However, conclusions about changing diets inferred from stable isotopes can be complicated by expectations that stable isotope discrimination between prey and consumer scales with body size (Martínez del Rio et al., 2009; Pecquerie et al., 2010). Evidence for this from controlled diet studies of sea turtles is equivocal (Reich et al., 2008; Vander Zanden et al., 2012).

We investigated ontogenetic changes in the diet of *C. mydas* in a tropical coastal lagoon in north-western Australia. *C. mydas* at this location are long-term residents that show size-related changes in home range size, home range location, and diet (Pillans et al., 2022; Stubbs et al., 2022). Size is a good predictor of age (Mayne et al., 2022), and here we use size as a proxy for age to further explore ontogenetic patterns in the home range location and diet of *C. mydas*.

2 Methods

2.1 Study area and survey methods

The study was conducted in and around Mangrove Bay, in the Ningaloo Marine Park, north-western Australia (21.9 °S, 113.9 °E). Mangrove Bay is a small, shallow (<1.5 m at Highest Astronomical Tide) embayment located shoreward of a lagoon which is bordered on the seaward side by a fringing coral reef. The lagoon is approximately 2–3 km wide, and the reef flat is approximately 250–500 m wide (Cassata and Collins, 2008). The seabed in the lagoon is predominantly sand veneer over rock, interspersed with low-relief rocky surfaces and coral bommies. Seaward of the reef flat, coral extends to ~35 m; beyond this depth, the seabed is predominantly low-relief rock (Turner et al., 2018). Seagrass (*Halophila ovalis* and *Halodule uninervis*) occurs within Mangrove Bay, and *Halophila ovalis* occurs on sandy areas in the lagoon. Multiple species of large brown and red macroalgae occur on rocky surfaces throughout Mangrove Bay and the lagoon (Vanderklift et al., 2020a). Episodically, gelatinous zooplankton, especially scyphozoan jellyfish, are abundant (often in April–May: Keesing et al., 2016).

Several times each year, from 2013 to 2019, green turtles *Chelonia mydas* were sought in multiple habitats by observers in a boat, and once located were captured by hand and transferred into the boat. Turtles were then transferred to a beach, where they were measured (curved carapace length: CCL, to the nearest millimeter), and titanium tags (Stockbrands Co Pty Ltd, Australia) were attached to the left and right fore flippers. Individuals ranged from 36.5 to 105.6 cm, and included mature males and females, and immature individuals; the sex of individuals over 80 cm CCL were determined from external morphological characteristics.

Large females (>90 cm CCL) captured from October to February were excluded from analyses because of the possibility that they were present for nesting and therefore would not reflect patterns of resident individuals (M. Vanderklift & R. Pillans, unpublished data). If an individual was captured more than once, only data from the first occasion was included.

Nail clippings were taken from the distal edge of a fore flipper using surgical scissors (Vanderklift et al., 2020b). A 2-mL blood sample was taken by inserting a 22G × 1.5-inch needle attached to a 5-mL syringe into the dorsal surface of the neck and gently creating suction (following Owens and Ruiz, 1980); the sample was spun in a

portable centrifuge (Digital Zip-Spin; LW Scientific, Lawrenceville, GA, USA) at 6000 rpm for 2 min, and the red blood cell portion was extracted using a disposable pipette. All samples were kept on ice in microcentrifuge tubes, frozen at −20 °C later in the day, and then transported to CSIRO laboratories in Perth (Australia), where they were stored. All procedures were conducted according to permits issued by the CSIRO Wildlife and Large Animal Ethics Committee.

Seagrass and macroalgae were collected by hand from multiple places throughout the study area on nine occasions encompassing six years, stored on ice and then frozen at −20 °C later in the day, before being transported to CSIRO laboratories in Perth (Australia), where they were stored. Red jellyfish *Crambione mastigophora* were collected by hand, the mesoglea were then removed, rubbed in seawater, and frozen at −20 °C.

In a laboratory, samples were thawed at room temperature. Microcentrifuge tubes with red blood cells were placed directly in an air-circulating oven. Nail clippings were prepared according to Vanderklift et al. (2020b). Seagrass and macroalgae were cleaned with distilled water, and epiphytic organisms and detritus were scraped or picked off if necessary, and then placed into microcentrifuge tubes in an air-circulating oven. Jellyfish mesoglea were placed into aluminum foil trays in an air-circulating oven. All samples were dried in an air-circulating oven at 60 °C for at least 48 h (jellyfish mesoglea took longer, up to 72 h).

After drying, all samples were ground into a fine powder, either manually using a mortar and pestle, or using a mixer mill (MM200; Retsch, Dusseldorf, Germany), and 0.7–0.8 mg were placed into tin capsules. Elemental compositions (%C, %N, %S by weight) and stable isotope compositions (δ^{13}C, δ^{15}N and δ^{34}S) were measured at the West Australian Biogeochemistry Centre, The University of Western Australia (Perth, Australia).

The stable carbon and nitrogen isotope compositions were analyzed using a continuous-flow system consisting of an elemental analyser (EA Thermo Flash 1112) connected via a Conflo IV to a Delta V Plus mass spectrometer (Thermo-Finnigan, Germany). In the elemental analyser samples were combusted with oxygen added to the helium stream (grade 99.999% purity; BOC, Australia, 100 mL/min) at a temperature of 1000°C in a reactor comprised of chromium oxide and silvered oxides of cobalt (Thermo, Germany) and then NO_x gases were reduced at 650°C with electrolytic copper to produce N_2. N_2 and CO_2 were separated with a gas chromatography column and transferred into the isotope ratio mass spectrometer. Raw δ for CO_2 and N_2 were obtained relative to working gases in high-pressure cylinders (BOC, Australia) using Isodat 2.5 software (Thermo Scientific, Bremen, Germany). For CO_2 "SSH" ^{17}O correction was applied.

The stable sulfur isotope composition was analyzed using an Elemental Analyser and a 20-22 Sercon isotope ratio mass spectrometer (Sercon, UK). Samples were mixed with V_2O_5 and packed into tin capsules (Sercon, UK). Samples were converted to SO_2 in the reaction column filled with tungsten oxides on zirconium and copper (Sercon, UK) at 1020°C (Studley et al., 2002). The produced gases, after passing through the Nafion water trap, were separated using a gas chromatography column and introduced to an ion source as SO_2 gas in the stream of helium (grade 99.999% purity; BOC, Australia, 100 mL/min) and masses 48/49/50 of fragmented ions were measured.

Data were generated in standard δ-notation normalized to Vienna Pee Dee Belemnite (for δ^{13}C), atmospheric N_2 (for δ^{15}N) or Vienna Canyon Diablo Troilite (for δ^{34}S) after multi-point normalization to the stable isotope international reference scale. International standards provided by the International Atomic Energy Agency (IAEA, Vienna, Austria) and United States Geological Survey (USGS, Reston, VA, USA) (δ^{13}C: NBS22, USGS24, NBS19, LSVEC; δ^{15}N: N1, N2, USGS32; δ^{34}S: IAEA-S1, IAEA-S2, IAEA-S3, NBS127) and internal laboratory standards (glutamic acid) were used (Skrzypek et al., 2010; Skrzypek, 2013). The uncertainty associated with the repeated measurements of the internal standards (±1 standard deviation) was not more than 0.10 ‰ for δ^{13}C and δ^{15}N and <0.40 ‰ for δ^{34}S.

2.2 Acoustic telemetry

Acoustic receivers were deployed in an area encompassing ~28 km^2 from <1 m water depth near the shoreline to >50 m water depth beyond the reef slope, forming an array of 77 acoustic receivers spaced 200–800 m apart (Supplementary Figure 1). Detection ranges typically did not overlap (for a detailed description, see Pillans et al., 2014; Pillans et al., 2022).

Post marginal scutes of *C. mydas* were cleaned using a cloth soaked in a disinfectant mixture of 10 mL Hexacon, 90 mL distilled H_2O and 900 mL ethanol, and then either one or two 3-mm diameter holes were drilled through the carapace. Acoustic tags were secured by 3 mm stainless steel bolts soaked in the same disinfectant mixture. A 20-mm diameter rubber washer and a similar sized stainless-steel washer were placed over the bolts on the dorsal surface and secured with a nylon insert self-locking nut. The protruding ends of the bolts were cut off and a two-part epoxy resin (Sika AnchorFix®-3+, Sika Australia Pty Ltd) was placed over the bolts to smooth their profile. All acoustic tags were painted with antifouling paint before being attached. Depending on size, individuals were tagged with either a V13-1L, V16-4H or V16-6H Vemco coded transmitter (tag). These transmitters range in length between 36–98 mm and weigh between 11–37 g in air. The pulse rate of transmitters varied from 30–180 s and battery life varied from 1,090–3,650 d depending on the frequency of each ping and the power output of the tag. Receivers were downloaded every 12 months throughout the study, and the batteries were changed at the same time.

2.3 Home range measures

Home range measures were calculated for each individual that was detected for more than 30 days and on two or more receivers to ensure we excluded data from tags that might have detached immediately after release. The measures were calculated separately for day and night using the maptools package (Bivand and Lewin-Koh, 2013) in the R statistical software environment. A simple measure of roaming extent was provided by the total number of receivers at which a turtle was detected. Other measures were calculated from kernel utilization distributions (KUD), which were

calculated using the adehabitatHR package (Calenge, 2006) in R. The methods for applying the package to the acoustic array were as described in Pillans et al. (2021): the smoothing parameter was set to 200 m, detections were binned into 20-min intervals, and the output grid resolution was 50 m KUD (95%, in km^2). The average distance from shore of each turtle was calculated as the weighted average distance from shore of the KUD grid cells, where the weights were the kernel densities. The shoreline was defined by the mainland high water mark of the polygonised coast of Western Australia.

2.4 Statistical analysis

We had no *a priori* expectation of the shape of the relationship between the response and explanatory variables; indeed, there was some evidence that patterns might be complex and nonlinear. Consequently, we preferred a statistical framework that did not assume particular relationships, and so we used generalized additive models (Wood, 2011). We used the mgcv package in the R statistical software environment (Wood, 2017) to fit and test models, using restricted maximum likelihood to select the smoothing parameter, and a Gaussian probability distribution. We tested for patterns in metrics of roaming and location with turtle size (as CCL), patterns in stable isotope composition with CCL, and patterns in roaming and location with stable isotope composition. We compared models with and without a term for sex using Akaike's information Criterion (AIC); in each case sex did not improve model and so it was not included in final analyses.

For stable isotope mixing models, primary producers (i.e., seagrasses, macroalgae) were first grouped using k-means clustering (Borcard et al., 2011) using the vegan package in the R statistical software environment (Oksanen et al., 2022). All species of primary producers (Supplementary Table 1) were included. Two clusters were clearly defined, one containing only seagrasses, the other containing only macroalgae. Further subdivisions created classes in which samples from the same macroalgae taxa were split, and so did not create useful additional information. For subsequent mixing models seagrasses and macroalgae were considered separate diet categories. The red jellyfish *Crambione mastigophora* was included as a third category. Although benthic invertebrates are consumed by *C. mydas* in some places, we found no evidence of this in our study area. Mangrove leaves are also eaten by green turtles in some places but analysis of >80,000 accurate locations (Fastloc GPS) from n=35 satellite-tagged *C. mydas* in Mangrove Bay (74.6–108.6 cm CCL), showed no foraging among mangroves, so we did not include them (M. Vanderklift & R. Pillans, unpublished data). The source dataset, therefore, included seagrass (n=30), macroalgae (n=82) and jellyfish (n=13): we used the means and standard deviations for each of $\delta^{13}C$, $\delta^{15}N$ and $\delta^{34}S$.

The potential contributions of seagrass, macroalgae and jellyfish to the diet of *C. mydas* were analysed using the Bayesian tracer mixing model MixSIAR (Stock and Semmens, 2016; Stock et al., 2018). We included CCL as a covariate to explore how diet changes with the size of n=89 individuals for which $\delta^{13}C$, $\delta^{15}N$ and $\delta^{34}S$ of red blood cells were measured. We included residual and process error (following Stock et al., 2018 this model formulation is appropriate for applications in which a consumer effectively samples a prey source multiple times), and uninformative priors. For trophic discrimination factors (TDF) of $\delta^{13}C$ and $\delta^{15}N$, we used data for captive feeding experiments by Vander Zanden (2012): 0.3 ± 0.5 ‰ for $\delta^{13}C$ and 2.4 ± 0.5 ‰ for $\delta^{15}N$. We are not aware of any studies of TDF for $\delta^{34}S$ in comparable taxa, but the scant evidence available for other taxa (Florin et al., 2011) suggests that TDF for $\delta^{34}S$ might be negatively correlated with $\delta^{34}S$ of diet; noting this pattern we used a TDF of 1.5 ± 1.5 ‰, with the comparatively higher standard deviation reflecting the uncertainty in choice of TDF. We selected the "normal" MCMC parameters of chainLength=100,000, burn=50,000, thin=50, chains=3.

3 Results

More receivers received transmissions during the day than at night for 72 of the 74 acoustically-tagged individual *Chelonia mydas*; there was no difference for the other two individuals (Figure 1A).

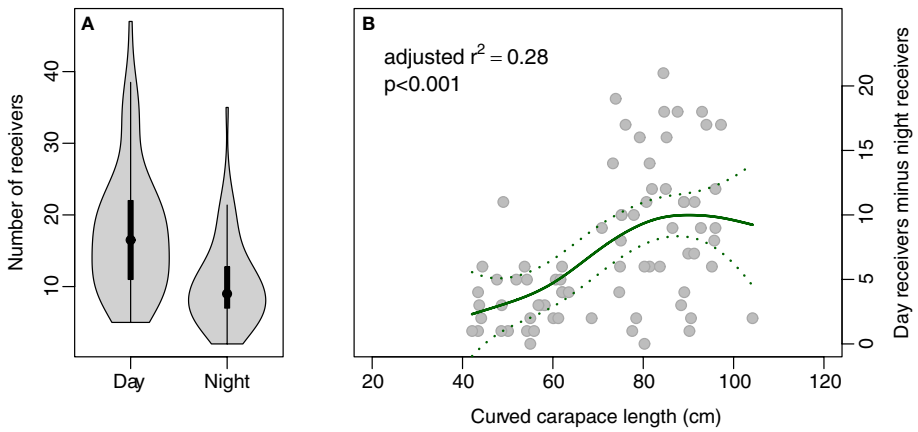

FIGURE 1
Plot of number of receivers at which each individual was recorded **(A)** during day and night, and **(B)** the difference in the number of receivers each individual was recorded on during day and night plotted against length (curved carapace length, cm).

No individuals were detected on more receivers at night than during the day. The absolute difference tended to be higher and more variable with length (Figure 1B), a reflection that larger individuals roam more widely (Pillans et al., 2022). Since turtles are more likely to move around when they are feeding, this result suggests that individuals were likely feeding during the day and so subsequent analyses focused on metrics of movement calculated from daytime detections only.

There was a substantial (but nonlinear) increase in 95% KUD with length, and an increase in average distance from shore with length (Figure 2): larger turtles tended to occupy larger areas and be found further from the shore. KUD tended to remain relatively constant at ~1.3–1.5 km^2 up to lengths of around 65 cm, then there was a steep increase in KUD between lengths of between 65 cm and 85 cm to ~5.0 km^2. There was a concomitant increase in average

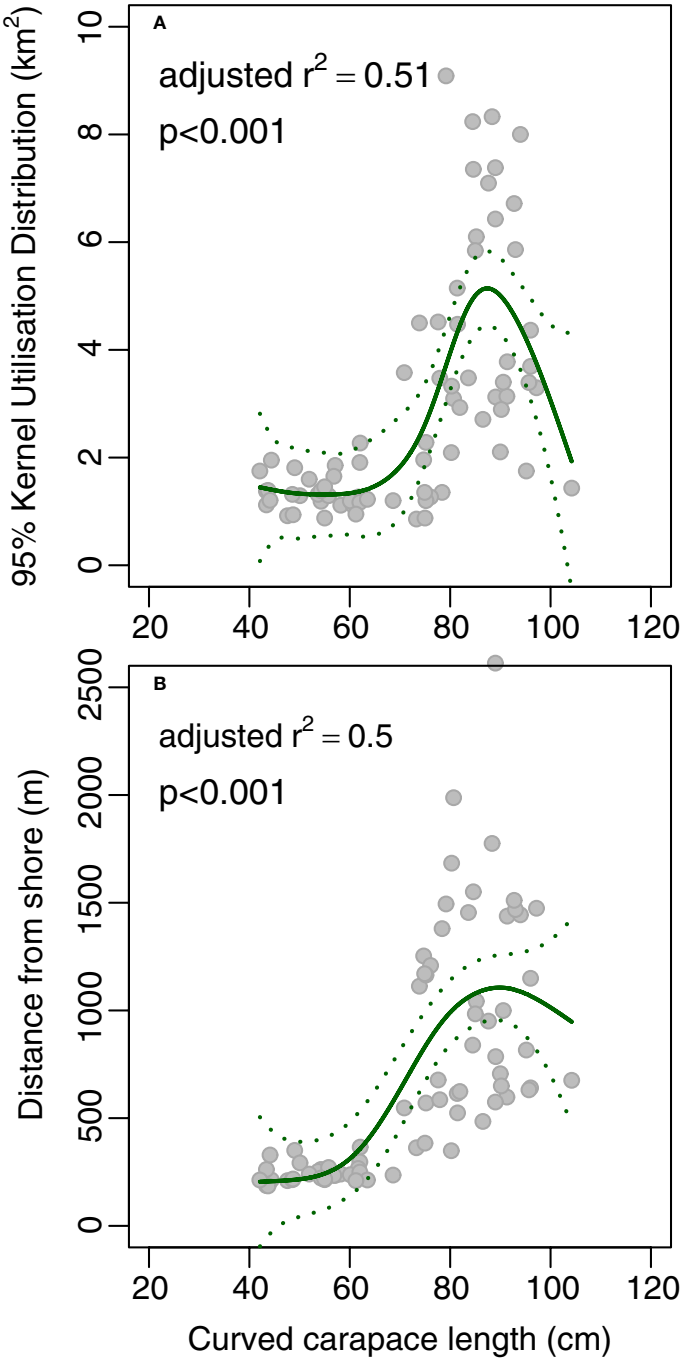

FIGURE 2
Plot of length (curved carapace length, cm) against **(A)** 95% Kernel Utilisation Distribution and **(B)** average distance from shore yielded by acoustic telemetry of green turtles *Chelonia mydas*. The solid line is the fit from a generalised additive model, and the dotted lines are the 95% confidence intervals for the fit.

distance from shore from ~200 m at 35–40 cm to ~1,100 m at 90 cm (Figure 2).

Red blood cells were collected from 128 individual *C. mydas* and nail clippings from 100 individual *C. mydas*. Each of δ^{13}C, δ^{15}N and δ^{34}S varied significantly in a nonlinear pattern with turtle length, although the amount of variation explained by length was greatest for δ^{15}N and δ^{34}S (Figure 3). The steepest changes in δ^{13}C and δ^{15}N occurred at the smallest lengths, and these were followed by more gradual changes towards maximum length. For example, from 36 cm (the length of the smallest individual captured) to 50 cm, δ^{13}C of red blood cells increased by 2.8 ‰, then decreased by 1.5 ‰ to 105 cm (the length of the largest individual). Similarly, δ^{15}N of red blood cells decreased by 3.4 ‰ from 36 cm to 50 cm before increasing by 2.5 ‰. δ^{34}S of red blood cells yielded similar patterns,

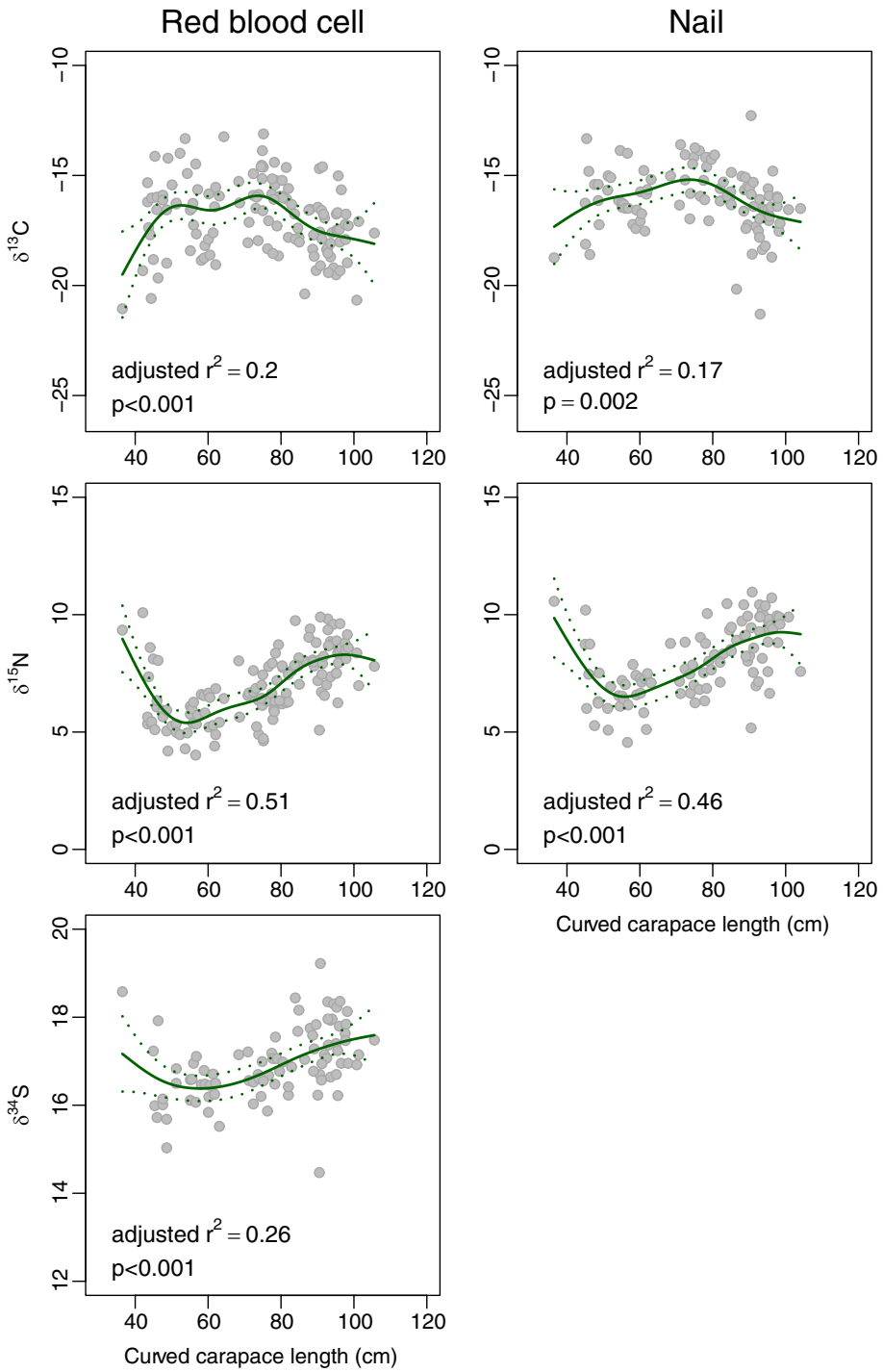

FIGURE 3
Plot of length (curved carapace length, in cm) against δ^{13}C, δ^{15}N and δ^{34}S of red blood cells (left panel) and nails (right panel) of green turtles *Chelonia mydas*. The solid line is the fit from a generalised additive model, and the dotted lines are the 95% confidence intervals for the fit.

but the change at smaller lengths was less, decreasing by 0.8 ‰ from 36 cm to 50 cm before increasing by 1.1 ‰ at 105 cm. Patterns for nails were similar.

Neither red blood cells nor nails showed significant variation in δ^{13}C with either KUD or distance from shore (r^2_{adj}<0.04 in each case; Figure 4). However, δ^{15}N and δ^{34}S of both red blood cells and nails (Figures 5, 6, respectively) increased monotonically with KUD and distance from shore (r^2_{adj}>0.25 in each case). To illustrate, δ^{15}N of red blood cells of turtles foraging ~1,600 m from shore was 2.4 ‰ higher than that of those foraging ~200 m from shore and δ^{34}S of red blood cells of turtles foraging further from shore was 1.7 ‰ higher than that of those foraging inshore. The amount of variation explained by models using δ^{15}N from nails was greater than that of models involving red blood cells.

Seagrass, macroalgae and jellyfish were distinguished by one or more of δ^{13}C, δ^{15}N and δ^{34}S (Figure 7). Seagrass tended to have lower δ^{15}N (range: −7.1 to 3.6 ‰) than macroalgae (range: 1.0 to 5.1 ‰), and lower δ^{34}S (range: 17.3 to 20.8 ‰) than macroalgae (range: 19.8 to 21.8 ‰). Jellyfish tended to have higher δ^{15}N (range: 5.3 to 7.2 ‰), and lower δ^{13}C (range: −22.4 to −19.7 ‰) than primary producers.

The mixing model supported inferences of ontogenetic changes in diet of *C. mydas* (Figure 8). Model results indicated that the proportion of seagrass was consistently high across the size range. The proportion of macroalgae was potentially substantial in small (< 60 cm CCL) individuals, but unlikely to be a major contributor to the diet of larger individuals. The proportion of jellyfish increased monotonically with size; this trend was present regardless of the TDF used, but the proportion was higher when a low TDF was tested (results not shown).

4 Discussion

Green turtles *Chelonia mydas* resident in a tropical lagoon in Ningaloo Marine Park exhibited size-related patterns in home range size, home range location, and diet. Small individuals tended to have small (<1.5 km^2) home ranges close to the shore and have a mixed

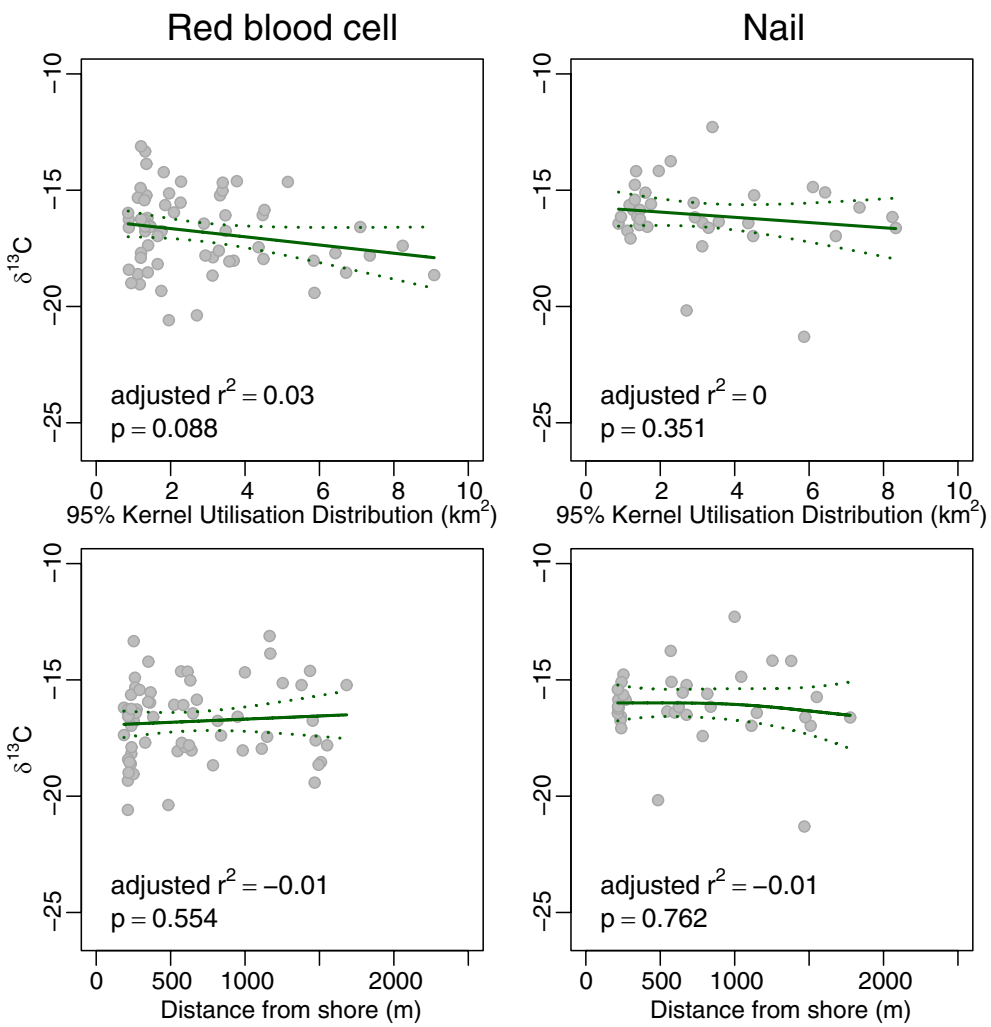

FIGURE 4
Plot of 95% Kernel Utilisation Distribution and average distance from shore yielded by acoustic telemetry against δ^{13}C of red blood cells (left panels) and nail (right panels) of green turtles *Chelonia mydas*. The solid line is the fit from a generalised additive model, and the dotted lines are the 95% confidence intervals for the fit.

10.3389/fevo.2023.1139441

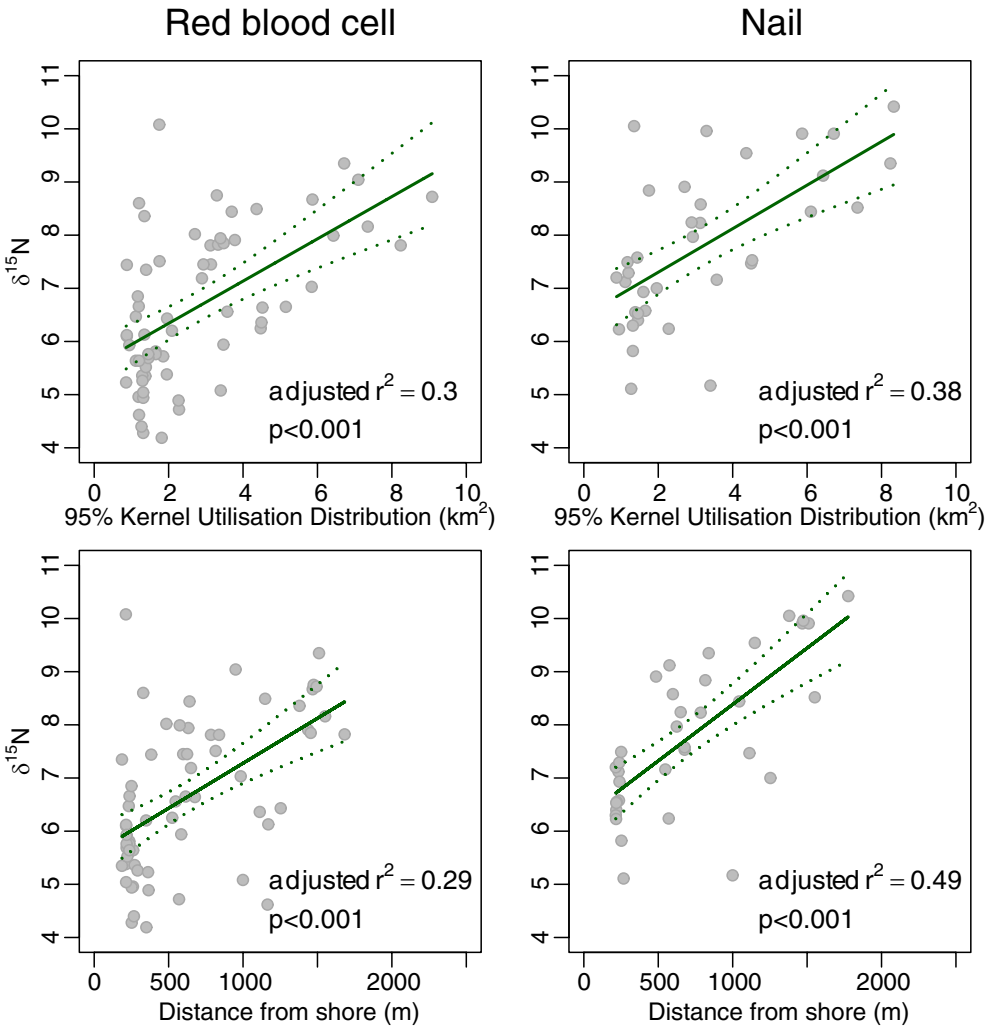

FIGURE 5
Plot of 95% Kernel Utilisation Distribution and average distance from shore yielded by acoustic telemetry against δ^{15}N of red blood cells (left panels) and nail (right panels) of green turtles *Chelonia mydas*. The solid line is the fit from a generalised additive model, and the dotted lines are the 95% confidence intervals for the fit.

diet including macroalgae, seagrass and scyphozoan jellyfish. Larger individuals tended to have larger (~5 km^2) home ranges located further from the shore, and a diet comprising mostly seagrass and jellyfish. Green turtle size is reliably correlated with age (Mayne et al., 2022), so these results confirm the presence of ontogenetic changes in habitat use and diet within the lagoon, across distances of ~1.5–2.0 km.

Ontogenetic changes in habitat use are a feature of green turtle life history — in particular, the migration of hatchlings from the beaches where they hatch to oceanic habitats, and then back again to shallow coastal habitats. Changes in diet associated with developmental migrations of turtles to shallow coastal habitats are well-established (e.g., Reich et al., 2007; Arthur et al., 2008). Our results were consistent with this, and further suggested that changes might continue to be reflected in tissues for some time after recruitment to coastal habitats — the stable isotope composition of all three elements included in this study changed between 40 cm and 50 cm CCL. The decrease in δ^{15}N was ~2 ‰ for red blood cells and nails, quite a substantial decrease equivalent to almost an entire trophic level (Seminoff et al., 2021). Mixing model results suggest that there is unlikely to be a substantial difference in diet at these lengths and they did not correspond with changes in home range size or location, so it seems plausible that the changes are due to continuation of the trajectory towards isotopic equilibrium. If so, noting that the span in size reflects several years of growth, it might imply that the residence times of elements in red blood cells are quite long. The residence times of elements within the tissues of sea turtles remains poorly known; Reich et al. (2008) found median residence times of 36–40 days for δ^{13}C and δ^{15}N in very small juvenile *C. mydas* (9.0–13.1 cm straight carapace length) but the residence times of turtles of sizes in our study are unknown. An alternative explanation, proposed by Cardona et al. (2010) following similar observations of patterns in stable isotope composition of scute layers, is that newly-recruited juveniles do not yet have the gut microbiome necessary to effectively digest

10.3389/fevo.2023.1139441

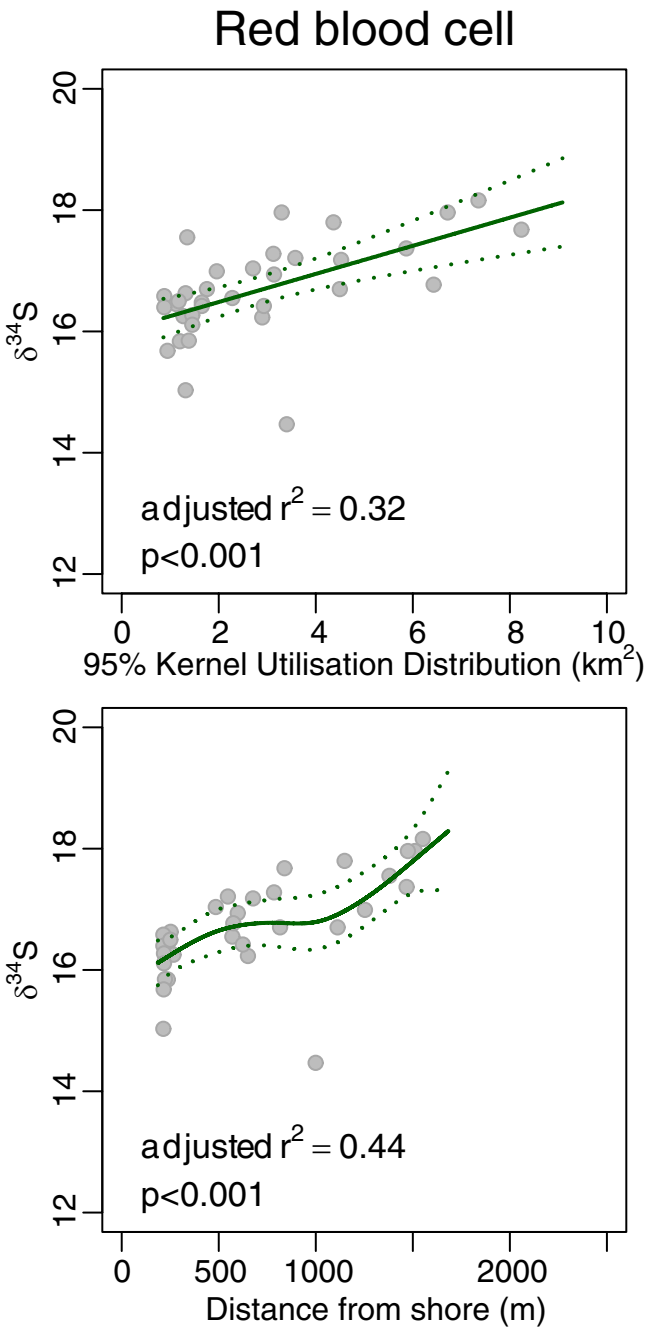

FIGURE 6
Plot of 95% Kernel Utilisation Distribution and average distance from shore yielded by acoustic telemetry with δ^{34}S of red blood cells of green turtles *Chelonia mydas*. The solid line is the fit from a generalised additive model, and the dotted lines are the 95% confidence intervals for the fit.

plants. Campos et al. (2018) subsequently found that patterns in microbiota of juvenile green turtles suggest that acquisition of polysaccharide fermenting microbiota (which allow turtles to extract nutrition from seagrass) in the gut occurs rapidly after recruitment to shallow coastal habitats.

Similar patterns of ontogenetic change in diet have been found in other populations of green turtles (Arthur et al., 2008; Howell et al., 2016; Roche et al., 2021). Stubbs et al. (2022) found that these patterns were reflected in the δ^{15}N of amino acids, suggesting that they are not due to size-related differences in discrimination; the inference from this is that the changes do reflect assimilated diet. Individuals at these sizes tended to have small home ranges located close to the shore and likely consumed a mixed diet of macroalgae, seagrass and jellyfish.

After recruitment to the lagoon, green turtles then exhibited further ontogenetic changes in home range size, home range location and diet as they grew. After lengths of approximately 60 cm CCL, home range size gradually increased, the location of the

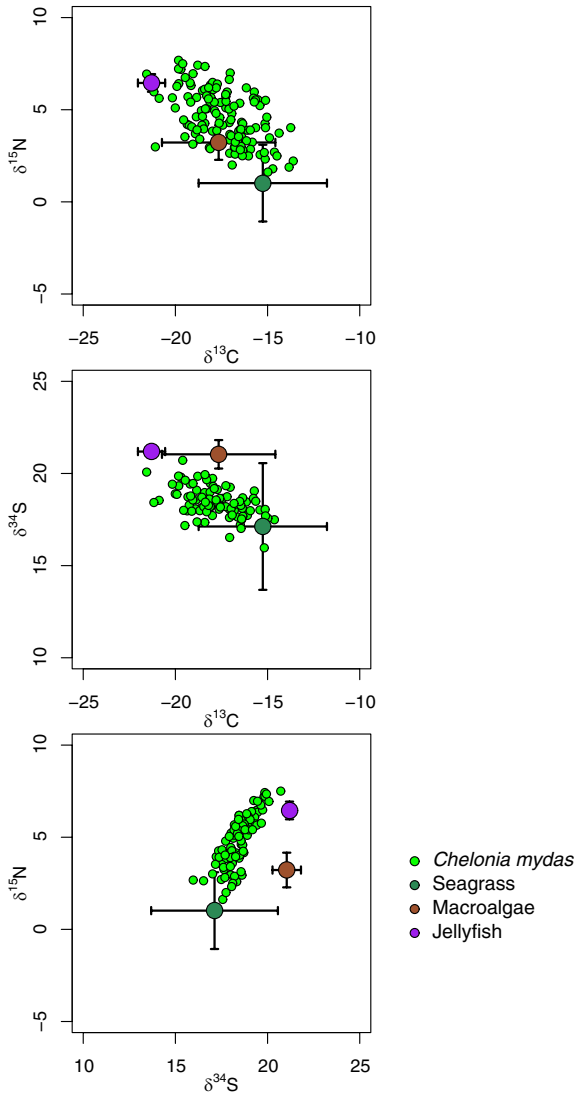

FIGURE 7
Plot of individual measurements of $\delta^{13}C$, $\delta^{15}N$ and $\delta^{34}S$ of green turtle *Chelonia mydas* red blood cells and mean ± SD of macroalgae, seagrass and the scyphozoan jellyfish *Crambione mastigophora*. $\delta^{13}C$, $\delta^{15}N$ and $\delta^{34}S$ of *C. mydas* are adjusted for TDF as follows: 0.3 ‰ for $\delta^{13}C$, 2.4 ‰ for $\delta^{15}N$, 1.5 ‰ for $\delta^{34}S$.

home range extended further from shore and diet likely became predominantly seagrass and jellyfish. Inferences about home range size and home range location are likely to be robust, because the durations of tag attachments were long (average detection span 372 days), and there was minimal emigration from the area encompassed by the array of receivers (three individuals: Pillans et al., 2022) These developmental changes occurred over relatively short distances (<2 km), and were detected by the extensive array of acoustic receivers. These shifts in home range occurred over very short distances compared to developmental changes from juvenile to adult habitats in some other green turtle populations (spanning hundreds of kilometers or more: e.g., Chambault et al., 2018; Doherty et al., 2020).

Despite the short distances, there are steep gradients in habitat type across the lagoon. Close to shore, water is very shallow (<1.5 m deep at Highest Astronomical Tide) and the seafloor is predominantly limestone pavement with macroalgae and sparse seagrass. Further from shore the water is deeper (up to 6 m) and the seafloor is predominantly sandy. The seagrass *Halophila ovalis* grows in the sandy habitats, which tend to be where larger turtles spend most time (Pillans et al., 2022). The mixing model suggests that seagrass is likely an important food for these individuals, a result that is supported by qualitative observations (M. Vanderklift, personal observations). Increases in seagrass consumption with size have also been reported for other populations of green turtles (e.g., Burgett et al., 2018; Palmer et al., 2021; Roche et al., 2021), and it might be common. However, there are also multiple examples of populations in which large green turtles consume other diets (e.g., see review by Jones and Seminoff, 2013), so the ecological context appears to play an important role in diet. Patterns in consumption

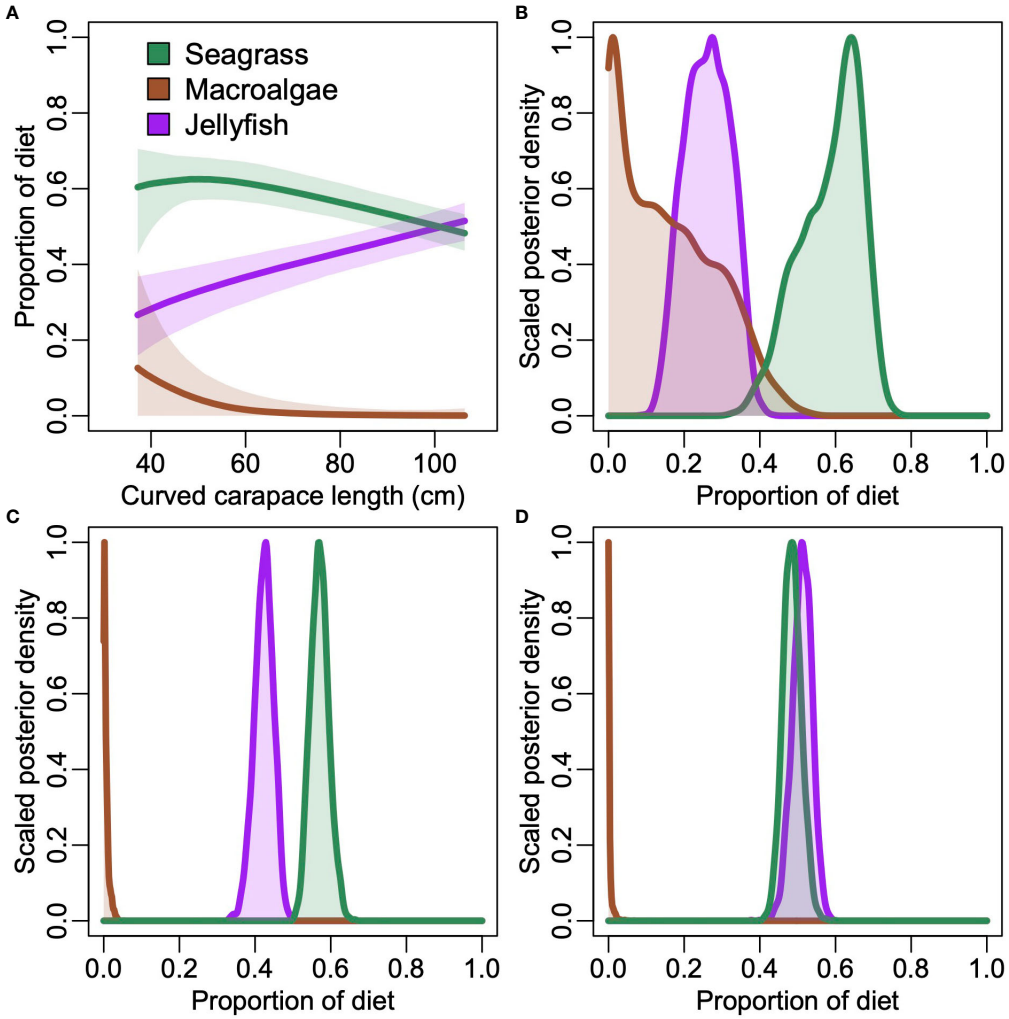

FIGURE 8
(A) Posterior distributions for estimated proportion of three likely foods of the green turtle *C. mydas* as a function of length. Lines depict medians and shaded area is 90% credible intervals. **(B–D)** Posterior plots showing the scaled probability for each potential food for the **(B)** smallest, **(C)** median, and **(D)** largest individuals.

of macroalgae are complex, with reports of greater consumption by small individuals (Howell and Shaver, 2021), by large individuals (Vélez-Rubio et al., 2016), or even selectively by only some individuals in a population (Burkholder et al., 2011; Vanderklift et al., 2021).

Jellyfish appear to be important to the diet of green turtles, and the proportion of jellyfish in the diet appears to increase with size. It is possible that other animals (such as crabs or bivalves) also contribute to their diet, but we saw no evidence of this. Jellyfish are not abundant for much of the year, but during April–May they can be superabundant, and occur in the water column above all habitats. It is possible that during these times consumption of jellyfish is nutritionally important. Some individuals fitted with satellite tags also showed episodic movements to deeper habitats outside the lagoon (M. Vanderklift & R. Pillans unpublished data), movements which might be related to a search for jellyfish or other prey. Consumption of gelatinous zooplankton has been observed in multiple green turtle populations, including to the extent where it forms a major component of the diet (González Carman et al., 2014). Facultative consumption of jellyfish when they are abundant might be advantageous if they can be quickly digested, offsetting their relatively low energetic value (Hays et al., 2018).

If the ontogenetic changes in habitat and diet reflect a trade-off between growth and mortality, then it follows that there should be differences among habitats in nutritional value of the food available, and in predation risk. We did not explicitly test for differences in predation risk, but they are plausible: probably the main predators of turtles at Ningaloo are tiger sharks *Galeocerdo cuvier*, which are present in the lagoon all year and tend to spend proportionally more time in the sandy lagoon habitat (R. Pillans unpublished data). In some contexts green turtles appear to select habitats based on predation risk (e.g., Smulders et al., 2023). It seems plausible that small turtles would be more vulnerable to predation by tiger sharks, and if so restricting home ranges to shallow areas beyond their reach would be a prudent strategy.

It is perhaps less obvious that the food sources in the lagoon are more nutritious. Seagrass is consumed by green turtles throughout much of their range (Esteban et al., 2020), but macroalgae is also

consumed even in places where seagrass is abundant (e.g., Burkholder et al., 2011; Vanderklift et al., 2021). Green turtles appear able to extract nutrition from seagrass and macroalgae through hindgut fermentation in which structural carbohydrates (such as cellulose) are broken down by microbes into compounds that can be digested (Bjorndal, 1979; Bjorndal et al., 1991). These microflora appear to provide the nutrition for green turtles eating seagrasses (Arthur et al., 2014). In our study area, the large meadow-forming seagrasses that typify many tropical lagoons are not present in the lagoon; the small-leaved seagrass *Halophila ovalis* is present, but in relatively low densities throughout the sandy areas of the lagoon. Macroalgae are abundant, but the most abundant macroalgae taxa in the lagoons at Ningaloo (*Sargassum* spp and other large brown algae) have very low nitrogen concentrations (M. Vanderklift unpublished data). Most of these large brown algae have nitrogen concentrations (a rough indicator of protein content) of <1%, while leaves of *H. ovalis* contain ~1.5% nitrogen. Red algae contain higher nitrogen concentrations, but are not abundant. It is possible that even with hindgut fermentation macroalgae do not provide the increasing energetic requirements as turtles grow, when proportionally more energy is needed for somatic maintenance (Stubbs et al., 2020). The increasing proportion of jellyfish in their diet as they grow suggests that they might increasingly rely on this food source for additional nutrition. The tissue of *Crambione mastigophora* has low nitrogen concentrations (~0.9%), but also much lower concentrations of carbon such that C:N ratios are potentially more favorable.

It is also possible that some individuals might select for specific foods more than the overall populations. In green turtles, multiple studies have found that individuals can select some food to the extent that they are considered specialists (e.g., Vander Zanden et al., 2013; Thomson et al., 2018). There is also evidence that this occurs in our study population (Stubbs et al., 2022).

The results here refine the initial diet estimates of Stubbs et al. (2022) by the addition of local measurements of jellyfish and the inclusion of δ^{34}S. The addition of δ^{34}S allows a clearer distinction of the contribution of seagrass and macroalgae, because the roots of seagrass allow uptake of sulfur from porewater which contains sulfides, which have substantially lower δ^{34}S than sulphate found in seawater (Fry et al., 1982), while macroalgae do not have roots and so obtain their sulfur from seawater. However, the model results are still sensitive to the potential foods included and the TDF used (Phillips et al., 2014). In particular, our decisions about what TDF to use for δ^{34}S were based on tenuous evidence (the negative correlation between δ^{34}S of diet and Δ^{34}S from experiments using mammals by Florin et al., 2011); tests using different TDF for δ^{34}S yielded qualitatively similar results, but lower TDF yielded a higher proportional contribution of jellyfish that was less plausible given the relatively low abundance of jellyfish for much of the year. We elected to exclude mangroves because we found no evidence that any individual was foraging in mangroves, but it is possible that mangroves might be a minor proportion of the diet of small turtles with home ranges close to the shore. Similarly, we did not include animals other than jellyfish because we saw no evidence that *C. mydas* consumed them. However, absence of evidence is not evidence of absence, and it is possible that some individual *C. mydas* in our study area might consume other animals.

5 Conclusion

Combining data from acoustic telemetry and stable isotope analysis revealed that the green turtle *Chelonia mydas* exhibits ontogenetic changes in home range size, home range location and diet across relatively short distances (~1.5 km) in a lagoon ecosystem at Ningaloo, north-western Australia. These changes are consistent with a hypothesis that they optimize a trade-off between risk of predation and nutrition for growth and reproduction.

Data availability statement

The raw data supporting the conclusions of this article will be made available by the authors, without undue reservation.

Ethics statement

The animal study was reviewed and approved by CSIRO Wildlife and Large Animal Ethics Committee.

Author contributions

MV and RP contributed to conception and design of the study. MV, RP, and WR conducted the statistical analyses. MV wrote the first draft of the manuscript. All authors contributed to data collection, manuscript revision, and read and approved the submitted version.

Funding

This research is funded by Ningaloo Outlook (a strategic marine research partnership between CSIRO and Woodside Energy to better understand Ningaloo Reef and its important ecological values). JS was supported by an Australian Government Research Training Program Scholarship and BHP Marine Research Scholarship at The University of Western Australia.

Acknowledgments

This study was done with the assistance of people too numerous to mention individually, but we thank them all. We thank Peter Barnes, Dani Rob and Keely Markovina from the Department of Biodiversity, Conservation and Attractions and Susie Bedford from the Exmouth District High School for their support. Animal handling procedures were conducted according to permits issued by the CSIRO Wildlife and Large Animal Ethics Committee.

Conflict of interest

The authors declare that the research was conducted in the absence of any commercial or financial relationships that could be construed as a potential conflict of interest.

Publisher's note

All claims expressed in this article are solely those of the authors and do not necessarily represent those of their affiliated organizations, or those of the publisher, the editors and the reviewers. Any product that may be evaluated in this article, or claim that may be made by its manufacturer, is not guaranteed or endorsed by the publisher.

Supplementary material

The Supplementary Material for this article can be found online at: https://www.frontiersin.org/articles/10.3389/fevo.2023.1139441/full#supplementary-material

References

Arthur, K. E., Boyle, M. C., and Limpus, C. J. (2008). Ontogenetic changes in diet and habitat use in green sea turtle (*Chelonia mydas*) life history. *Mar. Ecol. Prog. Ser.* 362, 303–311. doi: 10.3354/meps07440

Arthur, K. E., Kelez, S., Larsen, T., Choy, C. A., and Popp, B. N. (2014). Tracing the biosynthetic source of essential amino acids in marine turtles using $\delta^{13}C$ fingerprints. *Ecology* 95, 1285–1293. doi: 10.1890/13-0263.1

Bivand, R., and Lewin-Koh, N. (2013). *maptools: Tools for reading and handling spatial objects. R package version 0.8, 23.*

Bjorndal, K. A. (1979). Cellulose digestion and volatile fatty-acid production in the green turtle, *Chelonia mydas*. *Comp. Biochem. Physiol. A: Physiol.* 63, 127–133. doi: 10.1016/0300-9629(79)90638-8

Bjorndal, K. A., Suganuma, H., and Bolten, A. B. (1991). Digestive fermentation in green turtles, *Chelonia mydas*, feeding on algae. *Bull. Mar. Sci.* 48, 166–171.

Bolten, A. B. (2003). "Variation in Sea turtle life history patterns: neritic vs. oceanic developmental stages," in *The Biology of Sea Turtles volume 2.* Eds. P. L. Lutz, J. A. Musick and J. Wyneken (Boca Raton, CRC Press), 243–257.

Borcard, D., Gillet, F., and Legendre, P. (2011). *Numerical Ecology with R* (New York: Springer).

Burgett, C. M., Burkholder, D. A., Coates, K. A., Fourqurean, V. L., Kenworthy, W. J., Manuel, S. A., et al. (2018). Ontogenetic diet shifts of green sea turtles (*Chelonia mydas*) in a mid-ocean developmental habitat. *Mar. Biol.* 165, 33. doi: 10.1007/s00227-018-3290-6

Burkholder, D. A., Heithaus, M. R., Thomson, J. A., and Fourqurean, J. W. (2011). Diversity in trophic interactions of green sea turtles *Chelonia mydas* on a relatively pristine coastal foraging ground. *Mar. Ecol. Prog. Ser.* 439, 277–293. doi: 10.3354/meps09313

Calenge, C. (2006). The package adehabitat for the R software: a tool for the analysis of space and habitat use by animals. *Ecol. Model.* 197, 516–519. doi: 10.1016/j.ecolmodel.2006.03.017

Campos, P., Guivernau, M., Prenafeta-Boldú, F. X., and Cardona, L. (2018). Fast acquisition of a polysaccharide fermenting gut microbiome by juvenile green turtles *Chelonia mydas* after settlement in coastal habitats. *Microbiome* 6, 69. doi: 10.1186/s40168-018-0454-z

Cardona, L., Campos, P., Levy, Y., Demetropoulos, A., and Margaritoulis, D. (2010). Asynchrony between dietary and nutritional shifts during the ontogeny of green turtles (*Chelonia mydas*) in the Mediterranean. *J. Exp. Mar. Biol. Ecol.* 393, 83–89. doi: 10.1016/j.jembe.2010.07.004

Cassata, L., and Collins, L. B. (2008). Coral reef communities, habitats, and substrates in and near sanctuary zones of Ningaloo Marine Park. *J. Coast. Res.* 24, 139–151. doi: 10.2112/05-0623.1

Chambault, P., de Thoisy, B., Huguin, M., Martin, J., Bonola, M., Etienne, D., et al. (2018). Connecting paths between juvenile and adult habitats in the Atlantic green turtle using genetics and satellite tracking. *Ecol. Evol.* 8, 12790–12802. doi: 10.1002/ece3.4708

Doherty, P. D., Broderick, A. C., Godley, B. J., Hart, K. A., Phillips, Q., Sanghera, A., et al. (2020). Spatial ecology of sub-adult green turtles in coastal waters of the Turks and Caicos islands: implications for conservation management. *Front. Mar. Sci.* 7. doi: 10.3389/fmars.2020.00690

Esteban, N., Mortimer, J. A., Stokes, H. J., Laloë, J.-O., Unsworth, R. K. F., and Hays, G. C. (2020). A global review of green turtle diet: sea surface temperature as a potential driver of omnivory levels. *Mar. Biol.* 167, 183. doi: 10.1007/s00227-020-03786-8

Florin, S. T., Felicetti, L. A., and Robbins, C. T. (2011). The biological basis for understanding and predicting dietary-induced variation in nitrogen and sulphur isotope ratio discrimination. *Funct. Ecol.* 25, 519–526. doi: 10.1111/j.1365-2435.2010.01799.x

Fry, B., Scalan, R. S., Winters, J. K., and Parker, P. L. (1982). Sulphur uptake by salt grasses, mangroves, and seagrasses in anaerobic sediments. *Geochimica Cosmochimica Acta* 46, 1121–1124. doi: 10.1016/0016-7037(82)90063-1

González Carman, V., Botto, F., Gaitán, E., Albareda, D., Campagna, C., and Mianzan, H. (2014). A jellyfish diet for the herbivorous green turtle *Chelonia mydas* in the temperate SW Atlantic. *Mar. Biol.* 161, 339–349. doi: 10.1007/s00227-013-2339-9

Hays, G. C., Doyle, T. K., and Houghton, J. D. R. (2018). A paradigm shift in the trophic importance of jellyfish? *Trends Ecol. Evol.* 33, 874–884. doi: 10.1016/j.tree.2018.09.001

Hays, G. C., and Scott, R. (2013). Global patterns for upper ceilings on migration distance in sea turtles and comparisons with fish, birds and mammals. *Funct. Ecol.* 27, 748–756. doi: 10.1111/1365-2435.12073

Howell, L. N., Reich, K. J., Shaver, D. J., Landry, A. M., and Gorga, C. C. (2016). Ontogenetic shifts in diet and habitat of juvenile green sea turtles in the northwestern Gulf of Mexico. *Mar. Ecol. Prog. Ser.* 559, 217–229. doi: 10.3354/meps11897

Howell, L. N., and Shaver, D. J. (2021). Foraging habits of green sea turtles (*Chelonia mydas*) in the northwestern Gulf of Mexico. *Front. Mar. Sci.* 8. doi: 10.3389/fmars.2021.658368

Jones, T., and Seminoff, J. (2013). "Feeding biology: advances from field-based observations, physiological studies, and molecular techniques," in *Biology of Sea Turtles Volume III*. Eds. J. Wyneken, K. J. Lohmann and J. A. Musick (Boca Raton: Taylor & Francis), 211–247.

Keesing, J. K., Gershwin, L. A., Trew, T., Strzelecki, J., Bearham, D. , Liu, D. Y., et al. (2016). Role of winds and tides in timing of beach strandings, occurrence, and significance of swarms of the jellyfish *Crambione mastigophora* Mass 1903 (Scyphozoa: Rhizostomeae: Catostylidae) in north-western Australia. *Hydrobiologia Mass* 768, 19–36. doi: 10.1007/s10750-015-2525-5

Martínez del Rio, C., Wolf, N., Carleton, S. A., and Gannes, L. Z. (2009). Isotopic ecology ten years after a call for more laboratory experiments. *Biol. Rev.* 84, 91–111. doi: 10.1111/j.1469-185X.2008.00064.x

Mayne, B., Mustin, W., Baboolal, V., Casella, F., Ballorain, K., Barret, M., et al. (2022). Age prediction of green turtles with an epigenetic clock. *Mol. Ecol. Resour.* 22, 2275–2284. doi: 10.1111/1755-0998.13621

Musick, J. A., and Limpus, C. J. (1996). "Habitat utilization and migration in juvenile sea turtles," in *The Biology of Sea Turtles*. Eds. P. L. Lutz and J. A. Musick (Boca Raton: CRC Press), 137–163.

Oksanen, J., Guillaume Blanchet, F., Friendly, M., Kindt, R., Legendre, P., Dan McGlinn, P., et al. (2022). "Vegan: community ecology package." *R package version 2.5-7. 2020.*

Owens, D. W., and Ruiz, G. J. (1980). New methods of obtaining blood and cerebrospinal fluid from marine turtles. *Herpetologica* 36 (17), 17–20. Available at: http://www.jstor.org/stable/3891847.

Palmer, J. L., Beton, D., Çiçek, B. A., Davey, S., Duncan, E. M., Fuller, W. J., et al. (2021). Dietary analysis of two sympatric marine turtle species in the eastern Mediterranean. *Mar. Biol.* 168, 94. doi: 10.1007/s00227-021-03895-y

Pecquerie, L., Nisbet, R. M., Fablet, R., Lorrain, A., and Kooijman, S. (2010). The impact of metabolism on stable isotope dynamics: a theoretical framework. *Philos. Trans. R. Soc. B-Biological Sci.* 365, 3455–3468. doi: 10.1098/rstb.2010.0097

Phillips, D. L., Inger, R., Bearhop, S., Jackson, A. L., Moore, J. W., Parnell, A. C., et al. (2014). Best practices for use of stable isotope mixing models in food-web studies. *Can. J. Zool.* 92, 823–835. doi: 10.1139/cjz-2014-0127

Pillans, R. D., Bearham, D., Boomer, A., Downie, R., Patterson, T. A., Thomson, D. P., et al. (2014). Multi year observations reveal variability in residence of a tropical demersal fish, *Lethrinus nebulosus*: implications for spatial management. *PloS One* 10, e0118869. doi: 10.1371/journal.pone.0105507

Pillans, R. D., Rochester, W., Babcock, R. C., Thomson, D. P., Haywood, M. D. E., and Vanderklift, M. A. (2021). Long-term acoustic monitoring reveals site fidelity, reproductive migrations, and sex specific differences in habitat use and migratory timing in a large coastal shark (*Negaprion acutidens*). *Front. Mar. Sci.* 8. doi: 10.3389/fmars.2021.616633

Pillans, R. D., Whiting, S. D., Tucker, A. D., and Vanderklift, M. A. (2022). Fine-scale movement and habitat use of juvenile, subadult, and adult green turtles (*Chelonia mydas*) in a foraging ground at Ningaloo Reef, Australia. *Aquat. Conservation-Marine Freshw. Ecosyst.* 32, 1323–1340. doi: 10.1002/aqc.3832

Preisser, E. L., and Orrock, J. L. (2012). The allometry of fear: interspecific relationships between body size and response to predation risk. *Ecosphere* 3, art77. doi: 10.1890/ES12-00084.1

Reich, K. J., Bjorndal, K. A., and Bolten, A. B. (2007). The 'lost years' of green turtles: using stable isotopes to study cryptic lifestages. *Biol. Lett.* 3, 712–714. doi: 10.1098/rsbl.2007.0394

Reich, K. J., Bjorndal, K. A., and Martínez del Rio, C. (2008). Effects of growth and tissue type on the kinetics of ^{13}C and ^{15}N incorporation in a rapidly growing ectotherm. *Oecologia* 155, 651–663. doi: 10.1007/s00442-007-0949-y

Roche, D. C., Cherkiss, M. S., Smith, B. J., Burkholder, D. A., and Hart, K. M. (2021). Stable isotopes used to infer trophic position of green turtles (*Chelonia mydas*) from Dry Tortugas National Park, Gulf of Mexico, United States. *Regional studies in marine science* 48, 10211.

Seminoff, J. A., Komoroske, L. M., Amorocho, D., Arauz, R., Chacon-Chaverrı, D., Paz, N.D., et al. (2021). Large-scale patterns of green turtle trophic ecology in the eastern pacific ocean. *Ecosphere* 12, e03479. doi: 10.1002/ecs2.3479

Skrzypek, G. (2013). Normalization procedures and reference material selection in stable HCNOS isotope analyses: an overview. *Analytical Bioanalytical Chem.* 405, 2815–2823. doi: 10.1007/s00216-012-6517-2

Skrzypek, G., Sadler, R., and Paul, D. (2010). Error propagation in normalization of stable isotope data: a Monte Carlo analysis. *Rapid Commun. Mass Spectrom.* 24, 2697–2705. doi: 10.1002/rcm.4684

Smulders, F. O. H., Bakker, E. S., O'Shea, O. R., Campbell, J. E., Rhoades, O. K., and Christianen, M. J. A. (2023). Green turtles shape the seascape through grazing patch formation around habitat features: experimental evidence. *Ecology* 104, e3902. doi: 10.1002/ecy.3902

Snover, M. (2008). Ontogenetic habitat shifts in marine organisms: influencing factors and the impact of climate variability. *Bull. Mar. Sci.* 83, 53–67.

Stock, B., Jackson, A., Ward, E., Parnell, A., Phillips, D., and Semmens, B. (2018). Analyzing mixing systems using a new generation of Bayesian tracer mixing models. *PeerJ* 6, e5096. doi: 10.7717/peerj.5096

Stock, B. C., and Semmens, B. X. (2016). *MixSIAR GUI user manual, version 3.1*. Available at: https://github.com/brianstock/MixSIAR.

Stubbs, J. L., Marn, N., Vanderklift, M. A., Fossette, S., and Mitchell, N. J. (2020). Simulated growth and reproduction of green turtles (*Chelonia mydas*) under climate change and marine heatwave scenarios. *Ecol. Model.* 431, 109185. doi: 10.1016/j.ecolmodel.2020.109185

Stubbs, J. L., Revill, A. T., Pillans, R. D., and Vanderklift, M. A. (2022). Stable isotope composition of multiple tissues and individual amino acids reveals dietary variation among life stages in green turtles (*Chelonia mydas*) at ningaloo reef. *Mar. Biol.* 169, 72. doi: 10.1007/s00227-022-04055-6

Studley, S. A., Ripley, E. M., Elswick, E. R., Dorais, M. J., Fong, J., Finkelstein, D., et al. (2002). Analysis of sulfides in whole rock matrices by elemental analyzer–continuous flow isotope ratio mass spectrometry. *Chem. Geology* 192, 141–148. doi: 10.1016/S0009-2541(02)00162-6

Thomson, J. A., Whitman, E. R., Garcia-Rojas, M. I., Bellgrove, A., Ekins, M., Hays, G. C., et al. (2018). Individual specialization in a migratory grazer reflects long-term diet selectivity on a foraging ground: implications for isotope-based tracking. *Oecologia* 188, 429–439. doi: 10.1007/s00442-018-4218-z

Turner, J. A., Babcock, R. C., Hovey, R., and Kendrick, G. A. (2018). AUV-based classification of benthic communities of the Ningaloo shelf and mesophotic areas. *Coral Reefs* 37, 763–778. doi: 10.1007/s00338-018-1700-3

Turner Tomaszewicz, C., Seminoff, J., Avens, L., Goshe, L., Rguez-Baron, J., Peckham, S., et al. (2018). Expanding the coastal forager paradigm: long-term pelagic habitat use by green turtles *Chelonia mydas* in the eastern pacific ocean. *Mar. Ecol. Prog. Ser.* 587, 217–234. doi: 10.3354/meps12372

Vanderklift, M. A., Babcock, R. C., Barnes, P. B., Cresswell, A. K., Feng, M., Haywood, M. D. E., et al. (2020a). The oceanography and marine ecology of ningaloo, a world heritage area. *Oceanography and marine biology: an annual review*, vol 58. Eds. S. J. Hawkins, A. L. Allcock, A. E. Bates, L. B. Firth, I. P. Smith, S. E. Swearer, A. J. Evans, P. A. Todd, B. D. Russell and C. D. Mcquaid. (Taylor & Francis), 143–178.

Vanderklift, M. A., Pillans, R. D., Hutton, M., De Wever, L., Kendrick, G. A., Zavala-Perez, A., et al. (2021). High rates of herbivory in remote northwest Australian seagrass meadows by rabbitfish and green turtles. *Mar. Ecol. Prog. Ser.* 665, 63–73. doi: 10.3354/meps13657

Vanderklift, M. A., Pillans, R. D., Robson, N. A., Skrzypek, G., Stubbs, J. L., and Tucker, A. D. (2020b). Comparisons of stable isotope composition among tissues of green turtles. *Rapid Commun. Mass Spectrom.* 34, e8839. doi: 10.1002/rcm.8839

Vander Zanden, H. B., Bjorndal, K. A., and Bolten, A. B. (2013). Temporal consistency and individual specialization in resource use by green turtles in successive life stages. *Oecologia* 173, 767–777. doi: 10.1007/s00442-013-2655-2

Vander Zanden, H. B., Bjorndal, K. A., Mustin, W., Ponciano, J. M., and Bolten, A. B. (2012). Inherent variation in stable isotope values and discrimination factors in two life stages of green turtles. *Physiol. Biochem. Zool.* 85, 431–441. doi: 10.1086/666902

Vélez-Rubio, G. M., Cardona, L., López-Mendilaharsu, M., Martínez Souza, G., Carranza, A., González-Paredes, D., et al. (2016). Ontogenetic dietary changes of green turtles (*Chelonia mydas*) in the temperate southwestern Atlantic. *Mar. Biol.* 163, 57. doi: 10.1007/s00227-016-2827-9

Werner, E. E., and Gilliam, J. F. (1984). The ontogenetic niche and species interactions in size structured populations. *Annu. Rev. Ecol. Systematics* 15, 393–425. doi: 10.1146/annurev.es.15.110184.002141

Wood, S. (2011). Fast stable restricted maximum likelihood and marginal likelihood estimation of semiparametric generalized linear models. *J. R. Stat. Soc. B* 73, 3–36. doi: 10.1111/j.1467-9868.2010.00749.x

Wood, S. N. (2017). *Generalized Additive Models: an introduction with R. 2nd edition* (Boca Raton: Chapman and Hall/CRC), 496.

Frontiers in
Ecology and Evolution

Ecological and evolutionary research into our natural and anthropogenic world

This multidisciplinary journal covers the spectrum of ecological and evolutionary inquiry. It provides insights into our natural and anthropogenic world, and how it can best be managed.

Discover the latest Research Topics

See more →

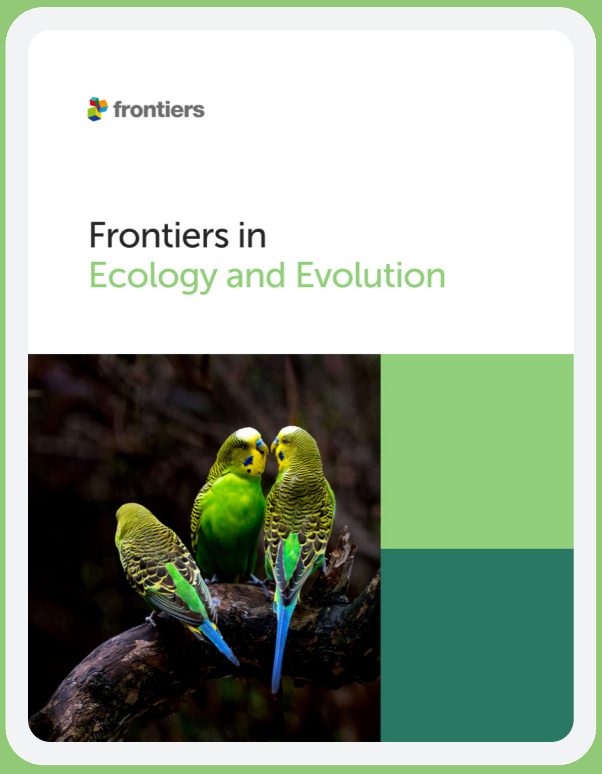

Frontiers

Avenue du Tribunal-Fédéral 34
1005 Lausanne, Switzerland
frontiersin.org

Contact us

+41 (0)21 510 17 00
frontiersin.org/about/contact